

This work is protected by copyright and other intellectual property rights and duplication or sale of all or part is not permitted, except that material may be duplicated by you for research, private study, criticism/review or educational purposes. Electronic or print copies are for your own personal, non-commercial use and shall not be passed to any other individual. No quotation may be published without proper acknowledgement. For any other use, or to quote extensively from the work, permission must be obtained from the copyright holder/s.

Investigating the impact of subchondral bone
health and activity levels on cartilage repair in
the knee.

Timothy HOPKINS

Doctor of Philosophy – Cell and Tissue Engineering

March 2021

Keele University

Abstract

Damage to the articular cartilage (AC) in the human knee, caused by physical trauma or degenerative disease, represents a common and complex clinical problem. AC has a very limited capacity for self-repair and, once damaged, rarely heals spontaneously. Several surgical interventions have been developed to restore the articular surface and prevent further AC damage and loss. Among these, cell therapies such as Autologous Chondrocyte Implantation (ACI) have demonstrated good mid- to long-term results in the treatment of chondral lesions. However, questions remain regarding the factors that influence a successful repair.

In this thesis, a Delphi consensus study among a panel of experts was used to identify research priorities in the cartilage repair field. The Delphi study highlighted factors that the panel agreed upon as being important in influencing the success of cartilage repair, some of which were used to develop or refine research questions for this thesis. The panel agreed that the subchondral bone (SB) was an important factor in cartilage repair and should be taken into account when planning therapeutic interventions, and that demographic and rehabilitative factors were also important factors.

An in vitro co-culture model was established and used to model the interaction between exogenous cells implanted as part of a cell-based, tissue engineering strategy for AC lesions, and the native endogenous cells of the SB. The co-culture model tested the effect of bone marrow-derived mesenchymal stromal cells (BM-MSCs), isolated from regions of the joint with varying degrees of SB degeneration, on the behaviour of allogeneic chondrocytes obtained from a donor with no history of OA. Chondrocytes co-cultured with BM-MSCs obtained from the more degenerated regions of the joint demonstrated a decrease in anabolic activity, with a downregulation of genes that

encode the major extracellular cartilage matrix proteins (collagen type 2 and aggrecan) and a corresponding decrease in the production of glycosaminoglycans (GAGs).

Transforming growth factor- β 1 (TGF- β 1) was identified as a protein that was differentially secreted by the BM-MSCs obtained from more and less degenerate SB regions and could be implicated in the differences in chondrocyte behaviour.

A preliminary study was carried out to investigate the histological and cellular characteristics of a clinically accessible measure of SB health, the presence of bone marrow oedema-like signals (BMELs) on magnetic resonance images (MRIs). Tissue from these areas, although similar in appearance on MRI, demonstrated a large amount of histological heterogeneity, although no cellular characteristics were identified that could explain these differences.

Finally, data collected as part of an on-going trial of cell therapies for the treatment of AC lesions, Autologous Chondrocytes, Stem Cells or the Two? (ASCOT), was analysed to investigate the relation between activity levels and knee function in the post-operative period. The influence of various demographic, anthropometric and psychological factors on this relation was also investigated. There was variation between patients in the relationship between activity levels and knee function, which correlated with the patients' negative affect (NA), a psychosocial construct that determines how an individual experiences negative emotions. NA was also found to be the best predictor of the primary outcome measure of the ASCOT trial, even when accounting for demographic, anthropometric and clinical factors. The results presented in this thesis add to current knowledge on the contribution of SB health, activity levels and psychosocial factors to the outcomes of cartilage repair therapy.

Contents

Abstract.....	ii
Contents.....	iv
List of Figures	xii
List of Tables	xvi
List of Appendices	xviii
Abbreviations	xix
Dissemination	xxiii
Acknowledgments.....	xxvii
1. Chapter 1: General Introduction	2
1.1 The Human Knee	2
1.1.1 Anatomical Overview.....	2
1.1.2 Articular Cartilage	4
1.1.2.1 Formation – Chondrogenesis	4
1.1.2.2 Structure	5
1.1.2.2.1 Zonal Organisation	5
1.1.2.2.2 Regional Organisation	8
1.1.2.2.3 Chondrocytes.....	11
1.1.2.2.4 The Extracellular Matrix	12
1.1.3 Subchondral Bone	21
1.1.3.1 Formation – Osteogenesis.....	21
1.1.3.2 Structure	22
1.1.3.3 Composition.....	25
1.1.3.3.1 Cellularity.....	25
1.1.3.3.2 The Extracellular Matrix	27
1.1.4 Cartilage Injury and Repair	29
1.1.4.1 Lesions of the Articular Cartilage	29
1.1.4.1.1 Epidemiology, Aetiology and Pathogenesis	29
1.1.4.2 Articular Cartilage Repair	30
1.1.4.2.1 Surgical Interventions.....	31
1.1.4.2.2 Factors that Influence a Successful Repair	39
1.1.5 Osteoarthritis	41
1.1.5.1 Epidemiology, Aetiology and Pathogenesis	41

1.1.5.2	Articular Cartilage in the Onset of Osteoarthritis	43
1.1.5.2.1	Osteoarthritic Changes in the Articular Cartilage	44
1.1.5.3	Subchondral Bone in the Onset of Osteoarthritis	46
1.1.5.3.1	Osteoarthritic Changes in the Subchondral Bone	48
1.1.6	The Osteochondral Junction	51
1.1.6.1	Tissue Interaction in Homeostasis.....	51
1.1.6.2	Tissue Interaction in Osteoarthritis.....	53
1.2	Aims and Objectives.....	55
2.	Chapter 2: Identifying Consensus and Research Priorities in the Field of Cartilage Repair: A Delphi Consensus Study.....	58
2.1	Introduction.....	58
2.1.1	Articular Cartilage Injury and Repair.....	58
2.1.2	The Delphi Technique	61
2.2	Materials and Methods.....	62
2.2.1	The Delphi Panel	62
2.2.2	The Delphi Process.....	63
2.2.3	Self-completed Questionnaires	64
2.2.4	Judging Consensus and Support or Importance	68
2.2.4.1	Likert-Scale Rated Single-statements	68
2.2.4.2	Ranked Series	68
2.2.5	Statistical Analyses.....	68
2.3	Results	70
2.3.1	The Delphi Panel	70
2.3.2	Responses	70
2.3.3	Items that Reached Consensus.....	70
2.3.3.1	Likert-Scale-Rated Single-Statements	70
2.3.3.2	Ranked Series	71
2.3.4	Items that did not Reach Consensus	79
2.3.4.1	Likert-Scale-Rated Single-Statements	79
2.3.4.2	Ranked Series	79
2.4	Discussion.....	83
2.4.1	Items that Reached Consensus.....	83
2.4.1.1	Likert-Scale-Rated Single-Statements	83
2.4.1.2	Ranked Statement Series.....	87

2.4.2	Statements That Did Not Reach Consensus	92
2.4.2.1	Likert-scale-rated Single-statements.....	92
2.4.2.2	Ranked Statement Series.....	94
2.4.3	The Delphi Panel	95
2.4.4	Study Limitations	98
2.5	Conclusion	98
2.6	Appendices	99
3.	Chapter 3: Investigating the Effect of Subchondral Bone Health on Articular Cartilage Repair in the Human Knee.	109
3.1	Introduction.....	109
3.2	Materials and Methods	115
3.2.1	Sample Collection	115
3.2.2	Macroscopic Sample Grading	115
3.2.3	Histological Assessment of Samples	117
3.2.3.1	Sample Processing and Sectioning	117
3.2.3.2	Dewaxing and Rehydrating Sections	117
3.2.3.3	Mayer’s Haematoxylin and Eosin Staining	117
3.2.3.4	Toluidine Blue Staining	118
3.2.3.5	Safranin O Staining	119
3.2.3.6	Microscopy	119
3.2.3.7	Histological Scoring Systems	120
3.2.3.7.1	The Osteoarthritis Research Society International (OARSI) Osteoarthritis Cartilage Histopathology Assessment System	120
3.2.3.7.2	Subchondral Bone Histological Grading System	120
3.2.3.7.3	Correlation Between Histological Scoring Systems.....	121
3.2.4	Primary Cell Isolation and Expansion.....	126
3.2.4.1	Media Formulations	126
3.2.4.1.1	Complete Culture Media	126
3.2.4.1.2	Chondrocyte Culture Media	126
3.2.4.1.3	Bone Marrow Mesenchymal Stromal Cell (BM-MS) Seeding Media ..	126
3.2.4.1.4	Chondrogenic Differentiation Media	126
3.2.4.1.5	Osteogenic Differentiation Media.....	126
3.2.4.2	Bone Marrow Derived Mesenchymal Stromal Cell (BM-MS) Isolation..	127
3.2.4.3	Chondrocyte Isolation	128

3.2.4.4	Passaging of Cells in Monolayer Culture	129
3.2.4.5	Cryopreservation of Cells	130
3.2.4.6	Recovery of Cells from Liquid Nitrogen.....	130
3.2.5	In-Vitro Co-Culture Model	131
3.2.5.1	Patients and Cell Populations.....	131
3.2.5.2	Co-Culture Model	132
3.2.5.2.1	Day -28 to Day 0	132
3.2.5.2.2	Day 0: Co-Culture Model Set-up.....	140
3.2.5.2.3	Experimental Endpoints: Day 0, Day 7, Day 14 and Day 21	148
3.2.6	Statistical Analyses.....	166
3.2.6.1	Flow Cytometry Data	167
3.2.6.2	qRT-PCR data	167
3.2.6.3	ELISA Data	168
3.2.6.4	Biochemistry Data	168
3.2.6.5	Statistical Software	168
3.3	Results	170
3.3.1	Patients	170
3.3.2	Sample Assessment and Grading.....	170
3.3.2.1	Samples obtained from TKR surgery at RJAH.....	170
3.3.2.1.1	Macroscopic Assessment	170
3.3.2.1.2	Histological Assessment	170
3.3.2.2	NHSBT Sample Obtained from Young Patient.....	176
3.3.2.2.1	Macroscopic Assessment	176
3.3.2.2.2	Histological Assessment	176
3.3.3	Co-Culture	179
3.3.3.1	Patients.....	179
3.3.3.2	Characterisation of Cells Prior to Co-culture.....	179
3.3.3.2.1	BM-MSC Characterisation by Flow Cytometry.....	179
3.3.3.3	Output from co-culture model	183
3.3.3.3.1	Chondrocyte-laden Agarose Scaffolds	183
3.3.3.3.2	Conditioned Media	211
3.3.3.3.3	Osteogenically Differentiated BM-MSCs.....	219
3.4	Discussion.....	226

3.5	Study Limitations.....	241
3.6	Conclusion.....	242
4.	Chapter 4: A preliminary investigation into the histological and cellular characteristics of regions with and without MRI-identified subchondral bone features.....	244
4.1	Introduction.....	244
4.2	Materials and Methods.....	253
4.2.1	Patient Identification.....	253
4.2.2	Sample Collection and Assessment.....	253
4.2.2.1	Subchondral Bone Region Identification.....	254
4.2.2.2	Macroscopic Cartilage Grading.....	257
4.2.2.3	Histological Assessment of Samples.....	257
4.2.2.3.1	Sample Processing and Sectioning.....	257
4.2.2.3.2	Dewaxing and Rehydrating Sections for Staining.....	257
4.2.2.3.3	Mayer’s Haematoxylin and Eosin Staining.....	258
4.2.2.3.4	Toluidine Blue Staining.....	258
4.2.2.3.5	Microscopy.....	258
4.2.2.3.6	Histological Scoring Systems.....	258
4.2.3	Primary Osteoblast Isolation and Expansion.....	259
4.2.3.1	Osteoblast Culture Media.....	259
4.2.3.2	Osteoblast Isolation.....	259
4.2.3.3	Cryopreservation of Osteoblasts.....	261
4.2.3.4	Osteoblast Yield.....	261
4.2.3.5	Alkaline Phosphatase Staining.....	262
4.2.4	Experimental Set-up.....	262
4.2.4.1	Recovery of Osteoblasts from Liquid Nitrogen Storage.....	262
4.2.5	Experimental Endpoint Analysis.....	263
4.2.5.1	Gene Expression Analysis.....	263
4.2.5.1.1	Ribonucleic Acid (RNA) Extraction.....	263
4.2.5.1.2	Reverse Transcription.....	264
4.2.5.1.3	Quantitative Real-time Polymerase Chain Reaction (qRT-PCR).....	264
4.2.5.1.4	dsDNA Quantification.....	265
4.2.5.2	Statistical Analyses.....	265
4.2.5.2.1	Correlation Between Histological Scores.....	265
4.2.5.2.2	Osteoblast Yield.....	265

4.2.5.2.3	qRT-PCR	266
4.2.5.2.4	dsDNA Quantification	266
4.3	Results	267
4.3.1	Patients	267
4.3.2	Macroscopic Cartilage Grading	267
4.3.3	Histological Assessment	268
4.3.3.1	The Osteoarthritis Research Society International (OARSI) Osteoarthritis Cartilage Histopathology Assessment System	268
4.3.3.2	Subchondral Bone Histological Grading System	268
4.3.3.2.1	Correlation and Differences in Scoring Systems	271
4.3.3.3	Morphological Features	271
4.3.3.3.1	Subchondral Bone Cyst – Patient 6	281
4.3.4	Osteoblast Outgrowth	281
4.3.5	Osteoblast Yield	281
4.3.6	Alkaline Phosphatase Staining	281
4.3.7	dsDNA Quantification	287
4.3.8	Gene Expression Profile	289
4.3.8.1	Alkaline Phosphatase (ALPL)	289
4.3.8.2	Bone morphogenic protein 2 (BMP2)	289
4.3.8.3	Collagen type 1, alpha 1 (COL1A1)	289
4.3.8.4	Bone gamma-carboxyglutamate (gla) protein (BGLAP) (Osteocalcin)	289
4.3.8.5	Secreted phosphoprotein 1 (SPP1) (Osteopontin)	289
4.3.8.6	Runt-related transcription factor 2 (RUNX2)	289
4.4	Discussion	291
4.5	Study Limitations	299
4.6	Conclusion	300
5.	Investigating the Relationship Between Activity Levels and Knee Function in the Post- Operative Period Following Cartilage Repair with Cell Therapy	302
5.1	Introduction	302
5.2	Materials and Methods	306
5.2.1	Patients	306
5.2.2	Autologous Stem Cells, Chondrocytes or the Two? (ASCOT) Trial	306
5.2.2.1	ASCOT Rehabilitation Program	307
5.2.2.2	Trial Assessments	307

5.2.2.2.1	The Lysholm Knee Scoring Scale	307
5.2.2.2.2	The Human Activity Profile (HAP)	311
5.2.2.2.3	The International Positive and Negative Affect Schedule Short Form (I-PANAS-SF)	316
5.2.3	Data Acquisition	319
5.2.4	Preparation of Data for Analysis	319
5.2.5	Data Analysis	321
5.2.5.1	General Analyses	321
5.2.5.2	Power Analysis	321
5.2.5.3	Assessing the Temporal Stability of the I-PANAS-SF	321
5.2.5.4	Numeric Coding of String Variables	322
5.2.5.5	Normality	322
5.2.5.6	Assessing Variation Between Patients	323
5.2.5.6.1	Centring AAS	323
5.2.5.6.2	Multilevel Modelling	323
5.2.5.7	Identifying Factors that Influence Variation Between Patients	324
5.2.5.7.1	Predictors of Individual Activity-Knee function Slopes	324
5.2.5.8	Identifying Factors that Predict Post-Operative Knee Function and Activity Levels	325
5.3	Results	326
5.3.1	Power Analysis	326
5.3.2	Patient Demographics and Clinical Characteristics	326
5.3.3	General Analyses	326
5.3.3.1	Lysholm Knee Score	326
5.3.3.2	Adjusted Activity Score	327
5.3.3.3	Negative Affect Score	330
5.3.3.4	Positive Affect Score	330
5.3.4	Assessing the Temporal Stability of the I-PANAS-SF for individual patients	333
5.3.4.1	Negative Affect	333
5.3.4.2	Positive Affect	333
5.3.5	Assessing Variation Between Patients	337
5.3.5.1	Multilevel Modelling	337
5.3.5.1.1	Centred vs Non-Centred AAS	337
5.3.5.1.2	All Timepoints	337

5.3.5.1.3	Removal of 2-Month Follow-up Data.....	337
5.3.6	Factors Influencing Slope.....	341
5.3.6.1	Psychosocial factors (PA and NA).....	341
5.3.6.1.1	All Timepoints.....	341
5.3.6.1.2	Removal of 2-Month Follow-up Data.....	341
5.3.6.2	Demographic and Psychosocial Factors.....	346
5.3.6.2.1	All Timepoints.....	346
5.3.6.2.2	Removal of 2-Month Follow-up Data.....	346
5.3.7	Predictors of Individual Outcome Measures at 15-Month.....	346
5.3.7.1	15-Month Lysholm Score.....	346
5.3.7.2	15-Month AAS.....	347
5.4	Discussion.....	348
5.5	Study Limitations.....	355
5.6	Conclusion.....	355
6.	General Discussion.....	367
6.1	Future Work.....	372
7.	References.....	374

List of Figures

Figure 1-1: Anatomy of the Human Knee Joint..	3
Figure 1-2: Zonal Organisation of Adult Articular Cartilage.	7
Figure 1-3: Regional Organisation of the Extracellular Matrix..	10
Figure 1-4: The Characteristic ‘Bottle-brush’ Configuration of the Aggrecan Large Aggregating Proteoglycan (PG).....	16
Figure 1-5: The Osteochondral Junction in a Normal Adult Knee Joint (aged 53 years).....	24
Figure 1-6: Osteoarthritic Changes in the Human Knee Joint..	42
Figure 1-7: A schematic overview of the thesis.....	56
Figure 2-1: 5-point Likert scale..	65
Figure 2-2: An example of the Likert-scale-rated single-statement question type layout from (A) the round 2 questionnaire and (B) the round 3 questionnaire..	66
Figure 2-3: An example of the ranked series question type layout from (A) the round 2 questionnaire and (B) the round 3 questionnaire.	67
Figure 2-4: APMO cut-off rate equation.....	69
Figure 2-5: Kendall’s Coefficient of Concordance (W) equation..	69
Figure 2-6: The Round 2 Likert-scale-rated single-statements.....	73
Figure 2-7: The round 3 Likert-scale-rated single-statements..	75
Figure 2-8: Change in APMO, between rounds 2 and 3, of the Likert-scale-rated single-statements that did not reach threshold consensus over the course of this Delphi study. ...	81
Figure 2-9: The change in Kendall's coefficient of concordance (W), between rounds 2 and 3, of the ranked series that did not reach consensus over the course of this Delphi study.	82
Figure 3-1: The International Cartilage Repair Society (ICRS) Cartilage Lesion Classification System.....	116
Figure 3-2: Example histological images for OARSI Osteoarthritis Cartilage Histopathology Grading System.....	123
Figure 3-3: Example histological images for the subchondral bone histological grading system.....	125
Figure 3-4: Overview of the novel in-vitro co-culture model.....	134
Figure 3-5: Flow chart to illustrate the timescale of the co-culture model with key events at relevant timepoints.....	135
Figure 3-6: Example analysis of flow cytometry data to determine immunopositivity of a number of cell surface markers.....	139
Figure 3-7: Photographs illustrating the set-up and harvest of the chondrocyte-loaded agarose scaffolds.....	143
Figure 3-8: Plate layout for the set up of the co-culture model.....	146
Figure 3-9: Schematic of the indirect co-culture model.....	147
Figure 3-10: Examples of the macroscopic appearance of knee condyles collected from patients following TKR surgery..	173
Figure 3-11: Macroscopic appearance of the condyle obtained from a young patient with no history of OA..	174

Figure 3-12: Graphical representation of the correlation between the OARSI OA Cartilage Histopathology Assessment System and the Subchondral Bone Histological Grading System.	177
Figure 3-13: Histological Staining of Normal Articular Cartilage from NHSBT Sample..	178
Figure 3-14: Flow cytometry data demonstrating the immunoprofile of healthy and unhealthy BM-MSC populations prior to seeding for the co-culture model.....	182
Figure 3-15: Representative images of a chondrocyte-agarose scaffold removed from the 24-well inserts in the co-culture model for analysis..	185
Figure 3-16: Representative images of stained sections from the chondrocyte-loaded agarose scaffolds at day 0.....	186
Figure 3-17: Representative images of stained sections from cell-free control agarose scaffolds at day 0..	187
Figure 3-18: Representative images of H&E and Alcian Blue stained sections from the top of day 21 chondrocyte-loaded agarose scaffolds co-cultured with healthy BM-MSCs.....	188
Figure 3-19: Representative images of H&E and Alcian Blue stained sections from the bottom of the day 21 chondrocyte-loaded agarose scaffolds co-cultured with healthy BM-MSCs.....	189
Figure 3-20: Representative images of H&E and Alcian Blue stained sections from the top of the day 21 chondrocyte-loaded agarose scaffolds co-cultured with unhealthy BM-MSCs. .	190
Figure 3-21: Representative images of H&E and Alcian Blue stained sections from the bottom of the day 21 chondrocyte-loaded agarose scaffolds co-cultured with unhealthy BM-MSCs.....	191
Figure 3-22: Representative images of H&E and Alcian Blue stained sections from the top of the day 21 chondrocyte-loaded agarose scaffolds from the chondrocyte-only control.....	192
Figure 3-23: Representative images of H&E and Alcian Blue stained sections from the bottom of the day 21 chondrocyte-loaded agarose scaffolds from the chondrocyte-only control.....	193
Figure 3-24: Representative images of H&E and Alcian Blue stained sections from the cell-free agarose scaffolds at day 21.	194
Figure 3-25: Wet weight of the agarose-chondrocyte scaffolds removed from the co-culture at the various timepoints.....	197
Figure 3-26: Mean chondrocyte number in scaffolds taken from the co-culture model at the four timepoints..	198
Figure 3-27: Mean total GAG content of agarose scaffolds taken from the co-culture model at the four timepoints.....	200
Figure 3-28: Average GAG/chondrocyte of the scaffolds taken from the co-culture model at the four timepoints.....	202
Figure 3-29: Relative fold change of SOX9 (top) and COL2A1 (bottom) between day 0 and day 21 of the co-culture.....	206
Figure 3-30: Relative fold change of ACAN (top) and ALK1 (bottom) between day 0 and day 21 of the co-culture..	207
Figure 3-31: Relative fold change of COL10A1 (top) and MMP-3 (bottom) between day 0 and day 21 of the co-culture.....	208

Figure 3-32: Relative fold change of MMP-13 (top) and ADAMTS4 (bottom) between day 0 and day 21 of the co-culture.....	209
Figure 3-33: Relative fold change of ADAMTS5 between day 0 and day 21 of the co-culture..	210
Figure 3-34: MMP-1 concentration in conditioned media at day 0, day 7 and day 21 of the co-culture model, as determined by ELISA.....	215
Figure 3-35: Mean MMP-13 concentration in conditioned media at day 0, day 7 and day 21 of the co-culture model, as determined by ELISA..	216
Figure 3-36: Mean TGF- β 1 concentration in conditioned media at day 0, day 7 and day 21 of the co-culture model, as determined by ELISA..	217
Figure 3-37: Mean VEGF concentration in conditioned media at day 0, day 7 and day 21 of the co-culture model, as determined by ELISA..	218
Figure 3-38: Mean dsDNA content for each of the two BM-MSCs types in the co-culture model, over the course of the experiment.....	220
Figure 3-39: Relative fold change of ALP (top) and BMP2 (bottom) in BM-MSCs between day 0 and day 21 of the co-culture.....	223
Figure 3-40: Relative fold change of COL1A1 (top) and BGLAP (bottom) in BM-MSCs between day 0 and day 21 of the co-culture.....	224
Figure 3-41: Relative fold change of SPP1 (top) and RUNX2 (bottom) in BM-MSCs between day 0 and day 21 of the co-culture.....	225
Figure 4-1: Overview of Experimental Procedure.	252
Figure 4-2: Example procedure for the location of SB abnormalities in excised osteochondral tissue using MRIs– Patient 1.....	255
Figure 4-3: Example procedure for the location of SB abnormalities in excised osteochondral tissue using MRIs – Patient 2.....	256
Figure 4-4: Correlation between histological scores.	273
Figure 4-5: Patient 1 histological findings.....	274
Figure 4-6: Patient 1 histological findings (continued).....	275
Figure 4-7: Patient 2 histological findings.....	276
Figure 4-8: Patient 2 histological findings (continued).....	277
Figure 4-9: Patient 3 histological findings.....	278
Figure 4-10: Patient 4 histological findings.....	279
Figure 4-11: Patient 5 histological findings.....	280
Figure 4-12: Identification of a subchondral bone cyst – Patient 6.....	282
Figure 4-13: Patient 6 histological findings (haematoxylin & eosin).....	283
Figure 4-14: Osteoblast outgrowth from subchondral trabecular bone chips.....	284
Figure 4-15: Mean osteoblast yield from lesioned and normal areas.....	285
Figure 4-16: Histochemical staining of alkaline phosphatase activity.....	286
Figure 4-17: Mean dsDNA content (pg) of osteoblast populations following experimental seeding.....	288
Figure 4-18: Fold difference in gene expression between osteoblasts isolated from lesioned and normal regions.	290
Figure 5-1: Lysholm Knee Scoring System used in the ASCOT Trial.....	309
Figure 5-2: Lysholm Knee Scoring System used in the ASCOT Trial (continued).....	310

Figure 5-3: The Human Activity Profile used in the ASCOT Trial..	313
Figure 5-4: The Human Activity Profile used in the ASCOT Trial (continued)..	314
Figure 5-5: The Human Activity Profile used in the ASCOT Trial (continued)..	315
Figure 5-6: The International Positive and Negative Affect Schedule - Short Form (I-PANAS-SF) used in the ASCOT Trial.	318
Figure 5-7: Mean Lysholm score over the course of the study.	328
Figure 5-8: Mean AAS score over the course of the study.	329
Figure 5-9: Mean NA over the course of the study..	331
Figure 5-10: Mean PA over the course of the study.	332
Figure 5-11: Bland-Altman plot of mean baseline and 15-month NA scores.	335
Figure 5-12: Bland-Altman plot of mean baseline and 15-month PA scores..	336
Figure 5-13: Plots of the individual patient plots resulting from robust linear multilevel modelling of the full data set.	339
Figure 5-14: Plots of the individual patient plots resulting from robust linear multilevel modelling of the data set excluding the 2-month follow-up.	340
Figure 5-15: Scatter plot to demonstrate the correlation between individual patient slopes, created using the full data set, and mean NA scores.	342
Figure 5-16: Scatter plot to demonstrate the correlation between individual patient slopes, created using the full data set, and mean PA scores.	343
Figure 5-17: Scatter plot to demonstrate the correlation between individual patient slopes, created with the 2-month follow-up data excluded, and mean NA scores.	344
Figure 5-18: Scatter plot to demonstrate the correlation between individual patient slopes, created with the 2-month follow-up data excluded, and mean PA scores.	345
Figure 6-1: An overview of the chapters that constitute this thesis, including a brief summary of key results.	367

List of Tables

Table 1-1: Zonal Organisation of Adult Articular Cartilage.....	6
Table 1-2: Non-collagenous Proteins and Glycoproteins in the ECM.....	20
Table 1-3: Factors that Influence Cartilage Repair.. ..	40
Table 2-1: Delphi study response rates.. ..	72
Table 2-2: The Likert-scale-rated single-statement items that reached threshold consensus in round 2.....	74
Table 2-3: The likert-scale-rated single-statement items that reached threshold consensus in round 3.....	76
Table 2-4: A summary of the consensus results for the ranked series in round 2 (Kendall's coefficient of concordance (W) and corresponding consensus level).....	77
Table 2-5: A summary of the consensus results for the ranked series in round 3 (Kendall's coefficient of concordance (W) and corresponding consensus level).....	78
Table 2-6: A summary of the Likert-scale-rated single-statement items that did not reach threshold consensus over the course of this Delphi study.....	80
Table 2-7: A Summary of the Likert-scale-rated single-statements that encompass parameters and considerations for the assessment of a structurally successful cartilage repair.....	88
Table 2-8: A Summary of the Likert-scale-rated single-statements that are considered to be factors that could influence a structurally successful repair.....	89
Table 2-9: A Summary of the Likert-scale-rated single-statements that encompass economic and ethical considerations of cartilage repair.	90
Table 2-10: The resulting 'Tissue Type' hierarchy based on the mean ranks of the items in the ranked series that reached threshold consensus.....	91
Table 3-1: OARSI Osteoarthritis Cartilage Histopathology Grading System. Key features for grades 0-6 (Pritzker et al., 2006).....	122
Table 3-2: Subchondral bone histological grading system. Key features for Grades 0-3 (Aho et al., 2017).	124
Table 3-3: Panel of cell surface markers interrogated to assess the immunoprofile of BM-MSCs prior to seeding for the co-culture model.	138
Table 3-4: Matrix used to calculate the number of chondrocytes and volumes of agarose and cell suspension required for the set up of each batch of the co-culture model.	142
Table 3-5: Lambda DNA standards used in DNA quantification.	151
Table 3-6: Chondroitin sulphate standards used in glycosaminoglycan quantification.....	151
Table 3-7: Volume of cDNA reverse transcription kit components and RNA required, per reaction, for the reverse transcription of RNA to cDNA.....	155
Table 3-8: Genes assessed by qRT-PCR in chondrocyte-agarose scaffolds from the co-culture model at day 0 and day 21.....	156
Table 3-9: Volume of SYBR green, primer and cDNA required per reaction for qRT-PCR. ...	157
Table 3-10: Thermal cycle used for qRT-PCR reaction.....	157
Table 3-11: Genes assessed by qRT-PCR in differentiated BM-MSCs from the co-culture model at day 0 and day 21.....	165

Table 3-12: Demographic information of the 16 patients from which knee condyles were obtained.....	172
Table 3-13: Macroscopic (ICRS Cartilage Lesion Grade) and histological scores (OARSI OA Cartilage Histopathology Grade and Subchondral Bone Histological Grade) of condyles obtained from patients undergoing TKR surgery.	175
Table 3-14: Demographic information of patients whose donated tissue was selected for use in the in-vitro co-culture model.....	180
Table 3-15: Flow cytometry results from BM-MSC characterisation..	181
Table 3-16: The lower limit of detection for each of the analytes quantified in the conditioned media using ELISAs.	214
Table 4-1: Patient demographic information and relevant MRI findings.....	269
Table 4-2: Macroscopic and histological scores of isolated regions of interest.....	270
Table 5-1: Prepared data utilised in this study..	320

List of Appendices

Appendix 2-1: A full list of the Likert-scale-rated single-statements and results from the round 2 questionnaire.	99
Appendix 2-2: A full list of the Likert-scale-rated single-statements and results from the round 3 questionnaire.	103
Appendix 2-3: A full list of the statement series and results from the round 2 questionnaire.	106
Appendix 2-4: A full list of the statement series and results from the round 3 questionnaire.	107
Appendix 5-1: Flow chart summarising the procedures involved in the ChALK study.	357
Appendix 5-2: Patient information sheet for the ChALK Study.	363
Appendix 5-3: Health Research Authority (HRA) Approval letter for the ChALK study.	365

Abbreviations

3D-MOCART – 3-Dimensional Magnetic Resonance Observation of Cartilage Repair Tissue

AAS – Adjusted activity score

AC – Articular cartilage

ACAN – Aggrecan

ACI – Autologous chondrocyte implantation

ACVRL1 – Activin A receptor type II-like 1

ADAMTS4 – A disintegrin and metalloproteinase with thrombospondin motifs 4

ADAMTS5 – A disintegrin and metalloproteinase with thrombospondin motifs 5

ALK1 – Activin receptor-like kinase 1

ALPL – Alkaline phosphatase

AMIC – Autologous Matrix-Induced Chondrogenesis

ANOVA – Analysis of variance

APC – Allophycocyanin

APMO – Average percentage majority opinions

BGLAP – Bone gamma-carboxyglutamate protein

BLC – Bone-lining cell

BMI – Body mass index

BML – Bone marrow lesion

BM-MSC – Bone marrow-derived mesenchymal stromal cell

BMP2 – Bone morphogenic protein 2

BSA – Bovine serum albumin

BV421 – Brilliant violet 421

cDNA – Complimentary deoxyribonucleic acid

CI – Confidence Intervals

COL10A1 – Collagen type 1 alpha 1

COL1A1 – Collagen type 1 alpha 1

COL2A1 – Collagen type 2 alpha 1

COMP – Cartilage oligomeric matrix protein

CROAKS – Cartilage Repair Osteoarthritis Knee Score

DMEM/F12 – Dulbecco's modified eagle medium: nutrient mixture F-12

DMMB – Dimethylmethylene blue

DNA – Deoxyribonucleic acid

ECM – Extracellular Matrix

ELISA – Enzyme-Linked Immunosorbent Assay

FACS – Fluorescence-activated cell sorting

FBS – Foetal bovine serum

FGFR3 – Fibroblast growth factor receptor 3

GAG – Glycosaminoglycan

GAPDH – Glyceraldehyde-3-phosphate dehydrogenase

GMP – Good Manufacturing Practice

H&E – Haematoxylin and Eosin

HA – Hyaluronan

HAP – Human Activity Profile

HPRT1 – Hypoxanthine phosphoribosyltransferase 1

ICRS – International Cartilage Regeneration and Joint Preservation Society

IFN- γ – Interferon Gamma

IPA – Isopropanol

I-PANAS-SF – International Positive and Negative Affect Schedule – Short Form

IQR – Inter-quartile range

ISCT – International Society for Cellular Therapy

ITS-X – Insulin-transferrin-selenium-ethanolamine

KS – Keratan Sulphate

LP – Link protein

MACI – Matrix-induced autologous chondrocyte implantation

MAS – Maximum Activity Score

MMP13 – Matrix metalloproteinase-13

MMP3 – Matrix metalloproteinase-13

MOAKS – MRI Osteoarthritis Knee Score

MRI – Magnetic Resonance Imaging

mRNA – Messenger Ribonucleic Acid

NA – Negative Affect

NHSBT – National Health Service Blood and Transplant Service

OA – Osteoarthritis

OARSI – Osteoarthritis Research Society International

OATS – Osteochondral Autograft Transplantation

OB – Osteoblast

OC – Osteoclast

OCA – Osteochondral Allograft...

P/S – Penicillin/Streptomycin

PA – Positive Affect

PBS – Phosphate Buffered Saline

PE – Phycoerythrin

PercP-Cy5.5 – Peridinin-chlorophyll-protein-Cyanine5.5

PG – Proteoglycan

PPIA – Peptidylprolyl isomerase A

PROM – Patient reported outcome measure

qRT-PCR – Quantitative real-time polymerase chain reaction

RNA – Ribonucleic acid

RUNX2 – Runt-related transcription factor 2

SB – Subchondral bone

SD – Standard deviation

SEM – Standard error of the mean

SOX9 – SRY-Box Transcription Factor 9

SPP1 – Secreted phosphoprotein 1

SPSS – Statistical package for the social sciences

TBP – TATA-binding protein

TGF- β 1 – Transforming growth factor- β 1

TKR – Total knee replacement

WORMS – Whole-Organ Magnetic Resonance Imaging Score

Dissemination

Publications

Full Manuscripts:

- Hopkins T., Richardson JB., Kuiper JH. **Identifying consensus and research priorities in the field of Cartilage Repair: a Delphi study** (in preparation)
- Wang JS., Wright K., Perry J., Tins B., Hopkins T., Hulme C., McCarthy H., Brown A., Richardson JB. **Combined Autologous Chondrocyte and Bone Marrow Mesenchymal Stromal Cell Implantation in the Knee: An 8-year Follow-up of Two First-In-Man Cases** (*Cell Transplantation*, 2019).
- Mennan C., Hopkins T., Channon A., Elliot M., Johnstone B., Kadir T., Loughlin J., Peffers M., Pitsillides A., Sofat N., Stewart C., Watt F.E., Zeggini E., Roberts S. **A Delphi study on the Use of Technology in the Subcategorisation of Osteoarthritis** (*Osteoarthritis and Cartilage*, 2020).
- Hopkins T., Richardson JB., Williams JM., Linklater-Jones B., Wales J., Roberts S., Kuiper JH. **The Effect of Affect: How a Patient’s Outlook Can Influence Their Recovery** (in preparation).
- Hareklea Markides, Jane S McLaren, Timothy Hopkins, Cameron Black, Richard Oreffo, Brigitte Scammel, Lisa White, Alicia El Haj. **Short term evaluation of cellular fate in an ovine bone injury model** (in preparation).
- Hopkins T., Wright, KT., Roberts S., Kuiper JH. **‘Investigating the effect of subchondral bone health on articular cartilage repair using a novel, in-vitro, co-culture model’**. (in preparation).

- Hopkins T., Wright, KT., Roberts S., Tins, B., Kuiper JH. **‘A preliminary investigation into the histological and cellular characteristics of regions with and without MRI-identified subchondral bone features’** (in preparation).

Abstracts:

- Hopkins T., Richardson JB., Kuiper, JH. (2018) Cartilage Repair: A Delphi Consensus Study. Submitted to International Cartilage Regeneration and Joint Preservation Society (ICRS) 14th World Congress in Macau, China. *In-press*.
- Hopkins, T., Richardson, J., Williams, M., Linklater-Jones, B., Wales, J., Roberts, S. and Kuiper, J. (2018). The effect of activity levels on the function of the human knee: preliminary examination of data collected as part of an ongoing cell therapy clinical trial. *eCM Online Periodical*, 4, p.120.
- Rotheram, M., Nahar, T., Goodman, T., Hopkins, T., Studd, A., Telling, N., Gates, M. and El Haj, A. (2018). Remote control of cell signalling using tagged magnetic nanoparticles for neuronal cell differentiation- emerging cell therapies for Parkinson’s disease. *eCM Online Periodical*, 4, p.20.
- Hopkins, T., Richardson, JB., Roberts, S., Williams, M., Linklater-Jones, B., Wales, J., Kuiper, JH. The Effect of Affect: Characterising the Relationship between Activity Levels, Knee Function and Emotion. Submitted to International Cartilage Regeneration and Joint Preservation Society (ICRS) 15th World Congress in Vancouver, Canada. *In-press*.

Awards

- **ICRS Young Investigator's Award 2018.** This accolade is awarded every 18 months for an individual who has demonstrated excellence in the field of cartilage repair and joint preservation research.

Conference Participation

Podium Presentations:

- Tissue Engineering Centre meeting for Arthritis Research UK (Newcastle, 2017).
- 11th Oswestry Cartilage Symposium (Oswestry, 2017) (co-organiser).
- Robert Jones and Agnes Hunt Orthopaedic Hospital Research Day (Oswestry, 2018).
- Keele University Postgraduate Symposium (Stoke-on-Trent, 2018).
- Robert Jones and Agnes Hunt Orthopaedic Hospital Research Day (Oswestry, 2019) (awarded 2nd place).
- International Cartilage Regeneration and Joint Preservation Society (ICRS) 15th World Congress. (Vancouver, 2019) (Presented by Prof. Roberts).

Poster Presentations:

- European Society of Tissue Regeneration in Orthopaedics and Traumatology (ESTROT) 3rd Congress (Leeds, 2017).
- Robert Jones and Agnes Hunt Orthopaedic Hospital Research Day (Oswestry, 2017).
- Keele University Postgraduate Symposium (Stoke-on-Trent, 2017).
- 10th Oswestry Cartilage Symposium (Oswestry, 2017).
- International Cartilage Regeneration and Joint Preservation Society (ICRS) 14th World Congress (Macau (China), 2018).

- The Institute of Liberal Arts and Sciences 3rd Annual Meeting: ‘Turning Heads: Changing Minds’ (Keele University, Stoke-on-Trent, 2018).
- 18th Annual Meeting of the Tissue and Cell Engineering Society (TCES) (Keele University, Stoke-on-Trent, 2018)
- Tissue Engineering Centre meeting for Arthritis Research UK (York, 2018)
- Mercia Stem Cell Alliance (MCSA) 8th Annual Scientific Meeting (Birmingham, 2018)
- Organ-on-a-Chip Technology Network Learning and Collaborative Event (London, 2019)
- The Institute of Liberal Arts and Sciences Postgraduate Conference: ‘Disrupting Disciplines: Sharing Perspectives’ (Keele University, Stoke-on-Trent, 2019).
- Versus Arthritis Musculoskeletal Pain Research in the UK (Nottingham, 2019).

Acknowledgments

I would like to express my sincere gratitude to my supervisor, Dr Jan Herman Kuiper. You inherited the additional workload and responsibility of this project and steadied the ship under difficult circumstances. Since then you have provided endless support and guidance, not to mention statistical wizardry! Your unwavering enthusiasm and optimism have helped me to no end, especially when experiments were not going entirely to plan. You have an incredible ability to explain complex concepts in an accessible way and I came away from every one of our meetings with a greater understanding and a number of new ways to tackle my research questions. Thank you for everything.

Additionally, I must thank our group lead Professor Sally Roberts, your unrelenting passion for research is truly inspirational. Several chapters of this thesis would not exist without your influence, invention and encyclopaedic knowledge of cartilage form and function. My PhD experience would not have been the same had I not been lucky enough to be a part of your research group and I can only hope to have outgrown the impression I made at my first ARUK TEC conference...

My thanks also go to Dr Karina Wright for your support, guidance and scientific creativity. The laboratory-based aspect of this thesis would not be the same without your input.

I would also like to thank Dr Nicola Kuiper. The co-culture work would not have been possible without your hypotheses and idea for the model.

To the rest of the spinal studies and cartilage research group, John, Claire, Mike, Helen, Jade, Charlotte, Kobe. I would firstly like to thank you all for your individual technical support over the course of my PhD. As a collective, I want to thank you all for making the

last four years so enjoyable, I am incredibly lucky to have you all as colleagues and to count you all as friends.

I must also thank all of the orthopaedic surgeons at the Robert Jones and Agnes Hunt Orthopaedic Hospital for the provision of tissue samples. I would like to particularly thank Mr Pete Gallacher, Mr Simon Roberts, Mr Andrew Barnett, Mr Paul Germin for their additional involvement in the ChALK study. My thanks also go to Teresa Jones for her help with the completion of the ChALK ethics. Additionally, I would like to thank Dr Bernhard Tins for help tracking down and locating subchondral bone features on MRIs. I would also like to thank all of those whom were involved in the inception of the ASCOT trial, and those who continue to collect data from participants, particularly Johanna Wales and Dr Andrea Bailey.

Finally, I would like to thank my family for their unending support, advice and motivation (and for allowing me to occupy your office for the last four months). Mum and Dad, I promise I am finished with education and will be looking for an actual job as soon as possible!

To Zoe, I could not have reached this stage in the process without your incredible support and understanding. I know I have been a bit absent for the last year or so, spending Christmas in the lab and every weekend in recent memory writing, thank you for bearing with me. I can't wait to see what the future holds.

This thesis is dedicated, in memoriam, to Professor James 'Prof' Richardson.

Chapter 1:
General Introduction

1. Chapter 1: General Introduction

1.1 The Human Knee

1.1.1 Anatomical Overview

The human knee is a synovial, diarthrodial, modified hinge joint that allows flexion and extension, as well as limited rotation, while providing stability during articulation (Vaughn et al., 2014; Vaienti et al., 2017; Ondrésik et al., 2017) (Figure 1-1). The knee comprises two separate articulations; the femorotibial joint, which bears the majority of the body weight, and the patellofemoral joint, which ensures a frictionless transfer of the forces generated by the contraction of the quadriceps muscle over the knee (Abulhasan & Grey, 2017). The femorotibial joint comprises the contact between femur and tibia at their respective articular surfaces: the medial and lateral femoral condyles with the medial and lateral tibial plateaux, separated by synovial fluid within the joint, to form the largest joint in the body (Ondrésik et al., 2017). Wedge-like menisci sit between the femoral condyles and tibial plateaux, increasing the contact area, preventing the lateral displacement of the bones and providing cushioning during impact loading (Abulhasan & Grey, 2017; Ondrésik et al., 2017). In the patellofemoral joint, the articular surface on the posterior patella is in contact with the trochlear groove (Vaienti et al., 2017). The movement of the osseous components is stabilised by a combination of ligaments, tendons, the joint capsule and the surrounding musculature of the upper and lower leg (Ondrésik et al., 2017). All articulating surfaces of the knee are covered by a layer of articular cartilage (AC), which is a specialised type of hyaline cartilage (Abulhasan & Grey, 2017; Vaienti et al., 2017).

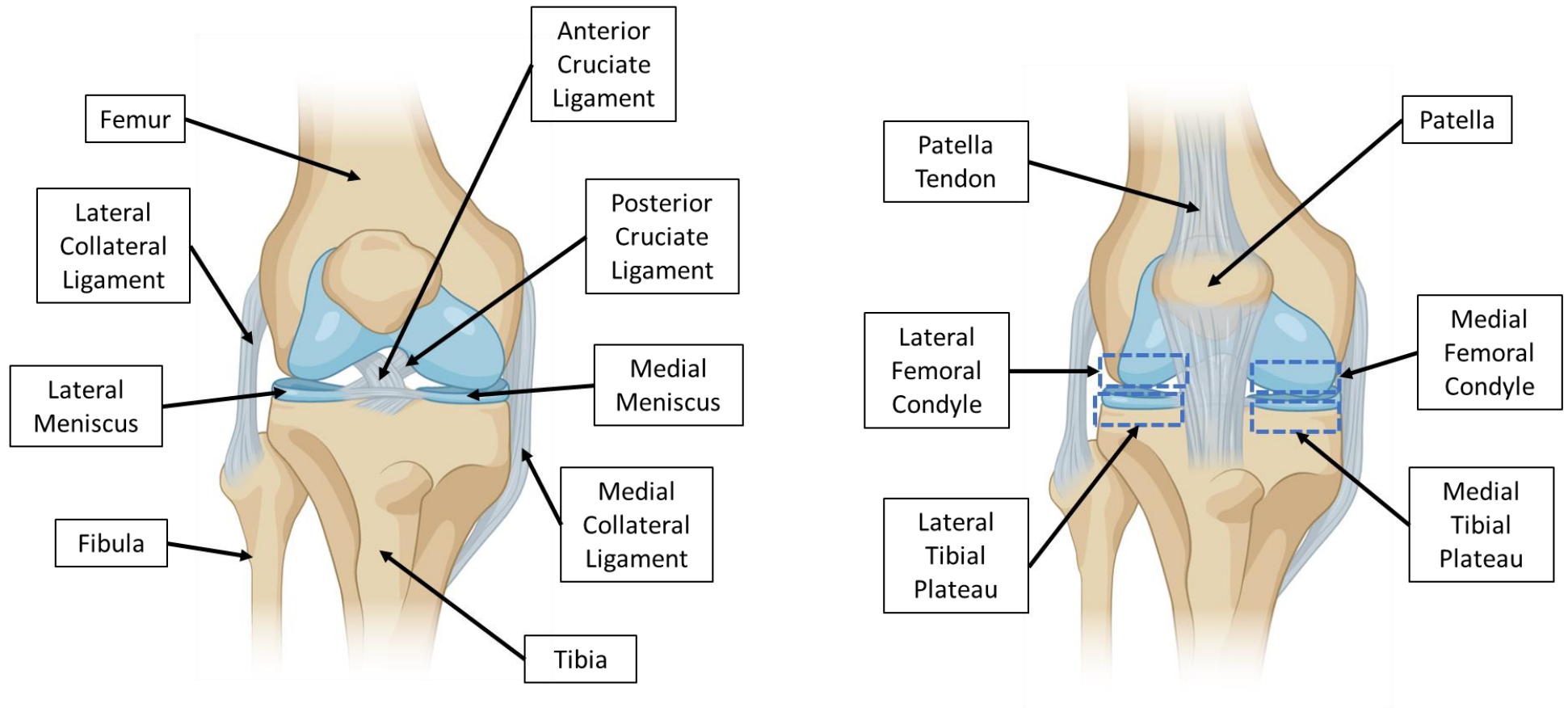


Figure 1-1: *Anatomy of the Human Knee Joint*. Left: Anterior plane with patella tendon removed to allow visualisation of the cruciate ligaments. Right: Anterior plane including the patella tendon. Created with BioRender.com.

1.1.2 Articular Cartilage

AC is critical for the functioning of the synovial joint and is uniquely adapted to provide a low-friction, lubricated and wear resistant surface for articulation, and to distribute compressive forces generated during locomotion (Fox et al., 2009; Klein et al., 2009; Athanasiou et al., 2013). AC is avascular, lacks innervation and lymphatics and contains only one cell type but the tissue is far from simple, representing a highly specialised connective tissue with a complex composition (Fox et al., 2009; Ondrésik et al., 2017). AC is characterised by a sparse distribution of highly specialised cells, chondrocytes, contained within a dense, hydrated extracellular matrix (ECM) (Ondrésik et al., 2017).

1.1.2.1 *Formation – Chondrogenesis*

Chondrogenesis occurs early in the embryonic formation of the skeletal system and is characterised by mesenchymal cell condensation and subsequent differentiation of chondroprogenitors (Goldring, 2012). In brief, mesenchymal cells migrate from the mesoderm and the neural crest and condense to form skeletal blastema, in a process regulated by mesenchymal-epithelial cell interactions (Goldring et al., 2006; Pitsillides & Ashhurst, 2008; Goldring, 2012). Chondroprogenitors within these pre-cartilage condensations then differentiate, adopting a chondrocyte phenotype that is characterised by the secretion of cartilage-matrix specific proteins, such as collagen types II, IX and XI and aggrecan, and a downregulation of collagen type I (Pitsillides & Ashhurst, 2008; Goldring, 2012). As a result, cartilaginous nodules arise in the middle of the blastema and elongate as the chondrocytes continue to proliferate and secrete matrix, eventually forming cartilage anlagen which act as a template for long bone formation (Pitsillides & Ashhurst, 2008). Following chondrogenesis, resting chondrocytes at the end of the opposing long bones form the articular cartilage by way of the continued secretion of matrix, eventually pushing the

cells apart (Goldring, 2012). Chondrocytes in the centre of the cartilage anlagen undergo continued proliferation, terminal differentiation, hypertrophy and apoptosis in a process termed 'endochondral ossification' whereby the hypertrophic cartilage is replaced by bone (Goldring, 2012).

1.1.2.2 *Structure*

1.1.2.2.1 *Zonal Organisation*

In the process of development, the AC acquires a layered structure that provides the tissue with its ability to resist compressive, tensile and shear forces and can be divided into four zones that vary in terms of composition, structure and function: 1) superficial zone, 2) middle (or transitional) zone, 3) deep zone, 4) calcified zone (Decker et al., 2015; Ondrésik et al., 2017). A summary of the ECM composition, function and cellular characteristics of each of these zones is given in table 1-1 and displayed in figure 1-2.

Chapter 1

Table 1-1: Zonal Organisation of Adult Articular Cartilage. A summary of the typical composition, cellular characteristics and function of each of the zones of normal human knee cartilage. (Eyre, David, 2001; Buckwalter et al., 2005; Fox et al., 2009; Athanasiou et al., 2013; Decker et al., 2015; Lee et al., 2015; Ondrésik et al., 2017).

Zone	Typical Thickness (% of total AC depth)	Function	Extracellular Matrix Components	Chondrocytes
Superficial (Tangential) Zone	~15%	Provides the AC with most of its tensile strength. Protects the deeper layers from shear stress and tensile forces.	Thin, tightly packed collagen fibrils (mainly type I, II and IX collagen) that run parallel to the articular surface. Low proteoglycan content compared to the other zones. Highest fibronectin and water content.	High number of flattened individual chondrocytes. Chondrocytes synthesise proteins that provide surface lubrication e.g. lubricin.
Middle (Transitional) Zone	~50%	Provides anatomical and functional transition between superficial and deep zones.	High concentration of proteoglycans (particularly aggrecan) and thicker collagen fibrils that are organised obliquely.	Low density but slightly larger in size compared to the superficial zone and oval/spherical in shape. Cells contain a higher concentration of synthetic organelles.
Deep Zone	~30%	Provides the greatest resistance to compressive forces.	Largest diameter fibrils arranged perpendicular to the articular surface in a radial disposition. Highest proteoglycan content and lowest water content of the three non-mineralised zones.	Sparse and spherical, organised into columns between collagen fibres.
Calcified Zone	~5%	Forms a boundary between the AC and SB, the start of it being marked by the basophilic tidemark. Secures cartilage to bone and redistributes forces acting at the surface.	Calcified matrix, types II and X collagen fibrils are abundant.	Cell population is scarce, chondrocytes are small and completely encased in mineralised ECM.

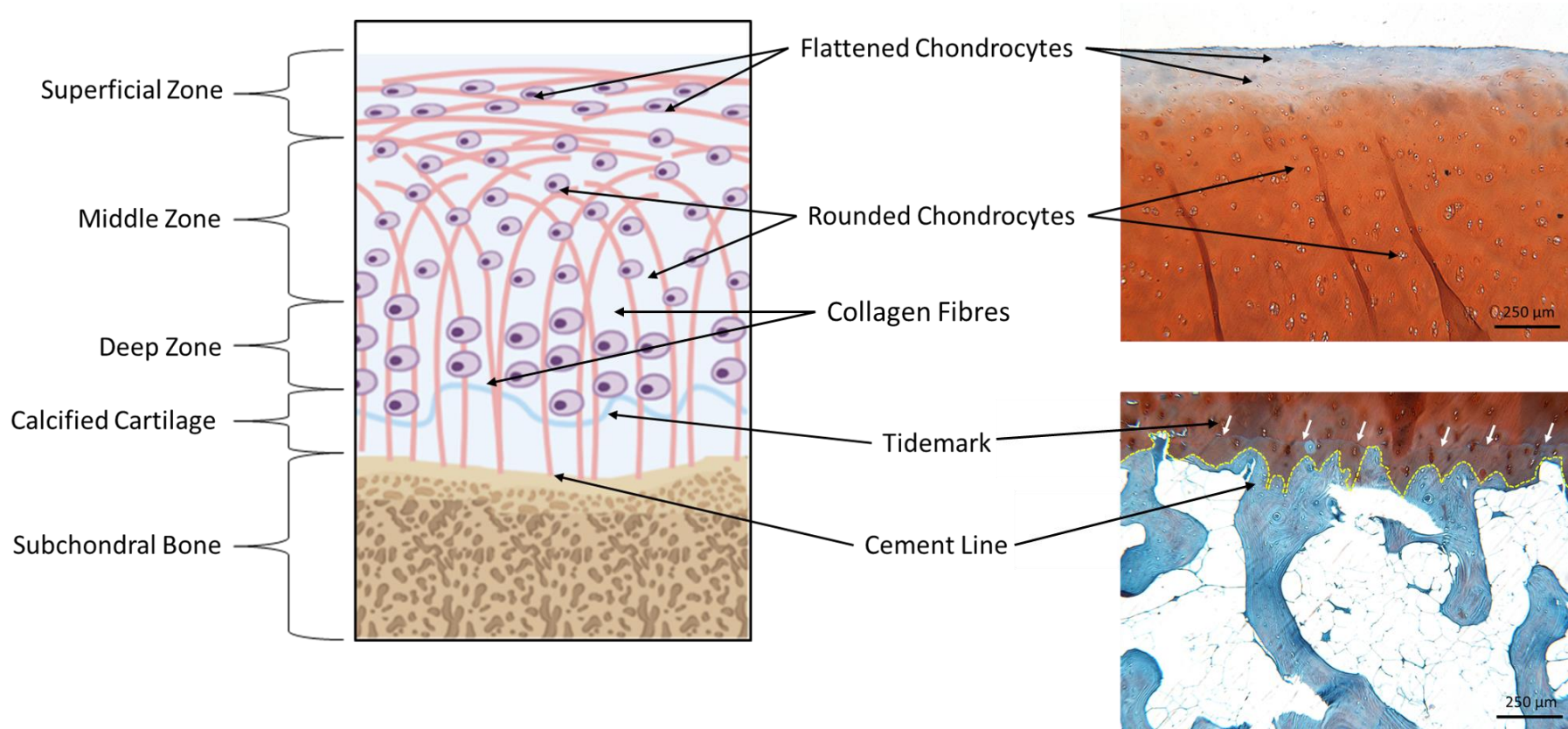


Figure 1-2: Zonal Organisation of Adult Articular Cartilage. Schematic (left; created with BioRender.com) and histological images of macroscopically normal AC from the knee of a 53-year-old, human male (right) demonstrating the zonal variations in the size, shape, number and distribution of chondrocytes, as well as zonal variations in the distribution of collagen fibres. Collagen fibres form the characteristic ‘arcade’ formation, running perpendicular to the articular surface in the deep zone, obliquely to the surface in the middle zone and parallel to the surface in the superficial zone. Rounded chondrocytes are arranged between collagen fibres in the deep zone and arranged randomly in the middle zone. The superficial zone is densely populated with flattened chondrocytes. The tidemark represents the separation between the non-calcified and calcified cartilage (white arrows). The cement line indicates the border between the calcified cartilage and subchondral bone plate (dashed, yellow line).

1.1.2.2.2 Regional Organisation

In addition to the horizontal, zonal subdivisions of the AC, the tissue also has a microscale structure that is orientated circumferentially around each chondrocyte (Poole, 1997; Athanasiou et al., 2013) (Figure 1-3). The composition and characteristics of the tissue matrix varies based on the proximity to the individual chondrocytes and can be separated into three, clearly discernible regions: the pericellular matrix, the territorial matrix and the interterritorial matrix (Poole, 1997; Athanasiou et al., 2013).

1. The Pericellular Matrix.

The pericellular matrix immediately surrounds the chondrocytes and comprises of a tightly woven, densely compacted enclosure of fine collagen fibres (primarily collagen type VI), forming an enclosure around each chondrocyte (Poole, 1997). The pericellular matrix is enriched with hyaluronan, sulphated proteoglycans (PGs), biglycan and a range of matrix glycoproteins including link protein, fibronectin, laminin and anchorin CII, which is associated with the binding of the cell matrix to collagen fibres (Poole, 1997; Buckwalter et al., 2005; Athanasiou et al., 2013). This region is thought to play a functional role in initiating the signal transduction of biomechanical signals within cartilage upon load bearing (Guilak et al., 2006).

In the deep and middle zones of the ECM, the pericellular matrix is also surrounded by a pericellular capsule, which contains a variety of fibrillar and filamentous components, and physically separates the chondrocyte and its pericellular matrix microenvironment from the more coarsely structured territorial matrix that surrounds it (Poole et al., 1987; Athanasiou et al., 2013). The chondrocyte, pericellular matrix and pericellular capsule comprises the

chondron, the basic functional, structural and metabolic unit of the AC (Poole et al., 1987; Poole, 1997).

2. The Territorial Matrix.

The territorial matrix is composed of fine collagen fibrils (primarily collagen type II) which are woven into a basket-like structure around the pericellular matrix (Poole, 1997; Athanasiou et al., 2013). The collagen fibres are interspaced with regions of chondroitin-sulphate (CS)-rich PGs, which are highly abundant in this region (Poole, 1997). The territorial region is thought to play a role in protecting the chondrocytes against mechanical stresses and may contribute to the ability of the AC to withstand mechanical loads (Buckwalter et al., 2005; Athanasiou et al., 2013).

3. The Inter-Territorial Matrix.

The inter-territorial matrix is the largest region and the furthest from the chondrocyte. This region contains thick (50nm or greater), densely packed collagen fibres and a high concentration of keratan-sulphate (KS)-rich PGs (Poole, 1997; Athanasiou et al., 2013). The inter-territorial matrix is typified by a gradient of increasing collagen fibril diameter with increasing distance from the chondrocyte (Hunziker et al., 1997). This region provides the bulk of the AC and is therefore thought to contribute most to the AC's mechanical properties (Athanasiou et al., 2013).

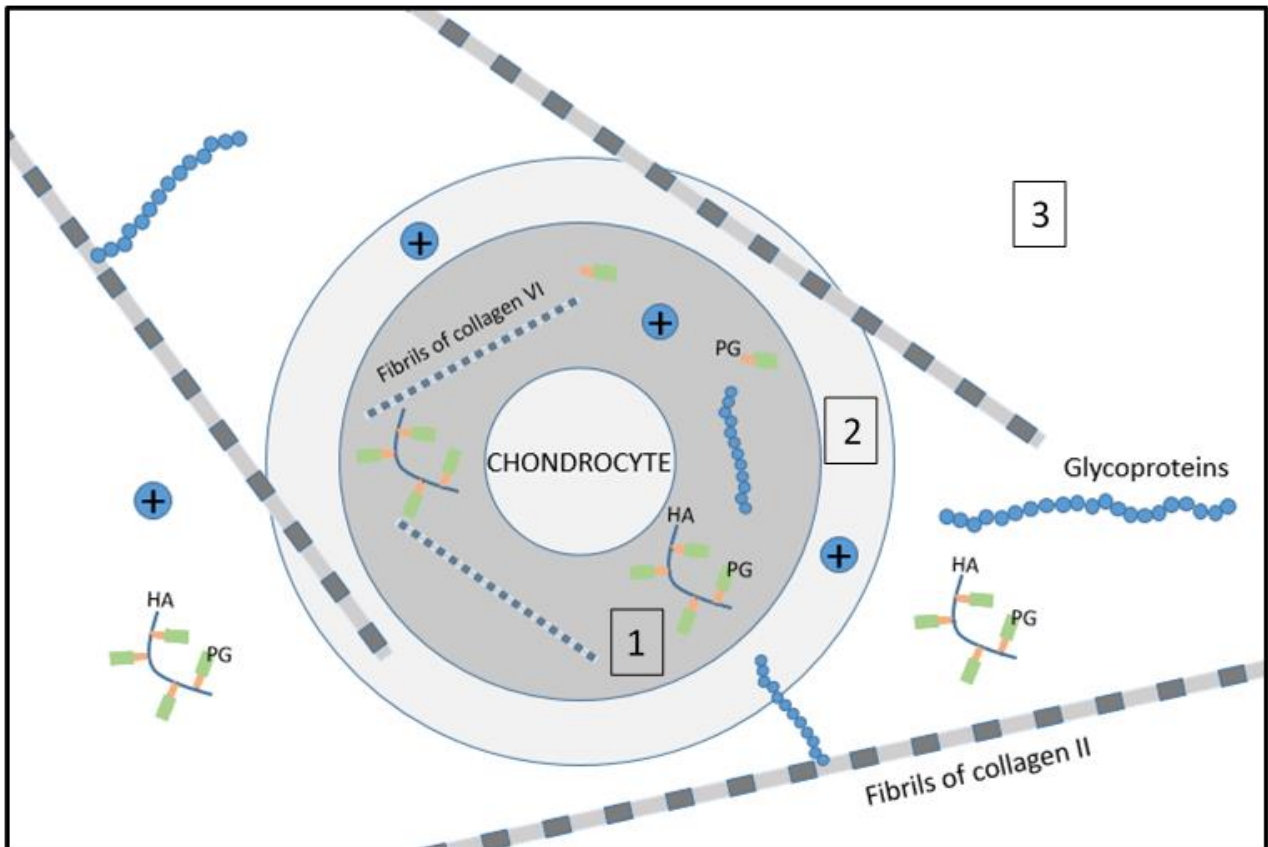


*Figure 1-3: Regional Organisation of the Extracellular Matrix. The extracellular matrix can be separated into distinct regions based on the distance from the chondrocyte. 1: Pericellular matrix, 2: Territorial matrix, 3: Inter-territorial Matrix. Large aggregating proteoglycan (aggrecan), made up of aggrecan subunits (**PG**) associated with a central hyaluronan filament (**HA**), are ubiquitous in all three of the ECM regions. GAGs on the PGs imbue a large negative charge which attracts positive ions (+) such as K^+ , Na^+ , H^+ , Ca^{2+} and Mg^{2+} , increasing the osmolarity and fluid flow into the ECM. Figure adapted from (Sobol et al., 2011).*

1.1.2.2.3 Chondrocytes

Chondrocytes are the sole resident cell of the AC and are highly specialised for the generation and maintenance of the various components that make up the ECM (Vaienti et al., 2017). Although chondrocytes are often quiescent, they can be metabolically active, even in the low oxygen tension environment of the joint and are able to synthesise and organise all of the necessary matrix proteins to form the macromolecular framework of the ECM (Akkiraju & Nohe, 2015). Chondrocytes are also able to respond to biochemical and biomechanical stimuli to modify matrix composition through the secretion of a number of catabolic and anabolic factors as well as signalling and transcription factors (Buckwalter et al., 2005; Guilak et al., 2006; Zhang et al., 2009).

Chondrocytes are typically oval or spheroidal in shape, with a diameter of $\sim 13\mu\text{m}$, but can vary in shape and size and depending on their resident zone within the AC (Hunziker, 2002; Buckwalter et al., 2005; Goldring, 2012). In comparison to other connective tissues, AC is sparsely populated with cells, with chondrocytes making up only 1-5% of the total tissue volume (Stockwell, 1967; Athanasiou et al., 2013). Chondrocytes reside within lacunae in the AC, ensuring that they are cytoplasmically separated from each other, and therefore cell-to-cell interaction is limited (Athanasiou et al., 2013).

1.1.2.2.3.1 Chondrocyte Mechanotransduction

Appropriate mechanical loading is important for both the formation and homeostasis of AC, with evidence that both reduced loading and overloading have a catabolic effect on the ECM (Leong et al., 2011; Dolzani et al., 2019). Conversely, specific mechanical loads have been shown to mitigate cartilage erosion, with compressive forces enhancing matrix-protein biosynthesis, remodelling and mechanical properties (Dolzani et al., 2019).

Mechanotransduction is the process by which biomechanical signals are able to regulate cell activity and behaviour (Leong et al., 2011). Chondrocytes are able to sense and respond to changes within the ECM that are induced by physical forces, such as shear stress, compressive loading, tension, hydrostatic pressure and fluid flow (Leong et al., 2011; Zhao, et al., 2020). Chondrocyte gene transcription, cell signalling and biosynthesis have been shown to change in response to mechanical forces in intact adult AC (Szafranski et al., 2004). Mechanical forces are able to regulate multiple steps along the biosynthetic pathway including transcription, translation and post-translational events, through the modulation of a number of pathways, including Indian hedgehog, Wnt and TGF- β 1 pathways (Szafranski et al., 2004; Zhao et al., 2020). Thus, mechanical signals are able to influence matrix composition (Kim et al., 1996).

Chondrocyte mechanotransduction is mediated by interactions between the cell membrane and the pericellular matrix (Leong et al., 2011). The structural properties of the pericellular matrix allow for the transmission of mechanical signals from the ECM environment to mechanoreceptors on the surface of the chondrocyte (Zhao et al., 2020). A series of mechanoreceptors exist on the cell surface, including primary cilium, mechanosensitive ion channels and integrins (Zhao et al., 2020).

1.1.2.2.4 The Extracellular Matrix

The main component of AC is the ECM, which makes up more than 90% of the tissue volume (Arkill & Winlove, 2008). The ECM is composed primarily of tissue fluid, collagens and proteoglycans with other non-collagenous proteins, glycoproteins, lipids and phospholipids at lower abundances (Buckwalter et al., 2005; Athanasiou et al., 2013). These components are broadly arranged into two groups: those that make up the tissue fluid, and those that make up the structural macromolecular framework. Components of the macromolecular

framework interact with the charged fluid environment to retain water within the ECM, thus preserving the biomechanical properties of the AC (Athanasίου et al., 2013).

1.1.2.2.4.1 Tissue Fluid

Tissue fluid is the most abundant component of the ECM and AC as a whole, making up 85% of the wet weight (Fox et al., 2009). The major component of the tissue fluid is water, the high proportion of which allows for the load dependant deformation of the AC. The relative water concentration of the ECM varies between zones, decreasing from the superficial zone (80%) to the deep zone (65%). Tissue fluid is found mainly in the molecular pore space of the ECM and is able to permeate through the whole tissue (Fox et al., 2009). It contains dissolved inorganic ions (sodium, calcium, chloride and potassium), gases, small proteins and metabolites (Buckwalter et al., 2005; Fox et al., 2009). The flow of water through the cartilage and across the articulating surface aids in the transport and distribution of nutrients to chondrocytes and lubrication at the articulating surface (Fox et al., 2009).

1.1.2.2.4.2 Glycosaminoglycans and Proteoglycans

Glycosaminoglycans (GAGs) are linear polysaccharides composed of varying numbers of repeating disaccharide units (Vynios, Karamanos & Tsiganos, 2002). They play an important role in the maintenance of AC structure and function through their modulation of osmolarity (Athanasίου et al., 2013). GAGs can be divided into two groups: non-sulphated, to which only hyaluronan (HA) belongs and sulphated, which comprise chondroitin sulphate (CS, types 4 and 6), keratan sulphate (KS), dermatan sulphate (DS) and heparan sulphate (HS) (Vynios, Karamanos & Tsiganos, 2002).

GAGs in aqueous solution occupy a large hydrodynamic volume. In AC, the GAG volume is constrained by the collagen type II fibres, forcing the GAG molecules closer together. This generates a high osmotic pressure; this in turn is caused by the large negative charges on

the GAGs (due to, for example, carboxyl, hydroxyl and sulphate groups) attracting neutralising cations, known as the Gibbs-Donnan effect (Maroudas, 1976). Typically, CS has two charges per disaccharide and KS one, although the degree of sulphation can vary with age and disease (Urban & Roberts, 1995). The osmotic pressure leads to the influx of fluid, which causes a swelling pressure and continues until the swelling pressure it is resisted by the tension arising in the surrounding macromolecular framework, formed primarily by type II collagen fibres.

Proteoglycans (PGs) are highly glycosylated protein monomers and form the second largest group of macromolecules in the ECM after collagens, making up 10-20% of the wet weight of cartilage. They consist of a protein core, to which 1 or more (maybe as many as 100-150) linear GAG side chains are covalently bound (Maroudas, 1976). PGs are produced and secreted into the ECM by chondrocytes and the main one in cartilage, aggrecan, helps to maintain the electrolyte and therefore fluid balance in the AC because of its GAG chains (Maroudas, 1976; Hardingham & Fosang, 1992).

There are two main types of PG in adult AC:

1. Large aggregating proteoglycans.

Of the large aggregating proteoglycans, the largest in size and the most abundant in cartilage ECM is aggrecan. Aggrecan has a primarily linear core protein but there are 3 globular regions: G1, G2 and G3 (Figure 1-4). G1 is the means whereby aggrecan monomers (~1-2M Da molecular weight) attach to hyaluronan, forming the typical and very large aggregate molecules of aggrecan. This G1-HA attachment is secured via the glycoprotein, link protein (Roughley, 2001; Athanasiou et al., 2013; Roughley & Mort, 2014). Aggrecan can possess more than 100 long, linear GAG side chains of chondroitin sulphate and keratan

sulphate covalently bound to its protein core (Athanasίου et al., 2013). This leads to the formation of the characteristic 'bottle-brush' configuration (Athanasίου et al., 2013; Roughley & Mort, 2014) (Figure 1-4).

2. Small, non-aggregating proteoglycans.

Small, non-aggregating PGs help to stabilise the matrix through their interaction with collagen fibrils (Buckwalter et al., 2005) as well as having other functions. The most abundant of these are decorin, fibromodulin and biglycan, all of which belong to a sub-group of PGs known as small leucine-rich proteoglycans (SLRPs). Decorin, which has one dermatan sulphate chain and fibromodulin which has several keratan sulphate chains, is able to interact with type II collagen and play a role in fibrillogenesis and interfibril interaction (Fox et al., 2009); a more important function of decorin, however, appears to be its binding with TGF β , perhaps contributing to its anabolic and protective effects against OA (Li et al., 2020). Biglycan which possesses 2 dermatan sulphate chains is found mainly in the pericellular matrix directly surrounding the chondrocytes and is thought to interact with collagen type VI (Buckwalter et al., 2005).

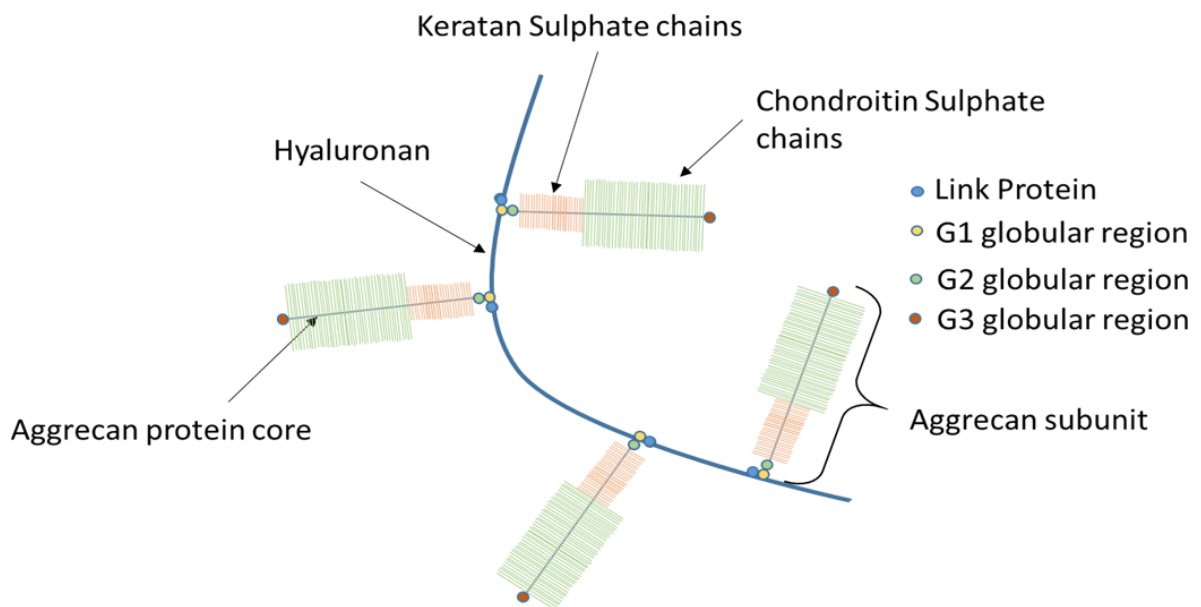


Figure 1-4: The Characteristic 'Bottle-brush' Configuration of the Aggrecan Large Aggregating Proteoglycan (PG). Aggrecan molecules which possess regions that are rich in keratan sulphate and chondroitin sulphate, are associated with the central hyaluronan filament via the G1 domain of the core protein, the binding of which is stabilised by link proteins.

1.1.2.2.4.3 Collagens

Collagens are the most abundant proteins of the body by weight, accounting for roughly two-thirds of the dry weight of adult AC (Eyre, 2001; Athanasiou et al., 2013). Collagen fibres are distributed uniformly throughout the cartilage, except in the collagen-rich superficial zone in which they are far more dense (Buckwalter et al., 2005). Collagen fibril organization and composition varies between zones, but collagen content per wet weight does not vary significantly with depth (Klein et al., 2009). Type II collagen is the predominant type, accounting for 90-95% of the collagen found in AC, with types III, VI, IX, X, XI, XII and XIV found in lower abundancies (Cohen et al., 1998; Eyre, 2001).

The fibrillar framework that frames the ECM of the AC is comprised of a heteropolymer of collagen types II, IX and XI (Eyre et al., 2006). Collagen type XI molecules are primarily crosslinked to each other and are thought to form an interconnecting, secondary network that provides links between, and constrains the lateral growth of, collagen type II fibrils (Eyre, 2001; Eyre et al., 2006). Collagen type IX molecules are covalently linked to the surface of the collagen type II fibres (Eyre et al., 2006).

Each collagen type has a specific function in the AC:

- Type II: is the predominant collagen type in AC comprising more than half the dry weight of the tissue, forming a fibrillary meshwork intertwined with proteoglycan aggregates supported by the less abundant collagens (types IX and XI) that gives cartilage its tensile strength and stiffness (Eyre, 2001; Eyre et al., 2006; Athanasiou et al., 2013). The extracellular framework formed by type II collagen also plays a part in resisting the swelling pressures created by the proteoglycans (Athanasiou et al., 2013).

- Type III: has been found to copolymerised and linked to collagen II fibrils in human cartilage (Eyre, 2001)
- Type VI: constitutes less than 1% of the total collagen and forms part of the pericellular matrix (immediately surrounding the chondrocytes) and is thought to aid in chondrocyte attachment to the matrix (Buckwalter et al., 2005). Collagen type VI self-assembles into a distinctive filamentous, basket-like network that is able to bind a number of ECM proteins, including type II collagen and decorin, forming a network which anchors the chondrocyte to the PCM in AC (Eyre et al., 2006; Luo et al., 2017).
- Type IX: constitutes 1-5% of total collagen in adult AC and is found crosslinked to the surface of the type II macrofibril (Eyre et al., 2006). Collagen type IX plays a part in regulating type II fibrillary diameter (Wotton et al., 1988; Eyre et al., 2006).
- Type X: constitutes 1% of the total collagen in adult AC and it closely related to the hypertrophic chondrocytes of the calcified layer, playing a key role in cartilage mineralisation (Eyre, 2001; Athanasiou et al., 2013). Also provides structural support and is a major component of the tidemark (Buckwalter et al., 2005; Athanasiou et al., 2013).
- Type XI: found mainly covalently bonded to each other, or to type II macrofibrils and makes up 3% of total collagen in adult AC (Eyre et al., 2006; Luo et al., 2017).

Collagen type XI is believed to form a template that constrains the lateral growth of the type II collagen hetero-fibril (Eyre, 2001; Buckwalter et al., 2005).

1.1.2.2.4.4 Non-Collagenous Proteins and Glycoproteins

AC contains a number of non-collagenous proteins and glycoproteins in its ECM, which differ greatly in structure, function and distribution (Roughley, 2001). The function of many of

these molecules is not fully characterized, however some of the suggested functions are listed in table 1-2 (Roughley, 2001; Athanasiou et al., 2013).

Table 1-2: Non-collagenous Proteins and Glycoproteins in the ECM. The specific function of many of these proteins has not been fully characterised but several authors report possible functions.

Protein	Reported Function
Cartilage oligomeric matrix protein (COMP)	Structural role in the ECM. Associates with collagen type IX (Roughley, 2001; Athanasiou et al., 2013).
Fibronectin	Component of the cell matrix adhesion complex and plays a role in the organisation of the ECM (Chevalier, 1993; Roughley, 2001).
Link protein	Stabilises the association between the aggrecan subunit and the central hyaluronan filament (Roughley & Mort, 2014).
Anchorin CII	Binds chondrocytes to type II and type X collagen fibres (Kirsch & Pfäffle, 1992).

1.1.3 Subchondral Bone

1.1.3.1 *Formation – Osteogenesis*

Human bone develops in two different ways depending on its type and location:

Intramembranous ossification, which is responsible for the formation of the craniofacial bones (Ortega et al., 2004).

Endochondral ossification, a complex, tightly controlled embryonic developmental process, which is responsible for the formation of the axial skeleton, including the long bones (Ortega et al., 2004; Mackie et al., 2008). Endochondral ossification involves a number of closely regulated steps which results in the replacement of hyaline cartilage with bone:

1. Initially, mesoderm-derived MSCs commit to a chondrogenic lineage and then condense into compact nodules before differentiating into chondroblasts (Gilbert, 2000; Ortega et al., 2004; Breeland et al., 2020).
2. The differentiated chondrocytes rapidly proliferate, secreting cartilage specific ECM and forming a cartilage template for bone morphogenesis, called cartilage anlagen (Gilbert, 2000; Ortega et al., 2004; Breeland et al., 2020).
3. Chondrocytes cease dividing and become hypertrophic, induced by fibroblast growth factor 18, Indian hedgehog and bone morphogenic proteins (Ortega et al., 2004).
4. This causes the cells to rapidly increase in volume and secrete an altered ECM containing more collagen type X and fibronectin. This allows the matrix surrounding the terminally differentiated chondrocytes to be mineralised (Gilbert, 2000; Ortega et al., 2004; Breeland et al., 2020).
5. Blood vessels invade the ECM and the hypertrophic chondrocytes in the neck of the bone die by apoptosis as the calcification of the ECM prevents nutrients from reaching the chondrocytes (Breeland et al., 2020).

6. As the chondrocytes die, a group of MSCs that surround the cartilage anlagen differentiate into osteoblasts (Ortega et al., 2004).
7. The newly differentiated osteoblasts begin forming bone matrix on the partially degraded cartilage, initially at the primary (epiphyseal) ossification site (Gilbert, 2000; Ortega et al., 2004). While the cartilage is replaced by bone in the diaphysis, the cartilage continues to proliferate at the ends of the bones, increasing bone length (Breeland et al., 2020).

1.1.3.2 *Structure*

The subchondral bone (SB) begins distally where the calcified cartilage ends, but has poor distal definition where it merges into the epiphysis of the bone (Figure 1-5) (Suri & Walsh, 2012; Li et al., 2013). The calcified cartilage consists of calcified collagen type II and type X and is also avascular and aneural, which is in contrast to the SB which has blood vessels and nerves. The SB is a highly dynamic structure (despite its inert appearance) and is specially adapted to cope with the mechanical forces created in the articular joints during locomotion (Suri & Walsh, 2012; Li et al., 2013; Florencio-Silva et al., 2015). SB has important roles in supporting the overlying AC and distributing forces across the joint with a gradual transition in stress and strain (Suri & Walsh, 2012; Li et al., 2013).

SB can be separated into two anatomically distinct regions:

1. The subchondral bone plate: A thin, cortical lamella lying directly beneath the calcified cartilage layer from which it is separated by the cement line (Li et al., 2013; Uygur et al., 2015). This layer is invaded by channels, that contain a large number of arterial and venous vessels, as well as nerves, providing a direct link between the calcified cartilage and subchondral trabecular bone (Holmdahl & Ingelmark, 1950; Madry et al., 2010; Li et al.,

2013). The subchondral bone plate consists of laminated sheets of parallel collagen fibrils (Finnilä et al., 2017).

2. Subchondral trabecular bone: Situated beneath the subchondral bone plate, this layer is made up of cancellous trabecular bone and serves important supporting and shock-absorbing functions (Madry et al., 2010; Castañeda et al., 2012; Li et al., 2013). Through bone remodelling processes, trabecular orientation can be altered in response to principal stresses (Li et al., 2013). This layer is both more porous and more metabolically active than the subchondral bone plate and is therefore thought to also play a role in the supply of nutrients and metabolic control to the AC (Castañeda et al., 2012; Suri & Walsh, 2012).

Beneath the subchondral bone plate is the epiphysis, which contains blood vessels, nerves endothelium and bone marrow, which is found in the spaces in the meshwork of trabecular bone (Suri & Walsh, 2012; Florencio-Silva et al., 2015; Travlos, 2016).

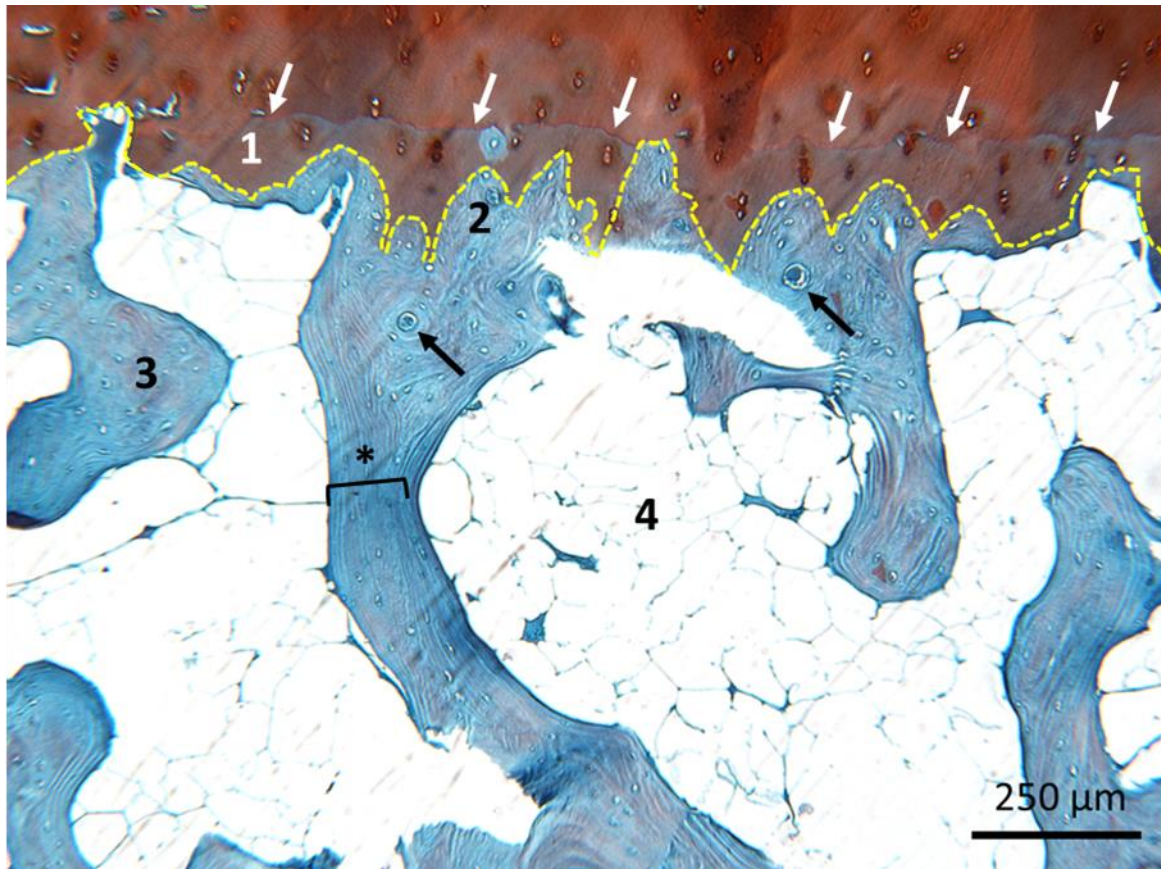


*Figure 1-5: The Osteochondral Junction in a Normal Adult Knee Joint (aged 53 years). The osteochondral junction extends from the deepest layers of the non-calcified cartilage down into the underlying trabecular bone. Histological section of osteochondral tissue was stained with Safranin O/Fast green 1: Calcified cartilage, 2: Subchondral bone plate, 3: Subchondral trabecular bone, 4: Bone marrow space. White arrows = tidemark. Yellow line = cement line. * = Bone Lamellae. Black arrows = Osteocytes.*

1.1.3.3 *Composition*

1.1.3.3.1 *Cellularity*

Mature subchondral bone contains five specialised cell types:

1. Osteoclasts (OCs) are large, terminally differentiated, multinucleated cells, derived from mononuclear precursor cells of the haematopoietic stem cell lineage (Florencio-Silva et al., 2015). Osteoclasts are phagocytic and are tasked with the resorption of bone during bone remodelling (Clarke, 2008; Mohamed, 2008). Osteoclasts are able to bind to the bone matrix via integrin receptors in the osteoclast membrane which interact with bone matrix peptides (Clarke, 2008). During the process of bone remodelling, osteoclasts polarise, forming 4 distinct regions: the sealing zone, the ruffled border (both of which are in contact with the bone matrix), the basolateral domain and the functional secretory domain. The ruffled border forms during bone resorption as a result of the intense trafficking of lysosomal and endosomal components which contain enzymes involved in the degradation of bone. The products of bone breakdown are then endocytosed across the ruffled border (Florencio-Silva et al., 2015).

2. Osteoblasts (OBs) make up roughly 4-6% of the total of resident bone cells and are derived from osteoprogenitor cells that originate from the MSC's found in the bone marrow (Mohamed, 2008; Florencio-Silva et al., 2015). Osteoblasts are specialised fibroblast-like cells, are normally cuboidal in shape and are responsible for bone formation by laying down osteoid which then mineralises (Mohamed, 2008; Clarke, 2008; Florencio-Silva et al., 2015). These cells contain an abundant rough endoplasmic reticulum and Golgi apparatus, which enable them to synthesise all of the proteins present in the bone matrix (Florencio-Silva et al., 2015).

3. Osteocytes are the most abundant cell type in the bone, constituting roughly 25,000 osteocytes per mm³ of bone (Mohamed, 2008; Florencio-Silva et al., 2015). Osteocytes are post-proliferative cells of the osteoblastic lineage and have a lifespan of up to 25 years in humans (Franz-Odenaal et al., 2006; Florencio-Silva et al., 2015). These cells were traditionally thought to be inactive, but are now recognised as having a number of important roles in the bone (Mohamed, 2008). Osteocytes are the main mechanoreceptor cells of the bone, receiving mechanical signals both directly, as a result of strain, or indirectly via fluid flow through the canaliculi (Florencio-Silva et al., 2015). These mechanical signals are converted into biochemical signals, secreting paracrine factors to direct bone remodelling (Mohamed, 2008; Florencio-Silva et al., 2015). Osteocytes reside in lacunae in the calcified matrix, which are regularly distributed throughout the bone and from which many fine channels, known as canaliculi, radiate (Knothe, 2003; Mohamed, 2008). Numerous cell process from the osteocytes run along the canaliculi, and connect to the processes of neighbouring osteocytes, osteoblasts and bone-lining cells by gap junctions (Florencio-Silva et al., 2015). Osteocytes vary in their morphology based on their location. Those found in the trabecular bone are more rounded and those in the cortical bone tend to be more elongated (Florencio-Silva et al., 2015).

4. Bone-lining cells (BLCs) have a flattened, elongated morphology in which their cytoplasm extends along the bone surface (Clarke, 2008; Mohamed, 2008; Florencio-Silva et al., 2015). These cells show very little sign of synthetic activity and are thought to be quiescent osteoblasts (Buckwalter et al., 2005). BLC's completely line the bone surfaces where neither bone resorption or formation is taking place and are therefore thought to play an important role in protecting the bone when remodelling is not required, by preventing the direct interaction of the osteoclasts and the bone matrix (Mohamed, 2008; Florencio-Silva et al.,

2015). They are also thought to play a part in the coupling of bone resorption and formation as well as the removal of bone collagen during resorption (Everts et al., 2002).

5. Mesenchymal Stromal Cells (MSCs)

MSCs are heterogenous progenitor cells that are capable of giving rise to a number of unique, differentiated mesenchymal cell types including osteogenic, chondrogenic and adipogenic lineages (da Silva Meirelles et al., 2008; Ilas et al., 2017). Although MSCs are present in virtually all organs, they were first identified in the bone marrow such as is found within the subchondral trabecular bone (Kfoury & Scadden, 2015; Ilas et al., 2017). The loosely woven and highly vascularised bone marrow provides a unique microenvironment for the MSCs that tightly controls the multi-potency and self-renewal of the cells (da Silva Meirelles et al., 2008; Méndez-Ferrer et al., 2010; Zhang, H. et al., 2018). MSCs are able to migrate out of the bone marrow and regenerate mesenchymal tissues as required by the body and can also demonstrate the ability to modulate both adaptive and innate immune responses (da Silva Meirelles et al., 2008; Kfoury & Scadden, 2015).

1.1.3.3.2 The Extracellular Matrix

Bone is composed of 50-70% mineral, 20-40% organic matrix (osteoid), 5-10% water and approximately 3% lipids (Clarke, 2008).

The mineral content of bone is primarily hydroxyapatite ($\text{Ca}_{10}(\text{PO}_4)_6(\text{OH})_2$), which is formed by the nucleation of calcium and phosphate ions (Clarke, 2008; Florencio-Silva et al., 2015).

There are also numerous other inorganic molecules present in the bone including: sodium, potassium, magnesium, zinc and barium (Florencio-Silva et al., 2015).

The organic matrix forms a scaffold for hydroxyapatite crystal deposition, providing bone with its characteristic stiffness and resistance to mechanical forces (Florencio-Silva et al., 2015). The matrix is continuously resorbed by osteoclasts (OCs) and reformed by osteoblasts (OBs), which synthesise all components of the organic bone matrix, including:

- Collagenous proteins (predominantly type I collagen), which make up 90% of the bone matrix, with trace amounts of types III and V (Clarke, 2008; Mohamed, 2008; Florencio-Silva et al., 2015).
- Noncollagenous proteins are the second most abundant component of the matrix, making up 10-15% of total bone protein, and include: osteocalcin, osteonectin, osteopontin, fibronectin, bone morphogenic proteins and growth factors (Mohamed, 2008; Clarke, 2008; Florencio-Silva et al., 2015).
- Small proteoglycans, including the SLRPs, decorin, biglycan, lumican and osteoadherin (Florencio-Silva et al., 2015).

1.1.4 Cartilage Injury and Repair

1.1.4.1 *Lesions of the Articular Cartilage*

1.1.4.1.1 Epidemiology, Aetiology and Pathogenesis

Lesions of the AC are very common in the human knee. A collection of studies, in which a combined total of more than 55,000 arthroscopies performed on patients with knee symptoms were reviewed, reported the presence of AC lesions in 60-66% (Curl et al., 1997; Hjelle et al., 2002; Årøen et al., 2004; Widuchowski et al., 2007). Defects in the AC can cause discomfort, pain, swelling and functional impairment, but their presence is not always reflected by clinical symptoms (Shelbourne et al., 2003; Cicuttini et al., 2005; Makris et al., 2014). In a systematic review and subsequent meta-analysis, Culvenor and colleagues reported that AC lesions were present in 24% of MRIs performed on asymptomatic, uninjured knees (Culvenor et al., 2018). It is estimated that AC lesions are present in 10-12% of the population as a whole (Sellards et al., 2002).

The most common cause of AC damage is high-impact, traumatic injury, leading to the formation of focal chondral or osteochondral defects (Ding et al., 2005; Camp et al., 2014). Focal AC lesions are recognised as a key predisposing risk factor for the early onset of OA. Although the natural history of AC defects is largely unconfirmed, common hypotheses suggest that cellular degradation and disruption of the ECM result from the continued, repetitive loading of the injured AC, which eventually leads to a decrease in cartilage volume and a narrowing of the joint space (Shelbourne et al., 2003; Ding et al., 2005; Wang et al., 2006; McAdams et al., 2010). AC lesions are also associated with increased bone volume and the formation of osteophytes, also common features of OA (Ding et al., 2005).

The lack of innervation, lymphatics and vascularisation in AC, in contrast to their presence in most other tissues of the body, is thought to be the main factor preventing the activation of the normal physiological response to injury and recruitment of extrinsic repair cells to the injury site (McAdams et al., 2010). Additionally, chondrocytes are limited in their migratory ability, due to their encapsulation in the dense ECM, and demonstrate relatively low synthetic activity, which is rarely sufficient for repair (Perera et al., 2012; Karuppall, 2017). Taken together, along with the harsh biochemical and biomechanical environment in the joint, these factors equate to a very limited capability for the AC to self-repair once injured (Perera et al., 2012; Karuppall, 2017). Therefore, without intervention, AC lesions often fail to spontaneously heal.

1.1.4.2 Articular Cartilage Repair

Once OA develops in the joint, treatment options are limited and the clinical focus shifts towards management while continued progression often leads to the necessity for joint replacement (Makris et al., 2014). Therefore, it is imperative to intervene earlier in the degenerative process, preventing the progression of AC lesions to OA. Although there are currently no pharmacological interventions that can heal AC defects, physiotherapy is often a recommended treatment, either prior to or accompanying surgical options that aim to repair, replace or regenerate lesioned AC with the aim to prevent further damage, restore knee function and prevent progression to OA.

1.1.4.2.1 Surgical Interventions

1.1.4.2.1.1 Palliative Approaches

Palliative approaches are often used as first-line surgical option and aim to reduce symptoms and improve function, but do not seek to regenerate or replace lesioned AC.

1.1.4.2.1.1.1 Lavage and Debridement

Lavage and debridement are procedures that can be performed successively during arthroscopic assessment of the knee joint. Lavage involves irrigation of the joint to wash out inflammatory mediators, loose cartilage and cartilage debris that may otherwise cause synovial irritation and functional impairment (Jackson & Dieterichs, 2003; Felson, 2009; Falah et al., 2010). Debridement involves the removal of loose flaps or edges of cartilage to create a smooth articular surface (Jackson & Dieterichs, 2003; Falah et al., 2010).

1.1.4.2.1.2 Intrinsic Repair Approaches

Intrinsic repair strategies (also collectively called marrow stimulation techniques) take advantage of the body's own repair mechanisms by exposing the lesioned AC to circulating blood and multipotent cells, to which they are normally deprived, by breaching the subchondral bone (Falah et al., 2010; Medvedeva et al., 2018). The creation of channels between the AC defect and bone marrow space ('marrow stimulation') allows for the influx of mesenchymal stromal cells and blood products such as platelets and growth factors from the bone marrow (Mithoefer et al., 2009; Makris et al., 2014). The result is the formation of a fibrin clot in the defect, which is gradually remodelled into fibrocartilage (Falah et al., 2010; Perera et al., 2012; Camp et al., 2014; Medvedeva et al., 2018). The first step of all of the marrow stimulation techniques is the debridement of the defect to create well-defined, smooth edges to allow the fibrin clot to adhere (Falah et al., 2010).

1.1.4.2.1.2.1 Abrasion Arthroplasty

Abrasion arthroplasty was popularised by Lanny Johnson in 1986 and involves the disruption of the superficial subchondral bone, using a surgical rasp to remove dead bone and expose viable bone and surface vascularity (Johnson, 1986; Johnson, 2001).

1.1.4.2.1.2.2 Subchondral Drilling

Subchondral drilling was popularised by Pridie in 1959 (Pridie, 1959; Falah et al., 2010).

Following debridement of the lesion edges, a high speed-drill is used to drill the subchondral bone, creating channels between the subchondral bone marrow and the AC lesion. The main drawback of this technique is necrosis of the subchondral bone caused by the thermal effect of using a high-speed drill (Falah et al., 2010). Tippet and colleagues reported that after more than five years follow-up, 70% of the patients had excellent results, 8% had good results and 22% fair to poor.

1.1.4.2.1.2.3 Microfracture

Microfracture is the most commonly performed marrow stimulation technique, developed by Steadman and colleagues in 1997 (Steadman et al., 1997; Mithoefer et al., 2009; Camp et al., 2014; Makris et al., 2014). In order to mitigate the thermal necrosis effects of using a high-speed drill, an arthroscopic awl is used to create channels through the SB plate, into the bone marrow, 3-4mm apart and 2-4mm deep. (Steadman et al., 1997; Steadman et al., 2010; Falah et al., 2010).

1.1.4.2.1.2.4 Nanofracture

Despite the widespread use of microfracture for AC repair, a consensus regarding a standardised procedure, with regard to methodology (depth, diameter and pattern of perforations) and device used, has not been reported (Benthien & Behrens, 2013). Several

studies have suggested that, in particular, the depth of the subchondral bone perforations can influence the composition of the generated repair tissue and the outcome of the procedure (Chen et al., 2009; Chen et al., 2011; Benthien & Behrens, 2013). For these reasons, Benthien and Behrens developed and reported on a new technique, Nanofracture (aka Subchondral Needling), which creates smaller and deeper channels compared to drilling and microfracture (Benthien & Behrens, 2013). Following debridement of the lesion borders, perforations are created 2-3mm apart, using a 1mm thick needle that is guided through a cannulated pick with a 15° angled tip (Benthien & Behrens, 2013). The cannulated pick facilitates access of the needle to the defect site and precisely restricts the depth of perforations to 9mm (Benthien & Behrens, 2013).

1.1.4.2.1.3 Tissue Replacement Strategies

Marrow stimulation techniques result in the formation of fibrocartilage, which is biomechanically and biochemically inferior to native hyaline AC, and therefore tends to deteriorate over time (Makris et al., 2014). This has led to the development of tissue replacement strategies that address this issue by transplanting whole tissue biopsies, matching the structure of the native tissue and allowing for immediate restoration of the articular surface (Camp et al., 2014).

1.1.4.2.1.3.1 Osteochondral Autograft Transfer (OATS)

Osteochondral autograft transfer was developed by Hangody and colleagues for the treatment of osteochondral defects (Hangody et al., 2010). The defect is prepared by the removal of unstable cartilage, and a cylinder of subchondral bone from the base of the defect (Falah et al., 2010). A cylindrical plug (or multiple plugs as in mosaicplasty) of the patient's own osteochondral tissue is harvested from a lesser-weight bearing area of the

joint, to match the depth of the lesion, and transferred into the defect (Falah et al., 2010; Camp et al., 2014). The use of the patients' own tissue mitigates the risk of disease transmission and of an immune response to the implanted tissue. However, donor-site morbidity must be taken into account and for this reason, OATS is limited to the treatment of smaller osteochondral defects (Camp et al., 2014).

1.1.4.2.1.3.2 Osteochondral Allograft Transplant (OCA)

OCA is performed in technically the same way as OATS, but eliminates the issues with donor site morbidity, and allows for treatment of larger lesions, by harvesting allograft osteochondral plugs from size-matched donor knees (Falah et al., 2010; Camp et al., 2014). However, compared to the use of autografts, there are a number of additional considerations surrounding allograft procurement, processing and storage (Torrie et al., 2015; Cook et al., 2016). It is widely reported that chondrocyte viability in the allograft at the time of implantation is an important determinant in the clinical success of OCA, as viable chondrocytes maintain the biochemical and biomechanical properties of the AC and enhance in vivo graft survival (Williams et al., 2004; Görtz & Bugbee, 2006; Gross et al., 2008; LaPrade et al., 2009; Bugbee et al., 2016). In a canine study of OCA transplantation, Cook and colleagues reported that all successful grafts had a chondrocyte viability >70% and conversely no graft with a chondrocyte viability <70% succeeded (Cook et al., 2016). For this reason, allograft transplantation was traditionally carried out within 7 days of the death of the donor (LaPrade et al., 2009). However, increasing safety concerns about the potential for recipient infection means that OCA are now harvested within 24 hours of donor death and preserved at 4°C for a minimum of 14 days to allow for a range of serological and microbiological tests to be carried out prior to transplantation (LaPrade et al., 2009; Torrie et al., 2015). It has been demonstrated that chondrocyte viability decreases over time spent

in storage, with one group reporting that chondrocyte viability in harvested ovine OC tissue decreased to 80.2% after 15 days (Williams et al., 2004). Similarly, Allen and colleagues reported a mean chondrocyte viability of 80% in human OCA tissue that had been stored for three weeks (Allen et al., 2005). This represents the key point of compromise in the use of OCA, in ensuring the safety of the OCA for transplantation, one must accept that chondrocyte viability is likely to be reduced. Research into storage conditions, including various temperatures, medias and storage times is ongoing, with a view to maximising chondrocyte viability over a longer period of time and increasing the availability of OCA for the treatment of AC lesions (Williams et al., 2004; Garrity et al., 2012; Torrie et al., 2015; Stoker et al., 2018).

1.1.4.2.1.4 Tissue Regeneration Strategies

Tissue engineering is used to generate new tissue that matches, as closely as possible, the native hyaline AC, by relying on implanted chondrocytes to proliferate and secrete ECM to form new cartilage in situ and provide the best possible biochemical and biomechanical properties (Falah et al., 2010; Makris et al., 2014).

1.1.4.2.1.4.1 Autologous Chondrocyte Implantation (ACI)

ACI is a two-stage cell therapy procedure that was first reported by Brittberg and colleagues in 1994 (Brittberg et al., 1994). In the first stage, a full-thickness sample of cartilage is harvested from a lesser-weight bearing area of the patient's knee joint, in an arthroscopic procedure (Roberts et al., 2003; Falah et al., 2010; Makris et al., 2014; Medvedeva et al., 2018). Chondrocytes are isolated from the excised cartilage and expanded ex vivo (Roberts et al., 2003; Falah et al., 2010; Makris et al., 2014). In the second stage, the expanded chondrocytes are implanted into the defect beneath either a periosteal patch (1st

generation ACI) or a biodegradable collagen membrane (2nd generation ACI), which is stitched and glued into place (Roberts et al., 2003; Falah et al., 2010; Medvedeva et al., 2018).

1.1.4.2.1.4.2 Matrix-induced Autologous Chondrocyte Implantation (MACI)

MACI, sometimes referred to as 3rd generation ACI, also involves a similar two-stage procedure similar to traditional ACI and was first carried out by the Verigen company, described by D'Anchise and colleagues (D'Anchise et al., 2005; Perera et al., 2012). MACI differs from traditional ACI in that, following culture expansion in monolayer, chondrocytes are seeded onto a three-dimensional scaffold, comprised of collagen type I and III, and cultured in vitro for 3 days to allow cell attachment (Perera et al., 2012). In the second stage of the procedure, the scaffold is sized to fit the prepared defect, fibrin glue is injected into the defect and the membrane is press-fit (Browne & Branch, 2000; Falah et al., 2010). The scaffold acts to provide a matrix preimplantation, eliminating the need for a periosteal or collagen patch to contain the chondrocytes, aiming to provide a microenvironment for the chondrocytes that more closely mimics that of native tissue (Perera et al., 2012; Makris et al., 2014)

1.1.4.2.1.4.3 Autologous Matrix Induced Chondrogenesis (AMIC)

AMIC is a single-stage procedure that combines the principles of microfracture with a supportive matrix and was developed by Peter Behrens (Behrens, 2005; Behrens et al., 2006). The subchondral bone is breached, as in microfracture, encouraging the influx of mesenchymal stromal cells and blood products (Behrens et al., 2006; Benthien & Behrens, 2010). A scaffold is then sutured into the defect and acts to contain the fibrin clot that forms, as well as permitting the ingrowth of MSCs that are encouraged by the

microenvironment to differentiate into chondrocytes (Benthien & Behrens, 2010; Falah et al., 2010; Hantes & Fylos, 2018). Several commercially available scaffolds are currently used in the AMIC procedure: Chondro-Gide® (a porcine-derived collagen type I/collagen type III scaffold (most commonly used)), Chondrotissue® (an absorbable polyglycolic acid textile treated with hyaluronan) and Hyalofast™ (a fibrous, semi-synthetic scaffold derived from hyaluronic acid) (Lee et al., 2014; Shaikh et al., 2017).

1.1.4.2.1.5 Alternative Cell Sources for Tissue Engineering

1.1.4.2.1.5.1 Allogeneic Chondrocyte Therapy

The main drawback of tissue engineering strategies such as ACI and MACI, that use autologous chondrocytes, is the need for a cartilage biopsy, from which chondrocytes can be isolated. The harvest of healthy cartilage for this purpose constitutes an additional surgery, inflicting additional trauma to the knee, and risking donor-site morbidity in the healthy AC (Verdonk et al., 2007; Matricali et al., 2010). As well as this, the culture expansion of chondrocytes *ex vivo* adds to the timescale and cost associated with the procedure. The use of allogeneic chondrocytes in procedures such as ACI, eliminates the need for a cartilage harvest and the *ex vivo* expansion of chondrocytes, providing an 'off-the-shelf' product that could be used across multiple patients.

Verdonk and colleagues reported on the development of a new technique for AC repair, using characterised, phenotypically stable, allogeneic chondrocytes encapsulated in alginate beads (Verdonk et al., 2007). The authors reported a case series of 21 patients treated with this method, with up to 24-months follow-up and found significant clinical improvement from 6 months onwards and no adverse reaction to the procedure (Verdonk et al., 2007;

Selmi et al., 2008). The authors also reported that the repair tissue was hyaline-like or mixed hyaline and fibrocartilage in 59.5% of patients treated (Almqvist et al., 2009).

Donor selection is critical in the use of allogeneic chondrocytes for cartilage repair. While the risk of rejection is minimal due to the immunoprivileged status of articular cartilage, there will be donor-to-donor variation in the behaviour of the chondrocytes and therefore their ability to regenerate articular cartilage in multiple recipient patients. Every effort should therefore be taken to screen the donor patient to ensure that there is no underlying disease that could affect chondrocyte behaviour. Screening should also be carried out on the isolated chondrocytes themselves to assess their cell surface marker profile, gene expression profile and ability to deposit and maintain matrix in vitro (at a minimum), to act as 'release criteria' to maintain standards and to exclude poor donors.

1.1.4.2.1.5.2 Mesenchymal Stromal Cells (MSCs)

MSCs offer a promising, alternative cell population for cartilage repair, and can be isolated from a number of sources including bone marrow, adipose tissue or synovial membrane (Medvedeva et al., 2018). MSCs are able to contribute to AC repair by differentiating into chondrocytes in situ and also through the secretion of paracrine factors and extracellular vesicles, that have anti-inflammatory and immunomodulatory effects in the joint (Makris et al., 2014; Lo Monaco et al., 2018). A number of pre-clinical and clinical trials have been carried out, using both autologous and allogenic MSCs from various sources, and have shown promising results for the repair of AC lesions (Zhang et al., 2019).

1.1.4.2.2 Factors that Influence a Successful Repair

Regardless of the technique employed, a number of factors are reported to influence the success or failure of AC repair. These factors and their purported effects on the outcomes of AC repair surgery are summarised in table 1-3.

Table 1-3: Factors that Influence Cartilage Repair. Factors that have been reported to influence the outcomes of surgical intervention for the treatment of AC lesions.

Category	Influencing Factor	Reported Effect
Demographic Factors	Age	In general, there is a consensus that superior clinical results can be obtained in younger patients. There is some debate over the cut-off for ‘younger’ patients. A number of studies reported superior results in patients <30 years old. One study reported superior outcomes in patients <41 years old. A further study reported only a slight tendency for patients <40 years old to demonstrate superior clinical outcomes compared to patients >40 years old. (Knutsen et al., 2004; Gudas et al., 2005; Krishnan et al., 2006; Knutsen et al., 2007; de Windt et al., 2009; Harris et al., 2010; Niemeyer et al., 2010)
	Gender	Incidence of joint failure following ACI was more common in females (Dugard et al., 2017).
Defect Factors	Defect Number	Patients with single defects demonstrate superior clinical results compared to those with multiple defects (Krishnan et al., 2006; Dugard et al., 2017).
	Defect Size	Success largely depends on treatment selection, with certain surgical options indicated for smaller and larger lesions. For one cohort of patients treated with ACI, clinical results were significantly better for lesions >3cm ² . For microfracture, patients with lesions >2cm ² had worse clinical outcomes than those with smaller lesions. For osteochondral transplantation, there is no difference in outcome based on defect size (Selmi et al., 2008; de Windt et al., 2009; Dugard et al., 2017).
	Defect Location	Several authors have found inferior results when defects are located on the medial femoral condyle or patellar compared to those on the trochlea and lateral femoral condyle, while others have reported superior clinical results for medial defects. (Krishnan et al., 2006; de Windt et al., 2009; Niemeyer et al., 2010).
	Duration of Symptoms	Patients with a clinical history <24 months reported superior clinical results (Krishnan et al., 2006; de Windt et al., 2009).
	Number of Previous Surgeries	Patients with less than 3 previous surgeries on the affected knee demonstrate superior results (Krishnan et al., 2006; Ruano-Ravina & Jato Díaz, 2006; de Windt et al., 2009; Dugard et al., 2017).
	Pre-op Knee Function Score	Improvement following surgery was significantly higher for patients with a high pre-operative score (Krishnan et al., 2006; Dugard et al., 2017).
Physical Factors	Physical Activity	Patients with more active lifestyles demonstrate greater clinical success following ACI. Increased post-operative activity levels was also associated with improved clinical outcomes. (Knutsen et al., 2004; Knutsen et al., 2007; Kreuz et al., 2007; Toonstra et al., 2013).
	Rehabilitation	Post-operative rehabilitation is an important determinant in return to normal function and return to sport (Hambly et al., 2012; Toonstra et al., 2013).

1.1.5 Osteoarthritis

1.1.5.1 *Epidemiology, Aetiology and Pathogenesis*

Osteoarthritis (OA) is the most common joint disease in the world, with symptomatic, radiographic knee OA occurring in 6% of the population over the age of 30 (Athanasίου et al., 2013). As well as the economic cost of intervention and care, the social cost of OA is high, with pain and other related symptoms having a profound effect on quality of life and affecting patients in both a physical and psychological manner (Goldring & Goldring, 2016). Contrary to longstanding beliefs, OA is not a predisposed consequence of ageing (Fox et al., 2009). Rather, age is one of a number of risk factors that increase the risk of OA onset and progression, including genetic predisposition, female gender, obesity and previous joint injury (Michael et al., 2010; Heidari, 2011). Our knowledge of the precise aetiology and pathogenesis of OA is still incomplete, but both intrinsic and extrinsic factors are believed to promote its development (Michael et al., 2010; Heidari, 2011). OA of joints is commonly considered a disease of the AC, but there is recognition that cartilage degeneration is one aspect of an organ-level failure, rather than the defining feature (Figure 1-6). OA is a complex disorder involving and affecting all tissues in the articular joint (Steinwachs et al., 2012); producing a spectrum of disease and symptomatic states (Ryd et al., 2015).

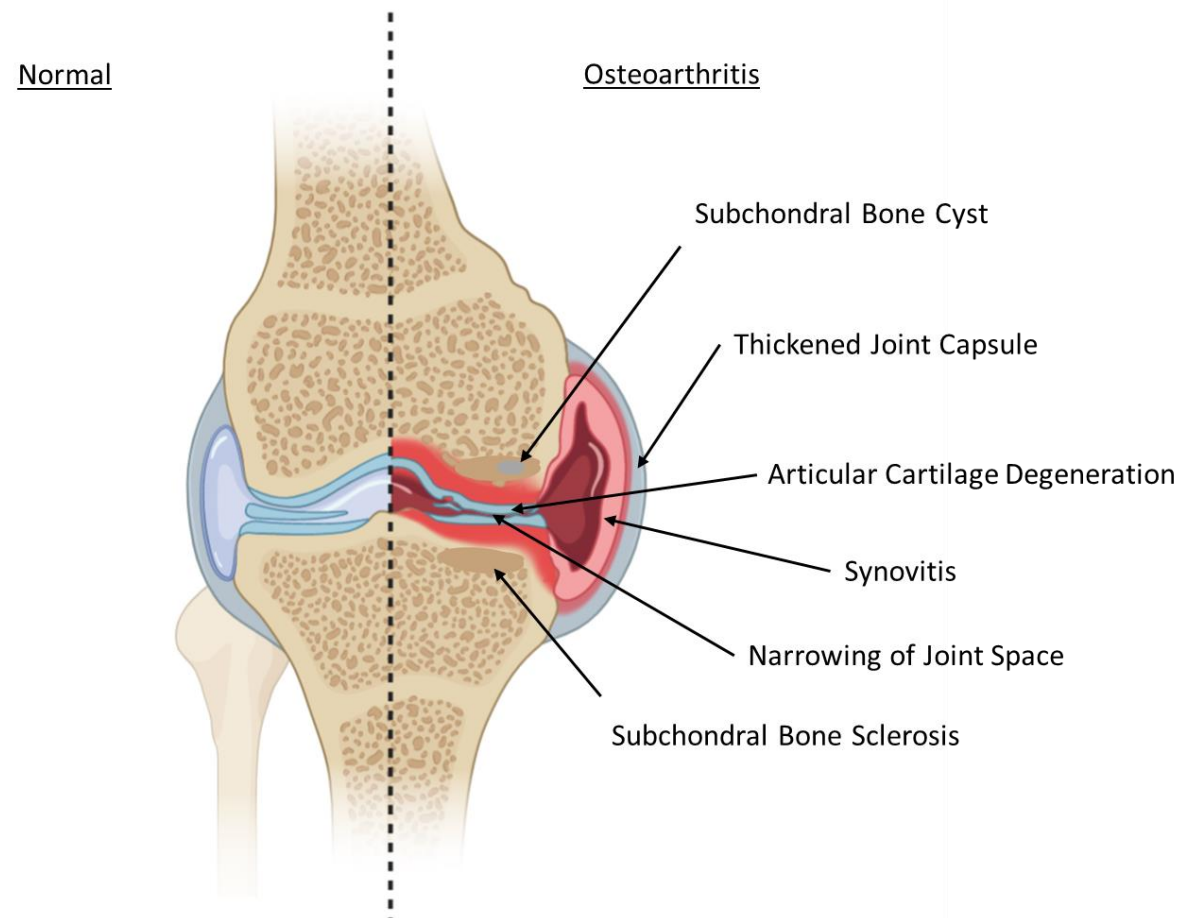


Figure 1-6: Osteoarthritic Changes in the Human Knee Joint. Osteoarthritis represents an organ-level failure of the joint in which all constituent tissues are involved and affected. Characteristic features include degeneration of the AC, subchondral bone sclerosis and the formation of subchondral bone cysts and inflammation of the synovial membrane.

1.1.5.2 *Articular Cartilage in the Onset of Osteoarthritis*

Of all the tissues that make up the knee joint, the cartilage is seemingly most affected by OA, with cartilage degeneration a characteristic feature (Fenwick et al., 1999; Steinwachs et al., 2012). The limited capacity for self-repair means that untreated injuries resulting from trauma and repetitive loading are likely to lead to OA over time (Steinwachs et al., 2012).

The homeostasis in the AC of the knee relies on a dynamic equilibrium between the on-going breakdown and formation of the ECM. This is regulated by the chondrocytes and a number of anabolic (for instance Insulin like growth factor (IGF) -1 and -2) and catabolic factors (in particular interleukin-1 (IL-1) and tumour necrosis factors-alpha (TNF- α) (Steinwachs et al., 2012). This regulatory system can, in part, compensate for harmful influences on the AC early in the process, through the increased synthesis by the chondrocytes of collagen type II, aggrecan and fibronectin (Sharma et al., 2013). However, if these harmful influences act over a long period of time or at a magnitude that exceeds the tissue's ability to compensate, the result is matrix degradation, initially due to the degeneration and suppression of synthesis of proteoglycans and further damage to the collagen network (Murphy & Nagase, 2008; Steinwachs et al., 2012). Traumatic injuries can also lead to the damage and destruction of chondrocytes (Murphy & Nagase, 2008). Due to the aforementioned lack of vascularization, there is no physiological inflammatory response to the tissue necrosis that follows injury, unlike in other, vascularized tissues of the body (Heidari, 2011). Therefore, there is a lack of recruitment of extrinsic, undifferentiated repair cells which, coupled with the low potential for repair by intrinsic mature chondrocytes, results in insufficient natural cartilage repair (Heidari, 2011).

Repetitive loading of the injured AC results in further cellular degeneration and a resulting accumulation of degradative enzymes and cytokines. This leads to the further disruption of the collagen structure, increased hydration and fissuring of the articular surface, which is commonly seen in arthroscopy in early stage OA (Michael et al., 2010; Heidari, 2011).

Changes to the articular cartilage and subchondral bone during the progression of OA are recognised as active components, contributing to the severity of the disease, rather than secondary consequences (Sharma et al., 2013).

1.1.5.2.1 Osteoarthritic Changes in the Articular Cartilage

As OA progresses, there are further changes to the composition and organisation of the ECM, leading to the deterioration in both the material properties and structural integrity of the AC (Goldring & Goldring, 2016). Various studies using animal models have shown that the progression of OA in cartilage tissue demonstrates relatively consistent features:

- The upregulation and increased production of specific ECM proteins (such as collagen type II and fibronectin) (Goldring & Goldring, 2016).
- A general reduction in chondrocyte number due to increased apoptosis, leading to a compensatory increase in cell proliferation which leads to chondrocyte clustering (Li et al., 2013; Goldring & Goldring, 2016). Chondrocytes have also been shown to exhibit reduced responsiveness to growth factors such as IGF-1 and transforming growth factor- β (TGF- β) leading to reduced matrix synthesis and a tip in the homeostatic balance towards catabolism (Loeser et al., 2012; Li et al., 2013).
- An increase in catabolic activity as a result of increased production of degradative enzymes such as matrix metalloproteinases (MMP) -1, -3, -9, -13 and -14 and aggrecanases (a disintegrin and metalloproteinase with thrombospondin-like motifs

(ADAMTS) 5, 4 and 9) (Murphy & Nagase, 2008; Goldring & Goldring, 2016). The increased production of these enzymes leads to the progressive loss of proteoglycans and, subsequently, collagen type II (Goldring & Goldring, 2016).

- An increase in the expression of regulatory proteins (IL-1, TNF- α , toll-like receptors), matrix proteins (collagen types II and X, aggrecan, link protein) and transcription factors ((SRY-box 9 (SOX9), runt-related transcription factor 2 (RUNX2), E74 like ETS transcription factor 3 (ELF3)). These changes lead to the fibrillation of the articulating surface and the localised production of fibrocartilage (Goldring & Goldring, 2016).

Another major change to the AC associated with the pathogenesis of OA is the invasion of the, normally avascular, tissue with blood vessels (Suri & Walsh, 2012). Due to the matrix composition and the secretion by the chondrocytes of anti-angiogenic factors (such as thrombospondin-1) and inhibitors of matrix degrading enzymes (such as tissue inhibitors of metalloproteinases (TIMPS), healthy AC is hostile to vascular invasion (Fenwick et al., 1999; Suri & Walsh, 2012). However, in OA cartilage, there is a loss of chondrocyte activity and secretion of these factors, a loss of proteoglycans and an increase in the production of vascular endothelial growth factor (VEGF), which together facilitate the invasion of blood vessels into the calcified cartilage. In addition, channels which normally exist between the subchondral bone and calcified cartilage begin to extend into the uncalcified cartilage in OA and are subsequently invaded by blood vessels (Suri & Walsh, 2012).

Signs of inflammation are evident during the progression of OA, with the overexpression of proinflammatory mediators noted in the synovial fluid of patients, during both early and late stage OA. The presence of these molecules in the synovial fluid is also likely to

contribute to the imbalance in homeostasis seen in the AC, in which the catabolic activity of the chondrocytes is increased (Sharma et al., 2013). The calcified cartilage layer also undergoes significant changes during the progression of OA, with an overall thickening of the calcified cartilage and an advancement or duplication of the tidemark contributing to the thinning of the AC and leading to further damage upon the application of mechanical force (Murphy & Nagase, 2008; Goldring & Goldring, 2016).

1.1.5.3 *Subchondral Bone in the Onset of Osteoarthritis*

As a consequence of recognising knee OA as a disease of the whole joint, involving all of its constituent tissues, there has been increased interest in the part played by the other tissues in the joint in the pathogenesis of OA. Of these tissues, the SB is of particular interest given its proximity and interaction with the AC. It is likely, however, that cellular and molecular changes are taking place in the various tissues of the joint even before tissue level AC degeneration is identified (Chubinskaya et al., 2015).

The SB is believed to play an important role in the onset of OA, and this is supported by the fact that many of the established risk factors associated with OA have a direct influence on the subchondral bone:

- Genetic predisposition: OA is considered to be polygenic with an important hereditary aspect (Li et al., 2013). Heritability of OA is estimated to be between 39% and 65% based on family and twin studies of OA in the hand and in the knee (Spector et al., 1996).
- Gender: OA is more common in men than in women, up to the age of 50, above which the trend is reversed, coinciding with the menopause, a feature of which is oestrogen deficiency (Li et al., 2013). In animal models in which oestrogen deficiency

is induced by ovariectomy, there is a reported increase in the rate of bone remodelling, as well as structural deterioration and weakened biomechanical properties in the subchondral trabecular bone (Sniekers et al., 2008; Li et al., 2013).

- Age: age is considered one of the most important risk factors in the onset of OA. There is an age-related decline in normal bone structure and microarchitecture as well as an accumulation of bone microdamage (Radin et al., 1973; Li et al., 2013).
- Obesity: obesity is a significant risk factor in the onset of OA, especially in the knee, partly due to increased compressive loading that lead to increased microfractures and bone sclerosis, increasing the bones stiffness and reducing the ability of the bone to absorb shock and to respond to mechanical forces (Cao, 2011; Li et al., 2013). Obesity is also a risk factor in the onset and development of OA in the hand, suggesting that increased mechanical loading cannot fully explain the influence of obesity on the onset of OA. Obesity is also associated with chronic inflammation, with increased levels of leptin secreting adipocytes, leading to an increase in circulating and tissue proinflammatory cytokines that are thought to promote bone resorption through modification of the OPG/RANK/RANKL pathway (Cao, 2011; Li et al., 2013).
- Physical activity: Moderate weight bearing activities are beneficial in protecting against OA and are reported to lead to an increase in cartilage volume (Wijayarathne et al., 2008). However, overloading of the joint, at a magnitude greater than normal physiological level, can be detrimental, leading to increased rates of bone remodelling and microdamage, eventually leading to subchondral bone sclerosis (Li et al., 2013).

- Previous joint injury: intra-articular fractures, meniscal tears, ligament damage and traumatic injury have also been shown to have a knock-on degradative effect on the subchondral bone, mainly caused by altered joint loading. Clinical studies of meniscal and ligamentous damage in humans have reported pathological changes in the subchondral bone, including increases in bone mineral density and the formation of bone cysts and bone marrow lesions (Lo et al., 2007; Meyer et al., 2008; Li et al., 2013).

1.1.5.3.1 Osteoarthritic Changes in the Subchondral Bone

Subchondral bone displays a number of, still not completely understood, changes in the pathogenesis of OA, most of which are structural consequences of an alteration to the bone remodelling process (Li et al., 2013):

- *Microfractures* (i.e microcracks), which are normally induced by overloading of the joint, have been widely detected in the mineralised tissues in the OA knee, including in the subchondral bone plate and the underlying trabecular bone (Castañeda et al., 2012). Microfractures have also been detected in the canaliculi, in which the osteocytes reside, leading to osteocyte apoptosis and altered bone remodelling (Li et al., 2013). Diffuse microdamage, a process which is similar, consists of a range of submicron-sized cracks which contribute to the reduction of biomechanical properties but not to osteocyte apoptosis or bone remodelling (Burr & Radin, 2003).
- *Angiogenesis*, the formation of new blood vessels which, in the OA joint leads to vessels breaching the tidemark and penetrating the calcified and non-calcified cartilage. Often these new vessels are accompanied by nerves, which may contribute to the symptomatic pain affecting OA patients (Suri & Walsh, 2012).

- *Osteophytes* are fibrocartilaginous and skeletal outgrowths that are localised to the joint margins (Goldring & Goldring, 2016). The proliferation of periosteal cells at the joint margin is implicated with the initiation of these outgrowths (Li et al., 2013). These cells subsequently differentiate into chondrocytes, which become hypertrophic and develop into an osseous outgrowth through the process of endochondral ossification (Goldring & Goldring, 2016).
- *Bone-marrow oedema-like signals (BMLs)* are identified using MRI and show as regions of increased signal intensity (Link & Li, 2011; Goldring, S. R. & Goldring, 2016). BML signal intensity has been reported to be proportional to the level of overlying cartilage degeneration (Zhao et al., 2010; Link & Li, 2011). BMLs are most commonly found distal to areas of chondropathy (Zhao et al., 2010; Kuttapitiya et al., 2017). BMLs are suspected to be a product of localised fibrous replacement of the bone marrow in an altered bone remodelling process following damage and are commonly identified in patients with OA. However they are also found in asymptomatic patients, in whom they are thought to predict an increased risk of OA (Wluka et al., 2009; Li et al., 2013; Goldring & Goldring, 2016). The precise causes of BMLs are still largely unknown but they are thought to be caused by an inflammatory reaction to cartilage breakdown products and microfractures caused by altered biomechanics of the joint (Garnero et al., 2005).
- *Bone cysts* are cavitory lesions in the subchondral bone which are thought to develop in areas with pre-existing BML (Carrino et al., 2006). Several groups have demonstrated that the presence of bone cysts directly correlates with the severity of joint pain and, similarly to BMLs, they are a key predictor for the progression of OA (Tanamas et al., 2010; Goldring & Goldring, 2016). The precise causes of bone cysts is

also unknown, but there are two main theories: synovial fluid intrusion, in which synovial fluid enters the bone through a damaged or breached osteochondral junction and bone contusion in which cysts originate from BML and subsequent necrotic bone resorption (Ondrouch, 1963; Tanamas et al., 2010).

- *Subchondral bone sclerosis* is commonly considered an indisputable sign of OA. The sclerosis of the subchondral bone is thought to be a biomechanical compensatory adaptation, acting to reduce the effect of the cysts and microdamage in subchondral bone, which both increase the fragility of the bone (Li et al., 2013). Thickening of the subchondral bone can be associated with the duplication of the tidemark, the advancement of the mineralisation front and the thinning of the AC (Li et al., 2013).

It still remains to be confirmed whether changes in the SB act as a trigger for the changes in the overlying cartilage, whether the changes observed in the bone are a secondary consequence of cartilage degeneration, or whether both can be possible in different patients (Castañeda et al., 2012; Li et al., 2013; Goldring & Goldring, 2016). Regardless of the order in which the SB and AC degrade, changes in either tissues affect the biomechanical properties of the knee joint, which leads to altered loading throughout the joint and subsequent damage to the other constituent tissues (Castañeda et al., 2012). This represents a circular pathogenesis in the joint, supporting the idea of an organ-level failure.

1.1.6 The Osteochondral Junction

The osteochondral junction of the human knee joint encompasses the deeper layers of the non-calcified cartilage, the calcified cartilage, the thin cement line, the SB plate and the directly underlying trabecular bone (Lyons et al., 2006; Suri & Walsh, 2012). The calcified and non-calcified cartilage are separated by the 'tidemark', a dynamic structure that represents the mineralisation front of calcified cartilage (Lyons et al., 2006). Figure 1-5 (page 24) demonstrates the proximity and interaction between the SB and AC in a normal human knee joint (Li et al., 2013).

1.1.6.1 *Tissue Interaction in Homeostasis*

Traditionally, the calcified layer of cartilage and the tidemark were considered impenetrable barriers, sealing the osteochondral junction and ensuring that there is a clear boundary between subchondral and synovial compartments (Suri & Walsh, 2012). Therefore, it was considered to be unlikely that any communication would take place between these two tissues. However, the close physical association between the SB and AC, as well as other suggestive factors, led to the hypothesis of biochemical and molecular crosstalk between the two tissues (Sharma et al., 2013). Since the cells of the AC and SB share a number of regulatory pathways, it was suspected that there existed crosstalk between these cells, but this remains unproven (Findlay & Kuliwaba, 2016).

Moreover, the avascular nature of AC, implies that the tissue has to possess an alternative mechanism for the provision of essential nutrients and signal molecules to the chondrocytes to ensure their survival (Athanasίου et al., 2013). Similarly, metabolites must be removed to prevent their build up. It is well established that solutes can be exchanged between capillaries of the synovial membrane and the articular surface via the synovial fluid, but it

was speculated that this may not be sufficient to supply the deeper areas of noncalcified cartilage or whether there is an additional transport from the bone microcirculation (Arkill & Winlove, 2008).

In light of this, Arkhill and Winlove used an *in vitro* diffusion cell system in horse metacarpal joints, in which they perfused the joint from the subchondral bone side using a fluorescent dye. The dye was shown to be present in the synovial fluid after one and a half hours, suggesting that both the tidemark and the calcified cartilage are permeable to low molecular weight solutes from the subchondral circulation (Arkill & Winlove, 2008). This was supported by results from other groups who showed, using fluorescent dyes, that small molecules could diffuse between the bone marrow and articular cartilage (Findlay & Kuliwaba, 2016). O'Hara and colleagues and Wang and colleagues showed that applying cyclic loading, mimicking physiological joint loading gave increased diffusion of larger molecules between the SB and cartilage (O'Hara et al., 1990; Wang et al., 2013).

Several groups published work to try and clarify the transport pathways from the subchondral circulation into the cartilage. Lyons and colleagues reported instances in which prolongations of uncalcified cartilage projected down into the calcified cartilage and touched the SB and marrow spaces, providing a potential route for molecular diffusion between the two tissues (Lyons et al., 2006).

It is now known that the calcified zone of articular cartilage is permeable to small molecules and plays an important role in the biochemical interaction between non-calcified cartilage and SB. There is a high number of arterial and venous vessels, often accompanied by nerves,

which can be seen branching into the calcified cartilage from the SB (Findlay & Kuliwaba, 2016). As well as this, the SB is invaded with hollow spaces that provide a direct link between the uncalcified cartilage and the bone marrow cavity, which have been shown to allow the passage of nutrients from the medullary cavity in the bone to nourish the cartilage in a number of animal models (Madry et al., 2010; Sharma et al., 2013).

1.1.6.2 *Tissue Interaction in Osteoarthritis*

The permeability of the subchondral bone plate and calcified cartilage which permits biochemical and molecular crosstalk between the SB and AC in homeostasis also plays a part in the knee joint degeneration of the OA pathogenesis (Pan et al., 2009; Goldring & Goldring, 2016). In OA there are well-described, destructive changes in the AC, which are often paralleled by less well-investigated changes in the SB (Findlay & Kuliwaba, 2016). While the thickness and mechanical integrity of the AC decreases, subchondral bone thickness and stiffness increases, with accelerated bone turnover and altered trabecular architecture (Hwang et al., 2008).

One of the characteristic changes to the osteochondral unit in OA pathogenesis is the formation of linear microcracks in the calcified cartilage, subchondral bone plate and trabecular bone, which can be induced by overloading (Burr & Radin, 2003; Hwang et al., 2008). These microcracks increase the permeability of the subchondral bone plate and calcified cartilage to molecular diffusion, particularly of catabolic agents, across the osteochondral junction (Burr & Radin, 2003; Li et al., 2013)

Increased subchondral osteoclastic activity in the early stages of OA, combined with the formation of microcracks, permits the formation of channels through the subchondral plate and into the non-calcified cartilage, which are often accompanied by venous and arterial vessels (Suri & Walsh, 2012). The invasion of blood vessels further increases the diffusion of molecules from the SB circulation. At the same time, fissuring of the AC extends down through the tidemark and the subchondral bone plate. There is also fragmentation of the articular cartilage along the tidemark (Suri & Walsh, 2012). As a result of these changes, subchondral and synovial compartments become increasingly well connected, with fluids, molecules, cells, tissues and physical forces transmitted with greater ease across the joint (Li et al., 2013).

This increase in the ability of fluid to flow between SB and AC has been shown in osteochondral plugs that demonstrate cartilage erosion along with subchondral bone plate thickening and increased vascularity (Hwang et al., 2008). Crosstalk between the bone and cartilage is thought to be dependent on the diffusion of factors from the subchondral vasculature, therefore any change to the rate of perfusion, will likely have an effect on this biochemical crosstalk and on the joint homeostasis (Sharma et al., 2013; Findlay & Kuliwaba, 2016). The increased permeability of the subchondral bone plate and calcified cartilage, leading to an increase in the ease of fluid flow, will also likely disrupt the joint biomechanics, which relies largely on fluid pressurisation in load bearing and shock absorbing (Hwang et al., 2008).

1.2 Aims and Objectives

An overview of the thesis chapters is provided in figure 1-7. The aim of this thesis was to address several aspects relating to the repair of a degenerate or injured joint, identifying and investigating several factors that may influence repair, at the cellular and whole organism level.

The specific objectives of this thesis were:

- To determine consensus and identify research priorities in the field of cartilage repair using an assembled panel of experts in a Delphi consensus study (Chapter 2).
- To investigate the influence of subchondral bone health on the structural outcome of cartilage repair in the knee using a novel, in-vitro model of the osteochondral unit (Chapter 3).
- To examine the histological and cellular characteristics of MRI-identified subchondral bone abnormalities (Chapter 4).
- To investigate the influence of activity levels and selected psychosocial factors on the clinical outcomes of cell therapy for articular cartilage repair (Chapter 5).

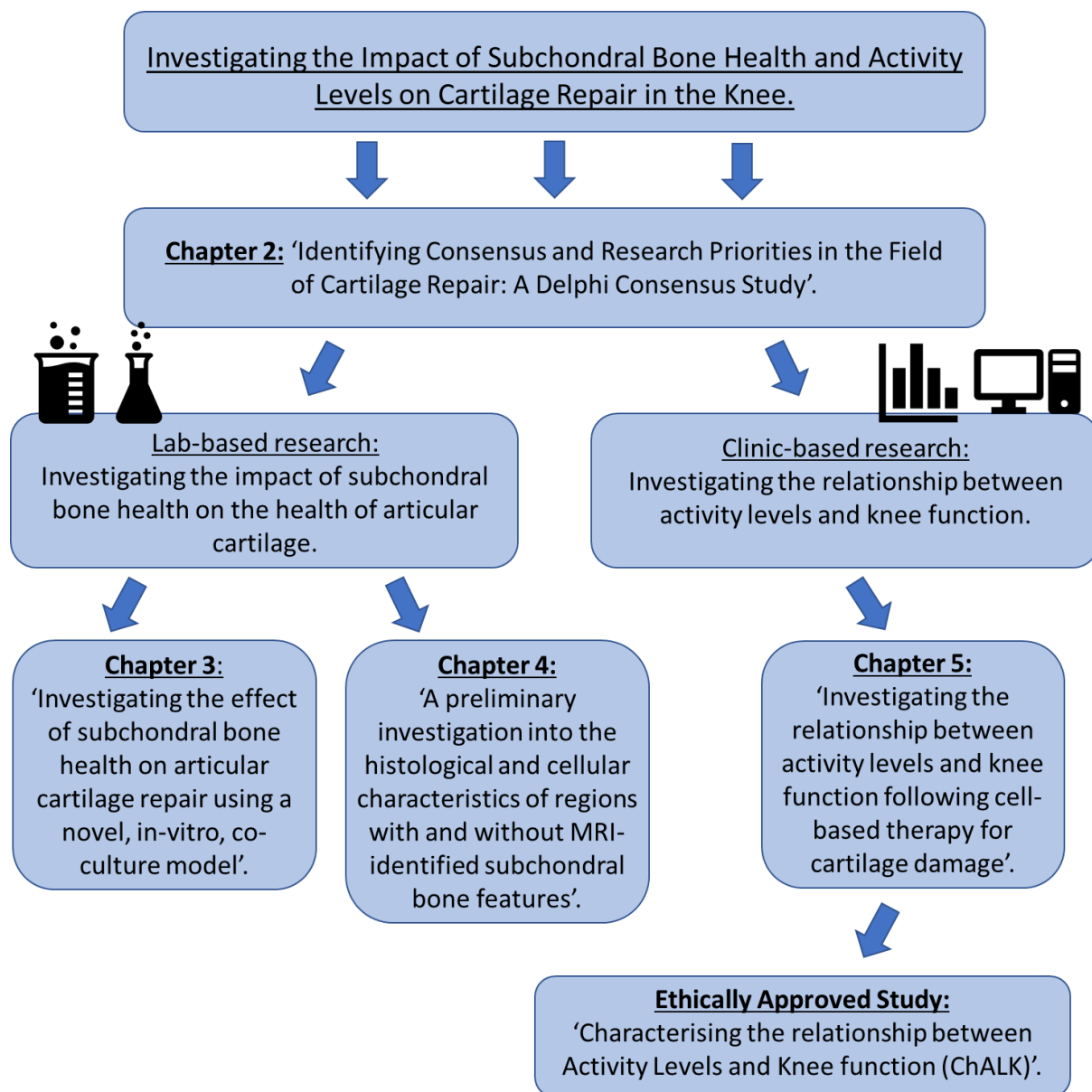


Figure 1-7: A schematic overview of the thesis. A flow chart to demonstrate the structure of the thesis and the interaction between chapters.

Chapter 2:
Identifying Consensus and Research Priorities
in the Field of Cartilage Repair: A Delphi
Consensus Study

2. Chapter 2: Identifying Consensus and Research Priorities in the Field of Cartilage Repair: A Delphi Consensus Study

2.1 Introduction

2.1.1 Articular Cartilage Injury and Repair

Articular cartilage (AC) lesions are very common in the human knee, with a reported incidence in 60-66% of arthroscopies carried out in patients presenting with knee symptoms, and 10-12% in the population as a whole (Curl et al., 1997; Hjelle et al., 2002; Sellards et al., 2002; Årøen et al., 2004; Widuchowski et al., 2007). Defects in the AC can cause discomfort, pain, swelling and functional impairment, although there is little correlation between the presence of clinical symptoms and AC status, and AC lesions have also been reported in 24% of MRIs carried out on asymptomatic knees (Shelbourne et al., 2003; Cicuttini et al., 2005; Ding et al., 2006; Saris et al., 2009; Culvenor et al., 2018). AC lesions can be separated by their aetiology. Focal lesions, which are well delineated, are usually attributed to trauma or conditions such as osteochondritis dissecans or osteonecrosis (Falah et al., 2010). On the other hand, degenerative defects are poorly demarcated and tend to result as a secondary consequence of other pathologies, including ligament instability, meniscus injury or as a consequence of OA (Falah et al., 2010). The natural history of AC lesions is still largely unconfirmed, but they are recognised as a predisposing risk factor for the early onset of OA, representing the circular nature of OA pathogenesis (Ding et al., 2006; Perera et al., 2012; Camp et al., 2014). The presence of AC lesions is associated with increased cartilage breakdown caused by repetitive loading of the injured AC that eventually leads to cellular degradation and disruption of the collagen ultrastructure, causing an associated decrease in cartilage volume and narrowing of the

joint space. (Shelbourne et al., 2003; Ding et al., 2005; Wang et al., 2006; Davies-Tuck et al., 2008; McAdams et al., 2010). The presence of AC lesions is also causally associated with the formation of tibial and fibular osteophytes and increasing bone volume, common features in the OA pathogenesis (Ding et al., 2005).

AC is characteristically aneural, devoid of lymphatics and avascular, the latter of which prevents the normal, physiological, inflammatory response to injury that leads to the recruitment of extrinsic repair cells to the injury site, as seen in other tissues of the human body (McAdams et al., 2010). Therefore, maintenance of the cartilage ECM is wholly reliant on the relatively low synthetic activity of resident chondrocytes, which is stimulated following injury but is rarely sufficient for repair (Fox et al., 2009; Karuppall, 2017). In combination, along with the harsh biomechanical environment to which the AC surface is subjected, these factors amount to a limited capacity for AC self-repair (Karuppall, 2017). Therefore, without intervention, AC lesions often fail to heal on their own.

The prevalence and poor self-reparative capabilities of AC lesions, and their association with the onset and progression of OA has necessitated the development of a number of surgical techniques aimed at repairing, replacing or regenerating lesioned AC (Steinwachs et al., 2012; Perera et al., 2012; Camp et al., 2014; Medvedeva et al., 2018). These techniques range from palliative approaches (debridement, lavage), intrinsic reparative strategies (marrow stimulation through abrasion, subchondral drilling and microfracture), whole tissue transplantation (osteochondral auto- and allografting) and tissue engineering strategies (Autologous Chondrocyte Implantation, Matrix-induced Autologous Chondrocyte Implantation, Autologous Matrix-Induced Chondrogenesis) (Brittberg et al., 1994; Clair et al.,

2009; Peretti et al., 2011; Seo et al., 2011; Steinwachs et al., 2012; Camp et al., 2014; Medvedeva et al., 2018; Vaishya et al., 2018).

There has also been an associated increase in the development of new scoring systems to assess the outcome of cartilage repair techniques. A multitude of histological, arthroscopic and imaging-based scoring systems have been established to assess the structural quality of repair cartilage, each with a number of different parameters (O'Driscoll et al., 1986; O'Driscoll et al., 1988; Pineda et al., 1992; Wakitani et al., 1994; Peterson et al., 2000; Moojen et al., 2002; Roberts et al., 2003; Peterfy et al., 2004; Knutsen et al., 2004; Smith et al., 2005; Marlovits et al., 2006; Grogan et al., 2006; Saris et al., 2008; Rutgers et al., 2010; Trattig et al., 2011; Camp et al., 2014; Roemer et al., 2014; Guermazi et al., 2017; Oei et al., 2018).

Perhaps unsurprisingly, given the wide variety of treatment options and scoring systems for AC repair, the published literature displays a wide range of opinions regarding the most important parameters in the structural assessment of cartilage repair, and in the possible factors that may influence a successful repair. There is currently no evidence-based consensus regarding the best treatment option and little guidance as to which are the most important criteria to be taken into account when selecting a treatment option (Saris et al., 2008; Bekkers et al., 2009).

The combined expertise of a panel of experts could be used to identify areas in the cartilage repair field where consensus exists and collate these ideas to form a framework of important parameters and factors. A gathered panel of experts could also be used to highlight areas where consensus is lacking and therefore identify topics where more research is required.

2.1.2 The Delphi Technique

The Delphi technique is a method for acquiring group knowledge by consolidating individual opinions into group consensus (Dalkey & Helmer, 1963; Hsu & Sandford, 2007). The technique was primarily developed in the 1950's by Norman Dalkey and Olaf Helmer and found publication for the first time in 1963 following the declassification of the military projects for which the technique was established (Dalkey & Helmer, 1963; Hsu & Sandford, 2007). The Delphi technique is based on the assumption that the opinion of a group is more valid and reliable than that of the individual or, 'two heads are better than one' (Dalkey, 1969; Linstone & Turoff, 1975; Keeney et al., 2011). The Delphi technique aims to collate existing beliefs and ideas surrounding a specific topic where previously there was little agreement and determine levels of consensus among a group of relevant experts (Keeney et al., 2011). The Delphi technique has been widely used to identify research priorities and gain consensus in many different areas of health research (Keeney et al., 2011). A number of variations on the original technique have been developed and utilised, but the four main features of the technique remain largely unchanged:

1. *Anonymity of participants*, which is designed to eliminate drawbacks associated with face-to-face consensus methods, such as the domination of confident participants over weak members, the pressure to agree with the opinions expressed by superiors or by the group and the underdog effect, in which there is a tendency to vote for unpopular or uncommon opinions (Dalkey, 1969; Habibi et al., 2014; Kauko & Palmroos, 2014).
2. *Controlled feedback* is provided to reduce the effect of noise and bias in the process, and sets the Delphi apart from other consensus gathering methods (Hsu & Sandford, 2007). Feedback is supplied to participants between rounds and is designed to

extract the reasoning and to re-appraise the factors that went into the first answer, leading to more considered, revised answers in successive rounds (Dalkey & Helmer, 1963; Linstone & Turoff, 1975; Powell, 2003; Hsu & Sandford, 2007).

3. *Iteration* enables a group of individuals to deal with and eventually achieve a general agreement of opinion around a central, often complex, problem, over several rounds (Lynn & Layman, 1996; Powell, 2003; Habibi et al., 2014).
4. *A statistical group response* is the desired final output of a Delphi study and enables the combination of behavioural and mathematical techniques, turning a qualitative issue into quantitative data (Ang & O'Connor, 1991). The statistical analysis allows for the objective and impartial analysis and summary of the collected data (Hsu & Sandford, 2007).

The present Delphi study sought to compile items that were deemed to be important in the structural assessment of cartilage repair and factors that influence a structurally successful repair, and subsequently to determine the levels of consensus of these items amongst a panel of experts.

2.2 Materials and Methods

2.2.1 The Delphi Panel

Individuals attending the two-day Oswestry Cartilage Symposium (a UK ICERS meeting) (24th-25th November 2016) were invited to participate in the study. The delegation of this meeting was made up of research scientists, clinicians and industry representatives with expertise in cartilage repair, from a range of backgrounds including rheumatology, regenerative medicine, orthopaedic surgery, biomedical engineering, and stem cell biology. All participants in the study were based in the United Kingdom.

Attendees at the first day of the meeting were approached to participate in the idea-generating round of this Delphi study. Attendees at the second day of the meeting were approached to form the Delphi panel for the two subsequent self-completed questionnaire rounds.

True anonymity could not be ensured for this Delphi study as both the idea-generating round and the first questionnaire round were carried out at a face-to-face meeting.

However, a quasi-anonymity was maintained throughout the process. In this way, the members of the panel were aware of the identity of the other panel members, but the opinions and judgements of individual participants remained anonymous (McKenna, 1994).

The participants in the Delphi study will henceforth be referred to as the Delphi panel.

2.2.2 The Delphi Process

This Delphi study consisted of three rounds:

1. *Idea-generating focus-group*: Attendees at the first day of the symposium were invited to anonymously submit free-text opinions on factors that they considered to be important in terms of influencing, or being used to assess, the structural quality of repair cartilage. Participants were also invited to submit opinions relating to the cartilage repair field more generally. These opinions were then summarised and structured into the first self-completed questionnaire.
2. *First self-completed questionnaire round*: The first questionnaire was distributed to the Delphi panel. The panel were asked to complete the questionnaire to the best of their knowledge and to leave free-text comments to justify their answers. Completed questionnaires were collected and there followed a review and statistical analysis of the results. Items that were deemed to have reached an acceptable

threshold level of consensus (see 2.2.4 'Judging Consensus and Importance') were removed, and those that remained were used to create the second self-completed questionnaire. A summary of the group answers and directly quoted comments from the previous round were also included in the second self-completed questionnaire.

3. *Second self-completed questionnaire round*: The second questionnaire was distributed to the Delphi panel electronically. The panel were again asked to answer the questions to the best of their knowledge, this time considering the summary of the group answers and comments from the previous round. Again, the panel were invited to add free-text comments for each question to justify their answer, particularly if their answer lay outside of the trend of group answers from the previous round. Completed questionnaires were returned electronically.

2.2.3 Self-completed Questionnaires

The questionnaires that were distributed in rounds 2 and 3 contained two different types of items, single statements and statement series, both created using the ideas collected during the idea-generating focus group in round 1. The two types asked the panel:

- To rate their agreement with single statements, using a 5-point Likert Scale (Likert, 1932; Smith et al., 2005) (figure 2-1).
- To rank statements in order of their perceived importance.

An example of each item type from both the round 2 and round 3 questionnaires is shown in figure 2-2, and figure 2-3 respectively.

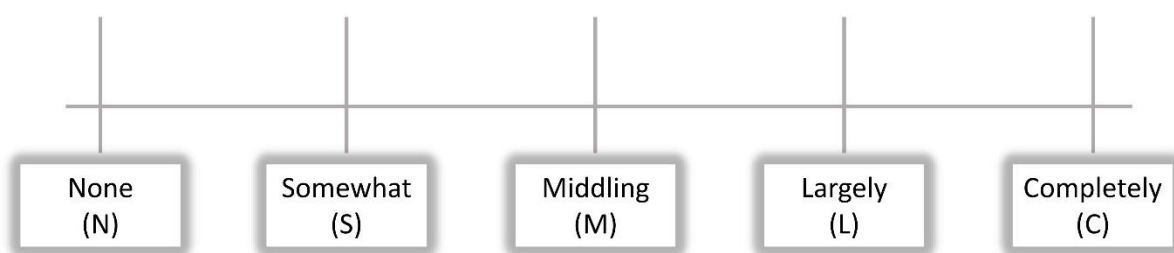


Figure 2-1: 5-point Likert scale. The 5-point Likert scale was used to rate agreement with single-statements on the round 2 and round 3 questionnaires.

A

I support the following statements :

None (N) Somewhat (S) Middling (M) Largely (L) Completely (C)

Reasons can be added below.

1. Ingoes (Patient Variables)

Measurements:

Size and depth of lesion should both be measured N S M L C

We measure the lacunae (cysts) in bone

N S M L C

We measure the area of the Bone Marrow oedema-like signal N S M L C

Reasons:

B

I support the following statements:

None (N) Somewhat (S) Middling (M) Largely (L) Completely (C)

Ingoes (Patient Variables)

1. Measurements

a. We should measure the lacunae (cysts) in the bone: N S M L C

Previous round: Responses (n) (1) (5) (3) (3) (9)
Median = L

a. We should measure the area of the Bone Marrow oedema-like (BML) signal:
N S M L C

Previous round: Responses (n) (2) (5) (3) (4) (6)
Median = M/L

Reasons/comments: _____

Figure 2-2: An example of the Likert-scale-rated single-statement question type layout from (A) the round 2 questionnaire and (B) the round 3 questionnaire. Note that in the round 3 questionnaire (B) the panel were provided with a summary of the previous round responses (a count of the answers and the median answer) as well as directly quoted comments from the previous round. Also note that the statement 'size and depth of the lesion should both be measured' is no longer present on the round 3 questionnaire as this statement reached threshold consensus in round 2 and was removed from the subsequent questionnaire.

A

What is the most important long term outcome for the patient? Please rank (1-4) by importance (1 being most important):

- Regain of function
- Movement without pain
- Return to baseline (or better) quality of life
- Patient specific goals-based on patient's expectations

B

Most important long-term outcome for the patient? (1-4)

- (2) Movement without pain
- (3) Return to baseline (or better) quality of life
- (4) Patient specific goals-based on patient expectations
- (1) Regain of function

Please select one	1	▼
Please select one	1	▼
Please select one	1	▼
Please select one	1	▼

Figure 2-3: An example of the ranked series question type layout from (A) the round 2 questionnaire and (B) the round 3 questionnaire. Note that in the round 3 questionnaire the Delphi panel were also provided with the rank of each item based on the previous round responses (in brackets to the left of each item).

2.2.4 Judging Consensus and Support or Importance

2.2.4.1 *Likert-Scale Rated Single-statements*

The average percentage of majority opinions (APMO) (figure 2-4) and the interquartile range (IQR), were used as cut-off values to examine the level of consensus achieved in the rating of single-statement items (Kapoor, 1987; von der Gracht, Heiko & Darkow, 2013; Habibi et al., 2014). The APMO was calculated separately for round 2 and round 3 and used as a cut-off rate to decide whether or not a statement had reached consensus (Kapoor, 1987; von der Gracht, Heiko & Darkow, 2013). The IQR threshold for significance was pre-set at ≤ 1 , which is deemed appropriate when using a 5-point Likert scale (Habibi et al., 2014).

The strength of support for each item to the panel was judged using the median and mode as measures of central tendency. Descriptive statistics such as mean and standard deviation would be inappropriate to use in this case as the Likert-scale is not delineated at regular intervals (Habibi et al., 2014).

2.2.4.2 *Ranked Series*

Kendall's coefficient of concordance (W) (figure 2-5), a consensus criterion representing the level of consensus between participants, was used to examine the degree of consensus in the ranked series questions (Kendall & Gibbons, 1990; Malone et al., 2004; von der Gracht, Heiko & Darkow, 2013). Resulting consensus-judged ranks were calculated using the mean rank.

2.2.5 Statistical Analyses

All statistical analyses were carried out using Microsoft® Office Excel 2013.

$$APMO = \frac{\text{majority agreements} + \text{majority disagreements}}{\text{total opinions expressed}} \times 100$$

Figure 2-4: *APMO cut-off rate equation.* The equation used to calculate APMO cut-off rate. APMO was used to determine the prescribed range of acceptable consensus (Kapoor, 1987; von der Gracht, Heiko & Darkow, 2013).

$$W = \frac{12S}{m^2(n^2 - n)}$$

Where:

$$s = \sum_{i=1}^n (R_i - \bar{R})^2$$

R_i = Total ranks of a factor
 m = Number of rank sets or judges
 n = Number of ranked factors or phenomena

When:
 $W = 1$: Complete consensus
 $W > 0.7$: Strong consensus
 $W = 0.5$: Moderate consensus
 $W < 0.3$: Weak consensus
 $W = 0$: No consensus

Figure 2-5: *Kendall's Coefficient of Concordance (W) equation.* (Kendall & Gibbons, 1990).

2.3 Results

2.3.1 The Delphi Panel

The resulting Delphi panel size, and associated response rate, in each of the three rounds is shown in table 2-1. There were 51 experts in attendance on the first day of the Oswestry Cartilage symposium who therefore made up the Delphi panel for first round: the idea-generating focus group. On the second day of the meeting there was a reduced attendance of 38, and of these, 24 completed the first questionnaire round. The attendees of the second day were then approached by email to complete the second questionnaire round, of which 15 did so.

2.3.2 Responses

A full list of the statements and responses for the two questionnaire rounds is provided in appendices 1 and 2 (single-statements) and appendices 3 and 4 (ranked series).

- Round 1 resulted in a collection of 54 statements and opinions.
- Round 2 resulted in the rating of 46 single-statements and the ranking of 4 statement series.
- Round 3 resulted in the rating of 30 single-statements and the ranking of 3 statement series.

2.3.3 Items that Reached Consensus

2.3.3.1 *Likert-Scale-Rated Single-Statements*

The 46 single-statements that were rated in round 2, the first questionnaire round, are presented graphically in figure 2-6, with the dashed line representing the APMO cut-off rate of 80.43% for this round. A total of 16 statements reached threshold consensus in this round, with a percentage of agreeing answers above the cut-off rate and an IQR of ≤ 1 .

These items are detailed in Table 2-2. The consensus of opinion for all 16 statements was supportive.

The remaining 30 single-statement items that were rated in round 3 are presented in figure 2-7, in which the dashed line represents the APMO cut-off rate of 66.67% for this round. A further 14 statements reached threshold consensus in round 3, with a percentage of agreeing answers above 66.67% and an IQR of ≤ 1 . These items are detailed in Table 2-3. Again, agreement for these statements was positive.

All 30 of the single-statements that reached consensus in this study were also largely or strongly supported by the Delphi panel with both the mode and median answers 'Largely' or 'Completely' agree (L or C) on the 5-point Likert-scale.

2.3.3.2 Ranked Series

One of the ranked statement series, 'Tissue type', reached consensus in round 2, demonstrating strong consensus $W=0.736$. No further ranked series reached consensus in round 3. A summary of the ranked series for round 2 and round 3 are shown in table 2-4 and table 2-5 respectively.

Table 2-1: Delphi study response rates. The number of experts that were invited to participate in each of the three rounds, the size of the resulting Delphi panel and the response rate as a percentage of the previous round respondents.

Round Number.	Invited to Participate	Respondents (n).	Response rate (% of previous round).
1	51	28	-
2	38	24	85.7
3	38	15	62.5

Consensus Level (APMO) of the Round 2 Likert-scale Rated
Single-Statements.

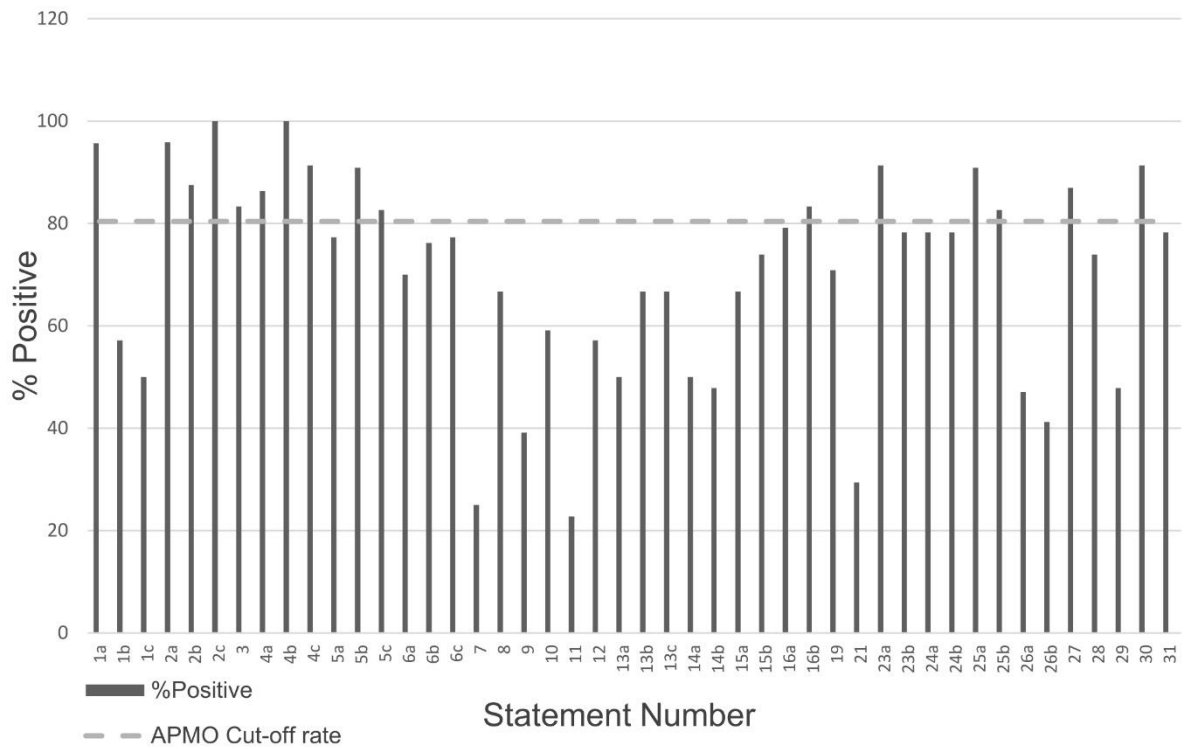


Figure 2-6: The Round 2 Likert-scale-rated single-statements. The dashed line represents the APMO cut-off rate for round 2 (80.43%).

Table 2-2: The Likert-scale-rated single-statement items that reached threshold consensus in round 2 (APMO > 80.43%, IQR ≤ 1).

Round 2 statement number	Statement	% Positive	Mode	Median	IQR
1a	The size and Depth of lesion should both be measured.	96	C	C	0
2a	We should take disease status (e.g. synovial fibrosis, bone sclerosis, inflammation) into account for efficient repair.	96	C	C	0
2b	Patients should be better stratified prior to clinical trial entry.	88	C	C	1
2c	Environmental factors are important in influencing repair (e.g. age, exercise, gender).	100	C	C	1
3	Access to specialist rehab programmes would be useful for all patients, pre- and post- cartilage repair	83	C	C	1
4a	An increase in collagen type II expression is a key marker of cartilage quality in pellet culture.	86	C	L	1
4b	An increase in collagen type II expression is a key marker of cartilage quality in animal models.	100	C	C	1
4c	An increase in collagen type II expression is a key marker of cartilage quality in humans.	91	C	C	1
5b	An increase in aggrecan expression is a key marker of cartilage quality in animal models.	91	L	L	1
5c	An increase in aggrecan expression is a key marker of cartilage quality in humans.	83	L	L	1
16b	It is important to assess all tissues in the joint in humans.	83	C	L/C	1
23a	It is important to assess the identity and quality of both the cartilage and the bone-cartilage interface in animal models.	91	C	C	1
25a	Determining the mechanism of damage repair is important in animal models.	91	C	C	1
25b	Determining the mechanism of damage repair is important in human research.	83	C	C	1
27	Treatment cost should be justifiable.	87	C	C	1
30	Lab research should push the boundaries, not slow down for clinics. There is a need for clinical innovation.	91	C	C	1

Consensus Level (APMO) of the Round 3 Likert-scale Rated Single-Statements.

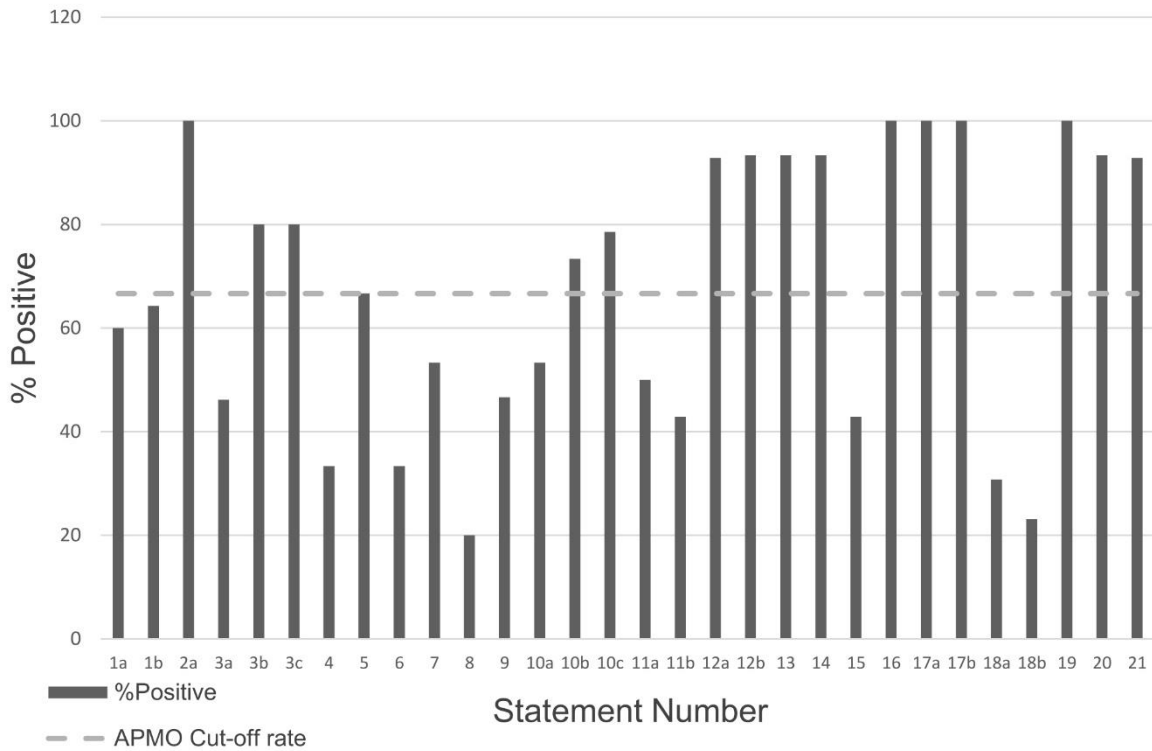


Figure 2-7: The round 3 Likert-scale-rated single-statements. The dashed line represents the APMO cut-off rate for round 3 (66.67%). Note that item 10b reached threshold APMO level but had an IQR of 1.5 and therefore was judged not to have reached threshold consensus overall.

Table 2-3: The likert-scale-rated single-statement items that reached threshold consensus in round 3 (APMO > 66.67%, IQR ≤ 1).

Round 3 statement number	Statement	% Positive	Mode	Median	IQR
2a	An increase in aggrecan expression is a key marker of cartilage quality in pellet culture.	100	L	L	1
3b	An increase in lubricin expression is a key marker of cartilage quality in animal models.	80	L	L	0
3c	An increase in lubricin expression is a key marker of cartilage quality in humans.	80	L	L	0
10c	A more extensive histology scoring system is needed for human tissue.	79	C	C	1
12a	Scoring systems should include both structural and inflammatory features in animal models.	93	L	L	1
12b	Scoring systems should include both structural and inflammatory features in human research.	93	C	L	1
13	It is important to assess all tissues in the joint in animal models.	93	C	C	0.5
14	Non-invasive measures provide a way to reduce time and cost.	93	C	C	0
16	It is important to assess the identity and quality of both the repair cartilage and the bone-cartilage interface in humans.	100	C	C	0.5
17a	The repair has an effect on the surrounding cells in animal models.	100	C	C	0
17b	The repair has an effect on surrounding cells in humans.	100	C	C	0
19	Any technique or product for cartilage repair has to be scalable.	100	C	C	1
20	The cell type should raise as few ethical and safety issues as possible.	93	C	C	1
21	More investment in cell therapies is needed.	93	C	C	0

Table 2-4: A summary of the consensus results for the ranked series in round 2 (Kendall's coefficient of concordance (W) and corresponding consensus level).

Round 2 Ranked Series	Tissue Type	Treatment Choice Basis	Repair Quality Assessment	Treatment Outcome
Kendall's Coefficient of Concordance (W)	0.736	0.049	0.182	0.172
Consensus	Strong	Very Weak	Very Weak	Very Weak

Table 2-5: A summary of the consensus results for the ranked series in round 3 (Kendall's coefficient of concordance (W) and corresponding consensus level). Note that the 'Tissue Type' ranked series has been removed from this round as it reached threshold consensus in the previous round.

Round 3 Ranked Series	Treatment Outcome	Treatment Choice Basis	Repair Quality Assessment
Kendall's Coefficient of Concordance (W)	0.437	0.376	0.287
Consensus	Weak/Moderate	Weak	Weak

2.3.4 Items that did not Reach Consensus

2.3.4.1 *Likert-Scale-Rated Single-Statements*

A total of 16 single-statements did not reach consensus threshold levels in this Delphi study (Table 2-6). Of these 16 items, 6 showed an increase in consensus (increase in APMO), 8 showed a decrease in consensus (decrease in APMO) and 2 showed no change between rounds 2 and 3 (figure 2-8).

2.3.4.2 *Ranked Series*

Three of the four ranked series in this Delphi study did not reach threshold consensus (Table 2-5). All three, however, demonstrated an increase in consensus levels between rounds 2 and 3 (figure 2-9).

Table 2-6: A summary of the Likert-scale-rated single-statement items that did not reach threshold consensus over the course of this Delphi study.

Round 3 statement number	Statement
1a	We should measure the lacunae (cysts) in the bone.
1b	We should measure the area of bone marrow oedema-like (BML) signal.
3a	An increase in lubricin expression is a key marker of cartilage quality in pellets.
4	Functional fibrocartilage is sufficient in the repair.
5	Hyaline cartilage is necessary in the repair.
6	Collagen type X expression should not be present in the repair at mRNA level.
7	Collagen type X expression should not be present in the repair.
8	Measuring cartilage changes is irrelevant, the pathogenic mechanisms that lead to the changes are more important and may be largely cartilage dependant.
9	Collagen type VI is a useful measure of cartilage quality.
10a	A more extensive histology scoring system is needed for pellets.
10b	A more extensive histology scoring system is needed for animal models.
11a	A simpler scoring system is best for MRI in animals.
11b	A simpler scoring system is best for MRI in humans.
15	Advancement of the bone front is negative
18a	MRI should be performed in short bursts to keep costs down in animal models.
18b	MRI should be performed in short bursts to keep costs down in human research.

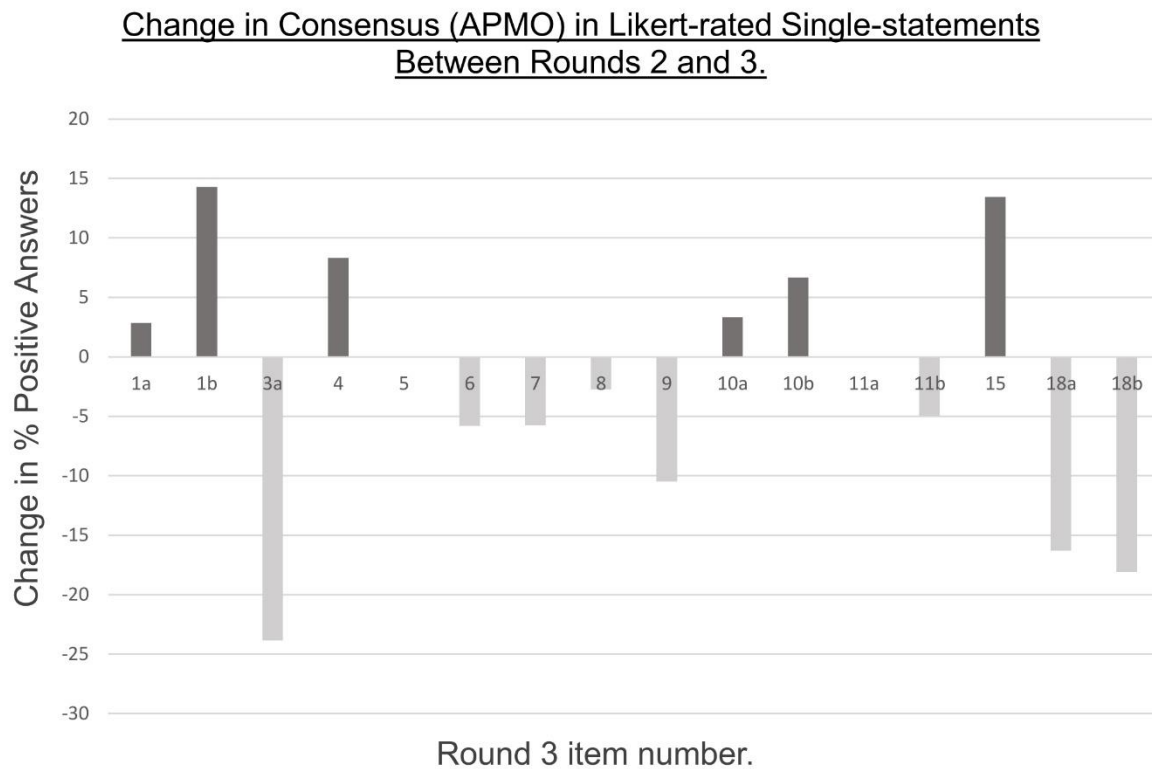


Figure 2-8: Change in APMO, between rounds 2 and 3, of the Likert-scale-rated single-statements that did not reach threshold consensus over the course of this Delphi study.

Change in Kendall's Coefficient of Concordance (W) of the Ranked Series Between Rounds 2 and 3.

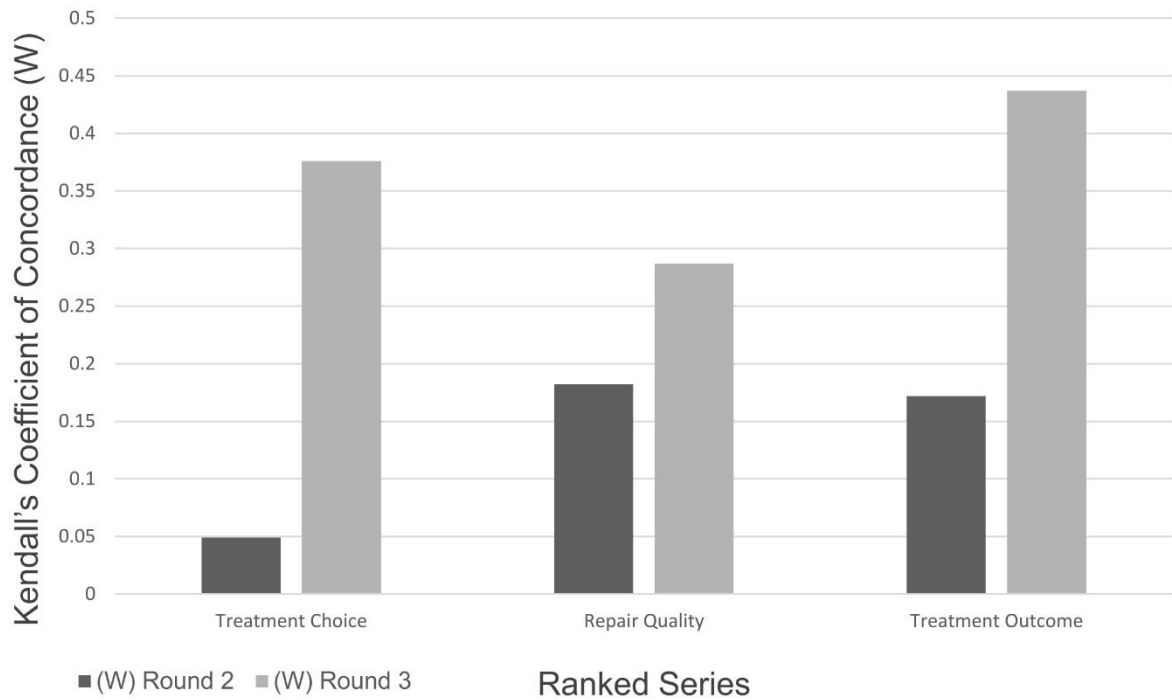


Figure 2-9: The change in Kendall's coefficient of concordance (W), between rounds 2 and 3, of the ranked series that did not reach consensus over the course of this Delphi study.

2.4 Discussion

2.4.1 Items that Reached Consensus

2.4.1.1 *Likert-Scale-Rated Single-Statements*

The items collected in the first round, and therefore the content of the subsequent questionnaires, varied widely in subtopic and scope within the cartilage repair field. The 30 single-statement items, recognised by the panel as being important factors in cartilage repair, were therefore separated into three distinct groups.

Table 2-7 contains statements relevant to assessing the structural quality of repair cartilage that, taken together, could act as a guide when developing a checklist to standardise structural assessment of cartilage repair across studies. Besides being agreed upon by the panel, the importance of these items is also supported by the literature. A number of these parameters are already assessed by one or several of the various, commonly used cartilage repair scoring systems. However, given the vast array of scoring systems and associated parameters, it can be hard to deduce which of the factors that are being assessed by each system is actually important. The Delphi panel agreed with the statements, 'A more extensive histology scoring system is required for human samples', and, 'Scoring systems for studies in humans and animals should include both structural and inflammatory features', reflecting the feeling that current scoring systems are inadequate in this regard. The utility of this output lies in the collation of the parameters that are agreed upon by the panel as important, regardless of which scoring system they belong to, that could serve as a starting point in the development of a checklist to standardise the structural assessment of cartilage repair across studies.

An increase in collagen type II, aggrecan and lubricin expression were agreed by the panel as important markers in determining the quality of repair cartilage in both human studies and animal models. An abundance of collagen type II, and proteoglycans such as aggrecan, in repair cartilage has long been considered a marker for repair cartilage quality and longevity, and therefore consensus on these items is unsurprising (Roberts et al., 2009; Roberts et al., 2010; Roughley & Mort, 2014). The prevalence of collagen type II in repair cartilage is considered to be a marker of the degree of differentiation towards hyaline cartilage and therefore can be indicative of a structurally successful repair (Mainil-Varlet et al., 2010). Lubricin has a less established history as a marker of cartilage quality but in a recent paper lubricin was found in the superficial zone of 84% of biopsies taken from repair cartilage following ACI (Roberts et al., 2010). Lubricin is known to reduce friction and prevent abnormal cell adhesion and overgrowth at the cartilage surface and therefore its presence in repair cartilage may be indicative of cartilage repair success and resemblance of the repair tissue to native articular cartilage (Schumacher et al., 1999; Roberts et al., 2010; Lee, Yunsup, Choi & Hwang, 2018).

The panel further agreed that all tissues in the joint should be considered when assessing the quality of cartilage repair in human and animal studies. This reflects the view of the knee as an organ in which the constituent tissues work together to maintain function, and multiple tissues are affected in times of dysfunction (Loeser et al., 2012). The agreement of the panel with this statement suggests that the knee should also be regarded as an organ when determining the success of cartilage repair techniques and all tissues of the joint should therefore be assessed. The statement, 'the repair has an effect on the other surrounding cells', also reached threshold consensus and conveys a similar message that the success of cartilage repair should not be judged solely on the quality of the repair cartilage

as this is not the only tissue affected by the repair. MRI scoring systems, such as the Whole-Organ Magnetic Resonance Imaging Score (WORMS) are able to assess the whole joint and it may be the case that standardising the assessment of cartilage repair across studies will require a multi-disciplinary approach that takes into account capabilities and parameters taken from histological and radiographic scoring systems (Rutgers et al., 2010; Roemer et al., 2014). Consensus was also reached on statements relating to the fact that non-invasive measures would reduce time and costs, suggesting that developing imaging-based cartilage repair scoring systems that are able to consider and assess all of the joint tissues. Such a scoring system could combine a whole-joint MRI scoring system such as the WORMS or MRI Osteoarthritis Knee Score (MOAKS) with a repair-specific system such as 3D-Magnetic Resonance Observation of Cartilage Repair Tissue (3D-MOCART) or the Cartilage Repair Osteoarthritis Knee Score (CROAKS) (Peterfy et al., 2004; Marlovits et al., 2006; Rutgers et al., 2010; Hunter et al., 2011).

The panel agreed that the bone-cartilage interface is another important marker of the structural quality of repair cartilage. It has been reported that cartilage repair strategies that lead to the formation of fibrocartilage often demonstrate little regeneration of the tidemark and calcified cartilage and therefore develop a less stable tissue-bone interface (Hoemann et al., 2012). The regeneration of the osteochondral interface and therefore the integration of the repair cartilage to the bone is necessary for a stable repair, with the calcified cartilage layer contributing not only to mechanical functionality and stability, but also to cartilage-bone homeostasis (Boushell et al., 2017). Thus, the quality of the cartilage-bone interface could be indicative of the quality of the repair as a whole.

The panel also agreed on baseline factors that may influence a structurally successful repair (Table 2-8). While the exact role of these factors in cartilage repair may not always be clear, the panel did agree they should be determined. Currently there is little guidance on criteria for the selection of appropriate cartilage repair technique and therefore defining baseline factors that could influence repair could be useful (Bekkers et al., 2009; Seo et al., 2011). The panel agreed that the disease status of the patient should be taken into account, as patients with chronic symptoms and related inflammation tend to have an increased failure rate of cartilage repair techniques or do not benefit at all (Scotti et al., 2016). Consensus was also reached on the influence of environmental factors, such as age, gender and BMI, on the success of cartilage repair. In the elderly, for example, the chondrogenic potency of bone marrow-derived mesenchymal stem cells is inferior to that of younger patients, which could lead to a reduced chance of success of marrow stimulation techniques such as microfracture (Miller et al., 2004; Brittberg et al., 2016).

The statement, 'Determining the mechanism of damage repair is important in both humans and animal models', also reached threshold consensus. Although it is well established that articular cartilage has a limited capacity for self-repair once injured, there is some evidence from joint distraction studies and longitudinal observational studies of the natural history of cartilage defects, that it is in fact possible in some cases, although the mechanisms underlying natural cartilage healing are largely unknown (Wang et al., 2006; Ding et al., 2006; Tiku & Sabaawy, 2015). In vitro studies using a wound model of both bovine and human cartilage have shown cellular responses that resemble those in other tissues that are able to repair (Seol et al., 2012; Tiku & Sabaawy, 2015). Similarly, the analysis of cartilage tissue from other animal models of OA have demonstrated molecular changes that parallel those seen in the repair of other wounds (Wong et al., 2013; Tiku & Sabaawy, 2015). It is

widely accepted that understanding the mechanisms that underpin the natural repair of tissue damage could lead to the development of new treatments, or the improvement of existing ones. This could also apply to the cartilage repair field.

The size and depth of the cartilage lesion were also agreed upon by the panel to be important factors to consider and may influence the outcome of cartilage repair surgery. Not only does the size and depth of the lesion often determine which repair technique is employed, but most procedures have a maximum size recommendation, beyond which success rates for that particular technique worsen (Gomoll et al., 2011). The panel also agreed upon a third group of statements that broadly related to the economical and ethical considerations around cartilage repair research, detailed in Table 2-9.

2.4.1.2 Ranked Statement Series

Only one of the four ranked series 'Tissue Type' reached consensus in this Delphi study (Table 2-10) providing a hierarchy of joint tissues based on their importance in the cartilage repair process, as perceived by our expert panel. This agreed hierarchy is particularly useful given the panel's opinion (Table 2-7) to regard cartilage degeneration and repair as processes that affect and involve all tissues in the joint, rather than the articular cartilage alone (Loeser et al., 2012). This hierarchy can therefore serve to aid in prioritising and deciding future directions of research in cartilage repair and its assessment.

Table 2-7: A Summary of the Likert-scale-rated single-statements that encompass parameters and considerations for the assessment of a structurally successful cartilage repair.

Factors that can be used to assess the structural quality of repair cartilage:

- An increase in collagen type II expression and aggrecan expression are key markers of cartilage production in pellets, animal models and humans.
- An increase in lubricin expression is a key marker of cartilage production in animal models and humans.
- Non-invasive measures provide a way to reduce time and cost.
- The repair has an effect on other surrounding cells in humans and in animal models.
- A more extensive histology scoring system is required for human samples.
- Scoring systems for studies in humans and in animal models should include both structural and inflammatory features.
- It is important to assess all tissues of the joint in humans and in animal models.
- It is important to assess the identity and quality of the cartilage and the bone-cartilage interface in humans and in animal models.

Table 2-8: A Summary of the Likert-scale-rated single-statements that are considered to be factors that could influence a structurally successful repair.

Factors that may influence a structurally successful cartilage repair:

- Size and depth of lesion should both be measured.
- Disease status (e.g. bone sclerosis, inflammation) should be taken into account.
- Determining the mechanism of damage repair is important in both humans and in animal models.
- Environmental factors (e.g. age, gender) are important in influencing repair.

Table 2-9: A Summary of the Likert-scale-rated single-statements that encompass economic and ethical considerations of cartilage repair.

Factors relating to research economics and ethics:

- More investment in cell therapies is needed.
- Any technique or product for cartilage repair must be scalable.
- Treatment cost should be justifiable.
- Cell type should raise as few ethical and safety issues as possible.
- Lab research should push boundaries, not slow down for the clinic. There is need for clinical innovation.
- Patients should be better stratified prior to clinical trial entry.
- Access to specialist rehabilitation programmes would be useful for all patients, pre and post repair.

Table 2-10: The resulting 'Tissue Type' hierarchy based on the mean ranks of the items in the ranked series that reached threshold consensus.

'Tissue Type' ranked series.

1. Cartilage.
2. Subchondral bone.
3. Synovium (focal to defect).
4. Synovium (general).
5. Meniscus.
6. Fat pad.

2.4.2 Statements That Did Not Reach Consensus

Some of the items in this Delphi study did not reach threshold consensus suggesting dissent amongst the panel and, by extension, within the field. There was an increase in consensus between rounds 2 and 3 in six of the remaining 16 single-statement items (Table 2-6), and in the remaining three ranked series (Table 2-5). In theory, a Delphi process can have an unlimited number of rounds and further rounds may have led to further convergence on these items. The lack of consensus more likely suggests a corresponding lack of knowledge surrounding the statements. These statements can therefore serve as a list of future research topics within the cartilage repair field.

2.4.2.1 *Likert-scale-rated Single-statements*

A total of ten of the Likert-scale rated statements, showed either no change or a decrease in consensus between rounds 2 and 3, suggesting that a difference in opinion in these topic areas remains (Table 2-6).

The panel was comprised of both scientists and clinicians and therefore some of the dissent could be attributed to a difference in priorities or a difference in knowledge between these two groups. An example is the two statements, 'hyaline cartilage is necessary in the repair' nor, 'functional fibrocartilage is sufficient in the repair', reached threshold consensus levels. These statements represent two of the major opposing arguments in the field of cartilage repair. The aim of any cartilage repair technique ultimately is to (re)generate a cartilage tissue that is as close as possible to native hyaline articular cartilage in order to provide the best possible biomechanical properties and longevity of the repair. Fibrocartilage is considered biomechanically inferior to hyaline cartilage and therefore is considered to provide a more temporary repair that only slows the progression from cartilage lesion to OA (Widuchowski et al., 2007; Mollon et al., 2013). The more the repair tissue resembles

hyaline cartilage, the better the repair quality is considered (Roberts et al., 2010). However, the fact that neither of these statements reached consensus, indicates that this idea is not as ingrained as expected. This may represent a difference in opinions and priorities between the basic scientists and the clinicians that make up the Delphi panel. A simpler surgical technique resulting in a functional cartilage that enables the patient to return to a similar quality of life as before their injury and delays arthroplasty may be sufficient from a clinical perspective. On the other hand, the regeneration of a true hyaline cartilage may be the ultimate goal for basic scientists working in the field. However, this remains speculation and a further, non-anonymised study would be required to shed light on this disagreement.

Neither, 'We should measure the lacunae (cysts) in the bone', nor, 'We should measure the area of bone marrow oedema-like (BML) signal', reached threshold consensus over the course of this Delphi study. This is interesting, and somewhat surprising given the fact the subchondral bone was placed second in the 'Tissue Type' hierarchy that reached threshold consensus levels with regard to its importance in cartilage repair. Thus, one may expect that pathological changes to the subchondral bone, such as cysts and oedema, would also be regarded as important considerations prior to cartilage repair, by the Delphi panel. The acceptance of OA as a disease of the whole joint, rather than exclusively of the articular cartilage, has increased interest in the other constituent tissues of the joint (Brandt et al., 2006; Loeser et al., 2012; Thysen et al., 2015). The subchondral bone is of particular interest given its proximity to the articular cartilage, and the demonstration of cellular, molecular and biochemical interaction between the two tissues (O'Hara et al., 1990; Wang et al., 2013; Findlay & Kuliwaba, 2016). Degenerative changes in the subchondral bone are often mirrored in the articular cartilage. For example, BML's are commonly found distal to areas of cartilage degeneration and the intensity of their signal on MRI has been shown to

correlate with the extent of cartilage degeneration (Garnero et al., 2005; Bhosale & Richardson, 2008; Wluka et al., 2009; Castañeda et al., 2012). However, the precise effect of pathological changes in the bone on articular cartilage health and repair is still unconfirmed. Work presented in chapters 3 and 4 seeks to address some of the unknowns in this area.

The fact that threshold consensus was not achieved regarding the presence of collagen type X in the repair, at protein nor at mRNA level, is also interesting. Collagen type X expression is associated with hypertrophic chondrocytes and has been shown to be upregulated in experimental animal OA models and in human osteoarthritic cartilage (Walker et al., 1995; G Shen, 2005; Matsumoto et al., 2009; Luo et al., 2017). However, other studies have reported that the expression of type X collagen was not significantly elevated in osteoarthritic cartilage in late stage rat and human OA (Appleton et al., 2007; Brew et al., 2010; Luo et al., 2017). Collagen type X also plays several important roles in healthy cartilage, supporting endochondral bone growth and development and matrix calcification (Luo et al., 2017). Thus, the significance of the presence of collagen type X in repair cartilage is unclear in the published literature, and further research is required. This is reflected by the lack of consensus amongst the Delphi panel.

2.4.2.2 Ranked Statement Series

The ranked statement series, 'Repair Quality Assessment', was compressed from ten options to six options between rounds 2 and 3 following comments from the panel that some of the options were too similar. For example, 'low friction surface' and, 'smooth surface', from the round 2 questionnaire, were combined into, 'surface', in the round 3 questionnaire.

Three of the four ranked statement series failed to reach threshold consensus levels in this Delphi study: 'Treatment Outcome', 'Treatment Choice Basis' and 'Repair Quality Assessment' (Table 2-5). This suggests that there remains disagreement over priorities in these areas and further research is required to determine priorities both in the clinic and in the laboratory.

2.4.3 The Delphi Panel

Throughout this Delphi process, the panel was composed entirely of individuals working in the United Kingdom. Although the study was therefore limited in its geographical scope, the results have potential international applicability. The Delphi panel was made up of individuals from a range of research, clinical and industrial backgrounds. Such a panel of experts, encompassing the different disciplines that make up the cartilage repair community, has the advantage of assessing the presented problem from a number of different perspectives.

To our knowledge, no guideline has been published for the selection of 'experts' to form a Delphi panel, and expertise itself is hard to define. In the case of this Delphi study, we used the criteria put forward by Adler and Ziglio (1996) to define expertise in the Delphi context: 'Knowledge and experience with the issue under investigation', 'capacity and willingness to participate', 'sufficient time to participate' and 'effective communication skills' (Adler & Ziglio, 1996). A large proportion of those that were invited to take part declined to do so (Table 2-1) and there was no attempt to encourage attendees to do so, as voluntary participation ensured that the entirety of the Delphi panel met these requirements.

Previously published Delphi studies vary widely in the size of the panel, from five participants, to around 400 (Malone et al., 2004; Kelly & Porock, 2005; Boulkedid et al.,

2011; Habibi et al., 2014). A larger panel size increases the variety of expertise but ultimately is likely to lead to diminishing responses (McMillan et al., 2016). The first-round panel size of 28 participants in this Delphi study allowed for the inclusion of a series of comments and opinions from a broad range of experts, without making the subsequent questionnaires overly time consuming. A recent systematic review, that aimed to evaluate previously published Delphi studies and produce guidance for future studies, detailed the number of experts that were invited to take part in 80 studies (Boulkedid et al., 2011). Of these studies, only 76 reported the number of individuals that were invited to participate and of these the median number invited was 17 (Q1:11-Q3:31), with a minimum of 3 and a maximum of 418 (Boulkedid et al., 2011).

As demonstrated in Table 2-1, there was some degree of participant attrition over the course of this Delphi process, with the panel size decreasing with each subsequent round. The lowest number of respondents (n=15) was observed in round 3, likely due to the distribution of this questionnaire electronically rather than in person as in previous rounds. While this may seem a small number of individuals, the lack of guidelines on the Delphi methodology means that no criteria exist for determining the number of participants that constitutes a small or large Delphi panel (Akins et al., 2005). The ability of the final round panel to reach consensus was not impeded by its size because a further 14 single-statement items reached consensus in this round.

The decrease in panel size came with an associated decrease in the response rate, presented in Table 2-1 as a percentage of the previous round respondents. The lowest response rate was observed in round 3. Once again, the lack of overreaching methodological guidelines for the Delphi process makes it difficult to appraise the response rates resulting

from this study. It is widely accepted that a 100% response rate is very rare in Delphi studies, particularly those which are at least partly carried out remotely, as in round 3 of our study (McKenna, 1994; Keeney et al., 2011). The previously mentioned systematic review reported that of the 80 Delphi studies that were interrogated, the median round 1 response rate was 90% (Q1:80%-Q3:100%) and the median final round response rate was 88% (Q1:69%-Q3:96%) (Boulkedid et al., 2011). However, only 31 of the 80 studies (39%) reported their response rates so these numbers could possibly suffer from publication bias (Boulkedid et al., 2011). A handbook recommends that a response rate of 70% should be maintained for each round but also acknowledges this is difficult to obtain (Keeney et al., 2011). This recommended response rate was obtained in the second round (85.7%) but not in the third round (62.5%), likely due to the electronic distribution of the third-round questionnaire. A higher response rate is easier obtained if all Delphi rounds are carried out face-to-face, which was not possible in this case (McKenna, 1994; Keeney et al., 2011).

Measuring and assessing the structural quality of repair cartilage, and determining the important influencing factors, is imperative. Here we report a 3-round Delphi process which resulted in the production of a set of guideline parameters by which to assess the structural quality of cartilage repair and a set of factors that may influence structurally successful cartilage repair. The items that failed to reach consensus in this study represent areas of incomplete knowledge and can therefore be used to formulate future clinical and fundamental science (laboratory) research questions with a view to filling gaps in knowledge, increasing consensus and determining priorities for the assessment of cartilage repair in the clinic and laboratory. Although the individual items interrogated in this Delphi study are not novel individually, the value of this study lies in their curation and interrogation by a diverse group of experts.

2.4.4 Study Limitations

The main limitation of this study was the low response number to the third-round questionnaire. Additionally, it would have been interesting to compare opinions between professions, which would have been possible to do while still maintaining quasi-anonymity, to determine if there is a difference in research priorities, particularly between clinicians and basic scientists.

2.5 Conclusion

Measuring and assessing the structural quality of repair cartilage, and determining the important influencing factors, is imperative. Here we report a 3-round Delphi process which resulted in the production of a set of guideline parameters by which to assess the structural quality of cartilage repair and a set of factors that may influence structurally successful cartilage repair. The items that failed to reach consensus in this study represent areas of incomplete knowledge and can therefore be used to formulate future clinical and fundamental science (laboratory) research questions with a view to filling gaps in knowledge, increasing consensus and determining priorities for the assessment of cartilage repair in the clinic and laboratory. Although the individual items interrogated in this Delphi study are not novel individually, the value of this study lies in their curation and interrogation by a diverse group of experts.

2.6 Appendices

Appendix 2-1: A full list of the Likert-scale-rated single-statements and results from the round 2 questionnaire.

Statement	Round 2 Statement Number	None (n)	Somewhat (n)	Middling (n)	Largely (n)	Completely (n)	Total answers (n)	Median	% Positive	IQR	Consensus Reached?
The size and depth of the lesion should both be measured.	1a	0	1	0	4	18	23	C	95.65	0	✓
We should measure the lacunae (cysts) in the bone.	1b	1	5	3	3	9	21	L	57.14	3	X
We should measure the area of bone marrow oedema-like (BML) signal.	1c	2	5	3	4	6	20	M/L	50	3	X
We should take disease status (e.g. synovial fibrosis, bone sclerosis, inflammation) into account for efficient repair.	2a	0	1	0	2	21	24	C	95.83	0	✓
Patients should be better stratified prior to clinical trial entry.	2b	0	1	2	8	13	24	C	87.5	1	✓
Environmental factors are important in influencing repair (e.g. age, exercise, gender).	2c	0	0	0	9	15	24	C	100	1	✓
Access to specialist rehabilitation programs would be useful for all patients, pre- and post- cartilage repair.	3	0	1	3	6	14	24	C	83.33	1	✓
An increase in collagen type II expression is a key marker of cartilage quality in pellet culture.	4a	0	1	2	9	10	22	L	86.36	1	✓
An increase in collagen type II expression is a key marker of cartilage quality in animal models.	4b	0	0	0	10	12	22	C	100	1	✓
An increase in collagen type II expression is a key marker of cartilage quality in humans.	4c	0	1	1	7	14	23	C	91.30	1	✓

An increase in aggrecan expression is a key marker of cartilage quality in pellet culture.	5a	0	1	4	9	8	22	L	77.27	1	X
An increase in aggrecan expression is a key marker of cartilage quality in animal models.	5b	0	1	1	12	8	22	L	90.91	1	✓
An increase in aggrecan expression is a key marker of cartilage quality in humans.	5c	0	2	2	10	9	23	L	82.61	1	✓
An increase in lubricin expression is a key marker of cartilage quality in pellet culture.	6a	0	0	6	9	5	20	L	70	1.25	X
An increase in lubricin expression is a key marker of cartilage quality in animal models.	6b	0	0	5	11	5	21	L	76.19	0	X
An increase in lubricin expression is a key marker of cartilage quality in humans.	6c	0	1	4	10	7	22	L	77.27	1	X
Any functional fibrocartilage is sufficient.	7	3	5	10	3	3	24	M	25	1.25	X
Hyaline cartilage is absolutely necessary.	8	2	0	6	10	6	24	L	66.67	1.25	X
Collagen type X expression should not be present at mRNA level.	9	2	2	10	6	3	23	M	39.13	1	X
Collagen type X expression should not be present in the repair.	10	1	1	7	9	4	22	L	59.09	1	X
Measuring cartilage changes is irrelevant, the pathogenic mechanisms that lead to the changes are more important and may be largely cartilage dependant.	11	3	6	8	4	1	22	M	22.72	1	X
Collagen type VI is a useful marker for cartilage repair quality.	12	2	0	4	0	8	14	C	57.14	2	X
A more extensive histology scoring system is needed for pellet culture.	13a	4	1	6	5	6	22	M	50	1.5	X

A more extensive histology scoring system is needed for animal models.	13b	4	2	2	8	8	24	L	66.67	2.25	X
A more extensive histology scoring system is needed for human tissue.	13c	4	2	2	7	9	24	L	66.67	2.25	X
A simpler scoring system is best for MRI in animal models.	14a	1	2	7	5	5	20	M/L	50	1.25	X
A simpler scoring system is best for MRI in human research.	14b	2	3	7	5	6	23	M	47.82	1.5	X
Scoring systems should include both structural and inflammatory features in animal models.	15a	2	2	3	8	6	21	L	66.67	2	X
Scoring systems should include both structural and inflammatory features in human research.	15b	2	2	2	9	8	23	L	73.91	1.5	X
It is important to assess all tissues in the joint in animal models.	16a	0	0	5	10	9	24	L	79.17	2	X
It is important to assess all tissues in the joint in human research.	16b	0	0	4	8	12	24	L/C	83.33	1.5	✓
Non-invasive measures provide a way to reduce time and cost.	19	1	1	5	5	12	24	L/C	70.83	1	X
The advancement of the bone front is negative.	21	1	2	9	2	3	17	M	29.41	1	X
It is important to assess the identity and quality of both repair cartilage and the bone-cartilage interface in animal models.	23a	0	0	2	8	13	23	C	91.30	2	✓
It is important to assess the identity and quality of both repair cartilage and the bone-cartilage interface in humans.	23b	0	1	4	7	11	23	L	78.26	1	X
The repair has an effect on the surrounding cells in animal models.	24a	0	0	5	5	13	23	C	78.26	1	X
The repair has an effect on the surrounding cells in humans.	24b	0	0	5	5	13	23	C	78.26	1	X

Determining the mechanism of damage repair response is important in animal models.	25a	0	2	2	6	13	22	C	90.91	1	✓
Determining the mechanism of damage repair response is important in human research.	25b	0	2	2	6	13	23	C	82.61	1	✓
MRI should be used in short bursts to keep costs down in animal models.	26a	2	2	5	6	2	17	M	47.06	1	X
MRI should be used in short bursts to keep costs down in human research.	26b	1	1	8	5	2	17	M	41.18	1	X
Treatment costs should be justifiable.	27	0	1	2	7	13	23	C	86.96	1	✓
Any technique or product for cartilage repair has to be scalable.	28	0	2	4	9	8	23	L	73.91	1.5	X
The cell type should raise as few ethical and safety issues as possible.	29	3	4	5	3	8	23	L	47.83	2	X
Laboratory research should push the boundaries, not slow down for clinics. There is a need for clinical innovation.	30	0	1	1	8	13	23	C	91.30	1	✓
More investment in cell therapies is needed.	31	0	1	4	5	13	23	C	78.26	1	X

Appendix 2-2: A full list of the Likert-scale-rated single-statements and results from the round 3 questionnaire.

Statement	Round 3 Statement Number	None (n)	Somewhat (n)	Middling (n)	Largely (n)	Completely (n)	Total answers (n)	Median	% Positive	IQR	Consensus Reached?
We should measure the lacunae (cysts) in the bone.	1a	1	1	4	3	6	15	L	60.00	2	X
We should measure the area of bone marrow oedema-like (BML) signal.	1b	0	2	3	5	4	14	L	64.29	1.75	X
An increase in aggrecan expression is a key marker of cartilage quality in pellet culture.	2a	0	0	0	8	7	15	L	100	1	✓
An increase in lubricin expression is a key marker of cartilage quality in pellet culture.	3a	0	0	7	4	2	13	M	46.15	1	X
An increase in lubricin expression is a key marker of cartilage quality in animal models.	3b	0	0	3	11	1	15	L	80.00	0	✓
An increase in lubricin expression is a key marker of cartilage quality in humans.	3c	0	0	3	9	3	15	L	80.00	0	✓
Any functional fibrocartilage is sufficient.	4	0	4	6	3	2	15	M	33.33	1.5	X
Hyaline cartilage is absolutely necessary.	5	1	1	3	7	3	15	L	66.67	1	X
Collagen type X expression should not be present in the repair at mRNA level.	6	0	4	6	5	0	15	M	33.33	1.5	X
Collagen type X expression should not be present in the repair.	7	0	2	5	7	1	15	L	53.33	1	X
Measuring cartilage changes is irrelevant, the pathogenic mechanisms that lead to the changes are more important and may be largely cartilage dependant.	8	3	4	5	2	1	15	M	20.00	1	X

Collagen type VI is a useful marker for cartilage repair quality.	9	0	2	6	1	6	15	M	46.67	2	X
A more extensive histology scoring system is needed for pellet culture.	10a	1	2	4	4	4	15	L	53.33	1.5	X
A more extensive histology scoring system is needed for animal models.	10b	1	1	2	4	7	15	L	73.33	1.5	X
A more extensive histology scoring system is needed for human tissue.	10c	1	1	1	2	9	14	C	78.57	1	✓
A simpler scoring system is best for MRI in animal models.	11a	1	0	6	6	1	14	M/L	50.00	1	X
A simpler scoring system is best for MRI in human research.	11b	1	0	7	5	1	14	M	42.86	1	X
Scoring systems should include both structural and inflammatory features in animal models.	12a	0	0	1	8	5	14	L	92.86	1	✓
Scoring systems should include both structural and inflammatory features in human research.	12b	0	0	1	7	7	15	L	93.33	1	✓
It is important to assess all tissues in the joint in animal models.	13	0	0	1	3	11	15	C	93.33	0.5	✓
Non-invasive measures provide a way to reduce time and cost.	14	0	0	1	0	14	15	C	93.33	0	✓
The advancement of the bone front is negative.	15	0	0	8	4	2	14	M	42.86	1	X
It is important to assess the identity and quality of both the repair cartilage and the bone-cartilage interface in humans.	16	0	0	0	4	11	15	C	100	0.5	✓
The repair has an effect on the surrounding cells in animal models.	17a	0	0	0	2	13	15	C	100	0	✓
The repair has an effect on the surrounding cells in humans.	17b	0	0	0	2	13	15	C	100	0	✓
MRI should be used in short bursts to keep costs down in animal models.	18a	1	0	8	4	0	13	M	30.77	1	X

MRI should be used in short bursts to keep costs down in human research.	18b	1	2	7	2	1	13	M	23.08	0	X
Any technique or product for cartilage repair has to be scalable.	19	0	0	0	7	8	15	C	100	1	✓
The cell type should raise as few ethical and safety issues as possible.	20	0	0	1	5	9	15	C	93.33	1	✓
More investment in cell therapies is needed.	21	0	0	1	1	12	14	C	92.86	0	✓

Appendix 2-3: A full list of the statement series and results from the round 2 questionnaire.

Round 2 Ranked Series	Options	Number of respondents	Number that ranked as most important	Mean Rank	Mode Rank	Kendall's coefficient of concordance	Consensus Reached?
Tissue Type	Cartilage	24	22	1.10	1	0.736	✓
	Meniscus		1	4.21	5		
	Fat Pad		0	5.79	6		
	Subchondral Bone		0	2.40	2		
	Synovium (focal to defect)		0	3.60	4		
	Synovium (general)		0	3.90	4		
Treatment Choice Basis	Patient Expectations	24	12	2.13	1	0.049	X
	Clinician Expectations		5	2.44	2		
	Biomarkers		4	2.67	3		
	Baseline		3	2.77	3		
Repair Quality Assessment	Filling of defect area	20	6	3.98	1	0.182	X
	Filling of defect depth		0	4.73	2		
	Quality measures by stiffness		0	6.60	10		
	Lateral integration		1	5.93	5		
	Attachment to bone		0	5.83	6		
	Smooth surface		0	7.15	9		
	Low friction surface		0	7.55	8		
	Durability over time		4	4.23	1		
	Functionality (lack of pain)		3	4.33	3		
	Functionality (delayed OA progression)		3	4.70	7		
Treatment Outcome	Regain function	24	9	1.96	2	0.172	X
	Movement without pain		7	2.13	2		
	Return to baseline (or better) quality of life		3	2.92	3		
	Patient specific goals		4	3.00	4		

Appendix 2-4: A full list of the statement series and results from the round 3 questionnaire.

Round 3 Ranked Series	Options	Number of respondents	Number that ranked as most important	Mean Rank	Mode Rank	Kendall's coefficient of concordance (W)	Consensus Reached?
Treatment Outcome	Movement without pain	15	6	1.77	1	0.437	X
	Return to baseline (or better) quality of life		0	3.10	3		
	Patient specific goals		1	3.37	4		
	Regain function		6	1.77	2		
Treatment Choice Basis	Biomarkers	15	0	2.87	3	0.376	X
	Patient expectations		10	1.73	1		
	Baseline imaging		1	3.43	4		
	Clinician expectations		3	1.97	2		
Repair Quality Assessment	Attachment	15	2	3.27	3	0.287	X
	Stiffness		1	4.27	5		
	Durability		6	2.23	1		
	Filling		1	2.53	2		
	Surface		1	4.80	6		
	Lateral integration		0	3.90	4		

Chapter 3:
Investigating the effect of subchondral bone
health on articular cartilage repair using a novel,
in-vitro, co-culture model

3. Chapter 3: Investigating the Effect of Subchondral Bone Health on Articular Cartilage Repair in the Human Knee.

3.1 Introduction

In the human knee, the articular cartilage (AC) forms a complex, functional unit with the subchondral bone (SB), the osteochondral unit, in which the components act together to dissipate forces generated during articulation (Goldring, 2012). The common biomechanical role and the close physical association between the tissues led to hypotheses of biochemical communication across the osteochondral junction (Luyten & Lories, 2011; Yuan et al., 2014). Although initially considered unlikely, due to the perceived impenetrability of the calcified cartilage to even small molecules, certain physical features were identified that demonstrated that the AC and SB are not as separate as previously thought (Duncan et al., 1987; Clark & Huber, 1990; Lyons et al., 2006; Luyten & Lories, 2011; Findlay & Kuliwaba, 2016). Subsequently, several groups used *ex vivo* models of the osteochondral junction to demonstrate that communication, through the calcified cartilage, was possible via the diffusion of both small and large molecules (O'Hara et al., 1990; Arkill & Winlove, 2008; Wang et al., 2013; Findlay & Kuliwaba, 2016). Biochemical communication between the AC and the SB is further supported by the presence of common biochemical pathways (such as the bone morphogenetic (BMP) and Wingless-related integration site (Wnt) pathways) that are able to activate cellular and molecular processes in both tissues (Luyten & Lories, 2011). The osteochondral unit can therefore be considered a biochemically and biomechanically functional unit and processes that disrupt homeostasis in either tissue will therefore alter the properties and function of the other (Goldring, 2012; Yuan et al., 2014). This is reflected in OA pathogenesis, in which SB thickening and AC degradation are two of the most

common features, and pathological changes in the SB often parallel those seen in the overlying AC (Li et al., 2013; Findlay, David & Atkins, 2014).

Recently, several authors have suggested that that changes to the SB may even precede those in the AC in degenerative diseases such as OA (Brandt et al., 2006; Burr & Gallant, 2012; Li et al., 2013; Chubinskaya et al., 2015; Grassel & Muschter, 2020). The importance of the SB in the development and progression of OA, and the potential for interventions that address the SB, has been demonstrated in two recently published studies, in which the authors applied performed cell-based therapies directly to the SB (Hernigou et al., 2020a; Hernigou et al., 2020b). In the first of these studies, the authors compared the subchondral injection of bone marrow-derived mesenchymal stromal cell (BM-MSCs) in one knee, with total knee replacement (TKR) of the contralateral knee, in 140 adults whom were scheduled for a bilateral TKR for medial OA (Hernigou, Delambre et al., 2020). The authors reported that, after two years, the volume of bone marrow lesions (BML) had reduced, and cartilage volume increased, compared to baseline, following treatment of the SB with BM-MSCs. After 15 years, 25 (18%) of the patients had undergone TKR on the BM-MSC treated knee, with an overall incidence of 1.19% per person-year, which was equivalent to the risk of revision of the primary TKR in the contralateral knee. In a second randomised controlled trial involving 120 patients with bilateral knee OA, the authors compared the injection of BM-MSCs into the subchondral bone of the femur and tibia, with the intra-articular injection of BM-MSCs in the contralateral knee (Hernigou et al., 2020). Clinical (Knee Society knee score and Visual Analog Scale pain score) and imaging (cartilage volume and synovitis score) outcomes were better in the knee that received BM-MSCs in the SB, in which there was an increase in cartilage volume, compared to the knee that received intra-articular BM-MSCs, in which there was a decrease in cartilage volume. A subsequent follow-up, at 15 years post-

op, revealed that of the 60 knees that had been treated with SB injection of BM-MSCs, 12 (20%) underwent TKR, whereas 42 (70%) of the 60 knees treated with intra-articular BM-MSCs underwent subsequent TKR. These studies concluded that the injection of BM-MSCs into the SB may halt the progressive loss of cartilage that is commonly observed in the progression of OA, demonstrating the importance of SB health in this process.

However, little consideration is given to the health status of the SB in influencing the outcomes of cell-based strategies for AC repair. According to the currently most widely held hypothesis in this area, SB remodelling is linked to cartilage degradation through the alteration of the architecture of the osteochondral unit and through altered biochemical crosstalk (Suri & Walsh, 2012; Yuan et al., 2014; Goldring & Goldring, 2016). While some authors have recently stressed the biomechanical importance of the SB in AC repair, there is, to our knowledge, no published work investigating the influence of cellular crosstalk from the SB on the AC repair tissue (Gomoll et al., 2010; Madry et al., 2016). The goal of cell-based tissue engineering strategies is to provide the optimal cell type with the optimal environment to be able to produce cartilaginous tissue that closely resembles the structure and composition of native tissue (Medvedeva et al., 2018). As the SB is not routinely addressed in any significant way by cell therapy, other than restoration of joint mechanics, any altered biochemical signalling that existed between the cells of the SB and the degenerated AC, will likely continue to act on cells that are implanted as the cell therapy and could influence the outcome. This study aims to investigate and characterise the cellular crosstalk between the resident cells of the SB and those that are implanted as a cell-based AC repair strategy, in order to determine the influence of said crosstalk on AC repair.

The ability of cells from the subchondral bone to modulate the behaviour of chondrocytes has been demonstrated by a number of in vitro studies. Westacott and colleagues demonstrated that the indirect co-culture of cartilage explants with primary osteoblasts taken from OA patients led to a significant increase in GAG secretion into the conditioned media, compared to those cultured with osteoblasts from non-arthritic patients (Westacott et al., 1997). This represented some of the first work to demonstrate that factors secreted by cells from the subchondral bone could directly influence cartilage metabolism, but was not directly comparable to cell-based cartilage repair due to the use of explanted cartilage, rather than a tissue engineered substitute.

A similar model was used by Sanchez and colleagues, in two studies published in 2005, to show that soluble factors secreted by human osteoblasts can modulate the phenotype of human OA chondrocytes. The authors reported a differential effect on chondrocyte phenotype when they were cultured with osteoblasts isolated from normal or sclerotic regions of the subchondral bone. In those chondrocytes that are cultured with the latter, there was a downregulation of aggrecan, SRY-Box Transcription Factor 9 (Sox9) and type II collagen and an upregulation of matrix metalloproteinase (*MMP*)-3 and *MMP*-13, suggesting a shift towards a catabolic phenotype (Sanchez et al., 2005a; Sanchez et al., 2005b).

However, the chondrocytes used in these studies were isolated from OA tissue and therefore were not representative of cells that may be employed in AC repair. In addition, samples were obtained from only three patients, all of whom were men, and therefore the conclusions reached should be accepted with caution.

The focus of the above in vitro studies was the contribution of the interaction between SB and AC cells to the progression of OA in the osteochondral unit rather than its influence on

AC repair. There is a need for representative modelling of AC repair to determine the effect of crosstalk in the repair tissue. In addition, previous research in this area focused mainly on the communication between osteoblasts and chondrocytes, and the contribution of the other resident cell types of the subchondral bone has been overlooked. Previous *in vitro* research involving a co-culture of MSCs and chondrocytes has focused on the unidirectional communication between the cell types, demonstrating the ability of chondrocytes to modulate the properties of MSCs, improving their chondrogenic characteristics and potential as a cell source for AC repair (Bian et al., 2011; Cooke et al., 2011). There has been little focus on the modulation of chondrocyte behaviour by signals produced by MSCs, either in the early phase following AC damage or in cartilage repair. MSCs are known to play a key role in bone remodelling, which is likely altered following AC damage, and therefore the properties of the cells, including signalling, may also be altered depending on the status of the SB (Kennedy, 2018; Donell, 2019).

Finally, the majority of AC repair techniques are indicated for traumatic lesions, or early degenerative lesions, and although cell-based treatments have been employed to address the symptoms of OA (Cho et al., 2016) (Invossa), there are no cell-based indications for cartilage repair in severe, end-stage OA (Brittberg et al., 2016). One of the difficulties in treating cartilage degeneration in end-stage OA is determining the contribution of the other tissues of the joint to the pathogenic changes in the AC, given that end-stage OA represents an 'organ-level' failure in which all joint tissues are involved. For reasons discussed above, the SB is of particular interest, and determining the contribution of the SB in AC repair at the various stages of OA is important for the future development of cell therapies for OA.

In this chapter, an in vitro, co-culture model of the osteochondral unit was developed to investigate the effect of SB health on a cell-based cartilage repair technique, in early and late stage OA. The bone component was represented by donor-matched BM-MSCs, isolated from the SB of regions of the knee joint that demonstrated the greatest and least AC degeneration, thus representing late- and early-stage OA respectively. The cartilage component was represented by allogeneic chondrocytes, obtained from a young patient with no history of OA. In a recent review of cartilage repair in the degenerative, ageing knee, Brittberg and colleagues reported that young chondrocytes outperform old chondrocytes in terms of regenerating a repair tissue that demonstrates the same structure and organisation of native tissue, and that an allogenic source would be preferable (Brittberg et al., 2016). The AC and SB components of the model were separated using a fine mesh, thus allowing for the investigation of cellular crosstalk between compartments.

3.2 Materials and Methods

3.2.1 Sample Collection

Knee femoral condylar samples of bone and cartilage were obtained from 16 patients undergoing total knee replacement (TKR) surgery at the RJAH Orthopaedic Hospital and whom provided written, informed consent. A sample of articular cartilage from the knee of a 'healthy' individuals (a young patient without OA) was obtained through the NHS Blood and Transplant (NHSBT) service. Favourable ethical approval was given by the National Research Ethics Service (NRES) (11/NW/0875) and all experiments were performed in accordance with the relevant guidelines and regulations.

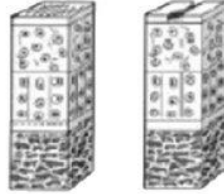
3.2.2 Macroscopic Sample Grading

Excised femoral cartilage and bone samples from patients undergoing TKR surgery were initially categorised based on the macroscopic appearance of the AC. This was carried out using the International Cartilage Repair Society (ICRS) Cartilage Lesion Classification System, a 5-grade macroscopic scoring system that was designed to be used by surgeons to assess cartilage lesions arthroscopically as part of a clinical Cartilage Injury Evaluation Package (Brittberg, Mats et al., 2000). In this system, cartilage is graded from Grade 0, 'Normal' cartilage, to Grade 4, 'Severely abnormal' cartilage. (Brittberg et al., 2000) (Figure 3-1). Two condyles, the one with the lowest grade (most normal) and highest grade (most abnormal) cartilage, were obtained for each patient.

ICRS grade 0—normal



ICRS grade 1—nearly normal
Superficial lesions. Soft indentation (A)
and/or superficial fissures and cracks (B)



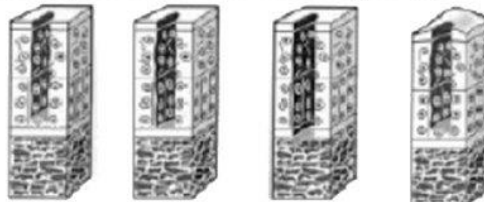
A

B

ICRS grade 2—abnormal
Lesions extending down to <50% of cartilage depth



ICRS grade 3—severely abnormal
Cartilage defects extending down >50% of cartilage depth (A) as well as
down to calcified layer (B) and down to but not through the subchondral
bone (C). Blisters are included in this grade (D)



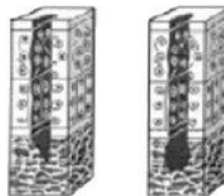
A

B

C

D

ICRS grade 4—severely abnormal



A

B

Copyright © ICRS

Figure 3-1: *The International Cartilage Repair Society (ICRS) Cartilage Lesion Classification System.*
Taken from the ICRS Cartilage Injury Evaluation Package (www.cartilage.org).

3.2.3 Histological Assessment of Samples

3.2.3.1 *Sample Processing and Sectioning*

A portion of the macroscopically-graded condyle was fixed in formalin overnight before being taken to the histopathology department at RJAH for processing and sectioning. In brief, tissue samples were dehydrated in 70% (v/v) isopropanol (IPA; Genta Medical, York, UK) in phosphate buffered saline (PBS; Gibco, Loughborough, UK), followed by two changes of 100% IPA (Genta Medical). Samples were then cleared in Xylene (Genta Medical), before being embedded in paraffin wax (Sigma-Aldrich, Dorset, UK) and sectioned at a thickness of 5µm. Cut sections were placed in a water bath, set at 45°C and collected onto poly-L-Lysine coated microscope slides (ThermoFisher Scientific, Loughborough, UK) before drying in an oven overnight at 37°C.

3.2.3.2 *Dewaxing and Rehydrating Sections*

Paraffin-wax sections were deparaffinised and rehydrated for further histological analysis as previously described (Roberts & Menage, 2004; Slaoui & Fiette, 2011). In brief, slides were warmed in an oven at 60°C for a minimum of 1 hour and subsequently dewaxed in two separate changes of xylene (Genta Medical) for 5 minutes each. Slides were then rehydrated through a series of decreasing concentrations of IPA (Genta Medical): two changes of 100% IPA followed by 90% IPA, 70% IPA and 50% IPA in distilled water, each for 5 minutes, before being washed in distilled water for 5 minutes.

3.2.3.3 *Mayer's Haematoxylin and Eosin Staining*

Haematoxylin and Eosin (H&E staining) is one of the most commonly used histological stains and can clearly demonstrate many different tissue structures (Roberts & Menage, 2004).

Haematoxylin is a basic dye that stains nuclear chromatin and other acidic cellular

components blue-black and eosin is an anionic dye that stains cell cytoplasm and connective tissue pink, red or orange (Roberts & Menage, 2004; Feldman & Wolfe, 2014). Paraffin-wax sections were dewaxed and rehydrated to distilled water (see 3.2.3.2 Dewaxing and Rehydrating Sections).

Slides were then immersed in filtered Mayer's Haemalum solution (VWR International Ltd, Poole, UK) for 1 minute before being drained and 'blued' in running tap water for 2-3 minutes. Next, slides were submerged in filtered 1% eosin yellowish solution (BDH, Dorset, UK) in distilled water for 30 seconds, followed by a quick rinse in tap water. Slides were then dehydrated through a series of increasing concentrations of IPA; 70% and 90% in distilled water for 2 minutes each and then two changes of 100% IPA for 5 minutes each before being cleared in two changes of xylene for 5 minutes each. Finally, glass coverslips (Scientific Laboratory Supplies Ltd, Nottingham, UK) were then mounted onto the tissue sections using Pertex mounting medium (Histolab Products AB, Gothenberg, Sweden), and the sections left to dry (Roberts & Menage, 2004; Schmitz et al., 2010).

3.2.3.4 *Toluidine Blue Staining*

Toluidine blue is a cationic dye that stains proteoglycans and glycosaminoglycans a deep violet colour, and other tissue elements appear in various shades of light blue. (Schmitz et al., 2010). Paraffin-wax sections were dewaxed and rehydrated to distilled water (see 3.2.3.2 Dewaxing and Rehydrating Sections). Slides were flooded with toluidine blue (1% aqueous) (VWR International Ltd, Poole, UK) for 30 seconds and then rinsed in tap water for 1 minute before being air-dried to prevent the stain from washing out in alcohol. Coverslips were then mounted onto the stained sections, using Pertex mounting medium, before being left to dry (Roberts & Menage, 2004; Schmitz et al., 2010).

3.2.3.5 *Safranin O Staining*

Safranin O is a cationic dye that stains cartilage orange-to-red. Fast green is used as a counter-stain and stains bone, connective tissue and cytoplasm green (Schmitz et al., 2010). Paraffin-wax sections were dewaxed and rehydrated to distilled water as previously described (see 3.2.3.2 Dewaxing and Rehydrating Sections). Slides were briefly dipped in Mayer's Haemalum solution (VWR International Ltd, Dorset, UK) before being washed in running tap water for 2 minutes. Slides were then quickly dipped twice in 2% acid alcohol (10ml concentrated Hydrochloric acid (HCl; VWR International Ltd, Dorset, UK) added to 490ml of 70% (v/v) IPA in distilled water) followed by a gentle rinse in running tap water for 5 minutes. Next, the slides were submerged in 0.2% (w/v) fast green solution (1g of fast green (FCF) (VWR International Ltd, Poole, UK) dissolved in 200ml of distilled water) for two minutes and then immediately rinsed with 1% (v/v) acetic acid solution (2.5ml of concentrated acetic acid (Sigma-Aldrich) added to 247.5ml of distilled water) for 30 seconds. The slides were then immersed in 0.7% (w/v) safranin O solution (3.5g of safranin (VWR International Ltd, Poole, UK) O in 500ml of distilled water) for 20 minutes. Finally, the slides were then dehydrated as previously described (see 3.2.3.1 Sample Processing and Sectioning)) and coverslips were mounted using Pertex mounting medium, and the slides left to dry.

3.2.3.6 *Microscopy*

Stained sections were viewed under a Leitz, Wetzlar light microscope (Leica Microsystems Ltd, Milton Keynes, UK) using x1.6, x6.3, x25 and x40 objective lenses. Images were captured using a DS-FiL camera (Nikon Corporation, Tokyo, Japan) and analysed using NIS-Elements BR software version 3.2 (Nikon Corporation) and Gnu Image Manipulation Programme (GIMP) version 2.10 (free software, gimp.org).

3.2.3.7 *Histological Scoring Systems*

Stained sections were imaged and scored using histological scoring systems to assess the structural quality of the cartilage and subchondral bone.

3.2.3.7.1 *The Osteoarthritis Research Society International (OARSI) Osteoarthritis Cartilage Histopathology Assessment System*

The OARSI OA Cartilage Histopathology Assessment System was developed by an OARSI working group in the year 2000 to standardise the assessment of OA cartilage pathology and is based on a series of target principles and designed for broad but defined applications (Pritzker et al., 2006). The assessment system is designed to address issues with common histopathological assessment methods, in particular poor reflection of mild or early phases of the disease, wide interobserver variation and lack of reproducibility and validity (Pritzker et al., 2006). The assessment system is based on the histological features of OA progression in the cartilage and comprises grades 0—6, with grade 0 representing normal articular cartilage, and an increasing grade indicating a more biologically aggressive disease. The key features of these grades are denoted in table 3-1, and example histological images are displayed in and figure 3-2.

3.2.3.7.2 *Subchondral Bone Histological Grading System*

The subchondral bone histological grading system is a simple system that was developed to specifically characterise histological changes occurring in the subchondral bone at the various stages of OA, which are poorly characterised in other histological scoring systems for OA (Aho et al., 2017). The grades in this scoring system were previously shown to have a significant relationship with the corresponding OARSI grades for cartilage. The scoring system comprises grades 0-3, with grade 0 representing early stage OA with no evident

subchondral bone changes and grade 3 representing subchondral bone changes that are associated with the late stages of OA (Aho et al., 2017). The key features of these grades are denoted in table 3-2 and representative histological images for each grade are shown in figure 3-3.

3.2.3.7.3 Correlation Between Histological Scoring Systems

The correlation between the two histological scoring systems was assessed using Pearson's correlation coefficient and a scatter plot was created to illustrate the data.

Table 3-1: *OARSI Osteoarthritis Cartilage Histopathology Grading System. Key features for grades 0-6 (Pritzker et al., 2006).*

Grade	Key Features
Grade 0	Normal articular cartilage. <ul style="list-style-type: none"> • Cartilage surface is smooth. • Matrix and chondrocytes organised into clear zones.
Grade 1	Surface intact. <ul style="list-style-type: none"> • There may be superficial fibrillation as well as cell death or proliferation. • The mid and deep zones are unaffected.
Grade 2	Surface discontinuity. <ul style="list-style-type: none"> • Fibrillation that extends through the superficial zone towards the superficial/mid zone boundary. • There may be cell proliferation and cell death in the mid zone.
Grade 3	Vertical fissures. <ul style="list-style-type: none"> • Matrix vertical fissures extending into the mid zone. • In latter stages, fissures may branch and extend into the deep zone. • Cell death and proliferation observed adjacent to fissures.
Grade 4	Erosion. <ul style="list-style-type: none"> • Cartilage matrix loss is observed. • In the early stages superficial zone cartilage is delaminated. • In the latter stages there is excavation and loss of matrix in fissured domains.
Grade 5	Denudation. <ul style="list-style-type: none"> • Unmineralized hyaline cartilage is completely eroded and articular surface is mineralised cartilage or bone. • Reparative fibrocartilage may result from microfracture through the bone.
Grade 6	Deformation. <ul style="list-style-type: none"> • The processes of microfracture, repair and bone remodelling reshape the contour of the articular surface. • Fibrocartilage has grown along the level of the previously eroded surface. • There may be marginal and central osteophytes.

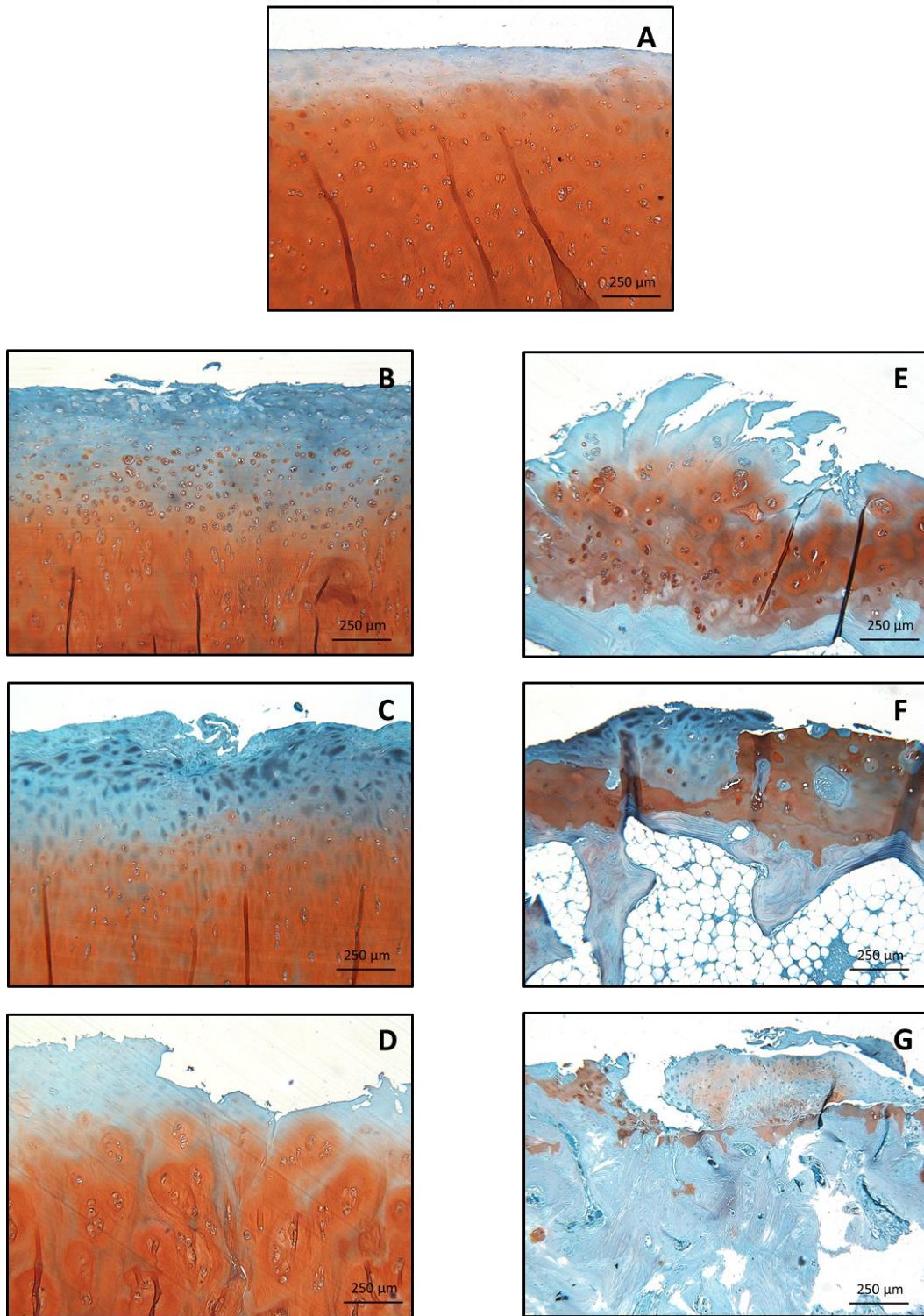


Figure 3-2: Example histological images for OARSI Osteoarthritis Cartilage Histopathology Grading System, Grades 0-6 (Pritzker et al., 2006). Sections were stained with Safranin O/Alcian blue. All images are at X6.3 magnification. The scale bar represents 250 μ m. A: Grade 0, B: Grade 1, C: Grade 2, D: Grade 3, E: Grade 4, F: Grade 5, G: Grade 6.

Table 3-2: Subchondral bone histological grading system. Key features for Grades 0-3 (Aho et al., 2017).

Grade	Key Features
Grade 0	<ul style="list-style-type: none"> • The early stages of OA. • No evident subchondral bone sclerosis with a thin subchondral bone plate and trabeculae. • Articular cartilage is directly connected to the bone marrow via open fenestrae in the subchondral bone.
Grade 1	<ul style="list-style-type: none"> • Some subchondral bone sclerosis. • Bone volume increased. • Thickened trabeculae. • Cartilage contact with bone marrow is maintained.
Grade 2	<ul style="list-style-type: none"> • Distinct increase in subchondral bone sclerosis and bone volume. • Fibrillation can be seen in the subchondral bone pate. • Cartilage is no longer in contact with bone marrow.
Grade 3	<ul style="list-style-type: none"> • Late stage disease. • Severe subchondral sclerosis and massive increase in bone volume. • Bone marrow distance from cartilage increases. • Subchondral bone plate flattens.

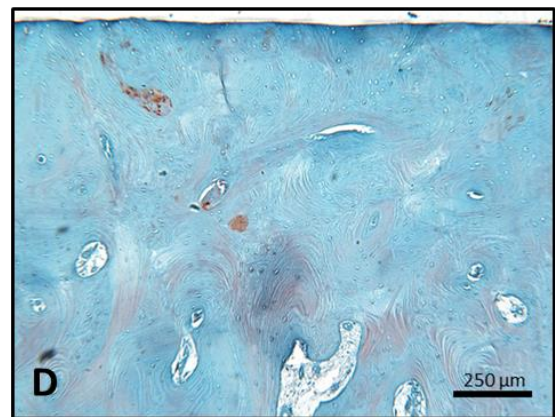
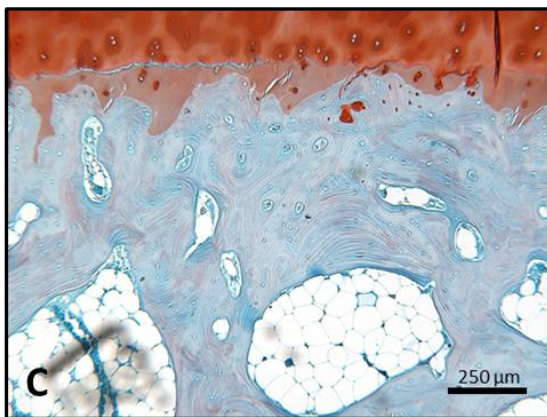
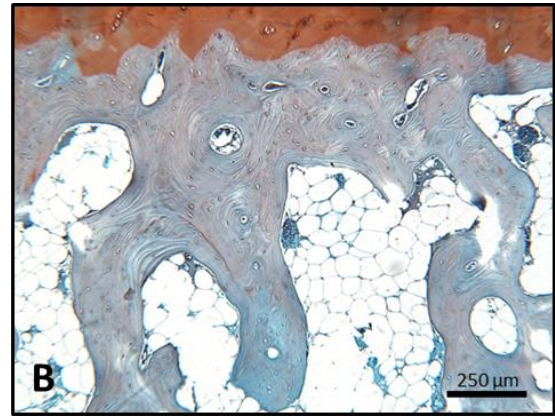
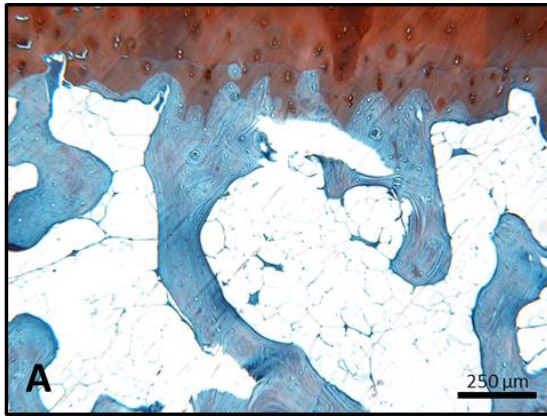


Figure 3-3: Example histological images for the subchondral bone histological grading system. Grades 0-3 (Aho et al., 2017). Sections were stained with Safranin O/Fast green. All images are at X6.3 magnification. The scale bar represents 250μm. A: Grade 0, B: Grade 1, C: Grade 2, D: Grade 3.

3.2.4 Primary Cell Isolation and Expansion

3.2.4.1 *Media Formulations*

3.2.4.1.1 Complete Culture Media

Dulbecco's modified eagle medium: nutrient mixture F-12 (DMEM/F12; 1:1) (Life Technologies, Paisley, UK) supplemented with 10% (v/v) foetal bovine serum (FBS; Life Technologies) and 1% (v/v) penicillin-streptomycin (P/S; 5,000 U/ml; Gibco).

3.2.4.1.2 Chondrocyte Culture Media

DMEM/F12 (1:1) (Life Technologies) supplemented with 10% (v/v) FBS (Life Technologies), 1% (v/v) P/S (5,000 U/ml; Gibco) and L-Ascorbic Acid-2-phosphate (Sigma-Aldrich) (final concentration: 62µg/ml).

3.2.4.1.3 Bone Marrow Mesenchymal Stromal Cell (BM-MS) Seeding Media

DMEM/F12 (1:1) (Life Technologies) supplemented with 20% (v/v) FBS (Life Technologies) and 1% (v/v) P/S (5,000 U/ml; Gibco).

3.2.4.1.4 Chondrogenic Differentiation Media

DMEM/F12 (1:1) (Life Technologies) supplemented with 2% (v/v) FBS (Life Technologies), 1% (v/v) P/S (5,000 U/ml; Gibco) and 1% (v/v) insulin-transferrin-selenium-ethanolamine (ITS-X; Gibco). Differentiation media was prepared freshly at time of use by supplementing the media with L-Ascorbic Acid-2-phosphate (1mM), dexamethasone (100nM) and sodium pyruvate (1mM) (all Sigma-Aldrich) and transforming growth factor-β1 (TGF-β1; PeproTech, London, UK) (10ng/ml) (Johnstone et al., 1998).

3.2.4.1.5 Osteogenic Differentiation Media

DMEM/F12 (1:1) (Life Technologies) supplemented with 10% (v/v) FBS (Life Technologies) and 1% (v/v) P/S (5,000 U/ml; Gibco). Differentiation media was prepared freshly at time of

use by supplementing the media with L-Ascorbic Acid-2-phosphate (50 μ M), β -glycerophosphate (10mM) and dexamethasone (100nM) (all Sigma-Aldrich) (Jaiswal et al., 1997).

3.2.4.2 *Bone Marrow Derived Mesenchymal Stromal Cell (BM-MSC) Isolation*

BM-MSCs were isolated from the subchondral bone of knee condyles obtained from 5 patients undergoing TKR surgery. Half of each condyle was left untouched to allow for histological assessment (see 3.2.3 Histological Assessment of Samples). BM-MSCs were extracted separately from the subchondral bone of knee condyles with the best and worst macroscopically graded articular cartilage (see 3.2.2 Macroscopic Sample Grading), using an adapted protocol for the extraction of MSCs from bone marrow aspirate (Mennan et al., 2013). In brief, the subchondral bone of each condyle was disrupted using scissor forceps to release bone marrow and create bone chips. The whole condyle, and any resulting bone chips, were then placed in a sterile, 60ml sample pot (Sarstedt, Leicester, UK) and 30ml of complete culture media (see 3.2.4.1 Media Formulations) was added. The pot was shaken vigorously for 5 minutes and the resulting media and bone marrow mix was then treated as one would bone marrow aspirate. The resulting aspirate from each condyle was then split between two sterile 50ml tubes (Sarstedt), carefully layered onto 10ml Lymphoprep™ (STEMCELL technologies, Cambridge, UK) and centrifuged for 20 minutes at 900 xg to isolate mononuclear cells by density gradient. The resulting buffy coat layer, containing the mononuclear cells, was aspirated using a 19 gauge needle and 5ml syringes (Becton Dickinson and Company, Wokingham, UK) and combined from the two tubes and supplemented with 10ml of BM-MSC seeding media before being centrifuged at 750 xg for 10 minutes to pellet cells. The resulting cell pellet was resuspended in BM-MSC seeding media and a viable cell count was performed by trypan blue exclusion. Cells were then

seeded at a density of 20×10^6 cells per 75cm^2 tissue culture flask (Sarstedt) in BM-MSC seeding media. After 24h, non-adherent cells were removed by PBS wash and media change and adherent cells were cultured in monolayer and maintained in a humidified atmosphere at 37°C , 5% CO_2 in complete culture media. When the cells reached 70% confluence, they were passaged by trypsinisation and a viable cell count was performed by trypan blue exclusion (see 3.2.4.4 Passaging of Cells in Monolayer Culture), before being re-seeded at a density 5×10^3 cells per cm^2 . BM-MSCs extracted from beneath the most and least macroscopically normal cartilage will henceforth be referred to as 'healthy' and 'unhealthy' BM-MSCs respectively for the purpose of simplicity.

3.2.4.3 *Chondrocyte Isolation*

Chondrocytes were isolated from a sample of cartilage taken from the knee of a 22-year old patient with no history of OA. Articular cartilage was excised from the femoral condyle of the donated knee and chondrocytes were extracted as previously described (Garcia, John et al., 2016). In brief, the cartilage was weighed and minced into small pieces (roughly 1mm^3) with a sterile scalpel and digested in type II collagenase (245 IU/ml; Worthington, New Jersey, USA) in DMEM/ F12 (1:1) (Life Technologies) containing 1% P/S (5,000 U/ml; Gibco) for 16 hours at 37°C (10ml type II collagenase mix per 200mg of cartilage). After 16 hours, the resulting suspension was filtered through $40\ \mu\text{m}$ cell strainers (ThermoFisher Scientific) and centrifuged at $350\ \text{xg}$ for 10 minutes to produce a cell pellet. The cell pellet was then resuspended in chondrocyte culture media (see 3.2.4.1.4 Chondrocyte Culture Media) and a viable cell count was performed by trypan blue exclusion (see 3.2.4.4 Passaging of Cells in Monolayer Culture), before the chondrocytes were seeded at a density of 5×10^3 cells per cm^2 .

3.2.4.4 *Passaging of Cells in Monolayer Culture*

Both cell types were routinely maintained in monolayer culture until 80% confluency, at which point, cells were passaged as previously described (ECACC & Merck, 2018). Cells were washed with Dulbecco's Phosphate Buffered Saline (PBS; Gibco) and then incubated with 0.05% (w/v) trypsin-ethylenediamine tetraacetic acid (trypsin-EDTA; Gibco) for 5 minutes at 37°C. The trypsin-EDTA activity was stopped by adding an equal volume of suitable culture media (complete culture media for BM-MSCs and chondrocyte culture media for chondrocytes). Tissue culture flasks were lightly tapped on the side of the lab bench to ensure that all cells had detached from the bottom of the flask and the resulting cell suspension was aspirated into sterile 50ml tubes and centrifuged at 179 xg for 10 minutes to pellet the cells. The resulting cell pellet was resuspended in suitable culture media and a viable cell count performed by trypan blue exclusion. Chondrocytes were not further expanded and were cryopreserved at this stage (see 3.2.4.5 Cryopreservation of Cells). BM-MSCs were seeded into fresh tissue culture flasks at a density of 5×10^3 cells per cm^2 .

Trypan blue exclusion was used to determine the estimated cell number in suspension following trypsinisation. This method is based on the principle that live cells have intact cell membranes that will exclude the Trypan blue dye, whereas dead cells do not have intact membranes and are therefore permeable to Trypan blue, will take up the dye and appear blue (Strober, 2015). In brief, 10 μ l of the cell suspension was diluted with 10 μ l of 0.4% (v/v) trypan blue (Sigma-Aldrich) in PBS (Gibco), in a 0.5ml microcentrifuge tube, and mixed thoroughly by pipetting. 10 μ l of the resulting mixture was then pipetted under a clean coverslip on a haemocytometer before live cells were counted (N) using an inverted light microscope. A minimum of 200 total cells were counted in the 16 squares in each corner of

the haemocytometer. The following calculation was used to give an estimate of the number of viable cells in the cell suspension:

$$\text{Number of cells} = N \times 2 \times 10000 \times V$$

Where N is the number of cells counted, 2 represents the dilution factor when the cell suspension was combined with trypan blue, and V represents the total volume of the cell suspension.

3.2.4.5 Cryopreservation of Cells

BM-MSCs were prepared for cryopreservation at passage 2-3 (P2-3) and chondrocytes were prepared for cryopreservation at passage 0-1 (P0-1), as previously described (ECACC & Merck, 2018). In brief, cells were harvested by trypsinisation and centrifugation (see 3.2.4.4 Passaging of Cells in Monolayer Culture) and the resulting pellet was resuspended in pre-cooled 10% (v/v) dimethyl sulphoxide (DMSO; Sigma-Aldrich) at a density of 1×10^6 cells per ml, in 1ml aliquots in 1.8ml cryovials (Sarstedt). Cryovials were then placed into a Mr Frosty™ cryofreezing container (ThermoFisher Scientific) that contains IPA and cools at a rate of $-1^\circ\text{C}/\text{minute}$, overnight at -80°C before being transferred to liquid nitrogen for long-term storage.

3.2.4.6 Recovery of Cells from Liquid Nitrogen

Cells were recovered from liquid nitrogen storage by rapidly thawing the cryovials under a running hot tap until there was only a small amount of ice left. 1ml of pre-cooled, suitable culture media was then added to the thawed cell suspension dropwise for 1 minute. Cell suspensions were then left to stand for a further minute before 20ml of the cooled media was added dropwise for 10 minutes to the cell suspension. The cells were then pelleted by centrifugation at 115 xg for 10 minutes. Cells were then resuspended in 20ml of cooled,

suitable medium and pelleted again by centrifugation before resuspension and a viable cell count was carried out. Cells were then seeded into tissue culture flasks at a density of 5×10^3 cells per cm^2 .

3.2.5 In-Vitro Co-Culture Model

A novel in-vitro model was set up, in which donor-matched healthy and unhealthy BM-MSCs were separately co-cultured with healthy, allogeneic chondrocytes to test the hypothesis that the two BM-MSC populations differ in their effect on the health and metabolic activity of the chondrocytes. Throughout the model, BM-MSC's were maintained in monolayer in 24-well plates (Sarstedt) and chondrocytes were encapsulated in agarose within transwell inserts (TC-Insert, 24-well, $0.4\mu\text{m}$ pore) (Sarsterdt) that were then placed into the BM-MSC containing wells. In this way, the two cell types were indirectly co-cultured, with no direct contact between the cells, but communication by soluble factors permitted. An overview of the co-culture model is shown in figure 3-4.

3.2.5.1 *Patients and Cell Populations*

The co-culture model was performed with donor-matched populations of healthy and unhealthy BM-MSCs from the five patients with the largest difference in subchondral bone histological grade between the two condyles (see 3.3.1 Patients and 3.3.2.1.2.2 Subchondral Bone Histological Grading System). Culture-expanded cells from the same population of chondrocytes, all isolated from the donated knee of the young, healthy donor (see 3.2.4.3 Chondrocyte Isolation) were used in the co-culture models of all five patients. Due to the complexity of the model and the labour-intensive set-up and endpoint preparation days, the patients were split into three batches that were staggered in their set-up by two weeks, with two patients in the first two batches, and the final patient in the third batch (Figure 3-

5). Each batch ran for approximately 50 days in total, dictated by the speed of proliferation of the various cell populations in culture.

3.2.5.2 *Co-Culture Model*

3.2.5.2.1 Day -28 to Day 0

3.2.5.2.1.1 BM-MSC Resurrection and Culture

Roughly 28 days before the set-up of the co-culture model (day -28), healthy and unhealthy BM-MSCs from each patient were recovered from long term storage in liquid nitrogen, resurrected and seeded in tissue culture flasks as previously described (see 3.2.4.6 Recovery of Cells from Liquid Nitrogen; figure 3-4, A). At this point all BM-MSC populations were at passage 3.

3.2.5.2.1.2 BM-MSC Experimental Seeding and Osteogenic Differentiation

Once the BM-MSCs populations reached 80% confluence (around day -21) they were trypsinised and a viable cell count was performed by trypan blue exclusion. Depending on the cell number available, a minimum of 100,000 cells were taken from each population and their immunoprofile was analysed by flow cytometry (3.2.5.2.1.3 BM-MSC Characterisation by Flow Cytometry). The remaining BM-MSCs were seeded at a density 5×10^3 cells per cm^2 in 24-well plates as required. For each patient, four experimental plates were seeded, one for each timepoint in the model, with 6 wells each of healthy and unhealthy BM-MSCs (figure 3-4 (B4 ad B6) and figure 3-6). Two further 24-well plates were also seeded to act as BM-MSC only controls, with 24 wells for each cell type (figure 3-6). Once the BM-MSC populations reached 80% confluence in the 24-well plates, osteogenic differentiation media (see 3.2.4.1.5 Osteogenic Differentiation Media) was added to the BM-MSCs and they were left to differentiate for three weeks. Media was changed three times per week.

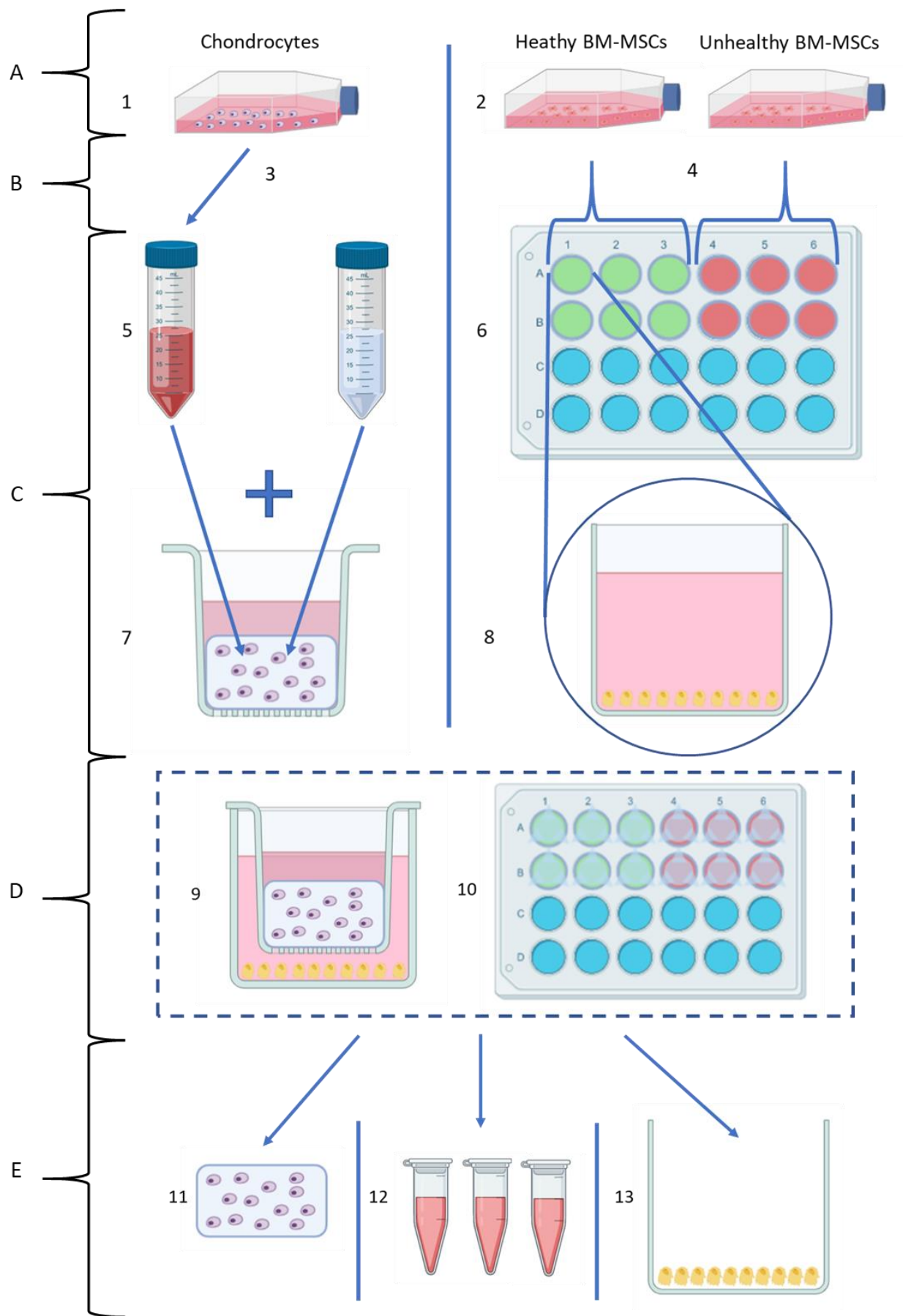


Figure 3-4: Overview of the novel in-vitro co-culture model. Created using biorender.com.

Key:

A. Recovery of cells from long-term storage:

1. Chondrocytes recovered from long-term storage. See (3.3.5.2.1.3 BM-MSC Characterisation by Flow Cytometry).
2. BM-MSCs recovered from long-term storage. See (3.3.5.2.1.1 BM-MSC Resurrection and Culture).

B. Cell characterisation:

3. Chondrocytes characterised by flow cytometry and qRT-PCR. See 3.3.5.2.2.1 Chondrocyte Characterisation.
4. BM-MSCs characterised by flow cytometry. See (3.3.5.2.1.3 BM-MSC Characterisation by Flow Cytometry).

C. Individual cell preparation for co-culture model:

5. Chondrocyte suspension combined with 4% agarose solution to form 1:1 mixture. See 3.3.5.2.2.2 Chondrocyte Encapsulation in Agarose.
6. BM-MSCs seeded in 24-well plates (top view). See (3.3.5.2.1.2 BM-MSC Experimental Seeding and Osteogenic Differentiation).
7. Agarose-chondrocyte mixture pipetted into 24-well plate transwell inserts. See 3.3.5.2.2.2 Chondrocyte Encapsulation in Agarose
8. BM-MSCs in 24-well plate (side-view) with osteogenic differentiation media added. See (3.3.5.2.1.2 BM-MSC Experimental Seeding and Osteogenic Differentiation).

D. Co-culture set-up:

9. Co-culture model (side view). See 3.3.5.2.2.3 Co-culture set-up.
10. Co-culture model (top view). See 3.3.5.2.2.3 Co-culture set-up.

E. Harvest of the co-culture model for analysis at endpoints (Day 0, Day 7, Day 14 and Day 21):

11. Chondrocyte-agarose scaffolds removed for gene expression analysis, histological analysis and biochemical analysis. See 3.3.5.2.3.1 Chondrocyte-laden Agarose Scaffolds.
12. Conditioned media removed for analysis of secreted protein abundance. See 3.3.5.2.3.1 Conditioned Media.
13. Osteogenically differentiated BM-MSCs removed for gene expression analysis and analysis of alkaline phosphatase activity. 3.3.5.2.3.1 Osteogenically Differentiated BM-MSCs.

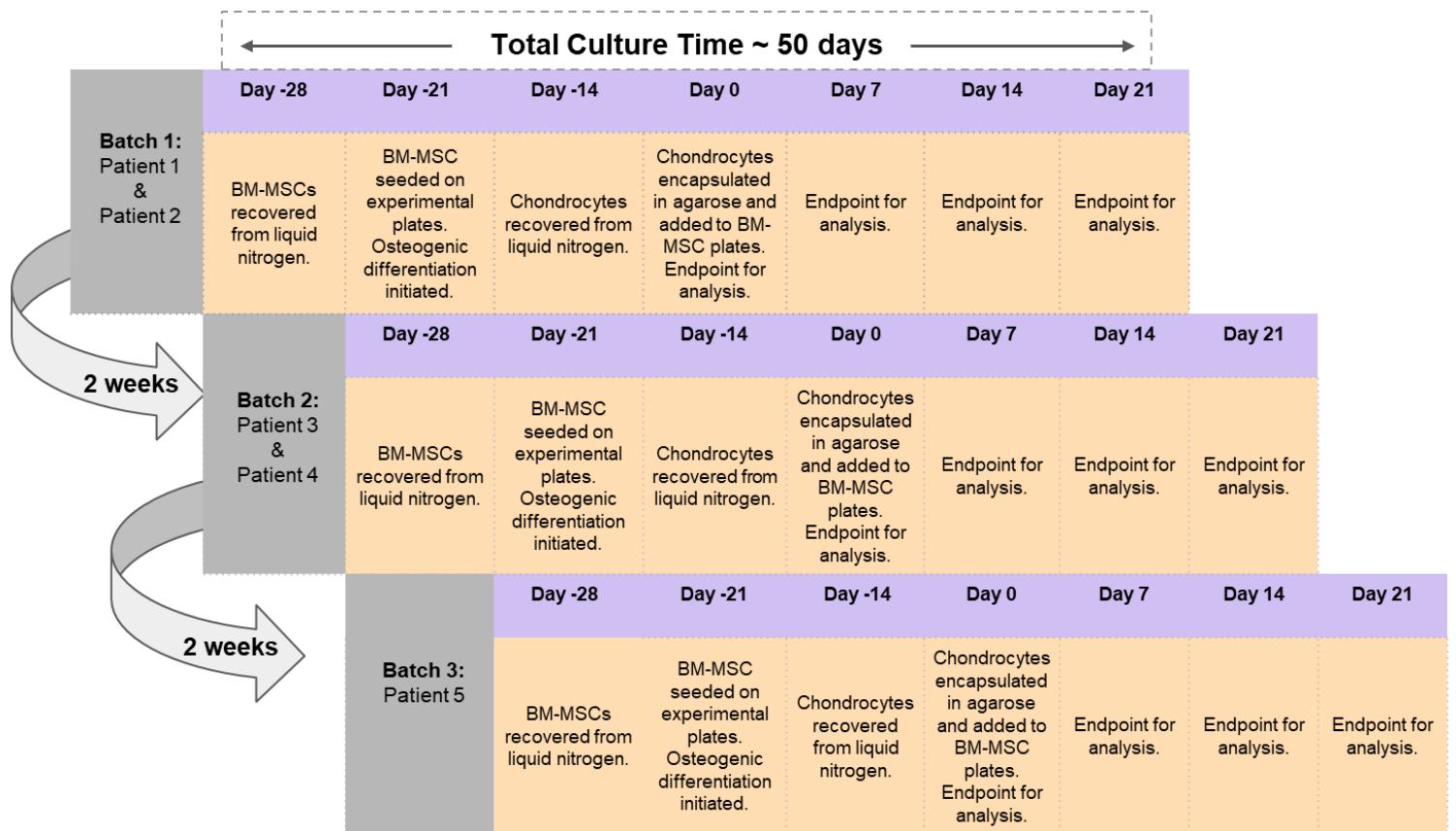


Figure 3-5: Flow chart to illustrate the timescale of the co-culture model with key events at relevant timepoints. The co-culture model was set-up in three batches; two batches with two patients and a final batch with one patient, which were each staggered in their set-up by approximately two weeks.

3.2.5.2.1.3 BM-MSC Characterisation by Flow Cytometry

Flow cytometry was carried out to assess the immunoprofile of the various BM-MSC populations. A minimum of 100,000 cells were taken from each population (healthy and unhealthy BM-MSCs) from each patient and pelleted by centrifugation at 500 xg for 5 minutes. The cell pellet was resuspended in 1ml 2% (w/v) bovine serum albumin (BSA; Sigma-Aldrich) in PBS. This was followed by a blocking step in which the cells were incubated in 10% (v/v) human IgG (Grifols, Spain) in 2% (w/v) BSA in PBS for 1 hour at 4°C, to prevent non-specific binding of the staining antibodies. The cells were then washed with 2% (w/v) BSA in PBS and centrifuged at 350 xg for 8 minutes. The resulting cell pellet was then resuspended in 500µl 2% (w/v) BSA in PBS. Cells were then stained for 30 minutes at 4°C with fluorochrome conjugated antibodies against the cell surface markers that constitute the immunoprofile indicative of MSCs, as described in the position statement by the International Society for Cellular Therapy (ISCT) (Dominici et al., 2006). Markers probed for were: CD90-phycoerythrin (PE), CD105-allophycocyanin (APC), CD73-brilliant violet 421 (BV421), CD19-BV421, CD34-APC, CD45-PE, HLA-DR (Human Leukocyte Antigen-D Related) - APC, and CD14-Peridinin-chlorophyll-protein-Cyanine5.5 (PerCP-Cy5.5) (presented as: cell surface marker-fluorochrome; BD Biosciences, Oxford, UK). Appropriate isotype-matched IgG controls were used throughout (BD Biosciences) (Table 3-3). At least 10,000 stained cells were acquired and analysed on a Fluorescence-activated cell sorting (FACS) Canto II flow cytometer (BD Biosciences). In order to match the ISCT profile, cells must express CD105, CD73 and CD90 (≥95% positivity) and lack expression of CD45, CD34, CD14, CD19 and HLA-DR (≤2% positivity) (Dominici et al., 2006).

3.2.5.2.1.3.1 *Analysis of Flow Cytometry Results*

Data was analysed using FACS Diva version 7.0 software (BD Biosciences). A scatter plot of all events was created, and cells were gated (figure 3-6, A). Doublets (two or more cells clustered together) and debris were excluded by gating around the single cells (figure 3-6, B) to exclude cell debris and doublets. A positivity gate, in which 99% of cells were negative, was established for each cell surface marker using scatterplots of the single cells stained with the corresponding isotype control (figure 3-6, C). The positivity gate was then applied to the test sample labelled with the marker of interest to determine the percentage of cells that were positive (figure 3-6, D).

Table 3-3: Panel of cell surface markers interrogated to assess the immunoprofile of BM-MSCs prior to seeding for the co-culture model.

Marker	Cell Selection	Clone	Fluorochrome	Marker Name and Reference
CD90	MSC (+ve)	5E10	PE	Thy-1 (Dominici et al., 2006).
CD105	MSC (-ve)	266	APC	Endoglin (Dominici et al., 2006).
CD73	MSC (+ve)	AD2	BV421	5'-nucleotidase (Dominici et al., 2006).
CD19	MSC (-ve)	HIB19	BV421	B-lymphocyte antigen (Dominici et al., 2006).
CD34	MSC (-ve/+ve)	581	APC	Haematopoietic progenitor cell antigen (Dominici et al., 2006; Bourin et al., 2013).
CD45	MSC (-ve)	HI30	PE	Protein tyrosine phosphatase receptor type C (Dominici et al., 2006).
CD14	MSC (-ve)	MφP9	PercP-Cy5.5	Monocyte differentiation antigen (Dominici et al., 2006).
HLA-DR	MSC (-ve)	TU36	APC/PE	Human leukocyte antigens-DR (Dominici et al., 2006)

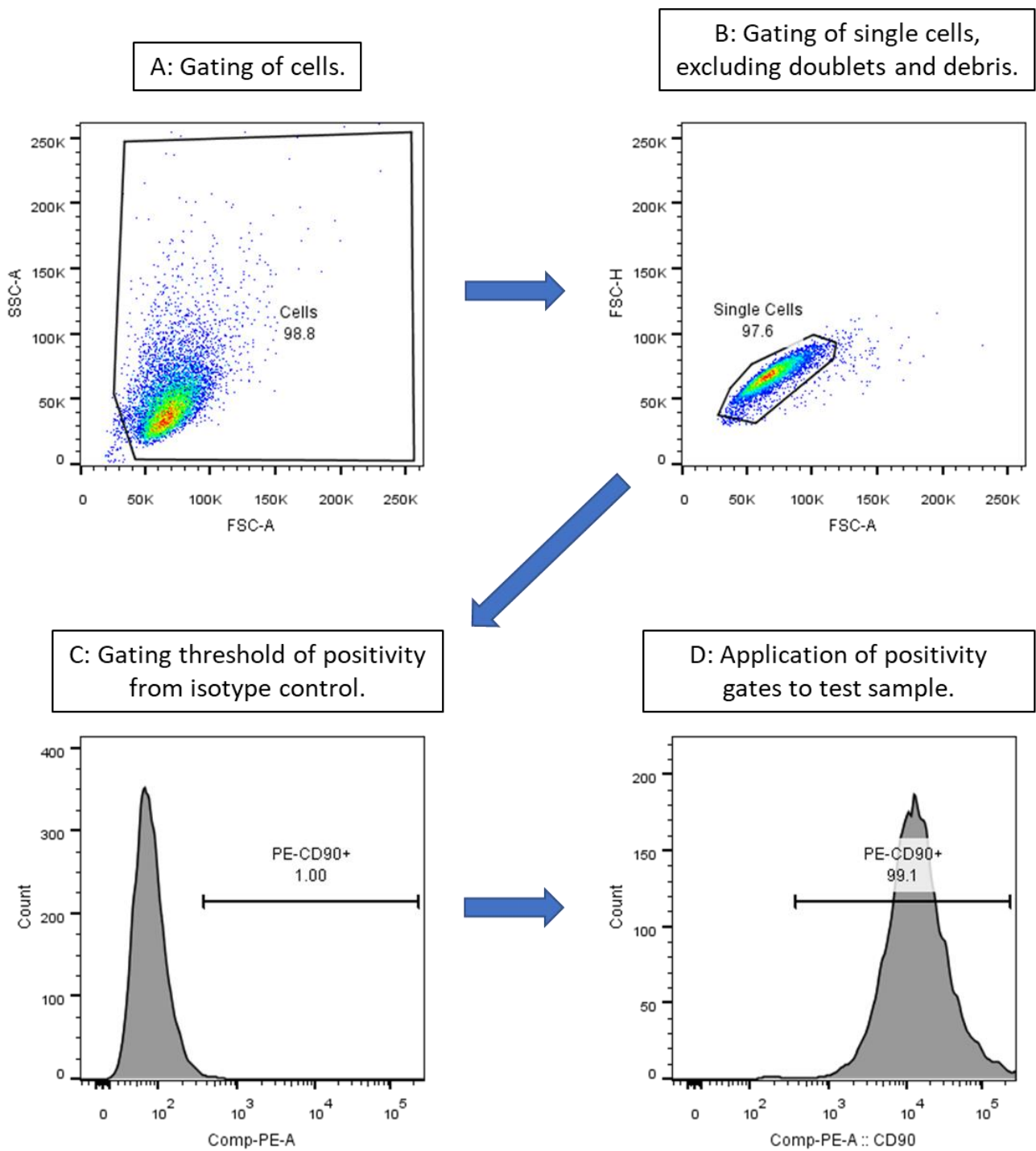


Figure 3-6: Example analysis of flow cytometry data to determine immunopositivity of a number of cell surface markers. A: Cells were gated. B: The single cells were gated to exclude doublets and debris. C: A positivity gate was established for each marker using scatterplots of the single cells stained with the corresponding isotype control D: The established positivity gate was applied to the test sample.

3.2.5.2.1.4 Chondrocyte Resurrection and Culture

Roughly 14 days before the set-up of the co-culture model (day -14) the chondrocytes were recovered from long term storage in liquid nitrogen, resurrected and seeded in tissue culture flasks as previously described (see 3.2.4.6 Recovery of Cells from Liquid Nitrogen and figure 3-4, A1). Chondrocytes were recovered separately for each batch of patients to ensure that all chondrocytes were at the same passage in the five co-culture models.

Chondrocytes were maintained in monolayer until 80% confluency and then passaged by trypsinisation as previously described (see 3.2.4.4 Passaging of Cells in Monolayer Culture).

At this point, chondrocytes were at P2.

3.2.5.2.2 Day 0: Co-Culture Model Set-up

Once the chondrocytes reached 80% confluence, they were again trypsinised and a viable cell count was performed by trypan blue exclusion.

3.2.5.2.2.1 Chondrocyte Encapsulation in Agarose

A 4% (w/v) solution of low gelling temperature (Type VII-A) agarose (Sigma-Aldrich) in PBS was prepared by adding 2g of agarose to 50ml PBS in a 100ml glass bottle containing a magnetic stirrer. The 4% agarose solution was autoclaved and then maintained at 37°C on a heat block (Stuart™ Sb162 Hotplate; Cole-Parmer™, Staffordshire, UK) with constant stirring. The number of chondrocyte-loaded agarose scaffolds required for each batch of the model was calculated, which subsequently allowed for the volume of chondrocyte suspension-agarose mixture required and therefore the cell number to be calculated, as the final cell concentration required was 1×10^6 cells per ml (Table 3-4). The corresponding volume of chondrocyte suspension following trypsinisation was aliquoted into a sterile 50ml tube and centrifuged at 179 xg for 10 minutes to pellet the chondrocytes. The required volume of cell

chondrocyte suspension was calculated, and the chondrocyte pellet was then resuspended in the corresponding volume of 2x chondrogenic differentiation media: DMEM/F12 (1:1) (Life Technologies) supplemented with 20% (v/v) FBS (Life Technologies), 2% (v/v) P/S (5,000 U/ml; Gibco) and L-Ascorbic Acid-2-phosphate (Sigma-Aldrich) (final concentration: 124 μ g/ml) Table 3-4). The cell suspension, which contained 2×10^6 chondrocytes per ml, was then quickly combined with an equal volume of the 4% (w/v) agarose in PBS to create a final mixture of 2% (w/v) agarose, which contained 1×10^6 chondrocytes per ml in 1x chondrogenic culture medium. The mixture was maintained at 37°C to prevent the agarose from setting and was stirred slowly throughout using a magnetic stirrer to prevent separation without introducing bubbles. Using a reverse pipetting technique with a 1000 μ l pipette (Sarstedt) and 1000 μ l pipette tips (Sarstedt), 200 μ l of the chondrocyte-loaded 2% agarose was carefully pipetted into 24-well plate transwell inserts (TC-Insert, 24 well, 0.4 μ m pore; Sarstedt) on sterile petri dishes (Sarstedt) (Figure 3-7, A). The agarose-containing inserts were allowed to set for 15 minutes at room temperature.

Table 3-4: Matrix used to calculate the number of chondrocytes and volumes of agarose and cell suspension required for the set up of each batch of the co-culture model.

Batch Number	Number of Patients	Experimental Scaffolds	Chondrocyte only control scaffolds	Total chondrocyte loaded scaffolds	Volume of 2% agarose-chondrocyte mixture	Number of Chondrocytes	Volume of 4% Agarose	Volume of cell suspension
1	2	96	24	120	24ml	24 million	12ml	12ml
2	2	96	24	120	24ml	24 million	12ml	12ml
3	1	48	24	72	14.4ml	14.4 million	7.2ml	7.2ml
Totals	5			312		62.4 million		

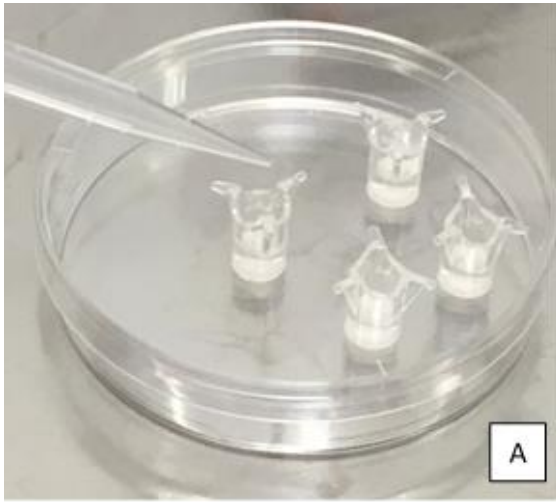


Figure 3-7: Photographs illustrating the set-up and harvest of the chondrocyte-loaded agarose scaffolds. A: Photograph demonstrating the pipetting of 200 μ l of the agarose-chondrocyte mixture into the transwell inserts. B: Photograph showing side view of transwell inserts containing 200 μ l of agarose-chondrocyte mixture. C: Photograph demonstrating how agarose-chondrocyte scaffolds were removed from the transwell inserts using 6mm biopsy punches.

3.2.5.2.2.2 Co-culture set-up

Once the agarose was set, inserts were randomly assigned, with 12 inserts added to each of the BM-MSC seeded experimental plates and 24 inserts to an empty 24-well plate to act as a chondrocyte only control plate (figure 3-8). 250µl of chondrogenic differentiation media was added on top of the agarose in the insert, and 1.5ml of osteogenic media was carefully added to the bottom of the well, avoiding mixing between the two media types. The resulting co-culture system, with osteogenically differentiated BM-MSCs in monolayer, and chondrocytes encapsulated in agarose within a transwell insert suspended above the differentiated BM-MSCs is shown in (figure 3-9). Both media types were changed every 2-3 days in all experimental and control plates.

3.2.5.2.2.3 Controls

Control plates were set up such that all four timepoints were contained on one plate (figure 3-8).

3.2.5.2.2.3.1 *BM-MSCs Only Control*

Patient-specific control plates were set-up for each of the two BM-MSC populations, healthy and unhealthy. Therefore each patient had a healthy BM-MSC only plate and an unhealthy BM-MSC only plate, which were both seeded at the same time as the experimental plates (see 3.2.5.2.1.2 BM-MSC Experimental Seeding and Osteogenic Differentiation) and were treated in exactly the same way in the set-up, other than that no transwell inserts were added to these plates. For each patient there were 6 BM-MSC only control wells per timepoint, per condition. Media was changed every 2-3 days. Three of the wells received 1.5ml of osteogenic media only, while the other three wells received 1.5ml of osteogenic media, with 250µl of chondrogenic media added to simulate the conditions in the

experimental plates and investigate the effect of the mixed media on the differentiated BM-MSCs.

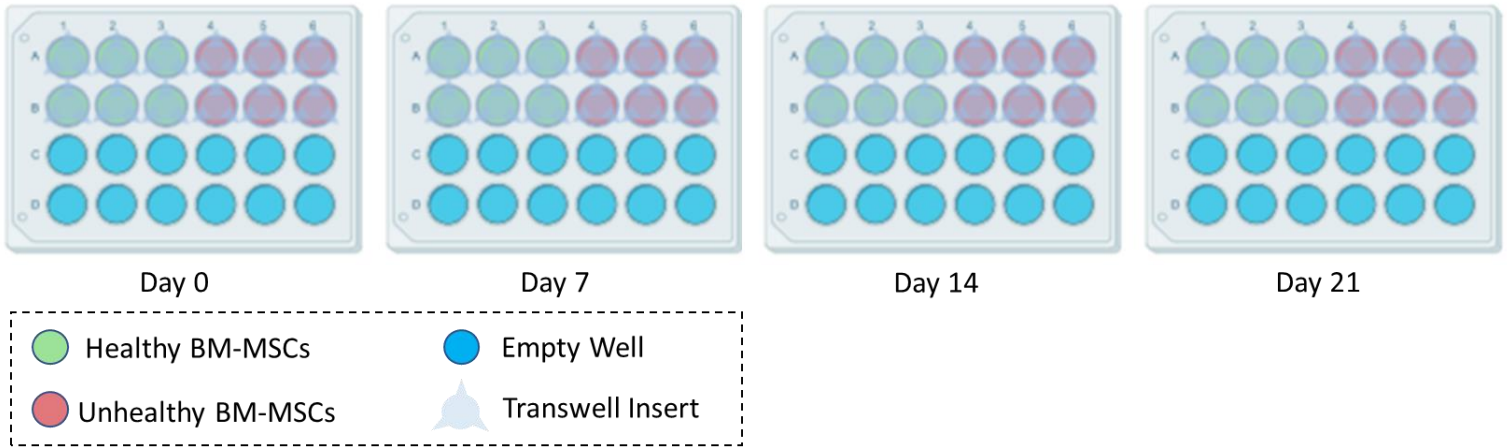
3.2.5.2.2.3.2 Chondrocyte Only Control

A chondrocyte only control plate was set up per batch, rather than per patient because the same chondrocytes were used throughout (figure 3-8). The chondrocyte-loaded scaffolds in the control plate were set up and treated in the same way as those in the experimental plates, other than the fact that they were placed into empty 24-well plates instead of those seeded with BM-MSCs. The purpose of the chondrocyte only control was to assess the effect of agarose encapsulation and culture on the behaviour of the chondrocytes.

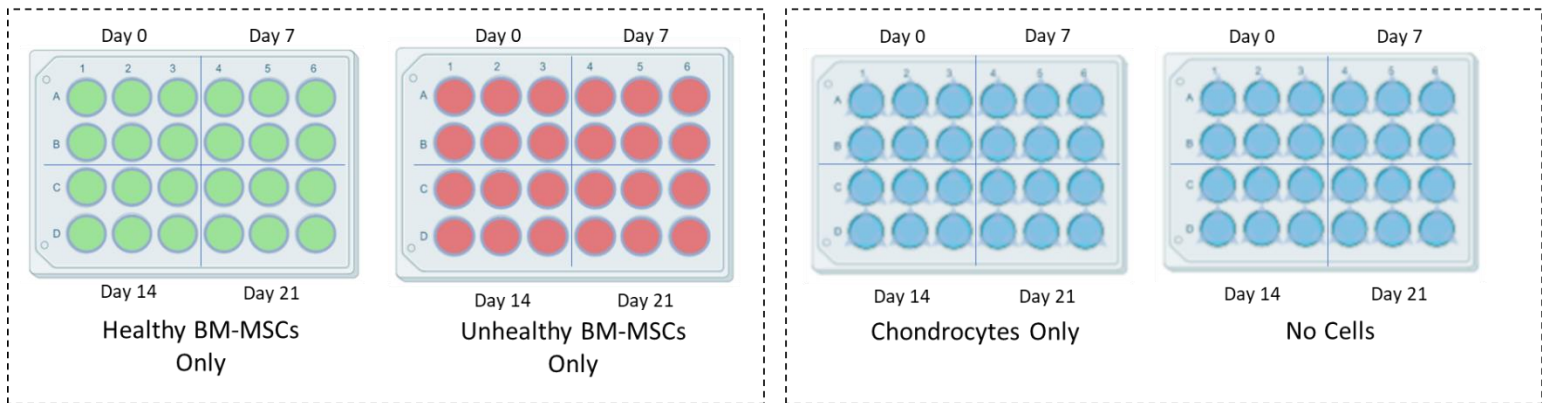
3.2.5.2.2.3.3 No Cell Control

A no cell control plate was set up per batch, rather than per patient because the same agarose was used throughout (figure 3-8). The no cell control consisted of transwell inserts containing 200µl of 2% (w/v) low gelling temperature (Type VII-A) agarose (4% (w/v) agarose in PBS mixed 1:1 with chondrogenic media), placed into empty 24-well plates. The no cell controls received the same media types and volumes as the experimental plates, which was exchanged every 2-3 days. The no cell control was established to act as an assay blank for each timepoint that had been treated in exactly the same way as the experimental samples throughout the culture period.

Experimental Plates



Control Plates



Per Patient

Per Batch

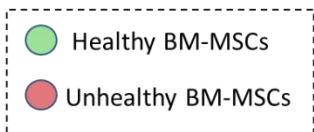


Figure 3-8: Plate layout for the set up of the co-culture model. For each patient, four experimental plates (day 0, day 7, day 14 and day 21) were seeded with both healthy and unhealthy BM-MSCs (6 wells each), as well as control plates for healthy and unhealthy BM-MSCs only. BM-MSCs were osteogenically differentiated and then chondrocyte-seeded agarose scaffolds in transwell inserts were added to the experimental plates and to the chondrocyte only control plate. Inserts containing agarose alone, with no chondrocytes, were added to the no cells control plate. Experimental plates and BM-MSC only control plates were set-up per patient, whereas the chondrocyte only and no cell control plates were set up per batch.

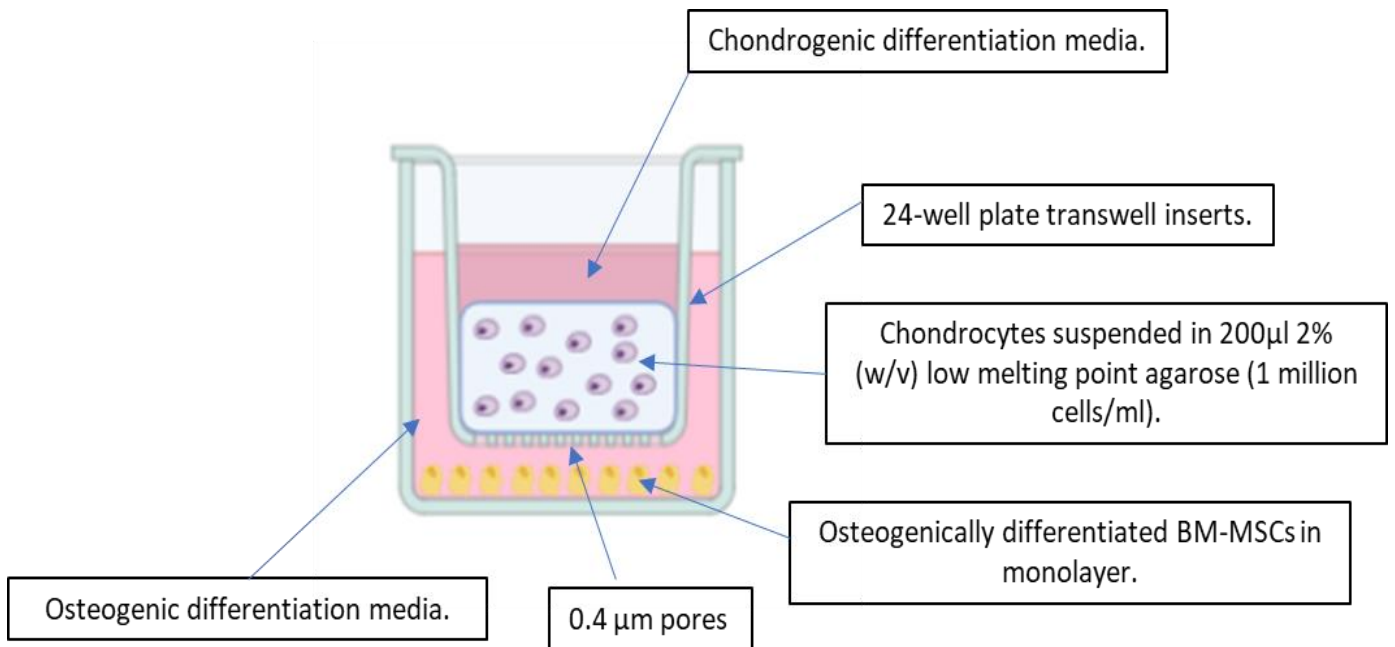


Figure 3-9: *Schematic of the indirect co-culture model. Side view of a well of an experimental plate.*

3.2.5.2.3 Experimental Endpoints: Day 0, Day 7, Day 14 and Day 21

At day 0 (immediately after set-up) and then 7, 14 and 21 days later, the co-culture model was stopped, and samples were prepared for various analyses.

3.2.5.2.3.1 Chondrocyte-laden Agarose Scaffolds

At each endpoint, the transwell inserts containing the agarose scaffolds were carefully removed from the 24-well plates using sterile forceps and transferred into sterile petri dishes. The agarose scaffolds were removed from the transwell inserts by gripping the insert with sterile forceps and pushing carefully through the bottom membrane of the insert using a 60mm Integra™ Miltex™ Biopsy Punches (ThermoFisher Scientific) to push the scaffold out of the top of the insert and into a sterile petri dish (Figure 3-7, B & C). For each condition, at each timepoint, scaffolds were collected into labelled, sterile petri dishes (Sarstedt). The scaffolds were washed three times with sterile PBS and any remaining membrane from the transwell insert was carefully removed from the scaffolds using sterile forceps. The scaffolds were carefully blotted dry using paper towels and then weighed. For each of the conditions described above, 4 of the 6 scaffolds were halved by weight and one half of each of the 4 scaffolds was processed for biochemical analyses, while the other half was processed for gene expression analysis. The remaining two whole scaffolds from each condition were processed for histological analysis.

3.2.5.2.3.1.1 Biochemical Analyses

For biochemical analyses, each agarose scaffold half (n=4) was digested in papain to release glycosaminoglycans and DNA. A digestion buffer that consisted of 0.01M cysteine hydrochloride (BDH), 0.05M ethylenediaminetetraacetic acid (EDTA; Sigma-Aldrich) and 0.2M sodium acetate (BDH) was prepared in distilled water and adjusted to pH6 using 1M

sodium hydroxide in distilled water (Sigma-Aldrich). Papain (Sigma-Aldrich) was then added to the digestion buffer to reach a final concentration of 125µg/ml. Each half scaffold was digested in 1ml of papain in a labelled 1.5ml Eppendorf tube, for 16 hours at 65°C, with regular vortexing, followed by 70°C for 10 minutes to melt the remainder of the agarose (Buschmann et al., 1992; Buschmann et al., 1995; Mauck et al., 2006; Estes & Guilak, 2011). The digested pellets were then immediately centrifuged at 10,000 rpm for 5 minutes to pellet any remaining fragments of agarose and other impurities, before being stored at -20°C for future use (DeKosky et al., 2010).

3.2.5.2.3.1.1.1 Scaffold DNA Quantification

DNA was quantified in the digested agarose scaffolds (n=4) using the PicoGreen® fluorescence assay (Invitrogen, Loughborough, UK) as per the manufacturer's instructions. In brief, DNA standards were prepared using a Lambda DNA stock solution (provided) which was diluted using Tris-EDTA (TE) buffer (10mM Tris-HCL, 1mM EDTA, pH7.5) (Table 3-5). 25µl of papain-digested agarose scaffold was diluted with 200µl of TE buffer and then mixed with 225µl of PicoGreen® dye (prepared from a stock solution in the kit). All standards and samples were plated in duplicate in a 96-well plate (Sarstedt) before the plate was covered in foil and incubate at room temperature for 4 minutes. Fluorescence was read on a FLUOstar Omega microplate reader (BMG LABTECH, Buckinghamshire, UK), configured to an excitation wavelength of 480nm and an emission wavelength of 520 nm. The mean fluorescence for the duplicate values was calculated and corrected for the average of the blank values. Unknown concentrations were interpolated from the standard curve, multiplied by the dilution factor (9), and by two to account for the whole scaffold to give a final value of the total DNA content in the whole scaffold in ng. Cell number was calculated

using the widely accepted value of 7.7pg of DNA per chondrocyte (Kim et al., 1988) and then an average cell number for each condition at each timepoint was calculated.

3.2.5.2.3.1.1.2 Glycosaminoglycan (GAG) Quantification

The dimethylmethylen blue (DMMB) assay was used to quantify GAG content in the papain-digested agarose scaffolds (n=4) (Farndale et al., 1982; Farndale et al., 1986). In brief, standards were prepared from a 1mg/ml stock solution of chondroitin sulphate (Sigma-Aldrich) from bovine trachea in distilled water (Table 3-6). DMMB staining solution was prepared by dissolving 4mg DMMB, 0.76g glycine and 0.595g sodium chloride (all Sigma-Aldrich) in 250ml distilled water and adjusting the pH to 3.0 with 10M HCl (BDH). The resulting solution was stored in a foil covered bottle at room temperature and filtered before use. To run the assay, 50µl of each standard and sample was added to a 96-well plate (Sarstedt) in duplicate. 200µl of DMMB staining solution was quickly added to each well and the absorbance was immediately read at 530nm and at 590nm on a FLUOstar Omega microplate reader (BMG, UK). Absorbance values for the standards were calculated $((A_{530nm}/A_{590nm})-(A_{530nmBlank}/A_{590nmBlank}))$ and total GAG values for samples were calculated using the equation of the resulting standard curve. The resulting values were multiplied by two, to account for the whole scaffold, to give a final value of the total GAG in the scaffold in µg. A mean total GAG value for each condition at each timepoint was calculated. Mean total GAG values and cell numbers were used to calculate a mean GAG/cell value for each condition at each timepoint.

Table 3-5: *Lambda DNA standards used in DNA quantification. A standard curve was plotted using the known concentration values and used to interpolate unknown concentrations in the samples.*

DNA Concentration (ng/ml)	Volume of Stock DNA (μ l)	Volume of TE Buffer (μ l)	Total Volume (μ l)
0	0	500	500
50	25	475	500
100	50	450	500
150	75	425	500
200	100	400	500
250	125	375	500

Table 3-6: *Chondroitin sulphate standards used in glycosaminoglycan quantification. A standard curve was plotted using the known concentration values and used to interpolate unknown concentrations in the samples.*

Glycosaminoglycan Concentration (μ g/ml)	Volume of Stock Chondroitin Sulphate (μ l)	Volume of Distilled Water (μ l)	Total Volume (μ l)
0	0	1000	1000
2	2	998	1000
10	10	990	1000
50	50	950	1000
100	100	900	1000
200	200	800	1000

3.2.5.2.3.1.2 *Gene Expression Analysis.*

For gene expression analysis, each scaffold half (n=4) was first dissolved in 1ml of dissolution buffer from a stock solution made up with 20ml Buffer RLT (Qiagen), 15ml Buffer QG (Qiagen) and 1% (v/v) β -mercaptoethanol in 1.5ml Eppendorf tubes (Bougault et al., 2008). The addition of the QG buffer, a solubilisation buffer, ensures complete dissolution of the agarose (Bougault et al., 2008). Upon the addition of the buffer mix, the samples were left at room temperature until complete dissolution and then stored at -20°C until ready to use.

3.2.5.2.3.1.2.1 Ribonucleic Acid (RNA) Isolation

In order to keep costs and time down, RNA was only extracted from day 0 and day 21 agarose scaffolds. After defrosting, the samples were homogenised by vortexing and 1ml of 70% ethanol (molecular biology grade; Sigma-Aldrich) in RNase free water was added. RNA was extracted using the RNeasy® Mini Kit (Qiagen) and by following the manufacturer's instructions. In brief, 700 μ l of the cell lysate-ethanol mixture was loaded into the RNeasy Mini spin column before a number of wash steps were performed to remove contaminants. Given the large volume of sample (2ml after the addition of 70% ethanol), it was necessary to repeat the first step of the manufacturer's protocol in which the sample is loaded into the spin column, which has a maximum volume of 700 μ l, to ensure extraction of RNA from the whole sample. The RNeasy® kit consists of a specialised spin column, that contains a silica membrane, and several proprietary buffers which were used to extract RNA using a number of centrifugation steps. In the final step, RNA was eluted from the spin column with RNase-free water (Qiagen) and stored at -80°C until required.

3.2.5.2.3.1.2.2 Reverse Transcription

Complementary DNA (cDNA) was generated from the extracted RNA by reverse transcription, using the High-Capacity cDNA Reverse Transcription Kit (Applied Biosystems,

Loughborough, UK) according to the manufacturer's instructions. In brief, the kit components (10X RT Buffer, 10X RT Random Primers, 25X dNTP Mix (100mM) and Multiscribe Reverse Transcriptase (50U/μl) were mixed to create a 2X reverse transcription master mix, which was kept on ice (Table 3-7). 25μl of the master mix was added to 25μl of RNA in a 0.2ml Eppendorf tube (Sarstedt) and mixed by pipetting to create a 50μl reaction. The Eppendorf tubes were then loaded into a Progene thermal cycler (Techne, Staffordshire, UK) which was set to run the following cycle: 25°C for 10 minutes, 37°C for 120 minutes, 85°C for 5 minutes and then a hold step at 4°C until tubes were removed. cDNA was stored at -20°C until required.

3.2.5.2.3.1.2.3 Quantitative Real-time Polymerase Chain Reaction (qRT-PCR)

Quantitative Real-time Polymerase Chain Reaction (qRT-PCR) was performed on the Quant Studio 3 Real-Time Quantitative PCR System (Applied Biosystems) using SYBR™ green QuantiTect primer assays (Qiagen) to assess a number of genes associated with chondrocyte health and extracellular matrix production: SRY-Box Transcription Factor 9 (Sox9), Collagen type 2 alpha 1 (*COL2A1*), aggrecan (*ACAN*), collagen type X (*COL10A1*) and activin receptor-like kinase 1 (*ALK1*), as well as genes associated with extracellular matrix breakdown; matrix metalloproteinase (*MMP*) -3 and -13 and A disintegrin and metalloproteinase with thrombospondin motifs (*ADAMTS*) -4 and -5 (Table 3-8). Glyceraldehyde-3-phosphate dehydrogenase (*GAPDH*) and hypoxanthine phosphoribosyltransferase 1 (*HPRT1*) were employed as housekeeping genes. qRT-PCR was carried out according to the manufacturer's instructions. In brief, a master mix was created for each gene of interest by mixing SYBR™ Green PCR Master Mix (Applied Biosystems™), with each QuantiTect Primer Assay and RNase free water (Qiagen) (Table 3-9). 18.4μl of the resulting mixture was then pipetted into wells of a MicroAmp™ Optical 96-well Reaction Plate (Applied Biosystems™). Each gene

of interest was plated on a new row of the plate (maximum 8 genes assessed per plate). 1.6µl of cDNA was then added to each well of the 96-well optical plate as required, with each new sample pipetted into a new column of the plate (maximum 12 samples assessed per plate) and mixed by pipetting to result in a 20µl reaction in each well of the plate. A MicroAmp™ Optical Adhesive Film (Applied Biosystems™) was then added to the plate and carefully sealed before the plate was loaded into the Quant Studio 3 Real-Time Quantitative PCR System (Applied Biosystems™) using the cycle detailed in table 3-10. Cycle threshold (Ct) values were collected at the end of the extension stage of each cycle. Sample gene expression levels were normalised to the geometric mean of their corresponding housekeeping genes (Vandesompele et al., 2002). Following normalisation to the reference genes, the relative expression of each gene at day 21 compared to day 0 was determined using the $\Delta\Delta C_t$ method and this was compared between healthy and unhealthy conditions (Schmittgen & Livak, 2008). A twofold change (up- or down- regulated) was deemed biologically significant.

Table 3-7: Volume of cDNA reverse transcription kit components and RNA required, per reaction, for the reverse transcription of RNA to cDNA.

Component	Volume per reaction (μl)
10X RT Buffer	5.0
25X dNTP Mix (100mM)	2.0
10X RT Random Primers	5.0
Multiscribe™ Reverse Transcriptase	2.5
RNase Free Water	10.5
RNA	25
Total per reaction	50

Table 3-8: Genes assessed by qRT-PCR in chondrocyte-agarose scaffolds from the co-culture model at day 0 and day 21.

Gene [Species]	Official Name	Amplicon Length	Entrez Gene ID
Housekeeping Genes			
<i>GAPDH</i> [Human]	Glyceraldehyde-3-phosphate dehydrogenase	95 (NM_001256799) 95 (NM_002046) 95 (NM_001289745) 95 (NM_001289746)	2597
<i>HPRT1</i> [Human]	Hypoxanthine phosphoribosyltransferase 1	130 (NM_000194)	3251
Genes of Interest			
<i>SOX9</i> [Human]	SRY (sex determining region Y)-box 9	111 (NM_000346)	6662
<i>COL2A1</i> [Human]	Collagen, type II, alpha 1	94 (NM_001844) 94 (NM_033150) 94 (XM_006719242)	1280
<i>ACAN</i> [Human]	Aggrecan	62 (NM_001135) 62 (NM_013227) 62 (XM_001131727) 62 (XM_001131734) 62 (XM_006720419)	176
<i>COL10A1</i> [Human]	Collagen, type X, alpha 1	91 (NM_000493)	1300
<i>ALK1</i> [Human]	Activin receptor-like kinase 1	102 (NM_000020) 102 (NM_001077401) 102 (XM_005269235)	94
<i>MMP3</i> [Human]	Matrix metalloproteinase 3 (stromelysin 1, progelatinase)	84 (NM_002422)	4314
<i>MMP13</i> [Human]	Matrix metalloproteinase 13 (collagenase 3)	97 (NM_002427)	4322
<i>ADAMTS4</i> [Human]	A disintegrin and metalloproteinase with thrombospondin type 1 motif, 4	100 (NM_005099) 100 (XM_006711635)	9507
<i>ADAMTS5</i> [Human]	A disintegrin and metalloproteinase with thrombospondin type 1 motif, 5	92 (NM_007038)	11096

Table 3-9: Volume of SYBR green, primer and cDNA required per reaction for qRT-PCR.

Component	Volume per reaction (μl)
SYBR™ Green PCR Master Mix	10
QuantiTect Primer Assay	1
RNase Free Water	7.4
cDNA	1.6
Total per reaction	20

Table 3-10: Thermal cycle used for qRT-PCR reaction.

Stage	Temperature (°C)	Time (minutes)	No. of Cycles
Activation	95	10:00	1
Denaturation	94	00:10	40
Annealing	55	00:30	
Extension	72	00:34	
Dissociation	94	00:15	1
	55	01:00	
	94	00:15	

3.2.5.2.3.1.3 *Histological Analyses*

The remaining 2 agarose scaffolds from each of the conditions, at each timepoint (2x healthy, 2x unhealthy, 2x chondrocyte only control and 2x no cell control) were processed for histological analysis using an adapted protocol for the preparation of various three-dimensional culture systems for histology (Estes & Guilak, 2011). Firstly, a 4% (w/v) paraformaldehyde solution was prepared. In brief, 40g paraformaldehyde powder was added to 800ml PBS on a heated magnetic stirrer in a fume cabinet. The solution was heated to 60°C and then 2N sodium hydroxide (Sigma-Aldrich) was added dropwise until the solution cleared. The solution was then topped up to 1L with PBS and pH was adjusted to 7.2 using HCl (BDH). The scaffolds were individually fixed overnight at 4°C in 10ml of 4% paraformaldehyde solution. The scaffolds were then slowly dehydrated through a series of increasing concentrations of IPA in PBS:

1. 30% IPA for 30 minutes.
2. 50% IPA for 30 minutes.
3. 70% IPA for 30 minutes (could be stored long-term at this step if required).
4. 80% IPA for 30 minutes.
5. 100% IPA for 30 minutes.
6. Replace 100% IPA for 30 minutes (could be stored overnight at this step if required).

This was followed by clearance of the scaffolds with xylene (Genta Medical):

1. Half of the 100% IPA was replaced with xylene for 15 minutes.
2. 100% xylene for 15 minutes.
3. Replace xylene for 15 minutes.

The scaffolds were then slowly permeated with paraffin wax (Sigma-Aldrich)

1. Half of the xylene was replaced with molten paraffin wax (maintained at 60°C) for 1 hour.
2. 100% paraffin wax for 1 hour.
3. Replace 100% paraffin wax for 1 hour.

The scaffolds were then transferred into individual metal moulds and paraffin wax was added, ensuring complete coverage of the scaffold. A pre-labelled, plastic cassette top was added to the top of the mould, additional paraffin wax was added, and the block was left to cool on a cold plate set at 4°C. Once cool, the metal mould was removed, and the block was trimmed of excess wax. Sections were then cut at a thickness of 8µm. Cut sections were placed in a water bath, set at 45°C and collected onto poly-L-Lysine coated microscope slides (ThermoFisher Scientific) before drying in an oven overnight at 37°C.

3.2.5.2.3.1.3.1 Mayer's Haematoxylin and Eosin Staining

Sections were dewaxed and rehydrated to distilled water and then stained with Mayer's Haematoxylin and Eosin as previously described (see 3.2.3.2 Dewaxing and Rehydrating Sections and 3.2.3.3 Mayer's Haematoxylin and Eosin Staining).

3.2.5.2.3.1.3.2 Alcian Blue Staining (pH1.0)

Alcian blue is a cationic dye that stains acid PGs by linking with sulphate and carboxyl groups of GAGs (Roberts & Menage, 2004). The stain was used at pH1.0 to ensure that both weakly and strongly sulphated GAGs were stained blue (Bancroft et al., 2018). Sections were dewaxed and rehydrated to distilled water (see 3.2.3.2 Dewaxing and Rehydrating Sections). The pH1.0 alcian blue stain was prepared by dissolving 1g of alcian blue 8GX (Sigma-Aldrich) in 100ml of 10% sulphuric acid (10ml concentrated sulphuric acid (Sigma-Aldrich) in 90ml distilled water). Slides were flooded with the alcian blue stain for 15 minutes before being

drained and blotted dry. Sections were then counterstained with neutral red (BDH) for 1 minute before being rapidly dehydrated in 100% IPA and cleared in xylene (Genta Medical) before coverslips were mounted using Pertex (Histolab Products AB). A section of articular cartilage, taken from a macroscopically normal area of a knee donated by a 53-year-old male following TKR surgery, was used as a positive control.

3.2.5.2.3.2 Conditioned Media

For each patient, at each endpoint, conditioned media was pooled for experimental repeat wells and collected in labelled, 1ml aliquots in sterile 1.5ml Eppendorf tubes (Sarstedt) before being stored at -20°C.

3.2.5.2.3.2.1 Enzyme-linked Immunosorbent Assays (ELISAs)

ELISAs were used to assess the abundance of several proteins of interest in the conditioned media, collected from the two co-culture conditions (healthy BM-MSCs and unhealthy BM-MSCs) and chondrocyte only controls at day 0, day 7 and day 21. Matrix metalloproteinase-13 (MMP-13) was assessed using a human Quantikine® ELISA kit (R&D Systems). Matrix metalloproteinase-1 (MMP-1), transforming growth factor-β1 (TGF-β1), interleukin-10 (IL-10) and vascular endothelial growth factor (VEGF) were assessed using duo-set ELISAs (R&D Systems). All ELISA's were carried out using neat conditioned media samples and in accordance with the manufacturer's instructions. In all cases, samples were assessed in duplicate and the mean optical density values were calculated, corrected for background interference and the average zero standard optical density. Graphpad Prism software, version 6.0 (GraphPad Software, USA) was used to plot dose-response standard curves of the log of the known concentration values against the optical density, which was then used to interpolate unknown values. For all analytes, the detection limit (DL), the lowest amount of analyte in a sample which can be detected, but not necessarily quantified as an exact value, was determined (ICH Expert Working group, 2006). The DL was based on the standard deviation of the response and the slope and can be expressed as:

$$DL = \frac{3.3\sigma}{S}$$

where σ = the standard deviation of the response, estimated as the residual standard deviation of the of the regression line between the analyte concentration and the optical density measurement (ICH Expert Working group, 2006).

S = the slope of the calibration curve, estimated from the curve of each analyte.

For all analyses presented, values below the DL were replaced with the detection limit value.

3.2.5.2.3.3 Osteogenically Differentiated BM-MSCs

At each experimental endpoint, for each patient, the differentiated BM-MSCs that were maintained in monolayer throughout the co-culture were assessed.

3.2.5.2.3.3.1 *BM-MSC DNA Quantification*

The DNA content of the differentiated BM-MSC populations in the co-culture was quantified at each of the four timepoints using the PicoGreen® fluorescence assay (Invitrogen, Loughborough, UK), as per the manufacturer's instructions. In brief, culture medium was removed from the differentiated BM-MSCs and stored in labelled aliquots (3.2.5.2.3.2 Conditioned Media). Cells in the 24-well plates were then carefully washed with chilled PBS. 350µl of buffer RLT (Qiagen), supplemented with 1% (v/v) β-mercaptoethanol (Sigma-Aldrich), was added to each well and incubated for 2 minutes at room temperature before being mixed thoroughly with a pipette and transferred into labelled, sterile 1.5ml Eppendorf tubes (Sarstedt). 25µl of each cell lysate was then used in the PicoGreen® assay and DNA was quantified as described in 3.2.5.2.3.1.1.1 Scaffold DNA Quantification.

3.2.5.2.3.3.2 RNA extraction and Gene Expression Analysis

RNA was extracted from four of the six experimental wells (n=4) and all 12 of the control wells. Culture medium was removed from the differentiated BM-MSCs and stored in labelled aliquots, as previously described. Cells in the 24-well plates were then carefully washed with chilled PBS. 350µl of buffer RLT (Qiagen), supplemented with 1% (v/v) β-mercaptoethanol (Sigma-Aldrich), was added to each well and incubated for 2 minutes at room temperature before being mixed thoroughly with a pipette and transferred into labelled, sterile 1.5ml Eppendorf tubes (Sarstedt). 350µl of 70% ethanol (molecular biology grade; Sigma-Aldrich) in RNase free water (Qiagen) was added. In order to keep costs and time down, RNA was only extracted from day 0 and day 21 BM-MSCs. RNA was extracted as previously described, using the RNeasy® Mini Kit (Qiagen) and following the manufacturer's instructions to eventually elute RNA in RNase free water (Qiagen) (see 3.2.5.2.3.1.2 Ribonucleic Acid (RNA) Isolation, Reverse Transcription and qRT-PCR). RNA was reverse transcribed to cDNA as previously described, using the High-Capacity cDNA Reverse Transcription Kit (Applied Biosystems) according to the manufacturer's instructions, and stored at -20°C until required. qRT-PCR was performed on the Quant Studio 3 Real-Time Quantitative PCR System (Applied Biosystems) using SYBR green QuantiTect primer assays (Qiagen) to assess a number of genes indicative of different stages of osteogenic differentiation: alkaline phosphatase (*ALPL*), bone morphogenic protein 2 (*BMP2*), collagen type 1 alpha 1 (*COL1A1*), bone gamma-carboxyglutamate protein (*BGLAP*), secreted phosphoprotein 1 (*SPP1*) and Runt-related transcription factor 2 (*RUNX2*) (Table 3-11). GAPDH and HPRT1 were employed as housekeeping genes and sample gene expression levels were normalised to the geometric mean of their corresponding housekeeping genes (Vandesompele et al., 2002). Following normalisation to the reference genes, the relative

expression of each gene at day 21 compared to day 0 was determined using the $\Delta\Delta C_t$ method (Schmittgen & Livak, 2008), which was then compared between the healthy and unhealthy conditions and the chondrocyte only control. A twofold change (up- or down-regulated) was deemed biologically significant.

Table 3-11: *Genes assessed by qRT-PCR in differentiated BM-MSCs from the co-culture model at day 0 and day 21.*

Gene [Species]	Official Name	Amplicon Length	Entrez Gene ID
Housekeeping Genes			
<i>GAPDH</i> [Human]	Glyceraldehyde-3-phosphate dehydrogenase	95 (NM_001256799) 95 (NM_002046) 95 (NM_001289745) 95 (NM_001289746)	2597
<i>HPRT1</i> [Human]	Hypoxanthine phosphoribosyltransferase 1	130 (NM_000194)	3251
Genes of Interest			
<i>ALPL</i> [Human]	Alkaline phosphatase	110 (NM_000478) 110 (NM_001127501) 110 (NM_001177520) 110 (XM_005245818) 110 (XM_005245820) 110 (XM_006710546)	249
<i>BMP2</i> [Human]	Bone morphogenetic protein 2	148 (NM_001200)	650
<i>COL1A1</i> [Human]	Collagen, type I, alpha 1	118 (NM_000088) 118 (XM_005257058) 118 (XM_005257059) 118 (XM_006721703)	1277
<i>BGLAP</i> [Human]	Bone gamma-carboxyglutamate (gla) protein	90 (NM_199173)	632
<i>SPP1</i> [Human]	Secreted phosphoprotein 1	115 (NM_000582)	6696
<i>RUNX2</i> [Human]	Runt-related transcription factor 2	101 (NM_001015051) 101 (NM_001024630) 101 (NM_004348) 101 (NM_001278478) 101 (XM_006715231) 101 (XM_006715233) 101 (XM_006715234)	860

3.2.5.2.3.3.3 Alkaline Phosphatase Staining

The remaining 2 wells of differentiated BM-MSCs for each condition were stained for alkaline phosphatase activity to assess osteogenic differentiation of the BM-MSCs (Mennan et al., 2019). In brief, 25mg naphthol AS-BI phosphate (Sigma-Aldrich) was dissolved in 0.5ml dimethyl formamide (Sigma-Aldrich) in a fume cabinet. This was then added to 50ml 0.2M Tris HCl buffer ((1.21g Tris-HCl (Sigma-Aldrich) in 50ml distilled water, adjusted to pH7.5 with 10M HCl (BDH). 50mg Fast Red TR (Sigma-Aldrich) was then added and the solution was mixed by vortexing before being filtered, using filter paper and a funnel, into a glass bottle. The cells were washed with PBS and fixed in 10% buffered formalin (Sigma-Aldrich) for 10 minutes. The cells were then washed again with PBS before 1ml of the staining solution was added to each well and incubated for 1 hour at room temperature. After 1 hour, the stain was washed off thoroughly with tap water and the cells were viewed immediately by phase contrast microscopy, using x4 and x20 objective lenses on a Nikon Eclipse TS100 bench-top microscope (Nikon Corporation). Images were captured using a Leica MC170 HD Microscope camera (Leica Microsystems Ltd).

3.2.6 Statistical Analyses.

For all analyses, statistical significance was considered at $p < 0.05$. The distribution of data was determined using the Shapiro-Wilk normality test. Normally distributed, continuous data were summarised as means, and standard errors of the mean. Throughout this thesis, we have presented data as mean \pm SEM rather than mean \pm SD. This was a conscious decision based on the experimental designs and statistical tests carried out throughout. SD is useful where results are descriptive, and one is attempting purely to communicate information about the mean and the variability between individuals (Altman & Bland, 2005; Kim, 2013). By contrast, if one is comparing means from different groups, such as different

experimental conditions or timepoints, then it is useful to communicate the level of precision of the group means. In this way, the standard error of the mean provides a measure of how much confidence one has that the calculated means are truly representative of the data (Altman & Bland, 2005). This is important as the calculated means are then compared in order to reject the null hypothesis and conclude that there are significant differences caused by experimental conditions (Altman & Bland, 2005; Kim, 2013). For this reason, we decided that the SEM was a more appropriate statistic for our work.

3.2.6.1 *Flow Cytometry Data*

In order to compare CD marker positivity between conditions, a two-way ANOVA of 'CD marker' and 'BM-MSC Type' was used with % positivity as the dependant variable (Fox & Weisberg, 2018; Lenth, 2018; R Core Team, 2019; jamovi, 2020). Post hoc Tukey tests were used to carry out multiple comparisons to interrogate individual relationships between BM-MSC types for each individual marker.

3.2.6.2 *qRT-PCR data*

The relative expression of each of the genes of interest to the geometric mean of their corresponding housekeeping genes was calculated using the ΔCt method, as described above (Vandesompele et al., 2002; Schmittgen & Livak, 2008).

The relative expression at day 0, to that at day 21, was calculated ($\Delta\Delta\text{Ct}$) (Schmittgen & Livak, 2008), where:

$$\Delta\Delta\text{Ct} = ((\text{Ct gene of interest} - \text{Ct housekeeping genes}) \text{ Day 0} - (\text{Ct gene of interest} - \text{Ct housekeeping genes}) \text{ Day 21})$$

Finally, fold change was calculated using the comparative Ct method ($2^{-\Delta\Delta Ct}$) (Schmittgen & Livak, 2008). Jamovi (version 1.2.8, jamovi.org) was then used to carry out an independent samples T-test with 'Fold Change' as the dependant variable and 'BM-MSC Type' as the grouping variable to compare fold change values between conditions across all patients.

3.2.6.3 *ELISA Data*

In any samples in which the protein concentration was below the detection limit, the concentration was replaced with the non-detect value. Linear mixed modelling was used to assess the ELISA data, for each of the analytes separately, with 'Concentration' as the dependant variable, 'BM-MSC type' and 'Timepoint' as factors and 'Patient' as the cluster variable. Post hoc Bonferroni tests were used to carry out multiple comparisons to interrogate individual relationships between BM-MSC types and timepoints for each analyte.

3.2.6.4 *Biochemistry Data*

Linear mixed modelling was used to assess the biochemistry data (DNA, GAG and GAG/cell) to determine differences between conditions. The quantified biochemistry data was used as the dependant variable, with 'BM-MSC type' and 'Timepoint' as factors, 'Patient' as the cluster variable and 'Patient|Intercept' as the random effects variable. Post hoc Bonferroni tests were used to carry out multiple comparisons to interrogate individual relationships between BM-MSC types and timepoints.

3.2.6.5 *Statistical Software*

All data were organised using Microsoft® Office Excel 2013 (Microsoft®, Washington, USA). For all analyses, data from the five patients was combined and comparisons were carried out between conditions and between timepoints, not between patients. Statistical analyses

were carried out using jamovi (version 1.2.8, jamovi.org) a free software interface that is built upon the R statistical package (R Core Team, 2019; jamovi, 2020).

3.3 Results

3.3.1 Patients

Medial and lateral femoral condylar tissue samples of cartilage and bone were collected from 16 patients undergoing TKR surgery at the RJAH Orthopaedic Hospital (Table 3-12), providing 32 femoral condyles in all (Figure 3-10).

Knee femoral condylar tissue was also obtained from a young patient (24 y/o) with no medical history of OA who had sadly passed away as the result of a road traffic collision (Figure 3-11).

3.3.2 Sample Assessment and Grading

3.3.2.1 *Samples obtained from TKR surgery at RJAH*

3.3.2.1.1 Macroscopic Assessment

All 32 knee femoral condyles were graded macroscopically using the ICRS Cartilage Lesion Classification System (Table 3-13). The cartilage of the excised condyles ranged in ICRS grade from grade 1; 'nearly normal' (12 condyles), to ICRS grade 4; 'severely abnormal' (9 condyles). None of the excised condyles from TKR patients had grade 0; 'normal' cartilage. The median ICRS grade was 2.

3.3.2.1.2 Histological Assessment

3.3.2.1.2.1 The Osteoarthritis Research Society International (OARSI) Osteoarthritis Cartilage Histopathology Assessment System

Stained sections of cartilage ranged in OARSI cartilage histopathology grade from grade 1; 'surface intact with superficial fibrillation' (7 condyles) to grade 6; 'deformation' (3 condyles) (Table 3-13). None of the excised condyles from TKR patients had grade 0; 'normal articular cartilage'. The median OARSI grade was 3.25.

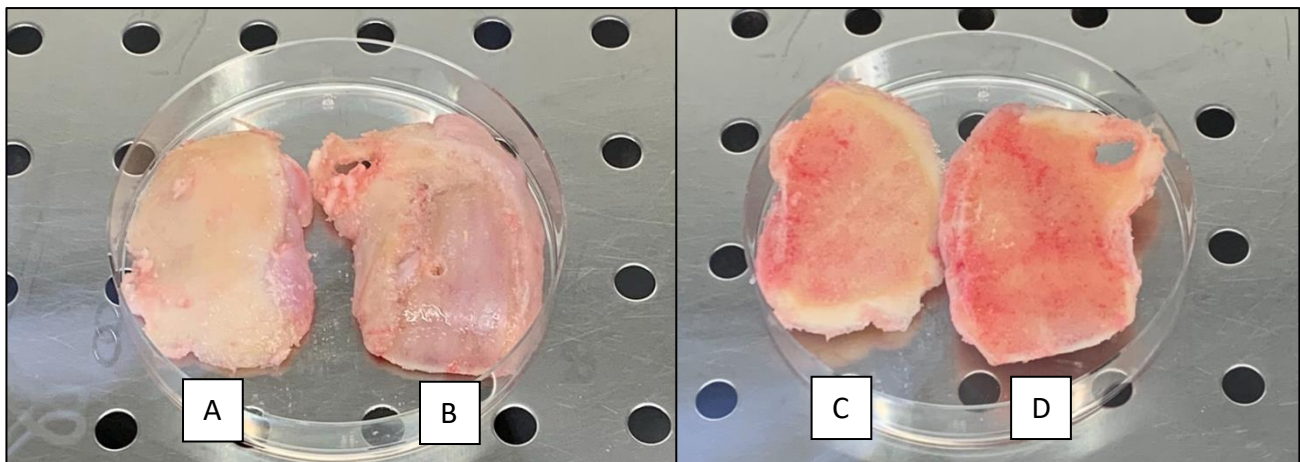
3.3.2.1.2.2 Subchondral Bone Histological Grading System

Stained sections of cartilage and subchondral bone ranged in subchondral bone histological grade from 0; 'early stages of OA' (18 condyles), to grade 3; 'late stage disease' (1 condyle) (Table 3-13). The median subchondral bone histological grade was 0.

Table 3-12: Demographic information of the 16 patients from which knee condyles were obtained.

Patient	Gender	Age (at time of TKR)	Operated Knee	Clinical Diagnosis (details where available)
1	Male	70	Left	OA (abnormal knee anatomy due to previous fracture)
2	Female	64	Right	OA (previous tibial fracture)
3	Male	72	Left	OA
4	Female	65	Right	OA
5	Male	53	Right	OA
6	Male	71	Right	OA
7	Female	67	Right	OA
8	Male	74	Right	OA
9	Male	66	Right	OA (bone on bone)
10	Male	72	Left	OA
11	Male	69	Right	OA (previous high tibial osteotomy (HTO))
12	Male	54	Left	OA (previous HTO)
13	Female	71	Left	OA (patellofemoral and medial compartment)
14	Male	76	Right	OA (varus)
15	Female	73	Right	OA (bilateral)
16	Female	74	Left	OA (medial compartment bone on bone)
	10 (M) 6 (F)	68.2±6.7	10 (R) 6 (L)	

Patient 14



Patient 15

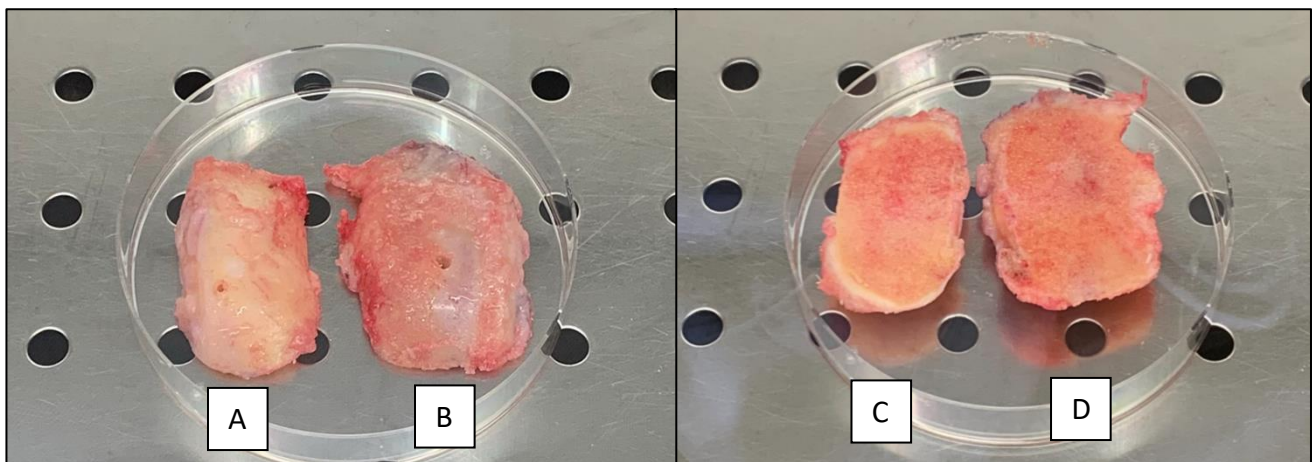


Figure 3-10: Examples of the macroscopic appearance of knee condyles collected from patients following TKR surgery. Patient 14 (top) and patient 15 (bottom). A: Condyle with the best (lowest) ICRS graded cartilage (cartilage side). B: Condyle with the worst (highest) ICRS graded cartilage (cartilage side). C: Condyle with the best ICRS graded cartilage (bone side). D: Condyle with the worst (highest) ICRS graded cartilage (bone side). Note that cartilage is eroded down to the bone in the worst graded condyles (B) of both patients.



Figure 3-11: Macrosopic appearance of the tibial plateau obtained from a young patient with no history of OA, sourced from the NHSBT. Right knee from posteroanterior view.

Table 3-13: Macroscopic (ICRS Cartilage Lesion Grade) and histological scores (OARSI OA Cartilage Histopathology Grade and Subchondral Bone Histological Grade) of condyles obtained from patients undergoing TKR surgery.

Patient	Condyle	ICRS Cartilage Lesion Classification System	OARSI Osteoarthritis Cartilage Histopathology Assessment System	Subchondral Bone Histological Grading System
1	A	2	3.5	0
	B	4	6	2
2	A	4	4	2
	B	2	2	0
3	A	3	3.5	1
	B	1	5.5	2
4	A	2	2	0
	B	3	4	1
5	A	0	2	0
	B	2	4.5	0
6	A	2	1	0
	B	1	1	0
7	A	2	6	2
	B	1	1	0
8	A	4	5	2
	B	1	3	1
9	A	1	2	0
	B	4	4.5	0
10	A	1	1	0
	B	4	3.5	1
11	A	1	2.5	0
	B	2	1.5	0
12	A	3	6	2
	B	1	1	0
13	A	1	1	0
	B	4	5	2
14	A	1	1	0
	B	4	5	3
15	A	1	2	0
	B	4	5	2
16	A	1	2	0
	B	4	5	2
Mode		2	3.25	0

3.3.2.1.2.3 Correlation Between Scoring Systems

The OARSI OA Cartilage Histopathology Assessment System and the Subchondral Bone Histological Grading System were strongly correlated (Pearson's $r=0.91$ (95%CI 0.75-0.97); $p<0.001$; Figure 3-12).

3.3.2.2 *NHSBT Sample Obtained from Young Patient*

3.3.2.2.1 Macroscopic Assessment

The tibial plateau obtained from the young patient demonstrated ICRS grade 0 'normal' cartilage with a smooth, glassy surface and no evidence of fibrillation, indentations or lesions (Figure 3-11). The AC of the healthy sample was white in colour and did not demonstrate any yellowing typically associated with ageing in cartilage and which was observed in the cartilage of all condylar samples obtained from TKR (Figure 3-10).

3.3.2.2.2 Histological Assessment

3.3.2.2.2.1 The Osteoarthritis Research Society International (OARSI) Osteoarthritis Cartilage Histopathology Assessment System

Stained sections of cartilage obtained from the young patient demonstrated an OARSI cartilage histopathology grade of 0, 'normal cartilage' (Figure 3-13).

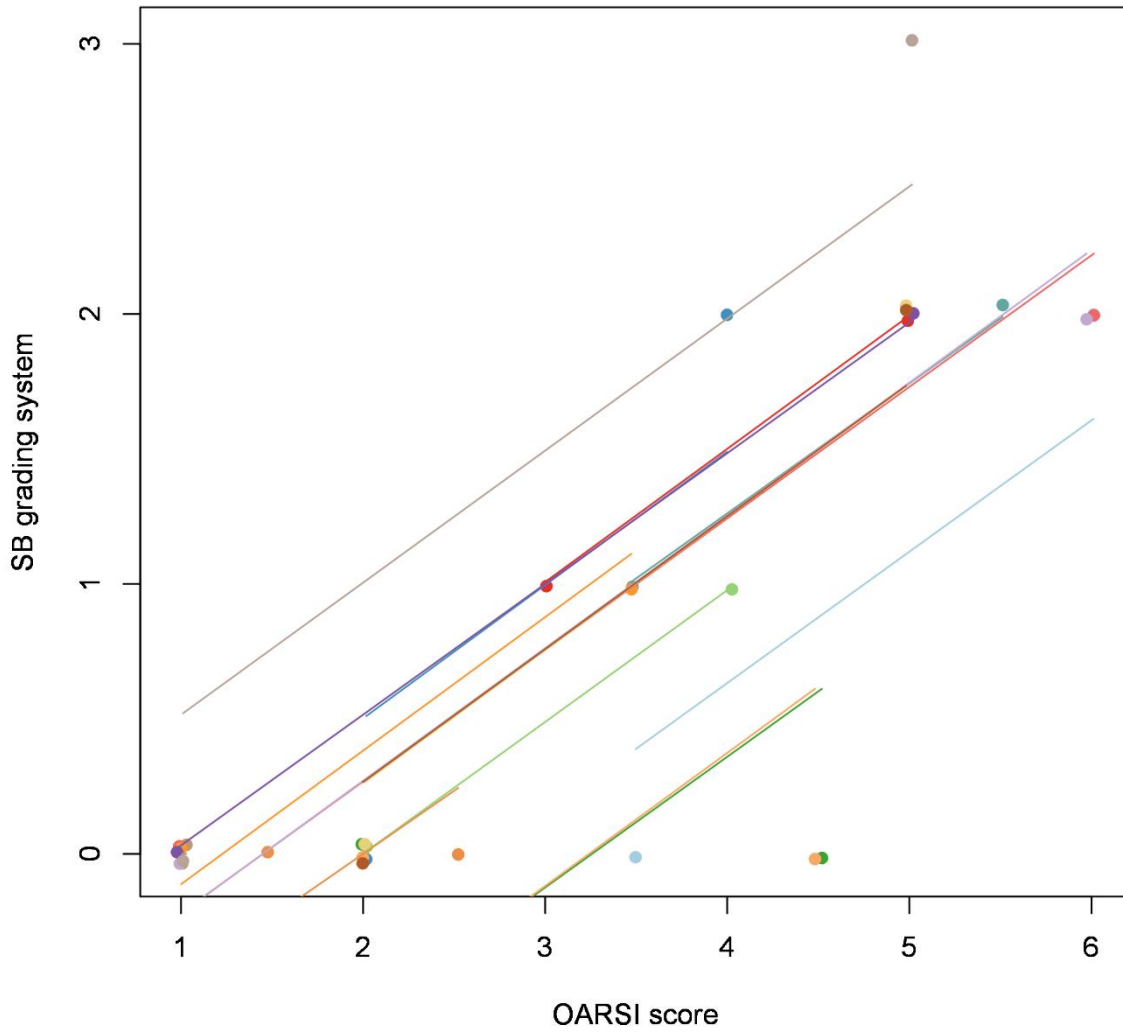


Figure 3-12: Graphical representation of the correlation between the OARSI OA Cartilage Histopathology Assessment System and the Subchondral Bone Histological Grading System. (Pearson's $r=0.91$ (95%CI 0.75-0.97); $p<0.001$).

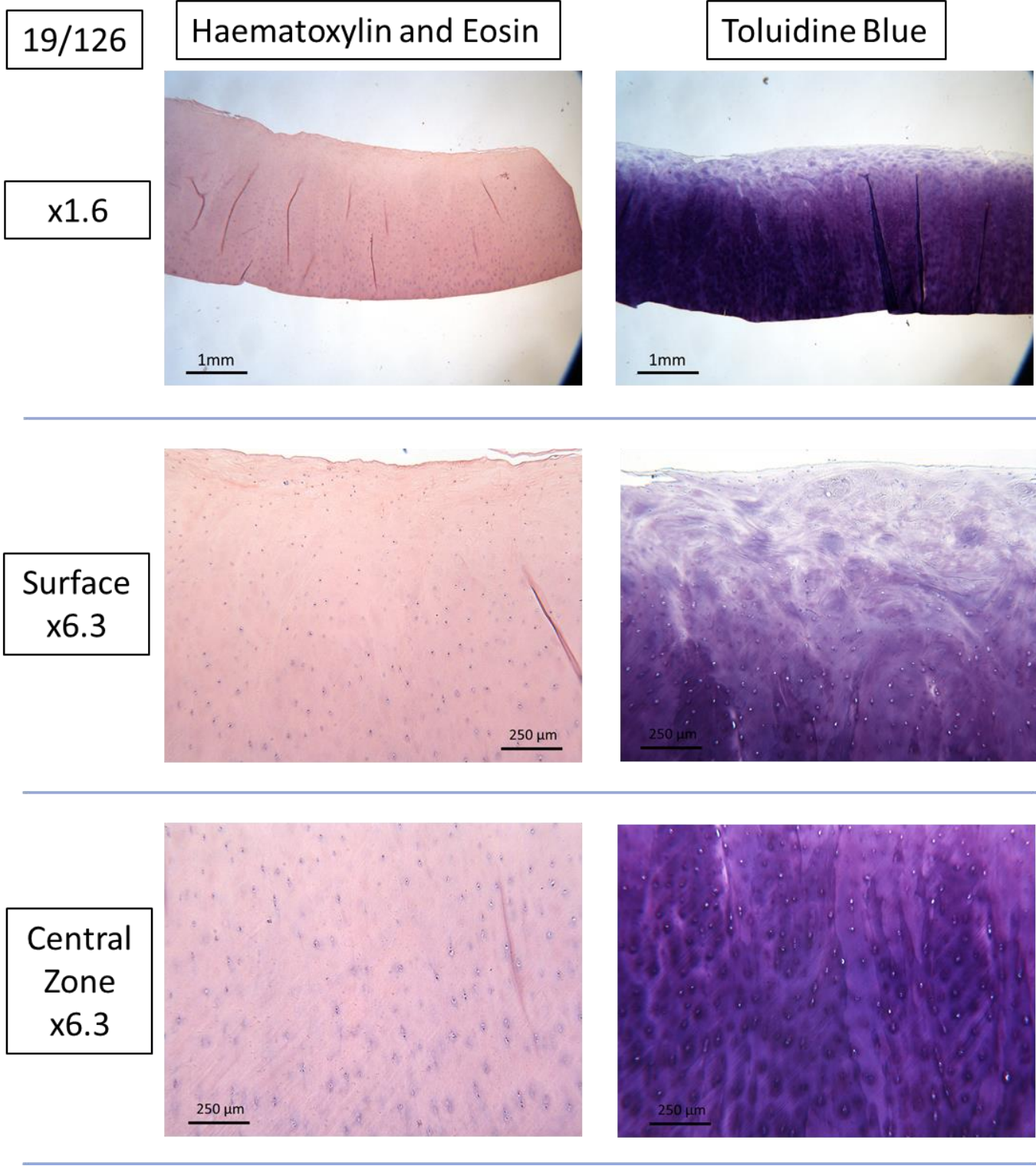


Figure 3-13: Histological Staining of Normal Articular Cartilage from NHSBT Sample. Left: H&E staining. Right: Toluidine blue staining.

3.3.3 Co-Culture

3.3.3.1 *Patients*

Five of the patients with the greatest difference in ICRS grade between the two excised condyles were selected for the co-culture model (Table 3-14).

3.3.3.2 *Characterisation of Cells Prior to Co-culture*

3.3.3.2.1 *BM-MSC Characterisation by Flow Cytometry*

Flow cytometry analyses demonstrated that both healthy and unhealthy BM-MSCs did not fulfil all ISCT criteria for MSC identification (Table 3-15, Figure 3-14). Both cell types demonstrated >95% positivity for CD73, CD90 and CD105. Both cell types also demonstrated <2% positivity for CD19 and CD45. However, there was some degree of positivity demonstrated in both healthy and unhealthy BM-MSCs for HLA-DR and CD34 which does not conform to recommendations by the ISCT in which these markers should be present in <2% of cells. CD14 was also present on both cell populations. There were no significant differences between healthy and unhealthy BM-MSCs in any of the cell surface markers interrogated (Table 3-15, Figure 3-14).

Table 3-14: Demographic information of patients whose donated tissue was selected for use in the in-vitro co-culture model.

Patient	Gender	Age	Knee	Condyle	ICRS Grade	OARSI Grade	SB Grade
10	Male	72	Left	A	1	1	0
				B	4	3.5	1
13	Female	70	Left	A	1	1	0
				B	4	5	2
14	Male	76	Right	A	1	1	0
				B	4	5	3
15	Female	73	Right	A	1	2	0
				B	4	5	2
16	Female	73	Left	A	1	2	0
				B	4	5	2
Mean±SD		72.8±2.2					

Table 3-15: Flow cytometry results from BM-MSC characterisation. The mean positivity of each marker in each condition is displayed along with the p-value resulting from independent t-tests between conditions for each marker assessed. The recommended immunopositivity suggested by the ISCT is also displayed.

Marker	ISCT Recommended Immunopositivity	% Positivity in Healthy BM-MSCs (mean±SEM)	% Positivity in Unhealthy BM-MSCs (mean±SEM)	Adherence to the ISCT Recommendations	Independent Samples T-test (p-value)
CD14	<2%	15.2% ± 6.66	15.6% ± 8.08	X	0.973
CD19	<2%	0.46% ± 0.108	0.9% ± 0.164	✓	0.055
CD34	<2%	3.26% ± 1.9	4.48% ± 2.64	X	0.718
CD45	<2%	0.86% ± 0.133	1.24% ± 0.136	✓	0.081
HLA-DR	<2%	3.94% ± 0.85	8.82% ± 2.61	X	0.114
CD73	>95%	99% ± 0.058	100% ± 0.02	✓	0.143
CD90	>95%	99.9% ± 0.032	99.9% ± 0.025	✓	0.347
CD105	>95%	96.1% ± 3.33	98.9% ± 0.705	✓	0.431

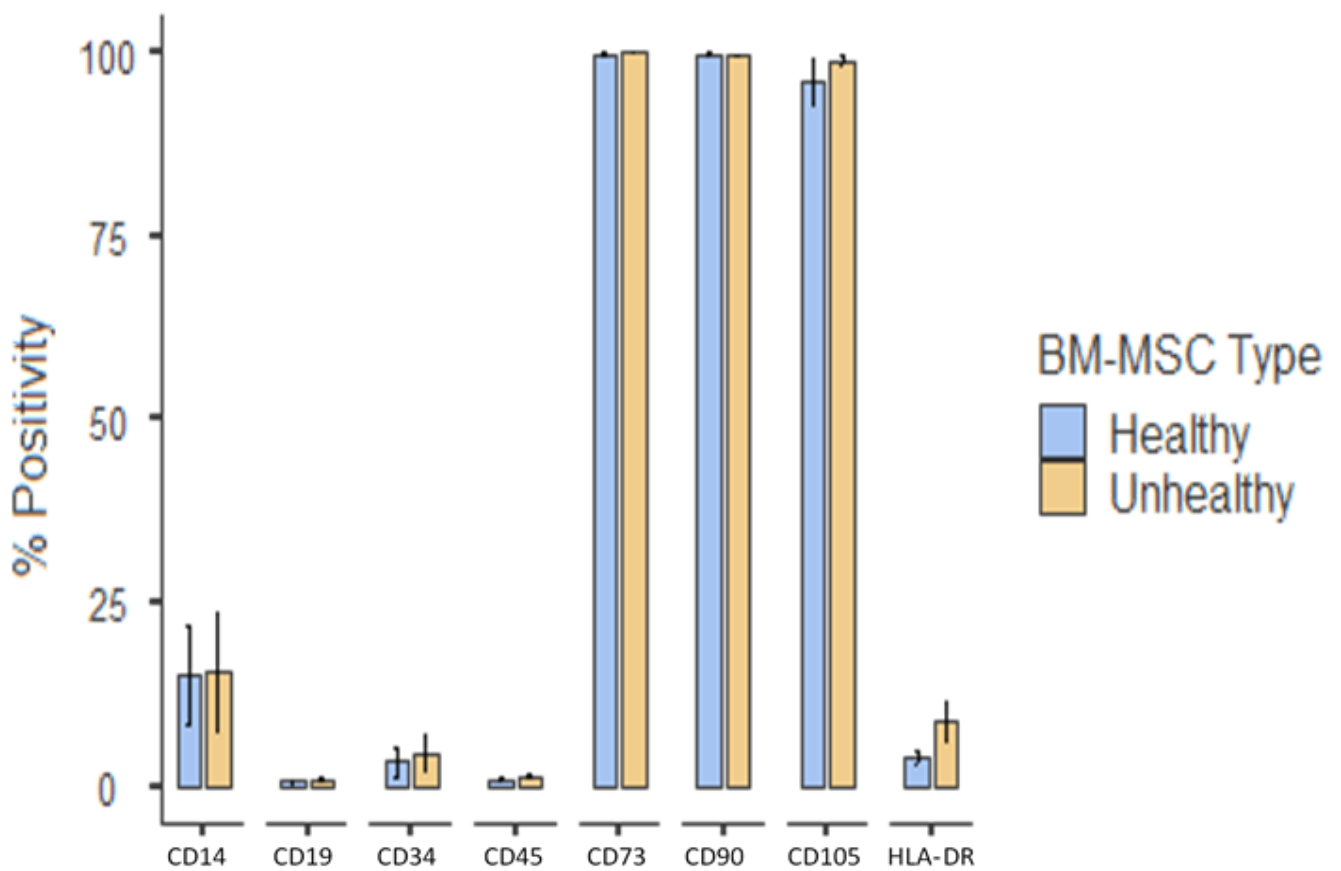


Figure 3-14: Flow cytometry data demonstrating the immunoprofile of healthy and unhealthy BM- MSC populations prior to seeding for the co-culture model. The mean abundance of a number of cell surface markers, recommended by the ISCT for the identification of MSCs, across the 5 patients, was assessed. The error bars represent the standard error of the mean.

3.3.3.3 *Output from co-culture model*

3.3.3.3.1 Chondrocyte-laden Agarose Scaffolds

At each of the experimental timepoints, agarose scaffolds were harvested from each of the conditions. The resulting scaffolds were cylindrical in shape, had a diameter of roughly 6mm and a height of roughly 7mm (Figure 3-15).

3.3.3.3.1.1 Histological Analysis

Sections from scaffolds at all timepoints and conditions showed some damage, caused during sectioning due to the fragile nature of the scaffolds, but otherwise the size and shape of the scaffold was maintained throughout histological processing (Figures 3-16 to 3-24).

Histological analysis of the chondrocyte-loaded agarose scaffolds at day 0 demonstrated that the cells were well-distributed throughout the scaffold and could be identified easily on the H&E stained sections, and also, to a lesser degree, on the alcian blue stained sections (solid arrows, Figure 3-16). The porous nature of the agarose could be appreciated on the higher magnification images. There was no evidence of GAG deposition in the alcian blue stained sections, at day 0 (Figure 3-16).

The stained sections of the day 0 cell-free scaffolds demonstrated that there is some degree of background staining for both stains, but it was clear to see that there were no cells present (Figure 3-17).

H&E stained sections from the chondrocyte-containing day 21 scaffolds showed that cells were still well-distributed throughout the scaffold (Figures 3-18, 3-19, 3-20, 3-21, 3-22 and 3-23). Alcian blue stained sections demonstrated the deposition of GAG in a circular pattern in the area immediately surrounding the chondrocytes. This was seen in the scaffolds that had been co-cultured with both healthy (Figures 3-18 & 3-19) and unhealthy (Figures 3-20 &

3-21) BM-MSCs and in the scaffolds that had been cultured without BM-MSCs (the chondrocyte-only control; Figures 3-22 & 3-23).

There were no obvious differences in either stain between the three conditions at day 21. There did, however, appear to be zonal differences. In both experimental conditions, and in the no BM-MSC control, the chondrocytes appeared to be larger at the top of the scaffold (Figures 3-18, 3-20 & 3-22) than at the bottom (Figures 3-19, 3-21 & 3-23). There also seemed to be more GAG deposition at the top of the scaffold (Figures 3-18, 3-20 & 3-22) compared to the bottom (Figures 3-19, 3-21 & 3-23), with alcian blue staining more intense and radiating further out from the chondrocytes.

The day 21 cell-free control demonstrated that there was still some degree of background staining but, again, it was clear that there were no cells when compared with the cell-containing scaffolds at the same timepoint (Figure 3-24).

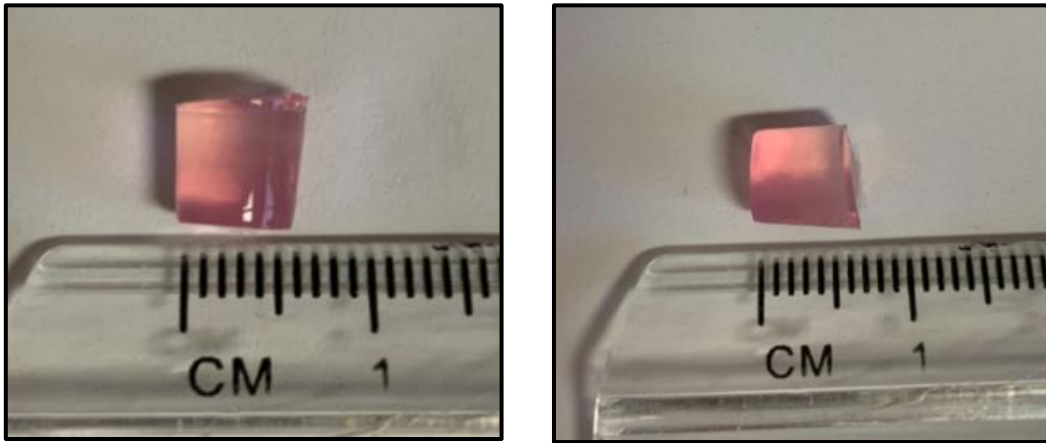


Figure 3-15: Representative images of a chondrocyte-agarose scaffold removed from the 24-well inserts in the co-culture model for analysis. The resulting scaffolds were cylindrical, with a diameter of approximately 6mm and a height of approximately 7mm.

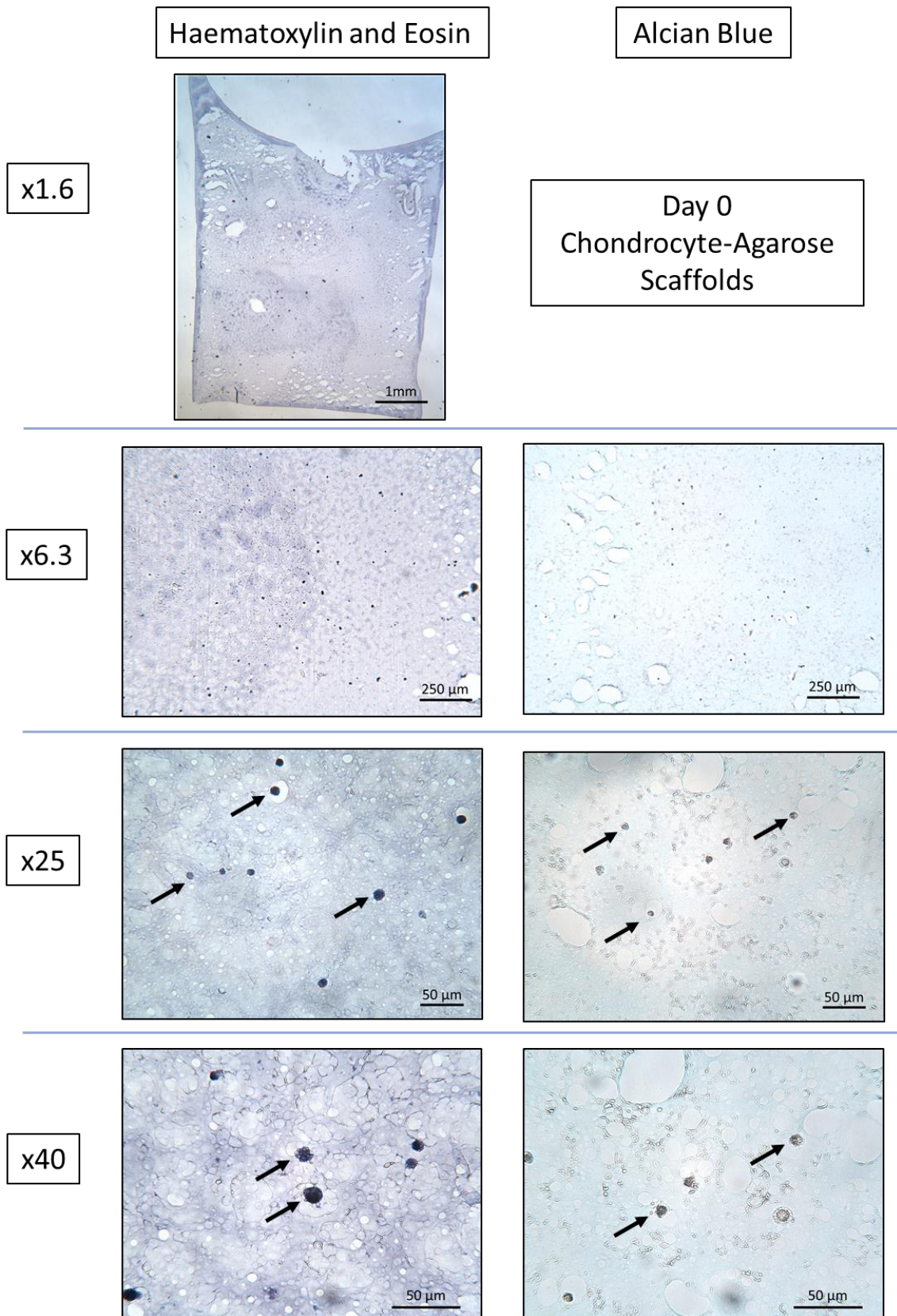
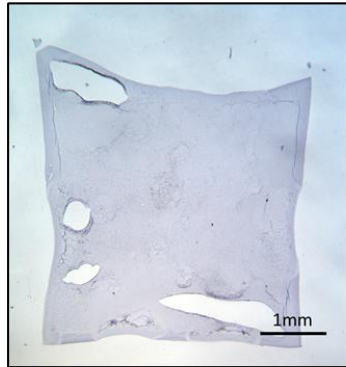


Figure 3-16: Representative images of stained sections from the chondrocyte-loaded agarose scaffolds at day 0. Left column: H&E stained sections. Right column: Alcian Blue stained sections. Solid arrows: chondrocytes.

Haematoxylin and Eosin

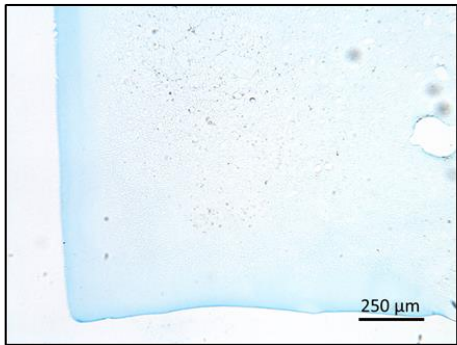
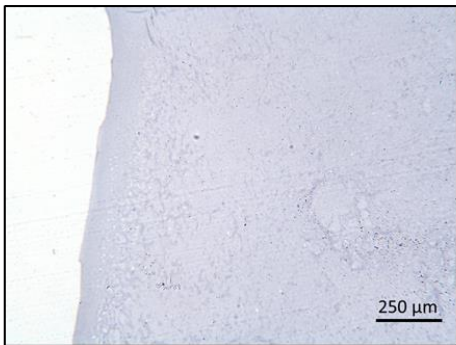
Alcian Blue

x1.6

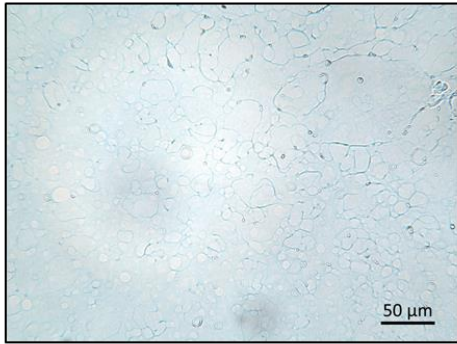
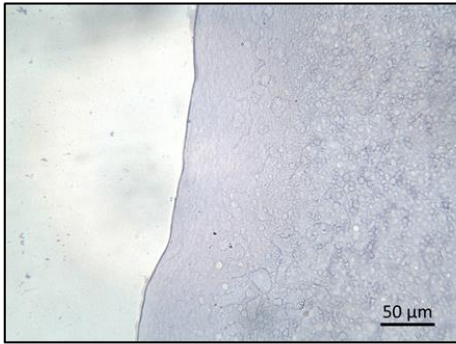


Day 0
Chondrocyte-Free
Scaffolds

x6.3



x25



x40

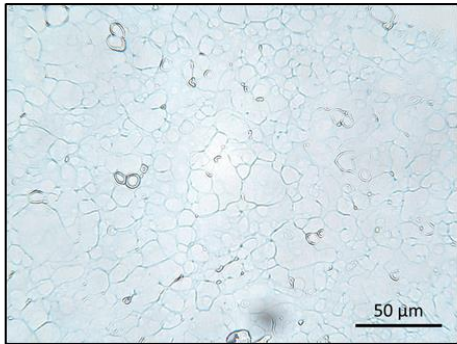
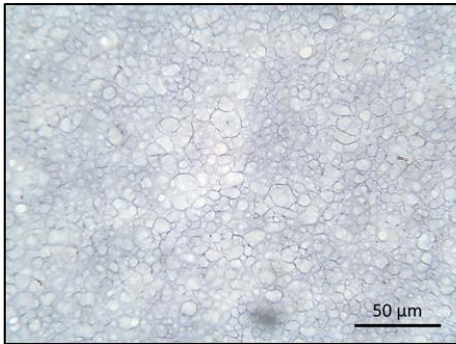


Figure 3-17: Representative images of stained sections from cell-free control agarose scaffolds at day 0. Left column: H&E stained sections. Right column: Alcian Blue stained sections.

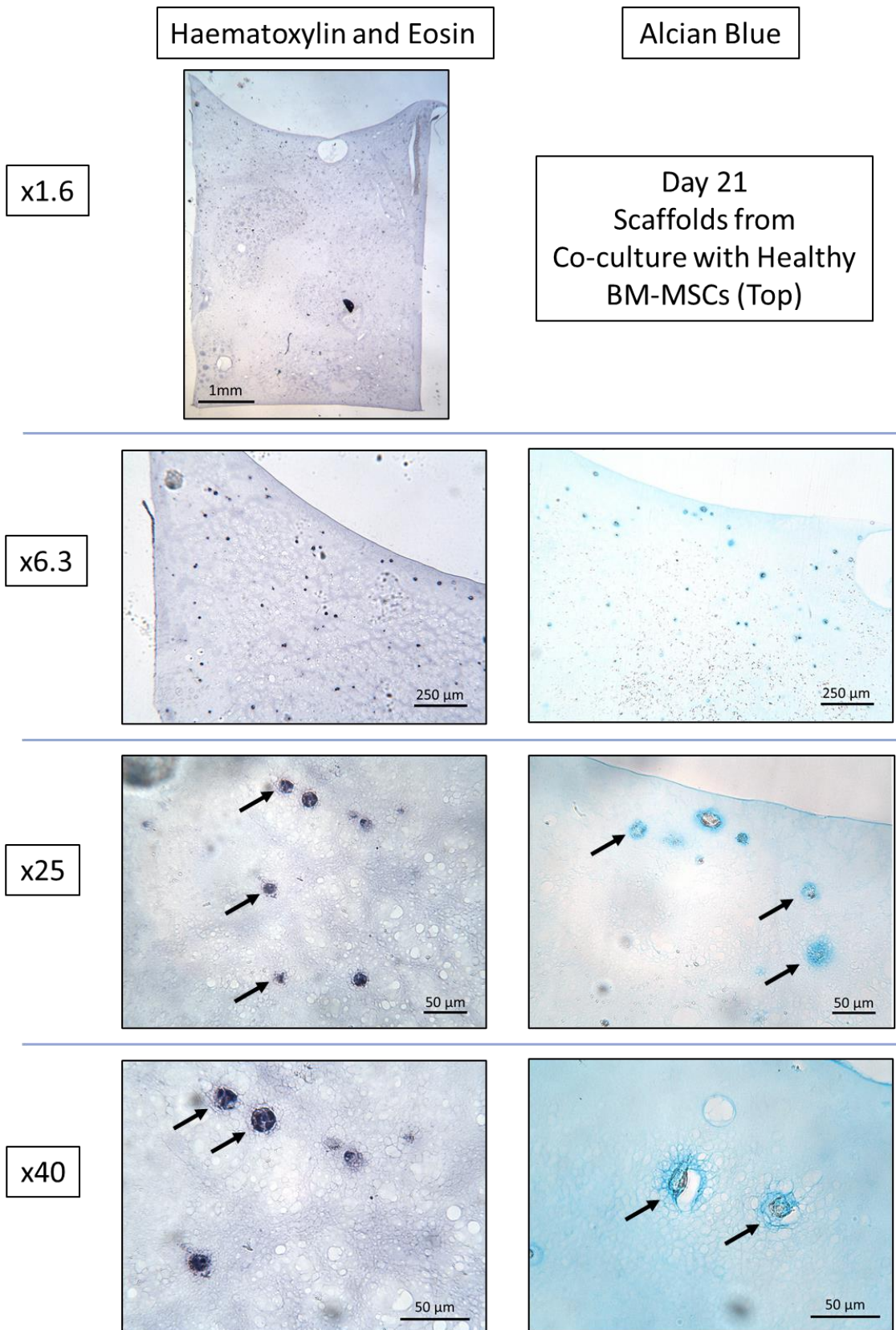


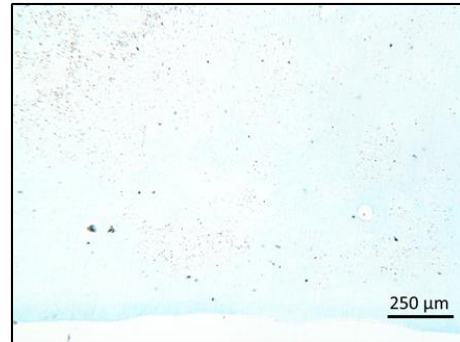
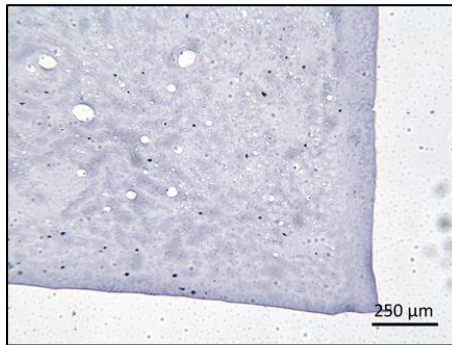
Figure 3-18: Representative images of H&E and Alcian Blue stained sections from the top of day 21 chondrocyte-loaded agarose scaffolds co-cultured with healthy BM-MSCs. Solid arrows: chondrocytes.

Day 21
Scaffolds from Co-culture with Healthy BM-MSCs
(Bottom)

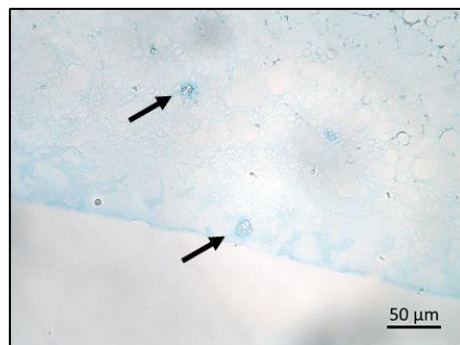
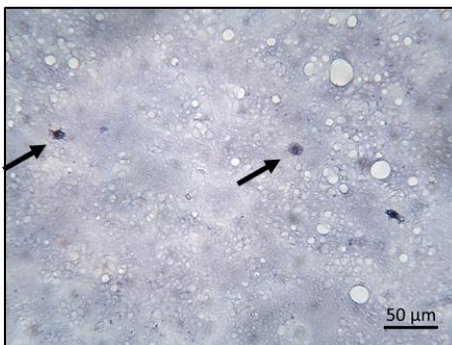
Haematoxylin and Eosin

Alcian Blue

x6.3



x25



x40

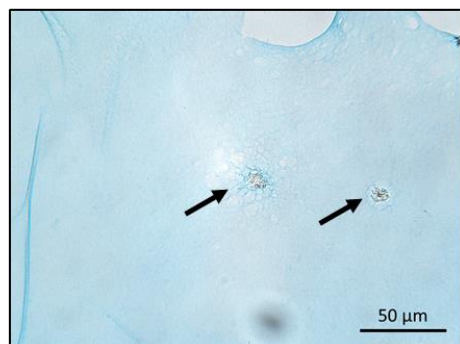
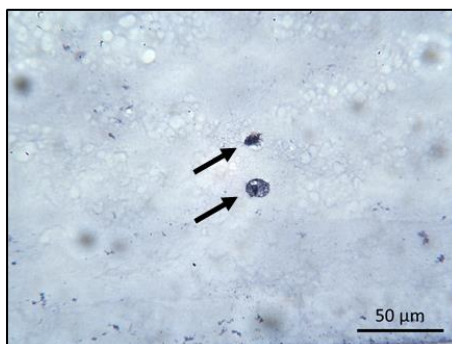


Figure 3-19: Representative images of H&E and Alcian Blue stained sections from the bottom of the day 21 chondrocyte-loaded agarose scaffolds co-cultured with healthy BM-MSCs. Solid arrows: chondrocytes.

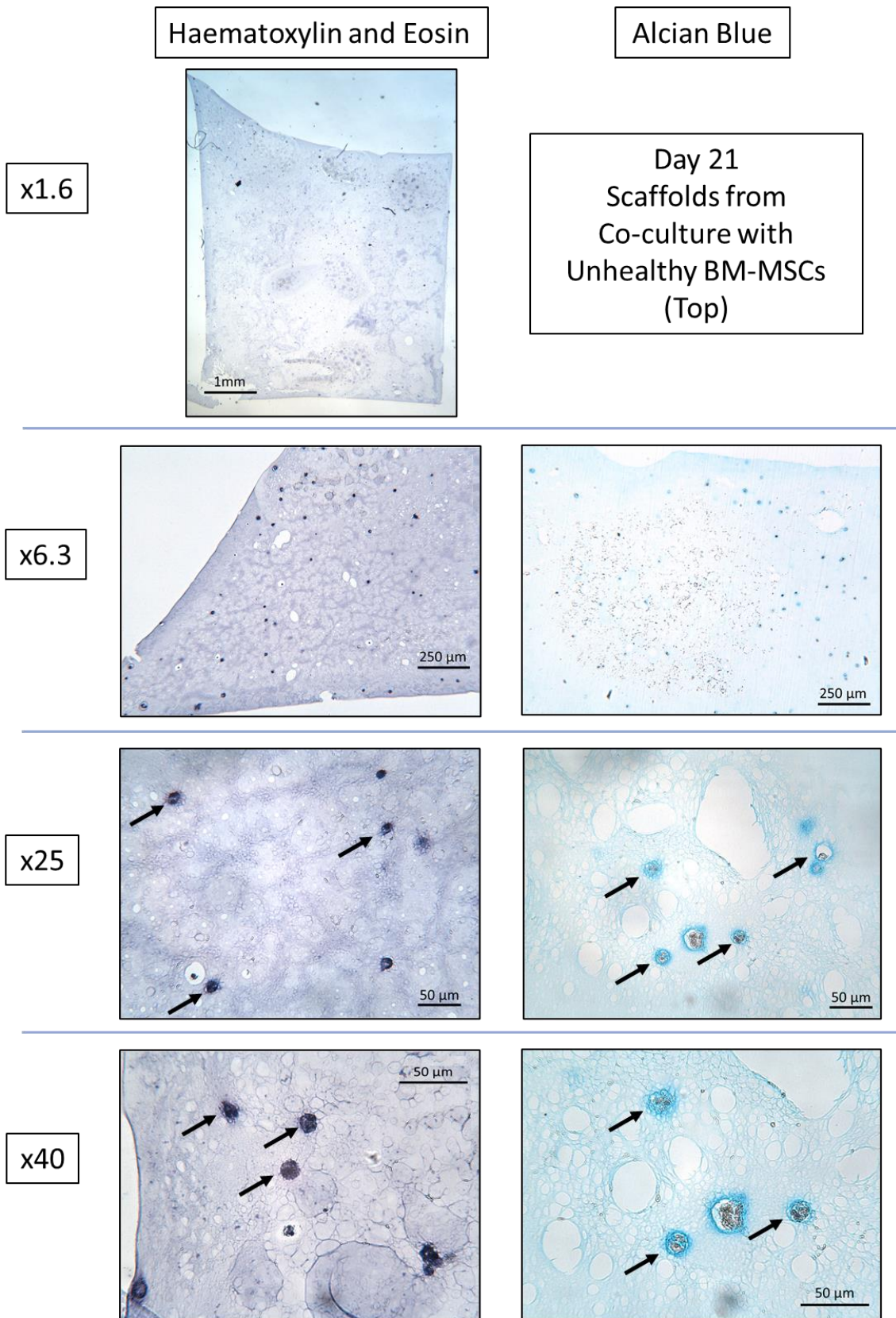


Figure 3-20: Representative images of H&E and Alcian Blue stained sections from the top of the day 21 chondrocyte-loaded agarose scaffolds co-cultured with unhealthy BM-MSCs. Solid arrows: chondrocytes.

Day 21
Scaffolds from Co-culture with Unhealthy BM-MSCs
(Bottom)

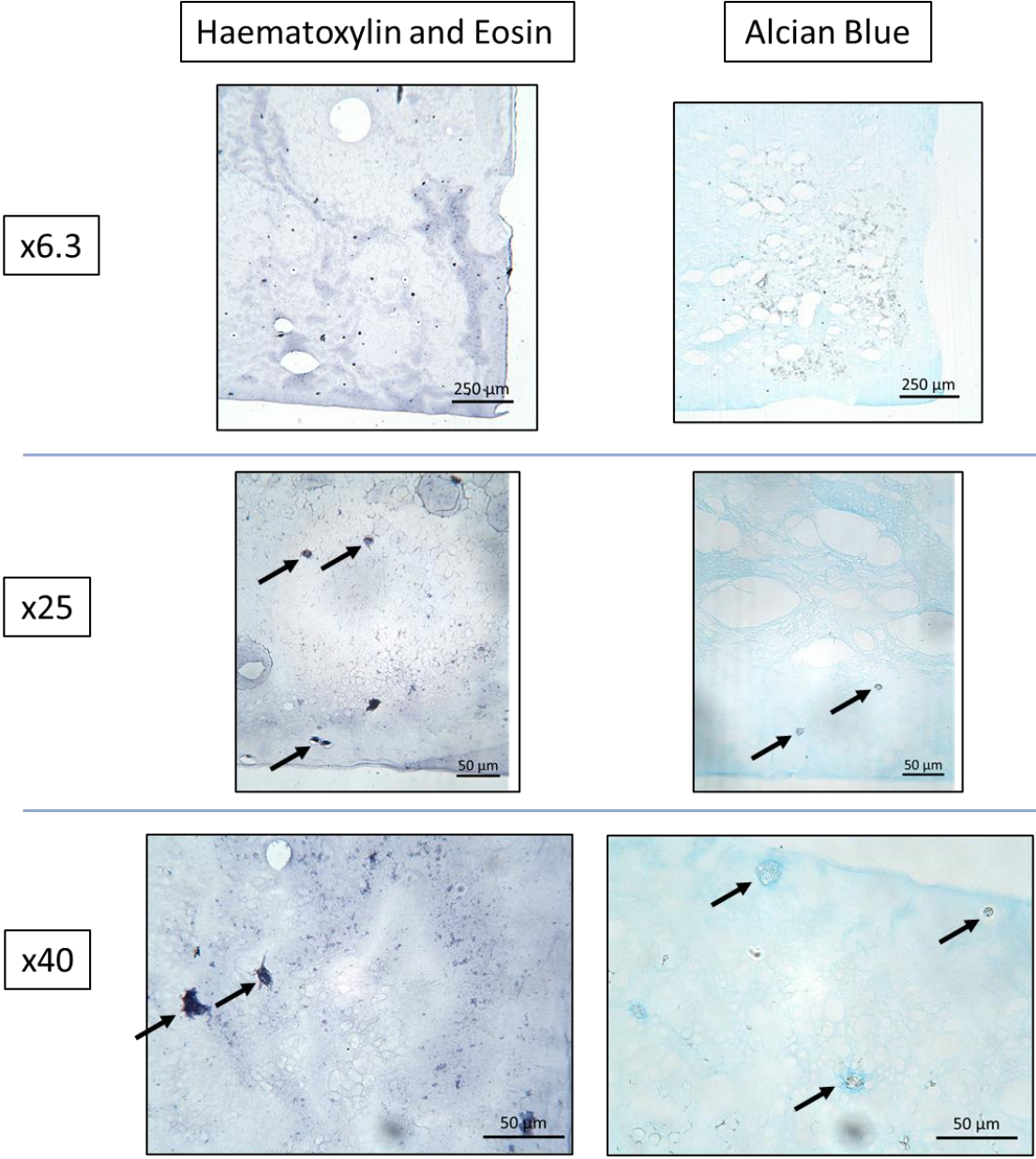


Figure 3-21: Representative images of H&E and Alcian Blue stained sections from the bottom of the day 21 chondrocyte-loaded agarose scaffolds co-cultured with unhealthy BM-MSCs. Solid arrows: chondrocytes.

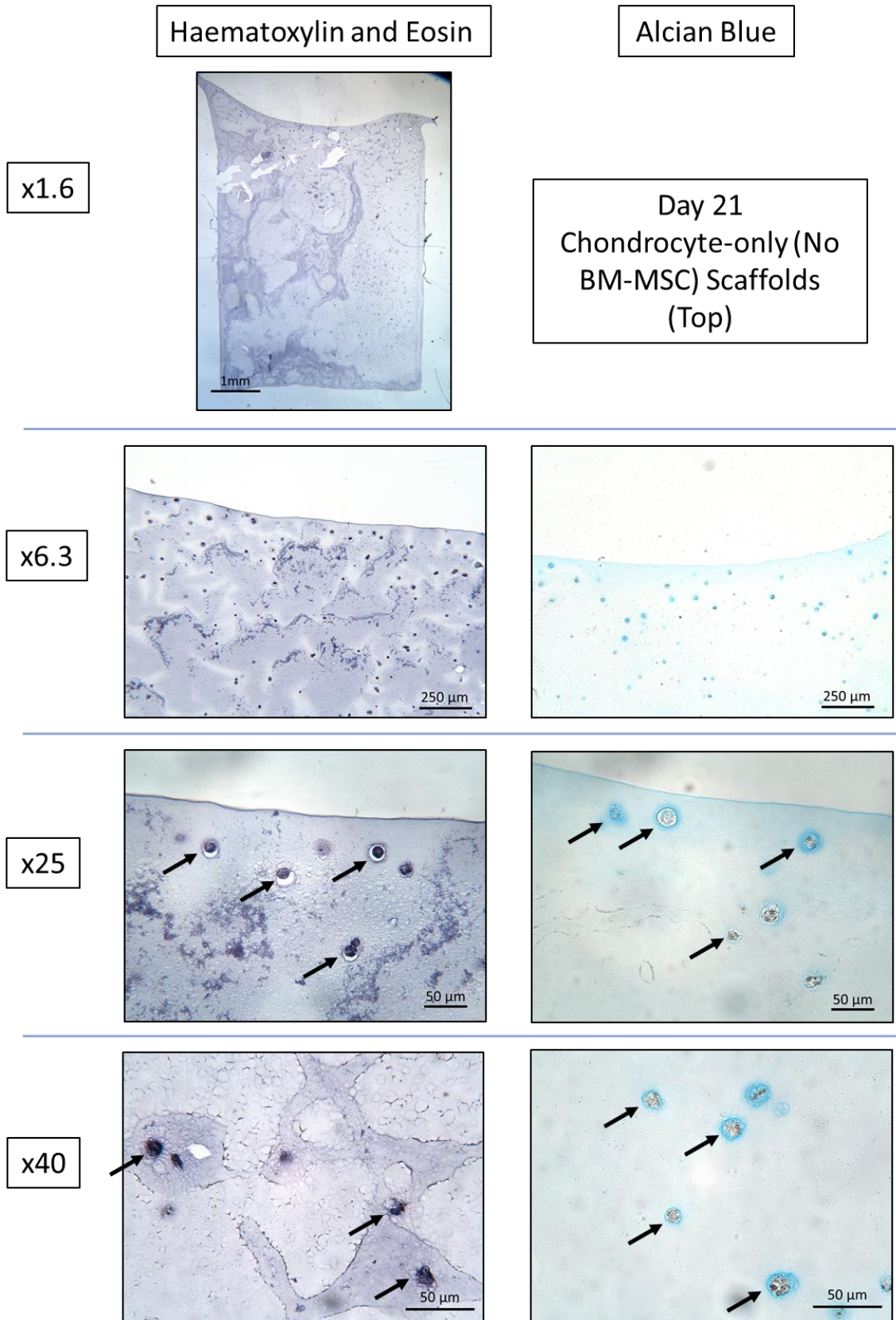


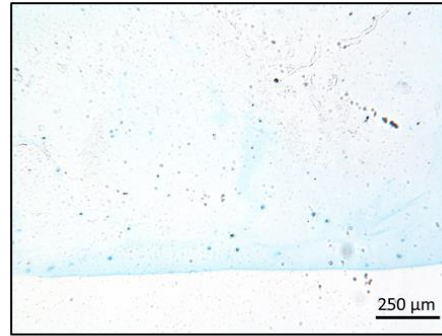
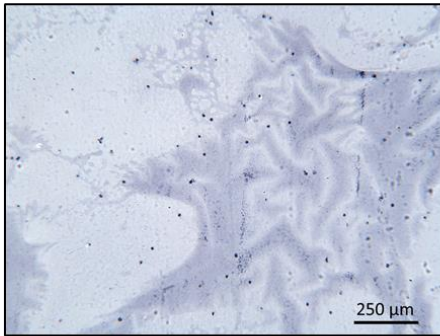
Figure 3-22: Representative images of H&E and Alcian Blue stained sections from the top of the day 21 chondrocyte-loaded agarose scaffolds from the chondrocyte-only control. Solid arrows: chondrocytes.

Day 21
Chondrocyte-only (No BM-MSC) Scaffolds
(Bottom)

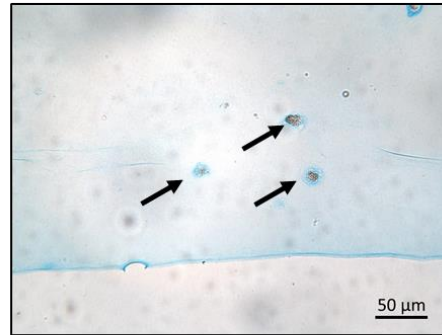
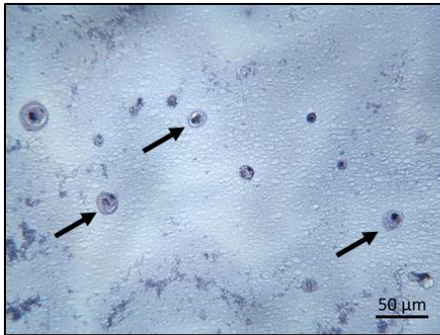
Haematoxylin and Eosin

Alcian Blue

x6.3



x25



x40

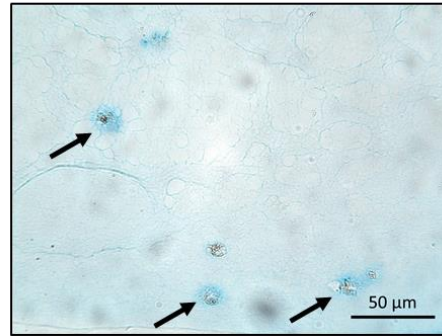
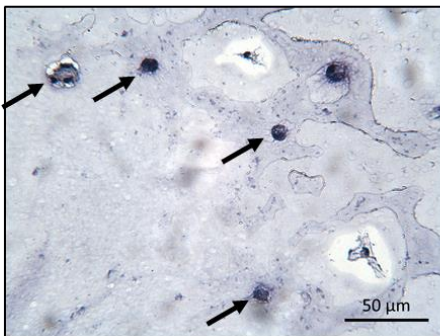
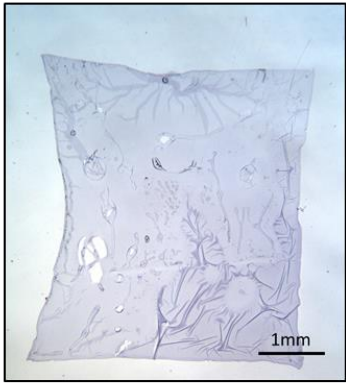


Figure 3-23: Representative images of H&E and Alcian Blue stained sections from the bottom of the day 21 chondrocyte-loaded agarose scaffolds from the chondrocyte-only control. Solid arrows: chondrocytes.

Haematoxylin and Eosin

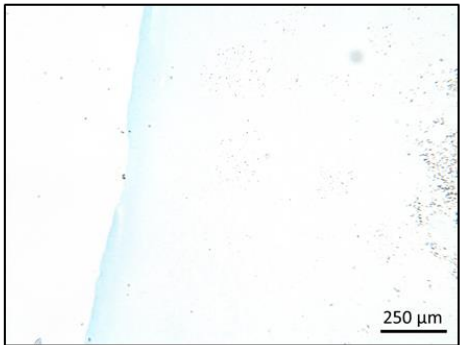
Alcian Blue

x1.6

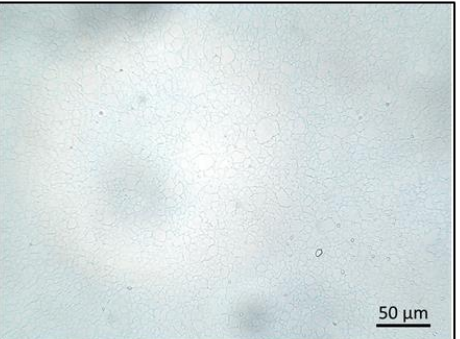
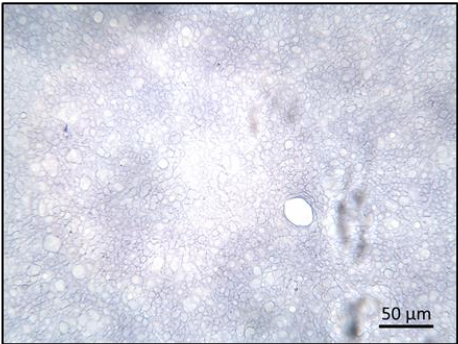


Day 21
Cell Free Scaffolds

x6.3



x25



x40

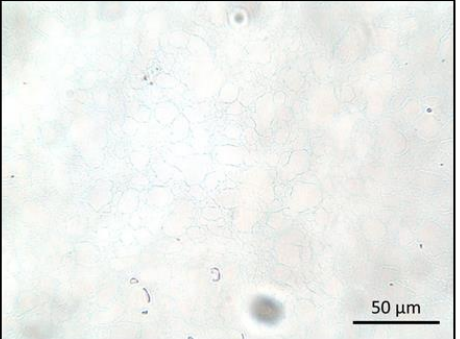
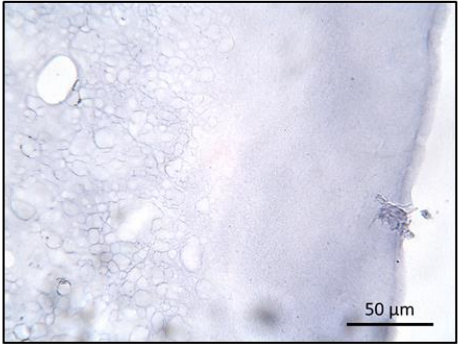


Figure 3-24: Representative images of H&E and Alcian Blue stained sections from the cell-free agarose scaffolds at day 21.

3.3.3.3.1.2 Scaffold Wet Weight

A total of 238 scaffolds were collected from the various conditions and timepoints of the co-culture model and weighed. The mean weight across all conditions was significantly higher in the scaffolds collected at day 0 ($0.236\text{g} \pm 0.002_{\text{SEM}}$), compared to those collected at day 7 ($0.225\text{g} \pm 0.002_{\text{SEM}}$; $p < 0.001$), day 14 ($0.228\text{g} \pm 0.002_{\text{SEM}}$; $p = 0.006$) and day 21 ($0.230\text{g} \pm 0.002_{\text{SEM}}$; $p = 0.025$; Figure 3-25). However, there was no significant difference in the mean weight of the scaffolds between conditions at any individual timepoint (all $p = 1.00$).

3.3.3.3.1.3 Biochemical Analysis

3.3.3.3.1.3.1 DNA Quantification for Cell number

The mean chondrocyte number in the co-culture model, across all three conditions, increased over time, with a significant increase between day 0 ($1.89 \times 10^5 \pm 5.36 \times 10^3_{\text{SEM}}$) and day 7 ($2.34 \times 10^5 \pm 5.21 \times 10^3_{\text{SEM}}$; $p < 0.001$), between day 7 and day 14 ($2.55 \times 10^5 \pm 6.5 \times 10^3_{\text{SEM}}$; $p = 0.024$) and between day 14 and day 21 ($3.28 \times 10^5 \pm 1.25 \times 10^4_{\text{SEM}}$; $p < 0.001$) (Figure 3-26).

Post hoc testing provided more detailed comparisons between conditions at individual timepoints. Neither at day 0 nor at day 7, there was no significant difference in mean chondrocyte number between the agarose scaffolds taken from healthy, unhealthy and chondrocyte-only ('none') conditions. At day 14, there was a significant difference in the mean chondrocyte number in agarose scaffolds taken from co-cultures with unhealthy BM-MSCs ($2.37 \times 10^5 \pm 7.38 \times 10^3_{\text{SEM}}$) and those taken from 'none' (chondrocyte-only) cultures ($2.86 \times 10^5 \pm 1.13 \times 10^4_{\text{SEM}}$; $p = 0.046$). There was no significant difference, at day 14, between scaffolds taken from co-culture with healthy BM-MSCs ($2.45 \times 10^5 \pm 1.18 \times 10^4_{\text{SEM}}$) and those taken from either the unhealthy ($p = 1.00$) nor chondrocyte-only conditions ($p = 0.153$). At day 21, there was a significant difference in mean chondrocyte number in scaffolds taken from

the no BM-MSC (none) condition ($3.82 \times 10^5 \pm 1.61 \times 10^4_{SEM}$) and those taken from both the healthy ($2.91 \times 10^5 \pm 2.19 \times 10^4_{SEM}$; $p < 0.001$) and unhealthy ($3.09 \times 10^5 \pm 2.19 \times 10^4_{SEM}$; $p < 0.001$) co-cultures. There was no significant difference at this timepoint between the healthy and unhealthy conditions ($p = 1.00$).

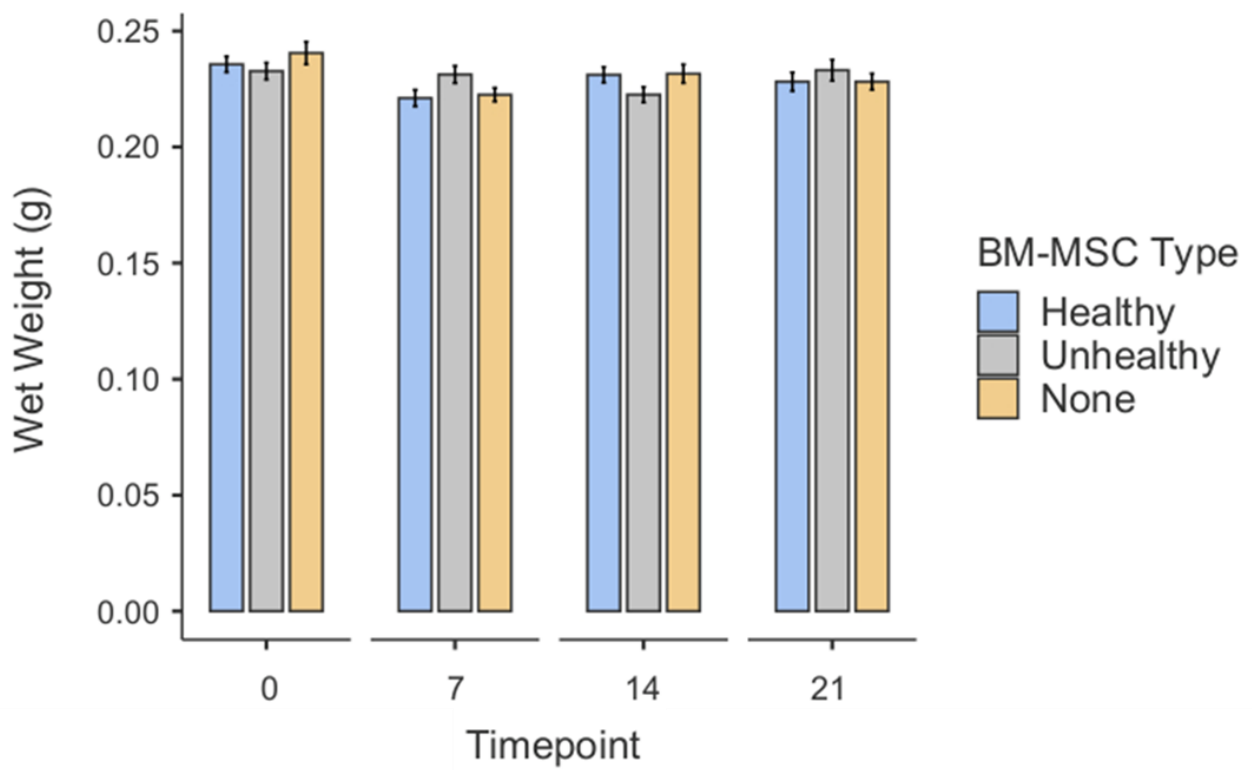


Figure 3-25: Mean wet weight of the agarose-chondrocyte scaffolds removed from the co-culture at the various timepoints. Error bars represent the standard error of the mean.

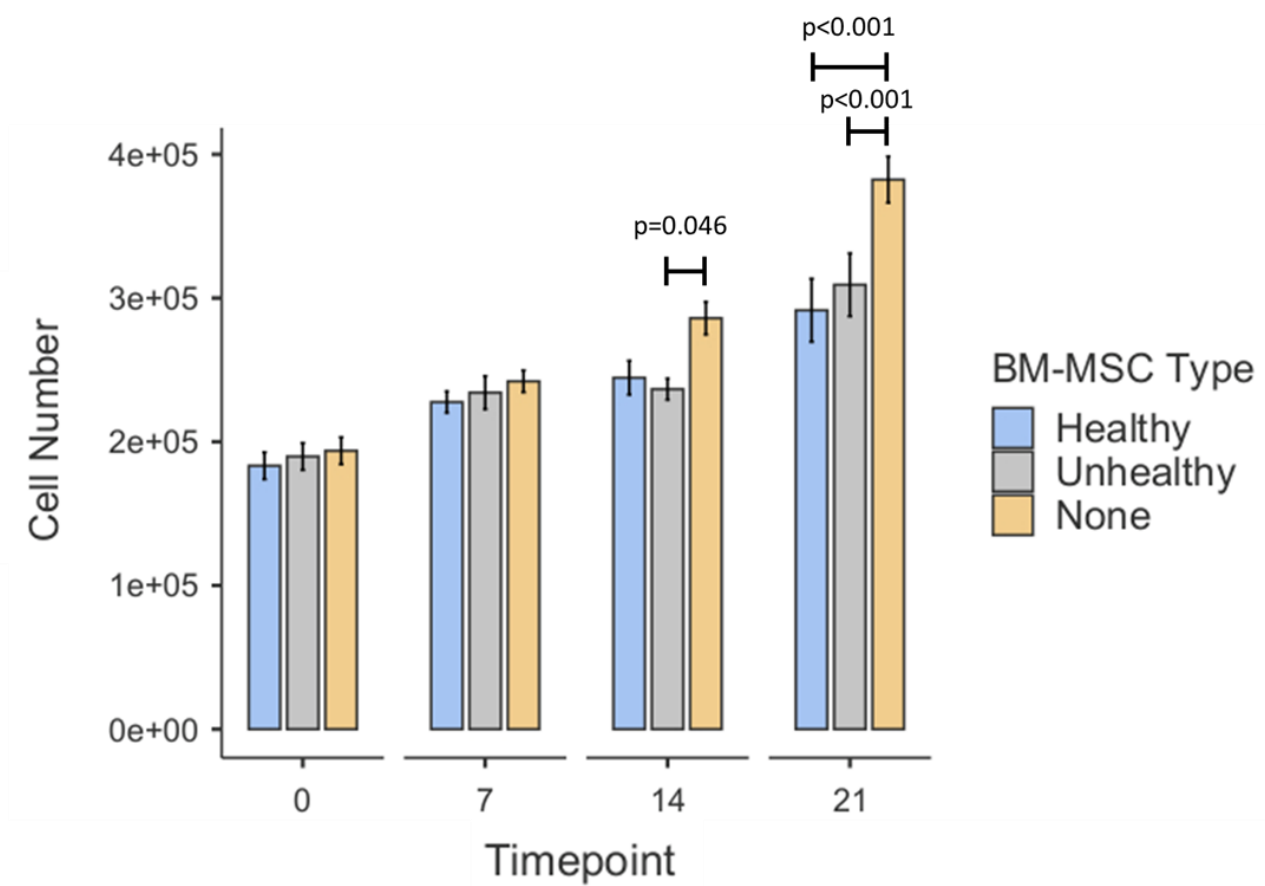


Figure 3-26: Mean chondrocyte number in scaffolds taken from the co-culture model at the four timepoints. Error bars represent standard error of mean. Significant differences are indicated by horizontal bars.

3.3.3.3.1.3.2 *Total Glycosaminoglycan (GAG) Content*

The mean GAG content of the scaffolds, across all conditions, increased over time with significant differences between day 0 ($9.09\mu\text{g} \pm 0.16_{\text{SEM}}$) and day 7 ($42.1\mu\text{g} \pm 1.09_{\text{SEM}}$; $p < 0.001$), between day 7 and day 14 ($78.7\mu\text{g} \pm 2.94_{\text{SEM}}$; $p < 0.001$) and between day 14 and day 21 ($129\mu\text{g} \pm 5.83_{\text{SEM}}$; $p < 0.001$; Figure 3-27).

Post hoc testing provided more detailed comparisons between conditions at individual timepoints. At day 0 and at day 7, there was no significant difference in mean total GAG between any of the conditions (all $p = 1.00$). At day 14 the mean total GAG content of the chondrocyte-only control scaffolds ($91.5\mu\text{g} \pm 4.41_{\text{SEM}}$) was significantly higher than that in scaffolds from both the healthy condition ($72.2\mu\text{g} \pm 3.21_{\text{SEM}}$; $p = 0.04$) and the unhealthy condition ($72.9\mu\text{g} \pm 6.13_{\text{SEM}}$; $p = 0.049$). There was no significant difference between the healthy and unhealthy conditions ($p = 1.00$). At day 21, the mean total GAG content of the chondrocyte-only control scaffolds ($153\mu\text{g} \pm 6.65_{\text{SEM}}$) was significantly higher than those from the healthy co-culture ($127\mu\text{g} \pm 12.2_{\text{SEM}}$; $p = 0.002$) and the unhealthy co-culture ($106\mu\text{g} \pm 7.88_{\text{SEM}}$; $p < 0.001$). Moreover, the mean total GAG content of the healthy co-culture scaffolds was significantly higher than that of the unhealthy co-culture scaffolds ($p = 0.02$).

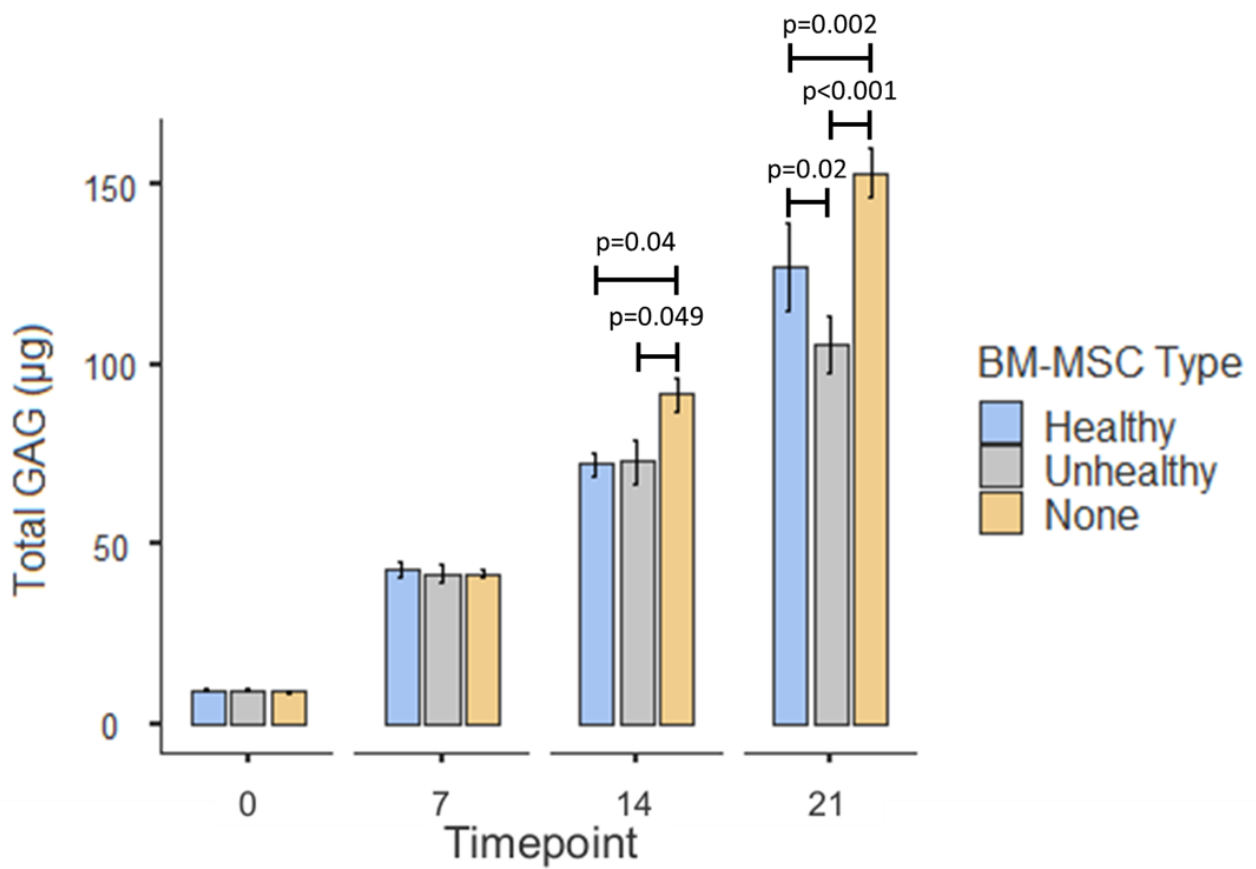


Figure 3-27: Mean total GAG content of agarose scaffolds taken from the co-culture model at the four timepoints. Error bars represent the standard error of the mean. Significant differences are indicated by horizontal bars.

3.3.3.3.1.3.3 GAG/Chondrocyte

The mean GAG content per chondrocyte was calculated for each scaffold, and then the mean for each condition at each timepoint was calculated. The mean GAG/chondrocyte across all conditions increased over time with a significant increase between day 0 ($5.02 \times 10^{-5} \mu\text{g}/\text{cell} \pm 1.55 \times 10^{-6} \text{SEM}$) and day 7 ($1.82 \times 10^{-4} \mu\text{g}/\text{cell} \pm 4.39 \times 10^{-6} \text{SEM}$; $p < 0.001$), between day 7 and day 14 ($3.09 \times 10^{-4} \mu\text{g}/\text{cell} \pm 9.14 \times 10^{-6} \text{SEM}$; $p < 0.001$) and between day 14 and day 21 ($3.99 \times 10^{-4} \mu\text{g}/\text{cell} \pm 1.30 \times 10^{-5} \text{SEM}$; $p < 0.001$; Figure 3-28).

There was no significant difference in mean GAG/chondrocyte between conditions at day 0, day 7 nor day 14 (all $p = 1.00$). At day 21 the average GAG/chondrocyte was significantly higher in the scaffolds from the healthy co-culture ($4.37 \times 10^{-4} \mu\text{g}/\text{cell} \pm 2.69 \times 10^{-5} \text{SEM}$) than in those from the unhealthy co-culture ($3.52 \times 10^{-4} \mu\text{g}/\text{cell} \pm 2.19 \times 10^{-5} \text{SEM}$; $p < 0.001$). The average GAG/chondrocyte in the chondrocyte-only scaffolds was borderline significantly higher ($4.07 \times 10^{-4} \mu\text{g}/\text{cell} \pm 1.36 \times 10^{-5} \text{SEM}$; $p = 0.05$) than in the unhealthy co-cultured scaffolds but there was no significant difference between the chondrocyte-only scaffolds and the scaffolds co-cultured with healthy BM-MSCs ($p = 1.00$).

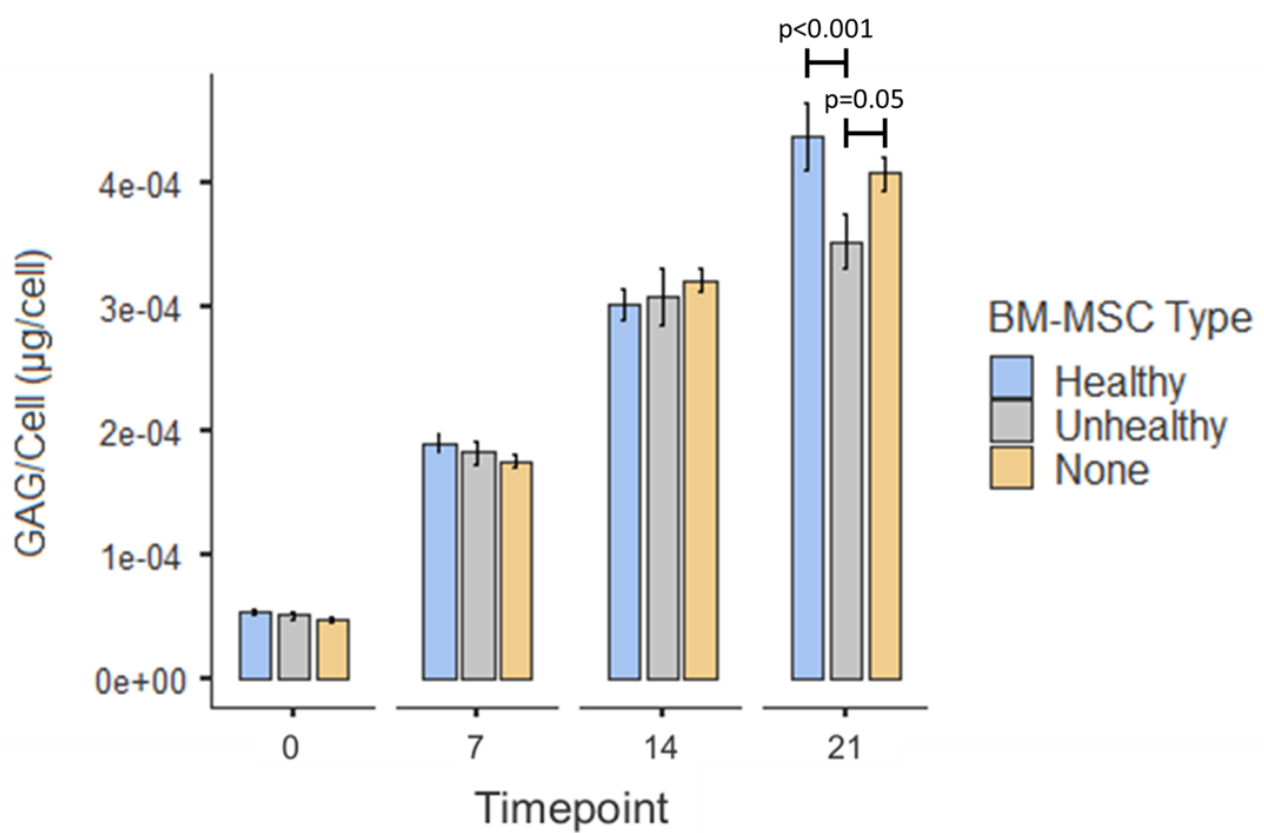


Figure 3-28: Mean GAG/chondrocyte of the scaffolds taken from the co-culture model at the four timepoints. Error bars represent the standard error of the mean. Significant differences are indicated by horizontal bars.

3.3.3.3.1.4 Gene Expression Analysis

qRT-PCR was used to assess the relative expression of nine genes in the chondrocytes encapsulated in agarose over the course of the co-culture model. The relative gene expression was then compared between conditions to assess the effect of healthy and unhealthy BM-MSCs, as well as no BM-MSCs ('none') on the gene expression profile of the encapsulated chondrocytes.

3.3.3.3.1.4.1 *SRY-Box Transcription Factor 9 (Sox9)*

None of the conditions demonstrated a biologically significant fold change in *sox9* expression (none: $-0.331 \pm 0.862_{SEM}$, healthy: $0.360 \pm 0.584_{SEM}$, unhealthy: $-0.884 \pm 0.586_{SEM}$; Figure 3-29 (top)).

3.3.3.3.1.4.2 *Collagen type 2 alpha 1 (COL2A1)*

All conditions demonstrated a biologically significant downregulation of *COL2A1* between day 0 and day 21 (Figure 3-29 (bottom)). There was a significantly greater downregulation of *COL2A1* in the unhealthy condition ($-32.8 \pm 12.9_{SEM}$) compared to both the healthy ($-7.82 \pm 4.46_{SEM}$; $p < 0.001$) and chondrocyte-only ($-2.32 \pm 0.74_{SEM}$; $p < 0.001$) conditions. There was no significant difference in relative expression of *COL2A1* between the healthy and the chondrocyte-only control ($p = 0.069$).

3.3.3.3.1.4.3 *Aggrecan (ACAN)*

A biologically significant upregulation of *ACAN* from day 0, to day 21 was observed in all conditions (Figure 3-30 (top)). The chondrocytes from the co-culture with unhealthy BM-MSCs ($1.51 \pm 0.51_{SEM}$) showed a significantly lower upregulation of *ACAN* between day 0 and day 21 than both the healthy ($4.05 \pm 0.49_{SEM}$, $p = 0.002$) and no BM-MSC ($3.57 \pm 0.36_{SEM}$; $p = 0.018$) conditions. There was no significant difference in *ACAN* fold change between the

scaffolds from the healthy co-culture and those from the no BM-MSC control condition (p=0.624).

3.3.3.3.1.4.4 *Activin receptor-like kinase 1 (ALK1)*

There was biologically significant upregulation of *ALK1* between day 0 and day 21 in the scaffolds taken from the healthy co-culture ($4.44 \pm 1.02_{SEM}$), unhealthy co-culture ($5.07 \pm 1.21_{SEM}$) and in the no BM-MSC control ($3.83 \pm 0.46_{SEM}$). There was no significant difference in fold change between any of the conditions: between healthy and unhealthy conditions (p=0.749), between healthy and chondrocyte-only conditions (p=0.942) nor between the unhealthy and chondrocyte-only control (p=0.531; Figure 3-30 (bottom)).

3.3.3.3.1.4.5 *Collagen type 10 alpha 1 (COL10A1)*

All conditions demonstrated biologically significant upregulation of *COL10A1* between day 0 and day 21 of the co-culture model (Figure 3-31 (top)). There was no significant difference between the healthy ($62.0 \pm 28.7_{SEM}$) and unhealthy conditions ($84.1 \pm 34.5_{SEM}$; p=0.595), between the healthy condition and the chondrocyte-only control ($85.0 \pm 41.1_{SEM}$; p=0.720), nor between the unhealthy and chondrocyte-only conditions (p=0.985).

3.3.3.3.1.4.6 *Matrix metalloproteinase-3 (MMP-3)*

Chondrocytes from all conditions demonstrated biologically significant upregulation of *MMP3* over the course of the co-culture (Figure 3-31 (bottom)). There was no significant difference in relative *MMP-3* expression between any of the conditions: between healthy ($11.4 \pm 2.72_{SEM}$) and unhealthy ($9.13 \pm 1.82_{SEM}$; p=0.517) conditions, between healthy and chondrocyte-only ($9.90 \pm 1.44_{SEM}$; p=0.965) conditions, nor between unhealthy and chondrocyte-only conditions (p=1.00)

3.3.3.3.1.4.7 *Matrix metalloproteinase-13 (MMP-13)*

Chondrocytes from all conditions demonstrated biologically significant upregulation of *MMP-13* over the course of the co-culture (Figure 3-32 (top)). There was no significant difference in fold change of *MMP-13* expression between the chondrocytes co-cultured with healthy BM-MSCs ($69.9 \pm 33.4_{SEM}$) and those cultured with unhealthy BM-MSCs ($61.6 \pm 29.4_{SEM}$; $p=0.977$), between those cultured with healthy BM-MSCs and those cultured with no BM-MSCs ($68.2 \pm 18.0_{SEM}$; $p=0.898$), nor between those cultured with unhealthy BM-MSCs and those cultured with no BM-MSCs ($p=0.805$).

3.3.3.3.1.4.8 *A disintegrin and metalloproteinase with thrombospondin motifs-4 (ADAMTS-4)*

None of the conditions demonstrated a biologically relevant fold change in *ADAMTS4* expression between day 0 and day 21 (healthy: $1.18 \pm 0.617_{SEM}$, unhealthy: $-0.377 \pm 0.545_{SEM}$, none: $-1.42 \pm 0.459_{SEM}$; Figure 3-32 (bottom)).

3.3.3.3.1.4.9 *A disintegrin and metalloproteinase with thrombospondin motifs-5 (ADAMTS5)*

All conditions showed biologically significant downregulation of *ADAMTS5* over the course of the co-culture model. There was no statistically significant difference in fold change in *ADAMTS5* expression between any of the conditions: between the healthy ($-11.3 \pm 1.57_{SEM}$) and unhealthy ($-9.69 \pm 1.25_{SEM}$; $p=0.924$) conditions, between the healthy and chondrocyte-only ($-8.56 \pm 0.955_{SEM}$; $p=0.244$) conditions, nor between the unhealthy and chondrocyte-only conditions ($p=0.427$; Figure 3-33).

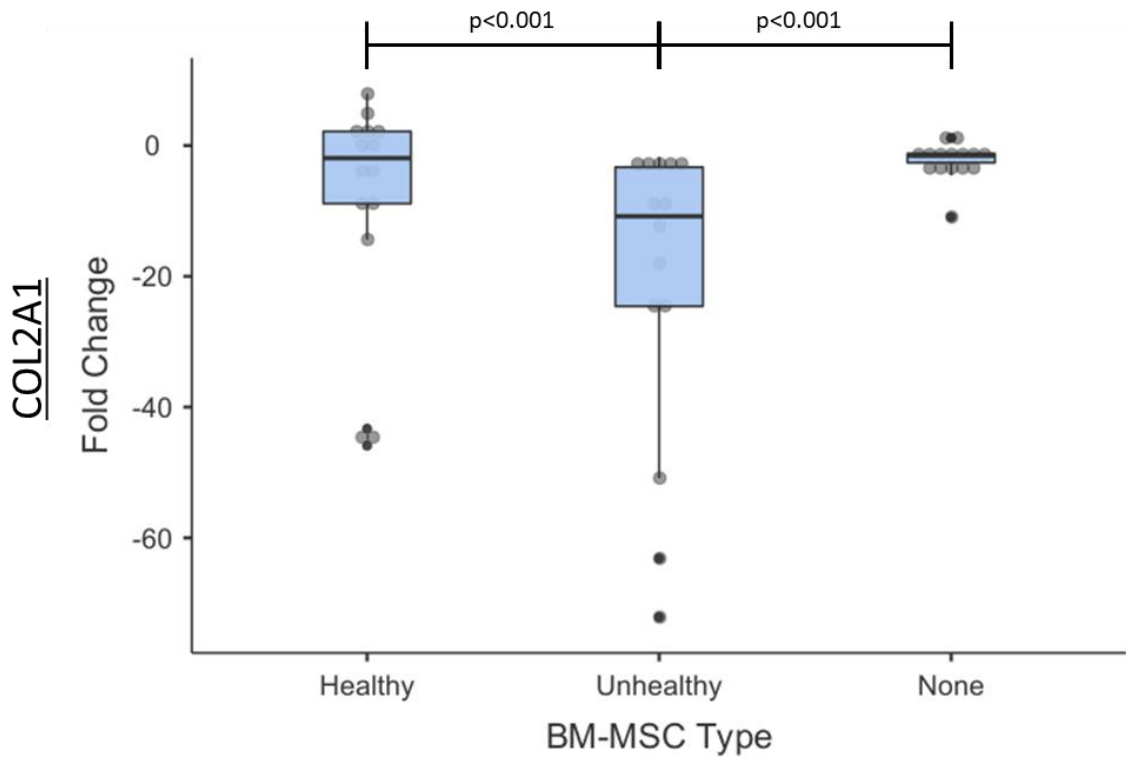
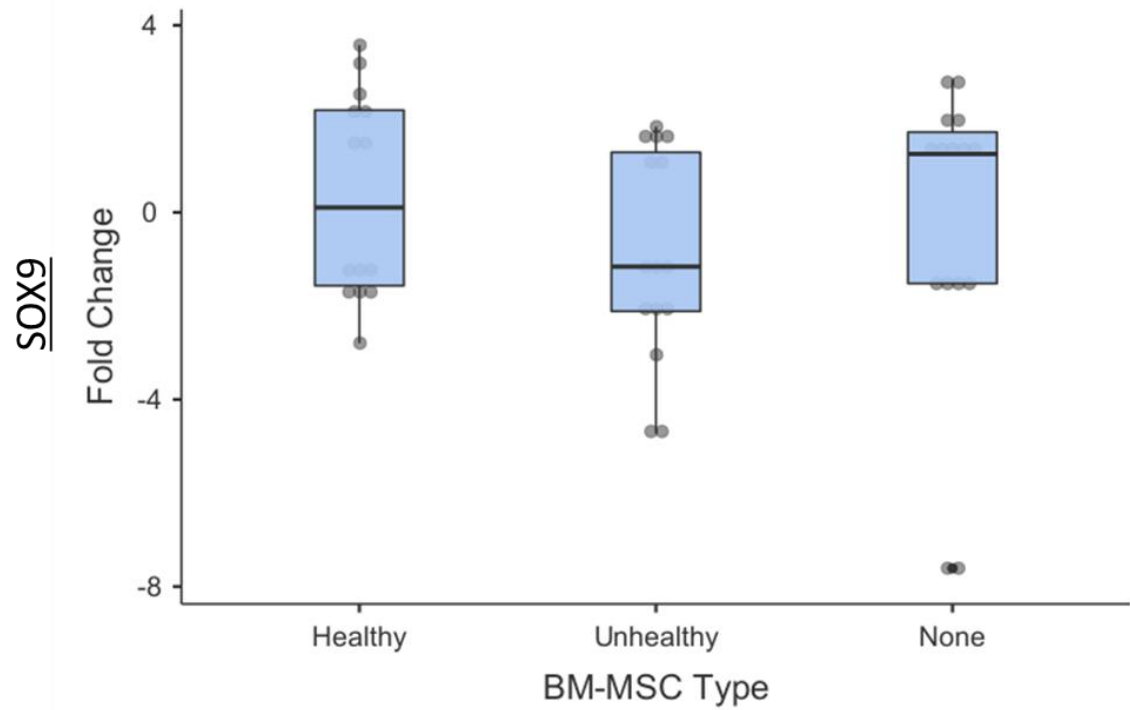


Figure 3-29: Relative fold change of *SOX9* (top) and *COL2A1* (bottom) between day 0 and day 21 of the co-culture. Error bars represent the standard error of the mean. Significant differences are indicated by horizontal bars.

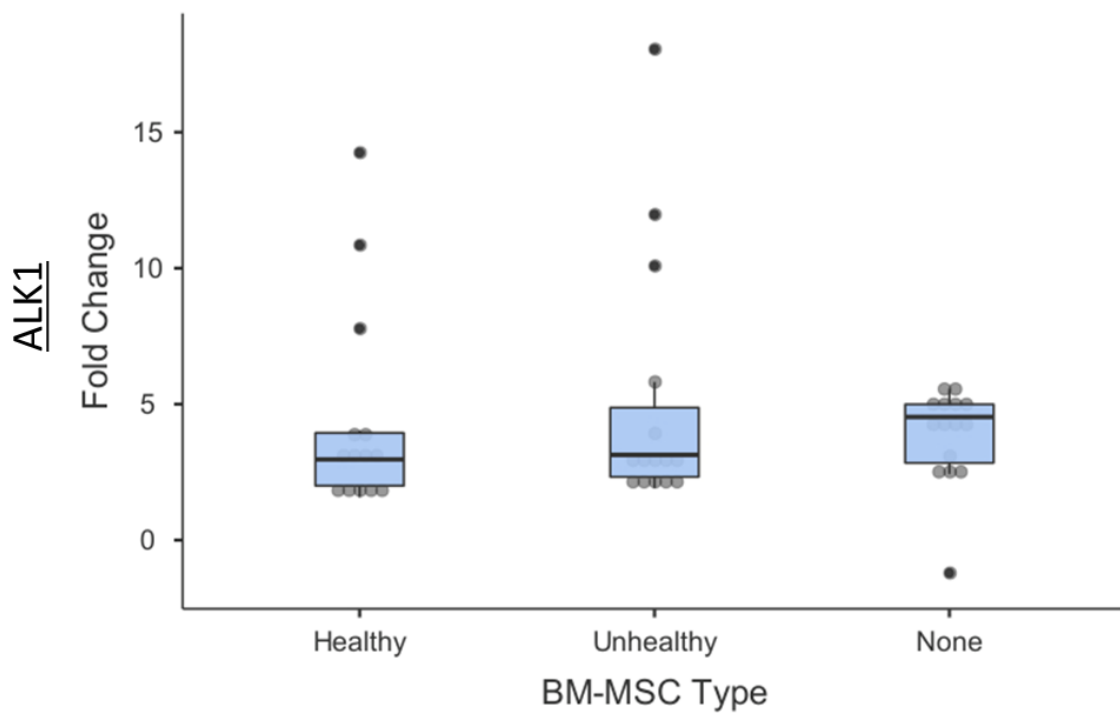
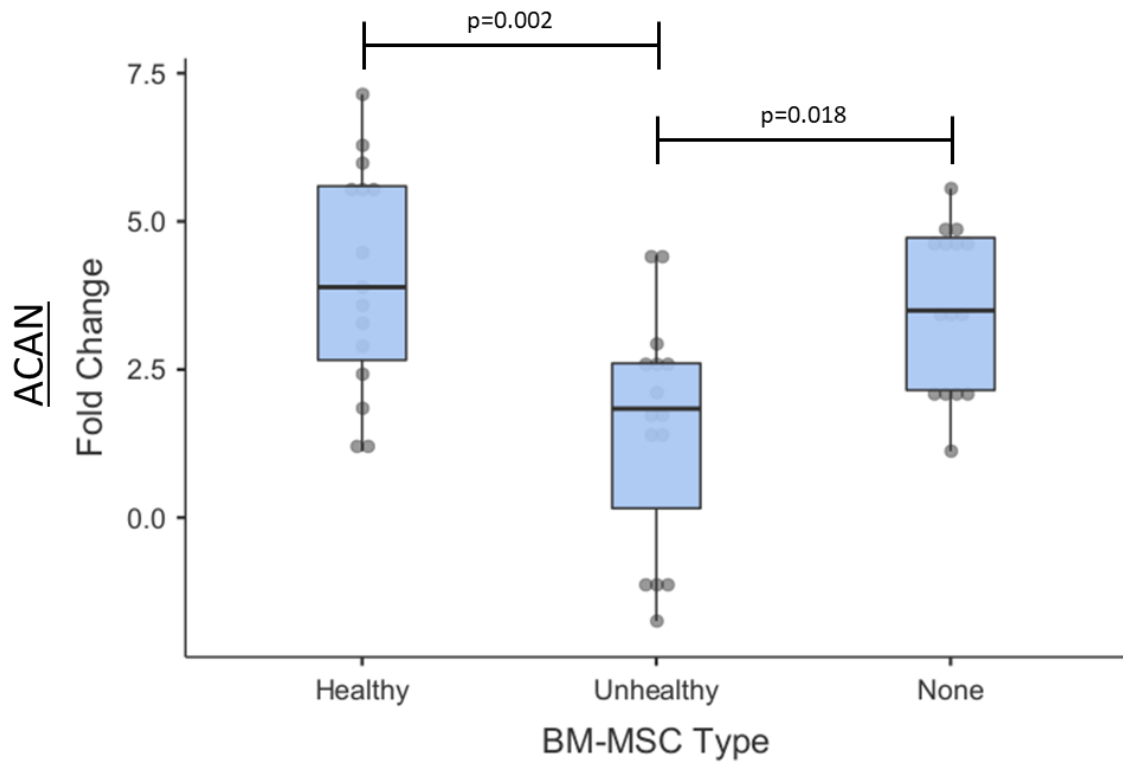


Figure 3-30: Relative fold change of ACAN (top) and ALK1 (bottom) between day 0 and day 21 of the co-culture. Error bars represent the standard error of the mean. Significant differences are indicated by horizontal bars.

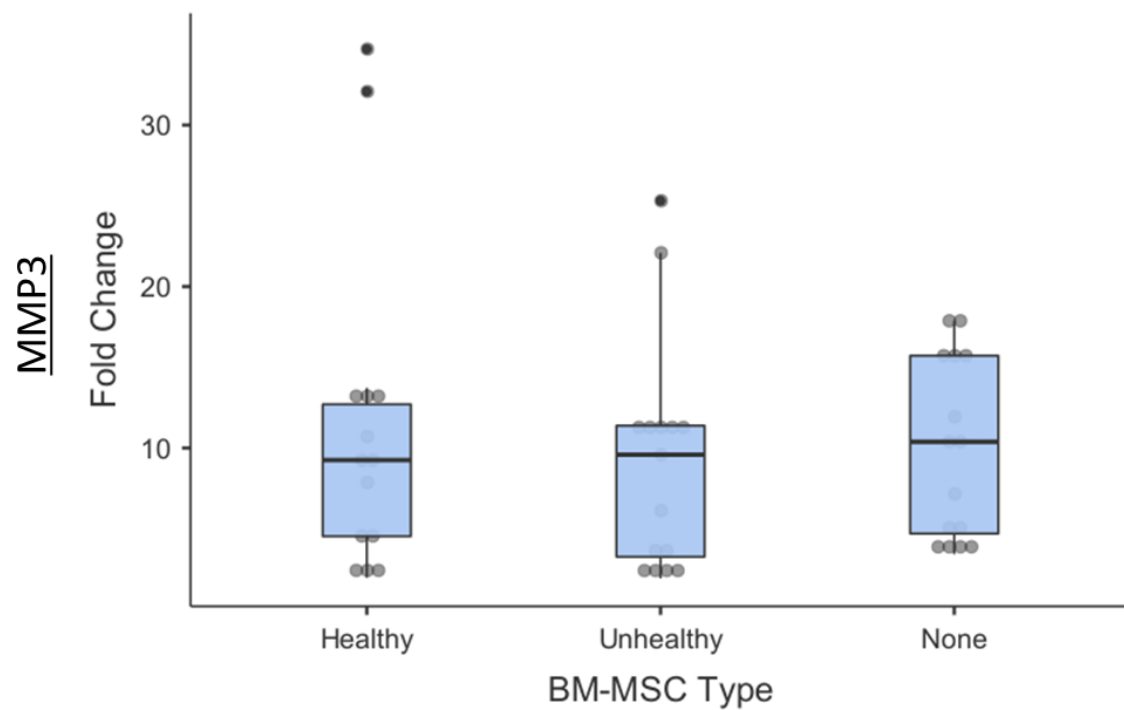
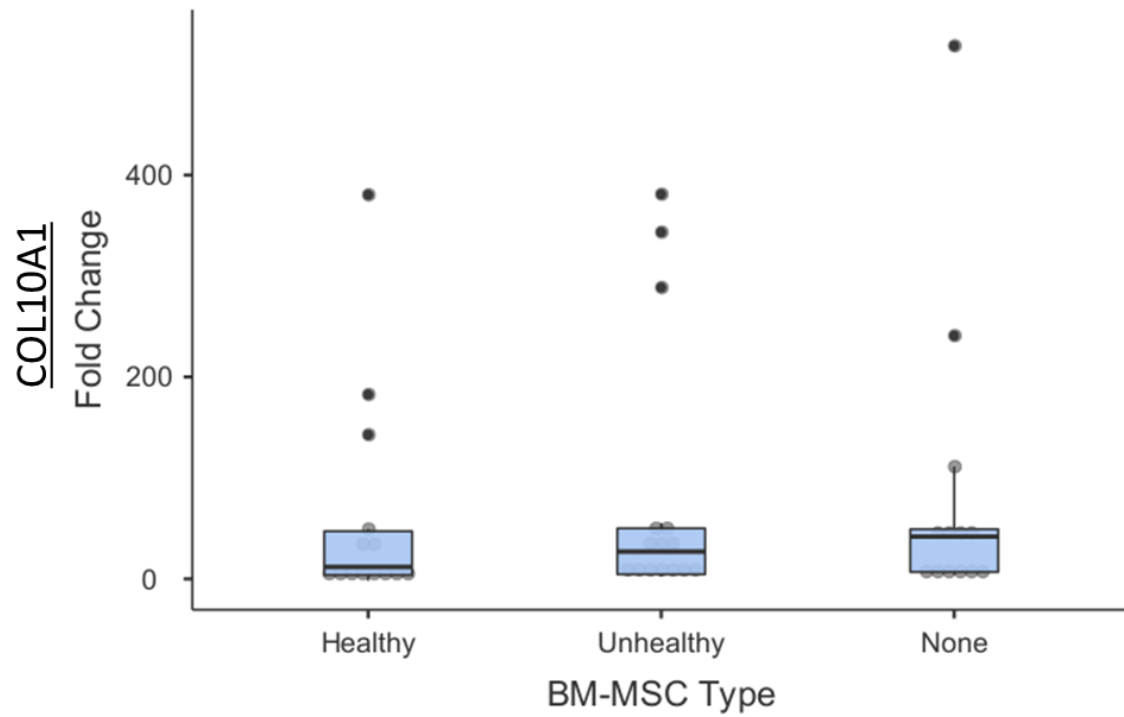


Figure 3-31: Relative fold change of *COL10A1* (top) and *MMP-3* (bottom) between day 0 and day 21 of the co-culture. Error bars represent the standard error of the mean. Significant differences are indicated by horizontal bars.

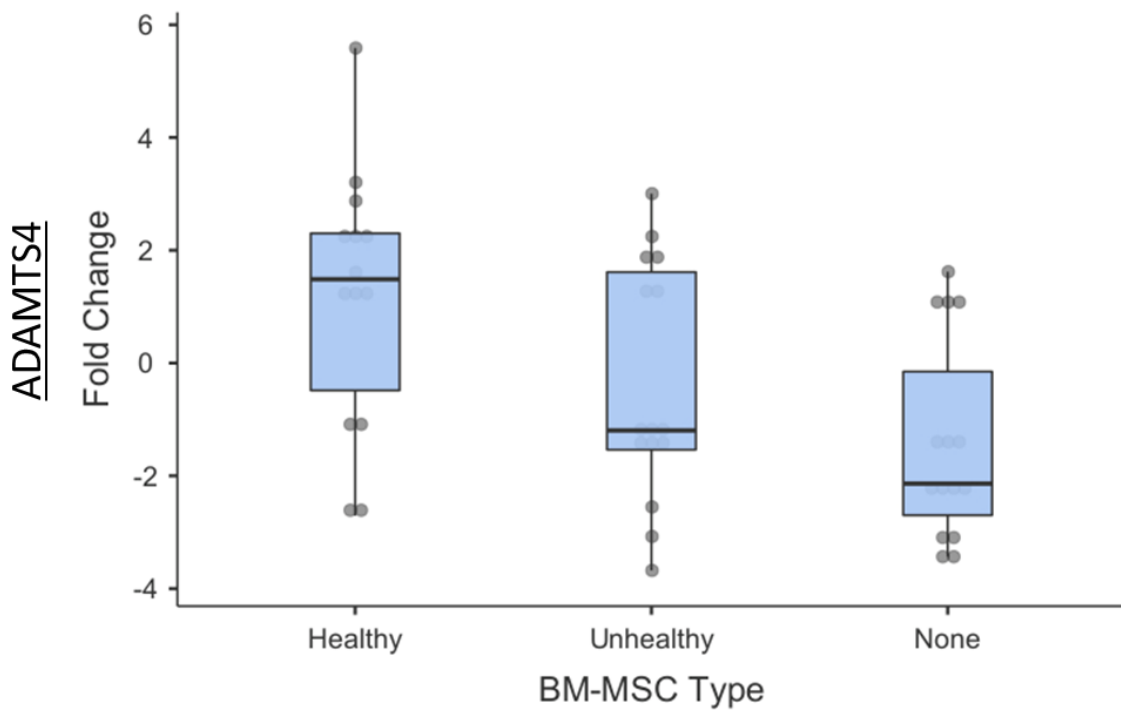
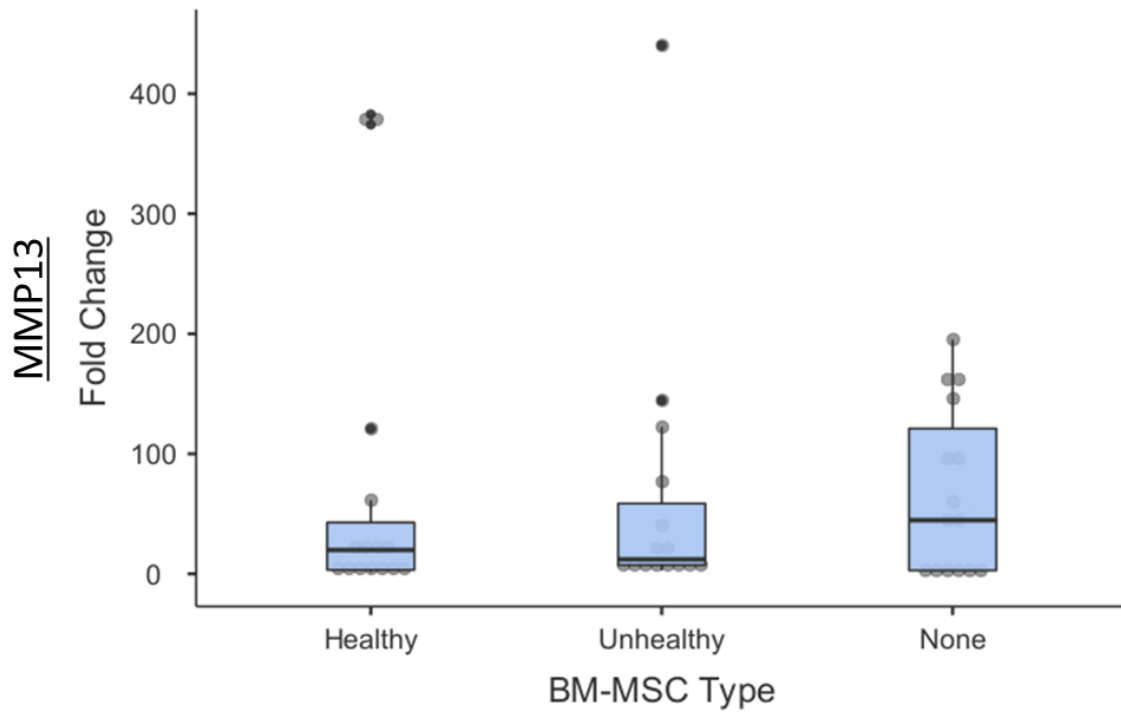


Figure 3-32: Relative fold change of MMP-13 (top) and ADAMTS4 (bottom) between day 0 and day 21 of the co-culture. Error bars represent the standard error of the mean. Significant differences are indicated by horizontal bars.

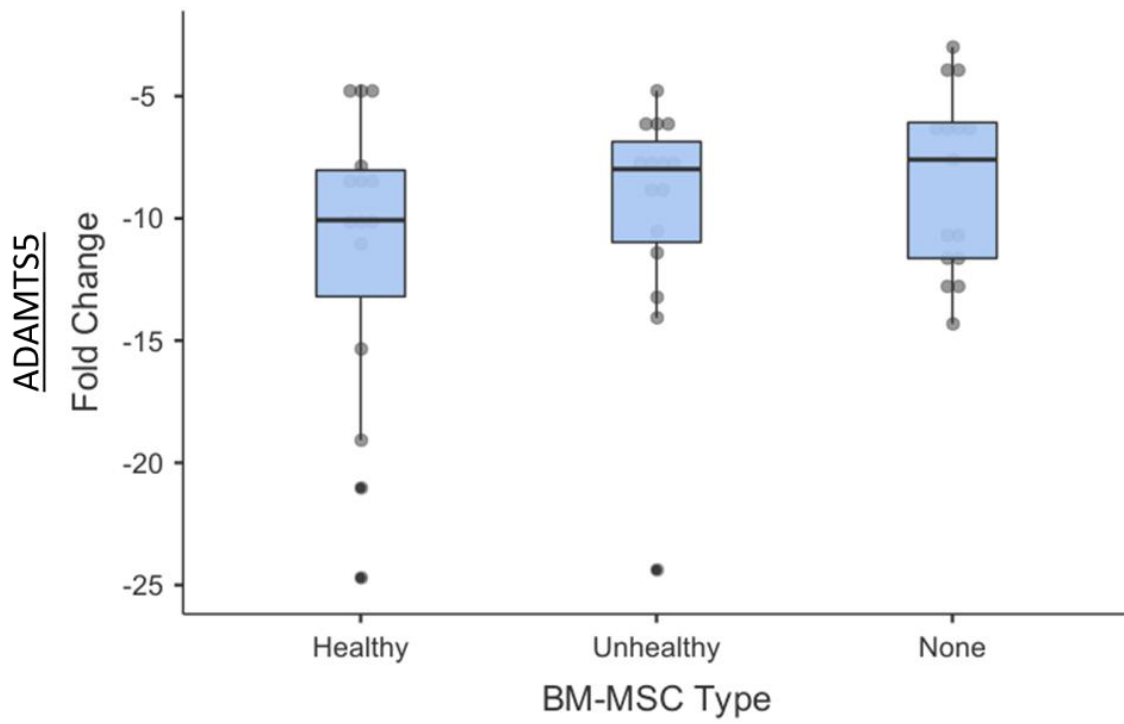


Figure 3-33: Relative fold change of *ADAMTS5* between day 0 and day 21 of the co-culture. Error bars represent the standard error of the mean. Significant differences are indicated by horizontal bars.

3.3.3.3.2 Conditioned Media

At each timepoint, conditioned media was collected from the 24-well plates and pooled between conditions.

3.3.3.3.2.1 ELISAs

ELISAs were carried out on conditioned media collected at day 0, Day 7 and day 21 from co-cultures containing healthy and unhealthy BM-MSCs as well as the chondrocyte only control (no BM-MSCs). The lower limit of detection for each analyte was calculated is shown in table 3-16.

3.3.3.3.2.1.1 *Interleukin-10 (IL-10)*

All conditioned media samples contained a concentration of IL-10 that was not detectable by the assay (below the concentration of the blank standard).

3.3.3.3.2.1.2 *Matrix Metalloproteinase-1 (MMP-1)*

A similar general pattern of MMP-1 concentration was demonstrated in all conditions over the course of the study, with an increase between day 0 and day 7, and a subsequent decrease between day 7 and day 21. At day 0, mean levels of MMP-1 were low all conditions, with no significant difference in MMP-1 concentration between conditioned media from the co-culture containing healthy BM-MSCs and unhealthy BM-MSCs, between the healthy and chondrocyte-only condition nor between the unhealthy and chondrocyte-only condition (all $p=1.00$; Figure 3-34). At day 7, the mean concentration of MMP-1 in the conditioned media from the chondrocyte only control ($883 \text{ pg/ml} \pm 260_{\text{SEM}}$) was significantly higher than in the conditioned media from both the healthy ($532 \text{ pg/ml} \pm 116_{\text{SEM}}$, $p=0.031$) and unhealthy ($351 \text{ pg/ml} \pm 119_{\text{SEM}}$, $p=0.01$) BM-MSC co-cultures. At day 21, there was no significant difference between conditions. Across all conditions, there was an overall

significant increase in mean MMP-1 concentration in the conditioned media between day 0 and day 7 ($p < 0.001$) and a significant decrease between day 7 and day 21 ($p < 0.001$). There was no significant difference in this pattern between conditions ($p = 0.058$).

3.3.3.3.2.1.3 *Matrix Metalloproteinase-13 (MMP-13)*

For all conditions, there was a consistent pattern in MMP-13 concentration over time (Figure 3-35), with a significant increase in mean MMP-13 concentration in the conditioned media across all conditions between day 0 and day 7 ($p < 0.001$), and a significant decrease between day 7 and day 21 ($p = 0.015$). There was no significant difference in mean MMP-13 concentration in the conditioned media between conditions at any of the individual timepoints (all $p = 1.00$).

3.3.3.3.2.1.4 *Transforming Growth Factor Beta 1 (TGF- β 1)*

The concentration of TGF- β 1 was very low in all conditions at day 0 and day 7, with majority of conditioned media samples were below the detection limit and therefore were replaced with the non-detect value (1.7 pg/ml). At day 0 and day 7, there was no significant difference in mean TGF- β 1 concentration in conditioned media between conditions (all $p = 1.00$; Figure 3-36). At day 21, there was a significant difference between the mean concentration of TGF- β 1 in conditioned media taken from the healthy BM-MSCs ($1178 \text{ pg/ml} \pm 589_{\text{SEM}}$) and that taken from the unhealthy BM-MSCs ($141 \text{ pg/ml} \pm 7.22_{\text{SEM}}$; $p = 0.014$) co-cultures and from the chondrocyte only control ($1.7 \text{ pg/ml} \pm 0_{\text{SEM}}$; $p = 0.006$). Between day 7 and day 21, conditioned media collected from the co-culture with healthy BM-MSCs demonstrated a significant increase in mean TGF- β 1 concentration (day 7: $83.1 \text{ pg/ml} \pm 81.4_{\text{SEM}}$, day 21: $1178 \text{ pg/ml} \pm 589_{\text{SEM}}$; $p = 0.018$).

3.3.3.3.2.1.5 *Vascular Endothelial Growth Factor (VEGF)*

There was no detectable VEGF in the conditioned media of the chondrocyte only controls at any of the timepoints, nor in a number of the BM-MSC samples and therefore these concentrations were replaced with the non-detect value (1.37 pg/ml; Figure 3-37). There was no significant difference in the mean concentration of VEGF in the conditioned media for any of the conditions at any of the individual timepoints interrogated. There was also no significant difference in the mean concentration of VEGF between timepoints for any of the conditions.

Table 3-16: The lower limit of detection for each of the analytes quantified in the conditioned media using ELISAs.

Analyte	Lower limit of detection (pg/ml)
IL-10	1.682932
MMP-1	3.26971
MMP-13	2.792356
TGF- β 1	1.69629
VEGF	1.369305

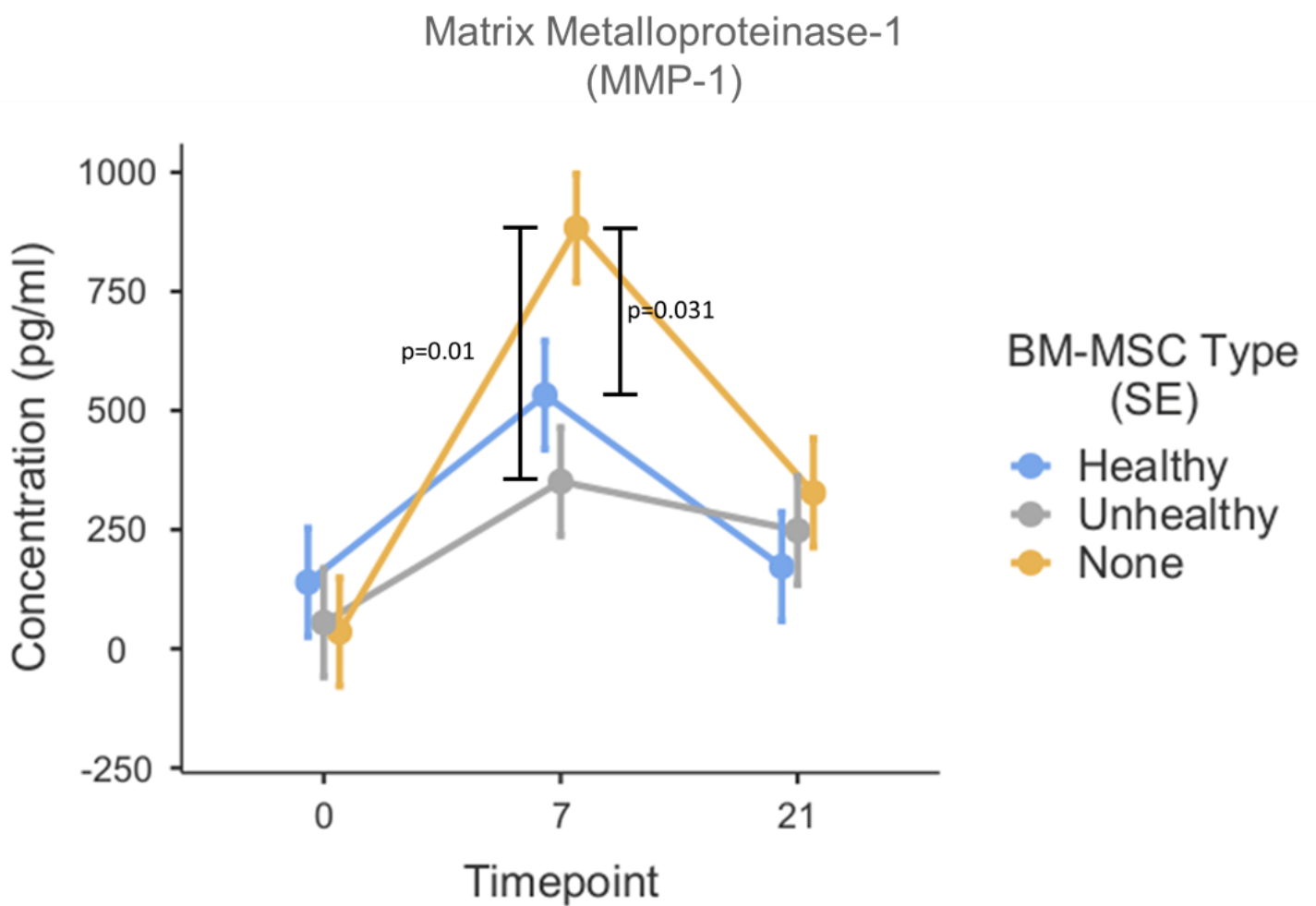


Figure 3-34: MMP-1 concentration in conditioned media at day 0, day 7 and day 21 of the co-culture model, as determined by ELISA. Error bars represent the standard error of the mean. Significant differences are indicated by vertical bars.

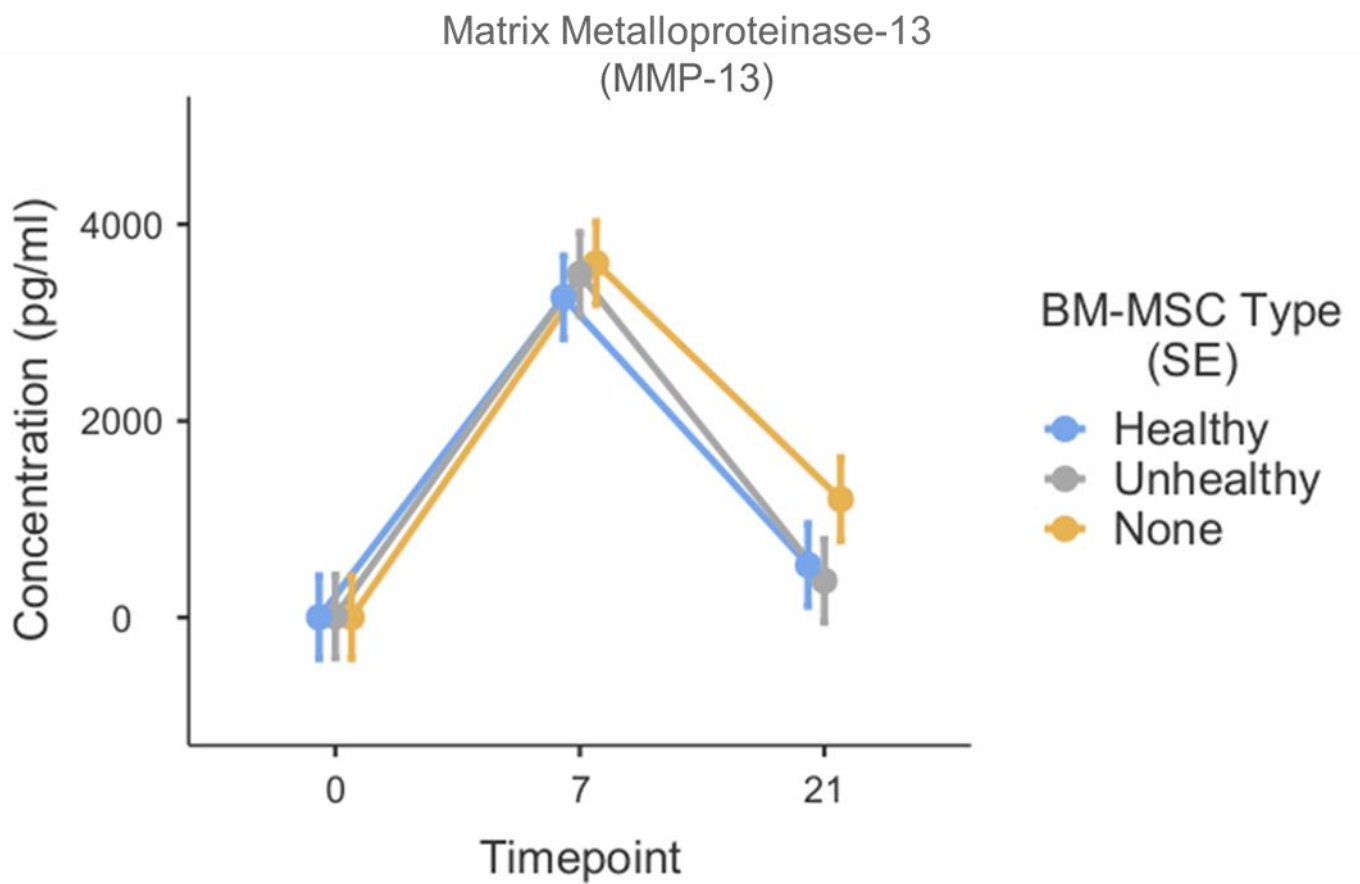


Figure 3-35: Mean MMP-13 concentration in conditioned media at day 0, day 7 and day 21 of the co-culture model, as determined by ELISA. Error bars represent the standard error of the mean. Significant differences are indicated by vertical bars.

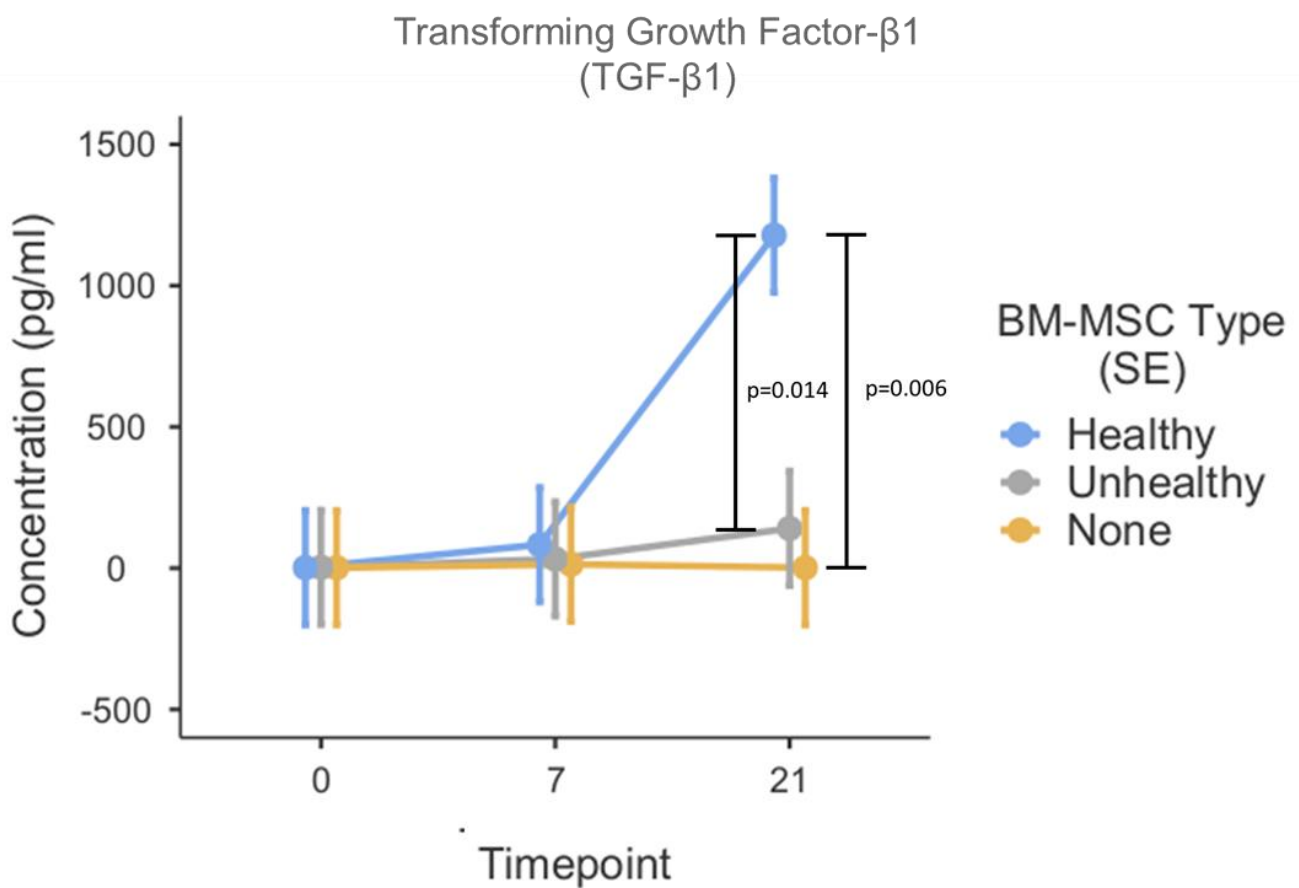


Figure 3-36: Mean TGF- β 1 concentration in conditioned media at day 0, day 7 and day 21 of the co-culture model, as determined by ELISA. Error bars represent the standard error of the mean. Significant differences are indicated by vertical bars.

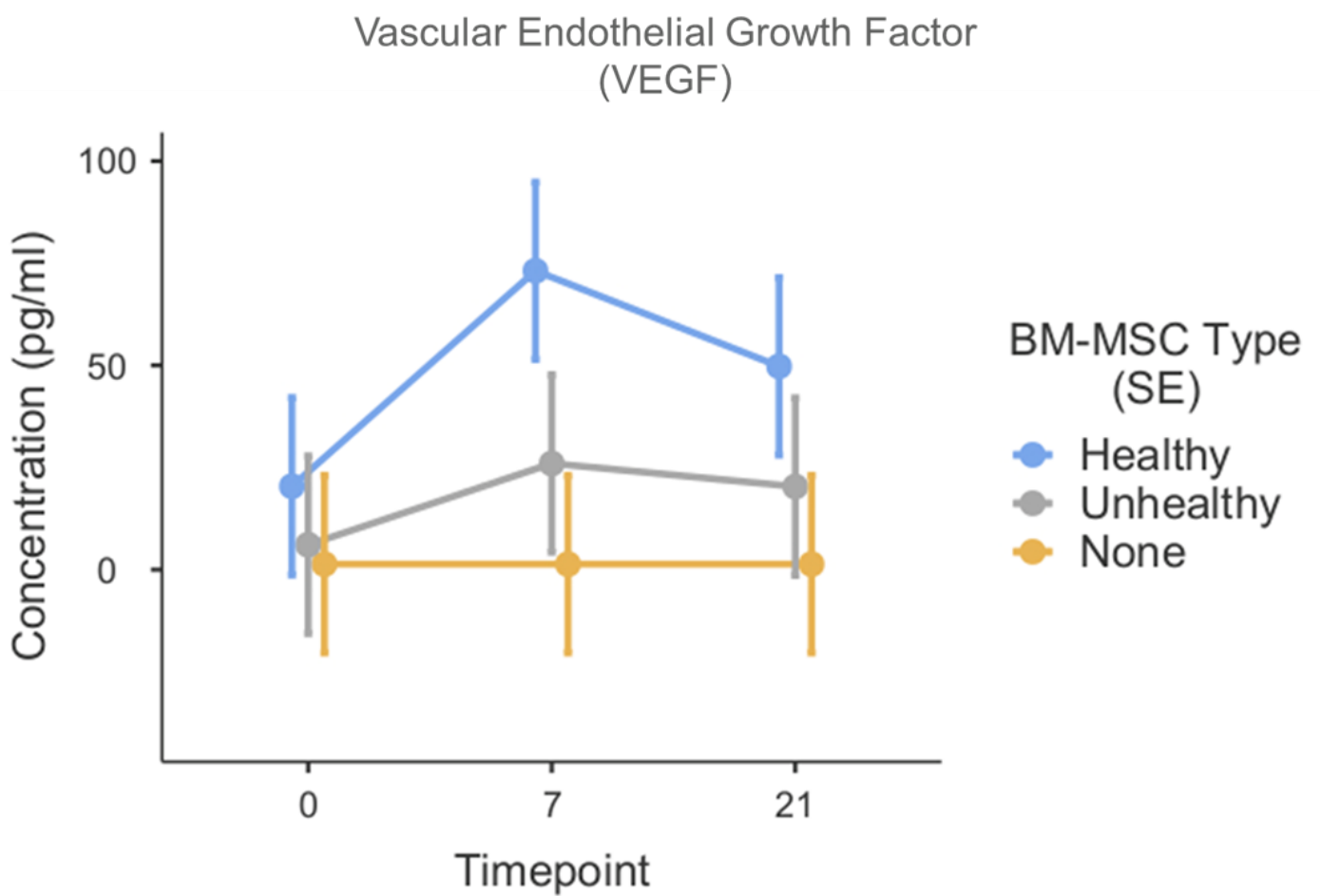


Figure 3-37: Mean VEGF concentration in conditioned media at day 0, day 7 and day 21 of the co-culture model, as determined by ELISA. Error bars represent the standard error of the mean. Significant differences are indicated by vertical bars.

3.3.3.3.3 Osteogenically Differentiated BM-MSCs

3.3.3.3.3.1 dsDNA Quantification

The mean dsDNA content of the BM-MSCs increased over time in both conditions, indicating a gradual increase in cell number. The mean dsDNA content increased from day 0 ($350.9\text{ng} \pm 37.9_{\text{SEM}}$), to day 7 ($484.4\text{ng} \pm 50.4_{\text{SEM}}$), but there was no evidence for statistical difference at this point ($p=0.166$). There was a statistically significant increase in mean dsDNA content between day 7 and day 14 ($651.4\text{ng} \pm 58.3_{\text{SEM}}$; $p=0.037$) and between day 14 and day 21 ($884.9\text{ng} \pm 86.5_{\text{SEM}}$; $p<0.001$). There was no significant difference in mean dsDNA content between conditions at any of the individual timepoints (all $p=1.00$), indicating that there was no difference in cell number (Figure 3-38).

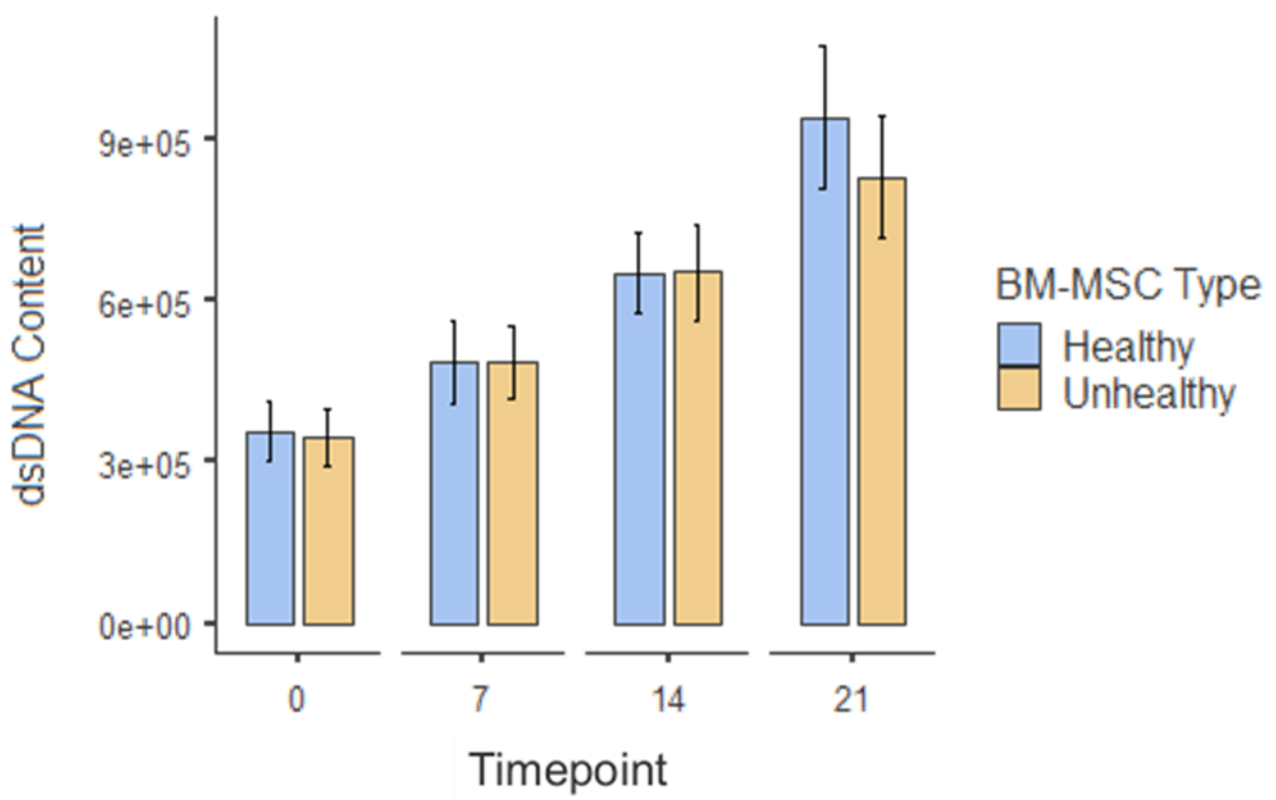


Figure 3-38: Mean dsDNA content for each of the two BM-MSC types in the co-culture model, over the course of the experiment. Error bars represent the standard error of the mean.

3.3.3.3.2 Gene Expression Profile

qRT-PCR was used to assess the relative expression of a number of genes in the two BM-
MSC types, over the course of the co-culture model. The relative gene expression was then
compared between the healthy and unhealthy BM-MSCs to try and identify differences in
their gene expression profiles.

3.3.3.3.2.1 *Alkaline phosphatase (ALPL)*

There was a slight downregulation of *ALPL* over the course of the co-culture, in both the
healthy ($-1.39 \pm 3.53_{SEM}$) and unhealthy ($-1.24 \pm 2.67_{SEM}$) BM-MSCs, but neither fold change
was biologically significant (Figure 3-39 (top)). There was no statistically significant
difference in relative expression between conditions.

3.3.3.3.2.2 *Bone morphogenic protein 2 (BMP2)*

There was a biologically significant down regulation of *BMP2* in both the healthy ($-6.35 \pm$
 7.78_{SEM}) and unhealthy ($-2.86 \pm 5.87_{SEM}$) BM-MSCs, over the course of the co-culture (Figure
3-39 (bottom)). There was no statistically significant difference in relative expression
between conditions.

3.3.3.3.2.3 *Collagen type 1 alpha 1 (COL1A1)*

Both the healthy ($1.32 \pm 2.17_{SEM}$) and unhealthy ($2.68 \pm 3.32_{SEM}$) BM-MSCs demonstrated
an upregulation of *COL1A1* between day 0 and day 21 of the co-culture, but this was only
biologically relevant in the healthy population (Figure 3-40 (top)). There was a statistically
significant difference in relative expression of *COL1A1* between the healthy and unhealthy
BM-MSCs ($p=0.003$).

3.3.3.3.2.4 *Bone gamma-carboxyglutamate (gla) protein (BGLAP) (Osteocalcin)*

Neither the healthy ($-0.874 \pm 2.19_{SEM}$), nor the unhealthy ($0.005 \pm 1.76_{SEM}$) BM-MSCs
demonstrated a biologically significant fold change in *BGLAP* expression over the course of

the co-culture (Figure 3-40 (bottom)). There was no statistically significant difference in relative expression between conditions.

3.3.3.3.2.5 *Secreted phosphoprotein 1 (SPP1) (Osteopontin)*

There was no biologically significant fold change in the expression of *SPP1* over time in either the healthy ($0.0572 \pm 3.18_{SEM}$) or the unhealthy ($0.633 \pm 2.01_{SEM}$) BM-MSCs (Figure 3-41 (top)). There was no statistically significant difference in relative expression between conditions.

3.3.3.3.2.6 *Runt-related transcription factor 2 (RUNX2)*

There was no biologically significant fold change in *RUNX2* expression in either the healthy ($1.39 \pm 1.99_{SEM}$) or the unhealthy ($1.16 \pm 1.74_{SEM}$) BM-MSCs (Figure 3-41 (bottom)). There was no statistically significant difference in relative expression between conditions.

3.3.3.3.3 Alkaline Phosphatase Staining

Alkaline phosphatase staining was positive in both the healthy and unhealthy BM-MSCs at all four timepoints. There was no observable difference in staining intensity between conditions or timepoints (data not shown).

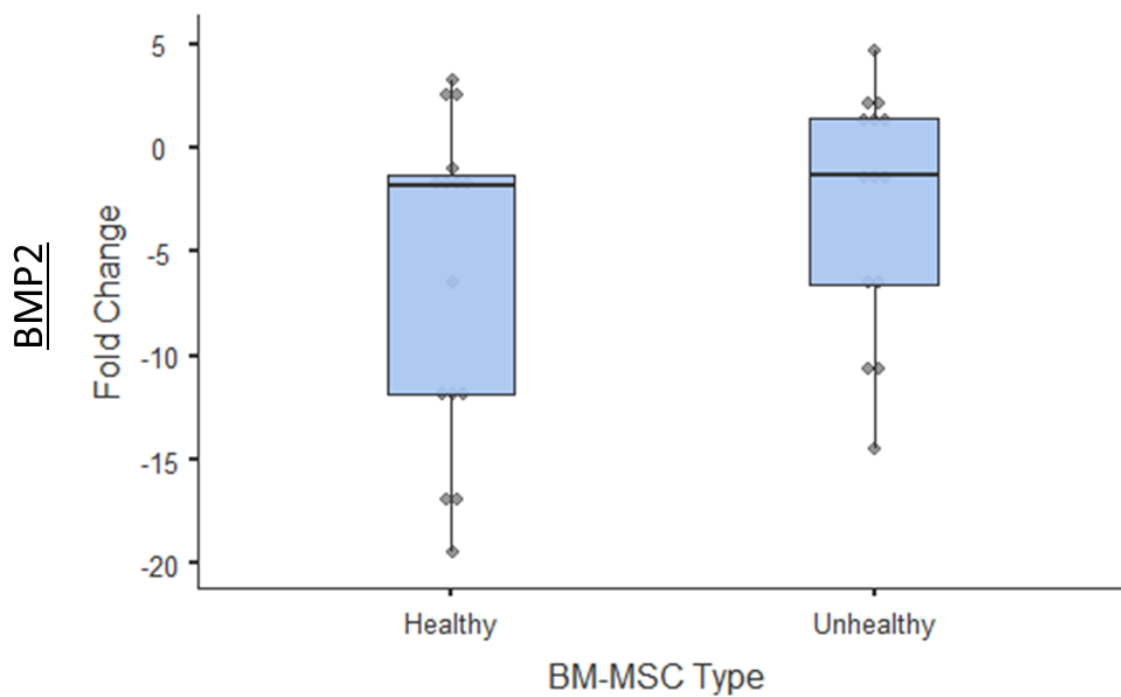
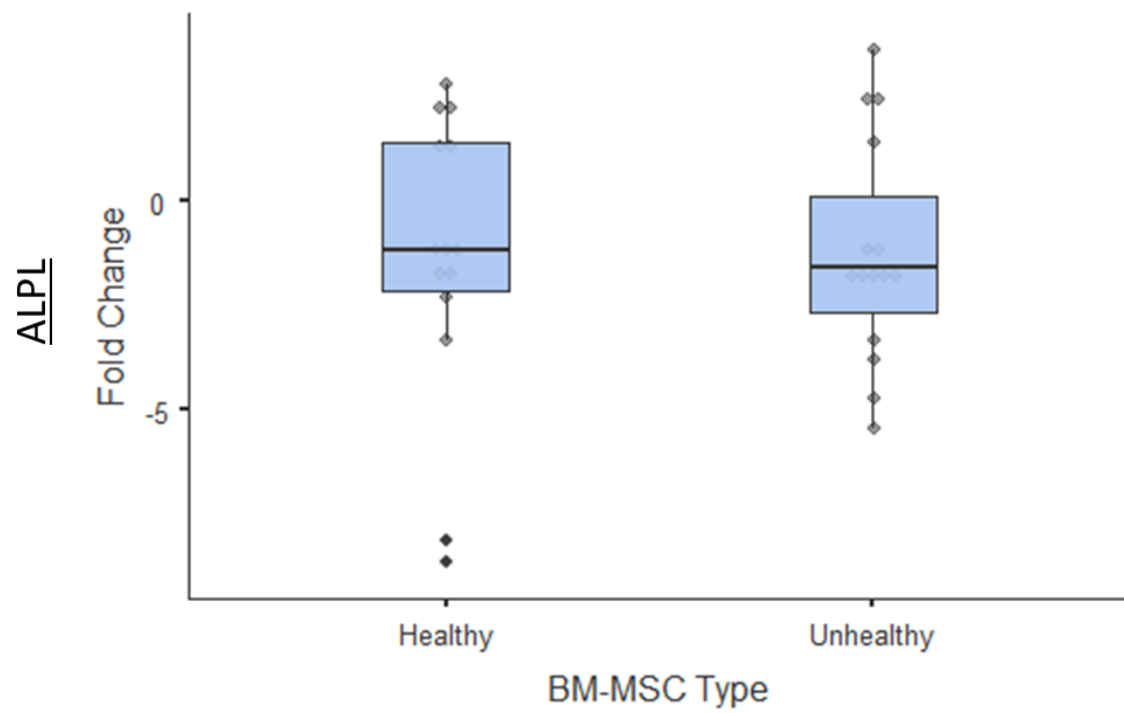


Figure 3-39: Relative fold change of *ALPL* (top) and *BMP2* (bottom) in BM-MSCs between day 0 and day 21 of the co-culture. Error bars represent the standard error of the mean. Significant differences are indicated by horizontal bars.

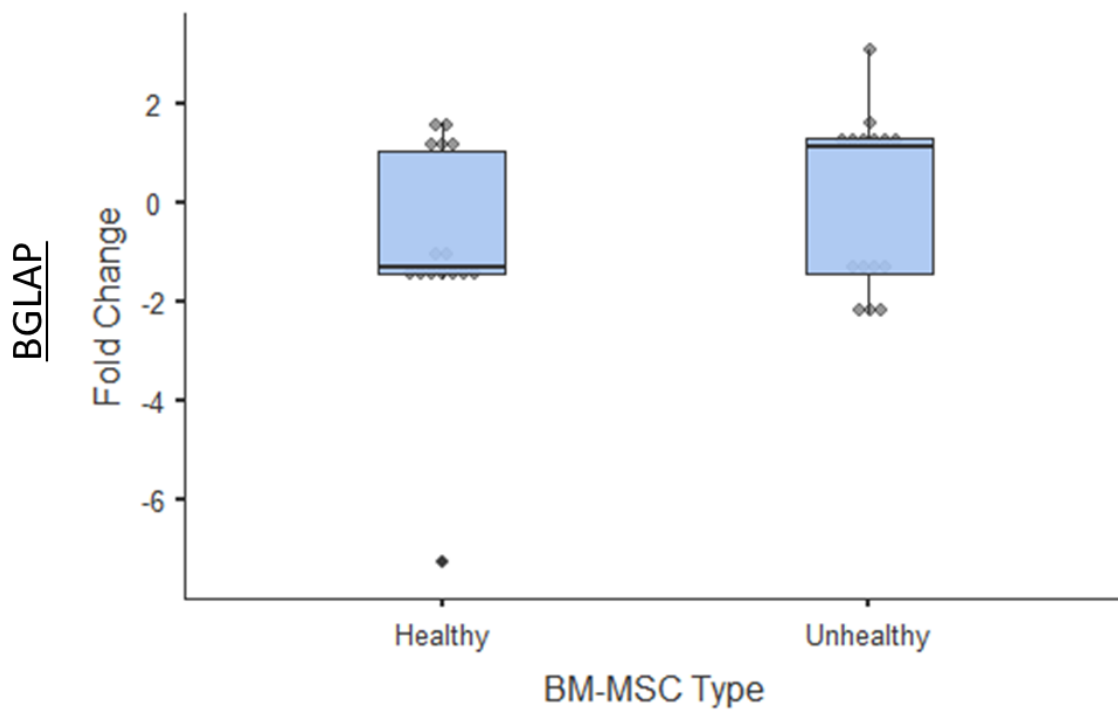
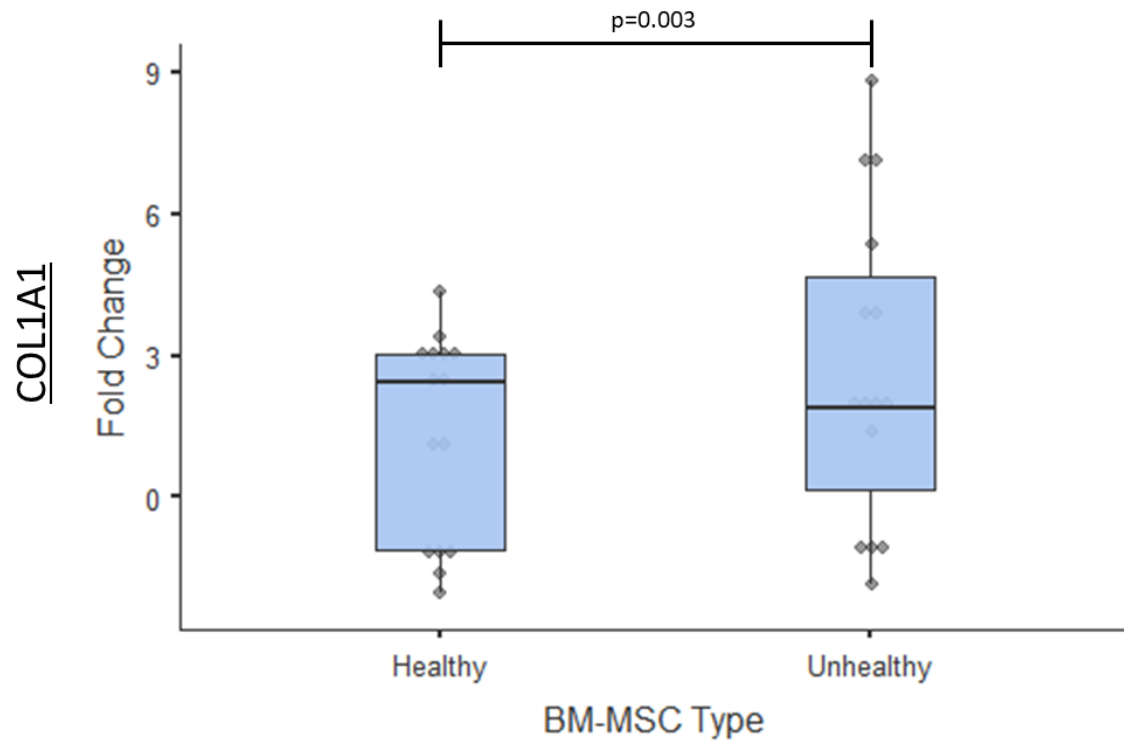


Figure 3-40: *Relative fold change of COL1A1 (top) and BGLAP (bottom) in BM-MSCs between day 0 and day 21 of the co-culture. Error bars represent the standard error of the mean. Significant differences are indicated by horizontal bars.*

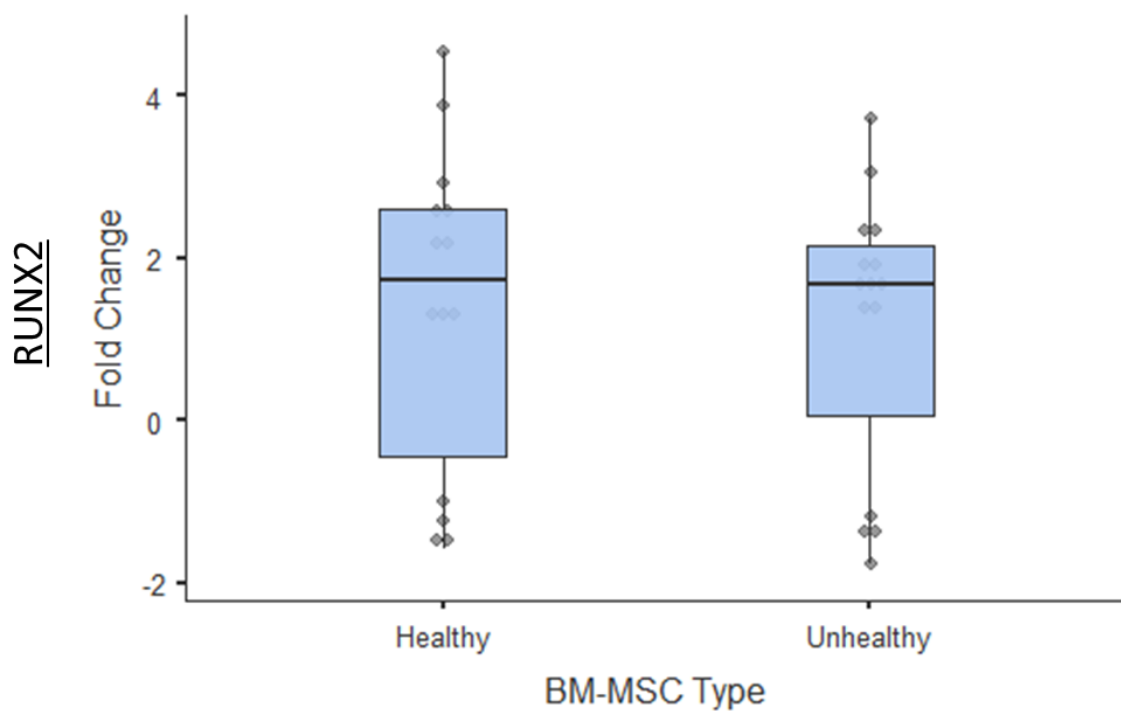
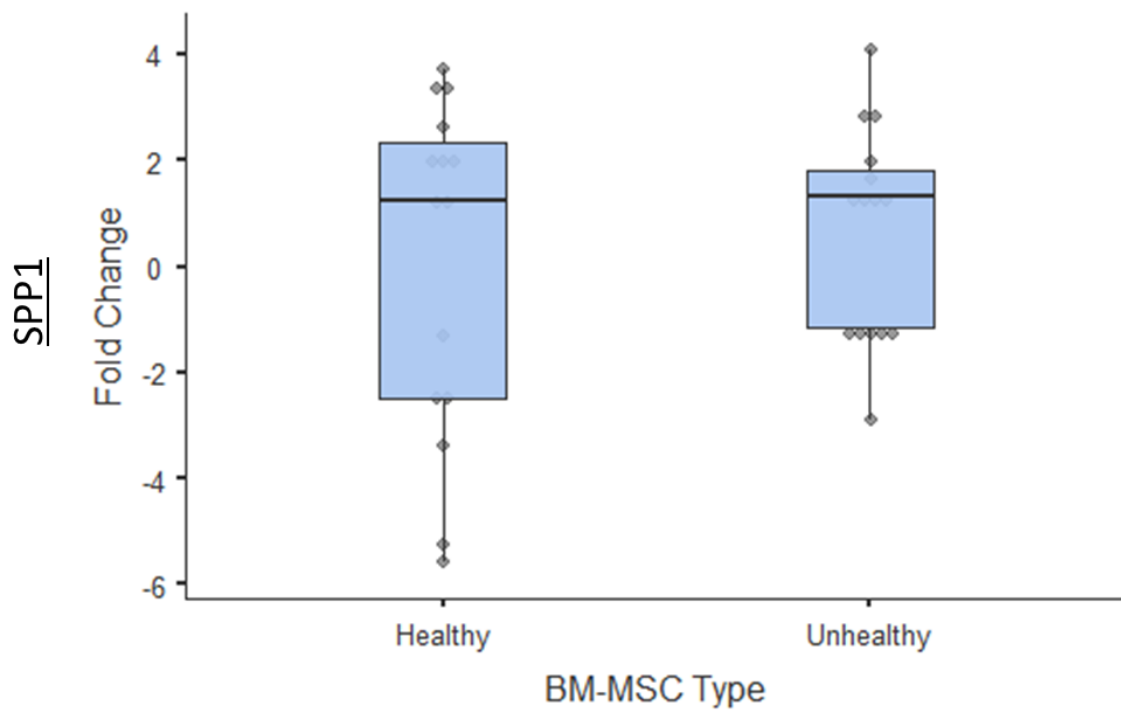


Figure 3-41: Relative fold change of *SPP1* (top) and *RUNX2* (bottom) in BM-MSCs between day 0 and day 21 of the co-culture. Error bars represent the standard error of the mean. Significant differences are indicated by horizontal bars.

3.4 Discussion

The aim of this study was to investigate the effect of subchondral bone health on articular cartilage repair. This was carried out using a novel, in vitro, co-culture model designed to mimic a cell-based tissue engineering strategy for the treatment of AC lesions located above SB with varying degrees of OA severity. The subchondral bone was represented in the model by BM-MSCs, isolated from donor-matched regions of five osteoarthritic joints that were deemed 'healthy' or 'unhealthy', based on macroscopic and histological features. The cartilage component of the model consisted of chondrocytes, isolated from non-OA cartilage in the donated knee of an otherwise healthy young donor, encapsulated in agarose. Using the same population of chondrocytes in the models for all five patients served two purposes: imitating an allogenic chondrocyte therapy and providing a consistent baseline of chondrocyte characteristics to allow for better comparisons between the subchondral bone of patients. The two tissue components of the model were separated by a porous membrane, creating an 'indirect' co-culture, in which the two cell types are not in direct contact but are able to communicate via soluble factors.

We demonstrated that the presence of BM-MSCs in the model, whether healthy or unhealthy, inhibited the proliferation and overall GAG production of the agarose-encapsulated chondrocytes. Proliferation and GAG deposition were evident in all conditions over the course of the experiment but at day 14 and day 21, both were significantly higher in the chondrocyte-only control (no BM-MSCs) than in either of the experimental conditions. One possible reason for these differences could be a lack of nutrient availability, because more cells rely on the same volume of media in the co-culture conditions compared to the chondrocyte-only condition. The increased number of cells in the same volume of

media could also have led to an increased build-up of waste products in the media.

However, media was exchanged every other day and there was no evidence that the phenol red in the medium changed colour to yellow, which would be indicative of a low pH caused by a build-up of acidic waste products. Another possible explanation for the reduction in chondrocyte activity by the presence of the BM-MSCs could be the effect of mediators produced by the BM-MSCs. It is well known that MSCs are able to secrete trophic factors that can exert modulating effects on chondrocytes, and this forms part of the basis for the use of MSCs in tissue repair. Xu and colleagues reported that indirect co-culture of rabbit articular chondrocytes with rabbit MSCs reduced proliferation of chondrocytes and production of cartilage ECM proteins, including GAGs, compared to monoculture of articular chondrocytes, and that this effect was mediated entirely via secreted factors (Xu et al., 2013). The identity of these secreted factors in the rabbit study and our study is unknown and further research is required.

More relevant to the aim of our work, we found that co-culture with unhealthy BM-MSCs led to a reduction in total GAG compared to co-culture with healthy BM-MSCs, as was evidenced by a significant difference in total GAG between the conditions at day 21. As there was no significant difference in chondrocyte number between the two conditions at any timepoint, we suspected that the difference in total GAG was caused by a difference in production per cell, rather than a difference in cell number. This was borne out when the total GAG was normalised to cell number, revealing a significant difference in GAG/cell between the healthy and unhealthy conditions at day 21 of the co-culture. This finding demonstrates that the health state of BM-MSCs can influence the metabolic activity of healthy chondrocytes in indirect co-culture, suggesting that the effect is mediated entirely via soluble factors. This represents a key finding of the study, indicating that the biochemical

composition of the repair cartilage is influenced by the health state of the subchondral bone. It is well established that the unique biomechanical properties of the AC are determined by its composition, and therefore a different composition of repair cartilage above healthy and unhealthy bone could lead to altered properties and altered outcome of the repair surgery. It would have been of interest to carry out mechanical testing of the constructs, but this was beyond the remit of the study. Interestingly, there was no significant difference in GAG/cell between the healthy co-culture condition and the chondrocyte-only control, indicating that the difference in total GAG between these conditions was due to a difference in chondrocyte number rather than a difference in the metabolic activity of the chondrocytes. This also suggests that unhealthy BM-MSCs have an inhibitory effect on GAG metabolism, rather than healthy BM-MSCs having a stimulatory effect. Westacott and colleagues similarly reported that the metabolism of explanted cartilage, quantified by GAG secretion, was modulated by the health of subchondral bone cells (Westacott et al., 1997). These authors found that co-culture of cartilage explants with nonarthritic bone cells had no effect on GAG secretion, whereas in half of those that were co-cultured with bone cells from osteoarthritic bone, there was an increase in GAG secretion.

Following encapsulation and culture for 21 days, there was a general upregulation of *ALK1*, *COL10A1*, *MMP-3*, *MMP-13*, but downregulation of *COL2A1* and *ADAMTS5* across all conditions. There was no biologically significant change in the relative expression of *SOX9* or *ADAMTS4*. It is widely accepted that the monolayer expansion of articular chondrocytes leads to the gradual loss of the chondrocyte phenotype and the acquisition of a more fibroblast-like phenotype, in a process termed, 'dedifferentiation' (Caron et al., 2012). It is also widely accepted that subsequent 3D culture of chondrocytes can ameliorate the effects

of monolayer culture and 'redifferentiate' chondrocytes, leading to a regain of the differentiated chondrocyte phenotype (expression of *SOX9*, *ACAN* and *COL2A1*) (Aulthouse et al., 1989; Caron et al., 2012). Therefore, in a model such as ours, one would expect to see an upregulation of *ACAN*, *COL2A1* and *SOX9* in all conditions following agarose encapsulation, representing redifferentiation and recapitulation of the chondrocyte phenotype following monolayer culture (Caron et al., 2012). This would be most clearly demonstrated in the chondrocyte-only control, in which any changes in the gene expression in chondrocytes from baseline can be attributed solely to encapsulation and culture in agarose. Chondrocytes are generally considered to be dedifferentiated after around five monolayer expansions, whereas our chondrocytes had only been subjected to two (P2) prior to encapsulation (Caron et al., 2012). We theorise that because the chondrocytes were used at a relatively low passage, there was minimal dedifferentiation and therefore subsequent 3D culture in agarose did not result in drastic redifferentiation. Thus, changes in gene expression of the key chondrocyte markers, over the course of the study, were minimal.

More interesting were the differences in gene expression between the chondrocytes that were co-cultured with healthy or unhealthy BM-MSCs. The relative expression of *ACAN* in the chondrocytes that were co-cultured with healthy BM-MSCs mirrored that of the chondrocyte only control, demonstrating a similar upregulation over the course of the study, with no significant difference between these conditions. However, there was no biologically significant change in *ACAN* expression, over the course of the experiment, in the chondrocytes that were co-cultured with unhealthy BM-MSCs. Although there is not direct correlation between gene expression and corresponding protein levels, this finding goes some way to explain the reduced GAG/cell in the unhealthy co-culture, as the *ACAN* gene encodes the aggrecan protein, a GAG that is highly abundant in the cartilage ECM. Work by

Sanchez and colleagues demonstrated similar results, showing that ACAN expression was inhibited in OA chondrocytes which were co-cultured with sclerotic osteoblasts, compared to those cultured with non-sclerotic osteoblasts, and that the effect was mediated by soluble factors (Sanchez et al., 2005a). Although this study is the most similar published work to our own, there are a number of methodological differences between our study and theirs, namely the use of osteoblasts rather than MSCs and OA chondrocytes in place of those from a healthy donor. In addition, their study was carried out using only three patients, all male. Therefore, comparisons between findings are useful, but are drawn with caution throughout.

The relative expression of *COL2A1*, which encodes another of the major proteins of the ECM, collagen type 2, was also found to differ between chondrocytes cultured with healthy and unhealthy BM-MSCs. Over the course of the study, there was an almost 33-fold downregulation in *COL2A1* expression in the chondrocytes that were cultured with unhealthy BM-MSCs (fold change = -32.8 ± 12.9). This was significantly different to both the healthy BM-MSC co culture ($p < 0.001$) and the chondrocyte-only control ($p < 0.001$). There was also a downregulation of *COL2A1* in the chondrocytes from the healthy co-culture (fold change = -7.82 ± 4.46), and in the chondrocyte-only control (fold change = -2.32 ± 0.74), but these were not significantly different from one another. A similar pattern of *COL2A1* expression in co-cultured chondrocytes was reported by Sanchez and colleagues, who demonstrated that the indirect co-culture of OA chondrocytes with either sclerotic or non-sclerotic osteoblasts caused a downregulation of *COL2A1* in both conditions after four days, but that the downregulation was significantly greater in the sclerotic condition (Sanchez et al., 2005b). They also showed that after 10 days, *COL2A1* expression was only downregulated in the co-culture with sclerotic osteoblasts (Sanchez et al., 2005b).

We also quantified a number of genes that encode matrix degrading enzymes to investigate whether co-culture with unhealthy BM-MSCs caused an increase in the catabolism of matrix components as well as a decrease in anabolism. The *ADAMTS4* and *ADAMTS5* genes encode two are the major aggrecan degrading enzymes of the same names. All conditions demonstrated a downregulation of *ADAMTS5* over the course of the study: healthy (-11.3 ± 1.57), unhealthy (-9.69 ± 1.25) and no BM-MSC (-8.56 ± 0.96). However, there was no significant difference between healthy and unhealthy conditions ($p=1.00$), nor between the chondrocyte-only control and either the healthy ($p=0.424$) nor the unhealthy co-culture ($p=1.00$). None of the conditions demonstrated a biologically significant change in *ADAMTS4* expression over the course of the study. The genes that encode the collagen degrading enzymes, *MMP-3* and *MMP-13* were also investigated. All conditions demonstrated upregulation in *MMP-13* over the course of the study but there were no significant differences, between the healthy (69.9 ± 33.4) and unhealthy conditions (61.6 ± 29.4 ; $p=1$), nor between the chondrocyte-only control (68.2 ± 18) and either the healthy ($p=1$) nor unhealthy conditions ($p=1$). Similarly, *MMP-3* was upregulated in all conditions over the course of the study, and there were no significant differences between healthy (11.4 ± 2.72) and unhealthy conditions (9.13 ± 1.82 ; $p=0.517$), nor between the chondrocyte-only control (9.90 ± 1.44) and either of the co-culture conditions. In the most similar published work to our own, Sanchez and colleagues reported an increased expression of *MMP-3* (1.6 times increase) and *MMP-13* (2 times increase) in OA chondrocytes cultured with sclerotic osteoblasts compared to normal osteoblasts (Sanchez et al., 2005a). While our results are contrary to those published by these authors, again it is difficult to compare directly due to methodological differences between the studies; we have investigated fold change over time in relative gene expression, and compared these values between conditions, whereas

Sanchez and colleagues compared copy number difference between the two conditions at a single timepoint (Sanchez et al., 2005a).

Taken together, the gene expression analyses suggest that decreased anabolic activity, rather than increased catabolic activity, inhibited GAG/cell production during co-culture with unhealthy BM-MSCs, compared to co-culture with healthy BM-MSCs. This is demonstrated by the differential regulation of genes that encode matrix proteins, but not of genes that encode matrix degrading enzymes.

Interestingly, *COL10A1*, *ALK1* and *MMP-13* were upregulated in all conditions, suggesting that the agarose-encapsulated chondrocytes were becoming hypertrophic over the course of the experiment (Dreier, 2010; Lian et al., 2019). This is likely due to the effect of β -glycerophosphate, a component of the osteogenic differentiation media, that is widely reported to induce chondrocyte hypertrophy both in vitro and in the developmental process of endochondral ossification in the formation of the long bones (Coe et al., 1992; Magne et al., 2003; Mueller & Tuan, 2008; Wu et al., 2017). This represents a limitation of the present study, as two different media types were used, both of which contain constituents that are potent drivers of differentiation of their respective cell types. However, this limitation does not negate the findings of this study, as the same media types and volumes were applied across all conditions and controls. Further investigation into the effect of this osteogenic media, and others, on the behaviour of the chondrocytes is required. As in vitro modelling continues to evolve, new media formulations are required that can support multiple cell types without phenotypic changes (Zhang et al., 2018).

We also sought to identify soluble mediators of the communication between the BM-MSCs and the chondrocytes by assessing the concentration of five potentially relevant proteins in

the conditioned media from the two co-culture conditions and the chondrocyte-only control. The concentration of secreted *MMP-1* and *MMP-13* demonstrated similar patterns across all conditions over the course of the study, with an increase in concentration from day 0 to day 7 and then a decrease from day 7 to day 21. Interestingly, the gene expression analysis of *MMP-13* indicated that there was a significant upregulation, in all conditions, between days 0 and 21. However, it is notoriously difficult to correlate gene expression levels and corresponding protein concentrations due to additional levels of regulation between transcript and protein i.e. not all DNA that is transcribed to mRNA (which is measured using PCR) is translated to protein (Koussounadis et al., 2015). At day 7, there was a significantly higher concentration of *MMP-1* in the media from the chondrocyte-only control culture, compared to both co-culture conditions, suggesting that the presence of BM-MSCs, healthy or unhealthy, led to a reduction in the quantity of *MMP-1* in the conditioned media. Unfortunately, we did not assess the expression levels of the *MMP-1* gene, and, as mentioned, there is poor correlation between gene expression and protein levels, so we cannot say whether the reduction in *MMP-1* or *MMP-13* at day 21 is caused by a downregulation in gene expression or another factor, such as the proteins binding to surface receptors on BM-MSCs.

The concentration of TGF- β 1 was below the detection limit (1.70 pg/ml) in all conditions at day 0 and day 7. At day 21, however, the concentration of TGF- β 1 in the conditioned media collected from the healthy co-culture condition (1178 \pm 589pg/ml) was significantly higher than in both the unhealthy co-culture (141 \pm 122; $p=0.014$) and the chondrocyte-only control ($p=0.006$), in which TGF- β 1 was still undetectable. The chondrogenic differentiation media, of which 250ul was added to the top of the agarose scaffold with every media change, contained TGF-B1 at a concentration of 10ng/ml. Therefore we were concerned that the

TGF- β 1 that was detected in the conditioned media was simply that which was added to the top of the agarose and had diffused through the scaffold and the transwell membrane into the media below, which was collected for analysis. However, the inability to detect TGF- β 1 in the conditioned media from the chondrocyte-only control condition, to which the same volumes and constituents of media were added as in the experimental conditions, suggested no evidence of TGF- β 1 diffusion through the scaffold.

Therefore, we concluded the TGF- β 1 detected in the conditioned media was produced by the BM-MSCs. At day 21 there was a significantly greater concentration of TGF- β 1 in the conditioned media collected from the healthy co-culture than the unhealthy co-culture. TGF- β is a potent inducer of cartilage ECM synthesis, as well as a suppressor of certain catabolic stimuli, found to be highly expressed in normal cartilage but absent in OA cartilage (Blaney Davidson et al., 2006; Blaney Davidson et al., 2007). Therefore, we hypothesise that the differential secretion of TGF- β 1 by the healthy and unhealthy BM-MSCs could, in part, explain the differential expression of ECM matrix genes and the difference in GAG/cell in the co-cultured chondrocytes. The concentration of TGF- β 1 detected in the conditioned media, even in the healthy co-culture (1178pg/ml (1.178ng/ml)), was considerably lower than that which was added to the chondrogenic media (10ng/ml), but still constituted an additional 10% in the healthy co-culture compared to the unhealthy co-culture and the chondrocyte-only control. The lack of evidence for TGF- β 1 diffusion from the top of the scaffold downwards, suggests that the TGF- β 1 added to the top of the scaffold acted mainly on the chondrocytes in the top of the agarose and that the TGF- β 1 secreted by the BM-MSCs acted on the chondrocytes in the bottom of the scaffold, causing an overall increase in GAG/cell once the entire depth of the scaffold was digested and analysed. The difference in TGF- β 1 concentration between the top and bottom of the scaffold seemed to be reflected in the

histological findings, in which the GAG staining surrounding the chondrocytes appeared more intense at the top of the scaffold compared to the bottom, in all conditions examined. Further investigation analysing the different zones of the scaffold separately, carrying out diffusion testing through the agarose or removing the TGF- β 1 from the media at the top of the scaffold would be required.

Analysis of the BM-MSCs demonstrated that there was proliferation in both the healthy and unhealthy conditions over the course of the experiment and that there were no significant differences in cell number between the conditions at any of the timepoints. We found that there was a significant upregulation of *COL1A1* in the unhealthy BM-MSCs but not in the healthy BM-MSCs over the course of the study. There were no significant differences in gene expression in any of the other genes assessed between conditions, suggesting that their phenotype was relatively stable. Sanchez and colleagues similarly reported that the gene encoding collagen type 1 was more highly expressed by osteoblasts from sclerotic bone, compared to those from non-sclerotic bone (Sanchez et al., 2008). However, in contrast to our study, they also found that osteocalcin and osteopontin were more highly expressed in the sclerotic osteoblasts. The difference between these findings may represent the phenotypic differences between primary osteoblasts and differentiated BM-MSCs as were used in our model, but further research is required.

An incidental finding of the comparative analysis of healthy and unhealthy BM-MSCs by flow cytometry was that neither condition wholly adhered to the ISCT profile of recommended immunopositivity for MSCs (Dominici et al., 2006). While the majority of our cells did meet the recommended criteria, there appears to have been a subpopulation of cells in each population that did not, with both conditions demonstrating a mean immunopositivity >2%

for CD14, CD34 and HLA-DR, all of which the ISCT recommends should be expressed on <2% of cells (Dominici et al., 2006). In practice, however, it is accepted that MSC specifications often deviate from the ISCT criteria, which represents a typical guide profile and should be used as such, rather than being exhaustive or wholly inclusive (Zachar et al., 2016; Grau-Vorster et al., 2018; Grau-Vorster et al., 2019). It is important to consider that BM-MSCs represent a highly heterogenous population of cells that are sensitive to intrinsic and extrinsic factors, and therefore restricting their identification to a strict set of cell surface markers may lead to the overzealous exclusion of MSCs (Zachar et al., 2016; Grau-Vorster et al., 2019). In the original position paper describing the minimum criteria for defining MSCs, the authors did concede that the criteria were likely to require modification as new knowledge became available (Dominici et al., 2006). Interestingly, our findings regarding CD14, CD34 and HLA-DR are mirrored by previous findings from our laboratory and in the wider research community.

CD14 is a monocyte/macrophage marker that has been previously reported to be present on BM-MSCs. In unpublished results from his thesis, my colleague Dr John Garcia reported a mean CD14 positivity of $14.8\% \pm 2.7_{SEM}$ in BM-MSCs tested ($n=20$) which was very similar to our findings, in which $15.2\% \pm 6.66_{SEM}$ and $15.6\% \pm 8.08_{SEM}$ CD14 positive cells were identified in healthy and unhealthy BM-MSCs respectively (Garcia, 2016). Both my work, and that of Dr Garcia, were carried out on BM-MSCs at passage 3, isolated and cultured using the same method. Further, a study carried out by Pilz and colleagues reported a positive signal for CD14 on early passage BM-MSCs and suggested a number of possible reasons for this signal, including macrophage contamination and technical issues with cross-reactivity of CD14 antibodies (Pilz et al., 2011). Further research is required to determine the nature of CD14 positivity in BM-MSC cultures and the implications for the ISCT profile.

Dr Garcia also demonstrated similar findings to ours with regards to CD34 immunopositivity, reporting in unpublished work from his thesis that $5.1\% \pm 1.2_{SEM}$ of BM-MSCs tested ($n=20$) were positive for CD34 (Garcia, 2016). Again this is similar to our findings that $3.26\% \pm 1.9_{SEM}$ and $4.48\% \pm 2.64_{SEM}$ of healthy and unhealthy BM-MSCs, respectively, were positive for CD34, a marker associated with perivascular or endothelial cells. Another researcher from our group, Dr Claire Mennan, also reported CD34 immunopositivity $>2\%$ in BM-MSCs obtained from commercial sources and cultured under normal conditions (Mennan et al., 2019).

Contrary to the ISCT recommendations, a great deal of variability in immunopositivity for HLA-DR has also been reported on BM-MSCs. In a retrospective analysis of 130 batches of BM-MSCs, manufactured for clinical use by two independent Good Manufacturing Practice (GMP) facilities, the authors reported that HLA-DR expression ranged from $<1\%$ to 77.7% (mean: $19.8\% \pm 15.6_{SD}$) at one site in Barcelona and from $<1\%$ to 60.5% (mean: $19.2\% \pm 17.4_{SD}$) at the second site in Helsinki (Grau-Vorster et al., 2019). The authors concluded that BM-MSCs do express HLA-DR under normal culture conditions and that this can prove to be an issue for researches that adhere strictly to the ISCT criteria (Grau-Vorster et al., 2019). The authors also reported that the HLA-DR positive cells were still fibroblastic in their morphology, still multipotent and were still able to modulate the behaviour of stimulate lymphocytes, thus demonstrating immunosuppressive properties, all of which are additional characteristics of MSCs (Grau-Vorster et al., 2019). Grau-Vorster and colleagues concluded that HLA-DR expression in BM-MSCs is largely unpredictable and variable despite production under tightly controlled conditions, in line with current GMP standards, and should therefore be considered as informative rather than definitive of BM-MSC identity (Grau-Vorster et al., 2019).

One possible explanation for the occasional deviation in cell surface marker expression compared to the ISCT recommendations is that immunopositivity is not constant for MSCs but rather is dynamic, changing over time and influenced by external stimuli (Zachar et al., 2016; Grau-Vorster et al., 2019). In this way, certain culture conditions and applications of MSCs may mean that immunopositivity is more likely to differ from the ISCT guidelines. This has been shown to be the case in certain therapeutic uses of MSCs. It has been reported that the efficacy of certain MSC-based treatments has been improved through priming of the MSCs prior to use (Noronha et al., 2019). There are a number of methods for the priming of MSCs that seek to generate cellular products with improved potential for clinical applications (Noronha, 2019). In one such example, priming of MSCs with interferon-gamma (IFN- γ) enhances their immunosuppressive properties, which has been shown to improve outcomes in the treatment of graft versus host disease in several murine models (Polchert et al., 2008; Kim, D. S. et al., 2018; Noronha et al., 2019). In comparative proteomic analyses of BM-MSCs primed with IFN- γ , 210 proteins with significantly altered expressions were identified (Wang, Q. et al., 2016; Noronha et al., 2019). One such protein that has been reported to increase in expression under the influence of IFN- γ is the cell surface marker HLA-DR (Le Blanc et al., 2003; Grau-Vorster et al., 2018; Grau-Vorster et al., 2019). Thus, strict adherence to the ISCT profile would suggest that IFN- γ primed MSCs could no longer be considered MSCs by definition. This is but one example but again suggests that that the ISCT profile should be regarded with flexibility and that additional guidelines for the recommended immunopositivity of MSCs for certain applications would be useful. Further research is required in this area.

Our study demonstrated that the co-culture of chondrocytes with BM-MSCs isolated from regions with more advanced OA changes inhibited the expression of genes encoding the

major ECM proteins and resulted in a decreased production of GAG. The application of these results, from the model to the clinical situation that it represents, suggests that the composition of repair cartilage that results from a cell-based therapy may vary depending on the health of the underlying SB. Thus, treatment of the SB prior to the implantation of cells, such as with the injection of BM-MSCs, as is described by Hernigou and colleagues, may result in a better repair cartilage (Hernigou et al., 2020a; Hernigou, et al., 2020b). However, we demonstrated that even in the presence of BM-MSCs from the most degenerated regions of OA joints, cartilage still formed, suggesting that there is a possibility that an allogenic chondrocyte therapy may be a viable option for AC repair in patients with even severe OA.

While not wholly relevant to the objectives of this research project, out of interest we also sought to isolate cells of the subchondral bone from the NHSBT sample from which our allogeneic chondrocytes were obtained in this study (see Section 3.2.1 Sample Collection, page 114 and figure 3-11, page 172). Using the methods described in section 3.2.4.2 Bone Marrow Derived Mesenchymal Stromal Cell (BM-MSC) Isolation and section 4.2.3 Primary Osteoblast Isolation and Expansion, we attempted to isolate BM-MSCs and osteoblasts respectively. However, neither method yielded cells from this sample despite successfully yielding cells from multiple samples obtained following TKR. While only an anecdotal finding based on a single sample, we thought that this warranted some discussion.

Tissue obtained from the NHSBT service would otherwise be used for osteochondral allografting (see section 1.1.4.2.1.3.2 Osteochondral Allograft Transplant) and was transported in serum-free media at 4°C. As discussed in this earlier section, a key focus of the harvesting and storage strategy of such samples is the maintenance of chondrocyte

viability and not necessarily that of the subchondral bone cells (Torrie et al., 2015). In fact, it has been proposed that one way to reduce the long-term immunological rejection of osteochondral allografts is through the devitalisation of the subchondral bone which, unlike the cartilage, is not immunologically privileged (Bastian et al., 2011). Thus, the maintenance of the viability of subchondral bone cells is not only not a priority in tissue such as this but doing so would be a possible hinderance to the success of the OCA procedure for which the tissue is harvested. Maintaining chondrocyte viability while allowing for a decrease in the vitality of subchondral bone cells is actually rather simple, owing to the different structure and function of the two tissues, and the different needs of the resident cells. AC is avascular and the sparse chondrocytes contained within are adapted to nutrition via diffusion, which would be required during storage and transport (Bastian et al., 2011). On the other hand, the subchondral bone is highly vascularised and the cells within are more metabolically active and not adapted to nutritional supply by diffusion. This could possibly explain the inability to isolate any viable cells from the subchondral bone. Finally, with regard specifically to the BM-MSC isolation procedure, a washout of the subchondral bone is performed to isolate the bone-marrow mononuclear cells, before additional processing steps are performed to isolate BM-MSCs. In effect, the storage and transport of the osteochondral tissue in media could have acted in a similar way to the washout step. Thus, in hindsight, it may have been of interest to try to isolate mononuclear cells from the media itself, but this was not attempted and given the disinclination of the subchondral bone cells to thrive at 4°C with nutrition by diffusion, the success of this idea may have been unlikely.

3.5 Study Limitations

The main limitation of this study, in terms of modelling the osteochondral unit in AC repair, was that we only considered one cell type from the subchondral bone, BM-MSCs. There are several other cell types present in the SB and future work will seek to include these in the model individually and in combination. We are also considering the use of bone chips in the model, in the place of the BM-MSCs. Another limitation was the use of two types of media, both of which are designed to induce differentiation in their respective cells. We were not able to characterise the effect of each of the media types on the other cell type in the model i.e. the effect of the osteogenic media on the chondrocytes and the effect of the chondrogenic media on the BM-MSCs. Future work will aim to address this. Additionally, time and financial constraints meant that we were unable to carry out gene expression analysis and ELISA on samples from all of the timepoints from the study. As such, we may have missed interesting changes in gene expression and protein secretion between the timepoints investigated. The requirement of a large number of BM-MSCs necessitated their culture expansion, over several passages, meaning that in vivo characteristics may have been lost or altered during culture. If we had been able to use the BM-MSCs at an earlier passage, we may have found greater phenotypic differences between the conditions. Finally, although we have modelled an allogeneic cell therapy for AC repair, we were not able to model, or to assess any immune response to the implantation of allogeneic cells that represents a key issue in the real-world use of allogeneic cells. An additional limitation of this study was the lack of robust screening and donor selection of the allogeneic chondrocytes used across the co-culture models. As discussed in the general introduction (see Section 1.1.4.2.1.5.1 Allogeneic Chondrocyte Therapy, page 37) donor selection is critical when utilising an allogeneic cell source. Ideally, we would have extensively tested several sources of healthy

chondrocytes to assess cell proliferation and extracellular matrix production, as well as immunoprofile and gene expression profile to then select the best donor for our experiments. In reality, however, we rarely have access to normal tissue, and that which does come is precious and limited. With additional donors in the future, and previous donor cells banked, this will become a possibility. This limitation is mitigated somewhat by the experimental design, in which the absolute cartilage forming ability of the allogeneic chondrocytes was not the primary outcome measure, but rather were the differences that could be attributed to co-culture with healthy and unhealthy BM-MSCs.

3.6 Conclusion

In summary, we have demonstrated that co-culture with unhealthy BM-MSCs resulted in a reduction in GAG deposition and a downregulation of the genes encoding collagen type 2 and aggrecan in healthy articular chondrocytes, compared to culture with healthy BM-MSCs. We also identified TGF- β 1 as a differentially secreted growth factor that could possibly mediate the differential effects of the two BM-MSC populations. Although this work was performed in vitro, there are clear implications for cartilage repair by cell-based tissue engineering, in which the health of the SB may influence the composition, and therefore properties of the repair tissue.

Chapter 4:
A preliminary investigation into the
histological and cellular characteristics of
regions with and without MRI-identified
subchondral bone features.

4. Chapter 4: A preliminary investigation into the histological and cellular characteristics of regions with and without MRI-identified subchondral bone features

4.1 Introduction

As discussed in the previous chapter, there is a growing body of evidence that highlights the influence of the biomechanical and biochemical interaction between the articular cartilage (AC) and SB in the onset and progression of osteoarthritis (OA) in the knee joint. In the previous chapter we demonstrated that BM-MSCs isolated from regions of the subchondral bone that demonstrated varying levels of OA severity were able to differentially modulate the behaviour of chondrocytes in a co-culture model of AC repair in the osteochondral unit. Our findings corroborated those in the literature, providing evidence to suggest that the health and function of the AC and SB are closely linked and that dysfunction in one can cause dysfunction in the other. However, the markers that demonstrated differential expression between healthy and unhealthy BM-MSCs isolated from the subchondral bone (*COL1A1* expression and TGF- β 1 secretion) are difficult to assess clinically and therefore have limited utility in predicting the success of AC repair. In this chapter, we sought to characterise a more clinic-friendly indicator of SB health, magnetic resonance imaging (MRI)-identified pathological features in the SB, bone marrow lesions (BMLs) and cysts. BMLs are of particular interest as their presence is a common feature of OA and is widely reported to correlate with both the location and severity of articular cartilage degeneration, pain, and even with the risk of future arthroplasty (Zhao et al., 2010; Li et al., 2013; Marcacci

et al., 2016). BMLs appear as diffuse, or ill-defined, areas of high signal intensity in the subchondral bone on T2-weighted, fat-suppressed MRI and low signal intensity on T1-weighted MRI (Hunter et al., 2006; Zhao et al., 2010; Link & Li, 2011). These features were first reported by Wilson and colleagues in 1988 and were termed 'bone marrow oedema' (Wilson et al., 1988). However, subsequent histological investigation revealed that oedema is not a major constituent in the majority of cases, hence they are commonly referred to as BMLs (Felson et al., 2003; Carrino et al., 2006; Li et al., 2013). It is now known that BMLs identified on MRI are representative of a wide range of histological subchondral bone abnormalities, including oedema, bone marrow and trabeculae necrosis, bone marrow fibrosis, increased vascular ingrowth, trabecular thickening, microfractures and cartilage ingrowth (Zanetti et al., 2000; Link & Li, 2011; Marcacci et al., 2016; Kuttapitiya et al., 2017; Loeff et al., 2018).

A number of studies have reported the association between BMLs and cartilage degeneration in OA. Felson and colleagues carried out a longitudinal natural history study of 256 patients with symptomatic knee OA and reported that BMLs were a powerful predictor of joint space narrowing, an MRI quantified proxy for cartilage loss at 30-month follow-up (Felson et al., 2003). They also showed that the effect was compartmentally dependent: BMLs in the medial compartment predicted medial cartilage loss and BMLs in the lateral compartment predicted lateral cartilage loss.

Garnero and colleagues also reported a longitudinal study of patients with painful knee OA and found that BMLs were present in 82% of 377 patients at baseline (Garnero et al., 2005). The authors reported that the presence of BMLs at baseline was associated with an increase in cartilage breakdown over the course of the study, as measured by both MRI and

biomarker quantification (urinary excretion of C-terminal crosslinking telopeptide of type II collagen (CTX-II)). The authors also showed that a reduction in BML size over the course of the study, which was observed in 37 patients (9.8%), was associated with a decrease in cartilage degradation, and conversely that an increase in BML which was observed in 71 patients (18.8%) was associated with an increase in cartilage breakdown at 3 month follow-up.

Similar findings were reported by Hunter and colleagues who also carried out a natural history study of patients with symptomatic knee OA (Hunter et al., 2006). The authors found that 57% of knees, from 217 patients, had BMLs at baseline and that their presence was associated with cartilage loss at follow-up compared to those with no BMLs at baseline. The authors also demonstrated that compartments with a higher baseline BML score (graded on a semiquantitative scale from 0-3 based on the extent of regional involvement) had increased cartilage loss at 30-month follow-up. Hunter and colleagues reported that the vast majority of BML's stayed the same size (72%) or increased in size (27%), and that an increase in BML score was strongly associated with increased cartilage loss.

Again, similar results were reported by Roemer and colleagues who studied the natural history of BMLs in 395 knees of subjects with OA, or those that were considered to be at a high-risk of developing OA, including those who were overweight or obese, those with knee symptoms or a history of knee injury (Roemer et al., 2009). At the time of baseline assessment, 265 (67%) knees demonstrated a Kellgren/Lawrence grade of 0 or 1, indicating 'none' or 'doubtful' OA, respectively, at which time 8.3% of subregions in the examined knees had BMLs. At the 30-month follow-up, 4.7% had new or increased BMLs and 4.1% of subregions showed regression or resolution of pre-existing BMLs. The authors reported that

the absence or resolution of BMLs over the course of the study was associated with a decreased risk of cartilage degradation, while the appearance of new BMLs, or an increase in the size of existing BMLs, was associated with an increased risk of cartilage loss in the same subregion.

More recently, BMLs have also been associated with cartilage loss in the healthy individuals with no history of knee injury or clinical knee OA. Wluka and colleagues reported the presence of BMLs on the baseline MRI of the dominant knee in 37 of 271 (14%) patients with no history of knee injury, knee pain or clinical knee OA. At two-year follow-up, the authors observed that the progression of cartilage defects in the tibiofemoral compartment was 2.6 times more likely when BMLs were present at baseline, compared to when they were absent. They also found that an increase in the size of BMLs over the course of the study was associated with increased annual tibial cartilage volume loss (Wluka et al., 2009). The same group also carried out a second analysis on the same cohort and found that of the 37 patients who had BMLs at baseline, 17 resolved by the time of the two-year follow-up, and that resolution was associated with reduced annual loss of tibial cartilage volume (Davies-Tuck et al., 2010).

Another subchondral bone abnormality, that is closely linked with BMLs, is subchondral bone cysts, which appear as well-defined, focal, high intensity signal changes on T2-weighted fat-suppressed MRI and are another common finding in OA patients (Crema et al., 2010; Link & Li, 2011). Histologically, cysts appear as cavitory lesions in the subchondral bone, the borders of which are composed of fibroconnective tissue (Li et al., 2013).

Areas of BML and cysts are closely related. It has been reported that prevalent BMLs strongly predict a subchondral bone cyst in the same subregion (Crema et al., 2010). This

was demonstrated by Carrino and colleagues, who carried out a retrospective study of BMLs and cysts in 32 patients with sequential MRIs (Carrino et al., 2006). The authors reported that bone cysts were present in 12 patients at baseline, 11 of which (92%) developed in a region of pre-existing BML. The authors also reported that 11 patients had developed new cysts between MRIs, and that all of these arose in regions of pre-existing BMLs. Although not all BMLs gave rise to cysts over the course of this study (average time between MRIs was 17.52 months), the authors suggest that BMLs may be an early 'pre-cyst' lesion. In a natural history study of subchondral bone cysts in a cohort of 132 patients with knee OA, Tanamas and colleagues found that cysts were present in 47.7% of patients, 98.1% of whom also had BMLs (Tanamas et al., 2010). They also found that cysts increased in size in 21 patients (including 6 in whom one or more new cysts developed) all of whom had pre-existing BMLs.

The two previously mentioned studies of subchondral bone cysts also reported their association with cartilage degradation. Carrino and colleagues reported that cartilage lesions were commonly seen overlying subchondral bone cysts and BMLs and that overall, 87% of subchondral bone cysts were adjacent to a visible cartilage abnormality on MRI (Carrino et al., 2006). In a natural history study performed by Tanamas and colleagues, it was observed that mean tibial cartilage volume was lower in patients with cysts compared to those without and that there was a significant reduction in lateral tibial cartilage volume loss in patients whose cysts regressed (10 patients) over the course of the study (Tanamas et al., 2010). Overall, the authors reported that the presence of subchondral bone cysts increases the risk of cartilage loss and future arthroplasty.

Abnormal subchondral bone remodelling has long been implicated in the pathological changes observed in the SB as part of the OA pathogenesis and has been proposed as a mechanism underlying the formation of BMLs and subchondral bone cysts (Carrino et al., 2006; Hopwood et al., 2007; Chen et al., 2015; Donell, 2019). The normal process of bone remodelling is a tightly controlled balance between bone deposition by osteoblasts and bone resorption by osteoclasts (Lajeunesse & Reboul, 2003). However, in late-stage OA, the balance of bone remodelling shifts to favour deposition, with osteoblast activity reported to increase by 96% (Burr & Gallant, 2012; Donell, 2019). Although the mechanisms behind this shift are unconfirmed, the resulting change in osteoblast activity and phenotype leads to the increased deposition of a modified form of collagen type I, the main organic component of the bone, in which the ratio of alpha-1 and alpha-2 chains is altered (Henrotin et al., 2012; Donell, 2019). The resulting form of collagen type I has a lower affinity for calcium and is associated with bone sclerosis, in which the overall bone volume increases but the bone is less mineralised (Burr & Gallant, 2012; Donell, 2019). In the subchondral bone, the result is an increase in trabecular thickness and volume and an increase in subchondral bone plate thickness. Local increases in abnormal bone remodelling have been noted both at the sites of BML and in the subchondral bone trabeculae surrounding SB cysts (Sabokbar et al., 2000; Hunter et al., 2009; Link & Li, 2011).

Recently, Kuttapitiya and colleagues employed microarray analysis to assess the transcriptome of BML tissue, which they identified in 100% of the TKR tissue assessed (n=72) (Kuttapitiya et al., 2017). The authors reported that 218 transcripts were differentially expressed between OA BML tissue and normal bone, including genes from a diverse range of regulatory pathways. This work provided interesting context and meaning to the transcriptomic findings, relating the differences discovered to the histological

features and clinical symptoms associated with BMLs. Interestingly, the group reported an increased expression in the BML tissue of both osteogenic and bone remodelling genes (Wnt, TGF, BMP, periostin), along with angiogenic genes (Notch), suggesting that bone formation and vascular proliferation are coupled in the formation of BMLs. The group also reported that the expression of a number of genes associated with neurodevelopment and pain pathway signalling (Notch, catenin, stathmin 2) were increased in the BML tissue, suggesting new nerve formation and a possible source for the source of pain associated with BMLs. Of particular interest to our research, Kuttapitiya reported on the upregulation of MMP-13, an enzyme involved in the breakdown of cartilage extracellular matrix components. The authors suggested that this finding, along with an increase in the detection of secreted MMP-13 cleavage products, might indicate a recapitulation of an embryonic bone development phenotype in OA BMLs, in which a cartilage template is first created and then gradually replaced with mineralised tissue (Kuttapitiya et al., 2017).

However, there has been little research on the cellular characteristics of regions with subchondral bone abnormalities. Given the profound changes to the subchondral bone architecture and histology associated with BMLs and cysts, and the wide range of genetic differences between BML and normal bone reported by Kuttapitiya and colleagues, it stands to reason that cells critically involved in bone production processes, namely osteoblasts, may themselves demonstrate altered behaviour and phenotypic characteristics.

Here we present an observational study in which we assessed the histological and cellular characteristics of regions of the subchondral bone that demonstrate abnormalities (BMLs and cysts) compared to normal regions of the subchondral bone.

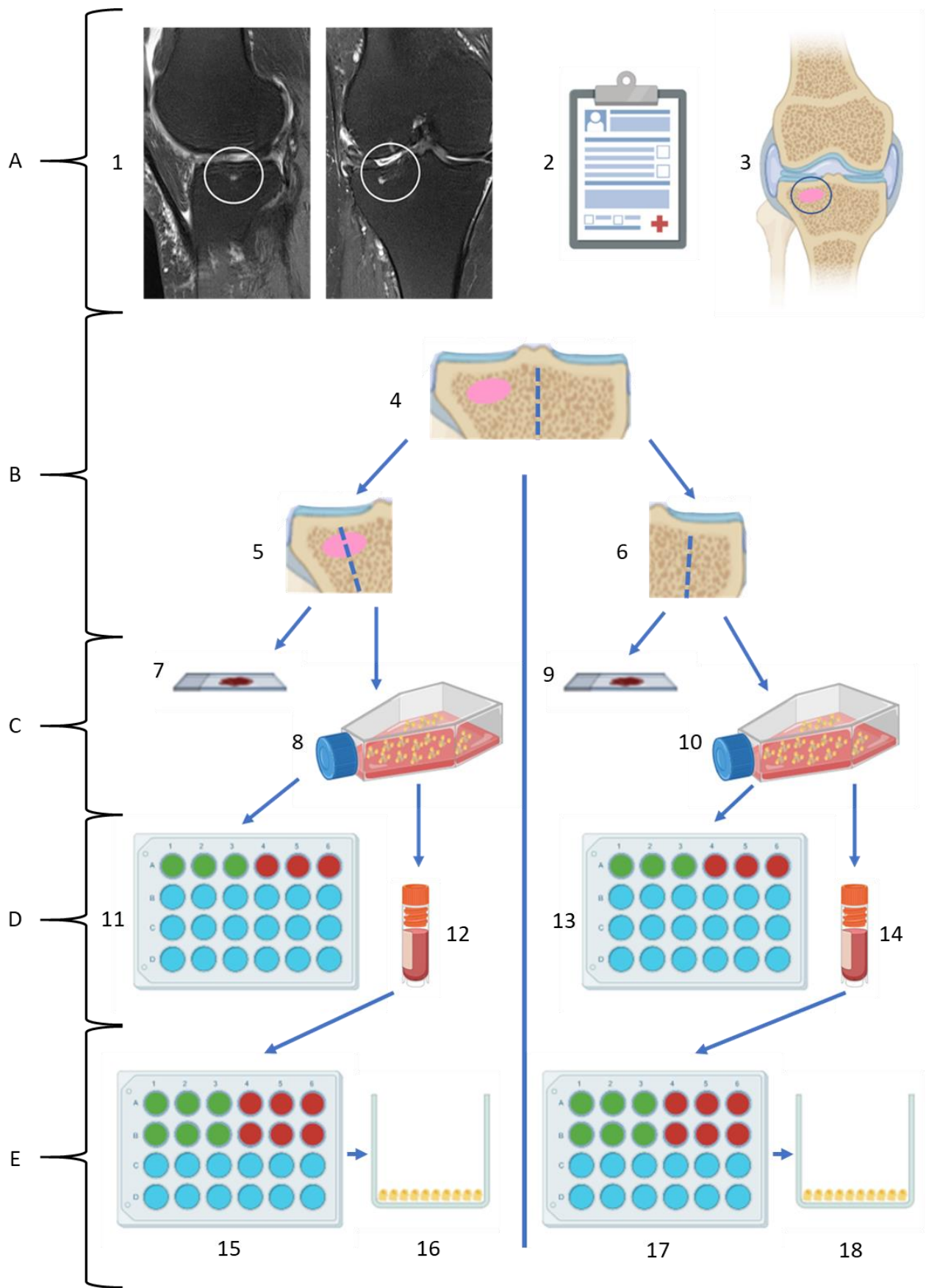


Figure 4-1: Overview of Experimental Procedure.

A. Identification of regions with and without subchondral bone abnormalities.

MRIs (1) and MRI reports (2) were used to identify regions in the affected knee with subchondral bone abnormalities (circled) and those without (3).

B. Separation of osteochondral tissue regions.

Excised osteochondral tissue (4) was separated into the identified regions: a region with subchondral abnormalities (5) and a region without (6).

C. Processing of osteochondral tissue for analysis.

Half of each isolated region was prepared for histological assessment (7 & 9) and the other half was used to create bone chips (8 & 10) for the outgrowth culture of osteoblasts.

D. Cryopreservation and seeding of osteoblasts for histochemical assessment.

Osteoblasts were seeded in 24 well plates for the histochemical assessment of alkaline phosphatase activity (11 & 13) and the remainder were prepared for cryopreservation (12 & 14).

E. Experimental seeding and analysis.

Osteoblasts were recovered from liquid nitrogen storage as required, seeded in 24 well plates (15 & 17) and cultured to 80% confluency before being prepared for analysis (16 & 18) of dsDNA content and gene expression.

4.2 Materials and Methods

An overview of the experimental procedure for this study is shown in figure 4-1.

4.2.1 Patient Identification

Patients who were scheduled for total knee replacement (TKR) surgery at the RJAH orthopaedic hospital were further screened by an NHS research nurse to identify those who had a recent (within the last 6 months) MRI on the knee that was to be replaced. Eligible patients were then further filtered by the research nurse using MRI reports to identify patients whose MRI findings included pathological subchondral bone abnormalities. MRI reports were either accessed by the research nurse on the electronic patient record (EPR) system or, for patients where an MRI report was not available on the EPR system, the report was kindly prepared by Dr Bernhard Tins, a consultant radiologist at the RJAH Orthopaedic Hospital. Five patients were identified who were scheduled for TKR surgery, had a recent MRI on the affected knee that identified SB abnormalities (oedema-like signal and cystic changes) and who provided written, informed consent. Favourable ethical approval was given by the National Research Ethics Service (NRES) (11/NW/0875) and all experiments were performed in accordance with the relevant guidelines and regulations.

4.2.2 Sample Collection and Assessment

Samples of bone and cartilage from the femoral condyles or tibial plateau, depending on the location of the abnormalities highlighted on MRI, were obtained from the five eligible patients following TKR surgery. Samples were initially assessed macroscopically before regions of interest in the SB were identified using MRIs. Samples were then processed for histological staining and assessment.

4.2.2.1 *Subchondral Bone Region Identification*

MRIs and corresponding MRI reports were used to identify the regions of the excised subchondral bone that corresponded to the pathological SB abnormalities identified on MRI (figure 1, A & B). Guidance on the anatomical organisation and orientation of excised tissue was provided by a colleague, Jingsong Wang, an orthopaedic surgeon from Dalian, China. For each patient a region was also identified that demonstrated no pathological features and was deemed normal tissue. Examples of this process are shown in figures 4-2 & 4-3. These regions are henceforth referred to as 'lesioned' and 'normal' respectively. A lesioned and normal region was identified for each of the five patients.

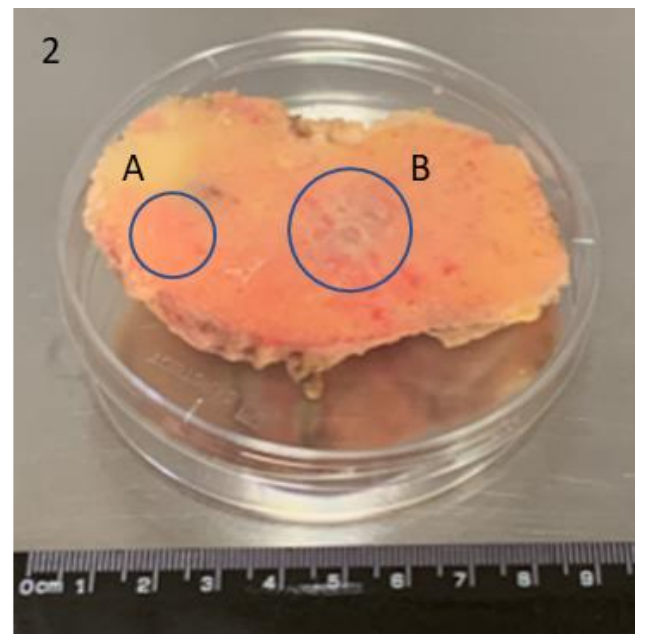
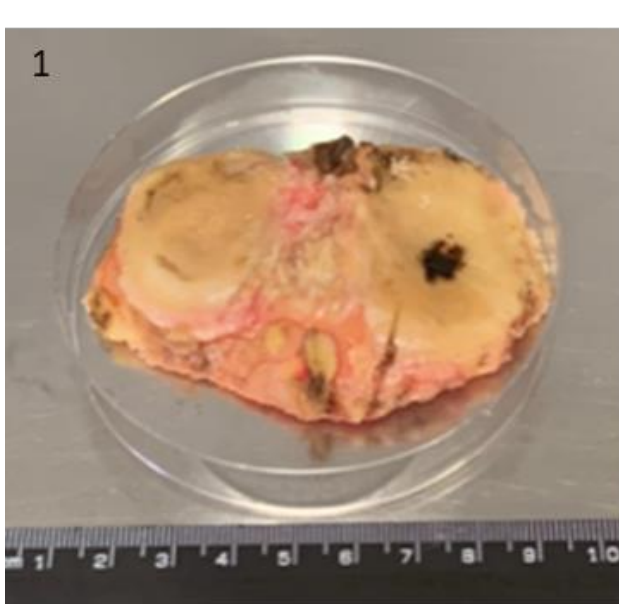
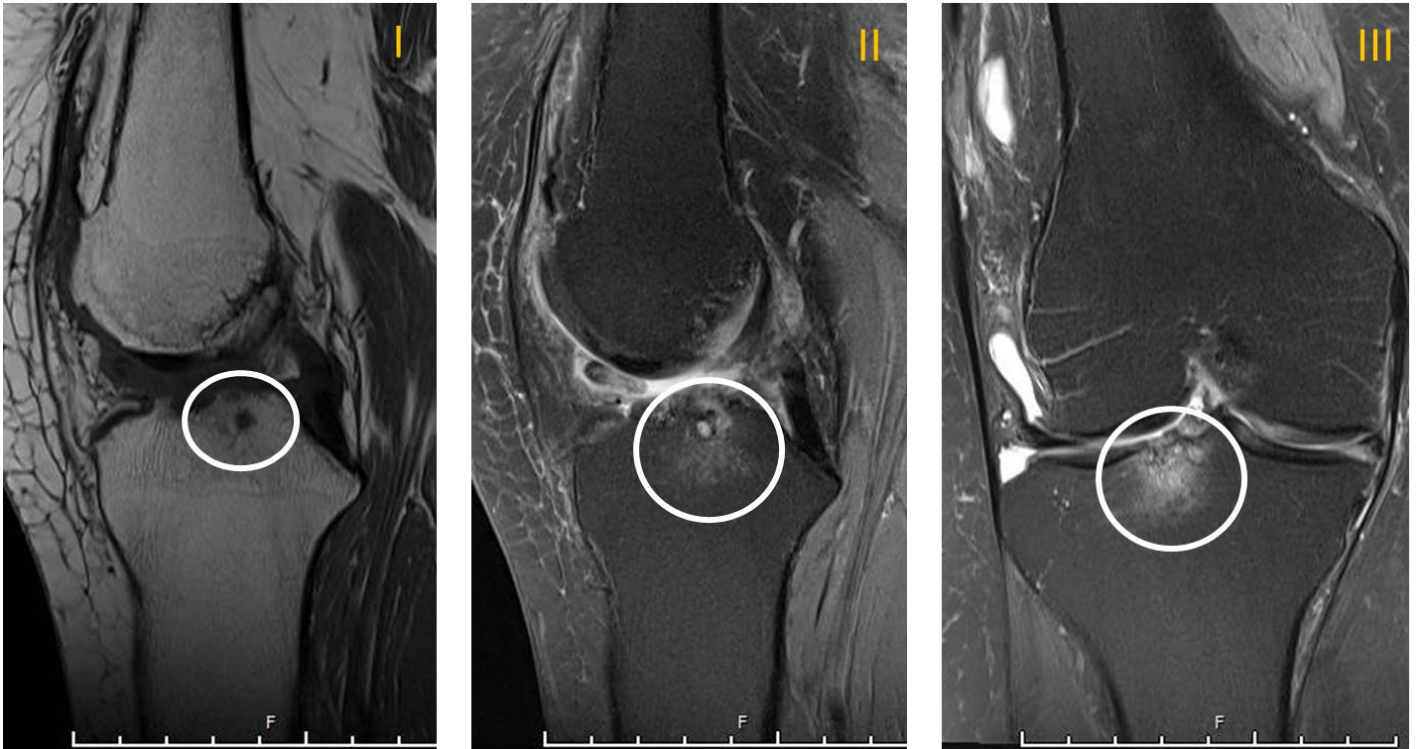


Figure 4-2: Example procedure for the location of SB abnormalities in excised osteochondral tissue using MRIs— Patient 1. Top: MRIs demonstrating signal abnormalities in the subchondral bone. I: T1-weighted (sagittal plain) II: T2-weighted (sagittal plain) III: T2-weighted (coronal plain). Bottom: Macroscopic appearance of excised tibial plateau. 1. Cephalic side 2. Caudal side A. ‘Normal’ region. B. ‘Lesioned’ region.

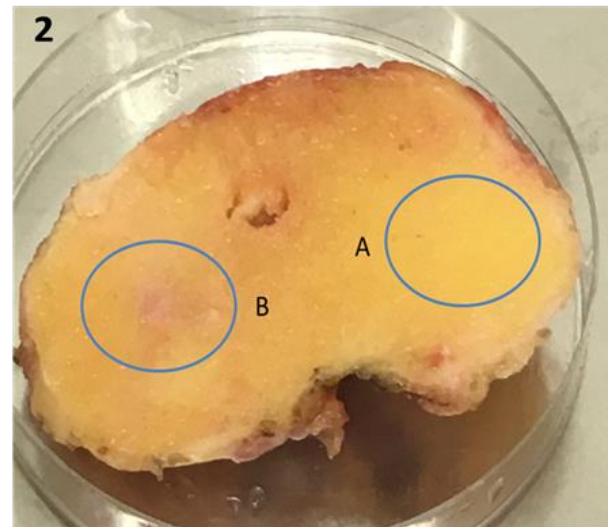
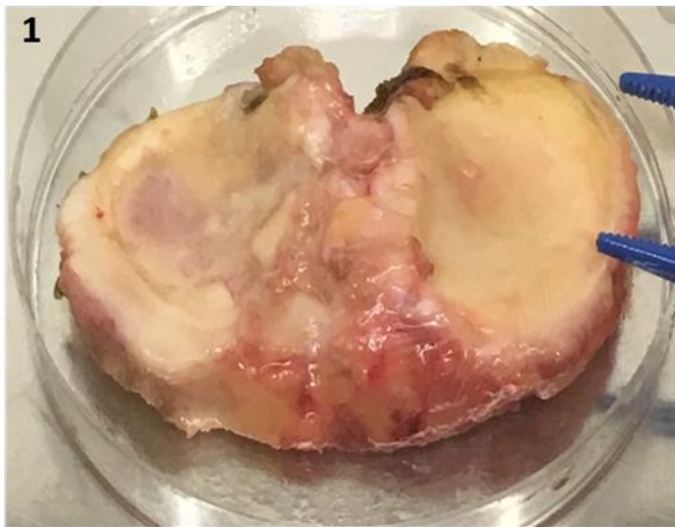
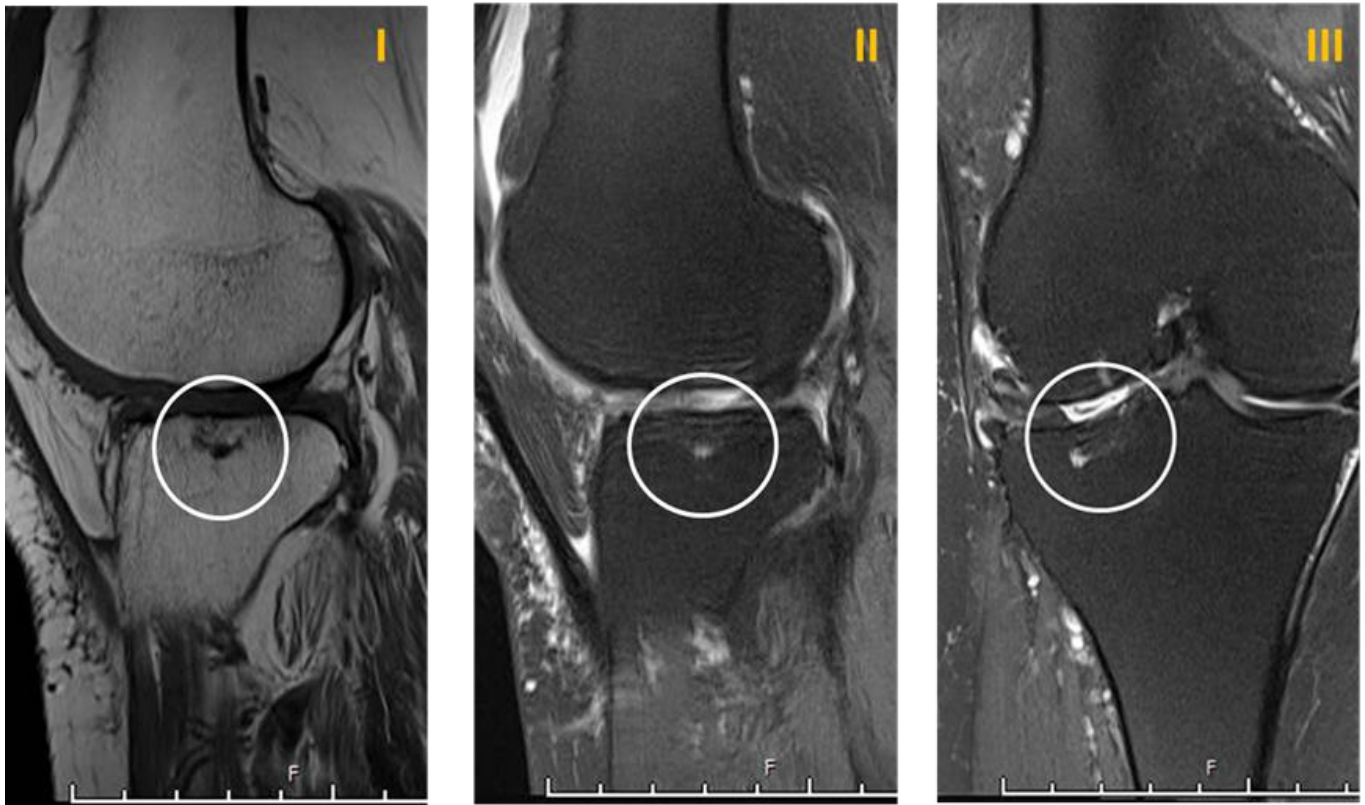


Figure 4-3: Example procedure for the location of SB abnormalities in excised osteochondral tissue using MRIs – Patient 2. Top: MRIs demonstrating signal abnormalities in the subchondral bone. I: T1-weighted (sagittal plain) II: T2-weighted (sagittal plain) III: T2-weighted (coronal plain). Bottom: Macroscopic appearance of excised tibial plateau. 1. Cephalic side 2. Caudal side A. 'Normal' region. B. 'Lesioned' region.

4.2.2.2 *Macroscopic Cartilage Grading*

The cartilage overlying the lesioned and normal regions was graded using the semi-quantitative International Cartilage Repair Society (ICRS) Cartilage Lesion Classification System (see 3.3.2 Macroscopic Sample Grading).

4.2.2.3 *Histological Assessment of Samples*

Histological staining and assessment were carried out to evaluate the morphological features of the osteochondral tissue isolated from the lesioned and normal regions.

4.2.2.3.1 *Sample Processing and Sectioning*

A portion of the lesioned and of the normal region of osteochondral tissue was fixed in formalin overnight before being taken to the histopathology department at RJAH for processing and sectioning, as detailed in chapter 3 (Section 3.2.3.1 Sample Processing and Sectioning, figure 4-1: C, 7 & 9). In brief, tissue samples were dehydrated through a series of increasing concentrations of isopropanol (IPA; Genta Medical, York, UK) in distilled water, before being cleared in Xylene (Genta Medical) and embedded in paraffin wax for sectioning. Sections of osteochondral tissue were cut at 5µm.

4.2.2.3.2 *Dewaxing and Rehydrating Sections for Staining*

Paraffin-wax sections were deparaffinised and rehydrated for further histological analysis as detailed in chapter 3 (Section 3.2.3.2 Dewaxing and Rehydrating Sections for Staining). In brief, paraffin wax was removed from the slides by heating and submersion in Xylene, and the sections were rehydrated through a series of decreasing concentrations of IPA to distilled water, in preparation for staining.

4.2.2.3.3 Mayer's Haematoxylin and Eosin Staining

Dewaxed and rehydrated sections were stained with Mayer's Haematoxylin (VWR International Ltd, Poole, UK) and Eosin (BDH, Dorset, UK), as detailed in chapter 3 (Section 3.2.3.3 Mayer's Haematoxylin and Eosin Staining). In brief, sections were submerged in each of the dyes in turn before being dehydrated through a series of increasing concentrations of IPA and mounted using Pertex mounting medium (Histolab Products AB, Gothenberg, Sweden).

4.2.2.3.4 Toluidine Blue Staining

Dewaxed and rehydrated sections were stained with Toluidine Blue (1% aqueous) (VWR International Ltd, Poole, UK), as detailed in chapter 3 (Section 3.2.3.4 Toluidine Blue Staining). In brief, sections were flooded with the dye, rinsed in tap water and air dried before being mounted using Pertex mounting medium.

4.2.2.3.5 Microscopy

Stained sections were viewed under a Leitz, Wetziar light microscope (Leica Microsystems Ltd, Milton Keynes, UK) using x1.6, x6.3, x25 and x40 objective lenses. Images were captured using a DS-FiL camera (Nikon Corporation, Tokyo, Japan) and analysed using NIS-Elements BR software version 3.2 (Nikon Corp., Tokyo, Japan) and Gnu Image Manipulation Programme (GIMP) version 2.10 (free software, gimp.org).

4.2.2.3.6 Histological Scoring Systems

4.2.2.3.6.1 The Osteoarthritis Research Society International (OARSI) Osteoarthritis Cartilage Histopathology Assessment System

The semi-quantitative OARSI OA Cartilage Histopathology Assessment system, detailed in chapter 3 (Section 3.2.3.7.1 The Osteoarthritis Research Society International (OARSI)

Osteoarthritis Cartilage Histopathology Assessment System), was used to score the cartilage on sections of bone and cartilage taken from the lesioned and normal regions.

4.2.2.3.6.2 Subchondral Bone Histological Grading System

The subchondral bone histological grading system, described in detail in chapter 3 (Section 3.2.3.7.2 Subchondral Bone Histological Grading System), was used to score the subchondral bone on sections of bone and cartilage taken from the lesioned and normal regions.

4.2.2.3.6.3 Correlation and Differences in Scoring Systems

The correlation between the two histological scoring systems was assessed using a repeated measures Pearson's correlation coefficient. A Wilcoxon-Pratt signed-rank test was used to test for differences between conditions in each of the individual scoring systems.

4.2.3 Primary Osteoblast Isolation and Expansion

4.2.3.1 *Osteoblast Culture Media*

Dulbecco's modified eagle medium: nutrient mixture F-12 (DMEM/F12; 1:1) (Life Technologies, Paisley, UK) supplemented with 10% (v/v) foetal bovine serum (FBS; Life Technologies) and 1% (v/v) penicillin-streptomycin (P/S) (5,000 U/ml; Gibco, Loughborough, UK).

4.2.3.2 *Osteoblast Isolation*

A portion of each region, lesioned or normal, was left untouched to allow for histological assessment (see 3.2.3 Histological Assessment of Samples). From the remainder of each region, osteoblasts were isolated using an established explant outgrowth method (Figure 4-1: C, 8 & 10) (Helfrich & Ralston, 2012). Excised osteochondral tissue from the normal and

lesioned regions were transferred into separate, sterile petri dishes (Sarstedt, Leicester, UK) and rinsed several times with 20ml of sterile PBS (Gibco) before being transferred into new, sterile petri dishes containing 20ml of sterile PBS. Fragments of the trabecular bone were removed from the regions identified as lesioned or normal, using sterile Liston bone cutting forceps (Leica Microsystems Ltd) and transferred into new, sterile petri dishes containing 5ml of sterile PBS. Bone fragments were then cut into 3-5mm pieces using a sterile scalpel and sterile fine scissors. The PBS was decanted and discarded, and the bone chips were transferred into a sterile, 60ml sample pot (Sarstedt). 20ml of PBS was added and the sample pot was vigorously vortex-mixed three times, for 10 seconds each, before being left to stand for 30 seconds to allow the bone chips to settle. The supernatant, which contained haematopoietic tissue and dislodged cells, was carefully aspirated and discarded, with care taken to not dislodge any of the bone chips. The process of adding 20ml of fresh PBS, vortex-mixing, resting and then aspirating the supernatant was repeated at least three more times, until no further haematopoietic marrow was visible, and the bone chips assumed a white, ivory-like appearance. At this point, the bone chips were weighed and then cultured as explants in tissue culture flasks at a density of 0.5g of bone chips per 75cm² tissue culture flask (Sarstedt). 10ml of osteoblast culture media (see 4.3.4.1 Osteoblast Culture Media) was added to each flask and they were incubated at 37°C in a humidified atmosphere, with 5% CO₂. The bone chips were cultured undisturbed for 7 days, at which point the media was replaced, taking care not to dislodge the explants. The outgrowth of osteoblasts from the bone chips was assessed at around 10 days. Media was exchanged after 14 days, and then twice weekly thereafter for 4-6 weeks until 80% confluence was attained (Helfrich & Ralston, 2012).

4.2.3.3 *Cryopreservation of Osteoblasts*

Osteoblasts were not further culture expanded once 80% confluence was attained after the initial seeding (passage 0 (P0)) and were cryopreserved at P0-1 (figure 4-1: D, 12 & 14). In brief, osteoblast monolayers were washed with 10ml PBS and then incubated with 8ml of 0.05% (w/v) trypsin-ethylenediamine (trypsin-EDTA; Gibco) for 5 minutes at 37°C. After 5 minutes, the detachment of the cells was assessed by examination under a microscope and flasks were gently tapped on the side of the lab bench to ensure that all the cells had dislodged. The trypsin-EDTA activity was stopped by adding 8ml of osteoblast culture media and the resulting suspension was aspirated into sterile 50ml tubes (Sarstedt) and centrifuged at 250 xg for 5 minutes to pellet the cells. The cell pellet was resuspended in complete media and a viable cell count performed by trypan blue exclusion (section 3.2.4.4 *Passaging Cells in Monolayer Culture*). At this point, 15,000 osteoblasts from each population were taken for the histochemical assessment of alkaline phosphatase activity (see 3.2.5.2.3.3.3 *Alkaline Phosphatase Staining*). The remaining cell suspension was again centrifuged at 250 xg and the cell pellet was resuspended in pre-cooled 10% (v/v) DMSO in FBS at a density of 1×10^6 cells per ml. The cell suspension was then distributed in 1ml (1 million cells) aliquots between 1.8ml cryovials (Sarstedt). Cryovials were placed into a Mr Frosty™ cryofreezing container (ThermoFisher Scientific, Loughborough, UK) that contains IPA and cools at a rate of 1°C/minute, overnight to -80°C before being transferred to liquid nitrogen for long-term storage.

4.2.3.4 *Osteoblast Yield*

The osteoblast cell count, calculated at the end of P0 immediately prior to cryopreservation (see section 4.2.3.3 *Cryopreservation of Osteoblasts*), was used to calculate osteoblast yield by normalising the cell count to the weight of the bone chips from which they were

cultured. The average osteoblast yield, expressed as number of osteoblasts per gram of trabecular bone chips, was compared between the lesioned and normal regions.

4.2.3.5 *Alkaline Phosphatase Staining*

Histochemical staining was performed to qualitatively assess alkaline phosphatase activity, which is considered a hallmark characteristic of osteoblasts, in the isolated cell populations (figure 4-1, D) (Anh et al., 1998; Helfrich & Ralston, 2012; Rutkovskiy et al., 2016). 15,000 cells from each population were taken from the cell suspension before it was prepared for cryopreservation, and re-seeded (P1) at a density of 5×10^3 cells/cm² in 24 well plates (Sarstedt) (3 wells of lesioned and normal osteoblasts per patient). The seeded osteoblasts were cultured until 80% confluency was attained, at which point they were fixed in 10% buffered formalin and stained using a mixture of naphthol AS-BI phosphate (Sigma-Aldrich) and Fast Red TR (Sigma-Aldrich), as described in chapter 3 (Section 3.2.5.2.3.3 Alkaline Phosphatase staining). Stained osteoblasts were viewed immediately by phase contrast microscopy, using x4 and x20 objective lenses on a Nikon Eclipse TS100 bench-top microscope (Nikon, Tokyo, Japan). Images were captured using a Leica MC170 HD Microscope camera (Leica Microsystems Ltd, Milton Keynes, UK).

4.2.4 Experimental Set-up

4.2.4.1 *Recovery of Osteoblasts from Liquid Nitrogen Storage*

Osteoblasts were recovered from liquid nitrogen storage as required, by rapidly thawing the cryovials under a running hot tap until there was only a small amount of ice left. Next, 1ml of pre-cooled, osteoblast culture media was added to the thawed cell suspension dropwise for 1 minute. Cell suspensions were then left to stand for a further minute before 20ml of the cooled media was added dropwise to the cell suspension for 10 minutes. After this, the

cells were pelleted by centrifugation at 250 xg for 2 minutes. Cells were then resuspended in 20ml of pre-cooled osteoblast culture medium and pelleted again by centrifugation before resuspension and a viable cell count was carried out by trypan blue exclusion (section 3.2.4.4 Passaging of Cells in Monolayer Culture).

Finally, osteoblasts were seeded in 24-well plates at a density of 5×10^3 cells/cm². Six wells were seeded per condition, per patient (Figure 4-1: E, 15 & 17) and cultured until 80% confluency was reached, at which point the osteoblasts were prepared for analysis.

4.2.5 Experimental Endpoint Analysis

Following experimental seeding and subsequent culture, cell populations were prepared for analysis (figure 4-1: E, 16 & 18)

4.2.5.1 Gene Expression Analysis

The gene expression profile of the osteoblasts isolated from lesioned and normal zones was assessed using Quantitative Real-time Polymerase Chain Reaction (qRT-PCR) following RNA extraction and reverse transcription.

4.2.5.1.1 Ribonucleic Acid (RNA) Extraction

RNA was extracted from three of the six wells containing the osteoblasts monolayers, for each osteoblast population and was performed as previously described (see chapter 3, section 3.2.5.2.3.1.2 Gene Expression Analysis). In brief, culture medium was aspirated, and the osteoblasts were carefully washed with 1.5ml of pre-cooled PBS. Next, 350µl of buffer RLT (Qiagen, Manchester, UK), supplemented with 1% (v/v) β-mercaptoethanol (Sigma-Aldrich), was added to each well and incubated for 2 minutes at room temperature before being mixed thoroughly with a pipette and transferred into labelled, sterile 1.5ml Eppendorf tubes (Sarstedt). After this, 350µl of 70% ethanol (molecular biology grade; Sigma-Aldrich) in

RNAse free water (Qiagen) was added to each sample and mixed thoroughly. RNA was then extracted from the cell lysate as previously described, using the RNeasy® Mini Kit (Qiagen) to eventually elute RNA with RNAse free water. RNA was stored at -80°C until required.

4.2.5.1.2 Reverse Transcription

Complementary DNA (cDNA) was generated from the extracted RNA by reverse transcription using the High-Capacity cDNA Reverse Transcription Kit (Applied Biosystems, Loughborough, UK) as previously described (section 3.2.5.2.3.1.2.2 Reverse Transcription). cDNA was stored at -20°C until required.

4.2.5.1.3 Quantitative Real-time Polymerase Chain Reaction (qRT-PCR)

qRT-PCR was performed on the Quant Studio 3 Real-Time Quantitative PCR System (Applied Biosystems) using SYBR green QuantiTect primer assays (Qiagen) to assess a number of genes in the osteoblast populations indicative of the different stages of osteogenic differentiation: bone morphogenic protein 2 (*BMP2*), alkaline phosphatase (*ALPL*), collagen type 1, alpha 1 (*COL1A1*), Runt-related transcription factor 2 (*RUNX2*), bone gamma-carboxyglutamate protein (*BGLAP*), secreted phosphoprotein 1 (*SPP1*) (table 3-11). GAPDH and HPRT1 were employed as housekeeping genes and sample gene expression levels were normalised to the geometric mean of their corresponding housekeeping genes (Vandesompele et al., 2002). Following normalisation to the reference genes, the relative expression of each gene in the osteoblasts isolated from the lesioned site expressed as a ratio compared to those isolated from the normal site, was determined using the comparative Ct method (Schmittgen & Livak, 2008). A twofold change (up- or down-regulated) was deemed biologically significant. Technical details relating to reagent

volumes, consumables and the thermal cycle used for qRT-PCR can be found in chapter 3 (Section 3.2.5.2.3.1.2.3 Quantitative Real-time Polymerase Chain Reaction (qRT-PCR)).

4.2.5.1.4 dsDNA Quantification

The dsDNA content of the cells in three of the six wells of each of the osteoblasts was quantified using the PicoGreen® fluorescence assay (Invitrogen, Loughborough, UK). In brief, the culture medium was aspirated, and the osteoblasts carefully washed with chilled PBS. Next, 350µl of buffer RLT (Qiagen), supplemented with 1% (v/v) β-mercaptoethanol (Sigma-Aldrich), was added to each well and incubated for 2 minutes at room temperature before being mixed thoroughly with a pipette and transferred into labelled, sterile 1.5ml Eppendorf tubes (Sarstedt). 25µl of each cell lysate was then used in the PicoGreen® assay and dsDNA was quantified as described in chapter 3 (Section 3.2.5.2.3.1.1.1 Scaffold DNA Quantification). The average dsDNA content was compared between the osteoblasts isolated from the normal and lesioned sites.

4.2.5.2 Statistical Analyses

4.2.5.2.1 Correlation Between Histological Scores

Jamovi (version 1.2.8, jamovi.org) was used to determine the repeated measures Pearson's correlation between the OARSI OA Cartilage Histopathology Assessment System and the Subchondral Bone Grading System (R Core Team, 2019; jamovi, 2020).

4.2.5.2.2 Osteoblast Yield

Microsoft® Office Excel 2013 (Microsoft®, Washington, USA) was used to calculate the osteoblast number per gram of trabecular bone for each of the osteoblast populations, and to calculate an average osteoblast yield (cells/gram) for trabecular bone chips isolated from the lesioned and from the normal regions. Jamovi was used to explore descriptive statistics

and to carry out a linear mixed model analysis on the osteoblast yield data with 'Osteoblast Number' as the dependant variable, 'Region' as a factor, 'Patient' as the cluster variable and 'Patient | Intercept' as the random effects variable (R Core Team, 2019; Gallucci, 2019; jamovi, 2020).

4.2.5.2.3 qRT-PCR

Microsoft® Office Excel 2013 (Microsoft®, Washington, USA) was used to calculate the relative expression of each of the genes of interest to the geometric mean of their corresponding housekeeping genes using the ΔC_t method (Vandesompele et al., 2002; Schmittgen & Livak, 2008). Jamovi was used to calculate the fold difference in gene expression in the osteoblasts from the lesioned site as a ratio to those from the normal site (Schmittgen & Livak, 2008; R Core Team, 2019; jamovi, 2020). A two-fold difference (up- or down-regulated) was considered biologically significant.

4.2.5.2.4 dsDNA Quantification

Microsoft® Office Excel 2013 (Microsoft®, Washington, USA) was used to calculate the quantity of dsDNA in each of the samples from the fluorescence values and the standard curve of known concentrations. Jamovi (version 1.2.8, jamovi.org) was then used to explore descriptive statistics and to carry out a linear mixed model analysis on the osteoblast dsDNA data with 'dsDNA Content' as the dependant variable, 'Osteoblast type' as a factor, 'Patient' as the cluster variable and 'Patient | Intercept' as the random effects variable (Gallucci, 2019; R Core Team, 2019; jamovi, 2020).

4.3 Results

4.3.1 Patients

Osteochondral tissue was collected from five OA patients following TKR surgery at the RJAH Orthopaedic Hospital that had MRIs in the last 6 months that demonstrated subchondral bone abnormalities.

Osteochondral tissue was also collected from a sixth patient, whose MRI was around 15 months old but did demonstrate a focal signal change in the medial tibial plateau. Tissue from this patient was used only for the histological demonstration of a well-defined subchondral bone cyst.

Demographic information and a relevant, brief excerpt from the MRI report for each patient is given in table 4-1.

4.3.2 Macroscopic Cartilage Grading

Ten areas of cartilage were graded, 5 located above subchondral bone regions with pathological changes that were indicated on MRI and 5 located above normal subchondral bone regions. The cartilage above these two regions ranged in ICRS grade from grade 1; 'nearly normal' (5 areas) to grade 4; 'severely abnormal cartilage (extending into the subchondral bone)' (1 area). In general, cartilage that was located above regions of the subchondral bone with no pathological features received a better ICRS cartilage grade (all received grade 1) than cartilage from areas above the MRI-identified subchondral bone pathologies (all received grade 2, 3 or 4) (Table 4-2).

4.3.3 Histological Assessment

4.3.3.1 *The Osteoarthritis Research Society International (OARSI) Osteoarthritis Cartilage Histopathology Assessment System*

Stained sections ranged in OARSI cartilage histopathology grade from grade 1, 'surface intact with superficial fibrillation' (4 areas) to grade 6; 'deformation' (1 area). In general, cartilage that was overlying the subchondral bone with no SB abnormalities received a better OARSI score (median: 1) than that which was overlying SB abnormalities (median: 5) (Table 4-2).

4.3.3.2 *Subchondral Bone Histological Grading System*

Stained sections ranged in subchondral bone histological grade from 0; 'early stages of OA' (4 regions), to grade 2; 'distinct increase in bone volume and loss of contact between cartilage and bone marrow' (4 regions). In general, the subchondral bone from regions with no MRI-identified SB abnormalities received a better SB histological grade (median: 0) than regions with SB abnormalities (median: 2) (Table 4-2).

Table 4-1: Patient demographic information and relevant MRI findings. Included are the five patients from the main study and the additional patient included for the histological assessment of a subchondral bone cyst.

Patient	Gender	Age (at time of TKR)	Operated Knee	Clinical Diagnosis (details where available)	MRI Findings of Note
1	Female	67	Right	OA (previous patellectomy)	Cystic change deep to the anterior meniscal root attachment with subchondral oedema.
2	Female	58	Right	OA (bilateral)	Subchondral bone marrow oedema-like signal/early cystic change.
3	Female	56	Right	OA	Moderate degree of subchondral bone marrow oedema noted within the medial tibial plateau.
4	Male	72	Left	OA	Prominent bone marrow signal change of the dorsal non weight-bearing lateral femoral condyle, bone cyst formation.
5	Female	57	Right	OA	Subchondral oedema adjacent to meniscal extrusion.
		62.0±7.1 (Mean±SD)			
6	Male	64	Left	OA	Bone marrow signal change medial tibia.

Table 4-2: *Macroscopic and histological scores of isolated regions of interest. ICRS Cartilage Lesion Grade, OARSI OA Cartilage Histopathology Grade and Subchondral Bone Histological Grade results for the osteochondral tissue isolated from regions with and without MRI-identified SB abnormalities. The median scores for the normal and lesion sites, and p-values resulting from the Wilcoxon-Pratt signed-rank test, are also presented (* indicates statistical significance).*

Patient	Region	ICRS Cartilage Lesion Classification System (0-4)	OARSI Osteoarthritis Cartilage Histopathology Assessment System (0-6)	Subchondral Bone Histological Grading System (0-3)
1	Normal	1	1	0
	Lesion	3	6	2
2	Normal	1	2	0
	Lesion	4	5	2
3	Normal	1	1	1
	Lesion	2	2	2
4	Normal	1	1	0
	Lesion	3	5	2
5	Normal	1	1	0
	Lesion	3	5	1
Median	Normal	1	1	0
	Lesion	3	5	2
Wilcoxon-Pratt signed-rank test (p-value)		0.039 *	0.039 *	0.039 *

4.3.3.2.1 Correlation and Differences in Scoring Systems

The OARSI OA Cartilage Histopathology Assessment System and the Subchondral Bone Histological Grading System were strongly correlated (Pearson's $r=0.95$, $p=0.004$; figure 4-4). For each of the scoring systems, there was a significant difference in scores between the lesioned and normal conditions (all $p=0.039$)

4.3.3.3 Morphological Features

The histological appearance of the normal sites was relatively consistent across patients, with the subchondral bone demonstrating only mild degenerative changes such as increased subchondral bone trabeculae thickness in patient 3, and no degenerative changes in the other four patients (Figures 4-5, 4-6, 4-7, 4-8, 4-9, 4-10 & 4-11).

There was a greater degree of heterogeneity in the morphological features of the lesioned sites. All patients demonstrated an increase in bone volume and trabecular thickness compared to their normal sites. Some evidence was found suggesting a loss of contact between the bone marrow and calcified cartilage as a result of increased thickness in the subchondral bone plate, which was particularly evident in patients 3 and 4 (Figures 4-9 & 4-10). The subchondral bone of the lesion site from patient 5 demonstrated only mild trabecular thickening compared to their normal site, along with some degree of bone marrow edema (Figure 4-11).

An ill-defined subchondral bone cyst, appearing as a cavitory lesion surrounded by dense, highly cellular, fibroconnective tissue, was identified in the lesioned area of patient 1 and was surrounded by thickened trabeculae (Figures 4-5 & 4-6). A second focal area of fibrous tissue between bone trabeculae was also evident in patient 1 and may represent further cystic changes.

A number of interesting features were also present in the lesion site of patient 2 (Figures 4-7 & 4-8). The calcified cartilage zone and underlying subchondral bone showed a great deal of discontinuity, including a pit in the surface that contained cartilage which was bordered by thickened trabeculae. Both sides of the pit had evidence of bone marrow fibrosis, between thickened bone trabeculae. Blood vessel infiltration was also present in the areas of bone marrow fibrosis. There were also islands of cartilage located in the subchondral bone, deep to the pit in the surface, which were surrounded by thickened subchondral bone trabeculae.

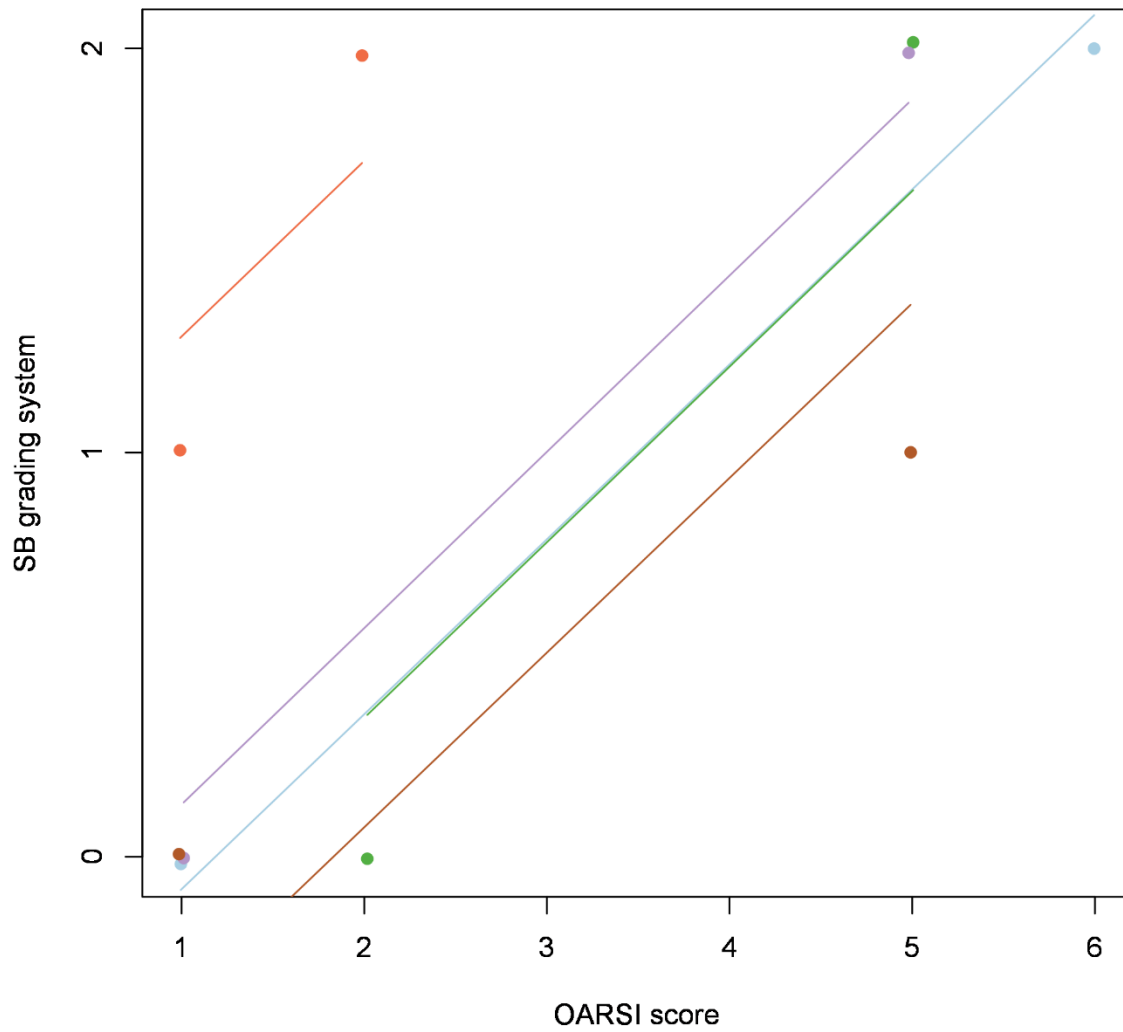


Figure 4-4: Correlation between histological scores. Graphical representation of the correlation between the OARS I OA Cartilage Histopathology Assessment System and the Subchondral Bone Histological Grading System (Pearson's $R=0.95$, $p=0.004$, $n=5$ pairs).

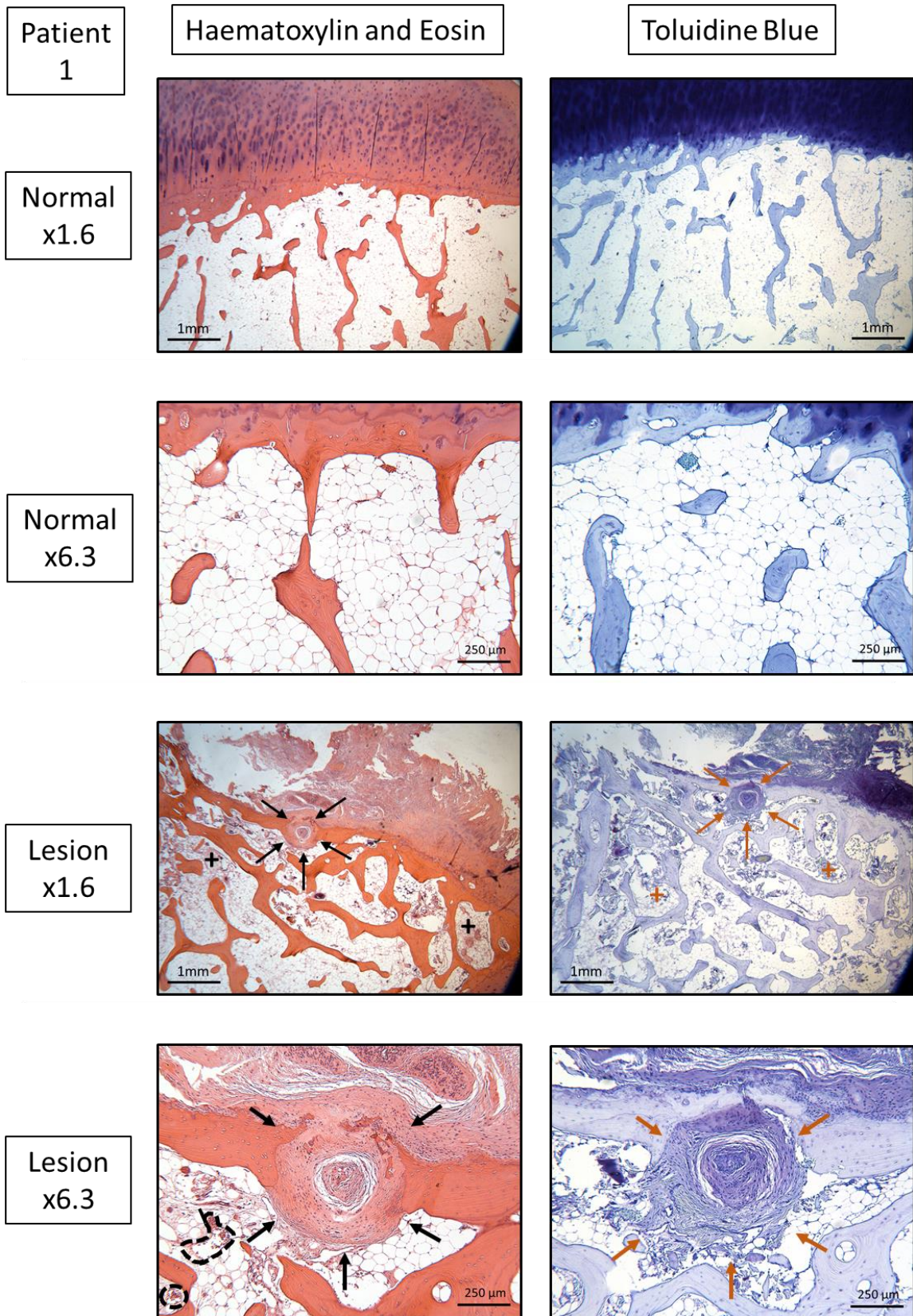


Figure 4-5: Patient 1 histological findings. Morphological features of normal (top) and lesioned (bottom) areas of the subchondral bone. Arrows: Focal area of fibrous tissue between bone trabeculae. Dotted line: blood vessel infiltration. +: bone marrow fibrosis.

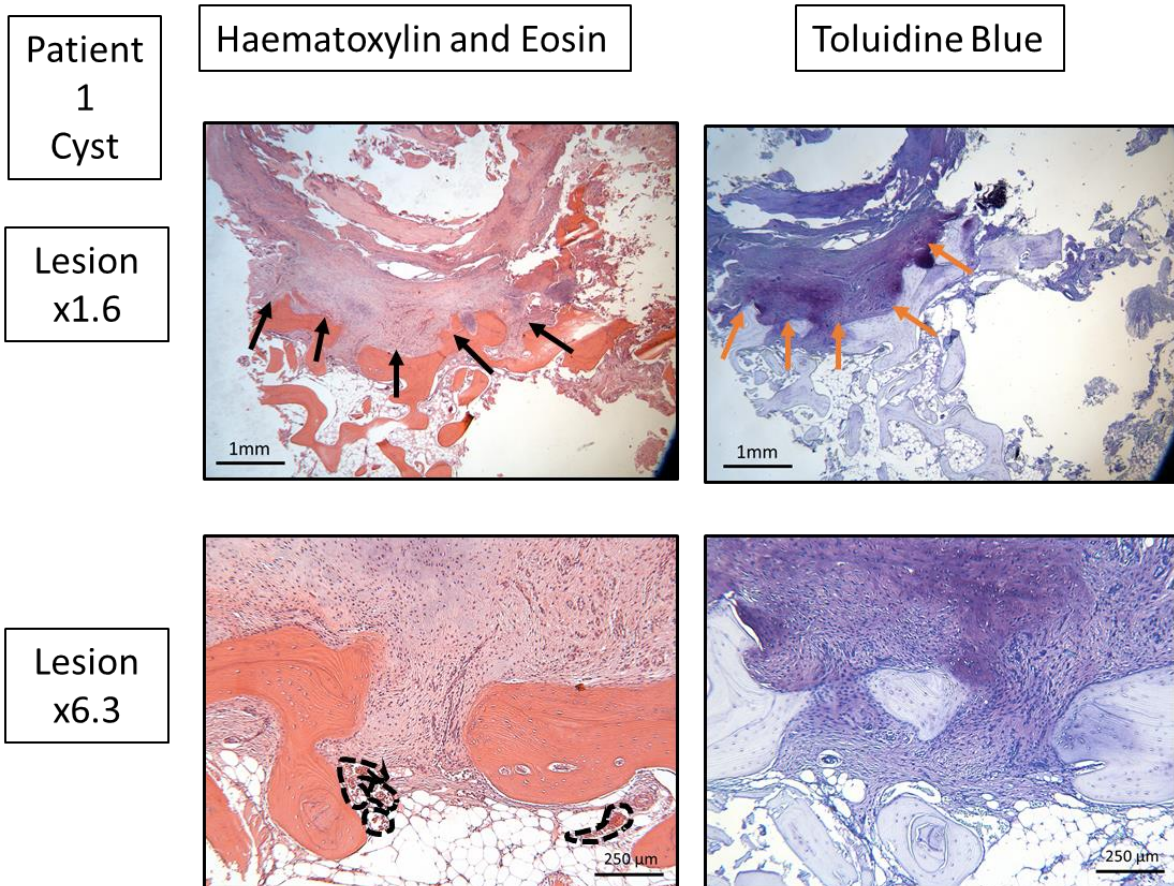


Figure 4-6: Patient 1 histological findings (continued). Arrows: Dense fibrous border of a subchondral bone cyst (arrows). Dotted line: blood vessel infiltration.

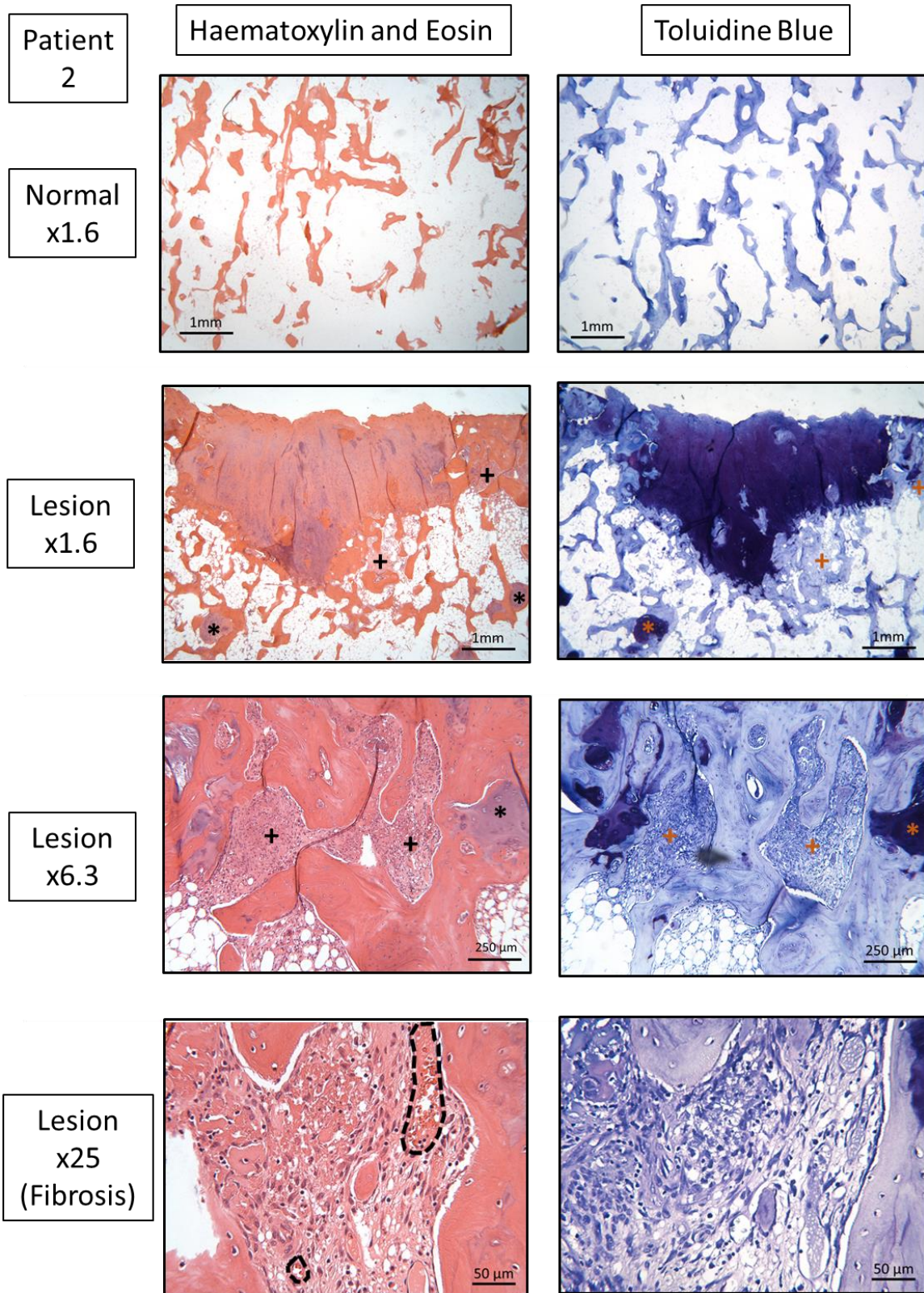


Figure 4-7: Patient 2 histological findings. Morphological features of normal (top) and lesioned areas of the subchondral bone. +: bone marrow fibrosis. *: cartilage islands. Dotted line: blood vessel infiltration.

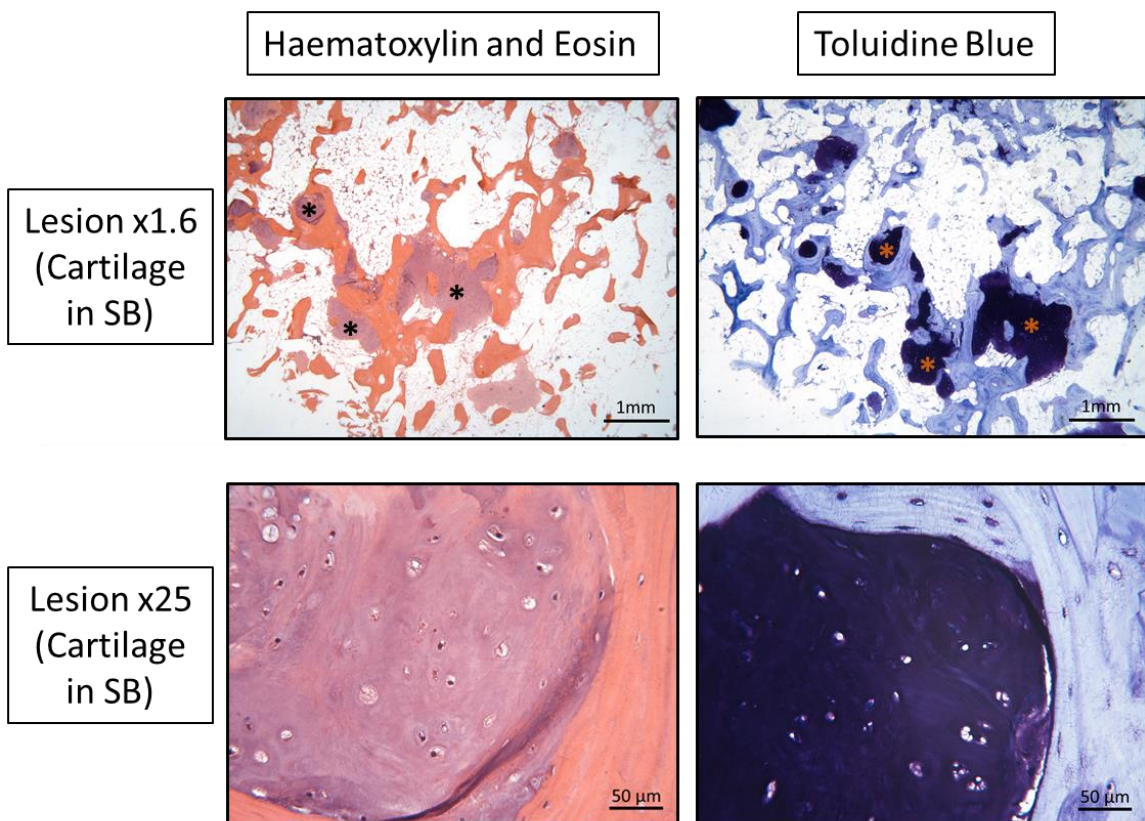


Figure 4-8: *Patient 2 histological findings (continued). Morphological features of the lesioned area of the subchondral bone. *: cartilage islands.*

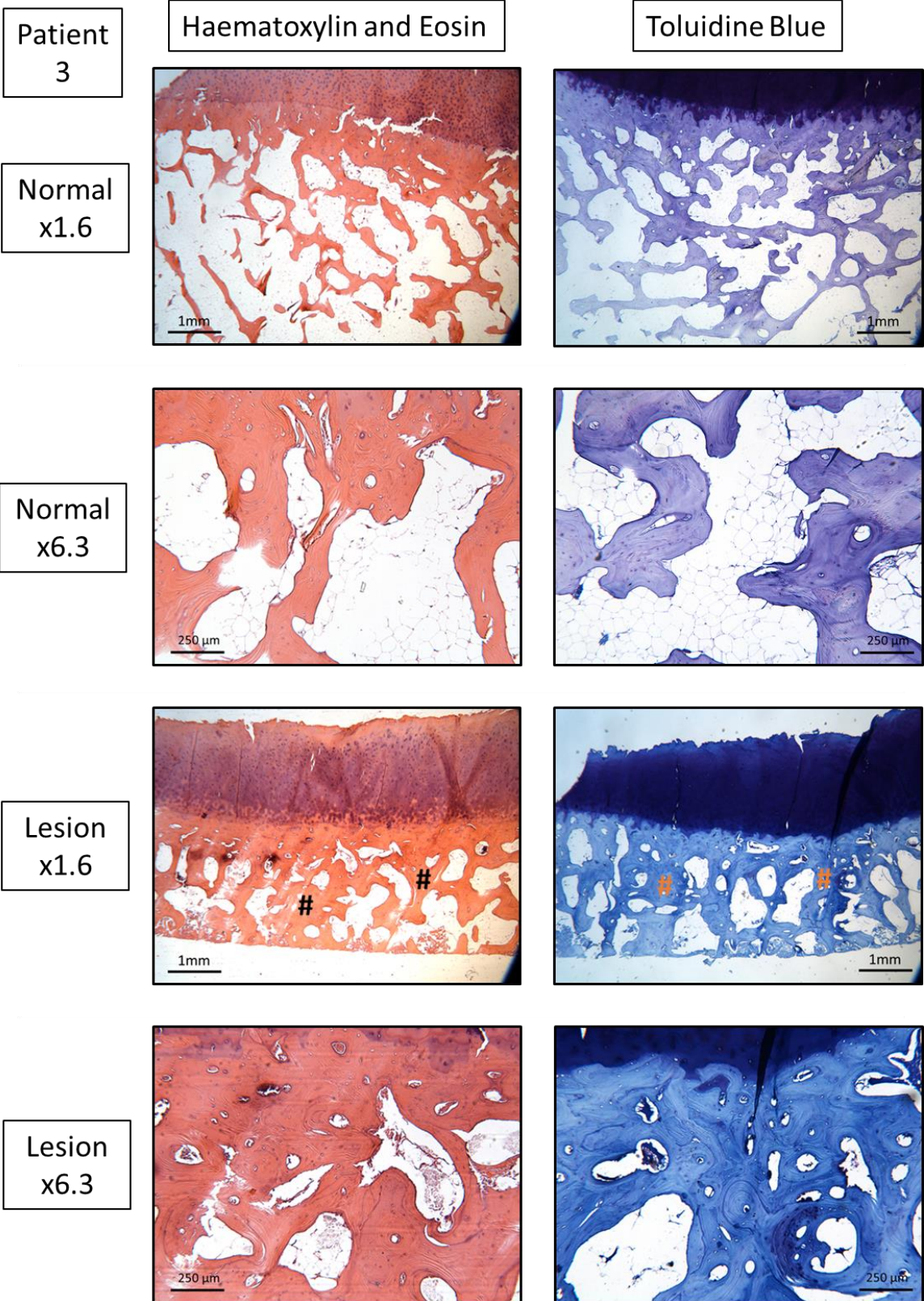


Figure 4-9: Patient 3 histological findings. Morphological features of normal (top) and lesioned (bottom) areas of the subchondral bone. #: trabecular thickening.

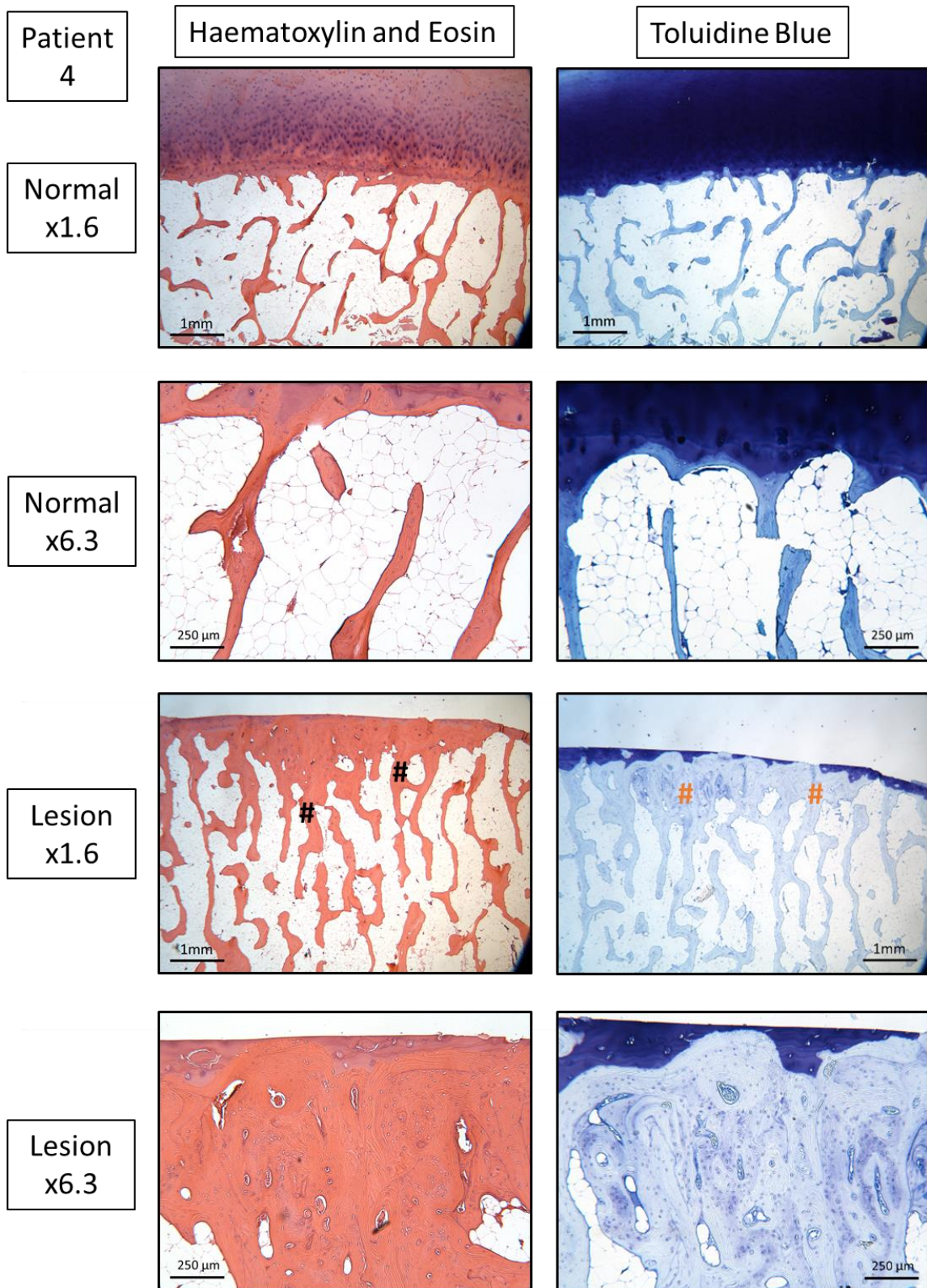


Figure 4-10: Patient 4 histological findings. Morphological features of normal (top) and lesioned (bottom) areas of the subchondral bone. #: trabecular thickening.

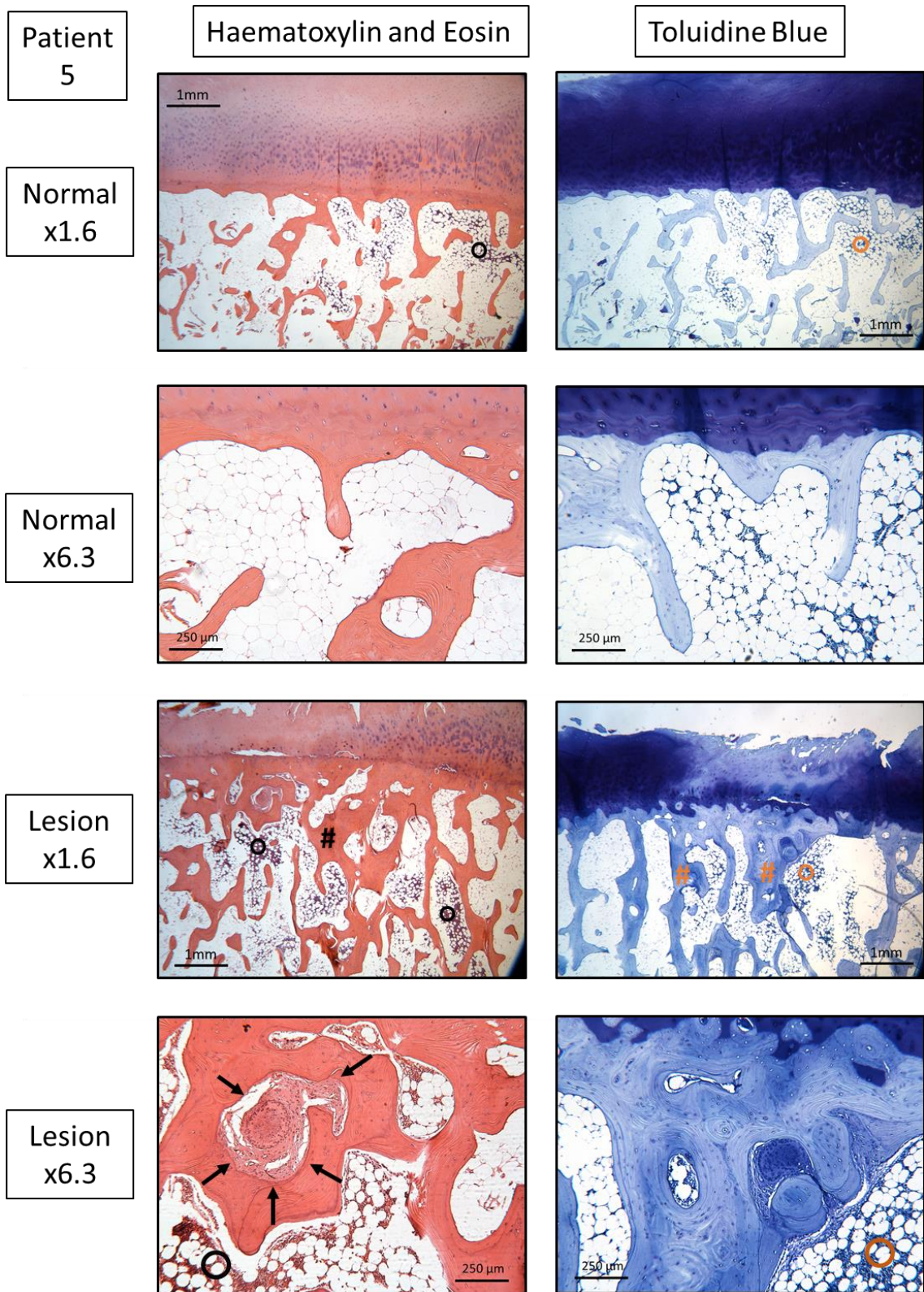


Figure 4-11: Patient 5 histological findings. Morphological features of normal (top) and lesioned (bottom) areas of the subchondral bone. #: trabecular thickening. O: bone marrow edema. Arrows: Focal area of fibrous tissue between bone trabeculae.

4.3.3.3.1 Subchondral Bone Cyst – Patient 6

A well-defined subchondral bone cyst was identified and isolated for histological assessment from a sixth patient. Although this patient was not included in the rest of the study, due to the exclusion of MRIs that were older than 6 months, the MRI, macroscopic tissue appearance and histological findings are included to demonstrate the characteristic features of an MRI-identified subchondral bone cyst (Figures 4-12 & 4-13 respectively). The cyst appeared as a small cavitory lesion surrounded by dense fibrous tissue and appeared to be roughly the same size (around 5mm) as the region of high-signal intensity on the MRI.

4.3.4 Osteoblast Outgrowth

Outgrowth of cells from the explanted bone chips was observed in all patients and conditions after 10-14 days (Figure 4-14).

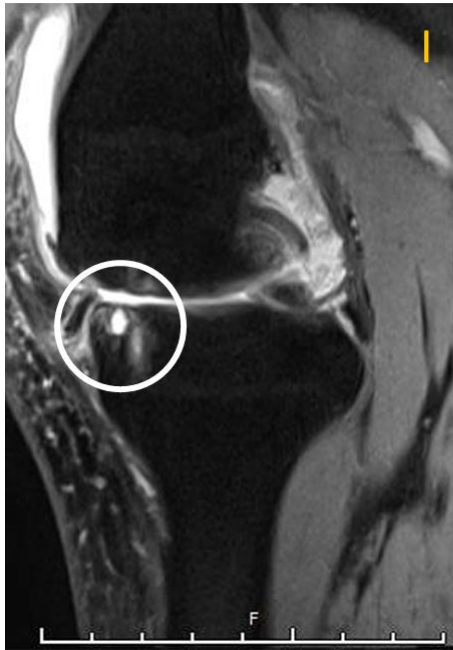
4.3.5 Osteoblast Yield

Osteoblast yield was calculated as the osteoblast number at the end of P0, normalised to the weight of the explanted bone chips from which they grew. There was no significant difference in the average osteoblast yield, expressed as cells per gram of trabecular bone, between bone chips from the normal ($1.51 \times 10^6 \pm 3.46 \times 10^5$ SEM osteoblasts/gram) and lesioned ($1.80 \times 10^6 \pm 6.73 \times 10^5$ SEM osteoblasts/gram) sites (Figure 4-15).

4.3.6 Alkaline Phosphatase Staining

Alkaline phosphatase activity, a characteristic feature of osteoblasts, was assessed by histochemical staining. All osteoblast populations demonstrated some degree of positivity for alkaline phosphatase and there was no discernible difference between patients or between conditions. Example images for one patient (patient 3) are shown in figure 4-16.

A



B

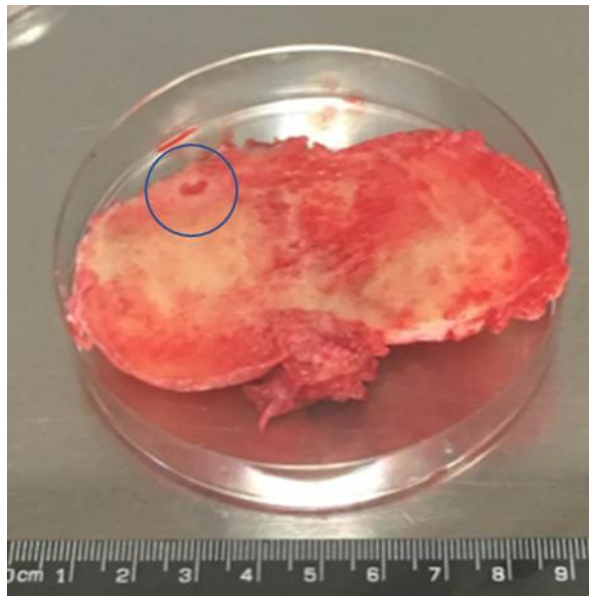
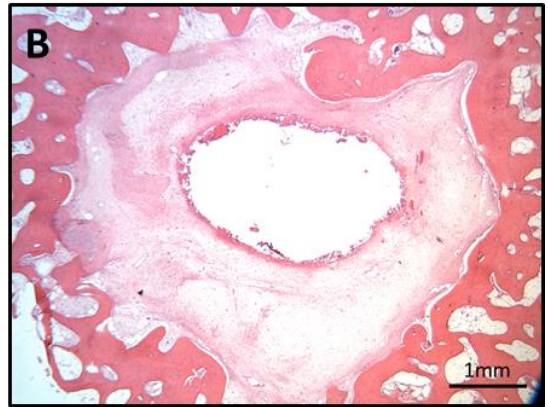
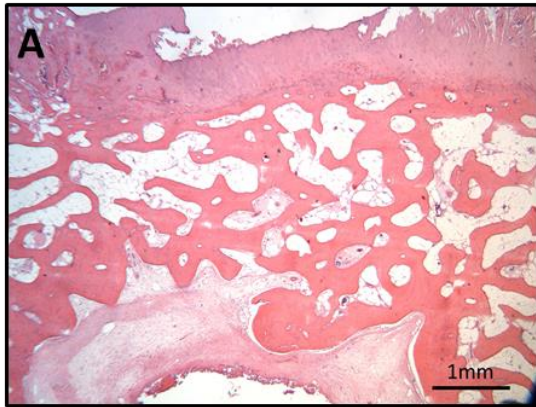


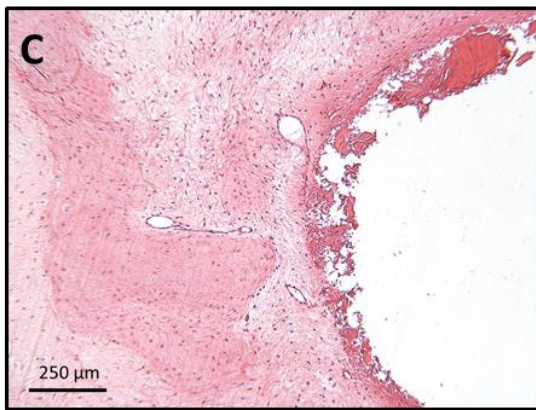
Figure 4-12: Identification of a subchondral bone cyst – Patient 6. A: MRIs demonstrating a focal signal abnormality in the subchondral bone. I: T2-weighted (sagittal plane). II: T2-weighted (coronal plane). B: Macroscopic appearance of excised tibial plateau, caudal side. Circled: subchondral bone cyst.

Patient
6
Cyst

x1.6



x6.3



x25

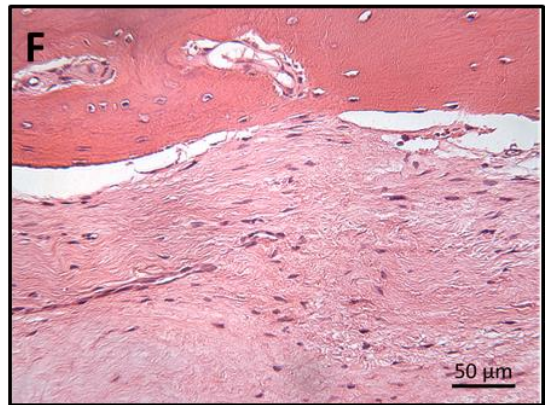
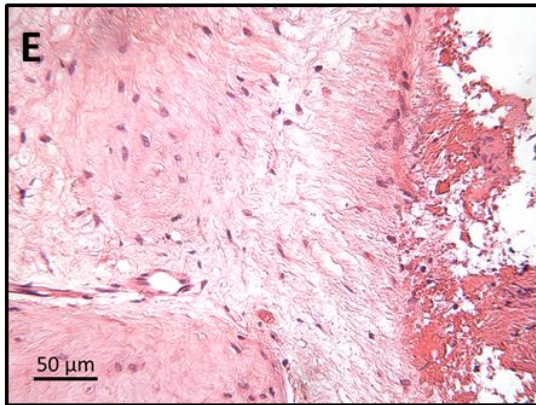


Figure 4-13: Patient 6 histological findings (haematoxylin & eosin). Morphological features of a subchondral bone cyst. A: Subchondral bone cyst beneath the articular surface. B: Appearance of entire subchondral bone cyst demonstrating cavitory lesion with dense fibrous border, surrounded by thickened bone trabeculae. C & E: Cellular, fibrous central border of the subchondral bone cyst. D & F: Transitional border between the edge of the subchondral bone cyst and the surrounding subchondral bone trabeculae.

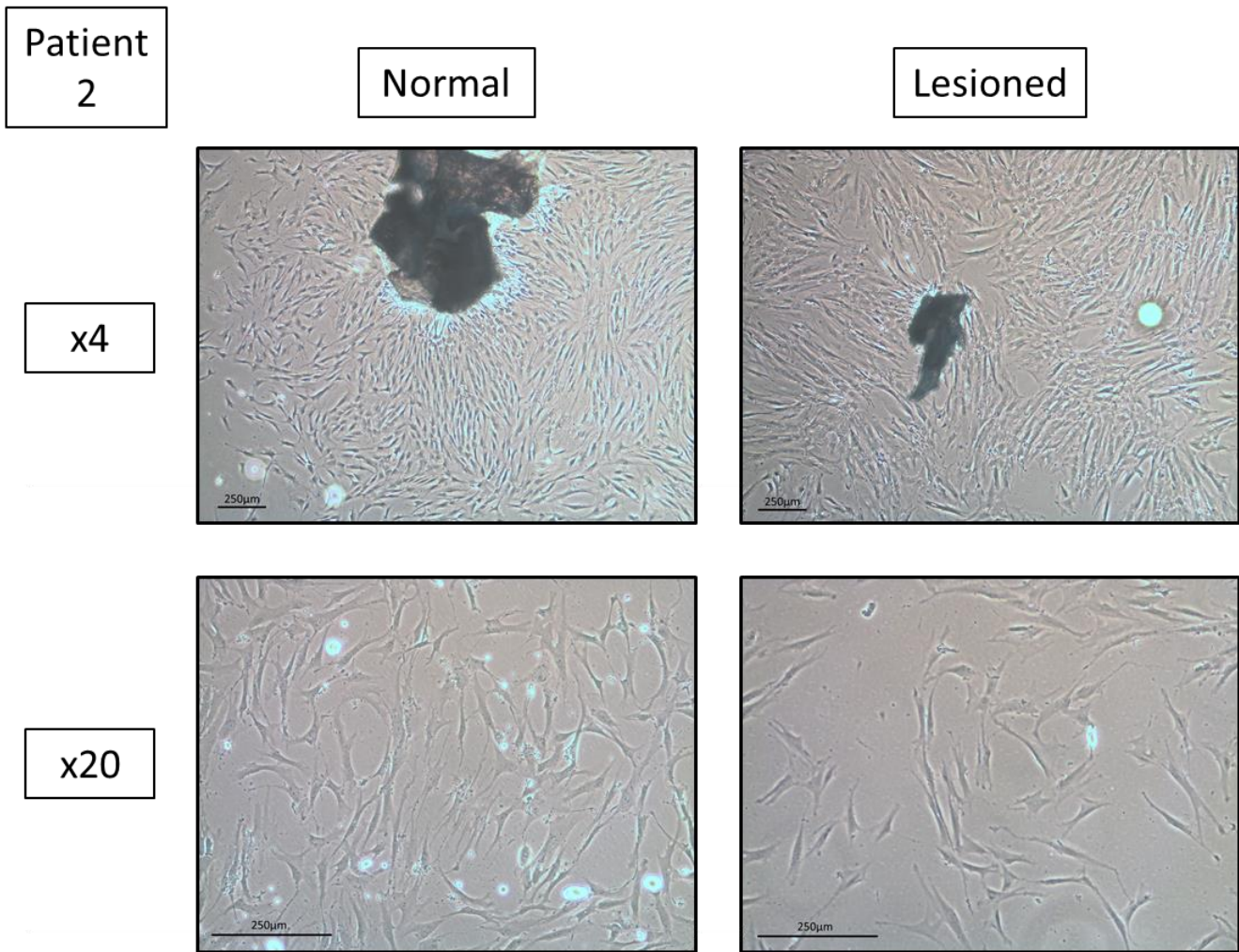


Figure 4-14: *Osteoblast outgrowth from subchondral trabecular bone chips. Bone chips were isolated from the normal region (left) and lesioned region (right) – Example taken from patient 2.*

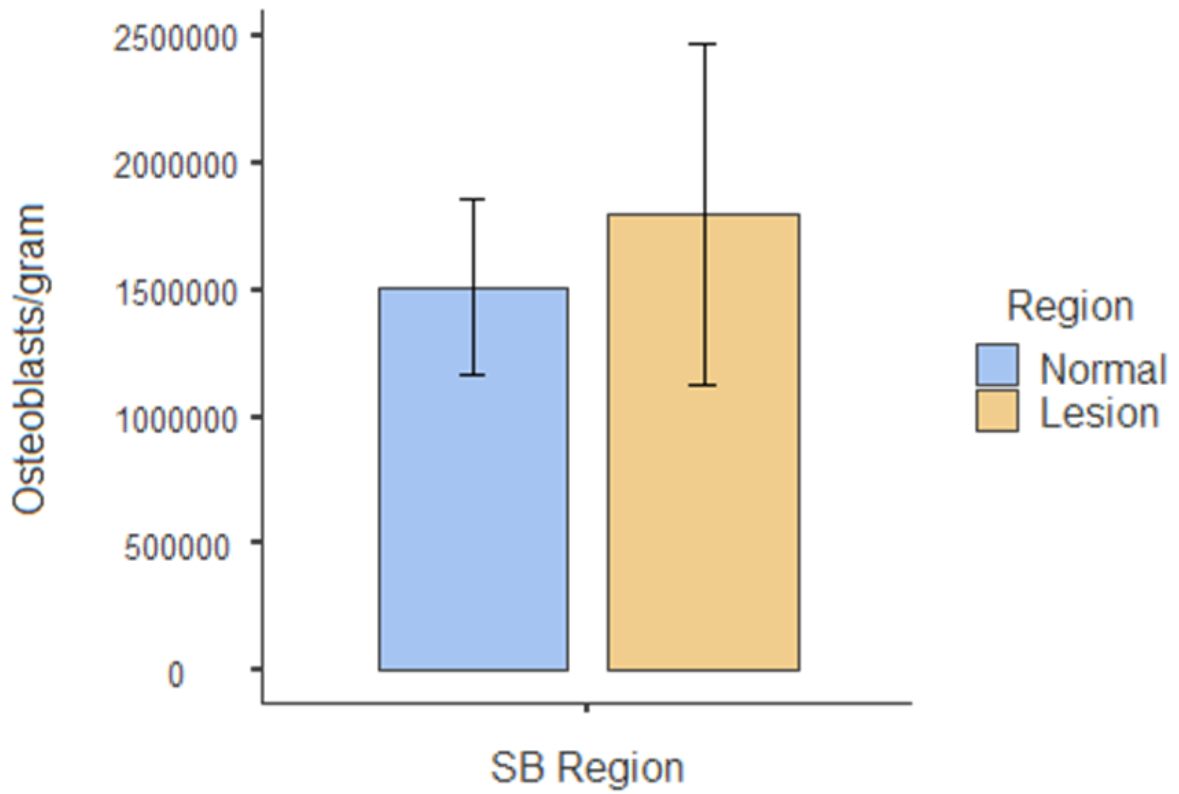


Figure 4-15: Mean osteoblast yield from lesioned and normal areas. Data is presented as the mean number of osteoblasts isolated per gram of bone chips from the lesioned and normal regions. Error bars represent the standard error of the mean.

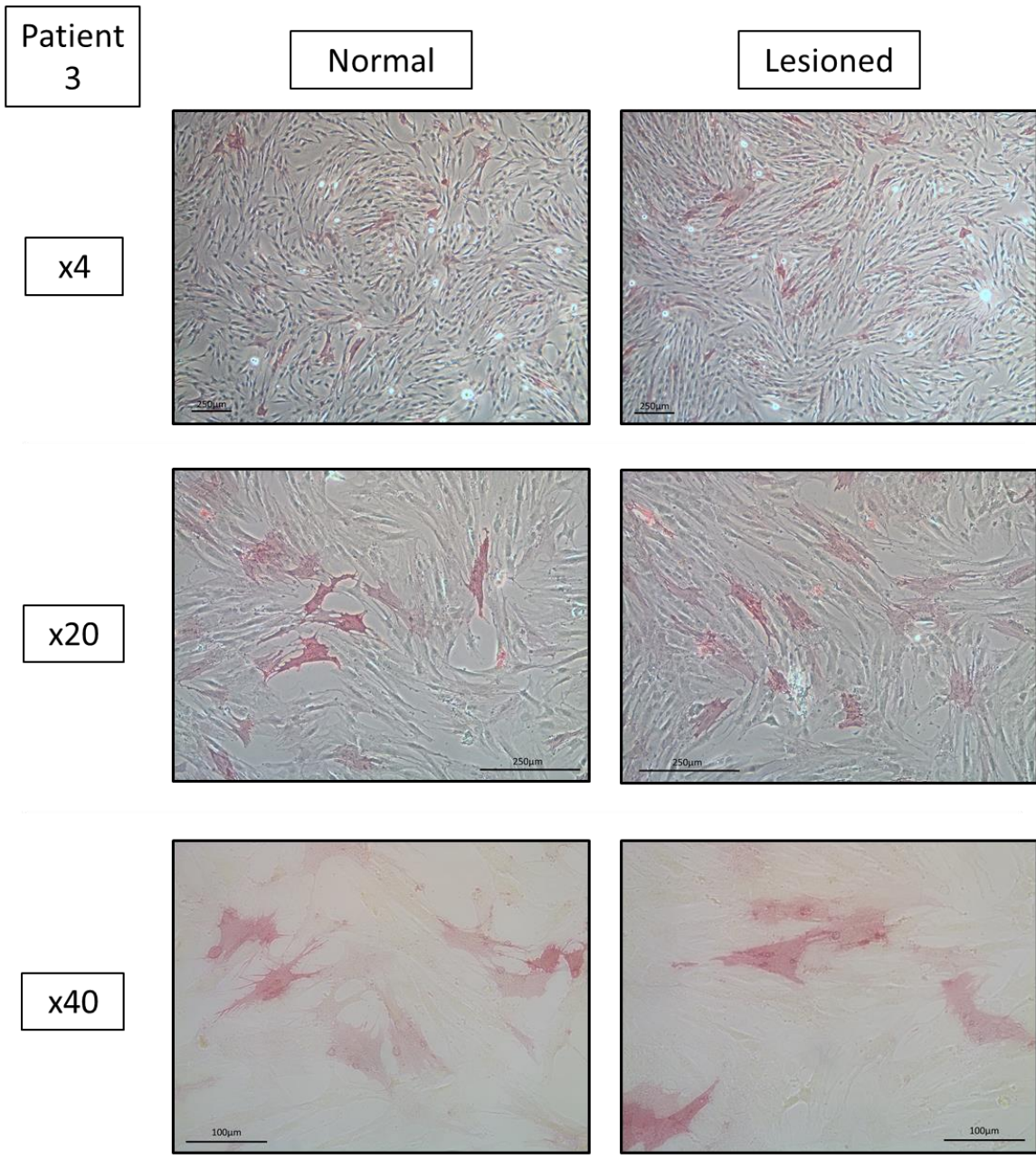


Figure 4-16: Histochemical staining of alkaline phosphatase activity. Some degree of staining was demonstrated in PO osteoblasts isolated from the normal (left) and lesioned (right) regions for all patients. Example shown is patient 3.

4.3.7 dsDNA Quantification

There was no significant difference in average dsDNA content between the cells isolated from the normal ($140\text{ng} \pm 10.7_{\text{SEM}}$) and lesioned ($156\text{ng} \pm 9.6_{\text{SEM}}$) sites (Figure 4-17).

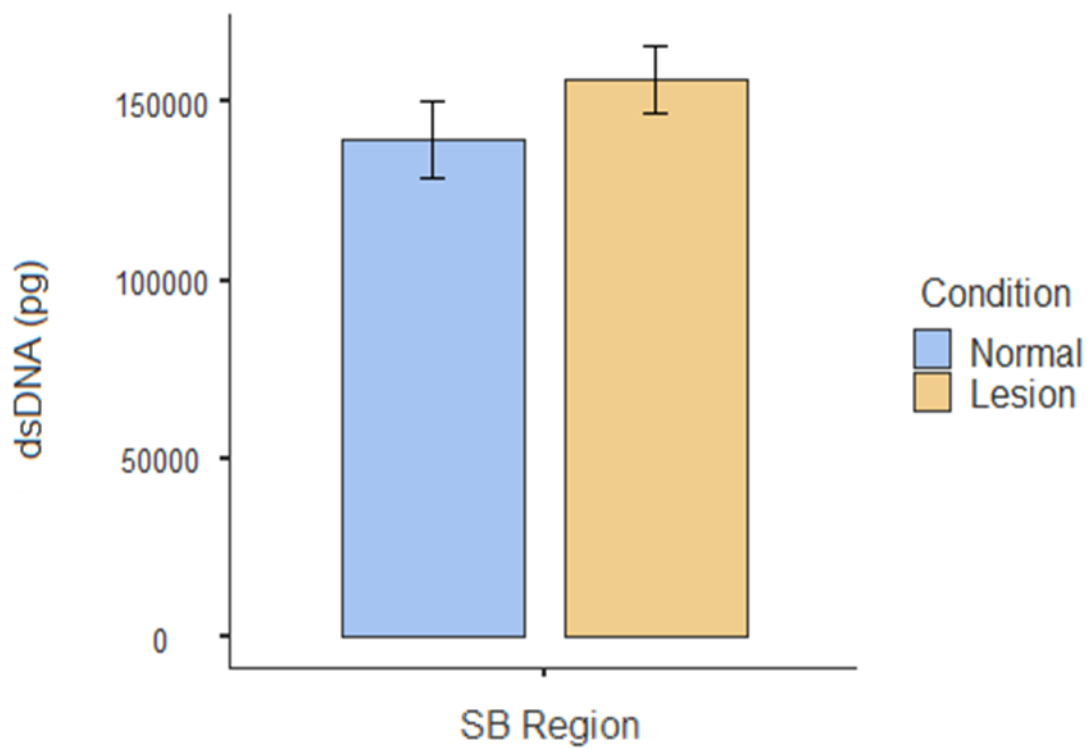


Figure 4-17: Mean dsDNA content (pg) of osteoblast populations following experimental seeding. Mean dsDNA content was calculated for osteoblasts isolated from lesioned and normal regions of the subchondral bone, following seeding at the same density and culture for the same period, for comparison. Error bars represent the standard error of the mean.

4.3.8 Gene Expression Profile

4.3.8.1 *Alkaline Phosphatase (ALPL)*

The mean fold difference in ALPL expression between osteoblasts from lesioned sites and normal sites was not biologically significant ($-0.374 \pm 0.744_{\text{SEM}}$; $p=0.946$; Figure 4-18, A).

4.3.8.2 *Bone morphogenic protein 2 (BMP2)*

The mean fold difference in BMP2 expression between osteoblasts from lesioned sites and normal sites was not biologically significant ($-0.532 \pm 0.566_{\text{SEM}}$; $p=0.564$; Figure 4-18, B).

4.3.8.3 *Collagen type 1, alpha 1 (COL1A1)*

There was a biologically significant fold difference in collagen type I expression between osteoblasts isolated from the lesioned site and those from the normal site ($-2.42 \pm 0.4_{\text{SEM}}$; Figure 4-18, C). However, there was no statistical evidence for this difference ($p=0.126$).

4.3.8.4 *Bone gamma-carboxyglutamate (gla) protein (BGLAP) (Osteocalcin)*

The mean fold difference in BGLAP expression between osteoblasts from lesioned sites and normal sites was not biologically significant ($-0.924 \pm 0.366_{\text{SEM}}$; $p=0.284$) (Figure 4-18, D).

4.3.8.5 *Secreted phosphoprotein 1 (SPP1) (Osteopontin)*

The mean fold difference in SPP1 expression between osteoblasts from lesioned sites and normal sites was not biologically significant ($0.440 \pm 0.554_{\text{SEM}}$; $p=0.928$) (Figure 4-18, E).

4.3.8.6 *Runt-related transcription factor 2 (RUNX2)*

The mean fold difference in RUNX2 expression between osteoblasts from lesioned sites and normal sites was not biologically significant ($-1.33 \pm 0.272_{\text{SEM}}$; $p=0.520$) (Figure 4-18, F).

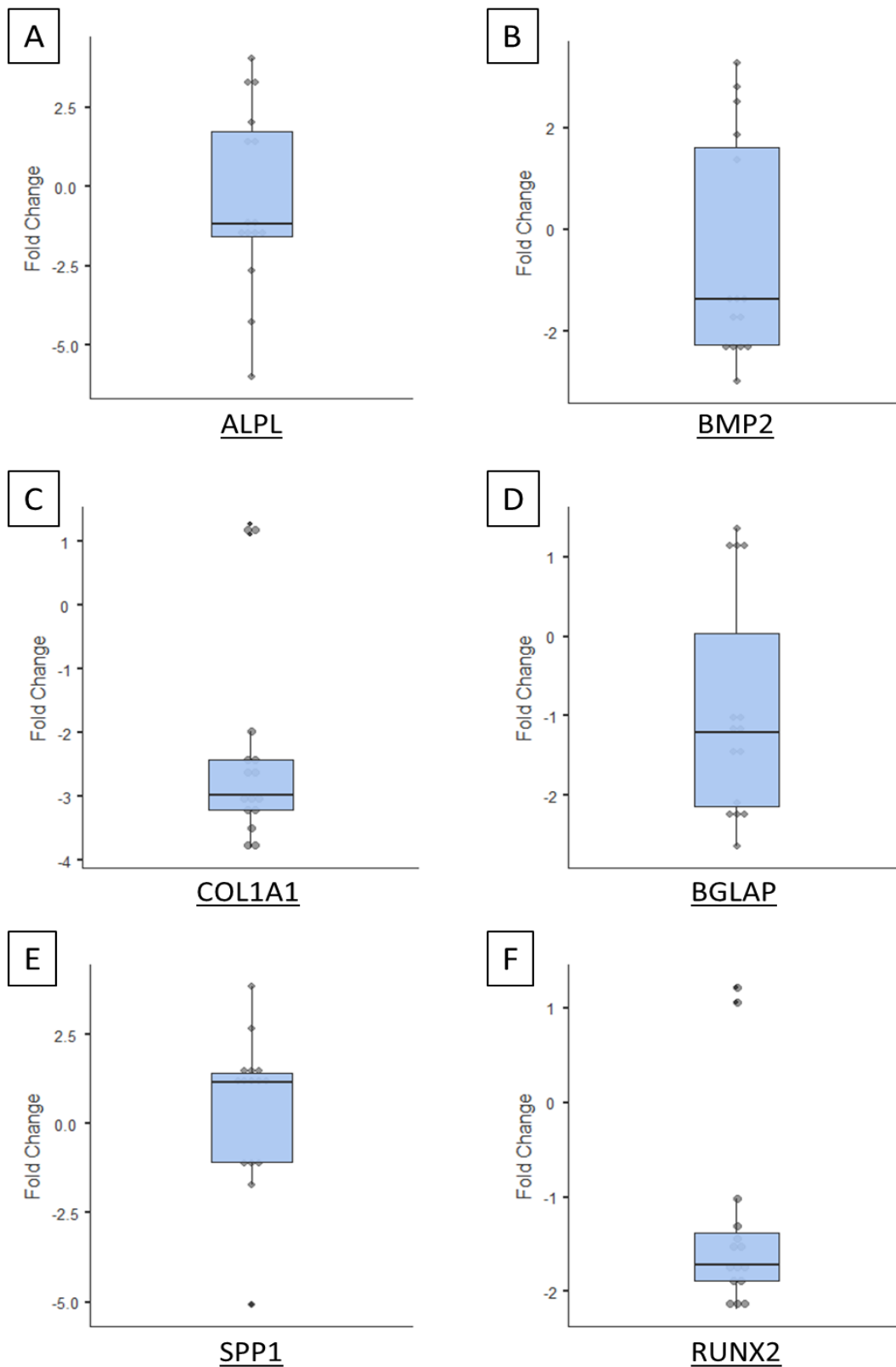


Figure 4-18: Fold difference in gene expression between osteoblasts isolated from lesioned and normal regions. Data is presented as fold difference, a ratio of gene expression in the lesioned osteoblasts compared to the normal osteoblasts. Error bars represent the standard error of the mean. A fold difference of 2 (up- or down-regulated) was judged as biologically significant.

4.4 Discussion

The aim of this observational study was to compare regions of the subchondral bone with, and without, MRI-identified subchondral bone abnormalities. We sought to identify differences in the histological features and osteoblast characteristics of regions with and without SB abnormalities. We demonstrated that histological features varied between normal and lesioned regions, and that within the lesioned regions there was a great deal of heterogeneity in histological features. We found no difference in osteoblast growth characteristics, nor did we not identify any differentially expressed genes, of those assessed, between the osteoblasts isolated from the lesioned and normal regions.

We were able to identify five patients who were scheduled for total knee replacement (TKR) surgery and who had a recent MRI on the affected knee that indicated the presence of subchondral bone abnormalities. All five patients had BMLs that were evident on MRIs and detailed in MRI reports, with three of the five patients also demonstrating subchondral bone cysts in the same location as the BML. The co-existence of BMLs and cystic changes in these patients agrees with a published report on the close association between these pathological features, which suggests that the majority of cysts arise in areas of pre-existing BMLs (Carrino et al., 2006).

Osteochondral tissue was isolated from regions identified as having SB abnormalities on MRI, and from regions in the same patients with no SB abnormalities for comparison. Macroscopic evaluation of the articular cartilage revealed that, in general, the cartilage overlying regions with SB abnormalities received a higher (worse) ICRS lesion grade than that overlying normal regions of the SB. This was also reflected in the histological analysis of cartilage quality, with cartilage overlying subchondral bone abnormalities generally

receiving a higher (worse) OARSI score than that overlying subchondral bone with no MRI-detected abnormalities. The OARSI score and SB histological score were strongly correlated. These findings provide further support for the close relationship between SB and AC and, as in the previous chapter, suggest that the interplay between the tissues is mediated locally as co-located differences in the quality of both tissues can be demonstrated in different regions in the knee from the same patient. This corroborates the large number of published reports that the presence of BMLs is associated with increased cartilage degradation in both OA and healthy populations, and that the effect is region specific (Felson et al., 2003; Garnero et al., 2005; Hunter et al., 2006; Roemer et al., 2009; Zhao et al., 2010).

Histological evaluation revealed distinct differences between the SB isolated from regions with and without SB abnormalities. For both histological scoring systems, there was a significant difference in scores between the lesioned and normal areas. Areas without SB pathological features generally demonstrated normal SB histology, with only mild trabecular thickening observed in one patient. By contrast, a great deal of heterogeneity was demonstrated in the histology of SB regions with MRI-identified abnormalities. In all of the patients there was some degree of subchondral bone sclerosis, indicated by thickening of the subchondral bone trabeculae and the subchondral bone plate compared to the normal regions from the same patients. Bone marrow fibrosis was demonstrated in several of the patients but was most abundant in the SB of patient number 2, where it was accompanied by blood vessels. Many histological studies of BML have reported the presence of bone marrow fibrosis, which is most commonly described as infiltration of the bone marrow space, and replacement of fatty marrow, by collagenous fibres (Zanetti et al., 2000; Taljanovic et al., 2008; Loeff et al., 2018). Leydet-Quillici and colleagues also reported the co-incidence of blood vessels with bone marrow fibrosis in some cases, as was demonstrated in

patient 2 (Leydet-Quilici et al., 2010). However, there is very little published literature on the aetiology and pathogenesis of bone marrow fibrosis and further research is required to determine the nature of the association between BML and bone marrow fibrosis. Bone marrow edema was evident in the subchondral bone of both the lesioned and normal region of patient number five but was more prominent in the subchondral bone from the lesioned site. Bone marrow edema is characterised by swollen fat cells, interspersed with eosinophilic extracellular fluid (Zanetti et al., 2000).

A study by Tanamas and colleagues reported that the presence of subchondral bone cysts at baseline assessment was associated with greater loss of tibial cartilage volume compared with the presence of BMLs only (Tanamas et al., 2010). While we found that the cartilage of the three patients for whom cystic changes were described on MRI did receive macroscopic and histological scores that were amongst the worst, a larger number of patients and a fully quantitative scoring system would be required to further appraise this relationship.

Of the three patients whose MRI reports described cystic changes, we were only able to identify cystic changes histologically in patient number 1, although the cyst borders were damaged during histological processing and therefore the feature was poorly defined. The cystic change in patient number 2, which we were unable to locate, was described as 'early cystic change'. BML have been described as pre-cysts due to the propensity for cysts to arise in pre-existing regions of BML, therefore early cystic changes may have been indistinguishable from BML histologically for this patient (Carrino et al., 2006). We were also unable to isolate the cystic change described in the subchondral bone of patient number 4 on macroscopic appraisal, as we had been able to for patient 2, and therefore isolated the region as close as possible to that which was indicated on MRI. Thus, we may have simply

missed the cyst site for this patient. A small, well-defined cyst was isolated from a sixth patient, showing a small cavitory lesion surrounded by dense, highly-cellularised, fibrous tissue which was surrounded by thickened bone trabeculae. The precise aetiology of cysts is unknown, although there are two predominant theories for their inception (Crema et al., 2010; Li et al., 2013). The first of these theories, termed 'synovial fluid intrusion' posits that a breach of the osteochondral junction allows synovial fluid to enter the subchondral bone and create a cystic lesion (Tanamas et al., 2010; Li et al., 2013). However, there are also published reports of subchondral bone cyst formation in the absence of damage to the osteochondral junction (Carrino et al., 2006). Thus, the more predominant contemporary theory, the 'bone contusion' theory, suggests that cysts originate from necrotic regions in the subchondral bone that are caused by abnormal mechanical stress, leading to microcracks and subsequent edema and focal bone resorption (Li et al., 2013).

We also identified distinct islands of cartilage deep within the SB in patient number 2, demonstrating the morphology and histological staining that one would expect of normal articular cartilage. However, while the chondrocytes were situated in lacuna, they were randomly arranged and did not demonstrate the columnar arrangement of chondrocytes in normal surface AC (Zhang et al., 2007; Fox et al., 2009; Kuttapitiya et al., 2017).

Cartilaginous regions within the subchondral bone have been described previously as incidental histological findings in the SB underlying AC denudation, as well as in BMLs (Zanetti et al., 2000; Zhang et al., 2007; Kuttapitiya et al., 2017). However, the source of chondrocytes and the mechanism that leads to the development of cartilaginous regions within the SB is still unknown. One theory is that the chondrocytes arise from differentiating BM-MSCs as a healing response to AC denudation (Zhang et al., 2007). A second theory was developed in consultation with a locum histopathologist at the RJAH Orthopaedic Hospital,

who suspected that the cartilage islands were local sites of endochondral ossification, as a healing response to a subchondral bone fracture (that was also noted in the MRI report for this patient). While this may be the case for this particular patient, and one possible mechanism of development, cartilaginous regions in the SB have been described previously in association with BML without a reported fracture (Zhang et al., 2007; Kuttapitiya et al., 2017). Further investigation is required to determine the aetiological mechanisms and characteristics of these features, and their relative frequencies.

The features identified in BML regions in this study corroborate those that have been previously described (Zanetti et al., 2000; Kuttapitiya et al., 2017; Loef et al., 2018). The heterogeneity of histological findings also reflects reports in the literature, and likely results from the historical use of 'BML' to describe any diffuse area of high-signal intensity on T2-weighted, fat-suppressed, MRI of the subchondral bone, for which there is a number of causes and therefore a range of histological findings (Zanetti et al., 2000; Carrino et al., 2006).

We found no difference in osteoblast growth characteristics, assessed by osteoblast yield from bone chip outgrowth and dsDNA content following monolayer seeding. A previous study by Campbell and colleagues suggested that MSCs derived from BML regions demonstrate slower proliferation in-vitro compared to those from normal tissue (Campbell et al., 2016). However, to our knowledge, there has been no published comparative study on the proliferation of BML-derived osteoblasts in-vitro.

Subsequently we investigated the gene expression profile of the osteoblast populations, interrogating characteristic osteoblast differentiation markers (*RUNX2*, *BMP2*, *ALP*) and markers of bone matrix proteins (*COL1A1*, *OPN*, *OCN*).

Of the six genes interrogated, we did not find any significant fold difference in the osteoblasts isolated from the lesioned and normal areas. BMLs are reported to be focal areas of increased bone remodelling, with increased osteoblast activity, and one would therefore expect upregulation in the expression of markers for matrix components (Lajeunesse & Reboul, 2003; Henrotin et al., 2012). Although there are no published studies on the characteristics of osteoblasts isolated from MRI-identified SB abnormalities, Sanchez and colleagues compared the gene expression profile of osteoblasts from sclerotic and non-sclerotic regions of the subchondral bone and reported upregulation in alkaline phosphatase, collagen type 1 (alpha 1), osteocalcin and osteopontin in the osteoblasts from the sclerotic region (Sanchez et al., 2008). However, subchondral bone sclerosis is but one feature of BMLs, and therefore the cell populations were likely more homogenous in that study than in the present study, in which a range of histological subchondral bone changes were noted.

Interestingly, Sanchez and colleagues reported that freshly isolated osteoblasts were poorly differentiated and showed low expression of osteoblast specific markers. The authors then cultured the osteoblast populations in medium that is known to promote osteoblast maturation and compared gene expression profiles at several timepoints (Sanchez et al., 2008). In the present study, freshly isolated osteoblasts were cultured in complete culture media (and for only one passage), in an attempt to maintain as many of the *in vitro* characteristics of the osteoblasts as possible without additional manipulation. Thus, it is possible that we have isolated and cultured poorly differentiated pre-osteoblasts, which are reported to express osteocalcin, osteopontin and alkaline phosphatase at lower levels than mature osteoblasts (Zhang et al., 2007; Miron & Zhang, 2012). Therefore, the gene expression levels in these markers may have been insufficient to discern any differences

between the populations without further osteogenic differentiation. It would be of interest to further differentiate the cells and assess the differences in gene expression in fully differentiated osteoblasts. Although, we were not able to identify any phenotypic difference between the osteoblasts isolated from regions with and without subchondral bone abnormalities, we studied only a very limited panel of genes. In a microarray analysis comparing BMLs and normal BMLs, Kuttapitiya and colleagues identified 218 differentially expressed genes, including those involved in cell adhesion, ECM organisation and signal transduction, that could be used to form the basis of additional gene expression comparisons in the future.

There are a number of treatments available for the treatment of BMLs, ranging from pharmaceutical options through the application of a bone substitute material to treatment with cells and cell products (Eriksen, 2015). In light of the histological findings in this study, it may be of interest to consider the mechanism of action and possible indications for use of some of these treatment options. Of the pharmaceutical options available for the treatment of BMLs, the prescription of bisphosphonates is the most common, although the mechanism of action is still unconfirmed (Eriksen, 2015). One theory is that bisphosphonates are able to inhibit osteoclast activity, thus uncoupling the process of increased bone resorption and deposition that leads to altered bone remodelling (Meier et al., 2014; Eriksen, 2015). Given that there was evidence for altered bone turnover and remodelling in the histological findings of all BML regions assessed in this study, it stands to reason that the inhibition of osteoclast activity may reduce the severity of these lesions. Treatment options that offer improved mechanical support are also available, such as the injection of calcium phosphate (bone cement), an osteoinductive bone substitute, directly into BML's. Several studies have demonstrated promising results using this method, reporting symptom reduction, functional

improvement and a delay in the need for total joint replacements (Rebolledo et al., 2018).

Considering the histological findings demonstrated in this study, in particular the changes to the trabecular structure that are associated with increased bone remodelling, it is easy to see why treatment options that offer mechanical support, and those that seek to recover normal bone turnover are successful. More recently, Hernigou and colleagues reported on the treatment of BMLs with the direct injection of BM-MSCs into the BML (Hernigou et al., 2020). In this elegant study, the authors recruited patients who were due to receive bilateral knee replacements, performing arthroplasty in the control knee and BM-MSC injection into the other. Hernigou and collaborators reported that not only did BML volume decrease over time in the BM-MSC treated knee, but cartilage volume also increased, resulting in a delay in the need for total knee replacement. By the 15 year follow-up, only 18% of patients had undergone a subsequent knee replacement on the BM-MSC treated knee (Hernigou et al., 2020). The findings of this study tie in with those of our study, in demonstrating that BMLs and the health of the overlying cartilage are inexorably linked and characterising this link may lead to better treatment options in the future. Given the vast range of histological features associated with BMLs in our study, even in such a limited number of patients, it is apparent that different treatments may be optimal for different patients. For example, the histological findings for patient 2 demonstrated that the calcified cartilage zone and underlying subchondral bone showed a great deal of discontinuity, which included a pit in the surface. This patient may therefore have benefitted from a treatment option that offered mechanical support and therefore may have prevented the pit formation.

4.5 Study Limitations

A major limitation of this study was the use of clinical-grade, rather than research-grade, MRIs. As such, we were unable to control for the length of time in between MRI and TKR. In order to address this, a 6-month cut-off period was used when selecting patients for the study. This cut-off period was implemented following published reports that a proportion of MRI-detected features in the SB change over a relatively short time period (Garnero et al., 2005; Roemer et al., 2009). We did, however, demonstrate that the subchondral bone cyst that was detected in patient 6, was roughly the same size as the MRI-detected signal change (figures 4-12 and 4-13), although the corresponding MRI was more than 15 months old at the time of TKR.

Additionally, a very limited panel of genes associated with osteoblastic differentiation and bone matrix composition was assessed, and future work would seek to interrogate a more extensive panel.

An additional limitation of this study, and also of the co-culture in the previous chapter (Chapter 3- Investigating the Effect of Subchondral Bone Health on Articular Cartilage Repair in the Human Knee) is the lack of power analysis carried out to determine the required number of patients to power this study. While we accept this observation as a limitation of our work, in our laboratory we do not tend to carry out power analyses for primary cell culture-based studies such as this. Rather, we base our patient numbers on what is feasible in terms of time required for sample acquisition, as well as similar studies previously carried out in our laboratory and in the wider literature. Our patient number of five for each of these studies is comparable to similar studies found in the literature, the majority of which utilise commercially sourced cells which are not donor matched, thus reducing the time and

labour required for culture (Westacott et al., 1997; Sanchez et al., 2005a; Sanchez et al., 2005b; Cooke et al., 2011; Bian et al., 2011). Of these studies, the greatest number of patients used to isolate and compare OA and normal bone cells was 15, but these were not donor-matched populations (Westacott et al., 1997). In the work that is most comparable to our own, Sanchez and colleagues isolated donor-matched populations of sclerotic and normal OBs, but only did so for 3 patients (Sanchez et al., 2005a; Sanchez et al., 2005b). Thus, while we appreciate that our studies may be underpowered statistically, they stand up to comparison with previously published work.

4.6 Conclusion

In the present study, we were able to demonstrate the spatial correlation between BMLs and articular cartilage degeneration, macroscopically and histologically, and to isolate histologically distinct regions of the subchondral bone, based on MRI findings. In a similar way to the previous chapter, these results provide further evidence for the close relationship and interaction between the articular cartilage and subchondral bone. Again, we were able to show that this interaction is mediated locally, as we were able to isolate histologically distinct regions of the subchondral bone from the same patient.

Chapter 5:
Investigating the relationship between activity
levels and knee function following cell-based
therapy for cartilage damage

5. Investigating the Relationship Between Activity Levels and Knee Function in the Post-Operative Period Following Cartilage Repair with Cell Therapy.

5.1 Introduction

Lesions of the articular cartilage (AC) are common in the human knee and can cause pain, swelling, functional impairment and a reduction in quality of life (Sellards et al., 2002; Widuchowski et al., 2007; Toonstra et al., 2013). Due to the avascular nature of the AC and the relatively low metabolic activity of the resident chondrocytes, the tissue has a limited capacity for self-repair once damaged (McAdams et al., 2010; Karuppal, 2017). If left untreated, AC lesions can predispose the joint to further cartilage loss and to the early onset of osteoarthritis (Ding et al., 2005; Fox et al., 2009; McAdams et al., 2010; Camp et al., 2014). A number of surgical techniques have been developed to treat AC lesions, ranging from palliative approaches (e.g. debridement), intrinsic reparative strategies (e.g. microfracture), tissue replacement strategies (e.g. osteochondral grafting) and cell or tissue engineering approaches (e.g. autologous chondrocyte implantation (ACI)) (Brittberg et al., 1994; Steinwachs et al., 2012; Perera et al., 2012; Camp et al., 2014; Medvedeva et al., 2018). Each of the surgical interventions has slightly different indications but they share the aims of restoring function and reducing symptoms. The outcomes of cartilage repair surgery are commonly assessed with objective clinical measures, subjective patient-reported outcome measures (PROMs) or a combination of the two, although there is little consensus on which type is the most useful, as discussed in Chapter 1.

Regardless of treatment or outcome measure, several factors are believed to contribute to the success or failure of cartilage repair surgery. Baseline demographic and clinical characteristics such as patient age, the number of defects, defect size and location, symptom duration and number of previous surgeries have all been suggested as prognostic or predictive factors that could alter the clinical outcome of cartilage repair surgery (Bekkers et al., 2009; Saris et al., 2009; Harris et al., 2010; de Windt et al., 2012; Toonstra et al., 2013; de Windt et al., 2017).

Several studies have suggested that post-surgical activity levels also contribute to the outcome of cartilage repair surgery, reporting that patients who are more active in the post-operative period are more likely to demonstrate clinical success (Toonstra et al., 2013).

Knutsen and colleagues reported two- and five-year follow-up of a randomised control trial comparing ACI to microfracture and found that patients who were more active as assessed by the Tegner activity scale had significantly better self-reported knee scores (Lysholm knee scoring scale) than those who were less active, regardless of which treatment they received (Knutsen et al., 2004; Knutsen et al., 2007). A similar positive relationship between post-operative activity levels and clinical outcome was reported by Kreuz and colleagues, who found that patients who exercise at least once a week following ACI achieved better clinically assessed and patient reported outcomes (ICRS and Cincinnati Scores) than did patients who exercise no more than 3 times per month (Kreuz et al., 2007). The authors report that the 'overall Pearson coefficient of correlation' between activity levels and outcomes scores, across several different defect locations, was significant from 6 months post-op (ICRS: $r=0.48$, Cincinnati: $r=0.37$; both $p<0.01$) and increased from 6 months post-op to 18 months post-op (ICRS: $r=0.72$, Cincinnati: $r=0.59$; both $p<0.01$) and again from 18

months to 36 months post-op (ICRS: $r=0.79$, Cincinnati: $r=0.66$; both $p<0.01$), suggesting that physical activity is beneficial after cartilage repair in the knee (Kreuz et al., 2007).

Although these studies report a general trend for a positive relationship between post-operative activity levels and clinical outcome across their patient cohorts, there is little investigation into this relationship for individual patients, or whether it varies between patients. In their 1985 publication describing the first revision of the Lysholm scoring system, Tegner and Lysholm also introduced an activity scale, the Tegner scale, to complement the Lysholm score (Tegner & Lysholm, 1985). They found a generally positive relationship between the two scores but commented that almost 20% of patients with a low activity level had a high functional score (>83), indicating in their eyes that limitations in knee function may be masked by an involuntarily low activity level. In a later publication, they further stressed that the functional score should be regarded in relation to the activity level: patients who have reached a desired high activity level and have a high score probably have better function than patients with a high score, but who have a low activity level (Tegner et al., 1988). Anecdotal reports from patients attending post-operative appointments at the RJAH Orthopaedic Hospital suggest even more variation between patients in this relationship, with some patients reporting a low Lysholm knee score precisely because they had been more active. This variability in functional outcome in relation to activity levels led the late Professor Richardson to hypothesise that patients could be stratified into two groups: those for whom the relationship is positive ('positive responders' [to activity]) and those for whom it is negative ('negative responders' [to activity]). The first aim of the present study was to investigate the patient-to-patient variation in their long-term relationship between activity levels and knee function over the

period from immediately before cartilage repair surgery to the end of the rehabilitative period, 15 months after surgery.

Psychosocial factors are another set of elements reported to influence functional outcomes of knee surgery, in addition to also influencing activity levels. Although these reports are heavily focused on rehabilitation outcomes following ACL reconstruction, it is suspected that the same factors could play a role in influencing outcome following AC repair surgery (Gobbi & Francisco, 2006; Chmielewski et al., 2008; Mithoefer et al., 2009; Chmielewski et al., 2011; Mithoefer et al., 2012). Psychological constructs such as the fear of reinjury, fear of movement, pain-catastrophising, self-efficacy, coping and the feeling of emotions are of particular interest and have been shown to influence post-operative activity levels, return to sport, functional outcome and pain (Thomee et al., 2006; Gobbi & Francisco, 2006; Tripp et al., 2007; Chmielewski et al., 2008; Chmielewski et al., 2011; George et al., 2012). Mithoefer and colleagues reported that some patient-reported measures of psychological constructs, such as the Knee Efficacy Scale and the Tampa Scale of Kinesiophobia, correlate with knee function scoring systems, such as the International Knee Documentation Committee - Subjective Knee Evaluation Form (IKDC-SKF), the Knee Injury and Osteoarthritis Injury Score (KOOS) and the Tegner-Lysholm Knee Scoring Scale, which are commonly used as outcome measures for AC repair surgery (Mithoefer et al., 2012). However, there is little to no research into the specific effect of psychological constructs on functional outcomes and activity levels following AC repair surgery. Thus, the second aim of the present study is to investigate the influence of one such construct, 'affect', the subjective experience of emotion, on post-operative knee function and activity levels.

5.2 Materials and Methods

5.2.1 Patients

All patients enrolled in the ASCOT (Autologous Stem Cells, Chondrocytes or the Two?) trial at the Robert Jones and Agnes Hunt (RJAH) Orthopaedic Hospital NHS Trust, who had completed their 15-month follow-up assessment by 1 August 2019, were included in this study. As per the inclusion criteria of the ASCOT study, all patients included in the current study had symptomatic articular AC defect(s) of the knee that extended down to, or into, the subchondral bone (ICRS grade 3 or 4; section 3.2.2) and which would have been appropriate for treatment by traditional autologous chondrocyte implantation (ACI). All patients were aged between 18 and 80 years and might have undergone a previous arthroscopic or open reparative procedure (e.g. debridement, microfracture, drilling/abrasion arthroplasty or osteochondral allograft/autograft) to which they had an inadequate response.

5.2.2 Autologous Stem Cells, Chondrocytes or the Two? (ASCOT) Trial

ASCOT is an ongoing, prospective, randomised controlled trial at the RJAH Orthopaedic Hospital with the aim of determining whether modification of the standard ACI procedure with other cell types improves outcomes. The trial compares three treatments: (1) traditional ACI (implantation of chondrocytes), (2) implantation of autologous bone marrow-derived stromal cells (BMSCs) and (3) implantation of a 1:1 combination of the two cell types. Patients are randomly allocated to one of the three treatments and all undergo a two-stage procedure, to which they are blinded. In the first stage, the required cells are harvested: chondrocytes are isolated from an arthroscopically collected cartilage biopsy and BMSCs are isolated from bone marrow aspirate collected from the iliac crest. Depending on

the allocated treatment, either or both cell types are then culture-expanded in monolayer to provide a sufficient number of cells for implantation. In the second stage, the cells are implanted into the defect beneath a periosteal flap or collagen membrane.

5.2.2.1 *ASCOT Rehabilitation Program*

All patients involved in the ASCOT study followed the same 'OsCell Rehabilitation Program' for 12 months following cell implantation (Bailey et al., 2003). This program was specifically developed for the rehabilitation of patients following ACI and consists of five successive phases, each with different goals depending on the time since cell implantation. The program comprised of exercises that are aimed at progressively increasing range of motion, weight-bearing and strength as the time since cell implantation increases (Bailey et al., 2003).

5.2.2.2 *Trial Assessments*

Baseline assessments were performed on the day of admission for stage 1 surgery. At this time, demographic information (age, gender, height, weight, affected knee, history of smoking) was collected, along with various knee scores, including the Lysholm Knee Scoring System and quality of life questionnaires including the International Positive and Negative Affect Schedule – Short Form (I-PANAS-SF) and the Human Activity Profile (HAP) to provide baseline data. The same knee scores and quality of life questionnaires were then completed at 2-month, 12-month and 15-month follow-up post cell implantation. Patients were asked to complete the knee scoring system separately for the affected and contralateral knee.


5.2.2.2.1 *The Lysholm Knee Scoring Scale*

The Lysholm knee scoring scale was first developed by Lysholm and colleagues in 1982, as a clinician-administered questionnaire to evaluate the outcomes of knee ligament surgery

(Lysholm & Gillquist, 1982). The scale was then revised in 1985 by Tegner and colleagues, to produce the 8-item version which has since been used in the assessment of a wide variety of conditions (e.g. knee ligament injury, meniscal tears, knee AC lesions, knee OA) and as an outcome measure to assess the efficacy of a number of interventions (e.g. ligament reconstruction, microfracture, high tibial osteotomy and osteochondral autografts) (Tegner & Lysholm, 1985; Collins et al., 2011). The 8-item scale assesses knee health and function using items about limp, support, locking, instability, pain, swelling, stair climbing and squatting. Patients are asked to indicate which of the options for each of the items best describes their knee symptoms, after which they are scored using weighted (delineated) scores, which add to give a maximum score of 100 (Tegner & Lysholm, 1985; Collins et al., 2011). Although originally designed for in-person, clinician administration, many studies report its use as an unsupervised PROM (Collins et al., 2011).

A further modification of the Lysholm knee scoring system based on patients with knee chondral damage was developed and validated by Smith and colleagues in 2008 (Smith et al., 2008). The authors removed the 'swelling' item, reporting that this item failed to discriminate across the underlying trait of knee impairment, and used unweighted scores for each of the remaining items (Smith et al., 2008). The resulting scoring system consists of 7 items, namely Pain (scored 0-5), Instability (0-5), Locking (0-4), Limp (0-2), Stair-climbing (0-3), Squatting (0-3) and Support (0-2), with possible total scores ranging from 0-24 (Smith et al., 2008). The authors reported that the 7-item version of the Lysholm knee scoring system is robust and can be either clinician administered or employed as a PROM (Smith et al., 2008) (Figures 5-1 & 5-2).

OSWESTRY 'Oscell' Cartilage KNEE LYSHOLM SCORE-FORM

Subject ID: Initials:..... Date form completed:..... Visit:.....		Robert Jones & Agnes Hunt Orthopaedic Hospital NHS Trust Oswestry, Shropshire SY10 7AG www.oscellenta.net
---	---	---

This questionnaire has been designed to give information as to how your knee has affected your ability to manage in everyday life. Please answer every section and tick the box to the left of the statement that applies to you. If more than one statement applies to you tick the one that most closely describes your situation.

Please complete the questionnaire for both knees.

PAIN

*	LEFT	RIGHT		
5	<input type="checkbox"/>	<input type="checkbox"/>	I have no pain in my knee	25
4	<input type="checkbox"/>	<input type="checkbox"/>	I have intermittent pain in my knee during severe exertion	20
3	<input type="checkbox"/>	<input type="checkbox"/>	I have marked pain in my knee during severe exertion	15
2	<input type="checkbox"/>	<input type="checkbox"/>	I have marked pain in my knee on or after walking more than 2km	10
1	<input type="checkbox"/>	<input type="checkbox"/>	I have marked pain in my knee on or after walking less than 2km	5
0	<input type="checkbox"/>	<input type="checkbox"/>	My knee is in constant pain	0

INSTABILITY

*	LEFT	RIGHT		
5	<input type="checkbox"/>	<input type="checkbox"/>	My knee never gives way	25
4	<input type="checkbox"/>	<input type="checkbox"/>	My knee rarely gives way during athletics or other severe exertion	20
3	<input type="checkbox"/>	<input type="checkbox"/>	My knee frequently gives way during athletics or other severe exertion	15
2	<input type="checkbox"/>	<input type="checkbox"/>	My knee occasionally gives way during daily activities	10
1	<input type="checkbox"/>	<input type="checkbox"/>	My knee often gives way during daily activities	5
0	<input type="checkbox"/>	<input type="checkbox"/>	My knee gives way with every step I take	0

LOCKING

*	LEFT	RIGHT		
4	<input type="checkbox"/>	<input type="checkbox"/>	I experience no locking or catching sensation	15
3	<input type="checkbox"/>	<input type="checkbox"/>	I do experience a catching sensation but not a locking sensation	10
2	<input type="checkbox"/>	<input type="checkbox"/>	I occasionally have a locking sensation	6
1	<input type="checkbox"/>	<input type="checkbox"/>	I frequently have a locking sensation	2
0	<input type="checkbox"/>	<input type="checkbox"/>	I have a locked knee now	0

SWELLING

*	LEFT	RIGHT		
-	<input type="checkbox"/>	<input type="checkbox"/>	My knee does not swell	10
-	<input type="checkbox"/>	<input type="checkbox"/>	My knee swells on severe exertion	6
-	<input type="checkbox"/>	<input type="checkbox"/>	My knee swells on ordinary exertion	2
-	<input type="checkbox"/>	<input type="checkbox"/>	My knee is constantly swollen	0

LIMP

*	LEFT	RIGHT		
2	<input type="checkbox"/>	<input type="checkbox"/>	I have no limp	5
1	<input type="checkbox"/>	<input type="checkbox"/>	I have a slight limp or periodical limp	3
0	<input type="checkbox"/>	<input type="checkbox"/>	I have a severe and constant limp	0

STAIR-CLIMBING

*	LEFT	RIGHT		
3	<input type="checkbox"/>	<input type="checkbox"/>	I have no problems climbing stairs because of my knee	10
2	<input type="checkbox"/>	<input type="checkbox"/>	My stair-climbing is slightly impaired because of my knee	6
1	<input type="checkbox"/>	<input type="checkbox"/>	I climb stairs one foot at a time because of my knee	2
0	<input type="checkbox"/>	<input type="checkbox"/>	Stair-climbing is impossible due to my knee	0

PTO

U:\CSIMcCarthy\Spinal Studies\Ethics\Questionnaires\lysholm.doc

Version2 - 03/11/2010

Figure 5-1: Lysholm Knee Scoring System used in the ASCOT Trial. Patients are required to score each parameter for both the affected and contralateral knee. The scoring system includes both the original (out of 100; right) and revised (out of 24; left). Parameters assessed are: Pain, Instability, Locking, Swelling, Limp and Stair-Climbing. Note that the Swelling item is included for both the original and revised lists but is not given a score for the revised version.

SQUATTING				
*	LEFT	RIGHT		
3	<input type="checkbox"/>	<input type="checkbox"/>	I have no problems squatting	5
2	<input type="checkbox"/>	<input type="checkbox"/>	My squatting is slightly impaired because of my knee	4
1	<input type="checkbox"/>	<input type="checkbox"/>	I can't squat beyond 90 ^o	2
0	<input type="checkbox"/>	<input type="checkbox"/>	Squatting is impossible because of my knee	0

SUPPORT				
*	LEFT	RIGHT		
2	<input type="checkbox"/>	<input type="checkbox"/>	I am not using any kind of support	5
1	<input type="checkbox"/>	<input type="checkbox"/>	I am using a stick or crutch	2
0	<input type="checkbox"/>	<input type="checkbox"/>	Weight-bearing is impossible for me due to my knee(s)	0

PLEASE ENSURE YOU HAVE ANSWERED ALL OF THE ABOVE QUESTIONS FOR BOTH KNEES

Has anything gone wrong with your knee complications such as:-

Blood clots (DVT etc) Yes Date: ___/___/___ No Side Left/ Right

Required hospitalisation Yes No

Infection Yes Date: ___/___/___ No Side Left/ Right

Required antibiotics Yes No

A revision operation? Yes Date: ___/___/___ No

Please list any other issues below

Please answer the following question only after you have had your operation

- 4 I am extremely pleased with the operation – would recommend it
- 3 I am pleased with the operation
- 2 I am no different to before the operation
- 1 I am worse than before the operation
- 0 I am much worse than before the operation – wouldn't recommend it

THANKYOU!

* Smith HJ, Richardson JB, Tennant A. Modification & validation of the Lysholm Knee Scale to assess articular cartilage damage. *Osteoarthritis & Cartilage*, 2009; 17(1): 53-8.
To convert 0 - 24 total score to 0 – 100 multiply the total score by 4.167



Figure 5-2: *Lysholm Knee Scoring System used in the ASCOT Trial (continued). Parameters assessed: Squatting and Support.*

5.2.2.2.2 The Human Activity Profile (HAP)

The Human Activity Profile (HAP) is a self-administered instrument used to assess physical activity by estimating energy expenditure. The HAP was developed by Daughton and colleagues in 1982 as an outcome measure of the quality of life achieved by patients undergoing rehabilitation for chronic obstructive pulmonary disease (Daughton et al., 1982; Bennell et al., 2004). The scoring system has since been used to assess physical activity in a variety of healthy and impaired populations, including those with cardiorespiratory, neurological and musculoskeletal conditions (Bennell et al., 2004). The HAP is comprised of a list of 94 activities that are ranked 1-94 according to the estimated energy expenditure that is required to perform each one, ranging from least to most physically demanding (Davidson & de Morton, 2007). The activities that comprise the HAP include day-to-day tasks (e.g. getting in and out of chairs or bed without assistance), self-care activities (e.g. dressing or undressing without assistance), work and social activities (e.g. going to see a film, play or sports activity) and exercise (e.g. swimming 25 yards, cycling 2 miles) and are designed to encompass the use of all muscle groups of the body (Bennell et al., 2004; Davidson & de Morton, 2007) (Figures 5-3, 5-4 & 5-5) . For each of the 94 activities in the HAP, respondents are required to indicate whether they (1) are still doing the activity, (2) have stopped doing the activity, or (3) never performed the activity (Davidson & de Morton, 2007).

Two aggregate scores can be calculated from the HAP: the Maximal Activity Score (MAS, also named Maximal Current Activity or MCA) and the Adjusted Activity Score (AAS, also named Normal Impairment Index or NII) (Hinman et al., 2002; Davidson & de Morton, 2007). MAS is defined as the rank number of the highest-ranked (physically most demanding) activity that the participant has indicated they are still doing, giving an idea of the most

strenuous, one-off activity that they are able to perform. AAS is derived by subtracting the number of activities that are physically less demanding than the MAS that the participant has indicated they have stopped doing (i.e. the number of items the participant has marked with a '2'), from the value of the MAS. Both the MAS and AAS have possible scores from 0-94. It has been reported that the MAS may provide unrealistically high estimates of normal physical activity, whereas the AAS is a more useful parameter for detecting change, is more reactive to impairment and helps to correct the MAS for individuals who may occasionally perform one energy intensive activity, but whom, day-to-day, have had to give up some less energy intensive activities (Bennell et al., 2004; Davidson & de Morton, 2007).

ASCOT Trial

**Human Activity Profile
questionnaire**

Subject ID:
Initials:
Date form completed:.....
Visit:.....

Please tick (using a ✓) each activity according to these directions:

Tick Column 1 ("Still Doing This Activity") if:
You completed the activity unassisted the last time you had the need or opportunity to do so.

Tick Column 2 ("Have Stopped Doing This Activity") if:
You have engaged in the activity in the past, but you probably would not perform the activity today even if the opportunity should arise.

Tick Column 3 ("Never Did This Activity") if:
You have never engaged in the specific activity.

	Still doing this activity	Have stopped doing this activity	Never did this activity
1. Getting in and out of chairs or bed (without assistance)			
2. Listening to the radio			
3. Reading books, magazines or newspapers			
4. Writing (letters, notes)			
5. Working at a desk or table			
6. Standing (for more than one minute)			
7. Standing (for more than five minutes)			
8. Dressing or undressing (without assistance)			
9. Getting clothes from drawers or wardrobes			
10. Getting in or out of a car (without assistance)			
11. Dining at a restaurant			

Figure 5-3: *The Human Activity Profile used in the ASCOT Trial. Patients are required to tick one column for each of the listed activities. Instructions for completion and items 1-11.*

	Still doing this activity	Have stopped doing this activity	Never did this activity
33. Making a bed (not changing sheets)			
34. Cleaning windows			
35. Kneeling, squatting to do light work			
36. Carrying a light load of groceries			
37. Climbing nine steps (non-stop)			
38. Climbing 12 steps (non-stop)			
39. Walking ½ block (50 yards or metres) uphill			
40. Walking ½ block (50 yards) uphill (non-stop)			
41. Shopping (by yourself)			
42. Washing clothes (by yourself)			
43. Walking 1 block (100 yards or metres) on level ground			
44. Walking 2 blocks (200 yards or metres) on level ground			
45. Walking 1 block (100 yards or metres) on level ground (non-stop)			
46. Walking 2 blocks (200 yards or metres) on level ground (non-stop)			
47. Scrubbing (floors, walls or cars)			
48. Making beds (changing sheets)			
49. Sweeping			
50. Sweeping (five minutes non-stop)			
51. Carrying a large suitcase or bowling (one game)			
52. Vacuuming carpets			
53. Vacuuming carpets (five minutes non-stop)			

Figure 5-4: The Human Activity Profile used in the ASCOT Trial (continued). Items 33-53.

	Still doing this activity	Have stopped doing this activity	Never did this activity
75. Walking three miles or golfing 18 holes without a golf buggy			
76. Walking three miles (non-stop)			
77. Swimming 25 yards			
78. Swimming 25 yards (non-stop)			
79. Cycling one mile			
80. Cycling two miles			
81. Cycling one mile (non-stop)			
82. Cycling two miles (non-stop)			
83. Running or jogging ¼ mile			
84. Running or jogging ½ mile			
85. Playing tennis or squash			
86. Playing football or basketball (game play)			
87. Running or jogging ¼ mile (non-stop)			
88. Running or jogging ½ mile (non-stop)			
89. Running or jogging one mile			
90. Running or jogging two miles			
91. Running or jogging three miles			
92. Running or jogging one mile in 12 minutes or less			
93. Running or jogging two miles in 20 minutes or less			
94. Running or jogging three miles in 30 minutes or less			

Daughton DM, Fix AJ, Kass I, Bell CW, Patil KD. Maximum oxygen consumption and the ADAPT quality of life scale. Arch Phys Med Rehabil 1982;63:620-2.

Figure 5-5: *The Human Activity Profile used in the ASCOT Trial (continued). Items 75-94.*

5.2.2.2.3 The International Positive and Negative Affect Schedule Short Form (I-PANAS-SF)

Affect is defined as ‘the feeling of emotion’ and is a subjectively experienced construct that has been reported as a primary cause and consequence of symptoms, coping, social activity and satisfaction (Serafini et al., 2016). The Positive and Negative Affect Schedule (PANAS) is a widely used measure of two distinct aspects of affect, positive affect (PA) and negative affect (NA) and was originally developed in 1988 by Watson and colleagues, using items from a list of descriptors for PA and NA developed by Zevon and Tellegen (Zevon & Tellegen, 1982; Watson et al., 1988). PA is described as the extent to which an individual feels enthusiastic, active and alert, with high PA associated with high energy, full concentration and pleasurable engagement and low PA with sadness and lethargy. NA is described as the general dimension of subjective distress and unpleasurable engagement, with high NA associated with anger, contempt and fear, and low NA with calmness and serenity (Watson et al., 1988; Serafini et al., 2016). PA and NA are reported to be largely independent and uncorrelated constructs; it has been shown that it is possible to simultaneously experience both very high PA and very high NA (Merz et al., 2013).

The original PANAS consisted of a list of 20 emotions, of which the participant is required to indicate the magnitude at which each had been experienced using a Likert-like scale: (1) very slightly or not at all (2) a little, (3) moderately, (4) quite a bit and (5) extremely (Watson et al., 1988). Watson and colleagues did not dictate a reference timeframe for participants to complete the questionnaire but tested a variety of timeframes e.g. ‘today’, ‘past few days’, ‘this week’, ‘past few weeks’, ‘this year’, ‘generally’ (Watson et al., 1988). The 20 emotions listed could be separated into two 10-item scales, one of which assessed PA and the other assessed NA, allowing for a separate score to be calculated for both aspects of affect.

More recently, Thompson and colleagues developed and validated a shortened version of the PANAS, the International Positive and Negative Affect Schedule Short Form (I-PANAS-SF) (Thompson, 2007). The authors reported that the original 20-item version constituted a significant time burden and contained items that were ambiguous in international English or used colloquial language that did not translate well. Following a qualitative, and subsequent quantitative, study to decide which of the original 20 items to retain, the authors created the I-PANAS-SF, which was validated and found to demonstrate acceptable levels of internal reliability, cross-sample stability and temporal stability over a period of two months (Thompson, 2007). The I-PANAS-SF consists of a list of 10 emotions which are listed in a random order but can be separated by researchers into two 5-item mood scales to assess PA and NA (Thompson, 2007) (Figure 5-6). The I-PANAS-SF is commonly used as a PROM, in which patients are asked to indicate the frequency at which they have felt each of the emotions listed, over the last few weeks: (1) never, (2) rarely, (3) sometimes, (4) most of the time and (5) always (Thompson, 2007). A score for NA and a score for PA can then be calculated, and for both aspects the score ranges from 5-25.

International Positive and Negative Affect Schedule Short Form (I-PANAS-SF)

Subject ID: Initials: Date form completed: Visit:		Robert Jones & Agnes Hunt Orthopaedic Hospital NHS Trust Oswestry, Shropshire SY10 7AG
--	---	---



This form consists of a number of words that describe different feelings and emotions. Read each word and then tick the appropriate box according to what extent you have felt this way during the past few weeks.

Thinking about yourself and how you normally feel, to what extent do you generally feel:

	1 (Never)	2 (Rarely)	3 (Sometimes)	4 (Most of the time)	5 (Always)
Upset					
Hostile					
Alert					
Ashamed					
Inspired					
Nervous					
Determined					
Attentive					
Afraid					
Active					

THANK YOU!

Figure 5-6: The International Positive and Negative Affect Schedule - Short Form (I-PANAS-SF) used in the ASCOT Trial. Patients are required to tick one column indicating the frequency at which they experience each of the listed items. Items that are used to calculate a score for NA (Upset, Hostile, Ashamed, Nervous and Afraid) and those that are used to calculate a score for PA (Alert, Inspired, Determined, Attentive, Active) are listed in a random order.

5.2.3 Data Acquisition

All completed knee function scores and quality of life scores were uploaded to the OsCell database, a purpose-built database for follow-up of cartilage defect patients, that is password protected and maintained on the RJAH servers. Following approval from Dr Johanna Wales, the ASCOT trial manager, raw data for the present study was obtained via download from the OsCell database by Mike Williams, our in-house data analyst. All researchers were blinded to treatment group throughout.

The acquired data comprised baseline demographic information and raw scores for the Lysholm, HAP and I-PANAS-SF at baseline, 2 months, 12 months and 15 months post-op.

5.2.4 Preparation of Data for Analysis

Where required, the data were prepared for subsequent analysis:

- Baseline Demographic Information: Height and weight data were used to calculate body mass index (BMI) for each of the patients at baseline.
- Lysholm Knee Scoring System: Individual items on the Lysholm knee scoring scale were added together to provide a total score for the affected knee for each patient at each of the four timepoints.
- HAP: The completed HAP scoresheets were used to calculate the MAS, which was then used to calculate the AAS for each patient at each of the four timepoints.
- I-PANAS-SF: The completed I-PANAS-SF scoresheets were used to calculate a value for NA and a value for PA for each patient at each of the four timepoints.

A summary of the processed data is shown in table 5-1

Table 5-1: Prepared data utilised in this study. A summary of the information collected and the scores that were calculated at each timepoint.

Timepoint	Demographic Information	Lysholm Knee Scoring Scale	Human Activity Profile (HAP)	International Positive and Negative Affect Schedule – Short Form (I-PANAS-SF)
Baseline	Age, gender, BMI, smoking status	Lysholm Score	Adjusted Activity Score (AAS)	Positive Affect (PA) score and Negative Affect (NA) score
2 months	-	Lysholm Score	AAS	PA & NA
12 months	-	Lysholm Score	AAS	PA & NA
15 months	-	Lysholm Score	AAS	PA & NA

5.2.5 Data Analysis

5.2.5.1 *General Analyses*

Descriptive statistics were used to assess general trends in the Lysholm, AAS, PA and NA data. A mixed model was used to test for differences in consecutive scores, as well as for differences between the primary endpoint and baseline scores.

5.2.5.2 *Power Analysis*

To test the primary hypothesis that the slope between activity levels and Lysholm scores varies between patients, sample size was calculated using Monte-Carlo simulations of a mixed effect model (using R (v3.3.3) and package “simr”) based on relevant pilot data from 28 patients who had data measured at 3 occasions (Green et al., 2016; R Core Team, 2019). As for the secondary objectives, to determine predictors of the slope, a sample size was determined to detect a significant correlation at the $p=0.05$ level if the variable explains at least 15% of the variation in slopes ($r^2=0.15$; $r=0.39$) using G*Power (v3.1.9.2) in R (v3.3.3) (Faul et al., 2007; R Core Team, 2019).

5.2.5.3 *Assessing the Temporal Stability of the I-PANAS-SF*

The temporal stability of PA and NA over the course of the study was assessed on the basis of differences over time in their mean values, their intra-rater reliability and on an individual level using Bland-Altman analysis of the NA and PA scores at baseline and 15-month follow-up. Intra-rater reliability was determined as the intraclass correlation coefficient (ICC) for agreement, based on a 2-way ANOVA model (McGraw & Wong, 1996). Bland-Altman plots were created by plotting the means of the paired baseline and 15-month scores ($(15\text{-month Score} + \text{Baseline Score})/2$) against the differences between the two scores ($15\text{-month Score} - \text{Baseline Score}$), for NA and PA separately. A value for the mean difference (estimated

bias) between the scores at the two timepoints, as well as values for the upper (mean + $1.96SD_{diff}$) and lower (mean - $1.96SD_{diff}$) limits of agreement, were determined from the plots, where SD_{diff} is the standard deviation of the difference. If data is normally distributed, 95% of the individual datapoints will fall within those limits. When a score is temporally stable, the bias will be close to zero, in which case the limits of agreement in Bland-Altman plots coincide with the Reliable Change Index (RCI), an index commonly used to find if patients have undergone a clinical meaningful change (Jacobson & Truax, 1991; Duff, 2012), but also used to demonstrate temporal stability by a lack of change (Vaidya et al., 2002; Elkins, 2017). Individual patients who fall above or below the limits of agreement have undergone a meaningful change, and conversely those within the limits are temporally stable.

As a result of these analyses, the average NA and PA for each patient across the four timepoints, were used in the subsequent analyses, rather than concurrent PA and NA scores.

5.2.5.4 *Numeric Coding of String Variables*

String variables were numerically coded to enable subsequent correlation analysis. Gender was coded as, 'Female=1', 'Male=0'. Smoking status was coded as an ordinal value: 'Non-smoker=0', 'Ex-smoker=1', 'Smoker=2'.

5.2.5.5 *Normality*

QQ-plots suggested that the AAS and PA data, as well as the values for the individual patient slopes between AAS and Lysholm were non-normally distributed, therefore non-parametric tests and robust analyses were used throughout.

5.2.5.6 *Assessing Variation Between Patients*

5.2.5.6.1 *Centring AAS*

Parameter estimations can be problematic with variables whose minimum value is well outside the range to be expected, as their slopes and intercepts in relations with other variables may be too highly correlated (Nezlek, 2001). Centring such variables will reduce the correlation between their slopes and intercepts in such relations. AAS values were therefore centred by group-mean centring, subtracting the overall mean value (65.00424) from the individual AAS data points. An additional advantage of centring the AAS value is that it facilitates interpretation of the intercept (Albright & Marinova, 2010). Instead of representing the mean predicted Lysholm score at AAS=0, an AS value well below that expected from our patients, it represented the mean predicted Lysholm score at the mean activity level of our patients.

5.2.5.6.2 *Multilevel Modelling*

A robust, linear multi-level analysis (random intercept and random slope) was carried out using the Lysholm score as dependent and the centred AAS as independent variable, at the four timepoints, to model the individual patient relationships between activity levels and knee function. The resulting patient-specific slopes were determined and used as summary measures for the relationship between Lysholm and AAS. These analyses were then repeated with the 2-month timepoint excluded. Multilevel modelling can be regarded as a method to compromise between two extreme approaches, namely completely separate regression models for each patient (no pooling) and a single regression model that completely ignores the fact that there are several patients (complete pooling; (Gelman et al., 2006). The no-pooling approach suffers from the problem that the individual sample

sizes for each patient are often too small to allow a regression analysis, whereas the complete pooling approach completely ignores the dependency between measurements of individual patients. Multilevel models provide a “partial pooling” approach. They determine weighted individual patient slopes (“random slopes”) by comparing the individual linear slope between AAS and Lysholm as obtained from the “no pooling” approach, to a single (“fixed effect”) slope that represents the completely pooled relationship across all patients, by taking into account the evidence supporting individual slopes. If there is strong evidence that the individual patient slope differs from the fixed effect slope (narrow 95% confidence intervals) then the model weighs that patient’s slope towards the individual value. Conversely, if there is little evidence that the patient’s slope differs from the fixed effects slope (wide 95% confidence intervals), then the model weights the new slope towards that of the fixed effects slope.

5.2.5.7 Identifying Factors that Influence Variation Between Patients

5.2.5.7.1 Predictors of Individual Activity-Knee function Slopes

Non-parametric correlation analysis was used to assess the correlation between patient-specific activity vs function slopes, obtained from the robust linear multi-level model, and the average NA and PA for each patient. Subsequent multiple linear regression and partial correlation analyses were performed to determine whether demographic factors (age, smoking status, gender and BMI) influenced the slope in addition to psychosocial factors (NA and PA). These analyses were initially carried out on the model data from all four timepoints, and then again with the 2-month follow-up removed.

5.2.5.8 *Identifying Factors that Predict Post-Operative Knee Function and Activity Levels*

Multiple linear regression and partial correlation analyses were performed to identify demographic and psychosocial factors that may influence the 15-month post-operative outcome scores (Lysholm and AAS) individually. Baseline values for each of the outcome scores were included as covariates for this analysis.

Unless otherwise stated, all data analysis was carried out using R vs 3.6.1 (R Foundation for Statistical Computing, Vienna, Austria) and the packages nlme, robustlmm and ppcor. A p-value below 0.05 was denoted to indicate statistical significance.

5.3 Results

5.3.1 Power Analysis

The power analysis revealed, for the primary hypothesis, that a sample size of 20 patients would give a 92% power to detect a significant slope at the $p=0.05$ level. The secondary objective, to determine predictors of the slope, required a sample size of 50 patients to give 80% power to detect a significant correlation at the $p=0.05$ level. To determine the limits of agreement ($d-1.96SD$ and $d+1.96SD$) with a precision of $0.5SD$, a sample size of 51 patients was required.

5.3.2 Patient Demographics and Clinical Characteristics

Data was collected from 62 patients, 23 female and 39 male. The mean age in the patient cohort was $38.26 \text{ years} \pm 9.53_{SD}$ (range: 18-62 years old). Of the 62 patients, 4 were smokers, 11 were ex-smokers and 47 were non-smokers. The mean BMI was $29.1 \pm 5.14_{SD}$ (range: 19.84-39.58). The mean baseline Lysholm was $11.5 \pm 4.15_{SD}$ (range: 3-21) and the mean baseline AAS was $61.9 \pm 17.2_{SD}$ (range: 13-92).

5.3.3 General Analyses

5.3.3.1 Lysholm Knee Score

Overall, the mean Lysholm score significantly increased in the patient cohort ($n=62$) over the course of the study from baseline to 15 months post-op (mean change: $5.81 \pm 0.767_{SEM}$; $p<0.001$; Figure 5-7). There was no statistical evidence for a change in Lysholm score between the baseline and 2-month follow-up ($p=0.866$). There was a significant increase in Lysholm score between the 2- and 12-month follow-ups (mean change $4.57 \pm 0.527_{SEM}$; $p<0.001$). The mean Lysholm scores at 12- and 15-months post-op were statistically identical, with no significant difference between timepoints ($p=1.00$).

5.3.3.2 *Adjusted Activity Score*

Overall, the mean AAS significantly increased in the patient cohort (n=62) over the course of the study from baseline to 15-months post-op (mean change: $10.9 \pm 2.67_{SEM}$; $p=0.027$; Figure 5-8). There was no statistical evidence for a change in AAS between the baseline and 2-month follow-up ($p=0.146$). There was a significant increase in AAS between the 2- and 12-month follow-ups (mean change $17.9 \pm 1.95_{SEM}$; $p<0.001$). There was no significant difference in mean AAS score between 12- and 15-months post-op ($p=0.935$).

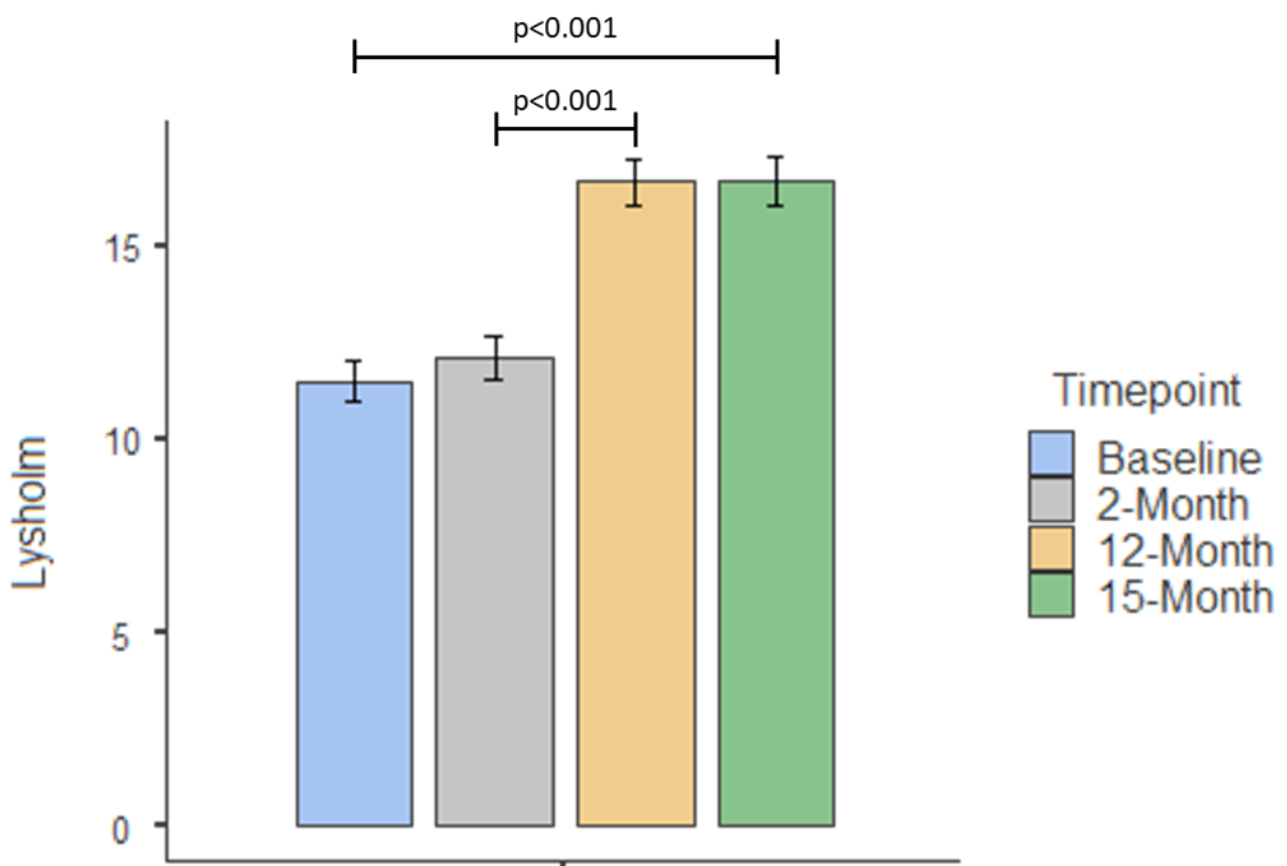


Figure 5-7: Mean Lysholm score over the course of the study. There were significant differences in mean Lysholm across the patient cohort (n=62), between baseline (pre-op) and the 15-month follow-up ($p<0.001$) and between the 2-month and 12-month follow-ups ($p<0.001$). Error bars represent the standard error of the mean. Significant differences are indicated by horizontal bars.

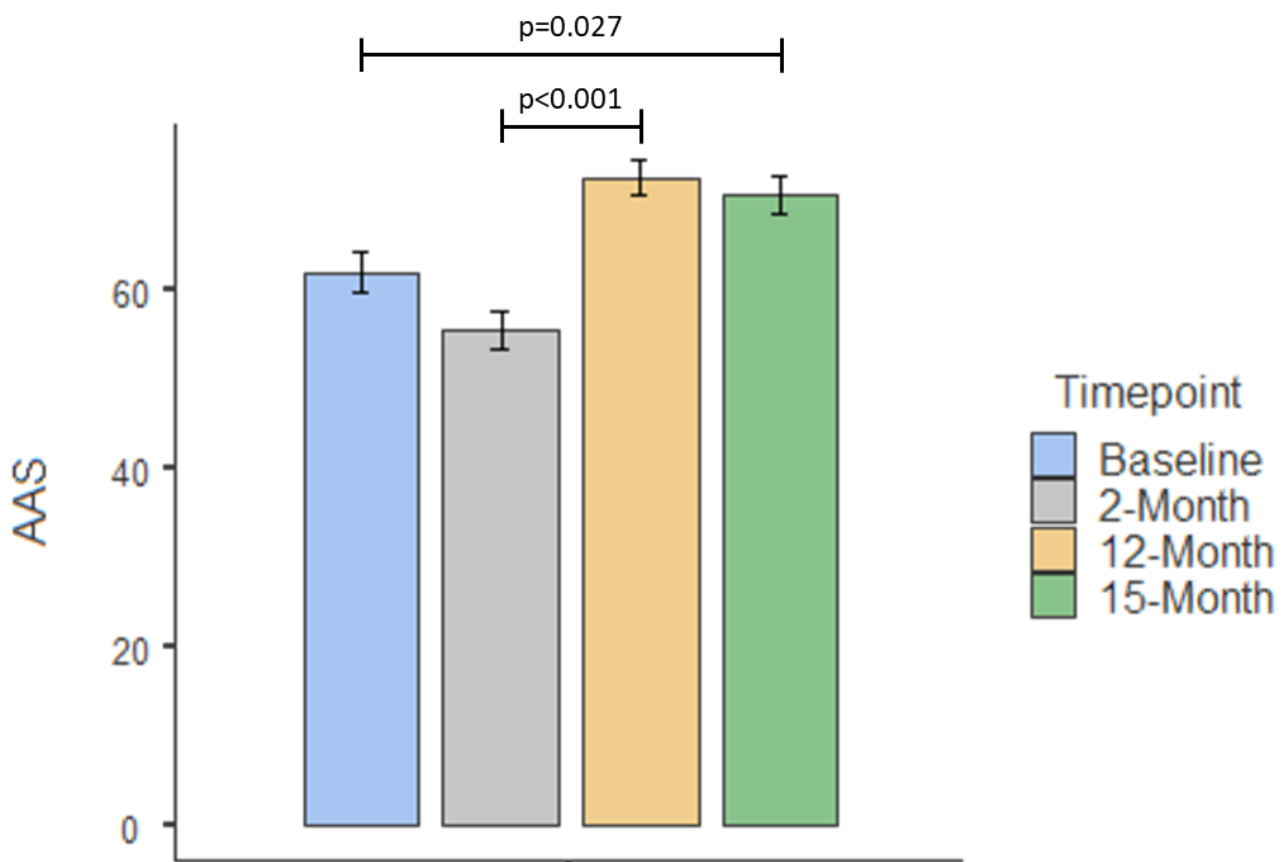


Figure 5-8: Mean AAS score over the course of the study. There were significant differences in mean AAS across the patient cohort (n=62), between baseline (pre-op) and the 15-month follow-up (p=0.027) and between the 2-month and 12-month follow-ups (p<0.001). Error bars represent the standard error of the mean. Significant differences are indicated by horizontal bars.

5.3.3.3 *Negative Affect Score*

Mean NA scores across the patient cohort demonstrated only minor fluctuations over the course of the study: baseline assessment ($10.6 \pm 0.298_{\text{SEM}}$; range: 5-17), 2-month follow-up ($9.87 \pm 0.359_{\text{SEM}}$; range: 5-16), 12-month follow-up ($9.72 \pm 0.429_{\text{SEM}}$; range: 5-20) and 15-month follow-up ($9.91 \pm 0.401_{\text{SEM}}$; range: 5-19). There were no statistically significant differences in average NA between any of the timepoints (Figure 5-9).

5.3.3.4 *Positive Affect Score*

Mean PA scores across the patient cohort demonstrated only minor fluctuations over the course of the study, and were almost identical at each of the four timepoints: baseline assessment ($17.8 \pm 0.398_{\text{SEM}}$; range: 9-24), 2-month follow up ($17.5 \pm 0.542_{\text{SEM}}$; range: 5-25), 12-month follow-up ($18.2 \pm 0.452_{\text{SEM}}$; range: 5-25) and 15-month follow-up ($18.1 \pm 0.559_{\text{SEM}}$; range: 5-25). There were no statistically significant differences in average PA between any of the timepoints (Figure 5-10).

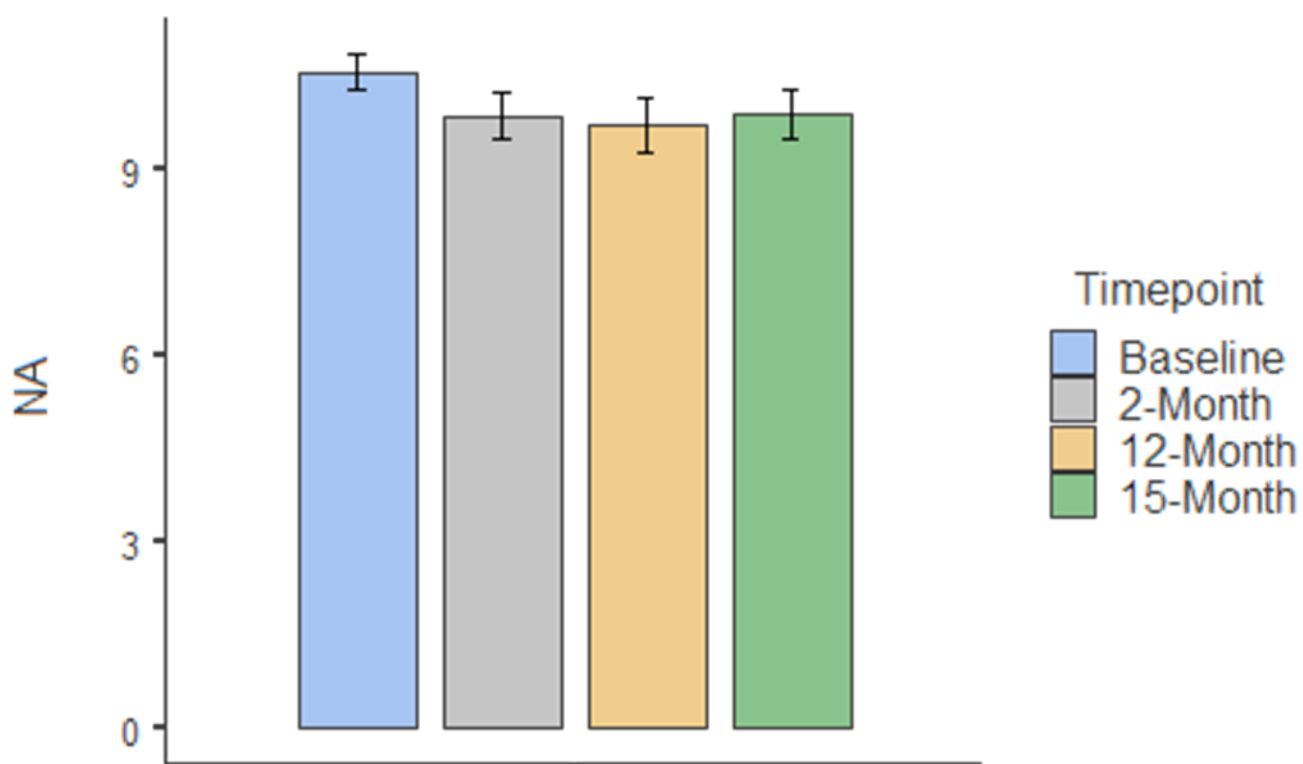


Figure 5-9: Mean NA over the course of the study. There were no significant changes in mean NA across the patient cohort (n=62) over the course of the study. Error bars represent the standard error of the mean.

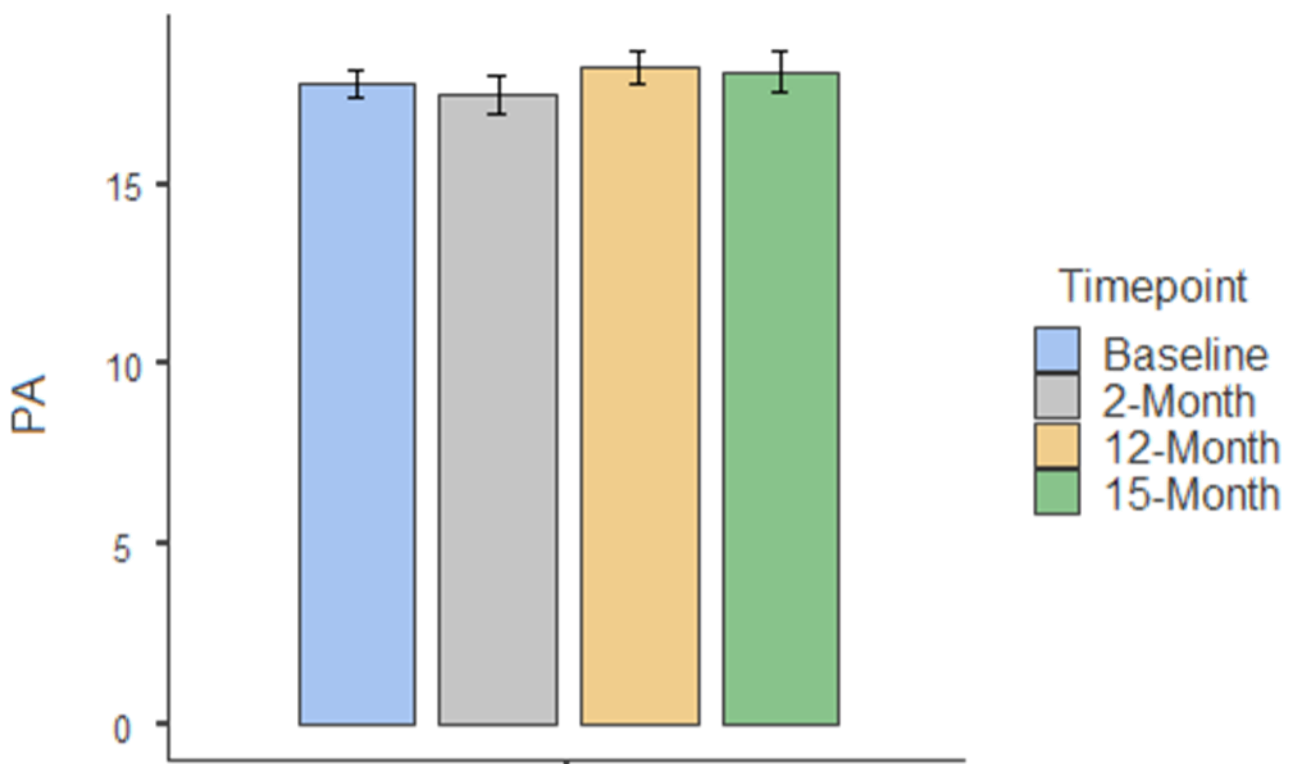


Figure 5-10: Mean PA over the course of the study. There were no significant changes in mean PA across the patient cohort (n=62) over the course of the study. Error bars represent the standard error of the mean.

5.3.4 Assessing the Temporal Stability of the I-PANAS-SF for individual patients

5.3.4.1 *Negative Affect*

Descriptive statistics and mixed modelling of the NA data indicated that there were no significant differences in mean NA, across the patient cohort, over time. Bland-Altman analysis demonstrated that there was good agreement between the baseline and 15-month NA scores. This was evidenced by the fact that the mean difference (estimated bias) was close to zero (0.75; 95% CI [-0.016, 1.52]) indicating that there was very little change in the scores from one timepoint to the other. The Bland-Altman plot also illustrated that there was a good spread of points above and below zero, suggesting no relationship between the difference and the mean value (Figure 5-11). The vast majority of points (51/52) lay between the upper (6.14; 95% CI [4.824, 7.46]) and lower (-4.64; 95% CI [-5.597, -3.32]) limits of agreement, and if one would centre these limits around the zero-difference line only three patients would have a clinically meaningful increase and one patient a clinically meaningful decrease, suggesting good agreement between the baseline and 15-month follow-up NA scores. Reliability analysis also demonstrated that there was good agreement between NA at the four timepoints (ICC(A,1)=0.58; $p < 0.001$; 95% CI 0.45-0.71).

5.3.4.2 *Positive Affect*

Descriptive statistics and mixed modelling of the PA data indicated that there were no significant differences in mean NA, across the patient cohort, over time. Bland-Altman analysis demonstrated that there was good stability between the baseline and 15-month PA scores. The mean difference (estimated bias) was close to zero (-0.231; 95% CI [-1.03, 0.566]) indicating that there was very little change in the scores from one timepoint to the other. The Bland-Altman plot displayed a good spread of points above and below zero,

suggesting that there was no relationship between the difference and the mean value (Figure 5-12). The vast majority of points (3/52) lay between the upper (5.375; 95% CI [4.01, 6.475]) and lower (-5.837; 95% CI [-7.21, -4.467]) limits of agreement, and if one would centre these limits around the zero-difference line only two patients would have a clinically meaningful increase and one patient a clinically meaningful decrease, again suggesting good agreement between the baseline and 15-month follow-up PA scores. This was again supported by the reliability analysis, which demonstrated that there was good agreement between PA at the four timepoints (ICC(A,1)=0.70; $p < 0.001$, 95% CI 0.58-0.80).

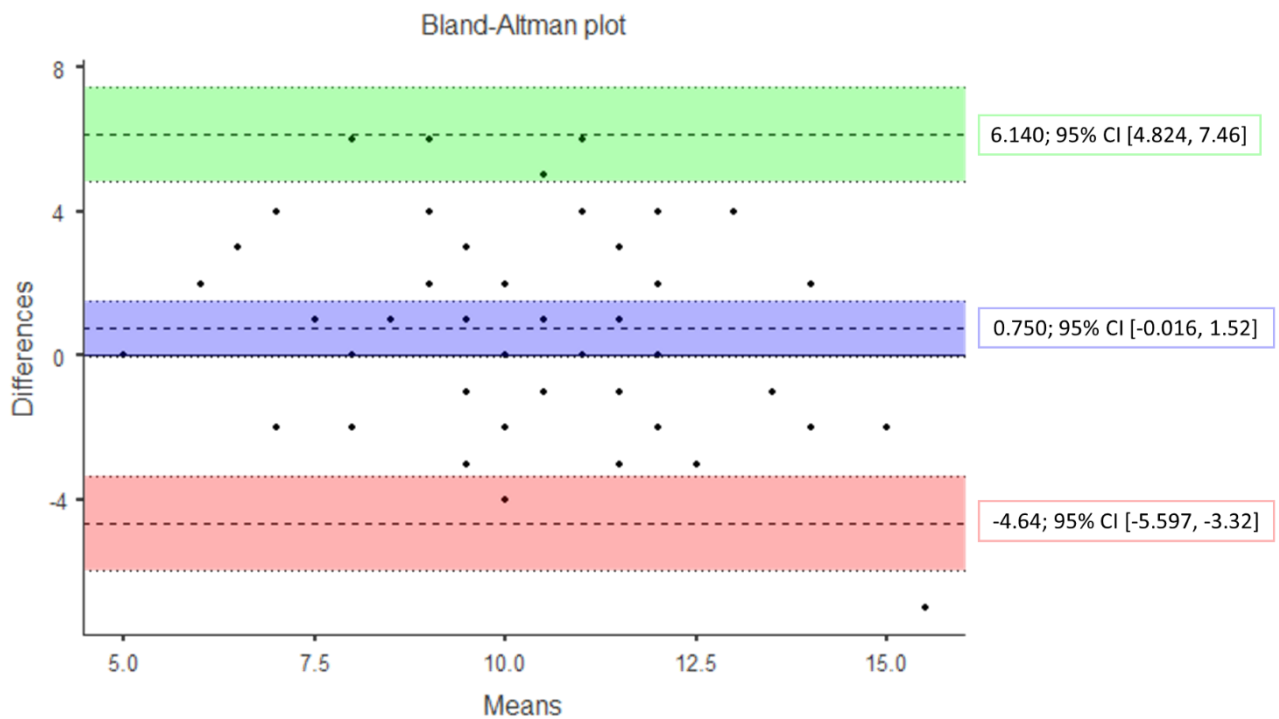


Figure 5-11: *Bland-Altman plot of mean baseline and 15-month NA scores. The horizontal axis represents the mean of the scores at the two timepoints and the vertical axis represents the mean of the scores from the two timepoints. The central dashed line represents the overall mean difference and 95% confidence intervals (blue area) between scores from the two timepoints. The upper dashed line represents the upper limit of agreement and associated 95% confidence intervals (green area) and the lower dashed line represents the lower limit of agreement and associated 95% confidence intervals (red area).*

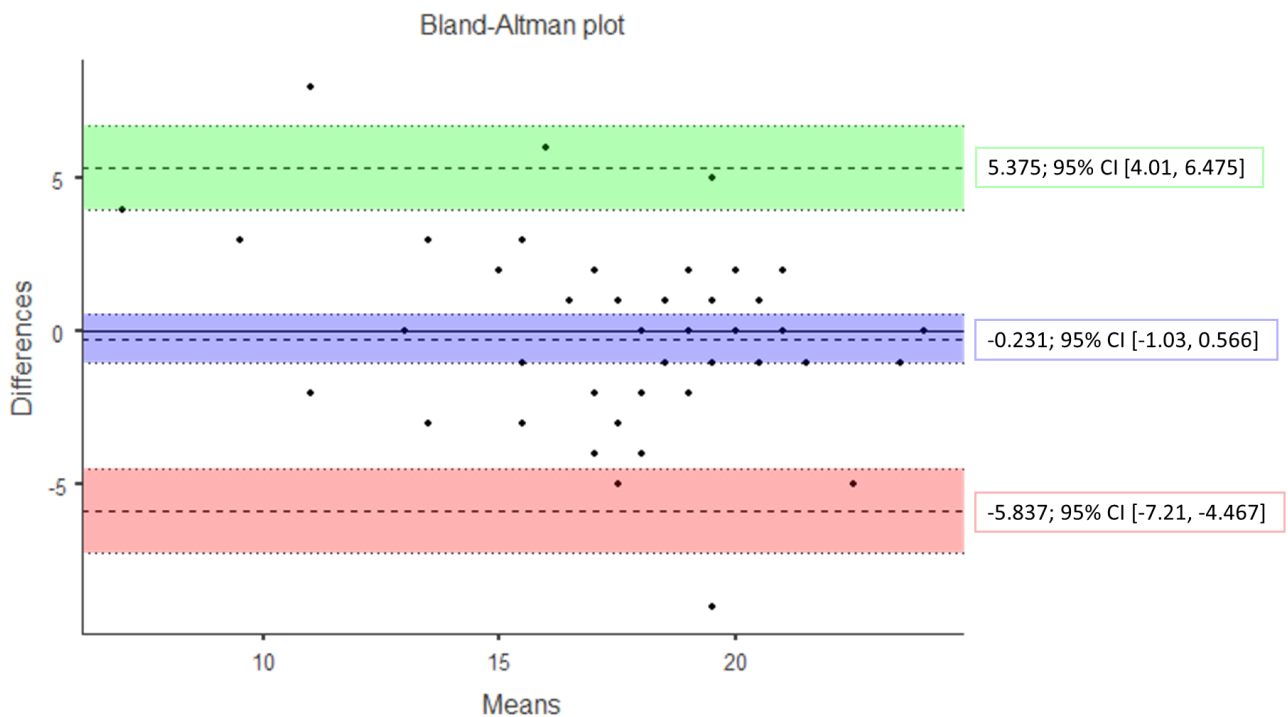


Figure 5-12: Bland-Altman plot of mean baseline and 15-month PA scores. The horizontal axis represents the mean of the scores at the two timepoints and the vertical axis represents the mean of the scores from the two timepoints. The central dashed line represents the overall mean difference and 95% confidence intervals (blue area) between scores from the two timepoints. The upper dashed line represents the upper limit of agreement and associated 95% confidence intervals (green area) and the lower dashed line represents the lower limit of agreement and associated 95% confidence intervals (red area).

5.3.5 Assessing Variation Between Patients

5.3.5.1 *Multilevel Modelling*

5.3.5.1.1 Centred vs Non-Centred AAS

The correlation between the random slopes and random intercepts of the patients' individual linear relationships between the non-centred AAS and the Lysholm scores was found to be almost perfect (Pearson's product-moment correlation: -0.98502 , $p=2.2e-16$, 95% CI $[-0.991, -0.9752]$). This would suggest that there were too many variables in the model, either the random slope or the random intercept should be dropped. The overall group mean of the AAS data was 65.0042 ± 17.9039 . Centring of the AAS data by subtracting the group mean reduced the correlation between the slope and intercept of the individual linear relationships (Pearson's product-moment correlation: -0.45563 , $p < 0.0002$, 95% CI $[-0.6333, -0.2323]$). The centred AAS data was therefore used for multi-level modelling.

5.3.5.1.2 All Timepoints

Following multilevel modelling, the fixed-effects value of the slope across all patients (0.1993 , $p < 0.0001$), suggested that, on average across the patient cohort, the relationship between activity levels and knee function was a positive one, with Lysholm increasing with increasing activity levels (AAS). Interpretation of the individual patient fits suggested that there was variation in the relationship between individual patients, however, with 54 (87.1%) demonstrating a positive relationship and 8 (12.9%) demonstrating a negative relationship (Figure 5-13).

5.3.5.1.3 Removal of 2-Month Follow-up Data

Following the removal of the AAS and Lysholm data from the 2-month follow-up, the positive fixed effect value of the slope across all patients (0.2117 , $p < 0.0001$), again

suggested that, in general, the relationship between activity levels and knee function was positive. However, interpretation of the individual patient fits suggested that there was variation in the relationship between patients, with 51 (82.3%) demonstrating a positive relationship and 11 (17.7%) demonstrating a negative relationship (Figure 5-14).

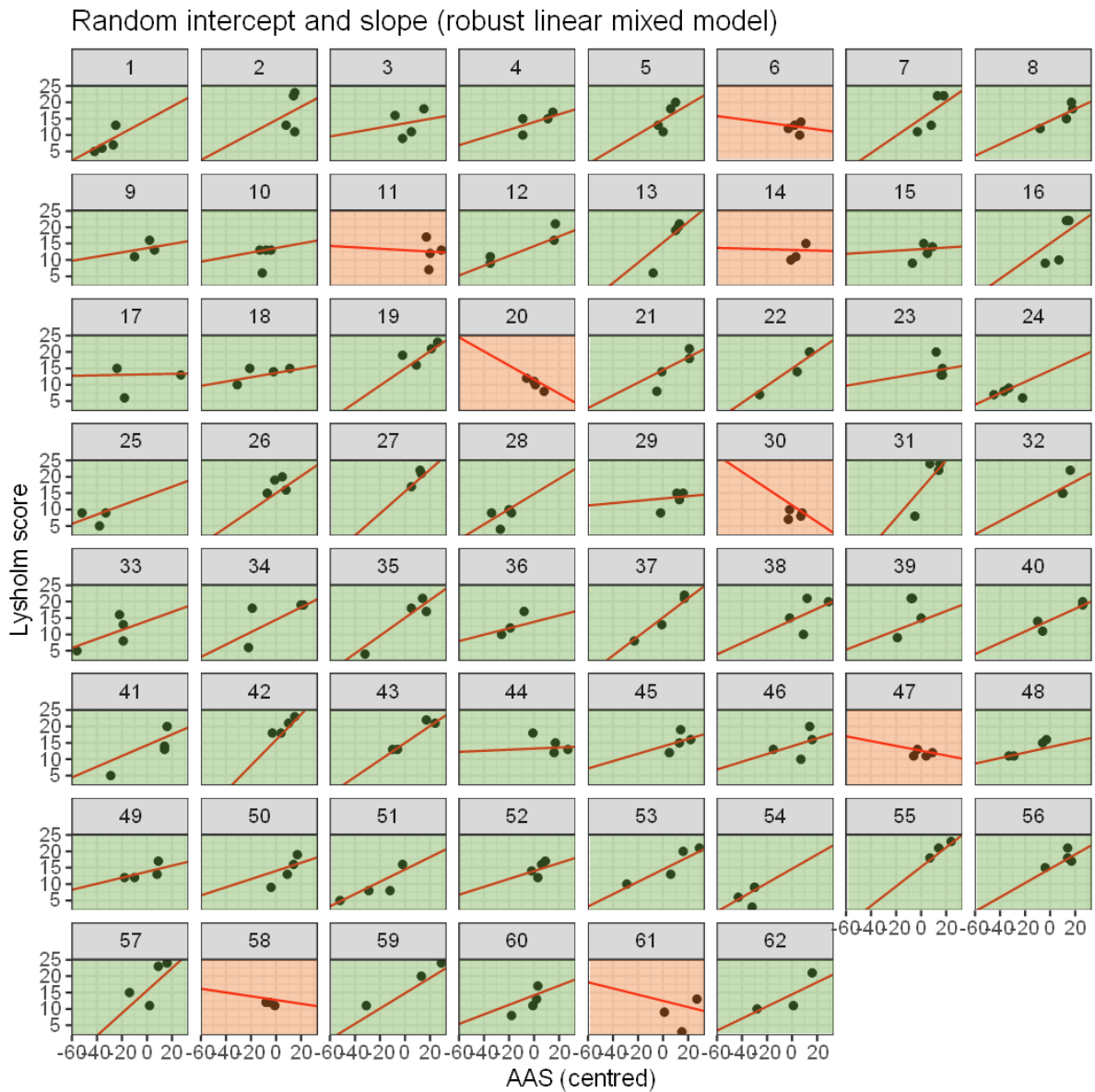


Figure 5-13: *Plots of the individual patient plots resulting from robust linear multilevel modelling of the full data set.* The individual plots represent the individual relationship between activity levels (AAS) and knee function (Lysholm score) at the four timepoint assessed in the study (baseline, 2 months, 12 months and 15 months). Following multilevel modelling, 54 patients demonstrated a positive relationship and 8 demonstrated a negative relationship. The value of the fixed-effect slope to which individual slopes were compared was determined to be 0.1993, $p < 0.0001$.

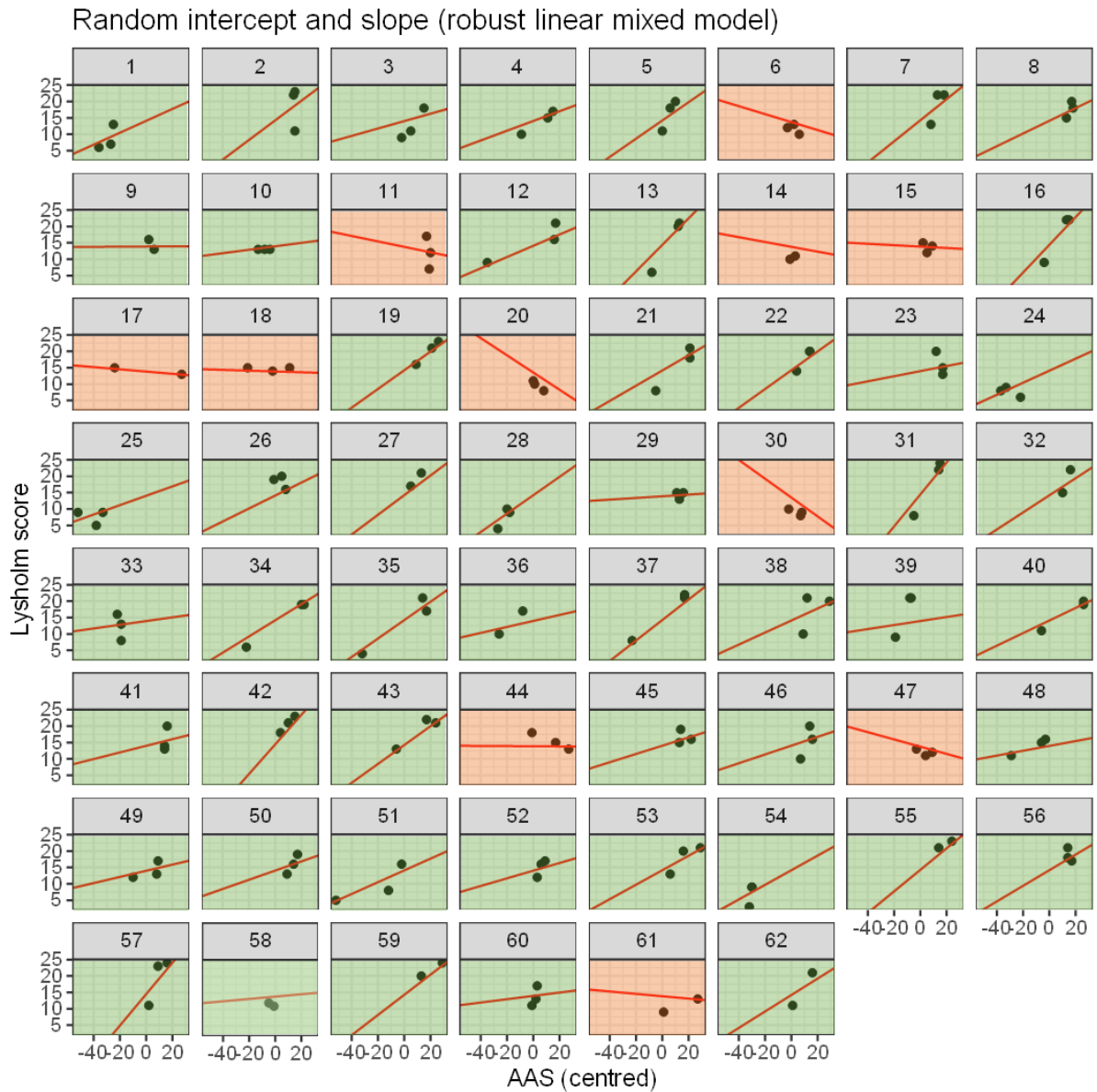


Figure 5-14: *Plots of the individual patient plots resulting from robust linear multilevel modelling of the data set excluding the 2-month follow-up. The individual plots represent the individual relationship between activity levels (AAS) and knee function (Lysholm score) at the four timepoint assessed in the study (baseline, 12 months and 15 months). Following multilevel modelling, 51 patients demonstrated a positive relationship and 11 demonstrated a negative relationship. The value of the fixed-effect slope to which individual slopes were compared was determined to be 0.2117, $p < 0.0001$.*

5.3.6 Factors Influencing Slope

5.3.6.1 Psychosocial factors (PA and NA)

5.3.6.1.1 All Timepoints

There was a significant correlation between the individual patient's mean NA and the individual patient slopes that resulted from the multilevel model, using the data from all four timepoints (Spearman's $\rho = -0.30$, 95%CI -0.05 to -0.51, $p = 0.018$; Figure 5-15). There was no significant correlation between mean PA and individual patient slopes from the multilevel model (Spearman's $\rho = 0.02$, 95%CI -0.23 to 0.27, $p = 0.8982$; Figure 5-16).

5.3.6.1.2 Removal of 2-Month Follow-up Data

When the AAS and Lysholm data from the 2-month follow-up were removed, the slopes from the multilevel model were significantly correlated with the patient's mean NA (Spearman's $\rho = -0.37$, 95%CI -0.57 to -0.14, $p = 0.0028$; Figure 5-17), but not mean PA (Spearman's $\rho = 0.13$, 95%CI -0.12 to 0.37, $p = 0.31$; Figure 5-18).

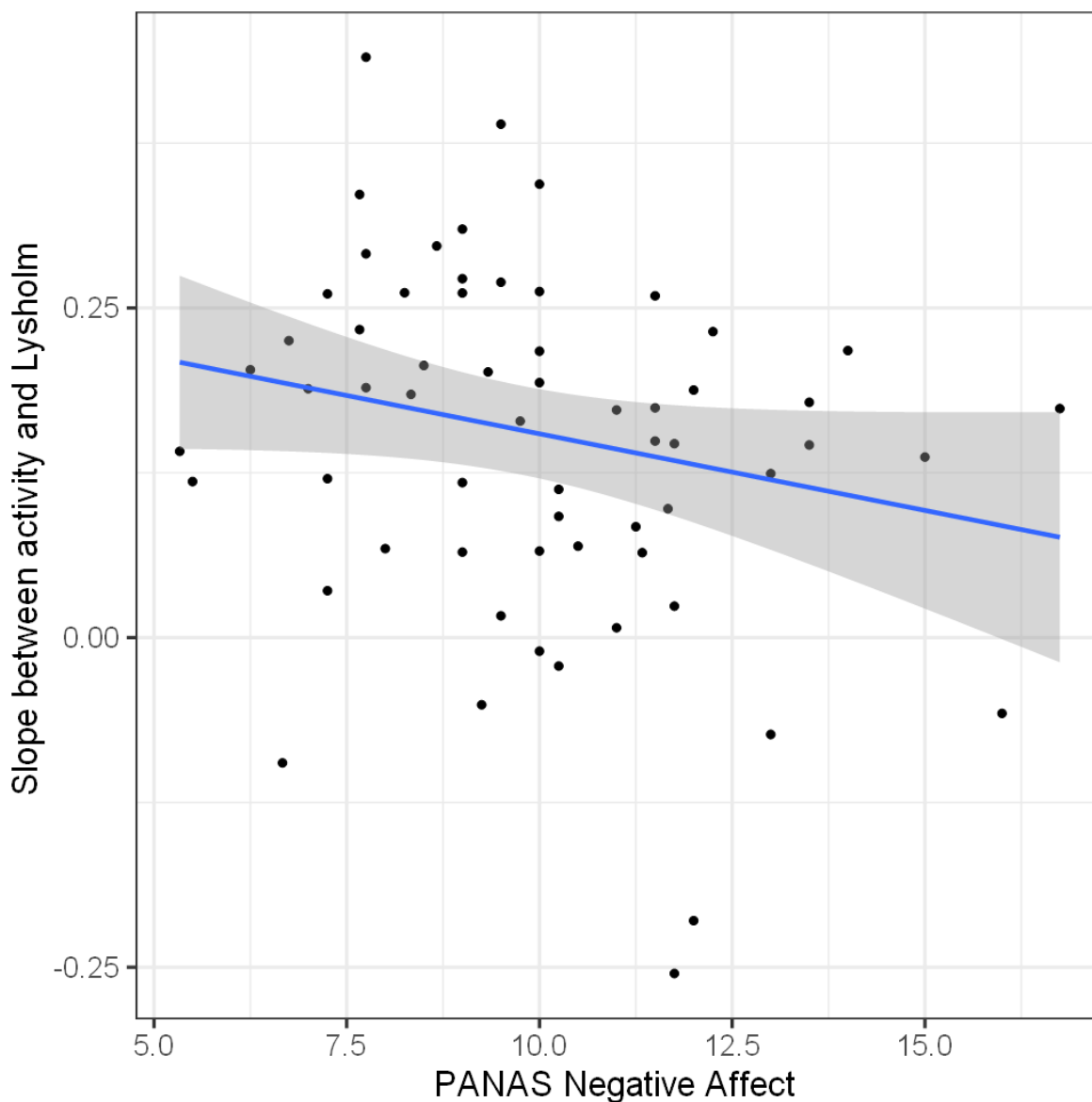


Figure 5-15: Scatter plot to demonstrate the correlation between individual patient slopes, created using the full data set, and mean NA scores. Slope was used as a measure with which to summarise the relationship between activity levels and knee function across the four timepoints used in the present study. The correlation of this summary measure with mean NA was assessed using Spearman's rank correlation. Slopes created using all four timepoints and mean NA were significantly correlated: Spearman's rho=-0.30, p=0.018.

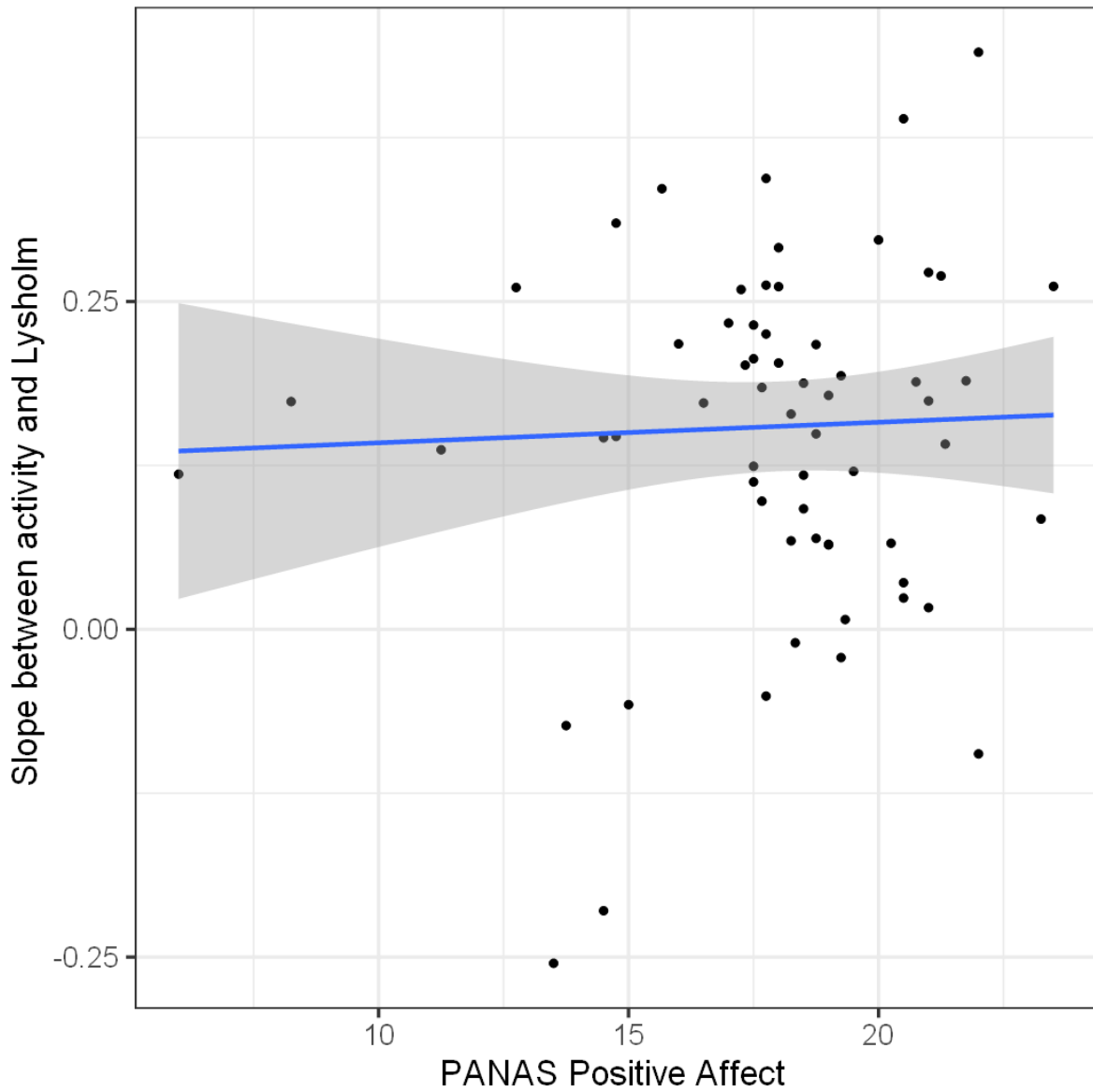


Figure 5-16: Scatter plot to demonstrate the correlation between individual patient slopes, created using the full data set, and mean PA scores. Slope was used as a measure with which to summarise the relationship between activity levels and knee function across the four timepoints used in the present study. The correlation of this summary measure with mean PA was assessed using Spearman's rank correlation. Slopes created using all four timepoints and mean PA were not significantly correlated: Spearman's $\rho=0.02$, $p=0.90$.

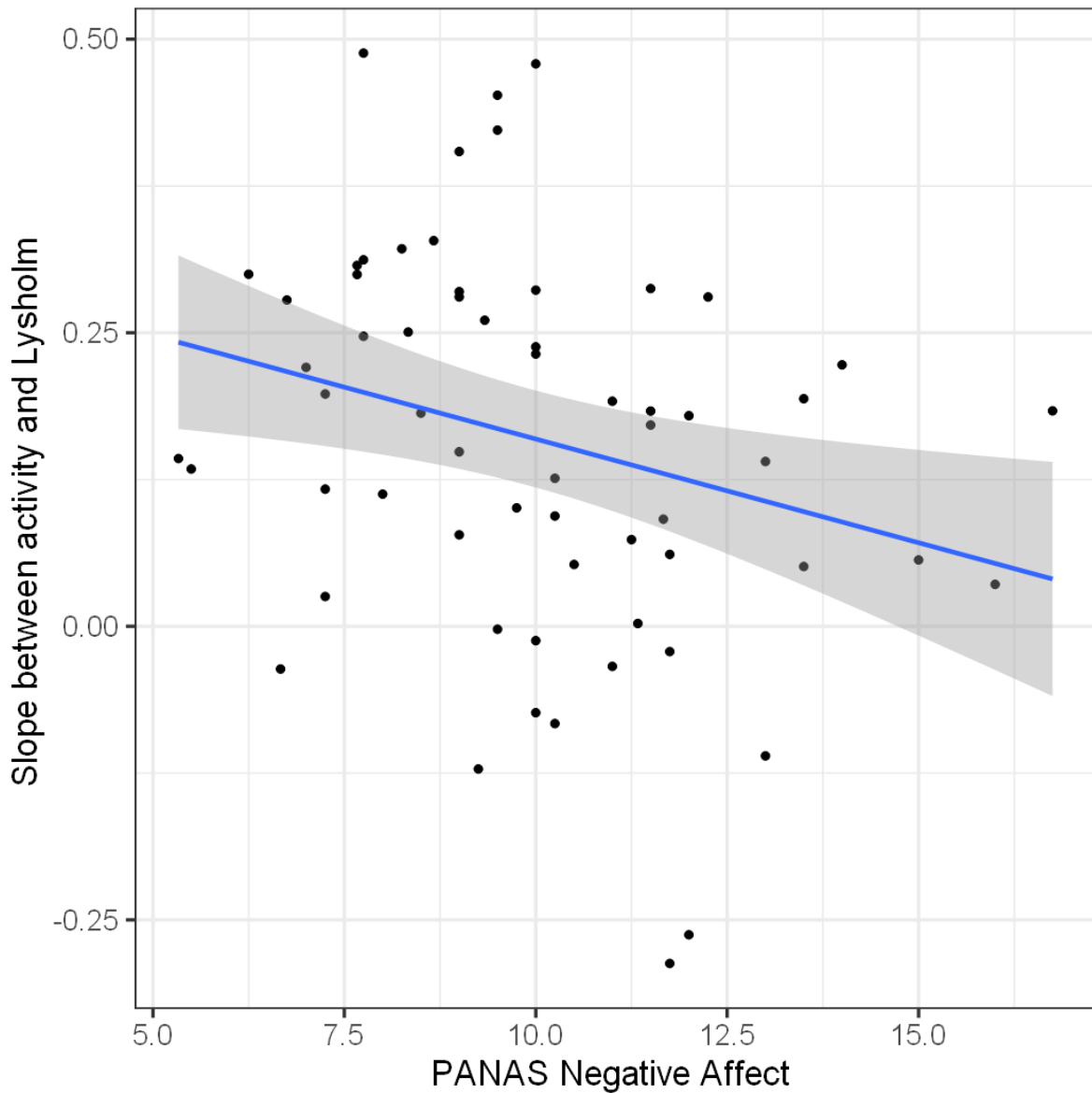


Figure 5-17: *Scatter plot to demonstrate the correlation between individual patient slopes, created with the 2-month follow-up data excluded, and mean NA scores. Slope was used as a measure with which to summarise the relationship between activity levels and knee function at baseline, 12-month and 15-month follow-up. The correlation of this summary measure with mean NA was assessed using Spearman's rank correlation. Slopes created from these three timepoints, and mean NA were significantly correlated: Spearman's rho=-0.37, p=0.0028.*

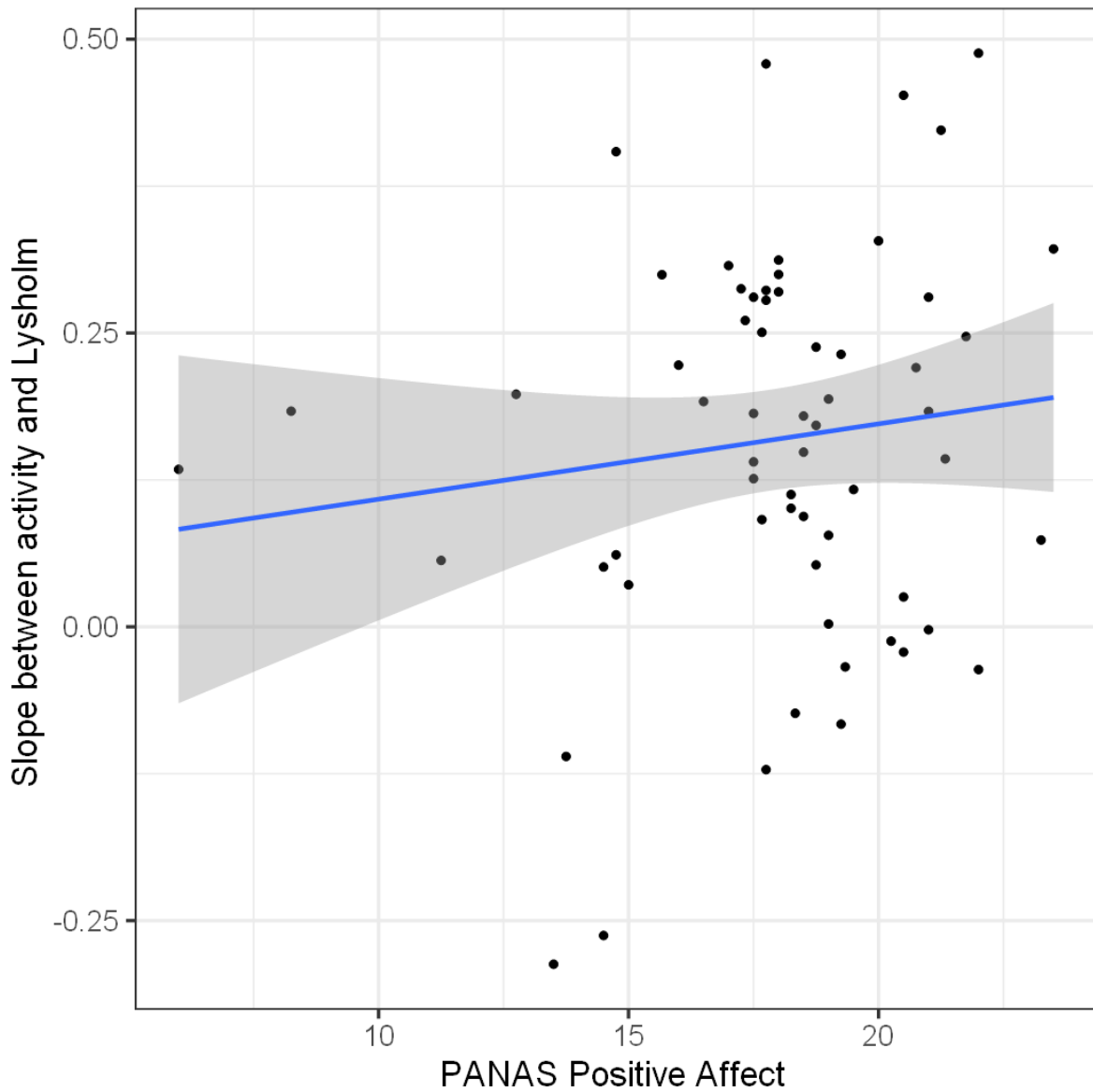


Figure 5-18: *Scatter plot to demonstrate the correlation between individual patient slopes, created with the 2-month follow-up data excluded, and mean PA scores. Slope was used as a measure with which to summarise the relationship between activity levels and knee function at baseline, 12-month and 15-month follow-up. The correlation of this summary measure with mean PA was assessed using Spearman's rank correlation. Slopes created from these three timepoints, and mean PA were not significantly correlated: Spearman's $\rho=0.13$, $p=0.31$.*

5.3.6.2 *Demographic and Psychosocial Factors*

5.3.6.2.1 All Timepoints

Multiple regression analysis did not identify any significant demographic (age, gender, smoking status, BMI) or psychosocial (PA and NA) predictors of the multilevel model slopes of the AAS and Lysholm data from all four timepoints. Partial correlation analysis revealed that average NA was significantly correlated with multilevel model slope (Spearman's $\rho = -0.33$, $p = 0.014$) when all other demographic and psychosocial factors were taken into account.

5.3.6.2.2 Removal of 2-Month Follow-up Data

Multiple regression and partial correlation analyses were also carried out on the resultant slopes from the multilevel modelling of the data after removing the 2-month AAS and Lysholm data. An increase in average NA was identified as the sole predictor of multilevel model slope (coefficient = -0.018 , $p = 0.0104$, 95% CI [-0.0321 , -0.004]) and was also found to be significantly correlated with slope when all psychosocial and demographic factors were taken into account using partial correlation analysis (Spearman's $\rho = -0.37$, $p = 0.0057$).

5.3.7 Predictors of Individual Outcome Measures at 15-Month

5.3.7.1 *15-Month Lysholm Score*

Multiple linear regression analysis revealed that the best individual predictors of the 15-month Lysholm score were mean NA (coefficient = -0.78 , $p = 0.0063$, 95% CI [-1.36 , -0.20]), mean PA (coefficient = 0.24 , $p = 0.026$, 95% CI [0.02 , 0.45]) and female gender (coefficient = 3.01 , $p = 0.040$, 95% CI [0.04 , 6.00]). However, when adjusted for all other demographic and psychosocial factors, as well as baseline Lysholm, only mean NA was

found to correlate significantly with the 15-month Lysholm (Spearman's rho=-0.34, p=0.027).

5.3.7.2 15-Month AAS

The best individual predictor of 15-month AAS, identified by multiple regression analysis, was baseline AAS (coefficient=0.29, p=0.043, 95% CI [0.0001, 0.58]). When adjusted for all other factors, however, there was no significant correlation with baseline AAS or any of the other psychosocial or demographic factors.

5.4 Discussion

The first objective of the present study was to assess the relationship between activity levels and knee function in a cohort of patients undergoing knee surgery and to determine if there was a significant variation in this relationship between patients.

We found that, across the patient cohort as a whole, the relationship between activity level (represented by AAS) and knee function (assessed by Lysholm knee function score) was positive, as was demonstrated by the positive fixed effects slopes from the multilevel model. In addition, the vast majority of individual slopes calculated using the multilevel model were positive. A positive relationship between activity levels and knee function is not a new finding. Tegner and Lysholm introduced the Tegner activity in 1985, when describing the first revision of the Lysholm scoring system, and demonstrated a positive relationship with the Lysholm scale (Tegner & Lysholm, 1985). Several more recent publications have specifically reported on the importance and beneficial effect of physical activity on knee function in the post-operative period following cartilage repair surgery (Knutsen et al., 2004; Knutsen et al., 2007; Kreuz et al., 2007; Toonstra et al., 2016).

However, in addition to the overall positive relationship across the study cohort, our results also showed that the activity-function relationship varied significantly between patients. We found not only a large variation in the magnitude of the individual patient slopes, but even some patients with a negative activity-function slope, indicating that there is indeed evidence that a proportion of patients (12.9% including all data and 17.7% following removal of the 2-month follow-up data) demonstrate a negative relationship between activity levels and knee function. This finding highlights the importance of individualised rehabilitation strategies, as patients with a negative relationship between AAS and Lysholm

are more likely to report decreased knee function with increased physical activity levels and therefore may require an alternative strategy for rehabilitation.

Removal of the data from the 2-month follow-up improved the fit of the robust multilevel model and revealed additional variation between patients, compared to using the full dataset. Removing the 2-month data may be justified due to its addition of several confounding variables that are not present in the pre-op or later follow-up assessments. Firstly, patients at the 2-month stage of the rehabilitative process are still recovering from major knee surgery, thus it is likely that the surgical intervention may affect both subjective knee function and activity levels to a greater degree than at the other timepoints assessed in the study. It has been reported that most patients do not fully recover knee function until at least 6 months post cell implantation, whereas patients can be expected to achieve full normal function, and even return to contact sport, at 12 months post-op (Bailey et al., 2003; Deszczynski & Slynarski, 2006). Our rehabilitation protocol is tailored to the patient's recovery, and hence at the 2-month timepoint the relation between knee function and activity is not only determined by the patient but also by the rehabilitation protocol.

Biological and biomechanical factors associated with cell implantation also add considerable additional variation at 2 months post-cell implantation, compared to the pre-op and later follow-up assessments. Following cell implantation, the new tissue forms in a series of repair stages, indicated by the degree of integration, maturation and mechanical properties (Hambly et al., 2012). In the early proliferative stage (0-6 weeks), a rapid cell response leads to the formation of a primitive soft repair tissue that then gradually firms up and integrates with native tissue during a transitional stage (7-26 weeks) (Bailey et al., 2003; Hambly et al., 2012; Toonstra et al., 2016). It has been reported that the early repair tissue is particularly

vulnerable to excess biomechanical forces during the first 3 months post-op (van Assche et al., 2010; Quatman et al., 2012). A remodelling stage (<27 weeks) follows, leading to the formation of a putty-like neocartilage (27-36 weeks), which is then gradually remodelled in a process characterised by increased cellular activity, matrix deposition and tissue stiffening to form a repair tissue that more closely resembles the mechanical properties of native articular cartilage (Bailey et al., 2003; Quatman et al., 2012; Toonstra et al., 2016). The remodelling phase can take as long as 3 years (Quatman et al., 2012; Hambly et al., 2012). The 2-month follow-up assessment in the present study is carried out during the early transition stage of the graft, whereas the later follow-ups at 12 and 15 month are carried out during the remodelling stage when the biomechanical properties of the repair tissue are likely to be very different. The soft tissue at 2-month post-op may thus introduce an additional confounding variable. This is reflected in the difference in rehabilitative strategy at 2-months post-op, in which full weight bearing is only just being introduced, compared to 12-months post-op, at which time some patients are able to return to contact sport. Further investigation into the acute post-operative phase, with additional timepoints that reflect biological, biomechanical and rehabilitative expectations is required but beyond the scope of the present study.

We have demonstrated that although there is an overall trend in the patient cohort for an improvement in subjective knee function score at increased activity levels, this is not the case for all patients, and some demonstrate a negative relationship. For these patients, an increase in activity level is associated with a decrease in subjective knee function score. It would be of use to be able to identify the patients for whom increased activity levels is associated with a negative response in knee function to enable patient stratification for rehabilitation and for treatment. The second aim of the present study was to identify and

examine demographic and psychosocial factors that could predict the magnitude and direction of the slope between AAS and Lysholm, and therefore predict the relationship between activity levels and knee function for individual patients.

We initially sought to assess the correlation between slopes and affect scores collected using the I-PANAS-SF. We were able to demonstrate the temporal stability of both constructs of the I-PANAS-SF, PA and NA, over the 15 months assessed in the present study using Bland-Altman, RCI and correlation analyses. Edmund Thompson, the researcher responsible for the development of the I-PANAS-SF from the original PANAS scales, reported that the scoring system was temporally stable over a period of 2 months with a significant test-retest correlation between NA and PA scores collected at baseline and at 2-months follow-up in a study of 143 patients ($r=0.84$, $p<0.01$ for both NA and PA) (Thompson, 2007). The intraclass correlation coefficient over the four scores collected in the present study was lower than the correlation coefficient reported by Thompson. However, the cohort assessed in the Thompson study consisted of volunteers with no reported health issues (Thompson, 2007). The present study not only assessed temporal stability over a longer time period, but the participants also suffered from a varying degree of knee pain and dysfunction and underwent major knee surgery during the time period over which stability was assessed. Judged by criteria commonly used to assess test-retest reliability (fair ICC 0.40-0.59, good ICC 0.60-0.74; (Cicchetti et al., 2006)), the NA would be regarded fair and the PA good, which is remarkable considering the patients' experiences. Moreover, we also demonstrated that the number of patients that did undergo a clinically and statistically relevant change, as indicated by the RCI, was not larger than one would expect by chance alone. Although the sample size of the present study was relatively small ($n=62$), the stability of the I-PANAS-SF over a 15-month period that included cell implantation surgery

and subsequent rehabilitation highlights the utility and robustness of the scoring system for use in research of surgical interventions. Based on these findings, our subsequent investigation of NA and PA as predictors of slope and individual outcomes used the mean NA and PA over the course of the study. The use of mean affect scores, as a stable indicator of affect over the course of a study, has been previously reported in a study of the effect of PA and NA on pain in patients with chronic OA (Finan et al., 2013).

The patient's mean NA score over the course of the study was found to correlate significantly with the slope between activity levels and knee function. Firstly, mean NA correlated significantly with the multilevel model slope, and a larger mean NA was found to be the best predictor of a decreased slope, accounting for demographic and clinical factors. Taken together, these results suggest that patients with a higher mean NA score are more likely to report a decrease in perceived knee function at higher activity levels, and vice versa. A number of psychosocial constructs, including negative affect, have been previously reported to correlate with knee function and activity levels independently, both in patients who had undergone surgery (Gobbi & Francisco, 2006; Thomee et al., 2006; Chmielewski et al., 2008; Chmielewski et al., 2011; Mithoefer et al., 2012; Seebach et al., 2012; Liao et al., 2015; Toonstra et al., 2016) and in patients not undergoing surgery (Tripp et al., 2007; Niermann et al., 2016). To our knowledge however, ours is the first study to report the influence of these constructs on the relationship between the two. Our findings suggest that NA acts as a mediator for the relationship between activity levels and knee function and therefore is very important in the rehabilitative period, in which success is commonly judged by an increase in activity levels and knee function.

Interestingly, mean PA was not significantly correlated with, nor shown to be a significant predictor of, slope by any of the analyses used in the present study. The published literature reports a range of findings regarding the relationship between PA, activity levels and knee function. Several published studies found a positive relationship between PA and activity levels (Carels et al., 2007; Dunton, Genevieve et al., 2009; Schwerdtfeger et al., 2010; Liao et al., 2015) and others found no significant relationship (Mata et al., 2012; Dunton, Genevieve F. et al., 2014) but the methods, patient cohorts and time periods examined vary widely. Finan and colleagues also reported that PA was predictive of knee OA pain (Finan et al., 2013). Our finding that only NA, but not PA, has significant relationship with slope, does corroborate reports that PA and NA are largely independent and uncorrelated constructs (Watson et al., 1988; Merz et al., 2013).

Finally, the present study sought to identify which of the demographic, clinical and psychosocial factors investigated in this study predict two of the 15-month trial outcomes, Lysholm (the primary outcome) and AAS (a secondary outcome). We found that mean NA was the sole significant predictor of 15-month Lysholm, whereas none of the other factors assessed was predictive of the 15-month AAS. We were surprised to find that the baseline Lysholm score, which could be taken as a proxy of pre-operative disease severity, had no predictive value for the outcome of cartilage repair. Other reports suggest that baseline Lysholm does influence outcome after 1 year (Krishnan et al., 2006; Dugard et al., 2017). Demographic factors that have previously been reported to influence the success of cartilage repair surgery also held no predictive value for the outcome in this study (Krishnan et al., 2006; Toonstra et al., 2013; Dugard et al., 2017). It should however be kept in mind that those earlier studies all used larger sample sizes than ours. Moreover, the patients in our cohort were treated using a mix of three different cell therapies, the allocation of which

was blinded to us. If the effectiveness of those therapies differs then this would add an additional variation that is not accounted for. Nevertheless, the strong predictive nature of the NA suggests that if one could improve a patient's NA score, one could improve the outcome of cell therapy. The stability of PA and NA (as assessed by the I-PANAS-SF), which in our study were not affected by knee pain, surgery and rehabilitation, may however preclude such an option.

Our results suggest that for the majority of patients, the relationship between activity levels and knee function is a positive one, but that there is variation between patients in the magnitude of this relationship, and for some, the direction of this relationship. We have shown that some of this variation can be explained by the patient's negative affect score, with patients whom have a higher NA score more likely to report decreased knee function with increasing activity levels, and that NA can also predict post-operative knee function, when all other demographic factors were taken into account. Taken together, our findings highlight the importance of an individualised approach to managing the expectation and rehabilitation of patients for the treatment of AC lesions with cell therapy, which could be based on the assessment of the patients' negative affect. As well as individualised rehabilitation, patients may benefit from psychological intervention prior to surgery. In this way, we may be able to increase the efficacy of existing rehabilitation programmes and the outcomes of surgery. Although we have shown in this study that NA is an incredibly stable construct, and therefore may not be influenced by counselling, there may be other psychological constructs that could be altered in this way. Further investigation into such constructs is required, along with the appraisal of our results and conclusions by a qualified clinical psychologist. For this reason, we have designed an observational study using wearable activity trackers to objectively and continuously monitor activity levels over the

course of a week, with twice-daily knee function scores and psychosocial scores (I-PANAS-SF and Survey of Pain Attitudes (SOPA)). The study is entitled, 'Characterising the relationship between Activity Levels and Knee Function (ChALK)' and has recently received ethical approval. The ChALK study flow chart, patient information sheet and letter of approval are included as appendices (appendix 5-1, 5-2 and 5-3 respectively).

5.5 Study Limitations

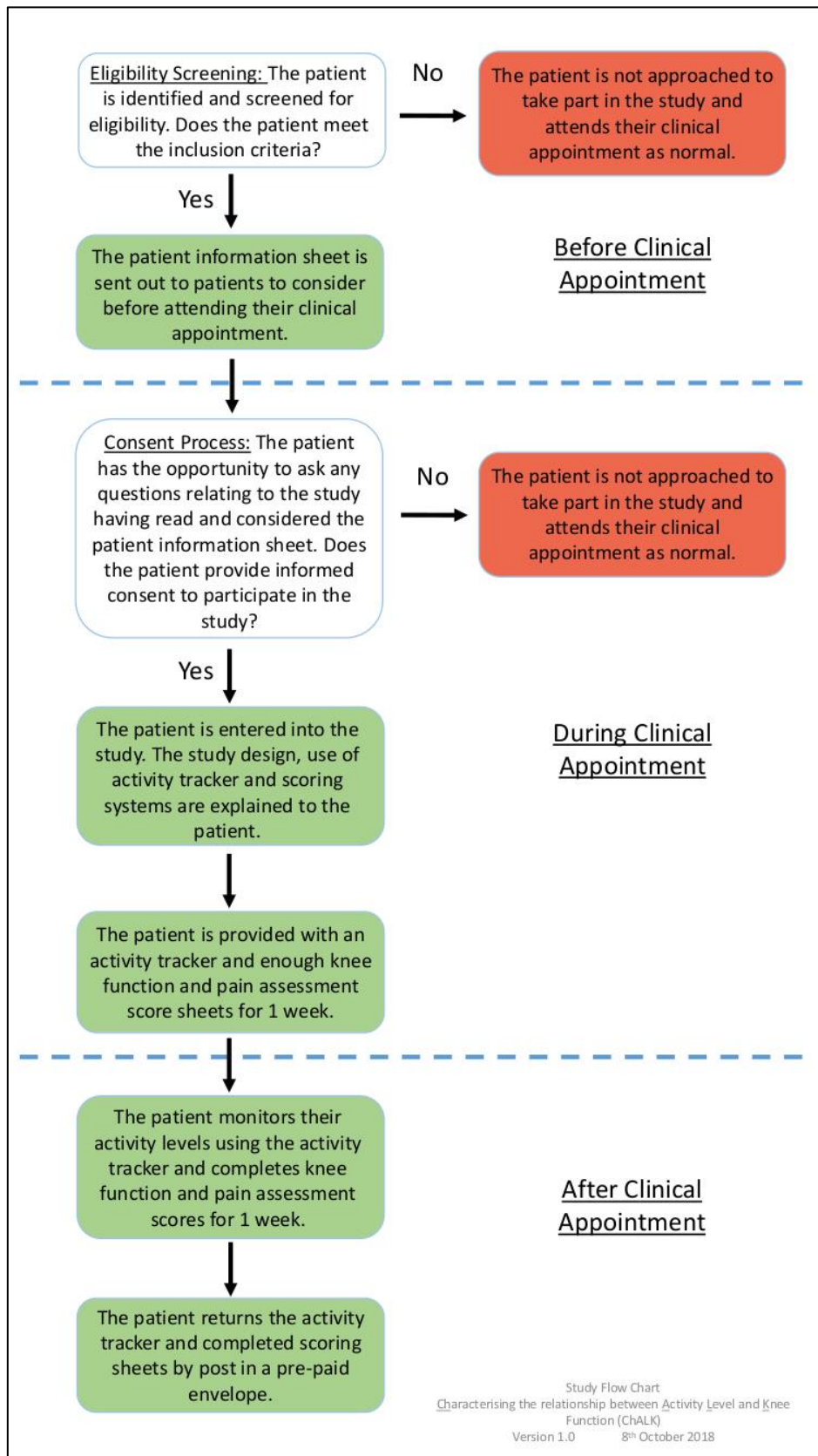
A major limitation of this study is the failure to include characteristics of the AC lesion such as the number of defects, defect size, defect location and defect age, which previous reports identified as predictive for the success of cartilage repair surgery, in the analyses (Krishnan et al., 2006; Toonstra et al., 2013; de Windt et al., 2017; Dugard et al., 2017). This will be the basis of future work in this area but does not diminish the importance of the finding that, of the reported demographic and psychosocial influences, NA is the most important.

A second potential shortcoming is the use in the present study of only three measurements (four before the removal of the 2-month follow-up data), taken over a relatively long time period, and of a subjective measure of activity levels (the HAP). While we were able to demonstrate and begin to pick apart the complex interaction between activity levels, knee function and psychosocial, clinical and demographic factors over the course of this study, we are also interested in the interaction between these factors over a shorter time period.

5.6 Conclusion

In the present study, we were able to demonstrate variation between patients in the relationship between activity levels and knee function, that was partially explained by the patients' negative affect score. Additionally, the patients' negative affect score was found to

be the best predictor of the primary outcome of the ASCOT trial, the 15-month Lysholm score. The results of this study led to the development of a further observational study investigating activity levels, using wearable activity trackers, and knee function, using a phone application.



Appendix 5-1: Flow chart summarising the procedures involved in the ChALK study.



**Orthopaedic
Institute**

The Robert Jones and Agnes Hunt **NHS**
Orthopaedic Hospital
NHS Foundation Trust



Patient Information Sheet

IRAS Project ID: 227476

Version 1.2, 6th December 2019

Study Title: Characterising the relationship between Activity Level and Knee Function

Acronym: ChALK

You have been invited to take part in a research study that is organised jointly by Keele University and the Robert Jones and Agnes Hunt Orthopaedic Hospital. The study will use wearable activity trackers to investigate and characterise the relationship between activity levels and knee function. This information sheet explains the reasoning behind the study and what would be involved should you choose to participate.

Background to the research:

Knee function is known to vary over the course of our lifetimes. We believe that knee function can also vary on a more short-term basis, day-to-day or even morning-to-night. This may pose a problem in clinic, because knee function scores are used to diagnose knee problems and to judge if treatments are effective. If the knee function varies day-to-day, how can one decide if the knee is better? One factor that we believe to play an important part in the short-term variation is activity level. The precise relationship between activity levels and knee function has not been fully characterised, but we know from previous research that this relationship varies between individuals. We think that patients' general disposition, their attitude to pain and their pain coping strategies may all determine the relationship, and therefore we will also investigate those.

Aim of the research:

We aim to use wearable activity trackers to measure activity levels, alongside knee function scores, to investigate the relationship between activity levels and knee function for individual patients. Secondly, we aim to find out if attitudes to pain and coping strategies, as well as general outlook can influence the relationship between activity levels and knee function.

Why was I chosen?:

You were invited to participate in this study because you are scheduled to attend a clinical appointment for knee-related symptoms with one of the consultant surgeons at The Robert Jones and Agnes Hunt Orthopaedic Hospital.

Timothy Hopkins

Patient Information Sheet V1.2

6th December 2019

What will be involved?

Your routine care will not be affected if you decide not to take part in this study. If you do decide to take part, you will not be required to attend any additional appointments. Reading and understanding the enclosed information should take no longer than 30 minutes.

You will receive a phone call before your clinical appointment in which a member of the research team will ask you whether or not you would like to take part in the study now that you have had chance to read and understand the enclosed information. At this point you will have the opportunity to ask questions.

If you indicate on your phone call that you would like to take part in the study, you will be asked to read and sign a consent form at your scheduled clinical appointment.

You will then be provided with an activity tracker (Withings Pulse HR) which a member of the research team will explain to you and help to set up. The activity tracker is worn on the wrist and is roughly the same size and weight of a watch. The tracker will monitor activity levels whenever it is being worn and therefore, once set up, will not require any further action other than being worn continuously for the week. You will be asked to download an accompanying application (Withings Health Mate) to your smart phone that will securely store your activity data on a secure server. You will be asked to input demographic data including your height, weight and age during the set-up of the phone application. This application will be password protected so that only you and the researchers can access the data.

The research team member will then explain the use of a web-based version of the Lysholm knee function scoring system. The web-based Lysholm knee function scoring system should take no longer than 2 minutes to complete the first time, and this time is likely to decrease to less than 30 seconds as you get used to the layout and questions. This electronic Lysholm knee function scoring system will need to be completed twice a day, ideally first thing upon waking, and last thing before you go to bed. Data collected using the electronic Lysholm scoring system will be stored on secure servers and accessed using a unique code that only you will know.

The research team member will also provide you with several scoring system sheets along with clear instructions as to how and when to complete these. These other scoring system sheets will take no longer than 5 minutes to complete in total.

Any data collected will not affect your routine care. Once you have worn the activity tracker and completed score sheets for one week, you will return the tracker and completed score sheets in the pre-paid envelope provided.

All information will remain strictly confidential and for use only for this research study. As this research study will not require any additional appointments, and activity trackers are provided, there will be no cost to the participant and therefore there will be no reimbursements made available for this study.

Will all participants have the same process?

Yes, all participants will go through the same process for the same length of time.

Do I have to take part?

No, you do not have to take part in the study. This study is voluntary, and if you decide not to take part there will be no effect on any aspect of your treatment or standard of care. If you do not wish to take part in the study, please ignore this letter and attend your upcoming appointment as normal.

If you do agree to take part, you are free to withdraw from the study at any time and without giving reason. Withdrawal from the study will not affect the standard of care you receive.

What are the benefits of taking part?

There are no direct benefits to your treatment from taking part in this study. You will however be actively contributing to research that could improve our understanding of the relationship between knee function, activity levels and attitudes to pain and pain management. This could influence research and clinical decisions in the future and so your contribution could benefit society and those with a similar condition.

What are the disadvantages/risks of taking part?

As this study involves only the monitoring of normal activity levels and the completion of questionnaires, there are no risks associated to your health or wellbeing.

What if I decide I no longer wish to take part after agreeing to the study?

You can withdraw from the study at the any time, without providing a reason. Your routine care will not be affected. Just contact a member of the research team, tell them that you no longer wish to take part in the study and return your activity tracker in the pre-paid envelope provided. No further data or information will be collected for the study purposes. We will still use data collected up to this point if possible. If you are no longer able to take part in the study, we will still use data collected up to the point of loss of capacity if possible.

Would you need to contact me in the future?

We may contact you in the future to clarify the information you provided if there is something unclear on the questionnaires you returned. For this reason, we will ask you to consent to allow us to store your contact details for the duration of the study and for 10 years after the completion of the study. This is entirely optional and is not required for participation in the study. If you consent to the retention of your contact details, they will be stored on a secure spreadsheet that is maintained on a password-protected Trust computer.

Is the information I provide kept confidential?

All information for this study is kept strictly confidential in line with the Data Protection Act 2018 and the General Data Protection Regulation (GDPR). Your personal information is only accessed by the research team, and will never be made available to anybody outside of the research study team. On consenting to the study, you will be allocated a unique identifying number (e.g. ChALK-123) that will be used on all documentation and records, and this will keep your identity anonymous and confidential. In the case of publication, there will be no identifiable data, such as names and other personal information, published. All information will be anonymous

Who is organising this study?

This research study is jointly organised by The Robert Jones and Agnes Hunt Orthopaedic Hospital and Keele University. The study is being led by Mr Timothy Hopkins, a PhD research student from the University of Keele, who is based at The Robert Jones and Agnes Hunt Orthopaedic Hospital. Timothy is investigating various aspects of the dysfunction of the

knee joint. The other members of the research team include the following healthcare and/or research professionals:

1. Dr Jan-Herman Kuiper, Senior Lecturer in Biomechanics.
2. Mr Peter Gallacher, Consultant Orthopaedic Knee Surgeon.
3. Professor Sally Roberts, Director of Spinal Research.
4. Mr Simon Roberts, Consultant Orthopaedic & Sports Injury Surgeon.
5. Mr Andrew Barnett, Consultant Orthopaedic Surgeon (Soft Tissue/Knee).
6. Mr Paul Germin, Consultant Knee Surgeon.

Who will have access to information about me?

Keele University is the sponsor for this study based in the United Kingdom. We will be using information from you in order to undertake this study. Keele University will act as the data controller and the RJAH hospital as the data processor for this study. This means that we are both responsible for looking after your information and using it properly. All the information you give to us will be treated in the strictest confidence.

Your data will be stored and safeguarded at RJAH Orthopaedic Hospital (Oswestry, Shropshire). The RJAH trust will keep your personal details (name, NHS number, date of birth and contact details) confidential and will not pass this information to anyone outside of RJAH. RJAH hospital trust will use this information as needed, to contact you about the research study, and make sure that relevant information about the study is recorded for your care, and to oversee the quality of the study. RJAH hospital trust will keep identifiable information about you from this study for 10 years after the study has finished and this is compliant with Keele University policies.

Each person who takes part in the study will be given a unique identifier number so any information that you give to us just for this study will not be associated with your personal details. The data published from this study will not contain any of your identifiable information and so cannot be traced back to you. All of the study-related information collected from you will be anonymised and saved on an NHS computer at RJAH that is secured, and password protected which can only be accessed by professionals involved in this study. All analysis will only be done on the anonymised data. The information will only be used for the purpose of health and care research and will not affect your care. It will not be used to make decisions about future services available to you, such as insurance.

The Health Mate application that is used to store activity data will require the input of personal information (name, date of birth, height, weight) but this will remain confidential and only yourself and the researchers will have access to this information. The electronic Lysholm score application will also require the input of personal data (age, gender) but this will also remain confidential and can only be accessed using a unique patient code that only yourself and the researchers will know.

Your healthcare records may be looked at by authorised individuals from the research team, RJAH, Keele University or the regulatory authorities to check that the study is being carried

out correctly. We are committed to protecting the privacy and security of the personal information of all participants in our research. For further information, please see the Keele University Privacy Notice for Research Participants and Keele University's Privacy Notice: <https://www.keele.ac.uk/business/privacynotice/>.

Your rights to access, change or move your information are limited, as we need to manage your information in specific ways in order for the research to be reliable and accurate. If you withdraw from the study, we will keep the information about you that we have already obtained. To safeguard your rights, we will use the minimum personally-identifiable information possible. You can find out more about how we use your information at: <https://www.keele.ac.uk/research/raise/governanceintegrityandethics/researchdatamanagement/#keele-research-data-management-policy> and/or by contacting the research team.

The contact details for the sponsor are as follows:

Dr Tracy Nevatte,
Head of Project Assurance,
David Weatherall Building,
Keele University,
Staffordshire.
ST5 5NH.

Telephone: 01782 732975

Email: research.governance@keele.ac.uk

Who is funding the study?

The study is funded by The Orthopaedic Institute Ltd. The Orthopaedic Institute Ltd is a charity that supports research and teaching at The Robert Jones and Agnes Hunt Orthopaedic Hospital NHS Foundation Trust.

What happens when the study finishes?

When the study is completed, all information will be stored for 10 years and then the information will be destroyed, as per the data protection act 2018. All stored information is only accessible by the research study team and will only be accessed in the case of new findings that may be relevant to this study and/or the results obtained.

What happens to my information if the study findings are published?

In the case of publication, the findings of the study will be published, but your personal information, including names, will not be made available. All information published will be kept confidential and anonymous. All correspondence regarding publication will be made through the funding body: The Orthopaedic Institute Ltd, Oswestry, or through the hospital, The Robert Jones and Agnes Hunt Orthopaedic Hospital, Oswestry. A study newsletter will be sent at the close of the study to disseminate any findings to all participants.

Contact details:

Principal investigator -

Mr. Timothy Hopkins

PhD Student

Institute of Science & Technology in Medicine (ISTM)

Keele University

Arthritis Research Centre (Building 10)

The Robert Jones and Agnes Hunt Orthopaedic Hospital NHS Foundation Trust

Oswestry

SY10 7AG

Tel: 01691 404699

Email: t.hopkins@keele.ac.uk

What happens now?

You will be contacted by a member of the research team by telephone before you attend your scheduled appointment to discuss whether or not you would like to take part in this study. During this phone call you will be able to ask questions and clarify anything that you do not fully understand from the information provided. If you indicate that you do wish to take part, a member of the research team will explain the next steps at your scheduled clinical appointment. If you indicate that you do not wish to take part, you will attend your scheduled appointment as normal and the study will not be discussed with you further.

For impartial advice and support at any stage, you can contact the Patient Advice and Liaison Service (PALS). Telephone: 01691404606. Email: pal.office@rjah.nhs.uk.

Thank you for reading through the information sheet. Please do not hesitate to contact us on the above details if you require any further information or have any questions regarding the study.

Timothy Hopkins

Patient Information Sheet V1.2

6th December 2019



Ymchwil Iechyd
a Gofal Cymru
Health and Care
Research Wales



Dr Jan Herman Kuiper
Institute for Science and Technology in Medicine,
University of Keele
Arthritis Research Centre, Robert Jones and Agnes
Hunt Orthopaedic Hospital NHS Trust
Oswestry, Shropshire
SY10 7AG

Email: hra.approval@nhs.net
HCRW.approvals@wales.nhs.uk

17 February 2020

Dear Dr Kuiper

**HRA and Health and Care
Research Wales (HCRW)
Approval Letter**

Study title:	Characterising the relationship between activity level and knee function, using wearable activity trackers, in patients presenting with knee pain at the Robert Jones and Agnes Hunt Orthopaedic Hospital.
IRAS project ID:	227476
Protocol number:	RG-0281-18
REC reference:	19/SC/0518
Sponsor	Keele University

I am pleased to confirm that [HRA and Health and Care Research Wales \(HCRW\) Approval](#) has been given for the above referenced study, on the basis described in the application form, protocol, supporting documentation and any clarifications received. You should not expect to receive anything further relating to this application.

Please now work with participating NHS organisations to confirm capacity and capability, in line with the instructions provided in the "Information to support study set up" section towards the end of this letter.

How should I work with participating NHS/HSC organisations in Northern Ireland and Scotland?

HRA and HCRW Approval does not apply to NHS/HSC organisations within Northern Ireland and Scotland.

If you indicated in your IRAS form that you do have participating organisations in either of these devolved administrations, the final document set and the study wide governance report

(including this letter) have been sent to the coordinating centre of each participating nation. The relevant national coordinating function/s will contact you as appropriate.

Please see [IRAS Help](#) for information on working with NHS/HSC organisations in Northern Ireland and Scotland.

How should I work with participating non-NHS organisations?

HRA and HCRW Approval does not apply to non-NHS organisations. You should work with your non-NHS organisations to [obtain local agreement](#) in accordance with their procedures.

What are my notification responsibilities during the study?

The standard conditions document "[After Ethical Review – guidance for sponsors and investigators](#)", issued with your REC favourable opinion, gives detailed guidance on reporting expectations for studies, including:

- Registration of research
- Notifying amendments
- Notifying the end of the study

The [HRA website](#) also provides guidance on these topics, and is updated in the light of changes in reporting expectations or procedures.

Who should I contact for further information?

Please do not hesitate to contact me for assistance with this application. My contact details are below.

Your IRAS project ID is **227476**. Please quote this on all correspondence.

Yours sincerely,

Maeve Ip Groot Bluemink
Approvals Specialist

Appendix 5-3: [Health Research Authority \(HRA\) Approval letter for the ChALK study.](#)

Chapter 6:
General Discussion

6. General Discussion

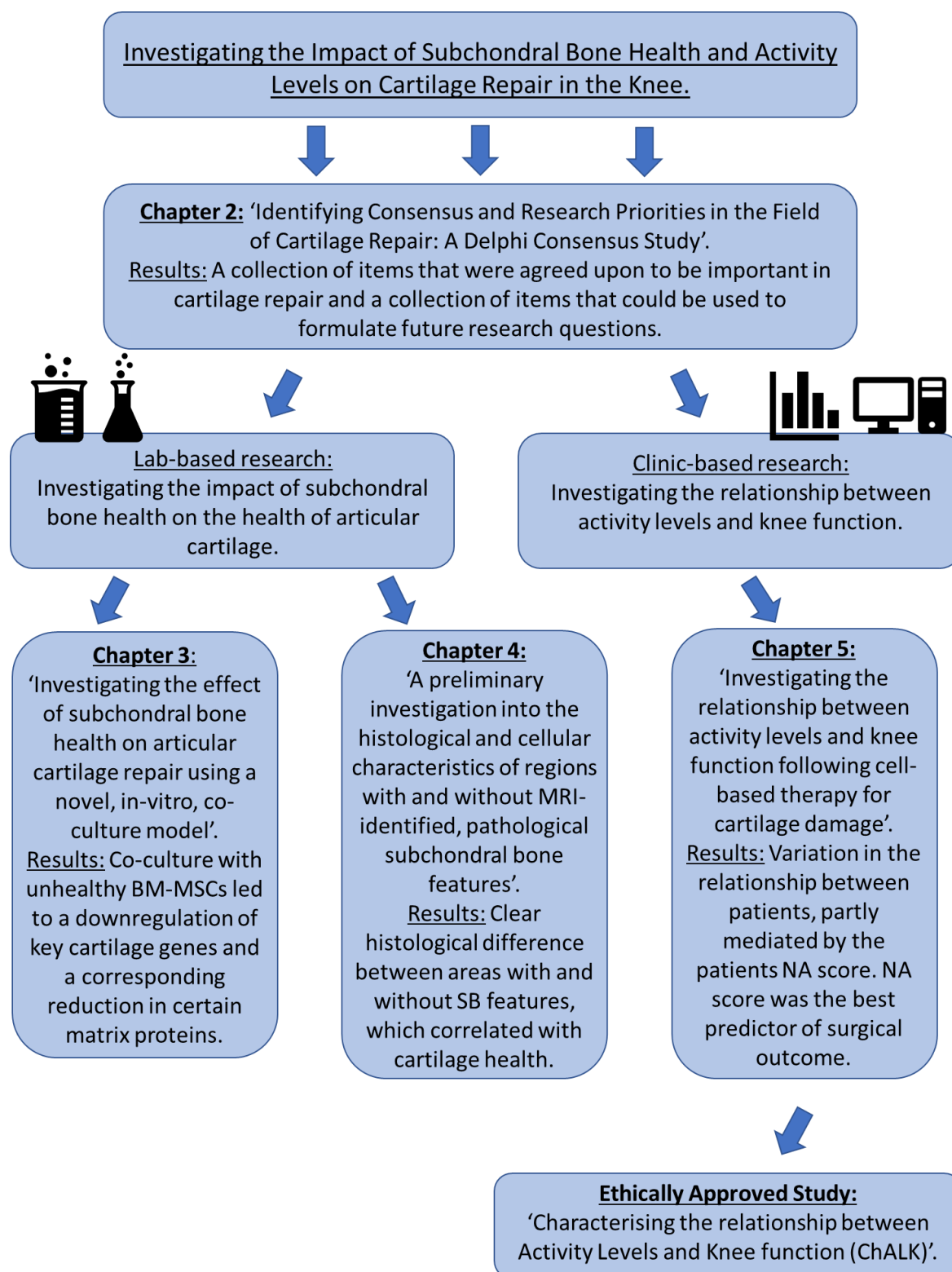


Figure 6-1: An overview of the chapters that constitute this thesis, including a brief summary of key results.

A reminder of the thesis chapters and key results is displayed in figure 6-1. This first aim of this thesis was to examine consensus and determine research priorities in the field of cartilage repair. Our results identified a number of statements that were agreed, across the board, to be important in influencing or assessing cartilage repair. A number of statements for which there was no consensus, were also identified and can be used to formulate future research questions. Items that arose from the Delphi study were implemented in the subsequent studies, reinforcing established research aims and helping to develop new ones. The Delphi panel agreed that 'It is important to assess all tissues of the joint in humans and in animal models [of cartilage repair]', that, 'It is important to assess the identity and quality of the cartilage and the bone-cartilage interface in humans and in animal models [of cartilage repair] and that the subchondral bone was second only to cartilage in terms of its importance in cartilage repair. These ideas reinforced the research hypotheses of chapter 3, in which the influence of the subchondral bone in cartilage repair was investigated. Consensus was not reached regarding the statements, 'we should measure the lacunae (cysts) in the bone', nor, 'we should measure the area of bone marrow oedema-like signal', contributing to the formation of the chapter 4 research hypotheses, in which the histological and cellular characteristics of these SB features was investigated. Finally, the Delphi panel agreed that, 'Access to specialist rehabilitation programmes would be useful for all patients, pre and post repair', and that 'Environmental factors (e.g. age, gender) are important in influencing repair'. Both of these ideas were investigated in chapter 5.

The second aim of the thesis was to examine the effect of subchondral bone health on articular cartilage repair. 'It is important to assess all tissues of the joint in humans and animal models [of cartilage repair]'. We hypothesised that any altered biochemical communication between the cells of the SB and AC, as a result of traumatic or degenerative

changes that cause AC damage, will continue to act on the implanted cells that constitute the repair cartilage. In this way, we hypothesised that the nature of the biochemical signalling and its effect on the implanted cells would differ based on the health of the SB. An in vitro co-culture system which mimicked an allogeneic chondrocyte-based cell therapy, was used to model this interaction.

Our findings demonstrate the differential effect on chondrocyte behaviour of BM-MSCs isolated from healthy and unhealthy regions of the knee. We found that co-culture with unhealthy BM-MSCs significantly altered the metabolism of the chondrocytes, leading to the downregulation of a number of genes encoding proteins of the ECM, including aggrecan and collagen type 2, and an associated decrease in the production of GAG per chondrocyte. The goal of any cell-based, tissue engineering strategy is the in-situ development of a cartilage repair tissue that closely mimics the composition and properties of the native tissue. Our results suggest that the composition, and therefore possibly the function and durability, of the repair cartilage as produced by healthy chondrocytes is influenced by biochemical signalling from cells of the subchondral bone, and that these signals vary based on the health of the subchondral bone. Therefore, subchondral bone health might be considered as an additional influencing factor for the success of AC repair.

However, unlike negative affect, for which validated score systems have been developed, identifying markers that could be used to indicate SB health and therefore be used predict the success of AC repair is difficult. Our study demonstrated that healthy and unhealthy BM-MSCs had a markedly different effect on matrix production by chondrocytes, but we did not find clear differences between the two BM-MSC groups themselves. Although we identified some minor phenotypic differences between the two groups, as well as the differential

secretion of TGF- β 1, these factors would be difficult to assess pre-operatively and therefore their utility in predicting the success of AC repair may be limited. For this reason, an additional aim of this thesis was to investigate the histological and cellular characteristics of a more clinic-friendly indicator of subchondral bone health: the presence of BMELs on MRI. While we demonstrated histological differences between areas of the SB with and without BMELs, we did not identify any differences in cellular characteristics. However, in both chapter 3 and chapter 4, a very limited panel of genes was assessed in an attempt to identify phenotypic differences between cell populations. Both studies would benefit from more widespread genetic analysis, such as DNA microarray analysis, to identify differentially expressed genes. However, such a data-driven approach was beyond the methodological remit of this thesis, which was based around pre-hypothesised proteins and genes.

Finally, this thesis aimed to characterise the relationship between activity levels and knee function in the post-operative period following cell therapy for articular cartilage lesions. Our work demonstrates, on average, a positive relationship between activity and knee function, which does however vary in magnitude and direction between patients. The Delphi study highlighted the importance of 'specialist' rehabilitation programmes, tailored specifically for cell therapies. The patients in our study, in fact, were prescribed a rehabilitation programme specifically designed for use following the cell therapy intervention, carried out as part of the ASCOT trial. While there was an overall increase in knee function scores over the course of the study, suggesting that the intervention and subsequent rehabilitation were successful, the variety between patients in the activity-knee function relationships suggests that a more individualised approach to the prescription of activity might result in improved outcomes. Our results in this section exceeded our aims. We were also able to demonstrate the powerful influence of the patients' negative affect

score, which was found to significantly correlate with the magnitude of the relationship between activity levels and knee function, suggesting the utility of this score in stratifying patients for rehabilitation. More surprising still was the finding that patients' NA scores were the best predictor of 15-month Lysholm score, the main outcome of the ASCOT trial. This was the case even when adjusted for common demographic factors and baseline scores for knee function and activity level. Based on our findings, we recommend that, at the least, NA should be included in pre-operative assessments and predictive modelling of cell therapies for AC repair, and also for tailoring rehabilitation programming in the future.

This thesis highlights that, while it is important to understand the cellular and molecular processes involved in cartilage repair, so that we can seek to influence these with external factors, it is important to remember that in complex being such as the human, the overriding and most powerful influence is often the mind.

6.1 Future Work

The results presented in this thesis contribute to the understanding of how a wide range of factors, namely subchondral bone health, activity levels and psychosocial factors, can influence the outcomes of cartilage repair. However, as is common in research studies, areas came to light which would benefit from further research. Future research that can build on the findings in this thesis includes:

- Further phenotypic characterisation of MSCs isolated from regions of more and less degenerated SB to try and identify characteristic differences between populations. This would involve the inclusion of a wider range of genes in gene expression analyses to try and identify phenotypic differences that could explain the histological differences of the tissue regions and/or the differential effect of these cells on chondrocyte behaviour in vitro. As mentioned in chapter 3, this research would particularly benefit from microarray analysis.
- Further phenotypic characterisation of osteoblasts isolated from regions of the SB with and without BMLs to try and understand the cellular factors that lead to the formation of BMLs, and how these factors may contribute to the corresponding AC degeneration. Again, this would involve the inclusion of a wider range of genes in analyses.
- Co-culture models that include additional subchondral bone cell types. Initially this should involve the osteoblasts described in chapter 3, to investigate whether those isolated from regions with BMLs will have a differential effect on chondrocyte behaviour than those isolated from regions with no BMLs. Besides investigating the relationship between BMLs and AC repair, it might also help to investigate the

relationship between BMLs and AC degeneration. Additionally, future research should consider using small pieces of SB in the form of bone chips, rather than cells proliferated in monolayer, to provide a more accurate representation of the in vivo SB in which all of the resident cells are present within the SB matrix. Future research should also consider media formulations that could support all cell types for the culture period, as well as the optimisation of protocols for standardising the co-culture between conditions without knowing bone cell numbers.

- Further characterisation of the relationship between activity levels, knee function and psychosocial factors through the execution of the ChALK study. The aim of ChALK is to characterise the relationship between activity levels and knee function in the short-term, over a period of a week, and investigate the influence of external factors, such as affect and attitude to pain, on the relationship.
- Inclusion of lesion characteristics and histological findings in the analysis of the relation between activity levels, knee function and psychosocial factors. While this thesis looked at demographic and psychosocial influences, lesion characteristics, such as size, number and location, have also been reported to influence the outcome of cartilage repair therapies and therefore should also be included in such analyses. Additionally, psychosocial factors might explain the known poor correlation between clinical and histological findings following cartilage repair.

7. References

- Abulhasan, J. & Grey, M. (2017). Anatomy and Physiology of Knee Stability. *Journal of functional morphology and kinesiology*. 2 (4): 34.
- Adler, M. & Ziglio, E. (1996). *Gazing into the Oracle: The Delphi Method and its Application to Social Policy and Public Health*. 1st edn. London, United Kingdom: Kingsley.
- Aho, O., Finnilä, M., Thevenot, J., Saarakkala, S. & Lehenkari, P. (2017). Subchondral bone histology and grading in osteoarthritis. *PLoS ONE*. 12 (3).
- Akins, R.B., Tolson, H. & Cole, B.R. (2005). Stability of response characteristics of a Delphi panel: application of bootstrap data expansion. *BMC medical research methodology*. 5 (1): 37.
- Akkiraju, H. & Nohe, A. (2015). Role of Chondrocytes in Cartilage Formation, Progression of Osteoarthritis and Cartilage Regeneration. *Journal of developmental biology*. 3 (4): 177-192.
- Albright, J.J. & Marinova, D.M. (2010). Estimating multilevel models using SPSS, Stata, SAS, and R. *Indiana University*. 1 (1): 1-35.
- Allen, R.T., Robertson, C., Pennock, A.T., Bugbee, W.D., Harwood, F.L., Wong, V.W., Chen, A.C., Sah, R.L. & Amiel, D. (2005). Analysis of Stored Osteochondral Allografts at the Time of Surgical Implantation. *The American journal of sports medicine*. 33 (10): 1479-1484.
- Almqvist, K.F., Aad A. M. Dhollander, Peter C. M. Verdonk, Ramses Forsyth, RenÅ© Verdonk & Gust Verbruggen (2009). Treatment of Cartilage Defects in the Knee Using Alginate Beads Containing Human Mature Allogenic Chondrocytes. *The American Journal of Sports Medicine*. 37 (10): 1920-1929.
- Altman, D.G. & Bland, J.M. (2005). Standard deviations and standard errors. *BMJ*. 331 (7521): 903.
- Ang, S. & O'Connor, M. (1991). The effect of group interaction processes on performance in time series extrapolation. *International Journal of Forecasting*. 7 (2): 141-149.
- Anh, D.J., Dimai, H.P., Hall, S.L. & Farley, J.R. (1998). Skeletal Alkaline Phosphatase Activity Is Primarily Released from Human Osteoblasts in an Insoluble Form, and the Net Release Is Inhibited by Calcium and Skeletal Growth Factors. *Calcified Tissue International*. 62 (4): 332-340.
- Appleton, C.T.G., Pitelka, V., Henry, J. & Beier, F. (2007). Global analyses of gene expression in early experimental osteoarthritis. *Arthritis & Rheumatism*. 56 (6): 1854-1868.
- Arkill, K.P. & Winlove, C.P. (2008). Solute transport in the deep and calcified zones of articular cartilage. *Osteoarthritis and Cartilage*. 16 (6): 708-714.

- Årøen, A., Løken, S., Heir, S., Alvik, E., Ekeland, A., Granlund, O.G. & Engebretsen, L. (2004). Articular Cartilage Lesions in 993 Consecutive Knee Arthroscopies. *The American Journal of Sports Medicine*. 32 (1): 211-215.
- Athanasίου, K.A., Darling, E.M., DuRaine, G.D., Hu, J.C. & Reddi, A.H. (2013). *Articular cartilage*. 1st edn. Boca Raton, Fla: CRC Press.
- Aulthouse, A.L., Beck, M., Griffey, E., Sanford, J., Arden, K., Machado, M.A. & Horton, W. (1989). Expression of the Human Chondrocyte Phenotype in vitro. *In Vitro Cellular & Developmental Biology*. 25 (7): 659-668.
- Bailey, A., Goodstone, N., Roberts, S., Hughes, J., Roberts, S., van Niekerk, L., Richardson, J. & Rees, D. (2003). Rehabilitation After Oswestry Autologous-Chondrocyte Implantation: The OsCell Protocol. *Journal of sport rehabilitation*. 12 (2): 104-118.
- Bancroft, J.D., Suvarna, K.S. & Layton, C. (2018). *Bancroft's theory and practice of histological techniques*. Elsevier.
- Bastian, J.D., Egli, R.J., Ganz, R., Hofstetter, W. & Leunig, M. (2011). Chondrocytes within Osteochondral Grafts Are More Resistant than Osteoblasts to Tissue Culture at 37°C. *Journal of investigative surgery*. 24 (1): 28-34.
- Behrens, P. (2005). Matrixgekoppelte Mikrofrakturierung. *Arthroscopie*. 18 (3): 193-197.
- Behrens, P., Bitter, T., Kurz, B. & Russlies, M. (2006). Matrix-associated autologous chondrocyte transplantation/implantation (MACT/MACI)—5-year follow-up. *The knee*. 13 (3): 194-202.
- Bekkers, J.E.J., Inklaar, M. & Saris, D.B.F. (2009). Treatment Selection in Articular Cartilage Lesions of the Knee. *The American Journal of Sports Medicine*. 37 (1): 148-155.
- Bennell, K.L., Hinman, R.S., Crossley, K.M., Metcalf, B.R., Buchbinder, R., Green, S. & McColl, G. (2004). Is the Human Activity Profile a useful measure in people with knee osteoarthritis? *Journal of rehabilitation research and development*. 41 (4): 621.
- Benthien, J.P. & Behrens, P. (2013). Reviewing subchondral cartilage surgery: considerations for standardised and outcome predictable cartilage remodelling: a technical note. *International orthopaedics*. 37 (11): 2139-2145.
- Benthien, J.P. & Behrens, P. (2010). Autologous Matrix-Induced Chondrogenesis (AMIC). *Cartilage*. 1 (1): 65-68.
- Bhosale, A.M. & Richardson, J.B. (2008). Articular cartilage: structure, injuries and review of management. *British Medical Bulletin*. 87 (1): 77-95.
- Bian, L., Zhai, D.Y., Mauck, R.L. & Burdick, J.A. (2011). Coculture of Human Mesenchymal Stem Cells and Articular Chondrocytes Reduces Hypertrophy and Enhances Functional Properties of Engineered Cartilage. *Tissue Engineering*. 17 (7-8): 1137-1145.

Blaney Davidson, E.N., van der Kraan, P. M & van den Berg, W. B (2007). TGF- β and osteoarthritis. *Osteoarthritis and Cartilage*. 15 : 597-604.

Blaney Davidson, E.N., Vitters, E.L., van den Berg, W. B & van der Kraan, P. M (2006). TGF β -induced cartilage repair is maintained but fibrosis is blocked in the presence of Smad7. *Arthritis research & therapy*. 8 (3): 65.

Bougault, C., Paumier, A., Aubert-Foucher, E. & Mallein-Gerin, F. (2008). Molecular analysis of chondrocytes cultured in agarose in response to dynamic compression. *BMC biotechnology*. 8 (1): 71.

Boulkedid, R., Abdoul, H., Loustau, M., Sibony, O. & Alberti, C. (2011). Using and Reporting the Delphi Method for Selecting Healthcare Quality Indicators: A Systematic Review. *PLoS one*. 6 (6): 20476.

Bourin, P., Bunnell, B.A., Casteilla, L., Dominici, M., Katz, A.J., March, K.L., Redl, H., Rubin, J.P., Yoshimura, K. & Gimble, J.M. (2013). Stromal cells from the adipose tissue-derived stromal vascular fraction and culture expanded adipose tissue-derived stromal/stem cells: a joint statement of the International Federation for Adipose Therapeutics and Science (IFATS) and the International Society for Cellular Therapy (ISCT). *Cytotherapy (Oxford, England)*. 15 (6): 641-648.

Boushell, M.K., Hung, C.T., Hunziker, E.B., Strauss, E.J. & Lu, H.H. (2017). Current strategies for integrative cartilage repair. *Connective Tissue Research*. 58 (5): 393-406.

Brandt, K.D., Radin, E.L., Dieppe, P.A. & van de Putte, L. (2006). Yet more evidence that osteoarthritis is not a cartilage disease. *Annals of the rheumatic diseases*. 65 (10): 1261-1264.

Breeland, G., Sinkler., M.A. & Menezes, R.G. (2020). *Embryology, Bone Ossification*. 1st edn. Florida, USA: StatPearls Publishing.

Brew, C.J., Clegg, P.D., Boot-Handford, R.P., Andrew, J.G. & Hardingham, T. (2010). Gene expression in human chondrocytes in late osteoarthritis is changed in both fibrillated and intact cartilage without evidence of generalised chondrocyte hypertrophy. *Annals of the Rheumatic Diseases*. 69 (1): 234-240.

Brittberg, M., Lindahl, A., Nilsson, A., Ohlsson, C., Isaksson, O. & Peterson, L. (1994). Treatment of deep cartilage defects in the knee with autologous chondrocyte transplantation. *The New England Journal of Medicine*. 331 (14): 889-895.

Brittberg, M., Aglietti, P., Gambardella, R., Hangody, L., Hauselmann, H.J., Jakob, R.P., Levine, D., Lohmander, S., Mandelbaum, B.R., Peterson, L. & Staubli, H. (2000). https://cartilage.org/content/uploads/2014/10/ICRS_evaluation.pdf. Available from: https://cartilage.org/content/uploads/2014/10/ICRS_evaluation.pdf. [Accessed: January 2019].

Brittberg, M. et al. (2016). *Cartilage repair in the degenerative ageing knee*. vol. 87. England: Taylor & Francis.

Browne, J.E. & Branch, T.P. (2000). Surgical Alternatives for Treatment of Articular Cartilage Lesions. *Journal of the American Academy of Orthopaedic Surgeons*. 8 (3): 180-189.

Buckwalter, J.A., Mankin, H.J. & Grodzinsky, A.J. (2005). Articular cartilage and osteoarthritis. *Instructional course lectures*. 54 : 465.

Bugbee, W.D., Pallante-Kichura, A.L., Görtz, S., Amiel, D. & Sah, R. (2016). Osteochondral allograft transplantation in cartilage repair: Graft storage paradigm, translational models, and clinical applications. *Journal of orthopaedic research*. 34 (1): 31-38.

Burr, D.B. & Gallant, M.A. (2012). Bone remodelling in osteoarthritis. *Nature reviews Rheumatology*. 8 (11): 665-673.

Burr, D.B. & Radin, E.L. (2003). Microfractures and microcracks in subchondral bone: are they relevant to osteoarthrosis? *Rheumatic Disease Clinics of North America*. 29 (4): 675-685.

Buschmann, M.D., Gluzband, Y.A., Grodzinsky, A.J. & Hunziker, E.B. (1995). Mechanical compression modulates matrix biosynthesis in chondrocyte/agarose culture. *Journal of Cell Science*. 108 (4): 1497-1508.

Buschmann, M.D., Gluzband, Y.A., Grodzinsky, A.J., Kimura, J.H. & Hunziker, E.B. (1992). Chondrocytes in agarose culture synthesize a mechanically functional extracellular matrix. *Journal of orthopaedic research : official publication of the Orthopaedic Research Society*. 10 (6): 745-758.

Camp, C.L., Stuart, M.J. & Krych, A.J. (2014). Current Concepts of Articular Cartilage Restoration Techniques in the Knee. *Sports Health: A Multidisciplinary Approach*. 6 (3): 265-273.

Campbell, T.M., Churchman, S.M., Gomez, A., McGonagle, D., Conaghan, P.G., Ponchel, F. & Jones, E. (2016). Mesenchymal Stem Cell Alterations in Bone Marrow Lesions in Patients With Hip Osteoarthritis. *Arthritis & Rheumatology*. 68 (7): 1648-1659.

Cao, J.J. (2011). Effects of obesity on bone metabolism. *Journal of orthopaedic surgery and research*. 6 (1): 30.

Carels, R.A., Coit, C., Young, K. & Berger, B. (2007). Exercise Makes You Feel Good, But Does Feeling Good Make You Exercise?: An Examination of Obese Dieters. *Journal of sport & exercise psychology*. 29 (6): 706-722.

Caron, M.M.J., Emans, P.J., Coolen, M.M.E., Voss, L., Surtel, D.A.M., Cremers, A., van Rhijn, L.W. & Welting, T.J.M. (2012). Redifferentiation of dedifferentiated human articular chondrocytes: comparison of 2D and 3D cultures. *Osteoarthritis and Cartilage*. 20 (10): 1170-1178.

Carrino, J.A., Blum, J., Parellada, J.A., Schweitzer, M.E. & Morrison, W.B. (2006). MRI of bone marrow edema-like signal in the pathogenesis of subchondral cysts. *Osteoarthritis and Cartilage*. 14 (10): 1081-1085.

Castañeda, S., Roman-Blas, J.A., Largo, R. & Herrero-Beaumont, G. (2012). Subchondral bone as a key target for osteoarthritis treatment. *Biochemical Pharmacology*. 83 (3): 315-323.

Chen, H., Hoemann, C.D., Sun, J., Chevrier, A., McKee, M.D., Shive, M.S., Hurtig, M. & Buschmann, M.D. (2011). Depth of subchondral perforation influences the outcome of bone marrow stimulation cartilage repair. *Journal of orthopaedic research*. 29 (8): 1178-1184.

Chen, H., Sun, J., Hoemann, C.D., Lascau-Coman, V., O, W., McKee, M.D., Shive, M.S. & Buschmann, M.D. (2009). Drilling and microfracture lead to different bone structure and necrosis during bone-marrow stimulation for cartilage repair. *Journal of orthopaedic research*. 27 (11): 1432-1438.

Chen, Y., Wang, T., Guan, M., Guo, X.E., Zhao, W., Leung, F., Cao, X. & Lu, W. (2015). Subchondral bone cysts complicated with bone remodeling turnovers in patients with knee osteoarthritis. *Osteoarthritis and Cartilage*. 23 : 128-130.

Chevalier, X. (1993). Fibronectin, cartilage, and osteoarthritis. *Seminars in Arthritis and Rheumatism*. 22 (5): 307-318.

Chmielewski, T.L., Giorgio Zeppieri Jr, Trevor A. Lentz, Susan M. Tillman, Michael W. Moser, Peter A. Indelicato & Steven Z. George (2011). Longitudinal Changes in Psychosocial Factors and Their Association With Knee Pain and Function After Anterior Cruciate Ligament Reconstruction. *Physical Therapy*. 91 (9): 1355-1366.

Chmielewski, T.L., Jones, D., Day, T., Tillman, S.M., Lentz, T.A. & George, S.Z. (2008). The Association of Pain and Fear of Movement/Reinjury With Function During Anterior Cruciate Ligament Reconstruction Rehabilitation. *The journal of orthopaedic and sports physical therapy*. 38 (12): 746-753.

Cho, J., Kim, T., Park, Y., Shin, J., Kang, S. & Lee, B. (2016). Invossa™(Tissuegene-C) in patients with osteoarthritis: A phase III trial. *Osteoarthritis and Cartilage*. 24 : 190.

Chubinskaya, S., Haudenschild, D., Gasser, S., Stannard, J., Krettek, C. & Borrelli, J. (2015). Articular Cartilage Injury and Potential Remedies. *Journal of Orthopaedic Trauma*. 29 Suppl 12 (Suppl 12): 47-52.

Cicchetti, D., Bronen, R., Spencer, S., Haut, S., Berg, A., Oliver, P. & Tyrer, P. (2006). Rating Scales, Scales of Measurement, Issues of Reliability: Resolving Some Critical Issues for Clinicians and Researchers. *The journal of nervous and mental disease*. 194 (8): 557-564.

Cicutini, F., Ding, C., Wluka, A., Davis, S., Ebeling, P.R. & Jones, G. (2005). Association of cartilage defects with loss of knee cartilage in healthy, middle-age adults: A prospective study. *Arthritis and rheumatism*. 52 (7): 2033-2039.

Clair, B., Johnson, A. & Howard, T. (2009). Cartilage Repair: Current and Emerging Options in Treatment. *Foot & Ankle Specialist*. 2 (4): 179-188.

Clark, J.M. & Huber, J.D. (1990). The structure of the human subchondral plate. *The Journal of bone and joint surgery. British volume*. 72 (5): 866-873.

Clarke, B. (2008). Normal Bone Anatomy and Physiology. *Clinical journal of the American Society of Nephrology*. 3 (Supplement 3): 131-139.

Coe, M.R., Summers, T.A., Parsons, S.J., Boskey, A.L. & Balian, G. (1992). Matrix mineralization in hypertrophic chondrocyte cultures. Beta glycerophosphate increases type X collagen messenger RNA and the specific activity of pp60c-src kinase. *Bone and mineral*. 18 (2): 91.

Cohen, N.P., Foster, R.J. & Mow, V.C. (1998). Composition and Dynamics of Articular Cartilage: Structure, Function, and Maintaining Healthy State. *The journal of orthopaedic and sports physical therapy*. 28 (4): 203-215.

Collins, N.J., Misra, D., Felson, D.T., Crossley, K.M. & Roos, E.M. (2011). Measures of knee function: International Knee Documentation Committee (IKDC) Subjective Knee Evaluation Form, Knee Injury and Osteoarthritis Outcome Score (KOOS), Knee Injury and Osteoarthritis Outcome Score Physical Function Short Form (KOOS-PS), Knee Outcome Survey Activities of Daily Living Scale (KOS-ADL), Lysholm Knee Scoring Scale, Oxford Knee Score (OKS), Western Ontario and McMaster Universities Osteoarthritis Index (WOMAC), Activity Rating Scale (ARS), and Tegner Activity Score (TAS). *Arthritis Care & Research*. 63 (S11): 208-228.

Cook, J.L., Stannard, J.P., Stoker, A.M., Bozynski, C.C., Kuroki, K., Cook, C.R. & Pfeiffer, F.M. (2016). Importance of Donor Chondrocyte Viability for Osteochondral Allografts. *The American journal of sports medicine*. 44 (5): 1260-1268.

Cooke, M.E., Allon, A.A., Cheng, T., Kuo, A.C., Kim, H.T., Vail, T.P., Marcucio, R.S., Schneider, R.A., Lotz, J.C. & Alliston, T. (2011). Structured three-dimensional co-culture of mesenchymal stem cells with chondrocytes promotes chondrogenic differentiation without hypertrophy. *Osteoarthritis and Cartilage*. 19 (10): 1210-1218.

Crema, M.D., Roemer, F.W., Zhu, Y., Marra, M.D., Niu, J., Zhang, Y., Lynch, J.A., Javaid, M.K., Lewis, C.E., El-Khoury, G.Y., Felson, D.T. & Guermazi, A. (2010). Subchondral Cystlike Lesions Develop Longitudinally in Areas of Bone Marrow Edema-like Lesions in Patients with or at Risk for Knee Osteoarthritis: Detection with MR Imaging—The MOST Study. *Radiology*. 256 (3): 855-862.

Culvenor, A.G., Øiestad, B.E., Hart, H.F., Stefanik, J.J., Guermazi, A. & Crossley, K.M. (2018). Prevalence of knee osteoarthritis features on magnetic resonance imaging in asymptomatic uninjured adults: A systematic review and meta-analysis. 53 (20): 1268-1278.

Curl, W.W., Krome, J., Gordon, E.S., Rushing, J., Smith, B.P. & Poehling, G.G. (1997). Cartilage injuries: a review of 31,516 knee arthroscopies. *Arthroscopy: The Journal of Arthroscopic &*

Related Surgery: Official Publication of the Arthroscopy Association of North America and the International Arthroscopy Association. 13 (4): 456-460.

D'Anchise, R., Manta, N., Prospero, E., Bevilacqua, C. & Gigante, A. (2005). Autologous implantation of chondrocytes on a solid collagen scaffold: clinical and histological outcomes after two years of follow-up. *Journal of Orthopaedics and Traumatology.* 6 (1): 36-43.

da Silva Meirelles, L., Caplan, A.I. & Nardi, N.B. (2008). In Search of the In Vivo Identity of Mesenchymal Stem Cells. *Stem cells (Dayton, Ohio).* 26 (9): 2287-2299.

Dalkey, N. & Helmer, O. (1963). An Experimental Application of the DELPHI Method to the Use of Experts. *Management Science.* 9 (3): 458-467.

Dalkey, N.C. (1969). *The Delphi Method: An Experimental Study of Group Opinion.* Santa Monica, CA: RAND Corporation.

Daughton, D.M., Fix, A.J., Kass, I., Bell, C.W. & Patil, K.D. (1982). Maximum oxygen consumption and the ADAPT quality-of-life scale. *Archives of physical medicine and rehabilitation.* 63 (12): 620.

David T. Felson, Sara McLaughlin, Joyce Goggins, Michael P. LaValley, M. Elon Gale, Saara Totterman, Wei Li, Catherine Hill & Daniel Gale (2003). Bone Marrow Edema and Its Relation to Progression of Knee Osteoarthritis. *Annals of Internal Medicine.* 139 (5 Part 1): 330.

Davidson, M. & de Morton, N. (2007). A systematic review of the Human Activity Profile. *Clinical Rehabilitation.* 21 (2): 151-162.

Davies-Tuck, M.L., Wluka, A.E., Wang, Y., Teichtahl, A.J., Jones, G., Ding, C. & Cicuttini, F.M. (2008). The natural history of cartilage defects in people with knee osteoarthritis. *Osteoarthritis and Cartilage.* 16 (3): 337-342.

Davies-Tuck, M.L., Wluka, A.E., Forbes, A., Wang, Y., English, D.R., Giles, G.G., O'Sullivan, R. & Cicuttini, F.M. (2010). Development of bone marrow lesions is associated with adverse effects on knee cartilage while resolution is associated with improvement - a potential target for prevention of knee osteoarthritis: a longitudinal study. *Arthritis research & therapy.* 12 (1): 10.

de Windt, T.S., Bekkers, J.E.J., Creemers, L.B., Dhert, W.J.A. & Saris, D.B.F. (2009). Patient Profiling in Cartilage Regeneration: Prognostic Factors Determining Success of Treatment for Cartilage Defects. *The American journal of sports medicine.* 37 (1_suppl): 58-62.

de Windt, T.S., Concaro, S., Lindahl, A., Saris, D.B.F. & Brittberg, M. (2012). Strategies for patient profiling in articular cartilage repair of the knee: A prospective cohort of patients treated by one experienced cartilage surgeon. *Knee surgery, sports traumatology, arthroscopy : official journal of the ESSKA.* 20 (11): 2225-2232.

Decker, R.S., Koyama, E. & Pacifici, M. (2015). Articular Cartilage: Structural and Developmental Intricacies and Questions. *Current osteoporosis reports.* 13 (6): 407-414.

DeKosky, B.J., Dormer, N.H., Ingavle, G.C., Roatch, C.H., Lomakin, J., Detamore, M.S. & Gehrke, S.H. (2010). Hierarchically Designed Agarose and Poly(Ethylene Glycol) Interpenetrating Network Hydrogels for Cartilage Tissue Engineering. *Tissue engineering. Part C, Methods*. 16 (6): 1533-1542.

Deszczynski, J. & Slynarski, K. (2006). Rehabilitation After Cell Transplantation for Cartilage Defects. *Transplantation Proceedings*. 38 (1): 314-315.

Ding, C., Cicuttini, F., Scott, F., Cooley, H., Boon, C. & Jones, G. (2006). Natural History of Knee Cartilage Defects and Factors Affecting Change. *Archives of Internal Medicine*. 166 (6): 651-658.

Ding, C., Garner, P., Cicuttini, F., Scott, F., Cooley, H. & Jones, G. (2005). Knee cartilage defects: association with early radiographic osteoarthritis, decreased cartilage volume, increased joint surface area and type II collagen breakdown. *Osteoarthritis and Cartilage*. 13 (3): 198-205.

Dolzani, P., Assirelli, E., Pulsatelli, L., Meliconi, R., Mariani, E. & Neri, S. (2019). Ex vivo physiological compression of human osteoarthritis cartilage modulates cellular and matrix components. *PloS one*. 14 (9): e0222947.

Dominici, M., Le Blanc, K., Mueller, I., Slaper-Cortenbach, I., Marini, F.C., Krause, D.S., Deans, R.J., Keating, A., Prockop, D.J. & Horwitz, E.M. (2006). Minimal criteria for defining multipotent mesenchymal stromal cells. The International Society for Cellular Therapy position statement. *Cytotherapy*. 8 (4): 315-317.

Donell, S. (2019). Subchondral bone remodelling in osteoarthritis. *EFORT open reviews*. 4 (6): 221-229.

Dreier, R. (2010). Hypertrophic differentiation of chondrocytes in osteoarthritis: the developmental aspect of degenerative joint disorders. *Arthritis research & therapy*. 12 (5): 216.

Duff, K. (2012). Evidence-Based Indicators of Neuropsychological Change in the Individual Patient: Relevant Concepts and Methods. *Archives of clinical neuropsychology*. 27 (3): 248-261.

Dugard, M.N., Kuiper, J.H., Parker, J., Roberts, S., Robinson, E., Harrison, P. & Richardson, J.B. (2017). Development of a Tool to Predict Outcome of Autologous Chondrocyte Implantation. *Cartilage*. 8 (2): 119-130.

Duncan, H., Jundt, J., Riddle, J., Pitchford, W. & Christopherson, T. (1987). The tibial subchondral plate. A scanning electron microscopic study. *The Journal of Bone & Joint Surgery*. 69 (8): 1212-1220.

Dunton, G.F., Huh, J., Leventhal, A.M., Riggs, N., Hedeker, D., Spruijt-Metz, D. & Pentz, M.A. (2014). Momentary assessment of affect, physical feeling states, and physical activity in children. *Health psychology*. 33 (3): 255-263.

Dunton, G., Atienza, A., Castro, C. & King, A. (2009). Using Ecological Momentary Assessment to Examine Antecedents and Correlates of Physical Activity Bouts in Adults Age 50+ Years: A Pilot Study. *Annals of Behavioral Medicine*. 38 (3): 249-255.

ECACC & Merck (2018). *Fundamental Techniques in Cell Culture. Laboratory Handbook. Fundamental Techniques in Cell Culture* 4th edn. Darmstadt, Germany: Public Health England.

Elkins, R.K. (2017). The stability of personality traits in adolescence and young adulthood. *Journal of economic psychology*. 60 : 37-52.

Eric G. Meyer, Timothy G. Baumer, Jill M. Slade, Walter E. Smith & Roger C. Haut (2008). Tibiofemoral Contact Pressures and Osteochondral Microtrauma During Anterior Cruciate Ligament Rupture Due to Excessive Compressive Loading and Internal Torque of the Human Knee. *The American Journal of Sports Medicine*. 36 (10): 1966-1977.

Eriksen, E.F. (2015). Treatment of bone marrow lesions (bone marrow edema). *BoneKEY reports*. 4 : 755.

Estes, B.T. & Guilak, F. (2011). Three-dimensional culture systems to induce chondrogenesis of adipose-derived stem cells. *Methods in molecular biology (Clifton, N.J.)*. 702 : 201-217.

Everts, V., Delaissé, J.M., Korper, W., Jansen, D.C., Tigchelaar-Gutter, W., Saftig, P. & Beertsen, W. (2002). The Bone Lining Cell: Its Role in Cleaning Howship's Lacunae and Initiating Bone Formation. *Journal of bone and mineral research*. 17 (1): 77-90.

Eyre, D.R., Weis, M.A. & Wu, J. (2006). Articular cartilage collagen: an irreplaceable framework? *European cells & materials*. 12 : 57-63.

Eyre, D. (2001). Articular cartilage and changes in arthritis: collagen of articular cartilage. *Arthritis Research*. 4 (1): 30-35.

Falah, M., Nierenberg, G., Soudry, M., Hayden, M. & Volpin, G. (2010). Treatment of articular cartilage lesions of the knee. *International orthopaedics*. 34 (5): 621-630.

Farndale, R.W., Sayers, C.A. & Barrett, A.J. (1982). A Direct Spectrophotometric Microassay for Sulfated Glycosaminoglycans in Cartilage Cultures. *Connective Tissue Research*. 9 (4): 247-248.

Farndale, R.W., Buttle, D.J. & Barrett, A.J. (1986). Improved quantitation and discrimination of sulphated glycosaminoglycans by use of dimethylmethylene blue. *BBA - General Subjects*. 883 (2): 173-177.

Faul, F., Erdfelder, E., Lang, A. & Buchner, A. (2007). GPower 3: A flexible statistical power analysis program for the social, behavioral, and biomedical sciences. *Behavior research methods*. 39 (2): 175-191.

- Feldman, A.T. & Wolfe, D. (2014). Tissue processing and hematoxylin and eosin staining. *Methods in molecular biology (Clifton, N.J.)*. 1180 : 31-43.
- Felson, D.T. (2009). Arthroscopy as a treatment for knee osteoarthritis. *Best Practice & Research: Clinical Rheumatology*. 24 (1): 47-50.
- Fenwick, S.A., Gregg, P.J. & Rooney, P. (1999). Osteoarthritic cartilage loses its ability to remain avascular. *Osteoarthritis and Cartilage*. 7 (5): 441-452.
- Finan, P.H., Quartana, P.J. & Smith, M.T. (2013). Positive and negative affect dimensions in chronic knee osteoarthritis: effects on clinical and laboratory pain. *Psychosomatic medicine*. 75 (5): 463-470.
- Findlay, D.M. & Kuliwaba, J.S. (2016). Bone–cartilage crosstalk: a conversation for understanding osteoarthritis. *Bone research*. 4 (1): 16028.
- Findlay, D. & Atkins, G. (2014). Osteoblast-Chondrocyte Interactions in Osteoarthritis. *Current Osteoporosis Reports*. 12 (1): 127-134.
- Finnilä, M.A.J., Thevenot, J., Aho, O., Tiitu, V., Rautiainen, J., Kauppinen, S., Nieminen, M.T., Pritzker, K., Valkealahti, M., Lehenkari, P. & Saarakkala, S. (2017). Association between subchondral bone structure and osteoarthritis histopathological grade. *Journal of orthopaedic research*. 35 (4): 785-792.
- Florencio-Silva, R., Sasso, Gisela Rodrigues da Silva, Sasso-Cerri, E., Simões, M.J. & Cerri, P.S. (2015). Biology of Bone Tissue: Structure, Function, and Factors That Influence Bone Cells. *BioMed research international*. 2015 : 1-17.
- Fox, A.J.S., Bedi, A. & Rodeo, S.A. (2009). The Basic Science of Articular Cartilage: Structure, Composition, and Function. *Sports Health*. 1 (6): 461-468.
- Fox, J. & Weisberg, S. (2018). *car: Companion to Applied Regression [R package]*. Available from: <https://cran.r-project.org/web/packages/car/index.html>. [Accessed: March 2020].
- Franz-Odendaal, T.A., Hall, B.K. & Witten, P.E. (2006). Buried alive: How osteoblasts become osteocytes. *Developmental dynamics*. 235 (1): 176-190.
- Shen, G. (2005). The role of type X collagen in facilitating and regulating endochondral ossification of articular cartilage. *Clinical Orthodontics and Research*. 8 (1): 11-17.
- Gallucci, M. (2019). *GAMj: General Analyses for Linear Models [jamovi module]*. Available from: gamlj.github.io. [Accessed: April 2020].
- Garcia, J. (2016). *An in vitro study of the chondrogenic and immunomodulatory properties of mesenchymal stem cells from the osteoarthritic joint*. Keele University, Staffordshire: .

- Garcia, J., Mennan, C., McCarthy, H.S., Roberts, S., Richardson, J.B. & Wright, K.T. (2016). Chondrogenic Potency Analyses of Donor-Matched Chondrocytes and Mesenchymal Stem Cells Derived from Bone Marrow, Infrapatellar Fat Pad, and Subcutaneous Fat. *Stem cells international*. 2016 : 6969726-11.
- Garnero, P., Peterfy, C., Zaim, S. & Schoenharting, M. (2005). Bone marrow abnormalities on magnetic resonance imaging are associated with type II collagen degradation in knee osteoarthritis: A three-month longitudinal study. *Arthritis and rheumatism*. 52 (9): 2822-2829.
- Garrity, J.T., Stoker, A.M., Sims, H.J. & Cook, J.L. (2012). Improved Osteochondral Allograft Preservation Using Serum-Free Media at Body Temperature. *The American journal of sports medicine*. 40 (11): 2542-2548.
- Gelman, A., Hill, J., Alvarez, R.M., Beck, N.L. & Wu, L.L. (2006). *Data Analysis Using Regression and Multilevel/Hierarchical Models*. Analytical methods for social research Cambridge: Cambridge University Press.
- George, S.Z., Lentz, T.A., Zeppieri, G., Lee, D. & Chmielewski, T.L. (2012). Analysis of shortened versions of the Tampa Scale for Kinesiophobia and Pain Catastrophizing Scale for patients following anterior cruciate ligament reconstruction. *The Clinical journal of pain*. 28 (1): 73-80.
- Gilbert, S.F. (2000). *Developmental Biology*. 6th edn. Massachusetts, USA: Sinauer Associates.
- Gobbi, A. & Francisco, R. (2006). Factors affecting return to sports after anterior cruciate ligament reconstruction with patellar tendon and hamstring graft: a prospective clinical investigation. *Knee surgery, sports traumatology, arthroscopy : official journal of the ESSKA*. 14 (10): 1021-1028.
- Goldring, M.B. (2012). Chondrogenesis, chondrocyte differentiation, and articular cartilage metabolism in health and osteoarthritis. *Therapeutic Advances in Musculoskeletal Disease*. 4 (4): 269-285.
- Goldring, M.B., Tsuchimochi, K. & Ijiri, K. (2006). The control of chondrogenesis. *Journal of cellular biochemistry*. 97 (1): 33-44.
- Goldring, S.R. (2012). Alterations in periarticular bone and cross talk between subchondral bone and articular cartilage in osteoarthritis. *Therapeutic Advances in Musculoskeletal Disease*. 4 (4): 249-258.
- Goldring, S.R. & Goldring, M.B. (2016). Changes in the osteochondral unit during osteoarthritis: structure, function and cartilage–bone crosstalk. *Nature reviews Rheumatology*. 12 (11): 632-644.
- Gomoll, A.H., Madry, H., Knutsen, G., van Dijk, N., Seil, R., Brittberg, M. & Kon, E. (2010). The subchondral bone in articular cartilage repair: current problems in the surgical

management. *Knee surgery, sports traumatology, arthroscopy : official journal of the ESSKA*. 18 (4): 434-447.

Gomoll, A.H., Yoshioka, H., Watanabe, A., Dunn, J.C. & Minas, T. (2011). Preoperative Measurement of Cartilage Defects by MRI Underestimates Lesion Size. *Cartilage*. 2 (4): 389-393.

Görtz, S. & Bugbee, W.D. (2006). Allografts in Articular Cartilage Repair. *Journal of bone and joint surgery. American volume*. 88 (6): 1374-1384.

Grässel, S. & Muschter, D. (2020). Recent advances in the treatment of osteoarthritis . *F1000Research*. 9 : 325.

Grau-Vorster, M., Laitinen, A., Nystedt, J. & Vives, J. (2019). HLA-DR expression in clinical-grade bone marrow-derived multipotent mesenchymal stromal cells: a two-site study. *Stem cell research & therapy*. 10 (1): 164.

Grau-Vorster, M., Rodriguez, L., Torrents-Zapata, S., Vivas, D., Condinach, M., Blanco, M., Oliver-Vila, I., Garcia-Lopez, J. & Vives, J. (2018). Levels of IL-17F and IL-33 correlate with HLA-DR activation in clinical-grade human bone marrow-derived multipotent mesenchymal stromal cell expansion cultures. *Cytotherapy (Oxford, England)*. 21 (1): 32-40.

Green, P., MacLeod, C.J. & Nakagawa, S. (2016). SIMR: an R package for power analysis of generalized linear mixed models by simulation. *Methods in ecology and evolution*. 7 (4): 493-498.

Grogan, S.P., Barbero, A., Winkelmann, V., Rieser, F., Fitzsimmons, J.S., O'Driscoll, S., Martin, I. & Mainil-Varlet, P. (2006). Visual Histological Grading System for the Evaluation of in Vitro-Generated Neocartilage. *Tissue engineering*. 12 (8): 2141-2149.

Gross, A.E., Kim, W., Las Heras, F., Backstein, D., Safir, O. & Pritzker, K.P.H. (2008). Fresh Osteochondral Allografts for Posttraumatic Knee Defects: Long-term Followup. *Clinical orthopaedics and related research*. 466 (8): 1863-1870.

Gudas, R., Kalesinskas, R.J., Kimtys, V., Stankevičius, E., Toliušis, V., Bernotavičius, G. & Smailys, A. (2005). A Prospective Randomized Clinical Study of Mosaic Osteochondral Autologous Transplantation Versus Microfracture for the Treatment of Osteochondral Defects in the Knee Joint in Young Athletes. *Arthroscopy*. 21 (9): 1066-1075.

Guermazi, A., Hayashi, D., Roemer, F.W., Niu, J., Quinn, E.K., Crema, M.D., Nevitt, M.C., Torner, J., Lewis, C.E. & Felson, D.T. (2017). Partial- and Full-thickness focal cartilage defects equally contribute to development of new cartilage damage in knee osteoarthritis - the Multicenter Osteoarthritis Study. *Arthritis & rheumatology (Hoboken, N.J.)*. 69 (3): 560-564.

Guilak, F., Alexopolous, L., Upton, M.L., Youn, I., Jae Bong Choi, Cao, L., Setton, L. & Haider, M.A. (2006). The pericellular matrix as a transducer of biomechanical and biochemical signals in articular cartilage. *Annals of the New York Academy of Sciences*. 1068 : 498-512.

- Habibi, A., Sarafrazi, A. & Izadyar, S. (2014). Delphi Technique Theoretical Framework in Qualitative Research. *International Journal of Engineering Science*. 3 (4): 8-13.
- Hambly, K., Silvers, H.J. & Steinwachs, M. (2012). Rehabilitation after Articular Cartilage Repair of the Knee in the Football (Soccer) Player. *Cartilage*. 3 (1_suppl): 50S-56S.
- Hangody, L., Kish, G. & Karpati, Z. (2010). Osteochondral plugs: autogenous osteochondral mosaicoplasty for the treatment of focal chondral and osteochondral articular defects. . *International Orthopaedics*. 34 (5): 621-630.
- Hantes, M.E. & Fylos, A.H. (2018). *Management of Knee Cartilage Defects with the Autologous Matrix-Induced Chondrogenesis (AMIC) Technique*. InTech Open.
- Hardingham, T.E. & Fosang, A.J. (1992). Proteoglycans: many forms and many functions. *The FASEB journal*. 6 (3): 861-870.
- Harris, J.D., Brophy, R.H., Siston, R.A. & Flanigan, D.C. (2010). Treatment of Chondral Defects in the Athlete's Knee. *Arthroscopy: The Journal of Arthroscopic and Related Surgery*. 26 (6): 841-852.
- Heidari, B. (2011). Knee osteoarthritis prevalence, risk factors, pathogenesis and features: Part I. *Caspian Journal of Internal Medicine*. 2 (2): 205-212.
- Helfrich, M.H. & Ralston, S. (2012). *Bone research protocols*. Methods in molecular biology vol. 816. Second edition. edn. New York, NY: Humana Press.
- Henrotin, Y., Pesesse, L. & Sanchez, C. (2012). Subchondral bone and osteoarthritis: biological and cellular aspects. *Osteoporosis International*. 23 (S8): 847-851.
- Hernigou, P., Delambre, J., Quiennec, S. & Poignard, A. (2020a). Human bone marrow mesenchymal stem cell injection in subchondral lesions of knee osteoarthritis: a prospective randomized study versus contralateral arthroplasty at a mean fifteen year follow-up. *International orthopaedics*. 45 (2): 365-373.
- Hernigou, P., Bouthors, C., Bastard, C., Flouzat Lachaniette, C., Rouard, H. & Dubory, A. (2020b). Subchondral bone or intra-articular injection of bone marrow concentrate mesenchymal stem cells in bilateral knee osteoarthritis: what better postpone knee arthroplasty at fifteen years? A randomized study. *International orthopaedics*. 45 (2): 391-399.
- Hinman, R.S., Bennell, K.L., Metcalf, B.R. & Crossley, K.M. (2002). Temporal Activity of Vastus Medialis Obliquus and Vastus Lateralis in Symptomatic Knee Osteoarthritis. *American journal of physical medicine & rehabilitation*. 81 (9): 684-690.
- Hjelle, K., Solheim, E., Strand, T., Muri, R. & Brittberg, M. (2002). Articular cartilage defects in 1,000 knee arthroscopies. *Arthroscopy: The Journal of Arthroscopic & Related Surgery: Official Publication of the Arthroscopy Association of North America and the International Arthroscopy Association*. 18 (7): 730-734.

Hoemann, C.D., Lafantaisie-Favreau, C., Lascau-Coman, V., Chen, G. & Guzmán-Morales, J. (2012). The cartilage-bone interface. *The Journal of Knee Surgery*. 25 (2): 85-97.

Holmdahl, D.E. & Ingelmark, B.E. (1950). The Contact Between the Articular Cartilage and the Medullary Cavities of the Bone. *Acta Orthopaedica*. 20 (2): 156-165.

Hopwood, B., Tsykin, A., Findlay, D.M. & Fazzalari, N.L. (2007). Microarray gene expression profiling of osteoarthritic bone suggests altered bone remodelling, WNT and transforming growth factor- β /bone morphogenic protein signalling. *Arthritis research & therapy*. 9 (5): 100.

Hsu, C. & Sandford, B. (2007). The Delphi Technique: Making Sense of Consensus. *Practical Assessment*. 12 (10): 1-8.

Hunter, D.J., Guermazi, A., Lo, G.H., Grainger, A.J., Conaghan, P.G., Boudreau, R.M. & Roemer, F.W. (2011). Evolution of semi-quantitative whole joint assessment of knee OA: MOAKS (MRI Osteoarthritis Knee Score). *Osteoarthritis and Cartilage*. 19 (8): 990-1002.

Hunter, D.J., Gerstenfeld, L., Bishop, G., Davis, A.D., Mason, Z.D., Einhorn, T.A., Maciewicz, R.A., Newham, P., Foster, M., Jackson, S. & Morgan, E.F. (2009). Bone marrow lesions from osteoarthritis knees are characterized by sclerotic bone that is less well mineralized. *Arthritis research & therapy*. 11 (1): 11.

Hunter, D.J., Zhang, Y., Niu, J., Goggins, J., Amin, S., LaValley, M.P., Guermazi, A., Genant, H., Gale, D. & Felson, D.T. (2006). Increase in bone marrow lesions associated with cartilage loss: A longitudinal magnetic resonance imaging study of knee osteoarthritis. *Arthritis and rheumatism*. 54 (5): 1529-1535.

Hunziker, E.B., Michel, M. & Studer, D. (1997). Ultrastructure of adult human articular cartilage matrix after cryotechnical processing. *Microscopy Research and Technique*. 37 (4): 271-284.

Hunziker, E.B. (2002). Articular cartilage repair: basic science and clinical progress. A review of the current status and prospects. *Osteoarthritis and cartilage*. 10 (6): 432-463.

Hwang, J., Bae, W.C., Shieu, W., Lewis, C.W., Bugbee, W.D. & Sah, R.L. (2008). Increased hydraulic conductance of human articular cartilage and subchondral bone plate with progression of osteoarthritis. *Arthritis & Rheumatism*. 58 (12): 3831-3842.

ICH Expert Working group (2006). *NOTE FOR GUIDANCE ON VALIDATION OF ANALYTICAL PROCEDURES: TEXT AND METHODOLOGY*. London, UK: .

Ilas, D.C., Churchman, S.M., McGonagle, D. & Jones, E. (2017). Targeting subchondral bone mesenchymal stem cell activities for intrinsic joint repair in osteoarthritis. *Future Science OA*. 3 (4): 228.

Jackson, R.W. & Dieterichs, C. (2003). The results of arthroscopic lavage and debridement of osteoarthritic knees based on the severity of degeneration: a 4- to 6-year symptomatic follow-up. *Arthroscopy*. 19 (1): 13.

Jacobson, N.S. & Truax, P. (1991). Clinical significance: a statistical approach to defining meaningful change in psychotherapy research. *Journal of consulting and clinical psychology*. 59 (1): 12-19.

Jaiswal, N., Haynesworth, S.E., Caplan, A.I. & Bruder, S.P. (1997). Osteogenic differentiation of purified, culture-expanded human mesenchymal stem cells in vitro. *Journal of Cellular Biochemistry*. 64 (2): 295-312.

jamovi (2020). *The jamovi project*. Available from: www.jamovi.org. [Accessed: April 2020].

Johnson, L.L. (2001). Arthroscopic abrasion arthroplasty: a review. *Clinical orthopaedics and related research*. 391 (391 Suppl): S306-S317.

Johnson, L.L. (1986). Arthroscopic abrasion arthroplasty historical and pathologic perspective: Present status. *Arthroscopy*. 2 (1): 54-69.

Johnstone, B., Hering, T.M., Caplan, A.I., Goldberg, V.M. & Yoo, J.U. (1998). In Vitro Chondrogenesis of Bone Marrow-Derived Mesenchymal Progenitor Cells. *Experimental Cell Research*. 238 (1): 265-272.

KAPOOR, P., 1987. *Systems approach to documentary maritime fraud*, University of Plymouth.

Karuppall, R., Dr (2017). Current concepts in the articular cartilage repair and regeneration. *Journal of Orthopaedics*. 14 (2): A1-A3.

Kauko, K. & Palmroos, P. (2014). The Delphi method in forecasting financial markets— An experimental study. *International Journal of Forecasting*. 30 (2): 313-327.

Keeney, S., Hasson, F. & McKenna, H.P. (2011). *The Delphi technique in nursing and health research*. Chichester: Wiley-Blackwell.

Kelly, K.P. & Porock, D. (2005). A survey of pediatric oncology nurses' perceptions of parent educational needs. *Journal of Pediatric Oncology Nursing: Official Journal of the Association of Pediatric Oncology Nurses*. 22 (1): 58-66.

Kendall, M.G. & Gibbons, J.D. (1990). *Rank correlation methods*. 5. ed. edn. New York: Oxford Univ. Pr.

Kennedy, O.D. (2018). The Role of Subchondral Bone Damage and Bone Marrow Lesions in Post-traumatic Osteoarthritis. *Orthopaedic Proceedings*. 100 (15).

Kfoury, Y. & Scadden, D. (2015). Mesenchymal Cell Contributions to the Stem Cell Niche. *Cell stem cell*. 16 (3): 239-253.

Kim, D.S., Jang, I.K., Lee, M.W., Ko, Y.J., Lee, D., Lee, J.W., Sung, K.W., Koo, H.H. & Yoo, K.H. (2018). Enhanced Immunosuppressive Properties of Human Mesenchymal Stem Cells Primed by Interferon- γ . *EBioMedicine*. 28 (C): 261-273.

Kim, H. (2013). Statistical notes for clinical researchers: Understanding standard deviations and standard errors. *Restorative dentistry & endodontics*. 38 (4): 263-265.

Kim, Y., Grodzinsky, A.J. & Plaas, A.H.K. (1996). Compression of Cartilage Results in Differential Effects on Biosynthetic Pathways for Aggrecan, Link Protein, and Hyaluronan. *Archives of biochemistry and biophysics*. 328 (2): 331-340.

Kim, Y., Sah, R.L.Y., Doong, J.H. & Grodzinsky, A.J. (1988). Fluorometric assay of DNA in cartilage explants using Hoechst 33258. *Analytical Biochemistry*. 174 (1): 168-176.

Kirsch, T. & Pfäffle, M. (1992). Selective binding of anchorin CII (annexin V) to type II and X collagen and to chondrocalcin (C-propeptide of type II collagen) Implications for anchoring function between matrix vesicles and matrix proteins. *FEBS Letters*. 310 (2): 143-147.

Klein, T., Malda, J., Sah, R. & Hutmacher, D. (2009). Tissue engineering of articular cartilage with biomimetic zones. *Tissue Engineering. Part B, Reviews*. 15 (2): 143-157.

Knothe Tate, M.L. (2003). "Whither flows the fluid in bone?" An osteocyte's perspective. *Journal of biomechanics*. 36 (10): 1409-1424.

Knutsen, G., Drogset, J., Engebretsen, L., Grøntvedt, T., Isaksen, V., Ludvigsen, T., Roberts, S., Solheim, E., Strand, T. & Johansen, O. (2007). A Randomized Trial Comparing Autologous Chondrocyte Implantation with Microfracture: Findings at Five Years. *The Journal of Bone & Joint Surgery*. 89 (10): 2105-2112.

Knutsen, G., Engebretsen, L., Ludvigsen, T., Drogset, J., Grøntvedt, T., Solheim, E., Strand, T., Roberts, S., Isaksen, V. & Johansen, O. (2004). Autologous Chondrocyte Implantation Compared with Microfracture in the Knee: A Randomized Trial. *The Journal of Bone & Joint Surgery*. 86 (3): 455-464.

Koussounadis, A., Langdon, S.P., Um, I.H., Harrison, D.J. & Smith, V.A. (2015). Relationship between differentially expressed mRNA and mRNA-protein correlations in a xenograft model system. *Scientific reports*. 5 (1): 10775.

Kreuz, P.C., Steinwachs, M., Erggelet, C., Lahm, A., Krause, S., Ossendorf, C., Meier, D., Ghanem, N. & Uhl, M. (2007). Importance of Sports in Cartilage Regeneration after Autologous Chondrocyte Implantation. *The American Journal of Sports Medicine*. 35 (8): 1261-1268.

Krishnan, S.P., Skinner, J.A., Bartlett, W., Carrington, R.W.J., Flanagan, A.M., Briggs, T.W.R. & Bentley, G. (2006). Who is the ideal candidate for autologous chondrocyte implantation? *Journal of bone and joint surgery. British volume*. 88 (1): 61-64.

- Kuttapitiya, A., Assi, L., Laing, K., Hing, C., Mitchell, P., Whitley, G., Harrison, A., Howe, F.A., Ejindu, V., Heron, C. & Sofat, N. (2017). Microarray analysis of bone marrow lesions in osteoarthritis demonstrates upregulation of genes implicated in osteochondral turnover, neurogenesis and inflammation. *Annals of the Rheumatic Diseases*. 76 (10): 1764-1773.
- Lajeunesse, D. & Reboul, P. (2003). Subchondral bone in osteoarthritis: a biologic link with articular cartilage leading to abnormal remodeling. *Current Opinion in Rheumatology*. 15 (5): 628-633.
- LaPrade, R.F., Botker, J., Herzog, M. & Agel, J. (2009). Refrigerated Osteoarticular Allografts to Treat Articular Cartilage Defects of the Femoral Condyles: A Prospective Outcomes Study. *Journal of bone and joint surgery. American volume*. 91 (4): 805-811.
- Le Blanc, K., Tammik, C., Rosendahl, K., Zetterberg, E. & Ringdén, O. (2003). HLA expression and immunologic properties of differentiated and undifferentiated mesenchymal stem cells. *Experimental hematology*. 31 (10): 890-896.
- Lee, W.D., Hurtig, M.B., Pilliar, R.M., Stanford, W.L. & Kandel, R.A. (2015). Engineering of hyaline cartilage with a calcified zone using bone marrow stromal cells. *Osteoarthritis and Cartilage*. 23 (8): 1307-1315.
- Lee, Y.H.D., Suzer, F. & Thermann, H. (2014). Autologous Matrix-Induced Chondrogenesis in the Knee. *Cartilage*. 5 (3): 145-153.
- Lee, Y. et al. (2018). *Regulation of lubricin for functional cartilage tissue regeneration: a review*. vol. 22. England: BioMed Central Ltd.
- Lenth, R. (2018). *emmeans: Estimated Marginal Means, aka Least-Squares Means [R package]*. Available from: <https://cran.r-project.org/web/packages/emmeans/index.html>. [Accessed: March 2020].
- Leong, D.J., Hardin, J.A., Cobelli, N.J. & Sun, H.B. (2011). Mechanotransduction and cartilage integrity. *Annals of the New York Academy of Sciences*. 1240 (1): 32-37.
- Leydet-Quilici, H., Le Corroller, T., Bouvier, C., Giorgi, R., Argenson, J.-., Champsaur, P., Pham, T., Maues de Paula, A. & Lafforgue, P. (2010). Advanced hip osteoarthritis: magnetic resonance imaging aspects and histopathology correlations. *Osteoarthritis and Cartilage*. 18 (11): 1429-1435.
- Li, G., Yin, J., Gao, J., Cheng, T.S., Pavlos, N.J., Zhang, C. & Zheng, M.H. (2013). Subchondral bone in osteoarthritis: insight into risk factors and microstructural changes. *Arthritis research & therapy*. 15 (6): 223.
- Li, Q., Han, B., Wang, C., Tong, W., Wei, Y., Tseng, W., Han, L., Liu, X.S., Enomoto-Iwamoto, M., Mauck, R.L., Qin, L., Iozzo, R.V., Birk, D.E. & Han, L. (2020). Mediation of Cartilage Matrix Degeneration and Fibrillation by Decorin in Post-traumatic Osteoarthritis. *Arthritis & rheumatology (Hoboken, N.J.)*. 72 (8): 1266-1277.

- Li, Y., Wei, X., Zhou, J. & Wei, L. (2013). The Age-Related Changes in Cartilage and Osteoarthritis. *BioMed research international*. 2013 : 1-12.
- Lian, C., Wang, X., Qiu, X., Wu, Z., Gao, B., Liu, L., Liang, G., Zhou, H., Yang, X., Peng, Y., Liang, A., Xu, C., Huang, D. & Su, P. (2019). Collagen type II suppresses articular chondrocyte hypertrophy and osteoarthritis progression by promoting integrin β 1-SMAD1 interaction. *Bone research*. 7 (1): 8.
- Liao, Y., Shonkoff, E.T. & Dunton, G.F. (2015). The Acute Relationships Between Affect, Physical Feeling States, and Physical Activity in Daily Life: A Review of Current Evidence. *Frontiers in psychology*. 6 : 1975.
- Likert, R. (1932). A technique for the measurement of attitudes. *Archives of Psychology*. 22 (140): 55-55.
- Link, T.M. & Li, X. (2011). Bone Marrow Changes in Osteoarthritis. *Seminars in Musculoskeletal Radiology*. 15 (3): 238-246.
- Linstone, H. & Turoff, M. (1975). *The Delphi Method*. Reading, Massachusetts: Addison-Wesley Publishing Company.
- Lo Monaco, M., Merckx, G., Ratajczak, J., Gervois, P., Hilkens, P., Clegg, P., Bronckaers, A., Vandeweerdt, J. & Lambrechts, I. (2018). Stem Cells for Cartilage Repair: Preclinical Studies and Insights in Translational Animal Models and Outcome Measures. *Stem cells international*. 2018 : 1-22.
- Lo, G.H., Niu, J., McLennan, C.E., Kiel, D.P., McLean, R.R., Guermazi, A., Genant, H.K., McAlindon, T.E. & Hunter, D.J. (2007). Meniscal damage associated with increased local subchondral bone mineral density: a Framingham study. *Osteoarthritis and Cartilage*. 16 (2): 261-267.
- Loef, M., van Beest, S., Kroon, F.P.B., Bloem, J.L., Dekkers, O.M., Reijnen, M., Schoones, J.W. & Kloppenburg, M. (2018). Comparison of histological and morphometrical changes underlying subchondral bone abnormalities in inflammatory and degenerative musculoskeletal disorders: a systematic review. *Osteoarthritis and Cartilage*. 26 (8): 992-1002.
- Loeser, R.F., Goldring, S.R., Scanzello, C.R. & Goldring, M.B. (2012). Osteoarthritis: A disease of the joint as an organ. *Arthritis and Rheumatism*. 64 (6): 1697-1707.
- Luo, Y., Sinkeviciute, D., He, Y., Karsdal, M., Henrotin, Y., Mobasher, A., Önerfjord, P. & Bay-Jensen, A. (2017). The minor collagens in articular cartilage. 8 (8): 560-572.
- Luyten, F.P. & Lories, R.J. (2011). The bone-cartilage unit in osteoarthritis. *Nature Reviews Rheumatology*. 7 (1): 43-49.
- Lynn, M. & Layman, E. (1996). The Nature of Nursing Administration Research Knowledge Building or Fire Stomping? *The Journal of Nursing Administration*. 26 (5): 9-14.

- Lyons, T.J., McClure, S.F., Stoddart, R.W. & McClure, J. (2006). The normal human chondro-osseous junctional region: evidence for contact of uncalcified cartilage with subchondral bone and marrow spaces. *BMC musculoskeletal disorders*. 7 (1): 52.
- Lysholm, J. & Gillquist, J. (1982). Evaluation of knee ligament surgery results with special emphasis on use of a scoring scale. *The American journal of sports medicine*. 10 (3): 150-154.
- Mackie, E.J., Ahmed, Y.A., Tatarczuch, L., Chen, K.-. & Mirams, M. (2008). Endochondral ossification: How cartilage is converted into bone in the developing skeleton. *International Journal of Biochemistry and Cell Biology*. 40 (1): 46-62.
- Madry, H., Orth, P. & Cucchiari, M. (2016). Role of the Subchondral Bone in Articular Cartilage Degeneration and Repair. *Journal of the American Academy of Orthopaedic Surgeons*. 24 (4): 45-46.
- Madry, H., van Dijk, C.N. & Mueller-Gerbl, M. (2010). The basic science of the subchondral bone. *Knee surgery, sports traumatology, arthroscopy*. 18 (4): 419-433.
- Magne, D., Bluteau, G., Faucheux, C., Palmer, G., Vignes-Colombeix, C., Pilet, P., Rouillon, T., Caverzasio, J., Weiss, P., Daculsi, G. & Guicheux, J. (2003). Phosphate Is a Specific Signal for ATDC5 Chondrocyte Maturation and Apoptosis-Associated Mineralization: Possible Implication of Apoptosis in the Regulation of Endochondral Ossification. *Journal of Bone and Mineral Research*. 18 (8): 1430-1442.
- Mainil-Varlet, P., Van Damme, B., Nestic, D., Knutsen, G., Kandel, R. & Roberts, S. (2010). A New Histology Scoring System for the Assessment of the Quality of Human Cartilage Repair: ICRS II. *The American Journal of Sports Medicine*. 38 (5): 880-890.
- Makris, E.A., Gomoll, A.H., Malizos, K.N., Hu, J.C. & Athanasiou, K.A. (2014). Repair and tissue engineering techniques for articular cartilage. *Nature reviews. Rheumatology*. 11 (1): 21-34.
- Malone, D.C., Abarca, J., Hansten, P.D., Grizzle, A.J., Armstrong, E.P., Van Bergen, R.C., Duncan-Edgar, B.S., Solomon, S.L. & Lipton, R.B. (2004). Identification of serious drug-drug interactions: results of the partnership to prevent drug-drug interactions. *Journal of the American Pharmacists Association: JAPhA*. 44 (2): 142-151.
- Marcacci, M., Andriolo, L., Kon, E., Shabshin, N. & Filardo, G. (2016). Aetiology and pathogenesis of bone marrow lesions and osteonecrosis of the knee. *EFORT open reviews*. 1 (5): 219-224.
- Marlovits, S., Singer, P., Zeller, P., Mandl, I., Haller, J. & Trattnig, S. (2006). Magnetic resonance observation of cartilage repair tissue (MOCART) for the evaluation of autologous chondrocyte transplantation: determination of interobserver variability and correlation to clinical outcome after 2 years. *European Journal of Radiology*. 57 (1): 16-23.
- Maroudas, A. (1976). Balance between swelling pressure and collagen tension in normal and degenerate cartilage. *Nature*. 260 (5554): 808-809.

Mata, J., Thompson, R.J., Jaeggi, S.M., Buschkuehl, M., Jonides, J. & Gotlib, I.H. (2012). Walk on the bright side: Physical activity and affect in major depressive disorder. *Journal of abnormal psychology (1965)*. 121 (2): 297-308.

Matricali, G.A., Dereymaeker, G.P.E. & Luyten, F.P. (2010). Donor site morbidity after articular cartilage repair procedures: a review. *Acta orthopaedica belgica*. 76 (5): 669.

Matsumoto, T., Cooper, G.M., Gharaibeh, B., Meszaros, L.B., Li, G., Usas, A., Fu, F.H. & Huard, J. (2009). Cartilage repair in a rat model of osteoarthritis through intraarticular transplantation of muscle-derived stem cells expressing bone morphogenetic protein 4 and soluble flt-1. *Arthritis & Rheumatism*. 60 (5): 1390-1405.

Mauck, R.L., Yuan, X. & Tuan, R.S. (2006). Chondrogenic differentiation and functional maturation of bovine mesenchymal stem cells in long-term agarose culture. *Osteoarthritis and Cartilage*. 14 (2): 179-189.

McAdams, T.R. et al. (2010). *Review: Articular Cartilage Injury in Athletes*. vol. 1. Los Angeles, CA: SAGE Publications.

McGraw, K.O. & Wong, S.P. (1996). Forming Inferences About Some Intraclass Correlation Coefficients. *Psychological Methods*. 1 (1): 30-46.

McKenna, H.P. (1994). The Delphi technique: a worthwhile research approach for nursing? *Journal of Advanced Nursing*. 19 (6): 1221-1225.

McMillan, S., King, M. & Tully, M. (2016). How to use the nominal group and Delphi techniques. *International Journal of Clinical Pharmacy*. 38 (3): 655-662.

Medvedeva, E.V., Grebenik, E.A., Gornostaeva, S.N., Telpuhov, V.I., Lychagin, A.V., Timashev, P.S. & Chagin, A.S. (2018). Repair of Damaged Articular Cartilage: Current Approaches and Future Directions. *International journal of molecular sciences*. 19 (8): 2366.

Meier, C., Meier, C., Kraenzlin, C., Kraenzlin, C., Friederich, N., Friederich, N., Wischer, T., Wischer, T., Grize, L., Grize, L., Meier, C., Meier, C., Kraenzlin, M. & Kraenzlin, M. (2014). Effect of ibandronate on spontaneous osteonecrosis of the knee: a randomized, double-blind, placebo-controlled trial. *Osteoporosis international*. 25 (1): 359-366.

Méndez-Ferrer, S., Michurina, T.V., Ferraro, F., Mazloom, A.R., MacArthur, B.D., Lira, S.A., Scadden, D.T., Ma'ayan, A., Enikolopov, G.N. & Frenette, P.S. (2010). Mesenchymal and haematopoietic stem cells form a unique bone marrow niche. *Nature (London)*. 466 (7308): 829-834.

Mennan, C., Garcia, J., Roberts, S., Hulme, C. & Wright, K. (2019). A comprehensive characterisation of large-scale expanded human bone marrow and umbilical cord mesenchymal stem cells. *Stem cell research & therapy*. 10 (1): 99.

- Mennan, C., Wright, K., Bhattacharjee, A., Balain, B., Richardson, J. & Roberts, S. (2013). Isolation and Characterisation of Mesenchymal Stem Cells from Different Regions of the Human Umbilical Cord. *BioMed research international*. 2013 : 916136-8.
- Merz, E.L., Malcarne, V.L., Roesch, S.C., Ko, C.M., Emerson, M., Roma, V.G. & Sadler, G.R. (2013). Psychometric properties of Positive and Negative Affect Schedule (PANAS) original and short forms in an African American community sample. *Journal of Affective Disorders*. 151 (3): 942-949.
- Michael, J.W., Schlüter-Brust, K.U. & Eysel, P. (2010). The Epidemiology, Etiology, Diagnosis, and Treatment of Osteoarthritis of the Knee. *Deutsches Arzteblatt international*. 107 (9): 152.
- Miller, B.S., Steadman, J.R., Briggs, K.K., Rodrigo, J.J. & Rodkey, W.G. (2004). Patient satisfaction and outcome after microfracture of the degenerative knee. *The Journal of Knee Surgery*. 17 (1): 13-17.
- Miron, R.J. & Zhang, Y.F. (2012). Osteoinduction. *Journal of Dental Research*. 91 (8): 736-744.
- Mithoefer, K., Hambly, K., Logerstedt, D., Ricci, M., Silvers, H. & Villa, S.D. (2012). Current Concepts for Rehabilitation and Return to Sport After Knee Articular Cartilage Repair in the Athlete. *The journal of orthopaedic and sports physical therapy*. 42 (3): 254-273.
- Mithoefer, K., McAdams, T., Williams, R.J., Kreuz, P.C. & Mandelbaum, B.R. (2009). Clinical Efficacy of the Microfracture Technique for Articular Cartilage Repair in the Knee. *The American Journal of Sports Medicine*. 37 (10): 2053-2063.
- Mohamed, A.M. (2008). An Overview of Bone Cells and their Regulating Factors of Differentiation. *Malaysian Journal of Medical Sciences*. 15 (1): 4-12.
- Mollon, B., Kandel, R., Chahal, J. & Theodoropoulos, J. (2013). The clinical status of cartilage tissue regeneration in humans. *Osteoarthritis and Cartilage*. 21 (12): 1824-1833.
- Moojen, D., Yang, K., Dhert, W., Verbout, A.J. & Saris, D. (2002). The correlation and reproducibility of histological scoring systems in cartilage repair. *Tissue Engineering*. 8 (4): 627-634.
- Mueller, M.B. & Tuan, R.S. (2008). Functional characterization of hypertrophy in chondrogenesis of human mesenchymal stem cells. *Arthritis & Rheumatism*. 58 (5): 1377-1388.
- Murphy, G. & Nagase, H. (2008). Reappraising metalloproteinases in rheumatoid arthritis and osteoarthritis: destruction or repair? *Nature clinical practice. Rheumatology*. 4 (3): 128-135.
- Nezlek, J.B. (2001). Multilevel Random Coefficient Analyses of Event- and Interval-Contingent Data in Social and Personality Psychology Research. *Personality & social psychology bulletin*. 27 (7): 771-785.

Niemeyer, P., Köstler, W., Salzmann, G.M., Lenz, P., Kreuz, P.C. & Südkamp, N.P. (2010). Autologous Chondrocyte Implantation for Treatment of Focal Cartilage Defects in Patients Age 40 Years and Older. *The American Journal of Sports Medicine*. 38 (12): 2410-2416.

Niermann, C.Y.N., Herrmann, C., von Haaren, B., van Kann, D. & Woll, A. (2016). Affect and Subsequent Physical Activity: An Ambulatory Assessment Study Examining the Affect-Activity Association in a Real-Life Context. *Frontiers in psychology*. 7 : 677.

Noronha, N.C., Mizukami, A., Caliári-Oliveira, C., Cominal, J.G., Rocha, J.L.M., Covas, D.T., Swiech, K. & Malmegrim, K.C.R. (2019). Priming approaches to improve the efficacy of mesenchymal stromal cell-based therapies. *Stem cell research & therapy*. 10 (1): 131.

Oei, E.H.G., Wick, M.C., Müller-Lutz, A., Schleich, C. & Miese, F.R. (2018). Cartilage Imaging: Techniques and Developments. *Seminars in Musculoskeletal Radiology*. 22 (2): 245-260.

O'Hara, B.P., Urban, J.P. & Maroudas, A. (1990). Influence of cyclic loading on the nutrition of articular cartilage. *Annals of the rheumatic diseases*. 49 (7): 536-539.

Ondršík, M., Oliveira, J.M. & Reis, R.L. (2017). Knee Articular Cartilage. In: Ondršík, M., Oliveira, J.M. (ed.) *Regenerative Strategies for the Treatment of Knee Joint Disabilities*. Cham, Switzerland: Springer International Publishing.

Ondrouch, A.S. (1963). Cyst formation in osteoarthritis. . *Journal of Bone and Joint Surgery*. 15 : 755-760.

Ortega, N., Behonick, D.J. & Werb, Z. (2004). Matrix remodeling during endochondral ossification. *Trends in cell biology*. 14 (2): 86-93.

O'Driscoll, S., Keeley, F. & Salter, R. (1988). Durability of regenerated articular cartilage produced by free autogenous periosteal grafts in major full-thickness defects in joint surfaces under the influence of continuous passive motion. A follow-up report at one year. *The Journal of Bone & Joint Surgery*. 70 (4): 595-606.

O'Driscoll, S., Keeley, F. & Salter, R. (1986). The chondrogenic potential of free autogenous periosteal grafts for biological resurfacing of major full-thickness defects in joint surfaces under the influence of continuous passive motion. An experimental investigation in the rabbit. *The Journal of Bone & Joint Surgery*. 68 (7): 1017-1035.

Pan, J., Zhou, X., Li, W., Novotny, J.E., Doty, S.B. & Wang, L. (2009). In situ measurement of transport between subchondral bone and articular cartilage. *Journal of Orthopaedic Research*. 27 (10): 1347-1352.

Perera, J.R., Gikas, P.D. & Bentley, G. (2012). The present state of treatments for articular cartilage defects in the knee. *Annals of the Royal College of Surgeons of England*. 94 (6): 381-387.

Peretti, G.M., Pozzi, A., Ballis, R., Deponti, D. & Pellacci, F. (2011). Current surgical options for articular cartilage repair. *Acta neurochirurgica. Supplement*. 108 : 213.

- Peterfy, C.G., Guermazi, A., Zaim, S., Tirman, P.F.J., Miaux, Y., White, D., Kothari, M., Lu, Y., Fye, K., Zhao, S. & Genant, H.K. (2004). Whole-Organ Magnetic Resonance Imaging Score (WORMS) of the knee in osteoarthritis. *Osteoarthritis and Cartilage*. 12 (3): 177-190.
- Peterson, L., Minas, T., Brittberg, M., Nilsson, A., Sjögren-Jansson, E. & Lindahl, A. (2000). Two- to 9-year outcome after autologous chondrocyte transplantation of the knee. *Clinical Orthopaedics and Related Research*. (374): 212-234.
- Pilz, G.A., Braun, J., Ulrich, C., Felka, T., Warstat, K., Ruh, M., Schewe, B., Abele, H., Larbi, A. & Aicher, W.K. (2011). Human mesenchymal stromal cells express CD14 cross-reactive epitopes. *Cytometry. Part A*. 79A (8): 635-645.
- Pineda, S., Pollack, A., Stevenson, S., Goldberg, V. & Caplan, A. (1992). A Semiquantitative Scale or Histologic Grading of Articular Cartilage Repair. *Cells Tissues Organs*. 143 (4): 335-340.
- Pitsillides, A.A. & Ashurst, D.E. (2008). A critical evaluation of specific aspects of joint development. *Developmental dynamics*. 237 (9): 2284-2294.
- Polchert, D., Sobinsky, J., Douglas, G.W., Kidd, M., Moadsiri, A., Reina, E., Genrich, K., Mehrotra, S., Setty, S., Smith, B. & Bartholomew, A. (2008). IFN- γ activation of mesenchymal stem cells for treatment and prevention of graft versus host disease. *European journal of immunology*. 38 (6): 1745-1755.
- Poole, C.A. (1997). Articular cartilage chondrons: form, function and failure. *Journal of anatomy*. 191 (Pt 1) : 1.
- Poole, C.A., Flint, M.H. & Beaumont, B.W. (1987). Chondrons in cartilage: Ultrastructural analysis of the pericellular microenvironment in adult human articular cartilages. *Journal of orthopaedic research*. 5 (4): 509-522.
- Powell, C. (2003). The Delphi technique: myths and realities. *Journal of Advanced Nursing*. 41 (4): 376-382.
- Pridie, A.H. (1959). The method of resurfacing osteoarthritic knee. *Journal of Bone and Joint Surgery*. 41 : 618-623.
- Pritzker, K.P.H., Gay, S., Jimenez, S.A., Ostergaard, K., Pelletier, J.-., Revell, P.A., Salter, D. & van den Berg, W.B. (2006). Osteoarthritis cartilage histopathology: grading and staging. *Osteoarthritis and Cartilage*. 14 (1): 13-29.
- Quatman, C.E., Harris, J.D. & Hewett, T.E. (2012). Biomechanical Outcomes of Cartilage Repair of the Knee. *The Journal of Knee Surgery*. 25 (3): 197-206.
- R Core Team (2019). *R: A Language and environment for statistical computing*. . Available from: cran.r-project.org. [Accessed: April 2020].

Radin, E.L., Parker, H.G., Pugh, J.W., Steinberg, R.S., Paul, I.L. & Rose, R.M. (1973). Response of joints to impact loading — III: Relationship between trabecular microfractures and cartilage degeneration. *Journal of Biomechanics*. 6 (1): 51-57.

Rebolledo, B.J., M.D, Smith, K.M., M.D & Dragoo, J.L., M.D (2018). Hitting the Mark: Optimizing the Use of Calcium Phosphate Injections for the Treatment of Bone Marrow Lesions of the Proximal Tibia and Distal Femur. *Arthroscopy techniques (Amsterdam)*. 7 (10): e1013-e1018.

Roberts, S., Menage, J., Sandell, L.J., Evans, E.H. & Richardson, J.B. (2009). Immunohistochemical study of collagen types I and II and procollagen IIA in human cartilage repair tissue following autologous chondrocyte implantation. *The Knee*. 16 (5): 398-404.

Roberts, S., Menage, J., Flannery, C.R. & Richardson, J.B. (2010). Lubricin: Its Presence in Repair Cartilage following Treatment with Autologous Chondrocyte Implantation . *Cartilage*. 1 (4): 298-305.

Roberts, S., McCall, I.W., Darby, A.J., Menage, J., Evans, H., Harrison, P.E. & Richardson, J.B. (2003). Autologous chondrocyte implantation for cartilage repair: monitoring its success by magnetic resonance imaging and histology. *Arthritis research & therapy*. 5 (1): R60-R73.

Roberts, S. & Menage, J. (2004). Microscopic Methods for the Analysis of Engineered Tissues. In: Hollander, A.P. & Hatton, P.V. (eds.) *Biopolymer Methods in Tissue Engineering*. Totowa, New Jersey, USA: Humana Press.

Roemer, F.W., Guerhazi, A., Javaid, M.K., Lynch, J., Niu, J., Zhang, Y., Felson, D.T., Lewis, C.E., Torner, J. & Nevitt, M.C. (2009). Change in MRI-detected subchondral bone marrow lesions is associated with cartilage loss: the MOST Study. A longitudinal multicentre study of knee osteoarthritis. *Annals of the Rheumatic Diseases*. 68 (9): 1461-1465.

Roemer, F.W., Guerhazi, A., Trattnig, S., Apprich, S., Marlovits, S., Niu, J., Hunter, D.J. & Welsch, G.H. (2014). Whole joint MRI assessment of surgical cartilage repair of the knee: Cartilage Repair OsteoArthritis Knee Score (CROAKS). *Osteoarthritis and Cartilage*. 22 (6): 779-799.

Roughley, P. (2001). Articular cartilage and changes in Arthritis: Noncollagenous proteins and proteoglycans in the extracellular matrix of cartilage. *Arthritis Res*. 3 (6): 1-6.

Roughley, P. & Mort, J. (2014). The role of aggrecan in normal and osteoarthritic cartilage. *Journal of Experimental Orthopaedics*. 1 (1): 1-11.

Ruano-Ravina, A. & Jato Díaz, M. (2006). Autologous chondrocyte implantation: a systematic review. *Osteoarthritis and cartilage*. 14 (1): 47-51.

Rutgers, M., van Pelt, M. J. P., Dhert, W.J.A., Creemers, L.B. & Saris, D.B.F. (2010). Evaluation of histological scoring systems for tissue-engineered, repaired and osteoarthritic cartilage. *Osteoarthritis and Cartilage*. 18 (1): 12-23.

Rutkovskiy, A., Stensl kken, K. & Vaage, I.J. (2016). Osteoblast Differentiation at a Glance. *Medical science monitor basic research*. 22 : 95-106.

Ryd, L., Brittberg, M., Eriksson, K., Jurvelin, J.S., Lindahl, A., Marlovits, S., M ller, P., Richardson, J.B., Steinwachs, M. & Zenobi-Wong, M. (2015). Pre-Osteoarthritis. *Cartilage*. 6 (3): 156-165.

Sabokbar, A., Crawford, R., Murray, D.W. & Athanasou, N.A. (2000). Macrophage-osteoclast differentiation and bone resorption in osteoarthrotic subchondral acetabular cysts. *Acta Orthopaedica*. 71 (3): 255-261.

Sanchez, C., Deberg, M.A., Piccardi, N., Msika, P., Reginster, J.-L. & Henrotin, Y.E. (2005a). Osteoblasts from the sclerotic subchondral bone downregulate aggrecan but upregulate metalloproteinases expression by chondrocytes. This effect is mimicked by interleukin-6, -1beta and oncostatin M pre-treated non-sclerotic osteoblasts. *Osteoarthritis and Cartilage*. 13 (11): 979-987.

Sanchez, C., Deberg, M.A., Piccardi, N., Msika, P., Reginster, J.-L. & Henrotin, Y.E. (2005b). Subchondral bone osteoblasts induce phenotypic changes in human osteoarthritic chondrocytes. *Osteoarthritis and Cartilage*. 13 (11): 988-997.

Sanchez, C., Deberg, M.A., Bellahc ne, A., Castronovo, V., Msika, P., Delcour, J.P., Crielaard, J.M. & Henrotin, Y.E. (2008). Phenotypic characterization of osteoblasts from the sclerotic zones of osteoarthritic subchondral bone. *Arthritis & Rheumatism*. 58 (2): 442-455.

Saris, D.B., Vanlauwe, J., Victor, J., Haspl, M., Bohnsack, M., Fortems, Y., Vandekerckhove, B., Almqvist, K.F., Claes, T., Handelberg, F., Lagae, K., van der Bauwhede, J., Vandenneucker, H., Yang, K.G.A., Jelic, M., Verdonk, R., Veulemans, N., Bellemans, J. & Luyten, F.P. (2008). Characterized Chondrocyte Implantation Results in Better Structural Repair When Treating Symptomatic Cartilage Defects of the Knee in a Randomized Controlled Trial Versus Microfracture. *The American Journal of Sports Medicine*. 36 (2): 235-246.

Saris, D.B.F., Vanlauwe, J., Victor, J., Almqvist, K.F., Verdonk, R., Bellemans, J. & Luyten, F.P. (2009). Treatment of Symptomatic Cartilage Defects of the Knee. *The American Journal of Sports Medicine*. 37 (1_suppl): 10-19.

Schmittgen, T.D. & Livak, K.J. (2008). Analyzing real-time PCR data by the comparative CT method. *Nature Protocols*. 3 (6): 1101-1108.

Schmitz, N., Laverty, S., Kraus, V.B. & Aigner, T. (2010). Basic methods in histopathology of joint tissues. *Osteoarthritis and Cartilage*. 18 : S113-S116.

Schumacher, B.L., Hughes, C.E., Kuettner, K.E., Caterson, B. & Aydelotte, M.B. (1999). Immunodetection and partial cDNA sequence of the proteoglycan, superficial zone protein, synthesized by cells lining synovial joints. *Journal of Orthopaedic Research: Official Publication of the Orthopaedic Research Society*. 17 (1): 110-120.

Schwerdtfeger, A., Eberhardt, R., Chmitorz, A. & Schaller, E. (2010). Momentary Affect Predicts Bodily Movement in Daily Life: An Ambulatory Monitoring Study. *Journal of sport & exercise psychology*. 32 (5): 674-693.

Scotti, C., Gobbi, A., Karnatzikos, G., Martin, I., Shimomura, K., Lane, J.G., Peretti, G.M. & Nakamura, N. (2016). Cartilage Repair in the Inflamed Joint: Considerations for Biological Augmentation Toward Tissue Regeneration. *Tissue Engineering. Part B, Reviews*. 22 (2): 149-159.

Seebach, C.L., Kirkhart, M., Lating, J.M., Wegener, S.T., Song, Y., Riley, L.H. & Archer, K.R. (2012). Examining the role of positive and negative affect in recovery from spine surgery. *Pain*. 153 (3): 518-525.

Sellards, R.A., Nho, S.J. & Cole, B.J. (2002). Chondral injuries. *Current Opinion in Rheumatology*. 14 (2): 134-141.

Selmi, T.A.S., Verdonk, P., Chambat, P., Dubrana, F., Potel, J., Barnouin, L. & Neyret, P. (2008). Autologous chondrocyte implantation in a novel alginate-agarose hydrogel: outcome at two years. *Journal of bone and joint surgery. British volume*. 90 (5): 597-604.

Seo, S., Kim, C. & Jung, D. (2011). Management of Focal Chondral Lesion in the Knee Joint. *Knee Surgery & Related Research*. 23 (4): 185-196.

Seol, D., McCabe, D.J., Choe, H., Zheng, H., Yu, Y., Jang, K., Walter, M.W., Lehman, A.D., Ding, L., Buckwalter, J.A. & Martin, J.A. (2012). Chondrogenic progenitor cells respond to cartilage injury. *Arthritis & Rheumatism*. 64 (11): 3626-3637.

Serafini, K., Malin-Mayor, B., Nich, C., Hunkele, K. & Carroll, K.M. (2016). Psychometric properties of the Positive and Negative Affect Schedule (PANAS) in a heterogeneous sample of substance users. *The American Journal of Drug and Alcohol Abuse*. 42 (2): 203-212.

Shaikh, N., Seah, M.K.T. & Khan, W.S. (2017). Systematic review on the use of autologous matrix-induced chondrogenesis for the repair of articular cartilage defects in patients. *World journal of orthopedics*. 8 (7): 588-601.

Sharma, A.R., Jagga, S., Lee, S. & Nam, J. (2013). Interplay between Cartilage and Subchondral Bone Contributing to Pathogenesis of Osteoarthritis. *International journal of molecular sciences*. 14 (10): 19805-19830.

Shelbourne, K.D., Jari, S. & Gray, T. (2003). Outcome of Untreated Traumatic Articular Cartilage Defects of the Knee. *The Journal of Bone and Joint Surgery-American Volume*. 85 : 8-16.

Slaoui, M. & Fiette, L. (2011). Histopathology Procedures: From Tissue Sampling to Histopathological Evaluation. In: Gautier, J. (ed.) *Drug Safety Evaluation: Methods and Protocols, Methods in Molecular Biology*. Totowa, New Jersey: Humana Press.

Smith, G.D., Taylor, J., Almqvist, K.F., Erggelet, C., Knutsen, G., Garcia Portabella, M., Smith, T. & Richardson, J.B. (2005). Arthroscopic assessment of cartilage repair: a validation study of 2 scoring systems. *Arthroscopy: The Journal of Arthroscopic & Related Surgery: Official Publication of the Arthroscopy Association of North America and the International Arthroscopy Association*. 21 (12): 1462-1467.

Smith, H.J., Ph.D, Richardson, J.B., M.D & Tennant, A., Ph.D (2008). Modification and validation of the Lysholm Knee Scale to assess articular cartilage damage. *Osteoarthritis and Cartilage*. 17 (1): 53-58.

Sniekers, Y.H., Weinans, H., Bierma-Zeinstra, S.M., van Leeuwen, J.P.T.M. & van Osch, G.J.V.M. (2008). Animal models for osteoarthritis: the effect of ovariectomy and estrogen treatment – a systematic approach. *Osteoarthritis and Cartilage*. 16 (5): 533-541.

Sobol, E.N., Baum, O.I., Shekhter, A.B., Guller, A. & Baskov, A.V. (2011). Laser-induced regeneration of cartilage. *Journal of Biomedical Optics*. 16 (8): 080902.

Spector, T.D., Cicuttini, F., Baker, J., Loughlin, J. & Hart, D. (1996). Genetic influences on osteoarthritis in women: a twin study. *BMJ*. 312 (7036): 940-943.

Steadman, J.R., Rodkey, W.G. & Briggs, K.K. (2010). Microfracture. *Cartilage*. 1 (2): 78-86.

Steadman, J., Rodkey, W., Singleton, S. & Briggs, K. (1997). Microfracture technique for full-thickness chondral defects: Technique and clinical results. *Operative Techniques in Orthopaedics*. 7 (4): 300-304.

Steinwachs, M.R., Engebretsen, L. & Brophy, R.H. (2012). Scientific Evidence Base for Cartilage Injury and Repair in the Athlete. *Cartilage*. 3 (1_suppl): 11S-17S.

Stockwell, R.A. (1967). Chondrocytes . *Journal of Clinical Pathology*. 31 (12): 7-13.

Stoker, A.M., Stannard, J.P. & Cook, J.L. (2018). Chondrocyte Viability at Time of Transplantation for Osteochondral Allografts Preserved by the Missouri Osteochondral Preservation System versus Standard Tissue Bank Protocol. *The Journal of knee surgery*. 31 (8): 772-780.

Strober, W. (2015). Trypan Blue Exclusion Test of Cell Viability. *Current Protocols in Immunology*. 111 (1): A3.B.1-A3.B.3.

Suri, S. & Walsh, D.A. (2012). Osteochondral alterations in osteoarthritis. *Bone*. 51 (2): 204-211.

Szafranski, J.D., Grodzinsky, A.J., Burger, E., Gaschen, V., Hung, H. & Hunziker, E.B. (2004). Chondrocyte mechanotransduction: effects of compression on deformation of intracellular organelles and relevance to cellular biosynthesis. *Osteoarthritis and cartilage*. 12 (12): 937-946.

Taljanovic, M., Graham, A., Benjamin, J., Gmitro, A., Krupinski, E., Schwartz, S., Hunter, T. & Resnick, D. (2008). Bone marrow edema pattern in advanced hip osteoarthritis: quantitative assessment with magnetic resonance imaging and correlation with clinical examination, radiographic findings, and histopathology. *Skeletal Radiology*. 37 (5): 423-431.

Tanamas, S.K., Wluka, A.E., Pelletier, J., Martel-Pelletier, J., Abram, F., Wang, Y. & Cicuttini, F.M. (2010). The association between subchondral bone cysts and tibial cartilage volume and risk of joint replacement in people with knee osteoarthritis: a longitudinal study. *Arthritis research & therapy*. 12 (2): R58.

Tegner, Y. & Lysholm, J. (1985). Rating systems in the evaluation of knee ligament injuries. *Clinical orthopaedics and related research*. (198): 43.

Tegner, Y., Lysholm, J., Odensten, M. & Gillquist, J. (1988). Evaluation of cruciate ligament injuries A review. *Acta Orthopaedica*. 59 (3): 336-341.

Thomee, P., Wahrborg, P., Borjesson, M., Thomee, R., Eriksson, B.I. & Karlsson, J. (2006). A new instrument for measuring self-efficacy in patients with an anterior cruciate ligament injury. *Scandinavian journal of medicine & science in sports*. 16 (3): 181-187.

Thompson, E.R. (2007). Development and Validation of an Internationally Reliable Short-Form of the Positive and Negative Affect Schedule (PANAS). *Journal of Cross-Cultural Psychology*. 38 (2): 227-242.

Thysen, S., Luyten, F.P. & Lories, R.J.U. (2015). Targets, models and challenges in osteoarthritis research. *Disease models & mechanisms*. 8 (1): 17-30.

Tiku, M.L. & Sabaawy, H.E. (2015). *Cartilage regeneration for treatment of osteoarthritis: a paradigm for nonsurgical intervention*. vol. 7. London, England: SAGE Publications.

Toonstra, J.L., Howell, D., English, R.A., Lattermann, C. & Mattacola, C.G. (2016). Patient Experiences of Recovery After Autologous Chondrocyte Implantation: A Qualitative Study. *Journal of athletic training*. 51 (12): 1028-1036.

Toonstra, J.L., Mattacola, C.G., English, R.A., Howard, J.S. & Uhl, T.L. (2013). The Role of Rehabilitation Following Autologous Chondrocyte Implantation: A Retrospective Chart Review. 8 (5): 670-679.

Torrie, A.M., Kessler, W.K., Elkin, J. & Gallo, A.G. (2015). Osteochondral allograft . *Current Reviews in Musculoskeletal Medicine*. 8 (4): 413-422.

Trattinig, S., Winalski, C.S., Marlovits, S., Jurvelin, J.S., Welsch, G.H. & Potter, H.G. (2011). Magnetic Resonance Imaging of Cartilage Repair. *Cartilage*. 2 (1): 5-26.

Travlos, G.S. (2016). Normal Structure, Function, and Histology of the Bone Marrow. *Toxicologic pathology*. 34 (5): 548-565.

- Tripp, D.A., Stanish, W., Ebel-Lam, A., Brewer, B.W. & Birchard, J. (2007). Fear of Reinjury, Negative Affect, and Catastrophizing Predicting Return to Sport in Recreational Athletes With Anterior Cruciate Ligament Injuries at 1 Year Postsurgery. *Rehabilitation Psychology*. 52 (1): 74-81.
- Urban, J.P. & Roberts, S. (1995). Development and degeneration of the intervertebral discs. *Molecular Medicine Today*. 1 (7): 329-335.
- Uygur, E., Kilic, B., Demiroglu, M., Ozkan, K. & Cift, H.T. (2015). Subchondral Bone and Its Role in Osteoarthritis. *Open journal of orthopedics*. 5 (11): 355-360.
- Vaidya, J.G., Gray, E.K., Haig, J. & Watson, D. (2002). On the Temporal Stability of Personality. *Journal of Personality and Social Psychology*. 83 (6): 1469-1484.
- Vaianti, E., Scita, G., Ceccarelli, F. & Pogliacomi, F. (2017). Understanding the human knee and its relationship to total knee replacement. *Acta bio-medica de l'Ateneo Parmense*. 88 (2S): 6-16.
- Vaishya, R., Maini, L. & Lal, H. (2018). A journey of the Journal of Clinical Orthopaedics and Trauma. *Journal of Clinical Orthopaedics and Trauma*. 9 (4): 277-280.
- van Assche, D., Staes, F., van Caspel, D., Vanlauwe, J., Bellemans, J., Saris, D.B. & Luyten, F.P. (2010). Autologous chondrocyte implantation versus microfracture for knee cartilage injury: a prospective randomized trial, with 2-year follow-up. *Knee surgery, sports traumatology, arthroscopy*. 18 (4): 486-495.
- Vandesompele, J., De Preter, K., Pattyn, F., Poppe, B., Van Roy, N., De Paepe, A. & Speleman, F. (2002). Accurate normalization of real-time quantitative RT-PCR data by geometric averaging of multiple internal control genes. *Genome biology*. 3 (7): 34-34.11.
- Verdonk, P., Almqvist, K., Verdonk, R., Verstraete, K. & Verbruggen, G. (2007). Allogeneic Chondrocyte-Based Cartilage Repair Using Alginate Beads. In: Anonymous *Cartilage Repair Strategies*. Totowa, NJ: Humana Press.
- von der Gracht, Heiko A & Darkow, I. (2013). The future role of logistics for global wealth – scenarios and discontinuities until 2025. *Foresight*. 15 (5): 405-419.
- Vynios, D.H. et al. (2002). *Advances in analysis of glycosaminoglycans: its application for the assessment of physiological and pathological states of connective tissues*. vol. 781. Netherlands: Elsevier B.V.
- Wakitani, S., Goto, T., Pineda, S., Young, R., Mansour, J., Caplan, A. & Goldberg, V. (1994). Mesenchymal cell-based repair of large, full-thickness defects of articular cartilage. *The Journal of Bone & Joint Surgery*. 76 (4): 579-592.
- Walker, G.D., Fischer, M., Gannon, J., Thompson, R.C. & Oegema, T.R. (1995). Expression of type-X collagen in osteoarthritis. *Journal of Orthopaedic Research*. 13 (1): 4-12.

- Wang, B., Zhou, X., Price, C., Li, W., Pan, J. & Wang, L. (2013). Quantifying load-induced solute transport and solute-matrix interaction within the osteocyte lacunar-canalicular system. *Journal of Bone and Mineral Research*. 28 (5): 1075-1086.
- Wang, Q., Yang, Q., Wang, Z., Tong, H., Ma, L., Zhang, Y., Shan, F., Meng, Y. & Yuan, Z. (2016). Comparative analysis of human mesenchymal stem cells from fetal-bone marrow, adipose tissue, and Warton's jelly as sources of cell immunomodulatory therapy. *Human vaccines & immunotherapeutics*. 12 (1): 85-96.
- Wang, Y., Ding, C., Wluka, A.E., Davis, S., Ebeling, P.R., Jones, G. & Cicuttini, F.M. (2006). Factors affecting progression of knee cartilage defects in normal subjects over 2 years. *Rheumatology (Oxford, England)*. 45 (1): 79-84.
- Watson, D., Clark, L.A. & Tellegen, A. (1988). Development and Validation of Brief Measures of Positive and Negative Affect. *Journal of Personality and Social Psychology*. 54 (6): 1063-1070.
- Waugh, A., Grant, A. & Chambers, G. (2014). *Ross & Wilson Anatomy and Physiology in Health and Illness*. 12th edition. edn. GB: Churchill Livingstone.
- Westacott, C.I., Webb, G.R., Warnock, M.G., Sims, J.V. & Elson, C.J. (1997). Alteration of cartilage metabolism by cells from osteoarthritic bone. *Arthritis and Rheumatism*. 40 (7): 1282-1291.
- Widuchowski, W., Widuchowski, J. & Trzaska, T. (2007). Articular cartilage defects: study of 25,124 knee arthroscopies. *The Knee*. 14 (3): 177-182.
- Wijayarathne, S.P., Teichtahl, A.J., Wluka, A.E., Hanna, F., Bell, R., Davis, S.R., Adams, J. & Cicuttini, F.M. (2008). The determinants of change in patella cartilage volume—a cohort study of healthy middle-aged women. *Rheumatology*. 47 (9): 1426-1429.
- Williams, R.J., Dreese, J.C. & Chen, C. (2004). Chondrocyte Survival and Material Properties of Hypothermically Stored Cartilage. *The American journal of sports medicine*. 32 (1): 132-139.
- Wilson, A.J., Murphy, W.A., Hardy, D.C. & Totty, W.G. (1988). Transient osteoporosis: transient bone marrow edema? *Radiology*. 167 (3): 757-760.
- Wluka, A.E., Hanna, F., Davies-Tuck, M., Wang, Y., Bell, R.J., Davis, S.R., Adams, J. & Cicuttini, F.M. (2009). Bone marrow lesions predict increase in knee cartilage defects and loss of cartilage volume in middle-aged women without knee pain over 2 years. *Annals of the rheumatic diseases*. 68 (6): 850-855.
- Wong, V.W., MD, Gurtner, G.C., MD & Longaker, Michael T., MD, MBA (2013). Wound Healing: A Paradigm for Regeneration. *Mayo Clinic Proceedings*. 88 (9): 1022-1031.
- Wotton, S.F., Duance, V.C. & Fryer, P.R. (1988). Type IX collagen: A possible function in articular cartilage. *FEBS letters*. 234 (1): 79-82.

- Wu, B., Durisin, E.K., Decker, J.T., Ural, E.E., Shea, L.D. & Coleman, R.M. (2017). Phosphate regulates chondrogenesis in a biphasic and maturation-dependent manner. *Differentiation*. 95 : 54-62.
- Xu, L., Wang, Q., Xu, F., Ye, Z., Zhou, Y. & Tan, W. (2013). Mesenchymal Stem Cells Downregulate Articular Chondrocyte Differentiation in Noncontact Coculture Systems: Implications in Cartilage Tissue Regeneration. *Stem cells and development*. 22 (11): 1657-1669.
- Yuan, X.L., Meng, H.Y., Wang, Y.C., Peng, J., Guo, Q.Y., Wang, A.Y. & Lu, S.B. (2014). Bone–cartilage interface crosstalk in osteoarthritis: potential pathways and future therapeutic strategies. *Osteoarthritis and Cartilage*. 22 (8): 1077-1089.
- Zachar, L., Bačenková, D. & Rosocha, J. (2016). Activation, homing, and role of the mesenchymal stem cells in the inflammatory environment. *Journal of inflammation research*. 9 : 231-240.
- Zanetti, M., Bruder, E., Romero, J. & Hodler, J. (2000). Bone Marrow Edema Pattern in Osteoarthritic Knees: Correlation between MR Imaging and Histologic Findings. *Radiology*. 215 (3): 835-840.
- Zevon, M.A. & Tellegen, A. (1982). The structure of mood change: An idiographic/nomothetic analysis. *Journal of personality and social psychology*. 43 (1): 111-122.
- Zhang, D., Johnson, L.J., Hsu, H. & Spector, M. (2007). Cartilaginous deposits in subchondral bone in regions of exposed bone in osteoarthritis of the human knee: Histomorphometric study of PRG4 distribution in osteoarthritic cartilage. *Journal of Orthopaedic Research*. 25 (7): 873-883.
- Zhang, H., Li, Z., Su, X., Ding, L., Li, J. & Zhu, H. (2018). Subchondral bone derived mesenchymal stem cells display enhanced osteo-chondrogenic differentiation, self-renewal and proliferation potentials. *Experimental Animals*. 67 (3): 349-359.
- Zhang, L., Hu, J. & Athanasiou, K.A. (2009). The Role of Tissue Engineering in Articular Cartilage Repair and Regeneration. *Critical reviews in biomedical engineering*. 37 (1-2): 1-57.
- Zhang, R., Ma, J., Jing, H., Weijie, Z. & Jianbing, M. (2019). Mesenchymal stem cell related therapies for cartilage lesions and osteoarthritis. *American journal of translational research*. 11 (10): 6275-6289.
- Zhang, Y., Guo, W., Wang, M., Hao, C., Lu, L., Gao, S., Zhang, X., Li, X., Chen, M., Li, P., Jiang, P., Lu, S., Liu, S. & Guo, Q. (2018). Co-culture systems-based strategies for articular cartilage tissue engineering. *Journal of Cellular Physiology*. 233 (3): 1940-1951.
- Zhao, J., Li, X., Bolbos, R., Link, T. & Majumdar, S. (2010). Longitudinal assessment of bone marrow edema-like lesions and cartilage degeneration in osteoarthritis using 3 T MR T1rho quantification. *Skeletal Radiology*. 39 (6): 523-531.

Zhao, Z., Li, Y., Wang, M., Zhao, S., Zhao, Z. & Fang, J. (2020). Mechanotransduction pathways in the regulation of cartilage chondrocyte homeostasis. *Journal of Cellular and Molecular Medicine*. 24 (10): 5408-5419.